

# TOWARDS UNDERSTANDING STRING COMPACTIFICATION

A Dissertation

Presented to the Faculty of the Graduate School

of Cornell University

in Partial Fulfillment of the Requirements for the Degree of

Doctor of Philosophy

by

Manki Kim

August 2021

© 2021 Manki Kim  
ALL RIGHTS RESERVED

# TOWARDS UNDERSTANDING STRING COMPACTIFICATION

Manki Kim, Ph.D.

Cornell University 2021

This thesis is mostly concerned with two questions: Is it possible to construct de Sitter solutions in string theory? How do strings make up spacetime in string theory? In this thesis, modest progress along those two directions is reported.

## BIOGRAPHICAL SKETCH

Manki Kim was born in 1994, in South Korea. His childhood memory is filled with one of his grandmothers, who was a famous shaman<sup>1</sup> in the local community. When Manki was of age to attend schools, he quasi-permanently moved back to parents' house until he attended high school.

Manki's attention was mostly captivated by computer games although he was not a good player, until he saw a flyer for a science high school<sup>2</sup>. As Manki was in desperate need of living away from his parents, getting accepted into the science high school became his imminent goal. This was the moment, when Manki seriously started his study, math and physics in particular.

After graduating the science high school, Manki attended KAIST (Korea Advanced Institute of Science and Technology) from 2011 to 2016, graduating *summa cum laude* with a double major in physics and mathematics. Manki's initial intention was to become a mathematician, but he soon realized that he was not gifted in math. This realization drove his attention away from pure mathematics to more down to earth physics.

In 2016, He became a graduate student in physics at Cornell University with the intention to study flavor physics. But, it was soon clear that he did not enjoy flavor physics. While he was contemplating quitting physics, he attended a colloquium given by his current advisor Liam McAllister.<sup>3</sup> On the very next day, Manki switched his field of study and since then Manki kept studying string theory. Manki will continue his research as a Pappalardo fellow at MIT.

---

<sup>1</sup>In Korean, female shamans are called *mudang*.

<sup>2</sup>In Korea, science high schools are public boarding schools.

<sup>3</sup>The title of the colloquium was "The Discrete Character of Physical Law from String Theory to the CMB."

This thesis is dedicated to my dearest friends who are more than families to me.

## ACKNOWLEDGEMENTS

My research progress for most of the time has resembled a random walk in the space of ideas in many ways. Without the constant driving force, which has been pointing towards correctness, provided by my advisor Liam McAllister, I may not have achieved what I did during the ph.d study. I would like to sincerely thank Liam for being a great mentor and giving me an opportunity to be his student in the first place.

Of course, all of this was possible thanks to my first advisor Yuval Grossman, who encouraged and supported me to follow my heart.

I would like to thank Tom Hartman for giving me countless advices and encouragement.

I would also like to thank Csaba Csaki, Maxim Perelstein, Michael Stillman, Seung Joon Lee for their positive influences on me.

I thank Michael Niemack, although he may not remember, for his very insightful question “can you compute the mass of electrons in string theory?” This question has echoed in my head for many days and it still does.

It is not an overstatement to say that I may not have been able to finish my ph.d study if I had not known my dearest friend Seuk Young Song. With all my heart, I sincerely thank you for being a great friend.

It would not have been possible to endure my time in Ithaca, if I did not have the support from my friends. Please forgive me if I failed to write your name. An incomplete list of friends of mine includes: Cheol Ho Jeon, Eugene Lee, Eunyong Go, Miso Myung, Gyutak Kim, Gwan Young Ahn, Dong Hwan Kim, Gowoon Cheon, Sooyeon Lee, Seungbin Park, Jiyoung Lee, Junghoon Han, YoungJu Jo, Euijin Jeon, Yoonsoo Bach Park, Kyeong-Ro Kim, Hyeongseop Kim, Shin Kim, Myungha Lee, Gang Ihn Kim, Daegwang Choi, Rebecca Da-In Choi, Aro Lee,

Minsoo Chung, Daeho Kwon.

My time in Ithaca is cherishable because of many friends I met in Ithaca. I thank Mehmet Demirtas, Jakob Moritz, Naomi Gendler, Andres Rios-Tascon, Geoffrey Fatin, Peter Cha, Ibrahim Shehzad, Gowri Kurup, Sungwoo Hong, Gabriel Lee, Yoonhyung Choi, Kyungsoo Kim, Jongil Kim, Sangwoo Park for being great friends to me.

I want to specially thank Yikun Jiang, for sharing his passion towards physics. I trully learned a lot from you.

I was able to learn unique approaches to physics thanks to many of my collaborators. I take this as a chance to thank Shamit Kachru, Max Zimet, Gabriel Wong, William Donnelly, Cody Long.

I cannot thank enough Youngsun Yoon and Sunku Kim for hosting me numerous times whenever I needed some time off in Karlsruhe, Germany.<sup>4</sup>

I also thank a faculty member, who shall not be named, for saying that I talk fluently unlike the other Asian students but I am terrible in using the articles.

I cannot thank the physics department enough as the department always demanded more than reasonable teaching load, especially for the autotutorial classes<sup>5</sup>, which well prepared me for the future workload one has to bear as an academic.

I acknowledge the tremendous effort of Cornell health in fighting depression. By being hospitalized against my will<sup>6</sup>, I learned how to eat up the emotion and

---

<sup>4</sup>Now I can finally admit that one of the primary reasons to visit Karlsruhe was this one pub Vogel Hausbräu. I even learned elementary German, just to order beer for myself in German.

<sup>5</sup>I remember waiting the route 10 bus at 10:20 pm on Monday, Wednesday, and Thursday and at 9:20 pm on Tuesday, because I had to teach three or four hours on each day until that late. It was a truly remarkable experience. It was one of the ample reasons to consider quitting physics.

<sup>6</sup>I went to Cornell health once concerning my depression. When I was asked if I will kill myself tomorrow, I answered “I don’t know, as I can’t predict the future.” This answer clearly was not meant to be a sign of a suicidal act rather an honest answer regarding my ability to predict the future. After this instant, the so called professionals concluded that I was suicidal and must be hospitalized. I clearly did not see it coming, as I am not an all-knowing deity who can predict the future.

pretend to act normal.

I sincerely thank my undergraduate advisor for refusing to write the recommendation letters because it does no good to him, although he finally gave in. He was the reason why I learned the importance of perseverance.



# TABLE OF CONTENTS

Biographical Sketch . . . . .	iii
Dedication . . . . .	iv
Acknowledgements . . . . .	v
Table of Contents . . . . .	viii
List of Tables . . . . .	xii
List of Figures . . . . .	xiii
<b>1 Introduction</b>	<b>1</b>
1.1 The cosmological constant in string theory . . . . .	3
1.1.1 The Dine-Seiberg problem . . . . .	5
1.1.2 The KKLT proposal . . . . .	7
1.1.3 The challenges to realize the KKLT proposal . . . . .	9
1.2 How is the spacetime made up? . . . . .	11
1.3 Organization of this thesis . . . . .	13
<b>2 Monodromy Charge in D7-brane Inflation</b>	<b>14</b>
2.1 Introduction . . . . .	15
2.2 Higgs-otic Inflation . . . . .	18
2.2.1 Setup . . . . .	19
2.2.2 Magnetized D-brane action . . . . .	20
2.2.3 Inflaton potential from induced charge . . . . .	22
2.2.4 An example . . . . .	23
2.2.5 An issue of orientation . . . . .	24
2.3 Backreaction of Monodromy Charge . . . . .	26
2.3.1 Perturbative computation of backreaction . . . . .	29
2.3.2 Effects on Euclidean D3-branes . . . . .	35
2.4 Implications . . . . .	38
2.4.1 Inflaton-dependence of the Pfaffian . . . . .	38
2.4.2 Comment on fluxbrane inflation . . . . .	41
2.5 Conclusions . . . . .	43
<b>3 de Sitter Vacua from Ten Dimensions</b>	<b>46</b>
3.1 Introduction . . . . .	47
3.2 Ten-dimensional Equations of Motion . . . . .	51
3.3 Stress-energy of Gaugino Condensate . . . . .	56
3.3.1 Four-dimensional effective theory . . . . .	58
3.3.2 D7-brane gaugino couplings . . . . .	60
3.3.3 Ten-dimensional stress-energy . . . . .	64
3.4 Anti-D3-branes and Gaugino Condensation . . . . .	66
3.4.1 Decompactification from anti-D3-branes . . . . .	66
3.4.2 Interactions of anti-D3-branes and gaugino condensation . . . . .	67
3.5 Conclusions . . . . .	71

<b>4</b>	<b>Vacua with Small Flux Superpotential</b>	<b>74</b>
4.1	Introduction . . . . .	75
4.2	A landscape of weakly coupled flux vacua with small $W_0$ . . . . .	76
4.3	An example . . . . .	80
4.4	Statistics of small $W_0$ . . . . .	82
4.5	Toward stabilizing all moduli . . . . .	83
4.6	Conclusions . . . . .	84
<b>5</b>	<b>Conifold Vacua with Small Flux Superpotential</b>	<b>86</b>
5.1	Introduction . . . . .	87
5.2	Vacua with small flux superpotential . . . . .	89
5.2.1	Setup . . . . .	89
5.2.2	The large complex structure patch . . . . .	93
5.2.3	Small flux superpotentials at large complex structure . . . . .	94
5.3	Stabilizing near the conifold . . . . .	95
5.3.1	The conifold prepotential from a shrinking curve . . . . .	97
5.3.2	Moduli stabilization in three steps . . . . .	101
5.3.3	Comments on the supergravity approximation . . . . .	104
5.4	An example . . . . .	104
5.4.1	A Calabi-Yau threefold and an orientifold . . . . .	106
5.4.2	The Greene-Plesser mirror dual . . . . .	109
5.4.3	Explicit flux vacua . . . . .	116
5.5	Discussion . . . . .	123
<b>6</b>	<b>Entanglement entropy and edge modes in topological string theory: I</b>	<b>126</b>
6.1	Introduction . . . . .	127
6.2	Summary, overview of GV duality and the Hartle-Hawking state . . . . .	133
6.2.1	Summary of the GV duality . . . . .	133
6.2.2	The Hartle Hawking state in string theory . . . . .	136
6.2.3	Outline of the paper . . . . .	139
6.3	The closed string Hilbert space and entanglement entropy from the replica trick . . . . .	141
6.3.1	The Hartle-Hawking state from the all-genus amplitude . . . . .	141
6.3.2	The chiral boson description of $\mathcal{H}_\Sigma$ and D branes . . . . .	145
6.3.3	Entanglement entropy from the replica trick . . . . .	149
6.4	The A-model closed TQFT and representation category of quantum groups . . . . .	153
6.4.1	General comments about factorization, E-brane axiom, and cobordisms . . . . .	153
6.4.2	A model TQFT on Calabi Yau manifolds . . . . .	158
6.4.3	Quantum traces and $q$ -deformation of the A model TQFT . . . . .	161
6.4.4	String theory origin of the $q$ -deformation . . . . .	164
6.5	Extension of the A-model closed TQFT . . . . .	166

6.5.1	The open string Hilbert space as the coordinate algebra $\mathcal{A}(U(\infty)_q)$ . . . . .	167
6.5.2	Quantum group symmetry on the open string Hilbert space . . . . .	170
6.5.3	A-model open-closed TQFT and factorization maps . . . . .	178
6.5.4	The open A-model TQFT and sewing relations . . . . .	181
6.5.5	The open closed sewing axioms and factorization of the Hartle-Hawking state . . . . .	183
6.5.6	The reduced density matrix for the Hartle-Hawking state and a canonical calculation of entanglement entropy . . . . .	188
6.5.7	Revisiting the replica trick on the resolved conifold . . . . .	190
6.6	Discussion . . . . .	196
<b>7</b>	<b>Entanglement entropy and edge modes in topological string theory II: The dual gauge theory story</b> . . . . .	<b>202</b>
7.1	Introduction . . . . .	203
7.2	Review of part 1 . . . . .	212
7.2.1	Generalized entropy for A model closed strings . . . . .	212
7.2.2	The closed string Hilbert space, A model TQFT, and the Hartle-Hawking state . . . . .	215
7.2.3	Shrinkable boundary condition and the Calabi Yau Cap . . . . .	219
7.2.4	Factorization and the q-deformed entanglement entropy . . . . .	223
7.2.5	Quantum group symmetry, defect operator and non-local boundary conditions . . . . .	231
7.3	Chern-Simons dual of the Hartle-Hawking state and the entanglement entropy . . . . .	233
7.3.1	Review of Chern-Simons theory . . . . .	235
7.3.2	Generating functional for Wilson loops and the $\Omega$ state . . . . .	238
7.3.3	Hartle-Hawking state in Chern-Simons theory . . . . .	239
7.3.4	Matching with the dual partition function and emergence of the bulk geometry . . . . .	243
7.3.5	Entropy from geometrical replica trick in Chern-Simons theory . . . . .	245
7.3.6	Factorization and edge modes in the dual Chern-Simons theory . . . . .	248
7.4	Large N expansion of Wilson loops and dual string worldsheets . . . . .	257
7.4.1	Mapping Wilson loops to worldsheets on the deformed conifold . . . . .	259
7.4.2	Applying the geometric transition to the resolved conifold geometry . . . . .	264
7.4.3	Dual description of the entanglement brane . . . . .	266
7.5	Discussion . . . . .	272
<b>A</b>	<b>Appendix for Chapter 2</b> . . . . .	<b>280</b>
A.1	Conventions for Differential Forms . . . . .	280
A.2	Green's Function on a Toroidal Orientifold . . . . .	284

<b>B</b>	<b>Appendix for Chapter 3</b>	<b>287</b>
B.1	Dimensional Reduction . . . . .	287
B.1.1	D7-brane gaugino action . . . . .	287
B.1.2	Reduction of the D7-brane action on a divisor . . . . .	290
B.1.3	Killing spinor equations and the superpotential . . . . .	297
B.1.4	Dimensional reduction and translation to four-dimensional terms . . . . .	307
B.1.5	Normalization of the Kähler potential . . . . .	309
B.2	Spectroscopy of Interactions . . . . .	310
B.2.1	Kaluza-Klein modes on $T^{1,1}$ . . . . .	311
B.2.2	Effect of anti-D3-branes on gaugino condensate . . . . .	313
B.2.3	Effect of gaugino condensate on anti-D3-branes . . . . .	318
B.3	Cancellation of Divergences, and the D3-brane Potential . . . . .	324
B.3.1	Cancellation of divergences . . . . .	324
B.3.2	D3-brane potential from flux . . . . .	328
<b>C</b>	<b>Appendix for Chapter 5</b>	<b>333</b>
C.1	The D3-brane tadpole in the orbifold . . . . .	333
C.1.1	Computation in the resolved orbifold . . . . .	333
C.1.2	Computation in the orbifold limit . . . . .	338
<b>D</b>	<b>Appendix for Chapter 6</b>	<b>342</b>
D.1	Topological twist and topological sigma model on the worldsheet . .	342
D.2	Topological String on Conifolds and Geometric Transition . . . . .	346
D.2.1	Blow up of the resolved conifold . . . . .	347
D.2.2	Lagrangian Submanifolds . . . . .	348
D.3	Quantum groups and their representations . . . . .	349
D.3.1	Hopf algebra structure . . . . .	349
D.3.2	R matrix and antipode for $SL_q(2)$ . . . . .	351
D.3.3	$*$ structure and unitary representations . . . . .	351
D.4	Spacetime non-commutativity from B fields . . . . .	352
<b>E</b>	<b>Appendix for Chapter 7</b>	<b>354</b>
E.1	Topological twist and topological sigma model on the worldsheet . .	354
E.2	Topological String on Conifolds and Geometric Transition . . . . .	358
E.3	$\mathbb{C}^3$ as a toric variety . . . . .	362
E.4	Replica trick in Chern-Simons theory . . . . .	365
E.5	Wilson loops in AdS/CFT . . . . .	368
	<b>Bibliography</b>	<b>371</b>

## LIST OF TABLES

5.1	Some interesting vacua. First line: smallest $W_0$ . Second line: smallest $W_0$ with $g_s M > 1$ . Third line: largest $g_s M$ . Fourth line: best alignment between $z_{\text{cf}}^{2/3}$ and $W_0$ . The parameter $\varepsilon$ is the magnitude of the neglected two-instanton contributions to the superpotential relative to the retained one-instanton terms. . . . .	123
A.1	Possible conventions. The first column denotes the quantity whose definition can be chosen. The variables $a$ and $b$ in parentheses equal $+1$ if the choice corresponds to the second column and $-1$ if the choice corresponds to the third column. We have taken $a = b = 1$ throughout this work. . . . .	283
C.1	Left: The curves $\mathcal{C}_{ij}$ invariant under subgroups $H_{ij} \subset G$ , their Euler characteristics $\chi$ , and the Euler characteristics $\hat{\chi}$ of the curves $\hat{\mathcal{C}}_{ij}$ obtained by removing toric points. Right: Analogous table for toric points. . . . .	340

## LIST OF FIGURES

4.1	The scalar potential on the positive $\text{Im } \tau$ axis. . . . .	82
5.1	The slice $\beta_3^C = 0$ in the Mori cone of the Calabi-Yau $X$ described in §5.4. Blue lattice points are populated by nonvanishing GV invariants $n_{(i,j,0)}^0$ . The red lattice point is GV-nilpotent of order one, and lies outside the closure of the interior cone (bounded by dashed purple lines). Near the origin of the Coulomb branch $z^1 \rightarrow 0$ , one retains a controlled expansion in $e^{2\pi i z^{2,3}}$ with coefficients $\sum_i n_{(i,j,k)}^0$ . These are the GV invariants on the Higgs branch, and are computable because the sum over $i$ terminates: each row in the figure has finite length. . . . .	98
5.2	Left: the slice $\{u = v = 0\} = \mathbb{C}^2/\mathbb{Z}_2$ and the position of the orientifold planes $x_1 = 0$ and $x_2 = 0$ . Two O7-planes intersect at the orbifold singularity $x_1 = x_2 = 0$ which also contains the conifold singularity. Middle and right: the same slice after the resolution of the orbifold singularity and a closeup of the exceptional divisor. The O7-planes intersect the exceptional divisor $\alpha = 0$ at antipodal points $[1 : 0]$ and $[0 : 1]$ . The conifold singularities reside at $[1 : i]$ and $[1 : -i]$ and are mapped into each other by the orientifold involution. . . . .	115
5.3	Left: the toric fan of the singular surface $\mathbb{C}^2/\mathbb{Z}_2$ with two vertices $v_x = (1, 2)$ and $v_y = (1, 0)$ . Right: the toric fan of the resolution of $\mathbb{C}^2/\mathbb{Z}_2$ by a resolution divisor $\alpha = 0$ associated with the vertex $v_\alpha = \frac{1}{2}(v_x + v_y) = (1, 1)$ . . . . .	115
5.4	Scatter plots showing the values of $2\ln(1/ W_0 )$ and $\frac{4}{3}\ln(1/ z_{\text{cf}} )$ with diagonal in red indicating the critical region where the uplift potential of an anti-D3-brane would compete efficiently with KKLT bulk moduli stabilization. Left: All vacua. Right: Only vacua that live close to the critical line. . . . .	119
5.5	A scatter plot as in Figure 5.4 but showing only vacua with $g_s M > 1.120$	
6.1	The partition function of the $A$ -model on a line bundle over $S^2$ has two interpretations. In the closed string channel (left), it represents the overlap $\langle HH^*   HH \rangle$ between the Hartle-Hawking state and its orientation reversal. In the open string channel (right), it represents a trace in the Hilbert space of open strings. Figure borrowed from Ref. [122]. . . . .	128
6.2	Gopakumar duality relates closed $A$ -model string on the resolved conifold to the open $A$ -model string on the deformed conifold . . .	136

6.3	The left figure shows the codimension-1 slice $\Sigma$ of the resolved conifold where a QFT state would be defined. In the closed string theory, the analogue of a time slice is a set $\mathcal{F}_\Sigma$ of loops configurations associated with $\Sigma$ . For the A-model string, we will restrict these loop configurations to lie in a Lagrangian submanifold $\mathcal{L} \subset \Sigma$ . The string wavefunctional assigns an amplitude to each configuration of such loops. . . . .	138
6.4	The left figure shows a D-brane on $\mathcal{L} \subset \Sigma$ which intersects the base $S^2$ along the equator and extends in to the fiber directions along a hyperbola. In the right figure, we show the string loops in the time slice $\mathcal{F}_\Sigma$ which lives in $\mathcal{L}$ . The state $ HH\rangle$ state is defined via worldsheets which end on these loops and wrap the upper hemisphere, as shown in the left figure. Similarly $\langle HH^* $ describes worldsheets on the southern hemisphere which end on anti-branes. . . . .	143
6.5	On the left, we show the splitting of the worldsheet boundary into $A$ and $B$ . On the right, the brane $\mathcal{L}$ on which the closed string configurations $X(\sigma)$ live is split into subregions by the entanglement branes. We show an open string configuration $X_{ij}(\sigma) \in \mathcal{F}_{\Sigma_A}$ . These end on the entanglement branes intersecting $\mathcal{L}$ along two open disks.	154
6.6	Quantizing the worldvolume gauge theory with time running around the non-contractible cycle of $\mathcal{L}$ , we have to impose Gauss's law on $M$ . The puncture on $M$ corresponds to the anyon charge on the Wilson loop which sources Gauss Law. . . . .	165
6.7	The state $ IJ\rangle$ represents a configuration of $n$ open strings with Chan-Paton factors $(i_1, j_1) \dots (i_n, j_n)$ . . . . .	170
6.8	The figure shows a state of two open strings. Antisymmetrization of the right and left indices can be expressed by fixing the Chan-Paton factors while changing the pattern of connection between them. In the figure we have put string number 1 on top of string number 2. When the open strings have bosonic statistics as imposed by the $S_n$ quotient in (6.97), the antisymmetrization of the left or the right endpoints give the same state, since the two operations are relating by commuting string number 1 and 2. However, the A-model open string has anyonic statistics, so the two orderings are not equal. This corresponds a nontrivial braiding structure in the diagrams above. . . . .	171
6.9	The reduced density matrix $\rho_A^C$ defined using a noncanonical trace operation fails to satisfy the E-brane axiom when it is replicated. It also does not commute with the edge mode symmetry group . . .	192
6.10	D-branes on $\mathcal{L}'$ intersect with D-branes on $\mathcal{L}$ . . . . .	198

7.1	The left figure shows the cigar geometry which is the saddle point that contributes the the area term in the generalized entropy. On the right we have removed a cap at the tip of the cigar and inserted a shrinkable boundary condition $e$ . . . . .	204
7.2	In this figure we have flattened out the cigar geometry into a disk. On the right figure, we can view the lower half of the annulus as a path integral preparation of a factorized state with a shrinkable boundary condition at the entangling surface. Quantizing $Z(\beta)$ with respect to the time variable around the origin shows that it can be viewed as the trace of a reduced density matrix on $V$ . . . .	205
7.3	Susskind and Uglum considered the generalized entropy of perturbative closed strings in flat space, viewed as a limit of the cigar geometry. Using off shell arguments, they computed generalized entropy by inserting a conical singularity in the background, corresponding to the tip of the cigar geometry. In perturbative string theory, the area term comes from the sphere diagram which intersects the conical singularity. Viewed in the open string channel, this is a one-loop open string diagram. This interpretation amounts to an open-closed string duality which identifies Bekenstein Hawking entropy as thermal entropy of open strings that end on the conical singularity. Figure borrowed from Ref. [122]. . . . .	207
7.4	Gopakumar-Vafa duality relates closed A-model string on the resolved conifold to the open A-model string on the deformed conifold . . . . .	209
7.5	The left figure shows worldsheet instantons ending on D-branes which cut the minimal volume $S^2$ of the resolved conifold along the equator. The branes extend into the non compact fiber directions and wrap a Lagrangian submanifold with the topology $\mathbb{C} \times S^1$ . . .	219
7.6	The closed string channel description of entanglement branes on the resolved conifold geometry. The total space is a six dimensional Calabi Yau manifold fibered over a sphere. We have shown only the base manifold and indicated the bundle structure with the Chern class labelling. . . . .	221
7.7	On the left, we show a closed string loop $X(\sigma)$ inside the non-compact Lagrangian manifold $\mathcal{L} = \mathbb{C} \times S^1$ where we put probe D branes. On the right $\mathcal{L}$ is split into subregions by the entanglement branes on $\mathcal{L}'$ . The factorization map embeds the closed string $X(\sigma)$ into open string configuration $X_{ij}^A(\sigma), X_{ij}^B(\sigma)$ which are glued together along the entanglement branes . . . . .	229



7.8	On the left, the blue disk corresponds to a $(0,0)$ cap with trivial bundle structure. To obtain the Calabi Yau cap, a defect operator is inserted to implement the nontrivial topology. In the first equality, we have integrated over the cap to obtain a non local shrinkable boundary condition $U = D$ . An equivalent A model amplitude on the disk can be obtained by moving the defect operator outside the hole and putting a local boundary condition on its boundary. . . .	233
7.9	The state $ R_{CS}\rangle$ is defined by the path integral on a solid torus with a Wilson loop operator inserted. . . . .	237
7.10	Separated solid torus with a Wilson loop operator inserted. . . . .	245
7.11	Geometric entanglement entropy in Chern-Simons theory is equivalent to left-right entanglement entropy in the WZW model. L and R in the diagram represents left and right moving chiralities for the WZW models. . . . .	249
7.12	The generating functional for Wilson loops can be viewed as the open string amplitude on the deformed conifold with dynamical branes wrapping $S^3$ and probe branes wrapping $\mathcal{L}$ . They intersect along a knot $C$ on $S^3$ , colored in blue. . . . .	260
7.13	Toric diagram for the deformed conifold with probe D-branes on $\mathcal{L}$ intersecting the $S^3$ . For the simplicity, we have not specified the frame of the D-brane and the probe brane is depicted as a red dot. . . . .	261
7.14	Toric diagram for the deformed conifold with M D-branes on $\mathcal{M}$ . Note that we have not specified the frame of the probe D-brane on $\mathcal{M}$ . . . . .	263
7.15	Displacing the probe branes away from $S^3$ gives rise to open string instantons of finite area, stretched between the branes. . . . .	264
7.16	The toric diagrams show the result of the geometric transition applied to the deformed resolved with probe branes displaced from $S^3$ . Under the transition the $S^3$ is replaced by a sphere of size $t'$ . On the right, we show the $t'$ limit in which that sphere $t'$ is sent to infinity. This results in “half” the resolved conifold geometry with probe branes inserted, which defines the Hartle-Hawking state. It is important to note that we have specified the framing for the probe D-brane for the HH state, which is determined by the direction of the arrow [4]. . . . .	265
7.17	The geometric transition, combined with the $t' \rightarrow \infty$ limit maps the state on the deformed conifold (left figure) to the Hartle-Hawking state on the resolved conifold. . . . .	266
7.18	The dual thermal interpretation of the resolved conifold partition function is obtained by first introducing two $S^2$ with Kahler parameter $t'$ (left figure) and then applying a geometric transition to the deformed geometry on the right with branes on two $S^3$ . The worldsheets stretched between these branes describe open string loop diagrams . . . . .	268

7.19	Annihilation of the probe branes gives rise to the partition function $Z_{\text{deformed}}(t, t')$ , which describes world worldsheet instantons stretched between D branes on the two $S^3$ 's. The quantum dimensions which lead to the q-deformation of the edge modes arise from the ribbon diagrams (red) interacting with the boundary of the instanton worldsheets. We have shown one term in the ribbon diagram expansion corresponding to the “theta” diagram. . . . .	269
7.20	Duality between Wilson loop and worldsheet in AdS/CFT. On the left figure, we showed the open string frame, where displacing a probe brane away from a stack of D branes leads to stretched worldsheets ending on Wilson loops. On the right we applied a geometric transition to obtain the closed string $AdS \times S^5$ geometry where the worldsheet has only one boundary ending on the probe brane. This is a direct analogue of the duality between Wilson loops and worldsheets in topological string theory . . . . .	277
7.21	Duality between Wilson loop and worldsheet in topological string. There is an $S^3$ at asymptotic infinity that has been omitted from the picture. [156] . . . . .	278
7.22	Toric diagram for the conifold geometry . . . . .	278
7.23	Thermo-field double state and the Penrose diagram for the dual AdS-Schwarzschild geometry. The horizontal line in the middle represents the $t = 0$ time slice. . . . .	279
7.24	Web of dualities for topological string theory. W/T: worldsheet/target space duality. O/C: open/closed duality (large N duality); M : mirror symmetry. . . . .	279
E.1	Solid torus with a Wilson loop operator inserted. . . . .	366
E.2	Separated solid torus with a Wilson loop operator inserted. . . . .	366
E.3	Geometric representation of the reduced density matrix . . . . .	367
E.4	Geometric representation of $Z_1$ . . . . .	368

# CHAPTER 1

## INTRODUCTION

Our universe on large scale is spatially flat, homogeneous, and isotropic. Not only our universe is highly symmetric, but it is also expanding at an accelerating rate. The standard model of cosmology that explains such a large-scale structure of our universe is the so-called  $\Lambda$ -CDM model supplemented with inflationary initial conditions.

As a phenomenological model, the standard model of cosmology is a tremendous success.<sup>1</sup> But, successful phenomenological models do not always come along with clean theoretical understanding. In fact, it has been notoriously difficult to understand the very fundamental assumption or input of the  $\Lambda$ -CDM model, the positive and small cosmological constant.

Let me illustrate the puzzle, the cosmological constant problem.<sup>2</sup> Consider an effective theory with the cutoff  $E_{cut}$ , and a massive field  $\phi$  whose mass  $m$  is smaller than  $E_{cut}$ . To compute the contribution to the cosmological constant from  $\phi$ , one can compute the vacuum expectation value of the vacuum energy which generically yields

$$\Lambda \sim \mathcal{O}(E_{cut}^4). \quad (1.1)$$

It should be noted that no matter what the mass and the spin of  $\phi$  are, the general expectation (1.1) always holds. Now the trouble comes. Below the energy cutoff  $E_{cut}$ , there are numerous fields and each of them give  $\mathcal{O}(E_{cut}^4)$  contribution to the

---

<sup>1</sup>Note that the Hubble constant measurements of the present and of the early universe are in strong tension. This Hubble tension may require a renovated understanding of cosmology. Even if the modifications to the  $\Lambda$ -CDM model are required, it does not change the fact that our current universe and inflation are still well approximated by quasi de Sitter solutions.

<sup>2</sup>More broadly, as we will see, the cosmological constant problem can be understood as an avatar of the hierarchy problem.

cosmological constant. This genericity of (1.1) therefore leads to an expectation that the cosmological constant itself will also be an order of the energy cutoff unless one has compelling evidence that numerous contributions to the cosmological constant somehow conspire to cancel each other.

Let us pretend for a moment that the standard model of particle physics works up to the Planck scale  $E_{cut} = M_{pl}$  at which quantum gravitational effects become unavoidable. (1.1) then tells us that the cosmological constant is evaluated to be

$$\Lambda \simeq 10^{76} \text{ GeV}^4. \quad (1.2)$$

Compared to the observed value of the cosmological constant,  $\Lambda_{obs} \simeq 10^{-44} \text{ GeV}^4$ , we realize that there is an order  $10^{120}$  discrepancy between the theoretical expectation and the observed value. Perhaps, one may argue that this tremendous failure is due to our arrogance that we know physics all the way up to the Planck scale. So, let us be more modest and suppose that the standard model of particle physics works up to the TeV scale. The troubling result is that the expected value of the cosmological constant is still order of  $\Lambda \simeq 10^{27} \text{ GeV}^4$ , which is still  $10^{71}$  times bigger than the observed value of the cosmological constant.

Something is awfully wrong.

## 1.1 The cosmological constant in string theory

All five approaches have one other thing in common: They show that any solution of the cosmological constant problem is likely to have a much wider impact on other areas of physics or astronomy. One does not need to explain the potential importance of supergravity and superstrings.

S. Weinberg [335].

It is conceivable that we are off by the factor of  $10^{120}$  because the cosmological constant is inherently a quantum gravitational effect and we do not understand much about the quantum gravity. Therefore, one reasonable approach is to study the cosmological constant in string theory.

String theory is a weird theory from quantum field theory point of view. Hence, it may be worth stating what it means to study the cosmological constant in string theory first before we delve into the details.

It is by now a well known fact that string theory lives in high dimensions: 10, 11, or 12 depending on how one view string theory. In order to connect string theory to our real world, we need to come up with a way to hide 6, 7, or 8 dimensions away. This procedure is so-called compactification.<sup>3</sup> In the context of weakly coupling string theories, this means that we consider a spacetime of a form

$$M_{10} \simeq M_4 \times M_6, , \tag{1.3}$$

where  $M_4$  is the non-compact spacetime and  $M_6$  is a six dimensional compactification manifold. Note that (1.3) should not be taken literally, as one may often find

---

<sup>3</sup>It is deeply disturbing that we still do not understand why string theory has to favor 4-dimensional non-compact spacetime.

that interesting solutions of string theory are non-trivial fibrations over spacetime.

In general, the compactification manifold  $M_6$  comes with many different modules that can control the volume and the shape of  $M_6$  for example. The abundance of those modules, which I will call moduli from now on, presents a tremendous technical challenge for string theory. Simply put, we do not understand how to compute scattering amplitudes of strings in such a background or how to build up non-trivial spacetime in string theory.<sup>4</sup>

To overcome such a difficulty, a common practice one performs is to take three major approximations. First, we approximate (1.3) as a controllable deviation from

$$M_{10} = M_4 \times X_3, \tag{1.4}$$

where  $X_3$  is a Calabi-Yau threefold. Second, we take a low energy effective theory of string theory on  $M_{10}$ , a common choice is ten-dimensional supergravity with extended objects on  $M_{10}$ . The third approximation is to integrate out all the heavy modes associated with high mass excitations of the compactification manifold. We take the first approximation because the moduli space of the Calabi-Yau is one of the best-understood moduli space. The second and the third steps are alike in that those approximations are justified in the spirit of effective field theory.

For example, physics would've been a mess if one has to bring string theory to understand a simple harmonic oscillator. Fortunately, we could understand a simple harmonic oscillator with Newton's theory of dynamics, which is a good approximation to string theory when quantum effects are small. It should be noted that it is not to imply that string theory or theories at high scales do nothing to our

---

<sup>4</sup>This is partly due to the intricacy to find a background independent formalism of string theory.

world. Theories at high energy scales do constrain the structure of the low energy effective theories, such as coupling constants and allowed terms. This constraining power of high energy theories is basically what we are after.

Coming back to the compactification, we can now state the task. To study the cosmological constant in string theory, we want to examine a meta-stable solution of the low energy supergravity of string theory of the form

$$M_{10} \simeq M_4 \times X_3, \tag{1.5}$$

where  $M_4$  is well approximated by the four-dimensional de Sitter space  $dS_4$ .

We must now ask, is finding de Sitter vacua in string theory even possible?

### 1.1.1 The Dine-Seiberg problem

In fact, classical or not, I don't know any clear-cut way to get de Sitter space from string theory or M-theory. This last statement is not very surprising given the classical no go theorem. For, in view of the usual problems in stabilizing moduli, it is hard to get de Sitter space in a reliable fashion at the quantum level given that it does not arise classically.

E. Witten [350].

It has been notoriously difficult to construct a de Sitter solution in string theory. In fact, no one has ever succeeded in finding one. In this section, we explain the challenges in the context of the Dine-Seiberg problem [111].

String theory is best understood in the weak coupling regime, where the string coupling is small  $g_s \ll 1$  and volume of the compactification manifold is large  $1/\mathcal{V} \ll 1$ .<sup>5</sup> Then the argument simply goes as follows. The effective potential of string compactification asymptotes to zero when the string coupling and inverse the compactification volume go to zero. If string theory ever admits de Sitter solutions, then there should be a deflection point at and beyond which higher order corrections to the tree-level supergravity approximations are equally important as the tree-level terms. Hence, even if string theory admits de Sitter solutions, Dine and Seiberg argued that those solutions may be in the strong coupling regime where we cannot easily explore with the current understanding of string theory.

There are a few loopholes in the argument. Despite the asymptotic behavior in the weak coupling limit of string theory, there could be tiny wiggles in the tree-level potential that can allow meta-stable de Sitter solutions. The other important loophole is that the tree-level potential in string theory is determined by discrete flux choices, which allows judicious fine-tuning [60].

Despite its attractiveness, it has been extremely challenging to find classical meta-stable de Sitter solutions in string theory in part due to the no-go theorems [254, 191, 354]. This should come as no surprise. We know the full classical action of stringy supergravity, and we all know that our life will be pretty boring if we know everything.

---

<sup>5</sup>In string theory with many supercharges, this restriction can be avoided due to strong-weak coupling dualities [328, 194, 344, 347, 294]. But, it is not clear how to take advantage of such dualities when there is no supersymmetry or too few supercharges.



### 1.1.2 The KKLT proposal

The vacua in [215] are not at all simple. They are jury-rigged, Rube Goldberg contraptions that could hardly have fundamental significance. But in an anthropic theory simplicity and elegance are not considerations. The only criteria for choosing a vacuum is utility, i.e. does it have the necessary elements such as galaxy formation and complex chemistry that are needed for life. That together with a cosmology that guarantees a high probability that at least one large patch of space will form with that vacuum structure is all we need.

L. Susskind [314].

The KKLT proposal [215] is the very first concrete proposal for the construction of de Sitter solutions in string theory.<sup>6</sup> To explain how the KKLT proposal circumvents the Dine-Seiberg problem, let us consider a type IIB string theory compactified on a CY3 orientifold with O3/O7-planes. The resulting 4d effective field theory is  $\mathcal{N} = 1$  supergravity with the following ingredients:

- Kähler moduli.
- Complex structure moduli.
- D3/D7-branes.

To simplify the discussion, let us assume that there is only one Kähler modulus, all the D3-branes are dissolved into the three form fluxes  $F$ ,  $H$ , and the D7-brane moduli are frozen by the worldvolume flux.

---

<sup>6</sup>For an alternative to the KKLT proposal, see [23].

The tree-level superpotential of the low energy supergravity is given by the so-called Gukov-Vafa-Witten (GVW) superpotential [176]

$$W_{\text{tree}} = \int (F - \tau H) \wedge \Omega, \quad (1.6)$$

where  $\tau$  is the axio-dilaton. Due to the non-renormalization theorem, (1.6) does not receive perturbative corrections. The leading non-perturbative corrections to the tree-level superpotential is due to the gaugino condensation on the D7-brane stack

$$W_{\text{np}} = \mathcal{A}e^{-aT} + \mathcal{O}(e^{-1/g_s}, e^{-2aT}), \quad (1.7)$$

where  $T$  is the Kähler modulus,  $\mathcal{A}$  is the one-loop pfaffian.

In order for the Kähler modulus to be stabilized near the F-term minimum, one must ensure that the non-perturbative superpotential is comparable in size to the tree-level superpotential. Naïvely, this will drive the Kähler modulus to the strongly coupled regime in which we lose control of the large volume expansion. Hence, to avoid this crisis, one should fine-tune the three form fluxes  $F$ ,  $H$  to yield an exponentially small value of the GVW superpotential.

Once this fine-tuning  $\langle W_{\text{tree}} \rangle \ll 1$  is achieved, we can finally stabilize the Kähler modulus at the F-term minimum and obtain a supersymmetric  $\text{AdS}_4$  vacuum of string theory, with exponentially small cosmological constant. We are not done yet, as the sign of the cosmological constant is negative.

To yield positive and small cosmological constant, we must break supersymmetry in a controllable way. A generic choice of supersymmetry breaking breaks supersymmetry at string scale, which is too high and quite hard to control. Furthermore, if we break supersymmetry at string scale, the cosmological constant will become string scale, albeit positive.

This calls for low-energy supersymmetry breaking. Fortunately, it was shown in [151] that in type IIB string theory one can engineer an exponential hierarchy which is like the RS model [298]. Once, one engineers the exponential hierarchy such that the IR scale is commensurate to the F-term potential, one can place an anti-D3 brane at the IR region to yield

$$V_{eff} = V_F + \text{SU/SY}, \quad (1.8)$$

where  $\text{SU/SY} = e^{4A_0} T_{\overline{\text{D3}}}$ , such that the effective potential is locally minimized at exponentially small and positive value. This last step achieves meta-stable de Sitter vacua of string theory.

### 1.1.3 The challenges to realize the KKLT proposal

It is thus fair to say that these scenarios have not yet been rigorously shown to be realized in string theory.

G. Obied, H. Ooguri, L. Spodyneiko, C. Vafa [283].

The blueprint for the construction of de Sitter solutions in string was put forward in 2003. But, we still have no explicit KKLT-like de Sitter solutions. In this section, we list some of the challenges that forbade the explicit realization of the proposal.

One relatively new challenge or issue is the mismatch between the ten-dimensional type IIB supergravity and the four-dimensional effective field theory [279]. More explicitly, there are two puzzles: divergences due to the gaugino condensation, the sign problem in the anti-D3-brane uplift. What was previously

known is that the gaugino condensation induces singularities in the compactification manifold in supergravity approximation [189, 27, 135]. In [279], it was pointed out that such a divergence can lead to a diverging cosmological constant of the four-dimensional effective field theory which is an indication of pathology. The other puzzle arises when one naïvely evaluates the contribution of the anti-D3-brane to the cosmological constant, which yields

$$\delta\Lambda \simeq -e^{8A_0}T_{\overline{D3}}. \quad (1.9)$$

Comparing to (1.8), we see two problems. The anti-D3-brane does not respect the supersymmetry of the susy AdS background, hence, one normally expects that the addition of an anti-D3-brane to the background will increase the energy hence the uplift. But, the naïve 10d supergravity computation tells us that actually the energy is lowered. The other problem is related to the supersymmetry breaking scale. The natural IR scale is given by  $e^{4A_0}$  not  $e^{8A_0}$ , but still, we see a much more small scale which was not present in the geometry. Those two problems, if they are true, indicate serious misunderstanding.

The second challenge is to realize the fine tunings required for the KKLT: finding three form fluxes  $F$ ,  $H$  such that  $\langle W_{\text{tree}} \rangle \ll 1$ , engineer the exponential hierarchy such that  $e^{4A_0} \simeq |V_F|$  while maintaining  $\langle W_{\text{tree}} \rangle \ll 1$ . From the statistical analysis, it was expected that there may exists a few flux choices that yield  $\langle W_{\text{tree}} \rangle \ll 1$  [21, 98, 99, 128]. But, due to the scarcity of such good flux choices, it was not possible to find such flux choices with  $\langle W_{\text{tree}} \rangle \ll 1$ . To illustrate the problem more vividly, let us take a relatively simple Calabi-Yau the mirror of  $\mathbb{P}_{[1,1,1,6,9]}$  [18] [69]. One can take an O3/O7 orientifold of the mirror of  $\mathbb{P}_{[1,1,1,6,9]}$  [18] which we will call  $\tilde{X}$  henceforth. Type IIB compactification on  $\tilde{X}$  has two complex structure moduli, and the D3-brane tadpole  $Q_{D3} = 138$ . Rough estimate tells us that there are at least  $6 \times 10^{13}$  different flux vacua. On the other hand the

number of flux vacua such that  $\langle W_{\text{tree}} \rangle \simeq \exp(-2\pi)$  is computed to be  $\mathcal{O}(1)$ . This clearly shows that in order to find good flux vacua, one has to perform an exponentially pricey numerical scan, unless one has an algorithm better than a brute force method.

The challenge to fine-tune  $\langle W_{\text{tree}} \rangle$  is closely tied with the problem to realize the exponential hierarchy. In order to realize exponentially small  $\langle W_{\text{tree}} \rangle$ , one must have the ability to compute the prepotential for the complex structure moduli as much as possible. Until recently, the computation of the prepotential near conifold singularities was severely limited. Because engineering the exponential hierarchy requires stabilizing at least one of the complex structure moduli near a conifold singularity, the computational limitation made it challenging to engineer the exponential hierarchy while maintaining  $\langle W_{\text{tree}} \rangle \ll 1$ .

The next challenge is to stabilize the Kähler moduli explicitly, in a vacuum with  $\langle W_{\text{tree}} \rangle \ll 1$  and the exponential hierarchy. In my opinion, this is a purely technical challenge that requires more rigorous and demanding computation.

The last challenge is to break supersymmetry such that an anti-D3-brane in the IR region does not jeopardize the whole solution. There is still much work to do to fully grasp when the supersymmetry breaking is mild enough.

In this thesis, we close the first two issues.

## 1.2 How is the spacetime made up?

Up until now, we have been ignoring one very important question by taking the supergravity approximation. Supergravity does not tell us how the universe or the

spacetime is formed. In this section, we give a brief overview on this question.

Because we lack the background-independent formalism of string theory, it is not easy to understand how the spacetime is formed in string theory. For example, in quantum field theory or quantum mechanics, one can construct the wave function by adding up the particles or the excitations to the vacuum state. But, in string theory we have no ability to construct the spacetime by adding up strings to the vacuum state.

To circumvent this difficulty, one can take an indirect route. Entanglement entropy between subregions  $A$  and  $A^c$  tells us how degrees of freedom in  $A$  are entangled with  $A^c$ . At the leading order, the entanglement entropy is  $\text{Min}(\text{Area}_{A \cap A^c})/4G_N$  [303, 243]. The entanglement entropy is a particularly appealing quantity to compute, because the area term, conjecturally, counts the number of edge modes across the horizon [115, 246]. Hence, rather than directly constructing spacetime out of a vacuum state in string theory, one can compute the entanglement entropy to understand the fine structure of the spacetime.<sup>7</sup>

Declaring that one can compute the entanglement entropy does not solve any problems. Because to compute the entanglement entropy access to the wavefunction or the partition function of the universe is still required and it is still extremely challenging to compute the wavefunction of the universe in physical string theory. Furthermore, it is not quite clear how to divide a region to obtain the extended Hilbert space in string theory because strings are extended objects [24].

As a first step towards understanding the origin of the spacetime, we study topological string theory which is a simplification of physical type II string theories.

---

<sup>7</sup>In the examples we consider in this thesis, we see a strong hint that the edge modes indeed correspond to the area term in the entanglement entropy.

Topological string theory is particularly appealing, as it is well known how to compute the partition function of topological string theory.<sup>8</sup> Furthermore, one can compute the wave function of the universe in the topological string theory [63]. Lastly, topological string theory is dual to various field theories. Because we understand how to compute the entanglement entropy in field theories, one can have a crosscheck from field theories.

### 1.3 Organization of this thesis

The organization of this thesis is as follows. In §2, we study how important it is to control the back-reaction from the monodromy charges to ensure the meta-stability of de Sitter solutions in string theory. In §3, we study the KKLT proposal in the ten-dimensional type IIB supergravity and show that ten-dimensional supergravity agrees exactly with the four-dimensional effective theory proposed in [215]. In §4, we show that it is possible to find flux vacua with exponentially small flux superpotential. We also give an explicit algorithm to find such flux vacua. In §5, we show a simple method to compute the prepotential near conifold singularities. We also extend the algorithm of §4 to find exponentially small flux superpotential with the exponential hierarchy. In §6, we study the entanglement entropy of topological A model on the resolved conifold. We compute the entanglement entropy via a replica trick and the extended TQFT for the topological string theory and show that those two independent results agree with each other. We also see an emergence of q-deformed symmetry. In §7, we study the entanglement entropy of the topological string theory from the dual Chern-Simons theory. We again obtain the result that agrees with the results found in §6.

---

<sup>8</sup>For review, see [258].

## CHAPTER 2

# MONODROMY CHARGE IN D7-BRANE INFLATION

### Abstract<sup>1</sup>

In axion monodromy inflation, traversing  $N$  axion periods corresponds to discharging  $N$  units of a quantized charge. In certain models with moving D7-branes, such as Higgs-otic inflation, this monodromy charge is D3-brane charge induced on the D7-branes. The stress-energy of the induced charge affects the internal space, changing the inflaton potential and potentially limiting the field range. We compute the backreaction of induced D3-brane charge in Higgs-otic inflation. The effect on the nonperturbative superpotential is dramatic even for  $N = 1$ , and may preclude large-field inflation in this model in the absence of a mechanism to control the backreaction.

---

<sup>1</sup>This chapter is published as M. Kim, L. McAllister, “Monodromy Charge in D7-brane Inflation,” JHEP 10 (2020) 060 [arxiv:1812.03532 [hep-th]].



## 2.1 Introduction

Inflationary models involving super-Planckian displacements provide a striking connection between quantum gravity and observable phenomena. Upper limits on primordial B-mode polarization in the CMB have excluded some models of large-field inflation, but others remain viable [12]. At the same time, the theoretical question of the status of super-Planckian displacements in quantum gravity remains unresolved, despite much activity.

Large-field inflation is readily described in effective field theory, but crucially relies on assumptions about symmetries in quantum gravity. A prototypical example is the shift symmetry of an axion with decay constant  $f \gg M_{\text{pl}}$  [143]. No assumption about quantum gravity that is sufficient to protect large-field inflation has yet been put on indisputably solid footing in string theory: on the contrary, general expectations about the destruction of global symmetry charges by black holes, as well as conjectures about Weak Gravity and about moduli spaces in quantum gravity [287, 19], suggest that controlling a super-Planckian displacement in a quantum gravity theory is difficult. In view of these results, ignoring the problem of ultraviolet completion and studying large-field inflation solely from the bottom up appears untenable.

A practical way forward is to search for candidate realizations of large-field inflation in compactifications of string theory, and to investigate their characteristics and limitations. To shed light on the question of interest, these realizations should be sufficiently explicit, and sufficiently well-controlled, so that quantum gravity corrections to the inflaton action can be computed.

In this work we study models of large-field inflation in string theory in which

the inflaton is the position of a D7-brane. We focus on D7-brane monodromy scenarios, such as Higgs-otic inflation [205], in which the D7-brane repeatedly traverses a loop in the internal space, discharging an induced charge or flux, and reducing the four-dimensional energy density, with each cycle. Compared to other scenarios for axion monodromy inflation in string theory, an advantage of existing D7-brane models is that the compactification can be a simple and comparatively explicit toroidal orientifold. In this setting, one can carefully examine effects that might interfere with achieving a super-Planckian displacement.

Arguably the most dangerous effect in axion monodromy inflation is *backreaction of monodromy charge*. Transporting the inflaton field  $N$  times around a loop in configuration space leads to the accumulation of  $N$  units of physical, quantized charge, corresponding for example to D-brane charge carried by branes or fluxes. This monodromy charge is the order parameter measuring displacement from the minimum of the inflaton potential. The stress-energy of the monodromy charge is a leading source in the four-dimensional Einstein equations, and in a successful model this stress-energy drives inflationary expansion. At the same time, the monodromy charge is a source for the Einstein equations in the internal six dimensions. We refer to the resulting effects on the internal space as ‘backreaction of monodromy charge’, and we use the term ‘probe approximation’ to describe the approach of neglecting the backreaction.

One of our main conclusions is that in D7-brane axion monodromy inflation, the probe approximation is *not* a valid or consistent approximation. The problem of backreaction of monodromy charge was already emphasized in [269] and its implications were the main subject of [140, 266], but because these works examined axion monodromy on NS5-branes [269] — a scenario requiring a rather

complicated warped throat compactification — some have suggested that backreaction of monodromy charge may be a particular defect of the NS5-brane model, and may be negligible in all F-term axion monodromy models [256]. Our analysis excludes this possibility. We find that the backreaction of monodromy charge is, if anything, even more visible and more dangerous in D7-brane monodromy on toroidal orientifolds than it is in the NS5-brane case: it was shown in [140, 266] that by fine-tuning the position of an NS5-brane pair in a warped throat, the leading backreaction effects can be mitigated, but there is no obvious analogue of this mechanism in a toroidal orientifold. We do not rule out the possible existence of a mechanism for ameliorating backreaction in D7-brane inflation, but in our view, inventing and establishing such a mechanism is a prerequisite to any claim of large-field inflation in this setting. On the other hand, although our work naturally generalizes to other models with monodromy charge localized on D-branes or NS-branes, backreaction may be less problematic in scenarios with delocalized monodromy charge, e.g. in the form of bulk fluxes [271].<sup>2</sup>

The ten-dimensional backreaction we consider here should be carefully distinguished from the four-dimensional backreaction studied in [31, 329, 57], which involves non-linear interactions among moduli fields in four-dimensional theories, e.g. shifts of saxion vevs following large axion displacements, along the lines of [113]. We are examining the effects of localized sources in the ten-dimensional equations of motion: these lead to couplings that are difficult or impossible to compute in the four-dimensional theory obtained by dimensional reduction in the probe approximation. In particular, ten-dimensional backreaction effects are not readily computed in a Kaloper-Sorbo [225] description of axion monodromy inflation in a four-dimensional effective theory, and should be understood instead as

---

<sup>2</sup>We thank E. Silverstein for emphasizing this point.

*ultraviolet inputs* to such a theory. In particular, a primary aim of the present work is to compute, in ten-dimensional supergravity, the precise form of the Pfaffian prefactors (2.78) that were approximated by constants in [31, 329, 57] and were modeled phenomenologically in [301]. Our results (2.78), (2.79) can then be taken as inputs for analyses in the frameworks of [31, 329, 57, 301].

The organization of this note is as follows. In §2.2 we review the construction of Higgs-otic inflation [205]. In §2.3 we compute the backreaction of induced D3-brane charge in configurations of moving D7-branes. We describe the impact of this effect on Higgs-otic inflation in §2.4, and we also comment on a related issue in fluxbrane inflation. Our conclusions appear in §5.5. Appendix A.1 gives our conventions for differential forms, and Appendix A.2 collects a few results about Green’s functions in toroidal orientifolds.

## 2.2 Higgs-otic Inflation

We begin by recalling key elements of the Higgs-otic inflation scenario [205, 49, 50]. For the phenomenology of these models, which we will not review, we refer the interested reader to the original references [205, 49, 50]. Related constructions include [86, 87, 177, 256, 186].

Higgs-otic inflation is a construction of chaotic inflation in type IIB string theory via monodromy. The inflaton field is identified as the position of a D7-brane wrapping a four-cycle in a flux compactification. As the D7-brane moves through a background of three-form flux, it accumulates induced anti-D3-brane charge, breaking supersymmetry and creating a potential. The idea is to choose the geometry and flux in such a way that the D7-brane can repeatedly travel

around a one-cycle in the compactification, acquiring more induced anti-D3-brane charge with each cycle. In other words, the D7-brane couplings to the background flux introduce monodromy, and the order parameter for the monodromy is the amount  $Q^{\overline{D3}}$  of induced anti-D3-brane charge on the D7-brane.

### 2.2.1 Setup

We will examine Higgs-otic inflation in the context of compactifications of type IIB string theory on toroidal orientifolds. In the conventions of [293], the type IIB supergravity action in Einstein frame takes the manifestly  $SL(2, \mathbb{Z})$ -invariant form

$$S_{IIB} = \frac{1}{2\kappa_{10}^2} \int_{\mathbb{R}^{1,3} \times X} \star_{10} \mathcal{R} - \frac{1}{2(\text{Im } \tau)^2} d\tau \wedge \star_{10} d\bar{\tau} - \frac{1}{2\text{Im } \tau} G_3 \wedge \star_{10} \bar{G}_3 - \frac{1}{4} \tilde{F}_5 \wedge \star_{10} \tilde{F}_5 \\ + \frac{1}{8i\kappa_{10}^2} \int_{\mathbb{R}^{1,3} \times X} \frac{1}{\text{Im } \tau} C_4 \wedge G_3 \wedge \bar{G}_3 + S_{loc}. \quad (2.1)$$

We consider an ansatz for the metric and Ramond-Ramond five-form of the form

$$ds^2 = h^{-1/2}(z) ds_{\mathbb{R}^{1,3}}^2 + h^{1/2}(z) ds_X^2, \quad (2.2)$$

$$\tilde{F}_5 = (1 + \star_{10}) d\alpha(z) \wedge \sqrt{-\det(g)} dx^0 \wedge dx^1 \wedge dx^2 \wedge dx^3,$$

where  $z$  denotes the coordinates on the internal space  $X$ . We denote the Hodge star operators in ten dimensions, on  $X$ , and on a divisor  $D \subset X$  by  $\star_{10}$ ,  $\star_6$ , and  $\star_4$ , respectively. We also define

$$G_{\pm} = \frac{(\star_6 \pm i)}{2} G_3, \quad (2.3)$$

and refer to  $G_+$  and  $G_-$  as imaginary self-dual (ISD) and imaginary anti-self-dual (IASD) flux, respectively. See Appendix A.1 for more details of our conventions.

In [205]  $G$  was assumed to be a constant ISD flux, while [50] generalized  $G$  to a linear combination of ISD and IASD fluxes. For simplicity, in this section we

consider an ISD background with  $G_- = 0$ ,  $h^{-1} = \alpha$ , and constant axio-dilaton field  $\tau$ ; our main analysis in §2.3 is robust to relaxing these restrictions.

### 2.2.2 Magnetized D-brane action

Consider a D7-brane that fills the noncompact spacetime and wraps a divisor  $D \subset X$ . A general two-form flux  $\mathcal{F}$  on the D7-brane can be written as the sum of self-dual (SD) and anti-self-dual (ASD) components:

$$\mathcal{F} = (1 + \star_4)\mathcal{F}/2 + (1 - \star_4)\mathcal{F}/2 = \mathcal{F}_+ + \mathcal{F}_-. \quad (2.4)$$

We will refer to a D7-brane carrying nontrivial worldvolume flux  $\mathcal{F}$  as being *magnetized*. In this section we examine the Dirac-Born-Infeld (DBI) and Chern-Simons (CS) actions of a magnetized D7-brane.

Viewing the two-form flux on  $D$  as a  $4 \times 4$  skew-symmetric matrix, and writing the metric on  $D$  as  $g$ , we have the identities

$$\det(I + g^{-1}\mathcal{F}) = 1 - \frac{1}{2} \text{tr}(g^{-1}\mathcal{F})^2 + \det(g^{-1}\mathcal{F}), \quad (2.5)$$

$$- \frac{1}{2} \int_D \text{Vol}_D \text{tr}(g^{-1}\mathcal{F})^2 = \int_D \mathcal{F} \wedge \star_4 \mathcal{F}. \quad (2.6)$$

It follows that

$$\det(I + g^{-1}\mathcal{F})^{1/2} = 1 - \frac{1}{4} \text{tr}(g^{-1}\mathcal{F})^2 + \frac{1}{2} \det(g^{-1}\mathcal{F}) - \frac{1}{32} [\text{tr}(g^{-1}\mathcal{F})^2]^2 + \mathcal{O}(\mathcal{F}^6). \quad (2.7)$$

Note that the above expansion is exact up to  $\mathcal{O}(\mathcal{F}^2)$  if  $\mathcal{F} = \pm \star_4 \mathcal{F}$ .

We can now expand the DBI+CS actions of a static D7-brane in an ISD back-

ground, written in Einstein frame, up to  $\mathcal{O}(\mathcal{F}^2)$ :

$$S_{D7} = -\mu_7 \int_{\mathbb{R}^{1,3} \times D} \text{Vol}_{\mathbb{R}^{1,3}} \wedge \text{Vol}_D (\text{Im } \tau)^{-1} \det(I + (\text{Im } \tau)^{1/2} g^{-1} \mathcal{F})^{1/2} \\ + \mu_7 \int_{\mathbb{R}^{1,3} \times D} C_8 + C_6 \wedge \mathcal{F} + \frac{1}{2} C_4 \wedge \mathcal{F} \wedge \mathcal{F} \quad (2.8)$$

$$= -\mu_7 \int_{\mathbb{R}^{1,3} \times D} \text{Vol}_{\mathbb{R}^{1,3}} \wedge \frac{1}{2} \left( (\text{Im } \tau)^{-1} \mathcal{J} \wedge \mathcal{J} + \mathcal{F} \wedge \star_4 \mathcal{F} \right) \\ + \mu_7 \int_{\mathbb{R}^{1,3} \times D} C_8 + \frac{1}{2} C_4 \wedge \mathcal{F} \wedge \mathcal{F} + \mathcal{O}(\mathcal{F}^4). \quad (2.9)$$

Here  $\text{Vol}_{\mathbb{R}^{1,3}}$  is the volume in the metric  $h^{-1/2} g_{\mu\nu}$ , and similarly the Hermitian form<sup>3</sup>  $\mathcal{J}$  corresponds to the full internal metric including the warp factor, and obeys  $\frac{1}{2} \mathcal{J} \wedge \mathcal{J} = \text{Vol}_D$ . We have dropped the  $C_6 \wedge \mathcal{F}$  term because  $C_6$  can be fixed to be zero in an ISD background. From the Chern-Simons term involving  $C_4$  in (2.9) it is clear that an SD flux on a D7-brane induces D3-brane charge, whereas an ASD flux induces  $\overline{D3}$ -brane charge.

The candidate inflaton potential arises from the terms in the D7-brane action (2.9) that are quadratic in  $\mathcal{F}$ :

$$S_{\mathcal{F}^2} = -\mu_7 \int_{\mathbb{R}^{1,3} \times D} (\text{Vol}_{\mathbb{R}^{1,3}} - C_4) \wedge \frac{1}{2} \mathcal{F}_+ \wedge \star_4 \mathcal{F}_+ - \mu_7 \int_{\mathbb{R}^{1,3} \times D} (\text{Vol}_{\mathbb{R}^{1,3}} + C_4) \wedge \frac{1}{2} \mathcal{F}_- \wedge \star_4 \mathcal{F}_-, \quad (2.10)$$

$$= -\mu_7 \int_{\mathbb{R}^{1,3} \times D} \text{Vol}_{\mathbb{R}^{1,3}} \wedge \mathcal{F}_- \wedge \star_4 \mathcal{F}_-. \quad (2.11)$$

In the last equality we used  $h^{-1} = \alpha$ , i.e.  $\text{Vol}_{\mathbb{R}^{1,3}} = C_4|_{\mathbb{R}^{1,3}}$ , which holds in an ISD background.

---

<sup>3</sup>The Hermitian form  $\mathcal{J}$  is a Kähler form if  $d\mathcal{J} = 0$ .

### 2.2.3 Inflaton potential from induced charge

Now suppose that the D7-brane position  $z_3$  is a modulus in the absence of fluxes, i.e. suppose that  $[D] \in H_4(X, \mathbb{Z})$  has a continuous family of representatives parameterized by  $z_3$ , which we write as  $D(z_3)$ . Displacing such a D7-brane in a background of three-form flux causes ASD flux to accumulate on the D7-brane worldvolume, as we will review below. This ASD flux carries anti-D3-brane charge, which interacts with the dissolved D3-brane charge carried by the background flux, and creates a potential for D7-brane motion. From (2.10), this potential is

$$V(z_3) = \mu_7 \int_{D(z_3)} h^{-1} \mathcal{F}_- \wedge \star_4 \mathcal{F}_-. \quad (2.12)$$

In the special case that  $h^{-1}$  is a constant, we have

$$V(z_3) = 2\mu_3 h^{-1} \frac{\mu_7}{\mu_3} \int_{D(z_3)} \frac{1}{2} \mathcal{F}_- \wedge \star_4 \mathcal{F}_-, \quad (2.13)$$

$$= 2\mu_3 h^{-1} Q^{\overline{D3}}(z_3), \quad (2.14)$$

Thus, the inflaton potential is proportional to the induced anti-D3-brane charge.

In the simplest incarnation of Higgs-otic inflation,  $D(z_3)$  is a family of effective divisors — i.e., a D7-brane rather than an anti-D7-brane wraps  $D(z_3)$  — and the flux that accumulates on the D7-brane is ASD, corresponding to anti-D3-brane charge. The inflaton potential in the probe approximation, and prior to including the effects of moduli stabilization, is given by (2.12). At the minimum of this potential, the induced ASD flux vanishes, and the D7-brane preserves the same supersymmetry as the background  $(2,1)$  flux. A system of this sort provides a realization of F-term axion monodromy inflation [256] in string theory [205].

In this note we will demonstrate that the relation (2.12) presents a strong constraint on model-building. We will see that as a D7-brane moves one or more



times around a one-cycle, the backreaction of accumulated anti-D3-brane charge on the compactification geometry is large and rapidly changing, precluding inflation.

## 2.2.4 An example

A prototypical example of Higgs-otic inflation given in [205] occurs in a toroidal orientifold for which the covering orbifold is of the form  $(T^4 \times T^2)/\mathbb{Z}_4$ , with the orbifold action

$$\theta : (z_1, z_2, z_3) \mapsto (-iz_1, -iz_2, -z_3). \quad (2.15)$$

No explicit orientifold action was given in [205]. In this section, we will take the orientifold action to be

$$\sigma : (z_1, z_2, z_3) \mapsto (z_1, z_2, -z_3). \quad (2.16)$$

This orientifold action is consistent with the presence of D7-branes and O7-planes whose position is described by the coordinate  $z_3$ . As  $\theta^2\sigma : (z_1, z_2, z_3) \mapsto -(z_1, z_2, z_3)$ , another choice of orientifold action,

$$\sigma' : (z_1, z_2, z_3) \mapsto -(z_1, z_2, z_3), \quad (2.17)$$

is equivalent to (2.16).

The constant ISD fluxes allowed by the orbifold action (2.15) are

$$G_+ = G^{(2,1)} dz^1 \wedge dz^2 \wedge d\bar{z}^3 + G^{(0,3)} d\bar{z}^1 \wedge d\bar{z}^2 \wedge d\bar{z}^3. \quad (2.18)$$

The NS-NS three-form flux is

$$H = \frac{i}{2\text{Im}\tau} \left( dz^1 \wedge dz^2 \wedge (G^{(2,1)} d\bar{z}^3 - G^{(0,3)*} dz^3) + d\bar{z}^1 \wedge d\bar{z}^2 \wedge (G^{(0,3)} d\bar{z}^3 - G^{(2,1)*} dz^3) \right). \quad (2.19)$$

We can choose a gauge (corresponding to the normal coordinate expansion in [212]) so that the NS-NS two-form field  $B$  is

$$B = \frac{i}{2 \operatorname{Im} \tau} \left( dz^1 \wedge dz^2 (G^{(2,1)} \bar{z}_3 - G^{(0,3)*} z_3) + d\bar{z}^1 \wedge d\bar{z}^2 (G^{(0,3)} \bar{z}_3 - G^{(2,1)*} z_3) \right). \quad (2.20)$$

If the background (2.20) pulled back to a D7-brane leads to ASD flux  $\mathcal{F}$ , then the key ingredients for Higgs-otic inflation are present.

### 2.2.5 An issue of orientation

We now explain a subtlety concerning orientation and the self-duality of flux. The most straightforward realization of the Higgs-otic scenario requires a flux background in which ASD flux is induced on a D7-brane that wraps a four-cycle  $D$ . However, we will show that a  $B$ -field of Hodge type  $(0, 2) + (2, 0)$ , such as (2.20), is SD, not ASD, when  $D$  is an effective divisor.

If one provisionally takes the orientation of  $D$  to be

$$dz^1 \wedge d\bar{z}^1 \wedge dz^2 \wedge d\bar{z}^2, \quad (2.21)$$

then a  $B$ -field of Hodge type  $(0, 2) + (2, 0)$  is indeed ASD, as desired for Higgs-otic inflation. A simple check of the anti-self-duality is that  $B \wedge B$  is negative relative to the orientation (2.21), as required for an ASD real two-form — see (A.13).

However, we will now argue that the correct orientation for an effective divisor differs from (2.21) by a sign: as recognized in [301], the orientation (2.21) corresponds to the orientation on an anti-D7-brane, not a D7-brane, wrapping  $D$ .

Suppose that  $X$  is a Kähler threefold with Hermitian metric  $i g_{a\bar{b}}$ , and let  $D$  be an effective divisor written as  $\{z_3 = a\}$  in local coordinates. We show in Appendix

A.1 that there are two possible choices of conventions for the Hodge star map, and correspondingly there are two choices of Kähler form, which in a unitary frame read

$$J = \pm i(g_{1\bar{1}}dz^1 \wedge d\bar{z}^1 + g_{2\bar{2}}dz^2 \wedge d\bar{z}^2). \quad (2.22)$$

Given either Kähler form in (2.22), the volume form of  $D$  is

$$\frac{1}{2}J \wedge J = -g_{1\bar{1}}g_{2\bar{2}}dz^1 \wedge d\bar{z}^1 \wedge dz^2 \wedge d\bar{z}^2. \quad (2.23)$$

The orientation (2.21) used in [205] has opposite sign relative to (2.23). This implies that the volume of  $D$  with the orientation (2.21) measured by the Kähler form (2.22) is negative. Note also that the eigenvalues of the four-dimensional Hodge star operator on  $D$  change sign under a change of the sign of the volume form. As a result, the NS-NS 2-form  $B$  (2.20), of Hodge type  $(2,0) + (0,2)$ , corresponds to a *self-dual* 2-form given the orientation (2.23).

We conclude that in the particular orbifold proposed in [205], the three-form fluxes allowed by the orbifold action (2.15) result from an NS-NS two-form  $B$  (2.20) of Hodge type  $(0,2) + (2,0)$ . Such a form is SD when pulled back to a D7-brane.<sup>4</sup> We therefore find that a D7-brane displaced in the  $z_3$  direction in the compactification proposed in [205], taking (2.16) to be the orientifold action, does not accumulate ASD flux, and does not lead to axion monodromy inflation. We have not found an alternative orientifold action that leads to a successful model based on the orbifold (2.15).

However, we now give an example of a toroidal orientifold that could support Higgs-otic inflation. Consider the toroidal orientifold  $T^6/\mathbb{Z}'_6$  studied in [40], T-

---

<sup>4</sup>We have argued above, and in more detail in Appendix A.1, that the orientation of the worldvolume of a D7-brane is given by (2.23), which differs by a sign from the orientation (2.21) used in [205]. Our choice of conventions is anchored by the requirement, almost ubiquitous in the literature, that  $G_3$  flux of Hodge type  $(0,3)$  should be ISD rather than IASD.

dualized six times in order to obtain O3-planes and O7-planes rather than O5-planes and O9-planes. The orbifold action  $\theta$  and the orientifold action  $\sigma$  are

$$\theta : (z_1, z_2, z_3) \mapsto (e^{i\pi/3} z_1, e^{-i\pi} z_2, e^{2\pi i/3} z_3), \quad (2.24)$$

$$\sigma : (z_1, z_2, z_3) \mapsto -(z_1, z_2, z_3). \quad (2.25)$$

As  $\theta^3 \sigma : (z_1, z_2, z_3) \mapsto (z_1, z_2, -z_3)$ , the position modulus of an inflationary D7-brane is  $z_3$ . The orbifold action (2.24) allows the bulk three-form flux

$$G = G^{(2,1)} dz^1 \wedge d\bar{z}^2 \wedge dz^3, \quad (2.26)$$

which generates an ASD  $B$ -field on the divisor  $\{z_3 = a\}$ :

$$B = \frac{ig_s}{2} (G^{(2,1)} z_3 dz^1 \wedge d\bar{z}^2 - G^{(2,1)*} \bar{z}_3 d\bar{z}^1 \wedge dz^2). \quad (2.27)$$

Thus the toroidal orientifold defined by (2.24), (2.25) could support a Higgs-otic inflation scenario. However, in the presence of bulk flux of Hodge type  $(0, 3)$ , which is required to induce a nonvanishing flux superpotential, the  $(2, 0) + (0, 2)$  components of  $\mathcal{F}$  do not vanish in general, and so the  $B$  field on the divisor is a linear combination of SD and ASD components. This leads to somewhat more complicated backreaction effects than purely ASD flux would produce, as we shall see.

## 2.3 Backreaction of Monodromy Charge

Having recalled the essential elements of Higgs-otic inflation, most notably the contribution (2.12) of ASD flux on the inflationary D7-brane to the inflaton potential, we can now study Higgs-otic inflation beyond the probe approximation. We will find that the accumulation of ASD flux sources significant changes in the super-

gravity solution for the internal space — changes that are omitted by assumption in the probe approximation.

In particular, we will see that the actions of Euclidean D3-branes, even those that are well-separated from the inflationary D7-brane, depend sensitively on the inflaton vev once backreaction is included. As a result, we will be able to draw strong conclusions about Higgs-otic inflation scenarios in which nonperturbative superpotential terms from Euclidean D3-branes<sup>5</sup> make important contributions to the potential for the Kähler moduli, as in [215, 23, 58]. The presence of perturbative contributions to the Kähler moduli potential, as in the Large Volume Scenario, does not affect our conclusion: all that matters is that the nonperturbative terms play a non-negligible role in moduli stabilization. On the flip side, our analysis does not directly constrain a hypothetical Higgs-otic inflation scenario stabilized by purely perturbative effects.

Although our computation will occur in ten-dimensional type IIB supergravity in the presence of localized and distributed sources, the results are efficiently expressed in four-dimensional  $\mathcal{N} = 1$  supergravity, with the superpotential

$$W = \int_X G \wedge \Omega + \sum_a \mathcal{A}_a e^{-2\pi Q_a^i T_i} . \quad (2.28)$$

Here  $\{T_i\}$  are the complexified Kähler moduli,  $i = 1, \dots, h^{1,1}(X)$ , and the coefficients  $Q_a^i \in \mathbb{Z}$  are the charges of Euclidean D3-branes under the shift symmetries of the Ramond-Ramond four-form axions. Determining which homology classes  $[D] \in H_4(X, \mathbb{Z})$  support Euclidean D3-brane superpotential terms is beyond the scope of this work, and so we do not specify the  $Q_a^i$  or the range of the index  $a$ .

---

<sup>5</sup>Precisely parallel results hold for superpotentials from gaugino condensation on D7-branes, but for simplicity of language we suppress the gaugino condensate case in our discussion.

It will suffice, in fact, to examine a single term, so we write

$$W = \int_X G \wedge \Omega + \mathcal{A} e^{-2\pi T} \quad (2.29)$$

henceforth. The Pfaffian prefactor  $\mathcal{A}$  depends on the complex structure moduli, on the positions of any D3-branes [146, 214, 40, 28], and, as we shall now show, *on the positions of magnetized D7-branes.*

Consider a Euclidean D3-brane wrapping a holomorphic divisor  $D$  in a general flux background. No essential generality is lost in assuming that the complexified volume of  $D$  is one of the Kähler moduli, denoted  $T$ . We allow ASD flux  $\mathcal{F}_D$  on the Euclidean D3-brane in accordance with the conditions for an instanton to preserve supersymmetry [259, 47].<sup>6</sup> The DBI action of such a magnetized Euclidean D3-brane is

$$S_{DBI} = \mu_3 \int_D \frac{1}{2} (\mathcal{J} \wedge \mathcal{J} + \text{Im } \tau \mathcal{F}_D \wedge \star_4 \mathcal{F}_D), \quad (2.30)$$

$$= \mu_3 \int_D \frac{1}{2} (\mathcal{J} \wedge \mathcal{J} - \text{Im } \tau \mathcal{F}_D \wedge \mathcal{F}_D). \quad (2.31)$$

One immediate observation is that the flux-induced D(-1)-brane charge  $\frac{\mu_3}{\mu_{-1}} \int_D \frac{1}{2} \mathcal{F}_D \wedge \star_4 \mathcal{F}_D$  is coupled to the axio-dilaton, and so the magnetized Euclidean D3-brane should be sensitive to the D7-brane position moduli in general.

The magnitude of the Euclidean D3-brane superpotential obeys

$$|\mathcal{A} e^{-2\pi T}| \propto e^{-S_{DBI}}. \quad (2.32)$$

One can therefore compute the Pfaffian  $\mathcal{A}$  by computing  $S_{DBI}$ , as in [28]. We will now do so to leading order in expansion around an ISD background.

---

<sup>6</sup>Notice that on a spacetime-filling D7-brane SD flux can be supersymmetric, while on a Euclidean D3-brane only ASD flux can be supersymmetric.

### 2.3.1 Perturbative computation of backreaction

We begin with the full equations of motion. Taking the ansatz (2.2) and defining the quantities

$$\Phi_{\pm} = h^{-1} \pm \alpha, \quad (2.33)$$

$$\Lambda = h^{-1} \star_6 G_3 - i\alpha G_3 = \Phi_+ G_- + \Phi_- G_+, \quad (2.34)$$

the type IIB supergravity action (2.1) leads to the following equations of motion and Bianchi identities, in the conventions of [27, 145]:

$$\nabla^2 \Phi_{\pm} = \frac{(\Phi_+ + \Phi_-)^2}{24 \operatorname{Im} \tau} G_{\pm, abc} \bar{G}_{\pm}^{abc} + \frac{2}{\Phi_+ + \Phi_-} \nabla_a \Phi_{\pm} \nabla^a \Phi_{\pm} + \kappa_{10}^2 \frac{(\Phi_+ + \Phi_-)^2}{2} \left( \frac{1}{4} (\hat{T}_i^i - \hat{T}_{\mu}^{\mu}) \pm \mu_3 \rho^{D3} \right) \quad (2.35)$$

$$\left( d\Lambda + \frac{id\tau}{\operatorname{Im} \tau} \wedge \operatorname{Re} \Lambda \right) \wedge dx^0 \wedge dx^1 \wedge dx^2 \wedge dx^3 = 2i\kappa_{10}^2 C_4 \wedge \frac{\delta S_{loc}}{\delta C_6} + 2i\kappa_{10}^2 \frac{\delta S_{loc}}{\delta B_2}, \quad (2.36)$$

$$d(G_3 + \tau H_3) = dF_3 = -2\kappa_{10}^2 \frac{\delta S_{loc}}{\delta C_6}, \quad (2.37)$$

$$\nabla^2 \tau = \frac{\nabla \tau \cdot \nabla \tau}{i \operatorname{Im} \tau} - \frac{i(\Phi_+ + \Phi_-)}{12} G_{+, abc} G_-^{abc} + 4i\kappa_{10}^2 (\operatorname{Im} \tau)^2 \frac{\delta S_{loc}}{\delta \bar{\tau}}, \quad (2.38)$$

$$\begin{aligned} R_{mn} = & \frac{\nabla_{(m} \tau \nabla_{n)} \bar{\tau}}{2(\operatorname{Im} \tau)^2} + \frac{2}{(\Phi_+ + \Phi_-)^2} \nabla_{(m} \Phi_+ \nabla_{n)} \Phi_- - g_{mn} \frac{\mathcal{R}_4}{2(\Phi_+ + \Phi_-)} \\ & - \frac{\Phi_+ + \Phi_-}{8 \operatorname{Im} \tau} \left( G_{+(m}{}^{pq} \bar{G}_{-n) pq} + G_{-(m}{}^{pq} \bar{G}_{+n) pq} \right) + \kappa_{10}^2 \left( \hat{T}_{mn} - \frac{1}{4} g_{mn} \hat{T}_i^i \right), \end{aligned} \quad (2.39)$$

where  $\hat{T}$  is the energy momentum tensor of localized objects such as D-branes and O-planes.

### Approximation scheme and simplifying assumptions

We would like to solve the system (2.35)-(2.39) to leading order in the effects of the two-form flux  $\mathcal{F}$  that accumulates on the inflationary D7-brane.

To this end, we consider a compactification of type IIB superstring theory on a toroidal orientifold<sup>7</sup> with local coordinates  $(z_1, z_2, z_3)$ , containing O7-planes, magnetized D7-branes, ISD flux, O3-planes, and possibly also D3-branes. We will first find a background solution containing ISD flux, O3-planes, and — optionally — D3-branes, with  $\Phi_- = 0$ . Then we will perturb the equations of motion by including the O7-planes and magnetized D7-branes as localized source terms.

Without loss of generality, we assume that the orientifold involution is  $\sigma : z_3 \mapsto -z_3$ , so that the O7-planes and D7-branes are extended over the  $z_1$  and  $z_2$  directions. We assume that each D7-brane  $\alpha$  wraps a holomorphic divisor  $D_\alpha = \{z_3 = z_{3,\alpha}\}$ , whose unwarped volume is  $\int_D \text{Vol}_D = \text{Re } T_D$ . The D7-brane charge density is then

$$\rho^{D7}(z_3) = \sum_{\alpha} \rho_{\alpha}^{D7} \delta_{(2)}(z_3 - z_{3,\alpha}), \quad (2.40)$$

where  $\rho^{D7} = 1$  for D7-branes and  $\rho^{D7} = -4$  for O7-planes. Because we have assumed that the background ISD flux includes nonzero components of Hodge types  $(0, 3)$  and  $(2, 1)$ , the two-form flux  $\mathcal{F}$  on a D7-brane may include both ASD and SD components — see (2.4). We do not consider any flux on the O7-planes.

The D3-brane charge density of D3-branes and O3-planes takes the form

$$\rho^{D3}(z) = \sum_i \rho_i^{D3} \delta_{(6)}(z - z_i), \quad (2.41)$$

where  $z_i$  is the position of the D3-brane or O3-plane,  $\rho_i^{D3} = 1$  for D3-branes, and  $\rho_i^{D3} = -1/4$  for O3-planes.

A primary focus of this note is the DBI action (2.30) of a Euclidean D3-brane at a fixed location. The NS-NS two-form  $B$  pulled back to the Euclidean D3-brane describes how NS-NS three-form flux  $H$  accumulates under a displacement of the

---

<sup>7</sup>The toroidal orientifold restriction makes it possible to compute the explicit Green's function, see (A.20). We expect, but will not show here, that our qualitative results hold more generally.



Euclidean brane along the normal direction. Thus for a Euclidean D3-brane at a fixed location, corrections to  $H$  do not significantly affect the DBI action (2.30). This allows us to consider only the fields  $\Phi_{\pm}$ ,  $\tau$ , and  $g_{mn}$  in the perturbed equations of motion.

To achieve considerable gains in simplicity, we will only focus on *localized* sources, such as those in (2.40) and (2.41), in the perturbed equations of motion. We will find that localized stress-energy and charge associated to ASD flux on the inflationary D7-brane strongly affects the solution at other locations in the compactification, including on the divisors wrapped by Euclidean D3-branes. While it is logically possible that including the backreaction of distributed sources, such as bulk three-form flux, could produce a counterbalancing effect on the Euclidean D3-brane action and leave the inflationary model unmodified in the final account, we find such a conspiracy to be most implausible.

Away from the minimum of the inflaton potential, the energy stored in the D7-brane configuration presents an obstacle to solving the ten-dimensional equations of motion with purely classical sources. We refer to such an obstacle as an NS-NS tadpole. In our ten-dimensional analysis we assume that there exist sources that cancel all NS-NS tadpoles, i.e. we assume that perturbative and nonperturbative corrections to the ten-dimensional equations of motion allow for consistent cosmological solutions. One leading candidate for an effect that cancels NS-NS tadpoles is gaugino condensation, as in [27, 279], but establishing NS-NS tadpole cancellation from specific quantum effects is beyond the scope of this work.

Practically, for a bosonic supergravity field  $A$ , we expand  $A = A^{(0)} + A^{(1)} + \dots$ , where  $A^{(0)}$  is the background field, and  $A^{(1)}$  is the perturbed field at leading order. Given this expansion, we rewrite the perturbed equations of motion schematically

as

$$\nabla^2 A^{(1)} = \rho_A^{bulk} + \rho_A^{D7} + \rho'_A, \quad (2.42)$$

where  $\rho_A^{bulk}$  is a bulk source term that involves bulk fields,  $\rho_A^{D7}$  is a source term that is localized on D7-branes, and  $\rho'_A$  is a source term added by hand to ensure tadpole cancellation. We write  $\rho_A^{NS} := \rho_A^{bulk} + \rho'_A$  and refer to  $\rho_A^{NS}$  as the NS-NS tadpole cancelling source.

As an example, we expand the equation of motion of  $\tau$ . The kinetic term  $\nabla^2 \tau$  is expanded as

$$(\nabla^2 \tau)^{(1)} = \nabla^{2(0)} \tau^{(1)} + \nabla^{2(1)} \tau^{(0)}, \quad (2.43)$$

where we often write  $\nabla^{2(0)}$  as  $\nabla^2$  when there is no ambiguity. Similarly, we expand the terms on the right hand side of (2.38) and treat the D7-brane density as a first-order term,

$$\nabla^{2(0)} \tau^{(1)} + \nabla^{2(1)} \tau^{(0)} = \left( \frac{\nabla \tau \cdot \nabla \tau}{i \operatorname{Im} \tau} \right)^{(1)} - \left( \frac{i(\Phi_+ + \Phi_-) \langle G_+, G_- \rangle}{2} \right)^{(1)} + 4i\kappa_{10}^2 (\operatorname{Im} \tau)^2 \frac{\delta S_{loc}}{\delta \bar{\tau}}. \quad (2.44)$$

Note that for  $\tau$  we do not have to add a term by hand to ensure tadpole cancellation at leading order. The localized source  $\rho_\tau^{D7}$  is

$$\rho_\tau^{D7} = 4i\kappa_{10}^2 (\operatorname{Im} \tau)^2 \frac{\delta S_{loc}}{\delta \bar{\tau}}. \quad (2.45)$$

Then we define  $\rho_\tau^{bulk}$  by

$$\rho_\tau^{bulk} = -\nabla^{2(1)} \tau^{(0)} + \left( \frac{\nabla \tau \cdot \nabla \tau}{i \operatorname{Im} \tau} \right)^{(1)} - \left( \frac{i(\Phi_+ + \Phi_-) \langle G_+, G_- \rangle}{2} \right)^{(1)}, \quad (2.46)$$

and  $\rho_\tau^{bulk}$  is identical to  $\rho_\tau^{NS}$  due to the absence of a  $\rho'_\tau$  term. Finally, we write down the perturbed equation of motion for  $\tau$  as

$$\nabla^2 \tau^{(1)} = \rho_\tau^{D7} + \rho_\tau^{NS}. \quad (2.47)$$

For further details of this perturbation scheme, see [145].

Strictly speaking, the perturbed dilaton could be negative in a small region around an O7-plane, and the perturbed metric could be negative around a magnetized D7-brane. To suppress effects of these singular regions on our solution, we will require  $\Phi_{+,c} \ll g_s \ll 1$ .

## Perturbed equations of motion

Consider first a compactification containing only ISD flux, D3-branes, and O3-planes, so that  $\Phi_-^{(0)} = \Lambda^{(0)} = 0$ . With the localized source terms (2.41), the equations of motion and Bianchi identities (2.35) are

$$d\left(G_3^{(0)} + \tau^{(0)} H_3^{(0)}\right) = 0, \quad (2.48)$$

$$\nabla^2 \tau^{(0)} = \frac{\nabla \tau^{(0)} \cdot \nabla \tau^{(0)}}{i \operatorname{Im} \tau^{(0)}}, \quad (2.49)$$

$$R_{mn}^{(0)} = \frac{\nabla_{(m} \tau^{(0)} \nabla_{n)} \bar{\tau}^{(0)}}{2(\operatorname{Im} \tau^{(0)})^2} + \frac{2}{\Phi_+^{(0)} + \Phi_-^{(0)}} \nabla_{(m} \Phi_+^{(0)} \nabla_{n)} \Phi_-^{(0)}, \quad (2.50)$$

$$\nabla^2 (\Phi_+^{(0)})^{-1} = - \sum_i \mu_3 \kappa_{10}^2 \rho_i^{D3} \delta_{(6)}(z - z_i) - \frac{|G_+^{(0)}|^2}{4 \operatorname{Im} \tau^{(0)}}. \quad (2.51)$$

The solutions for the ISD background are then

$$(\Phi_+^{(0)})^{-1} = \Phi_{+,c}^{-1} - \sum_i \mu_3 \kappa_{10}^2 \rho_i^{D3} G_{(6)}(z; z_i), \quad (2.52)$$

$$\tau^{(0)} = i/g_s, \quad (2.53)$$

$$g_{z_1 \bar{z}_1}^{(0)} = g_{z_2 \bar{z}_2}^{(0)} = g_{z_3 \bar{z}_3}^{(0)} = 1/2, \quad (2.54)$$

where  $\Phi_{+,c}^{-1}$  and  $g_s$  are constants. Denoting the unwarped volume of the compactification by  $\mathcal{V}$ , the warped volume  $\mathcal{V}_w$  is then

$$\mathcal{V}_w = \left( \frac{\Phi_{+,c}^{-1}}{2} \right) \mathcal{V}. \quad (2.55)$$

The D3-brane charge dissolved in ISD flux is

$$Q_{flux}^{D3} = \frac{|G_+^{(0)}|^2 \mathcal{V}}{4 \mu_3 \kappa_{10}^2 \operatorname{Im} \tau^{(0)}}. \quad (2.56)$$

Now we incorporate localized magnetized D7-branes, as well as O7-planes, as perturbations of the above background. The perturbed equations of motion are

$$\nabla^2 \Phi_-^{(1)} = -\frac{1}{4} \sum_{\alpha} \mu_7 \kappa_{10}^2 \rho_{\alpha}^{D7} \Phi_+^{(0)2} \text{tr}(g^{(0)-1} \mathcal{F}_{-, \alpha})^2 \delta_{(2)}(z_3 - z_{3, \alpha}) + \rho_-^{NS}, \quad (2.57)$$

$$\nabla^2 (\Phi_+^{(1)})^{-1} = \frac{1}{4} \sum_{\alpha} \mu_7 \kappa_{10}^2 \rho_{\alpha}^{D7} \text{tr}(g^{(0)-1} \mathcal{F}_{+, \alpha})^2 \delta_{(2)}(z_3 - z_{3, \alpha}) + \rho_+^{NS}, \quad (2.58)$$

$$\nabla^2 \text{Im } \tau^{(1)} = -2\mu_7 \kappa_{10}^2 \sum_{\alpha} \rho_{\alpha}^{D7} \delta_{(2)}(z_3 - z_{3, \alpha}) + \rho_{\text{Im } \tau}^{NS}, \quad (2.59)$$

$$\begin{aligned} \Delta_K g_{mn}^{(1)} = & \rho_{g, mn}^{NS}(z_3) - 2\mu_7 \kappa_{10}^2 (\text{Im } \tau^{(0)})^{-1} \sum_{\alpha} \rho_{\alpha}^{D7} \delta_{(2)}(z_3 - z_{3, \alpha}) \delta_{z_3(m} \delta_{n)} \bar{z}_3 \\ & + \mu_7 \kappa_{10}^2 \sum_{\alpha} \Phi_+^{(0)} \rho_{\alpha}^{D7} \delta_{(2)}(z_3 - z_{3, \alpha}) \left( \mathcal{F}_{ma, \alpha} \mathcal{F}_{nb, \alpha} g^{(0)ab} - \frac{1}{2} g_{mn}^{\parallel(0)} |\mathcal{F}_{\alpha}|^2 \right), \end{aligned} \quad (2.60)$$

where  $\rho_-$ ,  $\rho_+$ ,  $\rho_{\text{Im } \tau}$ , and  $\rho_g$  are NS-NS tadpole cancelling sources,  $g_{mn}^{\parallel(0)}$  is the background metric with legs parallel to the D7-brane divisor, and

$$\Delta_K g_{mn}^{(1)} := \nabla^2 g_{mn}^{(1)} + \nabla_m \nabla_n g^{(0)ab} g_{ab}^{(1)}. \quad (2.61)$$

Equation (2.60) can be separated into two equations,

$$\nabla^2 g^{(0)ab} g_{ab}^{(1)} = -4\mu_7 \kappa_{10}^2 (\text{Im } \tau^{(0)})^{-1} \sum_{\alpha} \rho_{\alpha}^{D7} \delta_{(2)}(z_3 - z_{3, \alpha}) + g^{(0)ab} \rho_{g, ab}, \quad (2.62)$$

$$\nabla^2 g_{mn}^{\parallel(1)} = \mu_7 \kappa_{10}^2 \sum_{\alpha} \Phi_+^{(0)}(z_{3, \alpha}) \rho_{\alpha}^{D7} \delta_{(2)}(z_3 - z_{3, \alpha}) \left( \mathcal{F}_{ma, \alpha} \mathcal{F}_{nb, \alpha} g^{(0)ab} - \frac{1}{2} g_{mn}^{\parallel(0)} |\mathcal{F}_{\alpha}|^2 \right) + \rho_{g, mn}^{NS, \parallel}(z_3). \quad (2.63)$$

## Solution incorporating backreaction

The solutions for the equations (2.57)-(2.59) and (2.62)-(2.63) are readily obtained in terms of the scalar Green's functions  $G_{(6)}(z; z')$  and  $G_{(2)}(z_3; z'_3)$  derived in Ap-

pendix A.2:

$$\begin{aligned}\Phi_-^{(1)}(z) = & -\frac{1}{4} \sum_{\alpha} \mu_7 \kappa_{10}^2 \rho_{\alpha}^{D7} \int_D d^4 z' G_{(6)}(z; z') \Phi_+^{(0)2}(z', z'_{3,\alpha}) \text{tr}(g^{(0)-1} \mathcal{F}_{-,\alpha})^2 \\ & + \int_X G_{(6)}(z; z') \rho_-^{NS}(z'),\end{aligned}\quad (2.64)$$

$$(\Phi_+^{(1)})^{-1}(z) = \frac{1}{4} \sum_{\alpha} \mu_7 \kappa_{10}^2 \rho_{\alpha}^{D7} G_{(2)}(z_3; z'_{3,\alpha}) \text{tr}(g^{(0)-1} \mathcal{F}_{+,\alpha})^2 + \int_X G_{(6)}(z; z') \rho_+^{NS}(z'), \quad (2.65)$$

$$\text{Im } \tau^{(1)}(z_3) = -2\mu_7 \kappa_{10}^2 \sum_{\alpha} \rho_{\alpha}^{D7} G_{(2)}(z_3; z_{3,\alpha}) + \int_X G_{(6)}(z; z') \rho_{\text{Im } \tau}^{NS}(z'), \quad (2.66)$$

$$g^{(0)ab} g_{ab}^{(1)} = -4\mu_7 \kappa_{10}^2 (\text{Im } \tau^{(0)})^{-1} \sum_{\alpha} \rho_{\alpha}^{D7} G_{(2)}(z_3; z_{3,\alpha}) + \int_{D^{\perp}} G_{(2)}(z_3; z'_3) g^{(0)ab} \rho_{R,ab}^{NS}, \quad (2.67)$$

$$\begin{aligned}g_{mn}^{\parallel(1)}(z_3) = & \mu_7 \kappa_{10}^2 \sum_{\alpha} \Phi_+^{(0)}(z_{3,\alpha}) \rho_{\alpha}^{D7} G_{(2)}(z_3; z_{3,\alpha}) \left( \mathcal{F}_{ma,\alpha} \mathcal{F}_{nb,\alpha} g^{(0)ab} - \frac{1}{2} g_{mn}^{\parallel(0)} |\mathcal{F}_{\alpha}|^2 \right) \\ & + \int_{D^{\perp}} G_{(2)}(z_3; z'_3) \rho_{g,mn}^{NS,\parallel}(z'_3),\end{aligned}\quad (2.68)$$

where  $D^{\perp}$  denotes the two-cycle dual to  $D$ .

### 2.3.2 Effects on Euclidean D3-branes

Now we examine the DBI action (2.31) for a Euclidean D3-brane wrapping a divisor  $D$  that is parallel<sup>8</sup> to the D7-brane divisors  $D_{\alpha}$ . In local coordinates, (2.31) can be written

$$S_{DBI} = \mu_3 \int_D h g_{z_1 \bar{z}_1} g_{z_2 \bar{z}_2} dz^1 \wedge dz^2 \wedge d\bar{z}^1 \wedge d\bar{z}^2 - \frac{\text{Im } \tau}{2} \mathcal{F}_D \wedge \mathcal{F}_D, \quad (2.69)$$

which to first order in the perturbations is

$$\begin{aligned}S_{DBI}^{(1)} = & 2\mu_3 \int_D d^4 z \left( \left( \Phi_+^{(1)} \right)^{-1} - \left( \Phi_+^{(0)} \right)^{-2} \Phi_-^{(1)} \right) + \left( \Phi_+^{(0)} \right)^{-1} \left( g_{z_1 \bar{z}_1}^{(1)} g_{z_1 \bar{z}_1}^{(0)-1} + g_{z_2 \bar{z}_2}^{(0)-1} g_{z_2 \bar{z}_2}^{(1)} \right) \\ & - \mu_3 \int_D \frac{\text{Im } \tau^{(1)}}{2} \mathcal{F}_D \wedge \mathcal{F}_D.\end{aligned}\quad (2.70)$$

---

<sup>8</sup>Our methods can also be applied when  $D$  is not parallel to the  $D_{\alpha}$ , though we will not present the non-parallel case in this note.

Evaluated in the perturbed solution given by (2.64)-(2.68), the DBI action (2.70) reads

$$\begin{aligned} S_{DBI}^{(1)} = & -\mu_3 \sum_{\alpha} \rho_{\alpha}^{D7} \int_D \left( \frac{1}{2} \mathcal{F}_{-,\alpha} \wedge \star_4 \mathcal{F}_{-,\alpha} + \frac{1}{2} \mathcal{F}_{+,\alpha} \wedge \star_4 \mathcal{F}_{+,\alpha} \right) G_{(2)}(z_3; z_{3,\alpha}) \\ & - \mu_3 \sum_{\alpha} \rho_{\alpha}^{D7} \int_D \frac{1}{2} \mathcal{F}_D \wedge \star_4 \mathcal{F}_D G_{(2)}(z_3; z_{3,\alpha}), \end{aligned} \quad (2.71)$$

where  $G_{(2)}(z_3; z_{3,\alpha})$  is the two-dimensional Green's function (A.30). If we express the induced D3-brane charge and  $\overline{D3}$  brane charge as

$$Q_{\alpha}^{D3} = \frac{\mu_7}{\mu_3} \int_D \frac{1}{2} \mathcal{F}_{+,\alpha} \wedge \star_4 \mathcal{F}_{+,\alpha}, \quad (2.72)$$

$$Q_{\alpha}^{\overline{D3}} = \frac{\mu_7}{\mu_3} \int_D \frac{1}{2} \mathcal{F}_{-,\alpha} \wedge \star_4 \mathcal{F}_{-,\alpha}, \quad (2.73)$$

and define

$$Q_D^{\overline{D3}} = \frac{\mu_7}{\mu_3} \int_D \frac{1}{2} \mathcal{F}_{-,D} \wedge \star_4 \mathcal{F}_{-,D}, \quad (2.74)$$

then (2.71) takes the form

$$S_{DBI}^{(1)} = -2\pi \sum_{\alpha} \rho_{\alpha} \left( Q_{\alpha}^{D3} + Q_{\alpha}^{\overline{D3}} + Q_D^{\overline{D3}} \right) G_{(2)}(z_3; z_{3,\alpha}). \quad (2.75)$$

We can now read off the effect of magnetized D7-branes on the nonperturbative superpotential. Writing (2.32) as

$$|\mathcal{A}e^{-2\pi T}| = \mathcal{A}_0 \exp(-S_{DBI}^{(0)} - S_{DBI}^{(1)}), \quad (2.76)$$

and noting that  $S_{DBI}^{(0)} = 2\pi T - 2\pi \sum_i \rho_i^{D3} G_{(2)}(z_3; z_{3,i})$ , we decompose the Pfaffian factor  $\mathcal{A}$  into  $\mathcal{A}_0$ ,  $\mathcal{A}_{D3}$ , and  $\mathcal{A}_{\mathcal{F}}$ :

$$\mathcal{A} = \mathcal{A}_0 \mathcal{A}_{D3} \mathcal{A}_{\mathcal{F}}, \quad (2.77)$$

where  $\mathcal{A}_0$  encodes the dependence on the complex structure moduli of the internal space,  $\mathcal{A}_{D3} = \exp(2\pi \sum_i \rho_i^{D3} G_{(2)}(z_3; z_{3,i}))$  encodes the dependence on the positions  $z_{3,i}$  of D3-branes, and  $\mathcal{A}_{\mathcal{F}}$  encodes the dependence on the positions  $z_{3,\alpha}$  of

magnetized D7-branes. From (2.75), the Pfaffian factor  $\mathcal{A}_{\mathcal{F}}$  takes the form

$$\boxed{\mathcal{A}_{\mathcal{F}} = \exp \left( 2\pi \sum_{\alpha} \rho_{\alpha} (Q_{\alpha}^{D3} + Q_{\alpha}^{\overline{D3}} + Q_D^{\overline{D3}}) G_{(2)}(z_3; z_{3,\alpha}) \right)}. \quad (2.78)$$

Equation (2.78) is one of our main results.

The final expression (2.78) is rather simple, especially in view of the intricate system of perturbed equations of motion presented in §2.3.1. The emergent simplicity can be understood as follows. Magnetized D7-branes can be viewed as bound states of D7-branes with D3-branes dissolved as the flux (2.4), and one should expect the Pfaffian to depend on the position moduli of this dissolved D3-brane charge (2.72), (2.73), just as the factor  $\mathcal{A}_{D3}$  depends on the positions of mobile D3-branes that are not bound to a D7-brane. Our explicit computation shows that this expectation is precisely fulfilled.

While the terms proportional to  $Q_{\alpha}^{D3}$  and  $Q_{\alpha}^{\overline{D3}}$  represent the backreaction of induced D3-brane charge on the warped volume of a Euclidean D3-brane, the term involving  $Q_D^{\overline{D3}}$  has a qualitatively different origin. It encodes the change in the action of a *magnetized* Euclidean D3-brane, with magnetization  $\mathcal{F}_D$ , that results from the dilaton profile due to the mobile D7-branes. With a slight abuse of language we may call  $Q_D^{\overline{D3}}$  the induced D(-1)-brane charge.

Using the explicit form (A.30) for  $G_{(2)}(z_3; z_{3,\alpha})$ , the Pfaffian (2.78) from a single magnetized D7-brane  $\alpha$  is

$$\mathcal{A}_{\mathcal{F}} = \prod_{i=1}^N \left[ \left| \vartheta_1 \left( \frac{z_3 - \theta^i z_{3,\alpha}}{L} \middle| U \right) \eta^{-1}(U) \right| \exp \left( \frac{-\pi \operatorname{Im} (z_3 - \theta^i z_{3,\alpha})^2}{L^2 \operatorname{Im} U} \right) \right]^{Q_{\alpha}^{D3} + Q_{\alpha}^{\overline{D3}} + Q_D^{\overline{D3}}}, \quad (2.79)$$

where  $L$  is the lattice size of the torus,  $U$  is the complex structure modulus of the torus, and  $\theta$  is the orientifold and orbifold action.

## 2.4 Implications

We have shown in §2.3 that the nonperturbative superpotential depends on the positions of magnetized D7-branes, as in (2.78) and (2.79), because the D3-brane charge induced on the D7-branes backreacts on the internal space. Thus, in D7-brane monodromy models, backreaction of monodromy charge leads to inflaton-dependence of the nonperturbative terms in the moduli potential.

### 2.4.1 Inflaton-dependence of the Pfaffian

To understand how these couplings affect inflation, we can relate the induced charges  $Q^{D3}$ ,  $Q^{\overline{D3}}$ , and  $Q_D^{\overline{D3}}$  in (2.79) to the position  $z_{3,\alpha}$  of the inflationary D7-brane, and in turn to the canonically-normalized inflaton field  $\varphi$ . From (2.79) it is clear that unless  $Q_{\text{tot}} := Q_\alpha^{D3} + Q_\alpha^{\overline{D3}} + Q_D^{\overline{D3}}$  is very small compared to unity, the dependence of  $\vartheta_1$  on  $z_{3,\alpha}$  causes  $\mathcal{A}_{\mathcal{F}}$  to oscillate strongly over a cycle  $z_{3,\alpha} \rightarrow z_{3,\alpha} + L$ . By definition, axion monodromy involves traversing  $N > 1$  periods of the axion, so the oscillations could in principle be repeated  $N$  times. In practice, the change in the moduli potential after a fraction of a cycle is large enough to destabilize the configuration, for example toward decompactification. Barring a mechanism that weakens the inflaton-dependence of the superpotential compared to what we have found, prolonged inflation — whether small-field or large-field — does not occur.

One could ask whether for fine-tuned values of the complex structure modulus  $U$  the dependence (2.79) might be mild enough to allow inflation. A numerical investigation has produced no evidence for this possibility, whereas fine-tuning of  $U$  can partially alleviate the eta problem [40, 177] in the related D3-D7 model [86]. The distinction is that in a small-field model, a problematic Pfaffian coupling



matters only very near a single point in field space, such as a hilltop or inflection point, and correspondingly can sometimes be fine-tuned to vanish by adjusting a single number, such as  $U$ . But for D7-brane monodromy to be possible despite the coupling (2.79), it would be necessary to fine-tune away the problematic terms along the entire trajectory, i.e. over one or more complete cycles. This is a concrete incarnation of the notorious problem of functional fine-tuning in large-field inflation.

A further perspective on our findings comes from [301], in which Ruehle and Wieck studied Pfaffian couplings in an effective supergravity theory. They considered a Kähler potential and superpotential of the form

$$K = -3 \log(T + \bar{T}) + \frac{1}{2}(\Phi + \bar{\Phi})^2, \quad (2.80)$$

$$W = W_0 + \mu \Phi^2 + A_0 \vartheta_3(i\Phi, q)^\delta e^{-\alpha T}, \quad (2.81)$$

where  $\Phi$  corresponds to a D7-brane position modulus,  $T$  is a Kähler modulus, and  $W_0$ ,  $\mu$ ,  $\alpha$ ,  $q$ ,  $\delta$ , and  $A_0$  are constants. It was shown in [301] that for  $\delta \gtrsim 1/2$ , the modulation of the potential via the inflaton-dependence of the Pfaffian is strong enough to adversely affect inflation.<sup>9</sup> Comparing (2.81) and (2.79), we have  $\delta = Q_{\text{tot}}$ .

To apply the results of [301], we can estimate  $Q_{\text{tot}}$ . For the benchmark values for the potential given in [205],  $V(\phi)\alpha'^2 \sim \mathcal{O}(1)$ , the induced  $\overline{D3}$  charge is

$$Q^{\overline{D3}} = 4\pi^3 h \frac{V}{M_S^4} \simeq \mathcal{O}(100h). \quad (2.82)$$

Since  $h \lesssim 1$ , we conclude that Pfaffian couplings due to the backreaction of induced D3-brane charge spoil Higgs-otic inflation for the benchmark parameters of [205].

---

<sup>9</sup>The results of [301] accord with the general finding, in the context of D3-brane inflation models, that the displacement of even a single unit of D3-brane charge typically causes a sizable correction to the Pfaffian of the nonperturbative superpotential [214, 40, 265, 28], and so precludes inflation.

To understand how the importance of backreaction depends on compactification parameters away from these benchmark values, we examine a simplified model. We consider the two-form flux (2.20) on the inflationary D7-brane divisor  $D$ , and we only include bulk fluxes of Hodge type  $(2, 1)$ .<sup>10</sup> The self-dual two-form flux (2.20) induces D3-brane charge on  $D$ :

$$Q^{D3} = \frac{\mu_7 \text{Re}(T)}{\mu_3} \frac{|B|^2}{2}, \quad (2.83)$$

$$= \frac{g_s^2 \text{Re}(T)}{4\mu_3/\mu_7} |G^{(2,1)} \bar{z}|^2. \quad (2.84)$$

Identifying the inflaton with  $\text{Im}(z)$ , the induced charge (2.84) simplifies to

$$Q^{D3} = \frac{g_s \mu_7 \text{Re}(T) \Phi_{+,c}^{-1}}{2M_p^2} Q_{flux}^{D3} \text{Im}(z)^2, \quad (2.85)$$

$$= \frac{1}{2} g_s Q_{flux}^{D3} N_w^2, \quad (2.86)$$

where  $N_w = \text{Im}(z)/L$ . In (2.86) we used the relation  $M_p^2 = (\Phi_{+,c}^{-1} \mathcal{V})/(2\kappa_{10}^2)$ . In terms of the canonically normalized field  $\varphi$ , for small field excursions  $\varphi \lesssim \mathcal{O}(M_p)$  the induced charge (2.84) is given by

$$Q^{D3} = \frac{1}{4} \Phi_{+,c}^{-2} Q_{flux}^{D3} \left| \frac{\varphi}{M_p} \right|^2, \quad (2.87)$$

whereas for large field excursions,  $\varphi \gtrsim \mathcal{O}(M_p)$ ,

$$Q^{D3} = \frac{1}{4} \Phi_{+,c}^{-2} \sqrt{g_s \mu_3 \Phi_{+,c}^{-1} \text{Re}(T) Q_{flux}^{D3}} \left| \frac{\varphi}{M_p} \right|. \quad (2.88)$$

Note that  $\mu_3 \Phi_{+,c}^{-1} \text{Re}(T)/2$  is the DBI action of a Euclidean D3-brane wrapping  $D$ .

To display the leading dependence of the Pfaffian (2.78) on  $\varphi$ , we make further simplifications: we set  $U \rightarrow 1$ , we omit the orientifold images of the magnetized D7- branes, and we expand  $\vartheta_1$  for small displacements  $z_3/L \ll 1$ . This yields

$$\mathcal{A}_{\mathcal{F}}(\varphi) \simeq \left[ c \frac{\varphi - \varphi_0}{M_p} \exp \left( -\pi c^2 \frac{(\varphi - \varphi_0)^2}{M_p^2} \right) \right]^{d \frac{\varphi^2}{M_p^2}}, \quad (2.89)$$

---

<sup>10</sup>As explained in §2.2.5, these restrictions are problematic in complete models, but they are innocuous for the present purpose of obtaining parametric scalings.

where  $d = \frac{1}{4}\Phi_{+,c}^{-2}Q_{flux}^{D3}$ , and  $\varphi_0$  is the location of the Euclidean D3-brane, expressed in terms of the canonically-normalized D7-brane position coordinate  $\varphi$ . For  $Q_{flux}^{D3} \gg 1$  we have  $d \gg 1$ , and even for the marginally controllable parameter choice  $\Phi_{+,c}^{-1} = 2$ ,  $Q_{flux}^{D3} = 1$  we have  $d = 1$ . Because the equations (2.51) and (2.56) imply that  $Q_{flux}^{D3}$  is integrally quantized,  $d$  cannot be made arbitrarily small. Evidently the Pfaffian (2.78) cannot be approximated by a constant independent of  $\varphi$ .

## 2.4.2 Comment on fluxbrane inflation

Even though the primary focus of this note has been on the backreaction of monodromy charge in the Higgs-otic model, the dependence of the Pfaffian (2.78) on the induced charge (2.72), (2.73) has broader applicability. We now discuss the implications of (2.78) for fluxbrane inflation.

Fluxbrane inflation [185, 184, 14] is a hybrid inflation scenario in string theory in which the inflaton field is the separation of a pair of spacetime-filling D7-branes. Suppose that  $X$  is an orientifold of a Calabi-Yau threefold, with  $[\Sigma] \in H_4(X, \mathbb{Z})$  a homology class that admits a continuous family of holomorphic representatives. Two D7-branes  $\mathcal{D}_a$  and  $\mathcal{D}_b$  can then be wrapped on distinct representatives  $\Sigma_a, \Sigma_b \in [\Sigma]$ . The proposal of [185] was to introduce a non-supersymmetric relative gauge flux  $\mathcal{F}$  on  $\mathcal{D}_a$  and  $\mathcal{D}_b$ , so that the D7-branes feel an attractive force and are driven to meet and fuse.

In order for inflation to be possible in this scenario, the flux  $\mathcal{F}$  must fulfill certain conditions. First,  $\mathcal{F}$  should be chosen to lie in the part of  $H^2(\Sigma)$  that descends from  $H^2(X)$ : this ensures the absence of a superpotential term of the

form  $\int_{\mathcal{C}_5} \Omega \wedge \mathcal{F}$ , with  $\mathcal{C}_5$  a five-chain ending on  $\Sigma$ . If such a term were present it could produce a problematically large F-term potential for the D7-brane position, cf. [211]. Next, some choices of  $\mathcal{F}$  will induce D3-brane charge on the D7-branes, and it is well-known that such D3-brane charge can lead to significant couplings in the nonperturbative superpotential [214, 40, 28, 255]. In order to avoid unwanted forces from induced D3-brane charge, the authors of [184] imposed the requirement

$$\int_{\Sigma} \mathcal{F} \wedge \mathcal{F} = 0. \quad (2.90)$$

Because  $\int_{\Sigma} \mathcal{F} \wedge \mathcal{F} = \int_{\Sigma} \mathcal{F}_+ \wedge \star_4 \mathcal{F}_+ - \int_{\Sigma} \mathcal{F}_- \wedge \star_4 \mathcal{F}_-$ , the condition (2.90) enforces that the *net* induced D3-brane charge vanishes, but allows D3-brane and anti-D3-brane charge density to be present in equal amounts. Thus, imposing (2.90) does not suffice to ensure that the backreaction of D3-brane charge vanishes: the SD and ASD components separately provide source terms.

Let us therefore examine the backreaction of induced charge on the Pfaffian in fluxbrane inflation. The induced D3 brane tension

$$\frac{\mu_7}{\mu_3} \int_{\Sigma} \frac{1}{2} \mathcal{F} \wedge \star_4 \mathcal{F} = Q_{\Sigma}^{D3} + Q_{\Sigma}^{\overline{D3}}, \quad (2.91)$$

which perturbs the warp factor  $h$  in the metric (2.2) significantly, does not vanish. As a result, the warped volume of a divisor in the internal space, and so too the Pfaffian, receive corrections depending on (2.91), and this leads to new inflaton-dependence of the moduli potential.

This effect is not necessarily the most stringent restriction on fluxbrane inflation. Examining a toroidal orientifold  $T^4 \times T^2/\mathbb{Z}_2$  for simplicity, (2.91) can be rewritten as

$$Q_{\Sigma}^{D3} + Q_{\Sigma}^{\overline{D3}} = 2 \frac{\mu_7}{\mu_3} \frac{\left( \int_{\Sigma} J \wedge \mathcal{F} \right)^2}{\frac{1}{2} \int_{\Sigma} J \wedge J}. \quad (2.92)$$

The quantity on the right-hand side is constrained [184] by upper bounds on the cosmic string tension [323], which put an upper bound on the D-term potential, and so on the scale of inflation. The resulting bound is

$$Q_{\Sigma}^{D3} + Q_{\Sigma}^{\overline{D3}} \lesssim 10^{-1}. \quad (2.93)$$

Thus, fluxbrane inflation scenarios whose D-term potential is small enough to avoid upper limits on cosmic strings involve the accumulation of a relatively small D3-brane dipole, and backreaction is not a severe problem. However, for any variations of fluxbrane inflation that evade cosmic string limits through a mechanism other than reducing the overall scale of inflation, and in which  $Q_{\Sigma}^{D3} + Q_{\Sigma}^{\overline{D3}}$  becomes significant, a detailed study of backreaction would be important.

## 2.5 Conclusions

Axion monodromy inflation proceeds via the progressive discharge of  $N > 1$  units of a quantized charge. The stress-energy of this monodromy charge sources curvature in the noncompact spacetime, leading to accelerated expansion, but also necessarily sources curvature in the internal six dimensions. The backreaction effects of monodromy charge on the internal solution are known to be important in the NS5-brane axion monodromy scenario of [269], and were extensively studied in that context in [269, 140, 266], but have not been examined at a comparable level in other models.

In this work we computed the backreaction of monodromy charge in Higgs-otic inflation, an axion monodromy scenario in which inflation is driven by the motion of a D7-brane that becomes magnetized as it travels through a background of three-form flux. Such a magnetized D7-brane is a localized source in the super-

gravity equations of motion, and its position and degree of magnetization affect the solution in the internal space. In §2.3 we obtained the resulting solution, to first order in the perturbation due to the D7-brane, in the case of a toroidal orientifold compactification. We found that nonperturbative superpotential terms from Euclidean D3-branes or from gaugino condensation depend on the position of the magnetized D7-brane, cf. (2.78) and (2.79). Thus, the moduli potential depends on the inflaton vev, via the backreaction of induced D3-brane charge on the supergravity solution in the internal space.

Our result echoes the situation in D3-brane inflation, where the position of a mobile D3-brane appears in a Pfaffian factor of the nonperturbative superpotential [146, 214, 40, 28], and leads to inflaton-dependence of the moduli potential. Here, however, the D3-brane charge in question is dissolved as flux in a mobile D7-brane; the amount of induced charge changes as the D7-brane moves; and both D3-brane and anti-D3-brane charges contribute. After a somewhat intricate calculation, our final result is the simple expression (2.78), in which D3-brane charge and anti-D3-brane charge on the D7-brane, and D(-1)-brane charge on the Euclidean D3-brane, enter on precisely equal footing.

The methods used here apply with little modification to any scenario of axion monodromy in which the inflaton is the position of a mobile brane, and in which there are important nonperturbative contributions to the moduli potential. We expect comparably strong backreaction effects in such models. However, our results do not constrain axion monodromy scenarios stabilized by purely perturbative effects, nor do they apply to scenarios such as [271] in which the monodromy charge is dispersed in the six-dimensional bulk rather than localized on a brane.

Our findings present an obstacle to achieving D7-brane axion monodromy in-

flation in a stabilized string compactification, but in our view they do not give such models a uniquely problematic status. Instead, our results show that F-term axion monodromy constructions such as Higgs-otic inflation face the same challenges as the NS5-brane models of [269], and manifest in these models the well-known couplings of moving branes to nonperturbative superpotential terms that plague D3-brane inflation scenarios [214, 40, 265, 28, 30]. In short, the backreaction problem that we find in D7-brane axion monodromy inflation has causes and severity that precisely match what we would expect based on studies of kindred models.

In view of our findings, it would be worthwhile to search for a mechanism that can alleviate the backreaction of monodromy charge in D7-brane monodromy models. More generally, exhibiting an explicit and arbitrarily well-controlled solution of string theory that supports large-field inflation remains an important problem.

# CHAPTER 3

## DE SITTER VACUA FROM TEN DIMENSIONS

— *Dedicated to the memory of Steven S. Gubser* —

### Abstract<sup>1</sup>

We analyze the de Sitter construction of [215] using ten-dimensional supergravity, finding exact agreement with the four-dimensional effective theory. Starting from the fermionic couplings in the D7-brane action, we derive the ten-dimensional stress-energy due to gaugino condensation on D7-branes. We demonstrate that upon including this stress-energy, as well as that due to anti-D3-branes, the ten-dimensional equations of motion require the four-dimensional curvature to take precisely the value determined by the four-dimensional effective theory of [215].

---

<sup>1</sup>This chapter is published as S. Kachru, M. Kim, L. McAllister, M. Zimet, “de Sitter Vacua from Ten Dimensions,” [arxiv:1908.04788 [hep-th]].



### 3.1 Introduction

A foundational problem in cosmology is to characterize de Sitter solutions of string theory. Tremendous efforts have been expended in the study of flux compactifications of weakly-coupled type II string theories on orientifolds (see e.g. the reviews [308, 162, 124, 56, 95, 268, 96, 30, 296]). Non-supersymmetric vacua necessarily remain more difficult to analyze than supersymmetric ones, if only because fewer theoretical tools can be applied there. However, we can take heart by recalling that the entirety of real-world physics is strictly non-supersymmetric, and progress has nonetheless been possible in a few areas, beginning with the work of the non-supersymmetric theorists of antiquity.

A paradigm for exhibiting realistic compactifications of string theory is to derive directly the properties of a four-dimensional effective theory in parametrically controlled limits, such as weak coupling, large volume, and small supersymmetry breaking, and then carefully argue for the form of corrections to the effective theory away from such limits. When the corrections are parametrically small, one expects the vacuum structure computed in the effective theory to be robust.

The couplings in such an effective theory can sometimes be computed in more than one way, e.g. on the string worldsheet and in ten-dimensional supergravity. When dual perspectives are available, they provide a cross-check that lends a degree of further support to the computation of the effective theory. However, it is rarely the case that everything that can be computed in one duality frame can also be computed in the other frame: instead, certain effects are manifest in one frame, and other effects are manifest in the other frame, as is familiar from famous strong-weak dualities in quantum field theory and holography.

The study of de Sitter vacua of type IIB string theory compactified on orientifolds of Calabi-Yau threefolds, as in [215], has relied heavily on computations of vacuum structure in the four-dimensional effective theory. However, certain questions about these theories are intrinsically ten-dimensional, and answering them requires a quantitative description of the de Sitter vacua in terms of configurations of ten-dimensional fields. For example, integrating the ten-dimensional equations of motion over the compact space reveals constraints on possible solutions (see e.g. [90, 151, 311, 279]), and it would be instructive to expose all such constraints. Similarly, the couplings between distinct sectors of the effective theory are often most readily computed by finding solutions for the massless fields in ten dimensions.

At the same time, it is not generally possible even in principle to derive all four-dimensional couplings through a purely ten-dimensional computation. Consider, for example, the infrared dynamics of a pure  $\mathcal{N} = 1$  super-Yang-Mills theory arising on a collection of D7-branes that wrap a four-cycle  $\Sigma$  in the compact space. The eight-dimensional gauge theory is not even asymptotically free, but at energies far below the Kaluza-Klein scale, the four-dimensional theory confines and generates a gaugino condensate. Attempting to compute the gaugino condensate from the ten-dimensional equations of motion, and rejecting the simplifications of the four-dimensional description, would be quixotically self-limiting.

A practical approach, then, is to compute the configuration of ten-dimensional fields that corresponds to a four-dimensional de Sitter vacuum, while taking specific expectation values — such as those of gaugino bilinears — to be those determined by the four-dimensional equations of motion. We refer to the result of this analysis as a *ten-dimensional description* of a de Sitter vacuum.

In this work we provide a ten-dimensional description of the de Sitter scenario of [215]. This problem has been examined in [279, 178, 147, 71, 148, 179, 37] (see also the earlier works [240, 27, 135]). As we will explain below, our analysis aligns with some aspects of these works, but also resolves certain puzzles that were implicit in the literature.

Our approach is a computation from an elementary starting point. Beginning with the ten-dimensional action of type I string theory, we derive the two-gaugino and four-gaugino couplings on D7-branes, and then compute the ten-dimensional stress-energy sourced by a gaugino bilinear expectation value  $\langle\lambda\lambda\rangle$ . Then, taking  $\langle\lambda\lambda\rangle$  to have the value predicted by the four-dimensional super-Yang-Mills theory — and we stress that this step is the only point at which information from four dimensions is injected — we compute the four-dimensional scalar curvature determined by the ten-dimensional equations of motion.

In order to evaluate the contribution of the D7-brane gaugino-flux coupling, we use the Killing spinor equations for compactification on a generalized complex geometry, with which we establish that in a supersymmetric configuration the generalized complex geometry superpotential equals the full superpotential of the four-dimensional theory. We then compare the scalar curvature resulting from the ten-dimensional configuration to the scalar curvature determined by the four-dimensional Einstein equations equipped with the scalar potential of [215]. We prove that the match is exact in the supersymmetric vacuum. Furthermore, provided that the generalized complex geometry superpotential continues to equal the full superpotential in off-shell configurations — which we find very plausible but do not prove here — our ten-dimensional computation of the scalar potential for the Kähler modulus continues to precisely match the four-dimensional theory, in

the presence of anti-D3-branes as well as off-shell.

The organization of this paper is as follows. In §3.2 we assemble the equations of motion of type IIB supergravity. In §3.3 we consider the effects of an expectation value for the gaugino bilinear on a stack of D7-branes. We show that couplings of the D7-brane gauginos, including the couplings to flux derived by Dymarsky and Martucci in [135] following [66], source a contribution  $T_{\mu\nu}^{(\lambda\lambda)}$  to the stress-energy tensor. Including this stress-energy in the ten-dimensional equations of motion, we compute the four-dimensional scalar curvature, and find perfect agreement with that determined by the F-term potential in the four-dimensional  $\mathcal{N} = 1$  supersymmetric effective theory of [215]. In §3.4 we consider the combined effects of an anti-D3-brane and a D7-brane gaugino bilinear. We examine the ten-dimensional supergravity solution with these sources and show that  $T_{\mu\nu}^{(\lambda\lambda)}$  continues to match the four-dimensional potential derived in [216]. Our conclusions appear in §5.5. In Appendix B.1 we first dimensionally reduce and T-dualize the type I action to obtain the couplings of D7-brane gauginos. We then analyze the ten-dimensional Killing spinor equations, correcting an inconsistency in the literature, and use them to demonstrate explicitly that the superpotential for compactification on a generalized complex geometry captures both the classical flux superpotential and the gaugino condensate superpotential. Appendix B.2 shows, based on the spectroscopy of  $T^{1,1}$ , that the interactions of an anti-D3-brane and a gaugino condensate mediated by Kaluza-Klein excitations of a Klebanov-Strassler throat can be neglected compared to the interaction mediated by the Kähler modulus. In Appendix B.3 we consider the singular contributions to the four-dimensional equations of motion, which originate in the fact that the D7-brane stack is localized to a divisor. We show that these divergent terms cancel each other, and the finite remainder is the four-dimensional scalar potential. We then repeat this computation for a

compactification containing a D3-brane, with analogous results.

### 3.2 Ten-dimensional Equations of Motion

In this section, we set our notation and collect useful forms of the ten-dimensional Einstein equations and five-form Bianchi identity. We then express the stress-energy tensor of the four-dimensional effective theory in terms of the ten-dimensional field configuration.

We consider type IIB string theory on  $X \times M$ , where  $X$  is a four-dimensional spacetime and  $M$  is a six-dimensional compact manifold that in the leading approximation is an O3/O7 orientifold of a Calabi-Yau threefold. We take the metric ansatz

$$ds^2 = G_{AB}dX^A dX^B = e^{-6u(x)+2A(y)}g_{\mu\nu}dx^\mu dx^\nu + e^{2u(x)-2A(y)}g_{ab}dy^a dy^b, \quad (3.1)$$

with  $x$  denoting coordinates in  $X$  and  $y$  denoting coordinates in  $M$ . Greek indices take values in  $\{0, \dots, 3\}$ , and Latin indices take values in  $\{1, \dots, 6\}$ . We use the abbreviations  $g_6 = \det g_{ab}$  and  $g_4 = \det g_{\mu\nu}$ , and note that  $\sqrt{-G} = \sqrt{-g}e^{-6u-2A} = \sqrt{-g_4 g_6}e^{-6u-2A}$ .

The ten-dimensional type IIB supergravity action is

$$S = \frac{1}{2\kappa_{10}^2} \int d^{10}X \sqrt{-G} \left( \mathcal{R}_{10} - \frac{\partial_A \tau \partial^A \bar{\tau}}{2(\text{Im } \tau)^2} - \frac{G_3 \cdot \bar{G}_3}{2\text{Im } \tau} - \frac{\tilde{F}_5^2}{4} \right) + \frac{1}{8i\kappa_{10}^2} \int \frac{C_4 \wedge G_3 \wedge \bar{G}_3}{\text{Im } \tau} + S_{\text{local}}, \quad (3.2)$$

where  $\mathcal{R}_{10}$  is the Ricci scalar computed from  $G$ ,  $\tau = C_0 + i e^{-\phi}$  is the axiodilaton,  $G_3 := F_3 - \tau H_3 \equiv dC_2 - \tau dB_2$ , and  $\tilde{F}_5 = F_5 - \frac{1}{2}C_2 \wedge H_3 + \frac{1}{2}B_2 \wedge F_3$ , with  $F_5 = dC_4$ .

The local term  $S_{\text{local}}$  encodes the contributions of D-branes and orientifold planes.

We work in units where  $(2\pi)^2 \alpha' = 1$ .

For the five-form  $\tilde{F}_5$  we take the ansatz

$$\tilde{F}_5 = (1 + \star_{10})e^{-12u}\sqrt{-g_4}d\alpha(y) \wedge dx^0 \wedge dx^1 \wedge dx^2 \wedge dx^3, \quad (3.3)$$

with  $\star_{10}$  the ten-dimensional Hodge star, and define the scalars

$$\Phi_{\pm} := e^{4A} \pm \alpha. \quad (3.4)$$

We also define the imaginary self-dual and imaginary anti-self-dual fluxes

$$G_{\pm} := \frac{(\star_6 \pm i)}{2} G_3, \quad (3.5)$$

with  $\star_6$  the six-dimensional Hodge star. We abbreviate (3.2) as

$$S = \frac{1}{2\kappa_{10}^2} \int d^{10}X \sqrt{-G} \mathcal{R}_{10} + \int d^{10}X \mathcal{L} \equiv S_{\text{EH}} + \int d^{10}X \mathcal{L}, \quad (3.6)$$

with  $\mathcal{L}$  encoding everything except for the Einstein-Hilbert term.

From (3.1) one computes the Ricci tensors

$$\mathcal{R}_{4,\mu\nu} = \mathcal{R}_{4,\mu\nu}[g] - e^{-8u+4A}g_{\mu\nu}\nabla^2 A + 3g_{\mu\nu}\square u - 24\partial_{\mu}u\partial_{\nu}u, \quad (3.7)$$

$$\mathcal{R}_{6,ab} = \mathcal{R}_{6,ab}[g] + \nabla^2 A g_{ab} - e^{8u-4A}g_{ab}\square u - 8\partial_a A \partial_b A, \quad (3.8)$$

where  $\mathcal{R}_{4,\mu\nu}[g]$  and  $\mathcal{R}_{6,ab}[g]$  are the Ricci tensors of  $g_{\mu\nu}$  and  $g_{ab}$ , respectively. Expanding the Einstein-Hilbert part of (3.2) using (3.7) and (3.8), we find

$$S_{\text{EH}} = \frac{1}{2\kappa_{10}^2} \int d^4x d^6y \sqrt{-g_4 g_6} \left( e^{-4A} \mathcal{R}_4[g] + e^{-8u} \mathcal{R}_6[g] - 24e^{-4A} \partial_{\mu}u \partial^{\mu}u - 8e^{-8u} \partial_a A \partial^a A \right),$$

where indices are raised using  $g_{\mu\nu}$  or  $g_{ab}$  as appropriate. The Planck mass is given by

$$M_{\text{pl}}^2 = \frac{\mathcal{V}}{\kappa_{10}^2}, \quad (3.9)$$

where  $\mathcal{V}$  is the warped volume of  $M$ , defined as

$$\mathcal{V} = \int_M d^6y \sqrt{g_6} e^{-4A}. \quad (3.10)$$

The equation of motion for the breathing mode  $u$  obtained from (3.6) is

$$24\Box u = 4e^{4A-8u}\left(\mathcal{R}_6[g] - 8\partial_a A\partial^a A\right) - \kappa_{10}^2 e^{4A}\frac{\delta\mathcal{L}}{\delta u}. \quad (3.11)$$

We next turn to the Einstein equations, in conventions where the stress-energy tensor is defined as

$$T_{AB} = -\frac{2}{\sqrt{-G}}\frac{\delta\mathcal{L}}{\delta G^{AB}}. \quad (3.12)$$

The four-dimensional components of the ten-dimensional Einstein equations are

$$\mathcal{R}_{4,\mu\nu} = \kappa_{10}^2\left(T_{\mu\nu} - \frac{1}{8}G_{\mu\nu}T\right). \quad (3.13)$$

Reversing the trace using the ten-dimensional metric  $G^{\mu\nu}$ , we have

$$\mathcal{R}_{4,\mu\nu}G^{\mu\nu} = -\kappa_{10}^2 T_{\mu\nu}G^{\mu\nu} - \frac{\kappa_{10}^2}{2}\left(T_{ab}G^{ab} - 3T_{\mu\nu}G^{\mu\nu}\right). \quad (3.14)$$

Integrating (3.14) over  $M$  and using (3.7) leads to

$$M_{\text{pl}}^2\left(\mathcal{R}_4[g] + 12\Box u - 24\partial_\mu u\partial^\mu u\right) = \int_M \sqrt{g_6}e^{-6u-2A}\left[-T_{\mu\nu}G^{\mu\nu} - \frac{1}{2}\left(T_{ab}G^{ab} - 3T_{\mu\nu}G^{\mu\nu}\right)\right]. \quad (3.15)$$

Similarly, the six-dimensional components of the ten-dimensional Einstein equations are

$$\mathcal{R}_{6,ab} = \kappa_{10}^2\left(T_{ab} - \frac{1}{8}G_{ab}T\right), \quad (3.16)$$

with trace-reversed form

$$\mathcal{R}_{6,ab}G^{ab} = \frac{\kappa_{10}^2}{4}\left(T_{ab}G^{ab} - 3T_{\mu\nu}G^{\mu\nu}\right). \quad (3.17)$$

Integrating (3.17) over  $M$  and using (3.8) gives

$$-6M_{\text{pl}}^2\Box u + \frac{1}{\kappa_{10}^2}\int_M \sqrt{g_6}e^{-8u}\left(\mathcal{R}_6[g] - 8\partial_a A\partial^a A\right) = \frac{1}{4}\int_M \sqrt{g_6}e^{-6u-2A}\left[T_{ab}G^{ab} - 3T_{\mu\nu}G^{\mu\nu}\right]. \quad (3.18)$$

Finally, we examine the Bianchi identity

$$d\tilde{F}_5 = 2\mu_3\kappa_{10}^2\rho_{D3}\text{dVol}_M = H \wedge F + 2\mu_3\kappa_{10}^2\rho_{D3}^{\text{loc}}\text{dVol}_M. \quad (3.19)$$

Here  $d\text{Vol}_M = \sqrt{g_6} dy^1 \wedge \cdots \wedge dy^6$ ,  $\rho_{D3}$  is the net D3-brane charge density, and  $\rho_{D3}^{\text{loc}}$  is the net D3-brane charge density of localized objects such as D3-branes and anti-D3-branes. (We use  $\rho_{\overline{D3}}$  to denote the contributions of anti-D3-branes specifically.) From (3.19) we derive the useful integrated form

$$0 = \int_M \sqrt{g_6} (e^{-8u-8A} \partial_a e^{4A} \partial^a \alpha + 2\mu_3 \kappa_{10}^2 e^{-12u} e^{4A} \rho_{D3}) . \quad (3.20)$$

Combining (3.15), (3.18), and (3.20) we obtain

$$\begin{aligned} M_{\text{pl}}^2 \mathcal{R}_4[g] &= 24M_{\text{pl}}^2 \partial_\mu u \partial^\mu u - \int_M \sqrt{g_6} (e^{-4A} \hat{T}_{\mu\nu} g^{\mu\nu} + 4\mu_3 e^{-12u+4A} \rho_{D3}) \\ &\quad - \frac{2e^{-8u}}{\kappa_{10}^2} \int_M \sqrt{g_6} \mathcal{R}_6[g] + \frac{e^{-8u}}{\kappa_{10}^2} \int_M \sqrt{g_6} e^{-8A} \partial_a \Phi_- \partial^a \Phi_- , \end{aligned} \quad (3.21)$$

where  $\hat{T}_{\mu\nu}$  denotes the stress-energy tensor excluding the contribution from  $\tilde{F}_5$ .

Substituting the type IIB supergravity action (3.2) into (3.21), and taking  $S_{\text{local}}$  in (3.2) to include D3-branes and D7-branes, we find

$$\begin{aligned} M_{\text{pl}}^2 \mathcal{R}_4[g] &= 24M_{\text{pl}}^2 \partial_\mu u \partial^\mu u + \frac{\partial_\mu \tau \partial^\mu \bar{\tau}}{(\text{Im } \tau)^2} + 8\mu_3 \int_M \sqrt{g_6} e^{-12u+4A} \rho_{\overline{D3}} - \int_M \sqrt{g_6} e^{-4A} T_{\mu\nu}^{D7} g^{\mu\nu} \\ &\quad - \frac{2e^{-8u}}{\kappa_{10}^2} \int_M \sqrt{g_6} \mathcal{R}_6[g] + \frac{e^{-8u}}{\kappa_{10}^2} \int_M \sqrt{g_6} e^{-8A} \partial_a \Phi_- \partial^a \Phi_- . \end{aligned} \quad (3.22)$$

To interpret (3.22), we consider a general four-dimensional action

$$S_4 = \frac{M_{\text{pl}}^2}{2} \int_X \sqrt{-g_4} \mathcal{R}_4[g] + \int_X \sqrt{-g_4} \mathcal{L}_4 . \quad (3.23)$$

The four-dimensional Einstein equations imply

$$M_{\text{pl}}^2 \mathcal{R}_4[g] = -\mathcal{T} , \quad (3.24)$$

where  $\mathcal{T}_{\mu\nu}$  is the *four-dimensional* stress-energy tensor, i.e. the stress-energy tensor computed from  $\mathcal{L}_4$ . The four-dimensional stress-energy tensor  $\mathcal{T}_{\mu\nu}$  and the four-dimensional components  $T_{\mu\nu}$  of the ten-dimensional stress-energy tensor  $T_{AB}$  are



related by

$$\begin{aligned} \mathcal{T}_{\mu\nu} = \int_M \sqrt{g_6} \left[ e^{-4A} \hat{T}_{\mu\nu} + \mu_3 e^{4A-12u} g_{\mu\nu} \rho_{D3} + \frac{e^{-8u}}{2\kappa_{10}^2} g_{\mu\nu} \mathcal{R}_6[g] - \frac{e^{-8A-8u}}{4\kappa_{10}^2} g_{\mu\nu} \partial_a \Phi_- \partial^a \Phi_- \right] \\ + M_{\text{pl}}^2 (24 \partial_\mu u \partial_\nu u - 12 g_{\mu\nu} \partial_\rho u \partial^\rho u). \end{aligned} \quad (3.25)$$

Comparing (3.22) and (3.24), the right-hand side of (3.22) can be identified with  $-\mathcal{T}$ , i.e. with minus the trace of the stress-energy tensor of the effective theory.

The master equation (3.22) thus encodes the relationship between the curvature  $\mathcal{R}_4[g]$  of the four-dimensional Einstein frame metric  $g_{\mu\nu}$  on the one hand, and the contributions of the ten-dimensional field configuration to the effective four-dimensional stress-energy tensor  $\mathcal{T}_{\mu\nu}$  on the other hand. This relation will be crucial in our analysis. We note that (3.22) matches the effective potential derived from the ten-dimensional Einstein equations in [152], see e.g. equation (5.30) of [152].

An equivalent route to deriving (3.22) is to first follow the steps leading to the Einstein-minus-Bianchi equation (2.30) of [151], which in our conventions reads

$$\nabla^2 \Phi_- = e^{-4A} \partial_a \Phi_- \partial^a \Phi_- + \frac{1}{2} \kappa_{10}^2 e^{2A+2u} (\hat{T}_{ab} G^{ab} - \hat{T}_{\mu\nu} G^{\mu\nu}) - 2\kappa_{10}^2 \mu_3 e^{8A-4u} \rho_{D3} + e^{8u} \mathcal{R}_4^{\text{Ref.}[12]}. \quad (3.26)$$

Because we have made explicit the breathing mode  $u$ , which was instead implicit in the metric ansatz of [151], the scalar curvatures there and here are related by

$$\mathcal{R}_4^{\text{Ref.}[149]} = \mathcal{R}_4[g] + 12 \square u - 24 \partial_\mu u \partial^\mu u. \quad (3.27)$$

Substituting (3.27) in (3.26) and using the Einstein equations and Bianchi identity, one arrives at (3.22). The point we would like to stress is that equation (2.30) of [151] — which has been the basis of a number of constraints on compact solutions — and the master equation (3.22) contain equivalent information, *provided* that one correctly accounts for the breathing mode as in (3.27).

### 3.3 Stress-energy of Gaugino Condensate

Our goal is to examine the de Sitter scenario of [215] using the ten-dimensional equations of motion. In the four-dimensional effective theory, the scalar potential has two components: an F-term potential for the moduli of an  $\mathcal{N} = 1$  supersymmetric compactification, and a supersymmetry-breaking contribution from one or more anti-D3-branes. We will examine these in turn: in this section we consider the ten-dimensional configuration without anti-D3-branes, and then in §3.4 we incorporate the effects of anti-D3-branes.

The relevant moduli at low energies are the Kähler moduli of the Calabi-Yau orientifold  $M$ , because the complex structure moduli and axiodilaton acquire mass from  $G_3$  flux at a higher scale.<sup>2</sup> For simplicity of presentation we will consider a single Kähler modulus, which we denote by  $T$ , but our method applies more generally.

The four-dimensional analysis of [215] established that in the presence of a suitably small<sup>3</sup> classical flux superpotential, combined with a nonperturbative superpotential from Euclidean D3-branes or from gaugino condensation on D7-branes, the Kähler modulus  $T$  is stabilized in an  $\mathcal{N} = 1$  supersymmetric  $AdS_4$  vacuum. To recover this result from ten dimensions, we need to understand how these two superpotential terms correspond to ten-dimensional field configurations.

---

<sup>2</sup>If D3-branes are present, their position moduli have masses parametrically comparable to those of the Kähler moduli, and the corresponding potential can be computed in ten dimensions [27]: see Appendix B.3.

<sup>3</sup>The statistical approach of Denef and Douglas [97] gives strong evidence that (in the spirit of [59]) one can fine-tune the classical flux superpotential  $W_0 = \langle W_{\text{flux}} \rangle$  to be small. This conclusion is supported by [94], which explicitly demonstrates that values of  $W_0$  small enough for control of the instanton expansion are achievable even with few complex structure moduli.

First of all, the Gukov-Vafa-Witten flux superpotential [176]

$$W_{\text{flux}} = \pi \int G \wedge \Omega \quad (3.28)$$

encodes in the four-dimensional effective theory the interaction corresponding to the term

$$S_{\text{flux}} = -\frac{1}{2\kappa_{10}^2} \int d^{10}X \sqrt{-G} \frac{G_3 \cdot \bar{G}_3}{2 \text{Im } \tau} \quad (3.29)$$

in the ten-dimensional action (3.2). In particular, the ten-dimensional stress-energy associated to  $W_{\text{flux}}$  is that computed from (3.29).

In the remainder of this section, we will describe the gaugino condensate superpotential in similarly ten-dimensional terms, and compute the contribution  $T_{\mu\nu}^{(\lambda\lambda)}$  of gaugino condensation on D7-branes to the ten-dimensional stress-energy tensor. We will see that the stress energy  $T_{\mu\nu}^{(\lambda\lambda)}$  arises from gaugino-flux couplings generalizing those derived by Cámara, Ibáñez, and Uranga in [66], and also from associated nonsingular four-gaugino terms. We will then show that this stress-energy<sup>4</sup> leads to a potential for the Kähler modulus that exactly matches the F-term potential of [215].

Because the gaugino condensate relies on the dynamics of the D7-brane gauge theory below the Kaluza-Klein scale, it is not entirely obvious that a ten-dimensional description of gaugino condensation should exist at all. However, as explained in [27], one can consider D7-branes wrapping a divisor that is very small compared to the entire compact space. A localized ‘observer’ far from the D7-branes, such as a distant D3-brane, should then be able to treat them as a fuzzy source. This approach turns out to be fruitful: we will exhibit below a precise correspondence between the ten-dimensional and four-dimensional computations

---

<sup>4</sup>In Appendix B.3 we account for the terms other than  $T_{\mu\nu}^{D7}$  in (3.22), and demonstrate that our conclusions remain unchanged.

of the potential for the Kähler modulus, just as the four-dimensional result for the potential of a D3-brane probe was obtained from ten dimensions in [27].<sup>5</sup>

### 3.3.1 Four-dimensional effective theory

We begin by recalling results from the four-dimensional effective theory that we aim to recover from ten dimensions. Dimensional reduction of the theory on a stack of D7-branes wrapping a divisor  $D$  leads at low energies, and in the limit that gravity decouples, to the  $\mathcal{N} = 1$  supersymmetric Yang-Mills Lagrangian density

$$\frac{1}{16\pi i} \int d^2\theta f(T) W_\alpha W^\alpha + c.c., \quad (3.30)$$

where we have adopted the conventions of [319], but suppress Lie algebra indices. We will denote the dual Coxeter number of the gauge group by  $N_c$ .

Classically, the  $\mathcal{N} = 1$  supergravity theory associated to (3.30), for D7-branes in a background whose moduli potential is described by a classical flux superpotential  $W_{\text{flux}}$ , has the Lagrangian density (see e.g. [221])

$$\begin{aligned} \mathcal{L} = & -\frac{1}{4} \text{Re} f(T) F_{\mu\nu} F^{\mu\nu} - i \bar{\lambda} \bar{\sigma}^\mu \partial_\mu \lambda \text{Re} f(T) - \frac{1}{4} \lambda \lambda e^{\kappa_4^2 K(T, \bar{T})/2} K^{T\bar{T}} \partial_T f(T) K_{\bar{T}} \bar{W}_{\text{flux}} + c.c. \\ & + \frac{3\kappa_4^2}{64} \left( \bar{\lambda} \bar{\sigma}^\mu \lambda \text{Re} f(T) \right)^2 - \frac{1}{16} \lambda \lambda \bar{\lambda} \bar{\lambda} K^{T\bar{T}} \partial_T f(T) \partial_{\bar{T}} \bar{f}(\bar{T}), \end{aligned} \quad (3.31)$$

which reduces to (3.30) in the limit  $\kappa_4 \rightarrow 0$ . We take the divisor  $D$  to be rigid, so that the Yang-Mills theory has no charged matter. Here, the D7-brane gauge coupling is given by the holomorphic expression<sup>6</sup>

$$f(T) = \frac{T}{4\pi} \quad \text{with } T := \int_D \sqrt{g_6} e^{-4A+4u} + i \int_D C_4. \quad (3.32)$$

<sup>5</sup>See Appendix B.3 for a computation of the D3-brane potential that extends the result of [27].

<sup>6</sup>The normalization  $f(T) = T/(2\pi)$  was used in the study of gaugino-flux couplings in [135, 279], but we take instead  $f(T) = T/(4\pi)$  for ease of comparison to the supergravity literature.

However, as explained by [226], in a quantum mechanical effective field theory treatment of supergravity (as opposed to classical supergravity) the gauge coupling function receives a non-holomorphic contribution from the Kähler potential:

$$f(T, \bar{T}) = \frac{T}{4\pi} - \frac{N_c}{16\pi^2} \kappa_4^2 K(T, \bar{T}) . \quad (3.33)$$

This term is present thanks to an anomaly in the Weyl rescaling that transforms fields from the normalization which has linearly realized supersymmetry (when one restores the auxiliary fields) and a holomorphic  $f(T)$  to the physical normalization employed in (3.4). Because of this, the usual expression for the gaugino bilinear expectation value in terms of the gauge coupling function depends non-holomorphically on  $T$  [226]:

$$\langle \lambda \lambda \rangle = -\frac{32\pi^2}{N_c} \mathcal{A} e^{-\frac{8\pi^2}{N_c} f(T, \bar{T})} . \quad (3.34)$$

Similarly, the classical Lagrangian (3.31) requires a number of modifications to account for the fact that  $f$  is not holomorphic.

After integrating out the vector multiplet, one obtains an effective field theory valid below the confinement scale that involves only the chiral superfield containing the Kähler modulus and the supergravity multiplet. This has the superpotential

$$W = W_{\text{flux}} + W_{\text{np}} , \quad (3.35)$$

where [226]

$$W_{\text{np}} = \mathcal{A} e^{-\frac{2\pi T}{N_c}} . \quad (3.36)$$

This leads to the relation

$$\langle \lambda \lambda \rangle = -\frac{32\pi^2}{N_c} e^{\kappa_4^2 K/2} W_{\text{np}} . \quad (3.37)$$

The Pfaffian prefactor  $\mathcal{A}$  depends on the complex structure moduli and the positions of any D3-branes: see [40, 28]. Finally, the Kähler potential is<sup>7</sup>

$$K = -3 \log(T + \bar{T}) - \log(-i(\tau - \bar{\tau})) - \log\left(i \int_M e^{-4A} \Omega \wedge \bar{\Omega}\right) + \log\left(2^7 \mathcal{V}^3\right). \quad (3.38)$$

In terms of these functions, the F-term potential in this effective field theory is

$$V = e^{\kappa_4^2 K} \left( K^{T\bar{T}} D_T W D_{\bar{T}} \bar{W} - 3 \kappa_4^2 W \bar{W} \right). \quad (3.39)$$

Our goal is now to show that the F-term potential (3.39), which we have just recalled as a result in four-dimensional supergravity, can also be derived from the *ten-dimensional* equations of motion, upon assigning the vev (3.34) and examining the ten-dimensional stress-energy.

### 3.3.2 D7-brane gaugino couplings

Now we turn to ten dimensions. To describe the backreaction of the gaugino condensate on the bulk fields, we must relax the Calabi-Yau condition and employ generalized complex geometry, as in [164, 38, 240, 239]. In particular, as reviewed in Appendix B.1, the single covariantly constant spinor is replaced by two internal Killing spinors  $\eta_1$  and  $\eta_2$ . We can combine these to form a bispinor  $\Phi_1$ , defined as

$$\Phi_1 := -\frac{8i}{|\eta|^2} \eta_1 \otimes \eta_2^\dagger, \quad (3.40)$$

and we also define

$$\mathfrak{t} := \text{Re}\left(e^{-\phi + (\phi/4 - A)\hat{p}} \Phi_1\right), \quad (3.41)$$

---

<sup>7</sup>Although the complex structure moduli and dilaton receive supersymmetric masses from the flux background, we retain the associated terms in (3.38) because their expectation values matter for the overall normalization. The Kähler potential (3.38) is consistent with that of [102, 240, 223] — see Appendix B.1 for details of our conventions.

where the operator  $\hat{p}$  is defined by

$$\hat{p} C_p := p C_p \quad (3.42)$$

for a  $p$ -form  $C_p$  [189]. In type IIB string theory compactified on an orientifold of a Calabi-Yau threefold, and in the absence of nonperturbative effects, one has  $\mathfrak{t} = 0$ . However, upon including the effects of gaugino condensation,  $\mathfrak{t}$  develops a nonvanishing two-form component [135], cf. (B.29), that will be important for our analysis.

We now study the action of D7-branes on such a generalized complex geometry. The eight-dimensional action describing a stack of D7-branes is derived in Appendix B.1 via dimensional reduction and T-dualization of the type I action. We will highlight the important changes that occur when, instead of dimensionally reducing these D7-branes on a divisor in a Calabi-Yau orientifold, one wraps a divisor in a generalized complex geometry. Our findings reproduce results of [240].

### Gaugino-flux couplings

To write the flux superpotential and the gaugino-flux couplings on D7-branes in a generalized complex geometry, we first define

$$\mathfrak{G} := G_3 + i d\mathfrak{t}, \quad (3.43)$$

and

$$\mathfrak{G}^{[2]} := G_3 + i d_2 \mathfrak{t}, \quad (3.44)$$

where  $d_2$  is a differential operator defined in terms of coordinates along the D7-brane, and is given in Appendix B.1.2.

The gaugino-flux couplings on D7-branes are determined by the supersymmetric Born-Infeld action. In the conventions of [249, 135], with the metric ansatz

(3.1), and recalling that we have set  $(2\pi)^2\alpha' = 1$ , these couplings – on a divisor *in a Calabi-Yau orientifold*, not a generalized complex geometry – are

$$S_{G\lambda\lambda} = \frac{i}{32\pi} \int \sqrt{-g_4 g_6} e^{\phi/2} e^{-2u} G_3 \cdot \Omega \bar{\lambda} \bar{\lambda} \delta^{(0)} + c.c. \quad (3.45)$$

We re-derive this interaction via dimensional reduction of the eight-dimensional D7-brane action in Appendix B.1.

In similar fashion, we find the action that one obtains from wrapping a divisor in a generalized complex geometry. The details are relegated to Appendix B.1; the result, in agreement with [38, 240], is that one should promote<sup>8</sup>

$$G_3 \rightarrow G_3 + i d_2 t \equiv \mathfrak{G}^{[2]}. \quad (3.46)$$

Thus, (3.45) becomes (cf. [135])

$$S_{\mathfrak{G}\lambda\lambda} = \frac{i}{32\pi} \int \sqrt{-g_4 g_6} e^{\phi/2} e^{-2u} \mathfrak{G}^{[2]} \cdot \Omega \bar{\lambda} \bar{\lambda} \delta^{(0)} + c.c. \quad (3.47)$$

One can likewise generalize the familiar flux superpotential (3.28). The superpotential in a generalized complex geometry has been studied in e.g. [163, 38, 277, 240, 249] from several angles, for example by computing the mass and supersymmetry transformation of the gravitino. In our class of solutions this superpotential takes the form

$$W_{\text{GCG}} = \pi \int_M \mathfrak{G} \wedge \Omega, \quad (3.48)$$

as we show in Appendix B.1.3.

To relate  $W_{\text{GCG}}$  to the superpotential  $W = W_{\text{flux}} + W_{\text{np}}$  given in (3.35), we impose the ten-dimensional Killing spinor equations that govern supersymmetric solutions. In Appendix B.1.3 we show that

$$\langle W_{\text{GCG}} \rangle = W_{\text{flux}} + W_{\text{np}}, \quad (3.49)$$

---

<sup>8</sup>Discussions of (3.46) in this context include [264] and the recent work [37].



where the brackets indicate evaluation in the supersymmetric configuration. The generalized complex geometry thus elegantly encodes the effects of the nonperturbative superpotential.

Evaluating the gaugino-flux coupling (3.47), one finds (see Appendix B.1.4 for details of the computation)

$$S_{\mathfrak{G}\lambda\lambda} = -\kappa_4^2 \int_X \sqrt{-g_4} e^{\kappa_4^2 K} K^{T\bar{T}} \partial_{\bar{T}} \bar{W} K_T W + c.c. + S_{\lambda\lambda}^{\text{sing}}, \quad (3.50)$$

where  $S_{\lambda\lambda}^{\text{sing}}$  is a singular contribution, given in (B.109), that is treated in Appendix B.3.

### Four-gaugino coupling

We similarly demonstrate in Appendix B.1, by dimensional reduction and T-dualization of the ten-dimensional type I action, that there is a four-gaugino coupling<sup>9</sup> on D7-branes given by

$$S_{\lambda\lambda\lambda\lambda} = -\frac{1}{6144\pi^3} \int \sqrt{-g_4} g_6 e^{-4A+8u} \nu \Omega \cdot \bar{\Omega} |\lambda\lambda|^2 \delta^{(0)}, \quad (3.51)$$

where  $\nu \equiv \mathcal{V}_\perp^{-1} = \mathcal{V}^{-1} \int_D \sqrt{g_6} e^{-4A}$  is the inverse of the volume  $\mathcal{V}_\perp$  transverse to the D7-branes. Upon assigning the gaugino bilinear vev (3.34), the four-gaugino term (3.51) dimensionally reduces to

$$S_{\lambda\lambda\lambda\lambda} = - \int_X \sqrt{-g_4} e^{\kappa_4^2 K} K^{T\bar{T}} \partial_T W \partial_{\bar{T}} \bar{W}. \quad (3.52)$$

See Appendix B.1 for details of the computation.

---

<sup>9</sup>The importance of four-gaugino couplings in this context was stressed in [178].

### 3.3.3 Ten-dimensional stress-energy

We can now obtain the F-term potential for the Kähler modulus  $T$  from the ten-dimensional field configuration. Upon assigning the gaugino bilinear vev (3.34) and using (3.50), the properly-holomorphic gaugino-flux coupling (3.47) evaluates to

$$\mathcal{L}_{\mathfrak{G}\lambda\lambda} = -\kappa_4^2 e^{\kappa_4^2 K} K^{T\bar{T}} \left( \partial_T W K_{\bar{T}} \bar{W} + c.c. \right) + \mathcal{L}_{\lambda\lambda}^{\text{sing}}. \quad (3.53)$$

The associated ten-dimensional stress-energy is

$$T_{\mu\nu}^{\lambda\lambda} := -\frac{2}{\sqrt{G}} \frac{\delta \mathcal{L}_{\mathfrak{G}\lambda\lambda}}{\delta G^{\mu\nu}} = \frac{i}{32\pi} e^{4A+\phi/2-2u} \mathfrak{G}^{[2]} \cdot \Omega \bar{\lambda} \bar{\lambda} \delta^{(0)} g_{\mu\nu} + c.c., \quad (3.54)$$

which integrates to

$$-\int_M \sqrt{g_6} e^{-4A} T_{\mu\nu}^{\lambda\lambda} g^{\mu\nu} = 4\kappa_4^2 e^{\kappa_4^2 K} K^{T\bar{T}} \partial_T W K_{\bar{T}} \bar{W} + c.c. - 4S_{\lambda\lambda}^{\text{sing}}. \quad (3.55)$$

Setting aside  $S_{\lambda\lambda}^{\text{sing}}$  for the moment, we see from (3.55) that the gaugino-flux coupling contributes a finite term in the F-term potential for the Kähler modulus  $T$ ,

$$V_{\lambda\lambda} = \kappa_4^2 e^{\kappa_4^2 K} K^{T\bar{T}} \partial_T W K_{\bar{T}} \bar{W} + c.c. \quad (3.56)$$

We now follow the same steps for the four-gaugino coupling. From (3.51),  $T_{\mu\nu}^{\lambda\lambda\lambda\lambda}$  is

$$T_{\mu\nu}^{\lambda\lambda\lambda\lambda} := -\frac{2}{\sqrt{G}} \frac{\delta \mathcal{L}_{\lambda\lambda\lambda\lambda}}{\delta G^{\mu\nu}} = -e^{8u} \frac{\nu \Omega \cdot \bar{\Omega}}{6144\pi^3} |\lambda\lambda|^2 \delta^{(0)} g_{\mu\nu}, \quad (3.57)$$

which integrates to

$$-\int_M \sqrt{g_6} e^{-4A} T_{\mu\nu}^{\lambda\lambda\lambda\lambda} g^{\mu\nu} = 4e^{\kappa_4^2 K} K^{T\bar{T}} \partial_T W \partial_{\bar{T}} \bar{W}. \quad (3.58)$$

The four-gaugino coupling (3.51) therefore contributes the term

$$V_{\lambda\lambda\lambda\lambda} = e^{\kappa_4^2 K} K^{T\bar{T}} \partial_T W \partial_{\bar{T}} \bar{W}. \quad (3.59)$$

The total ten-dimensional stress-energy is then

$$T_{\mu\nu}^{\langle\lambda\lambda\rangle} := T_{\mu\nu}^{\lambda\lambda} + T_{\mu\nu}^{\lambda\lambda\lambda\lambda}, \quad (3.60)$$

with  $T_{\mu\nu}^{\lambda\lambda}$  given by (3.54) and with  $T_{\mu\nu}^{\lambda\lambda\lambda\lambda}$  given by (3.57). Combining (3.56) and (3.59) to evaluate the integral of  $T_{\mu\nu}^{(\lambda\lambda)}$  over the internal space, and continuing to set aside the singular term  $S_{\lambda\lambda}^{\text{sing}}$ , we conclude that the ten-dimensional field configuration sourced by gaugino condensation on D7-branes gives rise to the four-dimensional scalar potential,

$$V = e^{\kappa_4^2 K} \left( K^{T\bar{T}} D_T W D_{\bar{T}} \bar{W} - 3\kappa_4^2 W \bar{W} \right), \quad (3.61)$$

and so precisely recovers the potential (3.39) computed in four-dimensional supergravity. In summary, we have shown that the *ten-dimensional* equation of motion (3.22), incorporating the stress-energy  $T_{\mu\nu}^{(\lambda\lambda)}$  in (3.60), requires that the Einstein-frame scalar curvature  $\mathcal{R}_4[g]$  takes exactly the value demanded by the *four-dimensional* Einstein equation (3.24) with the scalar potential (3.39), i.e. the value computed in the four-dimensional effective theory in [215]. This is one of our main results.

Before proceeding, we will comment briefly on the singularities in our solution, including  $S_{\lambda\lambda}^{\text{sing}}$ , deferring a complete treatment to Appendix B.3. The ten-dimensional configuration corresponding to gaugino condensation on D7-branes contains specific singular field profiles, because the D7-branes are localized to a complex hypersurface in the internal space. In particular, as shown in [27], the  $G_-$  flux sourced by gaugino condensation is

$$(G_-)_{a\bar{c}\bar{d}} = -ie^{-4A-\phi/2+8u} \frac{\lambda\lambda}{32\pi^2} \partial_a \partial_b G_{(2)}(z; z_{D7}) g^{b\bar{b}} \bar{\Omega}_{\bar{b}\bar{c}\bar{d}}, \quad (3.62)$$

where  $G_{(2)}$  is the Green's function on the internal space transverse to the D7-branes, with complex coordinate  $z$ . Similarly, it was shown in [135] that gaugino condensation sources  $G_+$  flux that is localized on the D7-branes:

$$G_+ = -i \frac{e^{-4A}}{64\pi^2} e^{-\phi/2} \lambda\lambda \bar{\Omega} \delta^{(0)}. \quad (3.63)$$

Upon evaluating the D7-brane action and the bulk supergravity action in the presence of these flux configurations, one finds divergent contributions to the stress-energy, and in turn to the six-dimensional curvature  $\mathcal{R}_6$  in (3.22). However, we show explicitly in Appendix B.3 that a highly nontrivial cancellation occurs: *all the divergences appearing in (3.22) cancel*, and the finite piece that remains gives exactly (3.61).

### 3.4 Anti-D3-branes and Gaugino Condensation

Thus far we have shown that the F-term potential in and around the  $\mathcal{N} = 1$  supersymmetric  $AdS_4$  vacuum of [215] can be obtained in two ways. The first is four-dimensional supergravity, as originally argued in [215]. The second derivation, as shown above, is from ten-dimensional supergravity, supplemented with the gaugino bilinear vev (3.34) substituted into the two-gaugino and four-gaugino terms in the D7-brane action.

We now turn to the effects of anti-D3-branes, and to the study of four-dimensional de Sitter vacua from ten dimensions.

#### 3.4.1 Decompactification from anti-D3-branes

We first consider the effects of an anti-D3-brane in a no-scale flux compactification, *without* a nonperturbative superpotential for the Kähler moduli.

The Dirac-Born-Infeld action of a spacetime-filling anti-D3-brane at position

$y_{\overline{D3}}$  in the internal space leads to the stress-energy tensor

$$T_{\mu\nu}^{\overline{D3}} = -\mu_3 e^{8A-12u} g_{\mu\nu} \delta(y - y_{\overline{D3}}). \quad (3.64)$$

Inserting (3.64) in (3.21), we learn that including a single anti-D3-brane in a no-scale background leads to a shift in the effective potential,<sup>10</sup>

$$\frac{1}{4} M_{\text{pl}}^2 \delta \mathcal{R}_4[g] = 2\mu_3 e^{-12u} e^{4A}(y_{\overline{D3}}). \quad (3.65)$$

The potential energy captured by (3.65) is minimized in the infinite volume limit  $u \rightarrow \infty$ , so in the absence of any other effects an anti-D3-brane will cause runaway decompactification. The expression (3.65) agrees with the four-dimensional analysis of [215].

### 3.4.2 Interactions of anti-D3-branes and gaugino condensation

To examine the ten-dimensional stress-energy, we write the ten-dimensional field configuration in the schematic form

$$\phi = \phi_{\text{bg}} + \delta\phi, \quad (3.66)$$

with

$$\delta\phi = \delta\phi|_{\langle\lambda\lambda\rangle} + \delta\phi|_{\overline{D3}}. \quad (3.67)$$

Here  $\phi$  is any of the ten-dimensional fields,  $\phi_{\text{bg}}$  is the field configuration when neither gaugino condensation nor anti-D3-branes are included as sources,  $\delta\phi|_{\langle\lambda\lambda\rangle}$  is the change in the field configuration when gaugino condensation is included as

---

<sup>10</sup>As explained in [214], if the anti-D3-brane is in a strongly warped region, the dependence on the breathing mode becomes  $e^{-8u}$  rather than  $e^{-12u}$ .

a source, and  $\delta\phi|_{\overline{D3}}$  is the change in the field configuration when  $p$  anti-D3-branes are included as a source.

The changes  $\delta\phi|_{\langle\lambda\lambda\rangle}$  and  $\delta\phi|_{\overline{D3}}$  are each parametrically small away from their corresponding sources:  $\langle\lambda\lambda\rangle$  is exponentially small by dimensional transmutation, and the anti-D3-brane is in a warped region. Because the anti-D3-branes and the D7-brane stack are widely-separated, we can safely neglect the nonlinear corrections to the field configuration resulting from simultaneously including both gaugino condensation and anti-D3-branes as sources.<sup>11</sup>

Separating the ten-dimensional Lagrange density as

$$\mathcal{L} = \mathcal{L}_{\text{SUSY}} + p \mathcal{L}_{\text{loc}}^{\overline{D3}}, \quad (3.68)$$

with  $\mathcal{L}_{\text{SUSY}} = \mathcal{L}_{\text{bulk}} + \mathcal{L}_{\text{loc}}^{D7}$ , the total ten-dimensional stress-energy can be written

$$T_{\mu\nu} = -\frac{2}{\sqrt{-G}} \frac{\delta\mathcal{L}_{\text{SUSY}}}{\delta G^{\mu\nu}} - \frac{2}{\sqrt{-G}} \frac{\delta\mathcal{L}_{\text{loc}}^{\overline{D3}}}{\delta G^{\mu\nu}} \equiv T_{\mu\nu}^{\langle\lambda\lambda\rangle}\Big|_{\phi} + T_{\mu\nu}^{\overline{D3}}\Big|_{\phi}, \quad (3.69)$$

which we write as

$$T_{\mu\nu} = T_{\mu\nu}^{\langle\lambda\lambda\rangle}\Big|_{\phi_{\text{bg}} + \delta\phi|_{\langle\lambda\lambda\rangle}} + p T_{\mu\nu}^{\overline{D3}}\Big|_{\phi_{\text{bg}}} + T_{\mu\nu}^{\text{int}}. \quad (3.70)$$

The first term on the right in (3.70) is the stress-energy (3.60) of gaugino condensation on D7-branes, computed in the field configuration  $\phi = \phi_{\text{bg}} + \delta\phi|_{\langle\lambda\lambda\rangle}$ , i.e. without including the backreaction of any anti-D3-branes, as in §3.3. The second term is the stress-energy (3.64) due to the Dirac-Born-Infeld action of  $p$  anti-D3-branes, computed as probes of the background  $\phi = \phi_{\text{bg}}$ , as in §3.4.1.

The interaction term  $T_{\mu\nu}^{\text{int}}$  is *defined* by (3.70), and captures the stress-energy due to the interactions of the anti-D3-branes and the condensate: specifically, the correction to  $T_{\mu\nu}^{\langle\lambda\lambda\rangle}$  from the shift  $\delta\phi|_{\overline{D3}}$ , and the correction to  $T_{\mu\nu}^{\overline{D3}}$  from the shift

---

<sup>11</sup>See [145] and Appendix B.2 for further details and references on nonlinear interactions.

$\delta\phi|_{\langle\lambda\lambda\rangle}$ .<sup>12</sup> We will now explain why  $T_{\mu\nu}^{\text{int}}$  can be neglected, so that  $T_{\mu\nu}$  is well-approximated by the first two terms on the right in (3.70). Since we have already shown in §3.3 and §3.4.1 that these two terms together precisely reproduce the four-dimensional effective potential of [215], establishing that  $T_{\mu\nu}^{\text{int}}$  is negligible will complete our demonstration that the ten-dimensional equations of motion recover the result of [215].

To show that the interaction  $T_{\mu\nu}^{\text{int}}$  is negligible, one can consider the leading effects of  $p$  anti-D3-branes on the ten-dimensional fields at the location of the the D7-branes, and evaluate the resulting correction to the ten-dimensional stress-energy  $T_{\mu\nu}^{\langle\lambda\lambda\rangle}$ .

As a cross-check, one can reverse the roles of source and probe, estimate the leading effects of the D7-brane gaugino condensate on the ten-dimensional fields at the location of the anti-D3-branes, and evaluate the resulting correction to the stress-energy  $p T_{\mu\nu}^{\overline{D3}}$  computed from the probe action of  $p$  anti-D3-branes.

The methodology for the computation is parallel in the two cases, and builds on investigations of supergravity solutions sourced by antibranes [219, 103, 273, 36, 33, 34, 134, 35, 75, 1, 20], and of D3-brane potentials in warped throats [214, 28, 104, 26, 27, 145]. One can approximate the Klebanov-Strassler throat as a region in  $AdS_5 \times T^{1,1}$ , and use the Green's functions for the conifold (see e.g. [232]) to compute the influence of a localized source — i.e., the anti-D3-branes or the D7-brane gaugino condensate — on distant fields. Far away from the source, the dominant effects appear as certain leading multipoles, corresponding to the lowest-dimension operators to which the source couples. Schematically (see Appendix B.2

---

<sup>12</sup>Corrections to  $T_{\mu\nu}^{\overline{D3}}$  from the shift  $\delta\phi|_{\overline{D3}}$  are subleading.

for details),

$$\delta\phi = \sum_{\Delta} \alpha_{\Delta} \left( \frac{r}{r_{\text{UV}}} \right)^{-\Delta} + \beta_{\Delta} \left( \frac{r}{r_{\text{UV}}} \right)^{\Delta-4}, \quad (3.71)$$

where  $\Delta$  is the dimension of an operator  $\mathcal{O}_{\Delta}$  in the dual field theory,  $r$  is the radial coordinate of the throat, and  $r_{\text{UV}}$  is the location of the ultraviolet end of the throat. The coefficients  $\alpha_{\Delta}$  and  $\beta_{\Delta}$  correspond to expectation values and sources, respectively, for the dual operator.

The spectrum of operators of the Klebanov-Witten theory [234] dual to  $AdS_5 \times T^{1,1}$  is well-understood, due to the pioneering work of Gubser [175] and of Ceresole et al. [72, 73] (see also [11, 27, 145, 144]), and moreover there are many quantitative cross-checks of the long-distance solutions created by anti-D3-branes [103, 218, 26, 36, 33, 134, 35, 27, 41] and by gaugino condensates [26, 27, 189, 135, 279]. In Appendix B.2 we assemble key results from this literature, and then apply them to compute the leading interactions of anti-D3-branes with a gaugino condensate. A brief summary is as follows.

In the linearized supergravity solution sourced by anti-D3-brane backreaction, as in [36, 33, 34, 134], the leading effects of anti-D3-branes in the infrared on the D7-brane gaugino condensate are mediated by expectation values for operators of dimension  $\Delta \geq 8$ , cf. (B.128),(B.129), and so can be neglected when the hierarchy of scales in the throat is large. Nonlinear effects are likewise negligible [145, 267].

Similarly, in the supergravity solution sourced by gaugino condensate backreaction, the leading effects of the D7-brane gaugino condensate on the anti-D3-branes are negligible compared to the probe anti-D3-brane action in the Klebanov-Strassler background, cf. (B.154),(B.155) [145, 144], both at the linear and the nonlinear level.



In sum, the dominant influence of the anti-D3-branes on the gaugino condensate is via the breathing mode  $e^u$ . All other interactions are suppressed by further powers of the warp factor. We have therefore established that

$$T_{\mu\nu} \approx T_{\mu\nu}^{\langle\lambda\lambda\rangle} + p T_{\mu\nu}^{\overline{D3}} + \dots, \quad (3.72)$$

where  $T_{\mu\nu}^{\langle\lambda\lambda\rangle}$  is given by (3.60),  $T_{\mu\nu}^{\overline{D3}}$  is given by (3.64), and the ellipses denote terms suppressed by powers of  $e^A$ .

It follows that the ten-dimensional equation of motion (3.22), incorporating the total stress-energy  $T_{\mu\nu}^{\langle\lambda\lambda\rangle} + p T_{\mu\nu}^{\overline{D3}}$  in (3.72), requires the Einstein-frame scalar curvature  $\mathcal{R}_4[g]$  to take exactly the value computed in the de Sitter vacuum of the four-dimensional theory in [215]. In other words, the precise quantitative match between ten-dimensional and four-dimensional computations that we established for the  $\mathcal{N} = 1$  supersymmetric theory in §3.3 continues to hold in the presence of anti-D3-branes.

### 3.5 Conclusions

We have derived the four-dimensional scalar potential in the de Sitter and anti-de Sitter constructions of [216] directly from type IIB string theory in ten dimensions, supplemented with the expectation value  $\langle\lambda\lambda\rangle$  of the D7-brane gaugino bilinear.

We first computed the two-gaugino and four-gaugino couplings on D7-branes, by dimensionally reducing and T-dualizing the ten-dimensional type I supergravity action. From these terms we computed the ten-dimensional stress-energy sourced by gaugino condensation on a stack of D7-branes, carefully accounting for the fact that the ten-dimensional solution in the presence of the condensate is a gener-

alized complex geometry. As a key step in this computation, we used the ten-dimensional Killing spinor equations to prove that in a supersymmetric configuration, the generalized complex geometry superpotential (3.48) is equal to the full superpotential, i.e. we established the relation (3.49). Upon dimensional reduction, the ten-dimensional stress-energy of the supersymmetric configuration then gives rise to the scalar potential of the  $\mathcal{N} = 1$  supersymmetric theory of [216], evaluated in its supersymmetric  $AdS_4$  vacuum. The match is exact, at the level of the approximations made in [216]. Furthermore, provided that (3.49) continues to hold off-shell — which we find plausible but have not established here — we recovered the complete scalar potential of the four-dimensional theory, even away from the supersymmetric minimum of the potential for the Kähler modulus.

To combine the stress-energy of the gaugino condensate with that of anti-D3-branes at the tip of a Klebanov-Strassler throat, we examined the Kaluza-Klein spectrum of  $T^{1,1}$ , and found the operators of the dual field theory that mediate the leading interactions between a condensate in the ultraviolet and anti-D3-branes in the infrared. We found that all such couplings via Kaluza-Klein excitations are suppressed by powers of the warp factor compared to the probe anti-D3-brane action. This left the interaction via the breathing mode, as in [216], as the only important one. We thus concluded that the ten-dimensional stress-energy of the gaugino condensate and the anti-D3-branes together lead to the scalar potential of the non-supersymmetric theory of [216]. The match is again exact, even away from the de Sitter minimum, in the same sense as above.

This work has not altered the evidence, which we judge to be robust [124], for the existence in string theory of the separate components of the scenario [216], namely a small classical flux superpotential, a gaugino condensate on a stack of D7-

branes, and a metastable configuration of anti-D3-branes in a Klebanov-Strassler throat. Instead, we showed that *provided* these components exist in an explicit string compactification, their effects can be computed either in ten dimensions or in the four-dimensional effective theory, with perfect agreement.

Progress in understanding the physics of de Sitter space in string theory continues. Our findings may aid in pursuing de Sitter solutions in ten dimensions.

## CHAPTER 4

### VACUA WITH SMALL FLUX SUPERPOTENTIAL

#### Abstract<sup>1</sup>

We describe a method for finding flux vacua of type IIB string theory in which the Gukov-Vafa-Witten superpotential is exponentially small. We present an example with  $W_0 \approx 2 \times 10^{-8}$  on an orientifold of a Calabi-Yau hypersurface with  $(h^{1,1}, h^{2,1}) = (2, 272)$ , at large complex structure and weak string coupling.

---

<sup>1</sup>This chapter is published as M. Demirtas, M. Kim, L. McAllister, J. Moritz, “Vacua with Small Flux Superpotential,” *Phys.Rev.Lett.* 124 (2020) 21, 211603 [arxiv:1912.10047 [hep-th]].

## 4.1 Introduction

To understand the nature of dark energy in quantum gravity, one can study de Sitter solutions of string theory. Kachru, Kallosh, Linde, and Trivedi (KKLT) have argued that there exist de Sitter vacua in compactifications on Calabi-Yau (CY) orientifolds of type IIB string theory [215]. An essential component of the KKLT scenario is a small vacuum value of the classical Gukov-Vafa-Witten [176] flux superpotential,

$$W_0 := \sqrt{\frac{2}{\pi}} \left\langle e^{\mathcal{K}/2} \int_X G \wedge \Omega \right\rangle. \quad (4.1)$$

Here  $X$  is the CY orientifold,  $G$  is the three-form flux,  $\Omega$  is the  $(3,0)$  form on  $X$ ,  $\mathcal{K}$  is the Kähler potential for the complex structure moduli and the axiodilaton, and the brackets denote evaluation on the vacuum expectation values of these moduli. The stabilized values of the Kähler moduli are proportional to  $\log(|W_0|^{-1})$ , so control of the  $\alpha'$  expansion is possible only if  $|W_0|$  is very small.

String compactifications are characterized by discrete data, including the topology of the internal space, and quantized fluxes within it. The number of distinct choices is vast, and although  $|W_0| \ll 1$  is evidently not typical, strong evidence for the existence of vacua with  $|W_0| \ll 1$  comes from the statistical treatment of [21, 98, 99, 128, 129], as reviewed in [125]. By approximating the integrally-quantized fluxes by continuous variables, one can compute the expected number of flux vacua with  $|W_0| \leq \delta$ , for  $\delta$  some chosen threshold. This approach predicts that in an orientifold with a sufficiently large value of the D3-brane charge tadpole  $Q_{\text{D3}}$  there should exist choices of flux giving vacua with exponentially small  $|W_0|$ .

We are not aware of any flaw in this statistical approach, but one can nevertheless ask: *do there in fact exist* orientifolds and choices of flux giving vacua with

$|W_0| \ll 1$ , as the statistical theory predicts? In this Letter we answer this question in the affirmative.

In §4.2 we present a general method for constructing vacua with small  $W_0$  at large complex structure (LCS) and weak string coupling, building on [155, 100]. In §4.3 we give an explicit example<sup>2</sup> where  $W_0 \approx 2 \times 10^{-8}$ , in an orientifold of a Calabi-Yau hypersurface in  $\mathbb{CP}_{[1,1,1,6,9]}$ . In §4.4 we show that our result accords well with the statistical predictions of [98]. We show in §4.5 that at least one complex structure modulus in our example is as light as the Kähler moduli. We explain why this feature occurs in our class of solutions, and we comment on Kähler moduli stabilization in our vacuum.

## 4.2 A landscape of weakly coupled flux vacua with small

$$W_0$$

Vacua with  $|W_0| \ll 1$  are rare elements in a large landscape. It is therefore impractical to exhibit vacua with  $|W_0| \ll 1$  by enumerating general vacua on a massive scale and filtering out the desired ones. Instead one should pursue algorithms that preferentially find fluxes that lead to vacua with small  $|W_0|$ .

One algorithm of this sort<sup>3</sup> [155, 100] proceeds by finding quantized fluxes that solve an *approximate* form of the F-term equations, with the corresponding approximate superpotential exactly vanishing, at some given point  $U_\star$  in moduli space. One then solves for nearby moduli values  $U = U_\star + \delta U$  that solve the *true*

---

<sup>2</sup>Pioneering work in this direction appears in [100, 101]. Issues related to the size of  $|W_0|$  are discussed in e.g. [74, 289].

<sup>3</sup>For an approach via genetic algorithms see [76].

F-term equations with the same choice of fluxes. When the approximation made in the first step is a good one, the true superpotential evaluated at  $U = U_\star + \delta U$  will be small.

We will construct a class of flux vacua along these lines. The approximate superpotential is obtained by neglecting nonperturbative corrections to the prepotential for the complex structure moduli around the LCS locus in moduli space.<sup>4</sup> Stabilization near LCS, where these nonperturbative terms are exponentially small, then yields an exponentially small flux superpotential.

We consider an orientifold  $X$  of a Calabi-Yau threefold with  $-Q_{\text{D3}}$  units of D3-brane charge on seven-branes and O3-planes. Let  $\{A_a, B^b\}$  be a symplectic basis for  $H_3(X, \mathbb{Z})$ , with  $A_a \cap A_b = 0$ ,  $A_a \cap B^b = \delta_a^b$ , and  $B^a \cap B^b = 0$ . We use projective coordinates  $\{U^a\}$  on the complex structure moduli space of dimension  $n \equiv h_-^{2,1}$ , and we work in a gauge in which  $U^0 = 1$ . Denoting the prepotential by  $\mathcal{F}$  and writing  $\mathcal{F}_a = \partial_{U^a} \mathcal{F}$ , we define the period vector as

$$\Pi = \begin{pmatrix} \int_{B^a} \Omega \\ \int_{A_a} \Omega \end{pmatrix} = \begin{pmatrix} \mathcal{F}_a \\ U^a \end{pmatrix}. \quad (4.2)$$

The integer flux vectors  $F$  and  $H$  are similarly obtained from the three-form field strengths  $F_3$  and  $H_3$  as

$$F = \begin{pmatrix} \int_{B^a} F_3 \\ \int_{A_a} F_3 \end{pmatrix}, \quad H = \begin{pmatrix} \int_{B^a} H_3 \\ \int_{A_a} H_3 \end{pmatrix}. \quad (4.3)$$

Defining the symplectic matrix  $\Sigma = \begin{pmatrix} 0 & I \\ -I & 0 \end{pmatrix}$ , the flux superpotential and the Kähler

---

<sup>4</sup>Recent discussions of flux potentials near LCS appear in [192, 169, 193].

potential are<sup>5</sup>

$$W = \sqrt{\frac{2}{\pi}} \left( F - \tau H \right)^T \cdot \Sigma \cdot \Pi, \quad (4.4)$$

$$\mathcal{K} = -\log \left( -i \Pi^\dagger \cdot \Sigma \cdot \Pi \right) - \log \left( -i(\tau - \bar{\tau}) \right). \quad (4.5)$$

The LCS expansion of the prepotential is  $\mathcal{F}(U) = \mathcal{F}_{\text{pert}}(U) + \mathcal{F}_{\text{inst}}(U)$  [197] with the perturbative terms

$$\mathcal{F}_{\text{pert}}(U) = -\frac{1}{3!} \mathcal{K}_{abc} U^a U^b U^c + \frac{1}{2} a_{ab} U^a U^b + b_a U^a + \xi, \quad (4.6)$$

and the instanton corrections

$$\mathcal{F}_{\text{inst}}(U) = \frac{1}{(2\pi i)^3} \sum_{\vec{q}} A_{\vec{q}} e^{2\pi i \vec{q} \cdot \vec{U}}. \quad (4.7)$$

Here  $\mathcal{K}_{abc}$  are the triple intersection numbers of the mirror CY,  $a_{ab}$  and  $b_a$  are rational, the sum runs over the homology classes  $\vec{q}$  of effective curves in the mirror CY, with amplitudes  $A_{\vec{q}}$  determined by the corresponding Gromov-Witten invariants, and  $\xi = -\frac{\zeta(3)\chi}{2(2\pi i)^3}$ , with  $\chi$  the Euler number of the CY. We write

$$W = W_{\text{pert}} + W_{\text{inst}}, \quad (4.8)$$

with  $W_{\text{pert}}$  the portion obtained by using  $\mathcal{F}_{\text{pert}}(U)$  in (4.4), and  $W_{\text{inst}}$  the correction from  $\mathcal{F}_{\text{inst}}(U)$ . We call  $W_{\text{pert}}$  the perturbative superpotential, and  $W_{\text{inst}}$  the nonperturbative correction, even though the full flux superpotential  $W$  is classical in the type IIB theory.

The real parts of  $\vec{U}$  are axionic fields that do not appear in the perturbative Kähler potential, enjoying discrete gauged shift symmetries  $\vec{U} \mapsto \vec{U} + \vec{\nu}$  with  $\vec{\nu} \in \mathbb{Z}^n$ . Under such a shift, the period and flux vectors undergo a monodromy

---

<sup>5</sup>We have set the reduced Planck mass to unity, and we omit here the Kähler potential for the Kähler moduli, which reads  $\mathcal{K}_K = -3 \log(2 \text{Vol}^{2/3})$ , with Vol the volume of  $X$  in ten-dimensional Einstein frame, in units of  $(2\pi)^2 \alpha'$ . Our conventions match those of [217] upon taking  $\mathcal{V} = 1/4\pi$  and  $b = 1$  in §A.3 of [217], cf. [101].



transformation  $\{\Pi, F, H\} \mapsto M_\infty^{\vec{\nu}}\{\Pi, F, H\}$  with the monodromy matrix  $M_\infty^{\vec{\nu}} \in Sp(2n+2, \mathbb{Z})$ . For generic choices of flux quanta, these discrete axionic shift symmetries are spontaneously broken, realizing axion monodromy [309, 270, 225]. A discrete shift symmetry remains unbroken if and only if there exists a monodromy transformation  $M_\infty^{\vec{\nu}}$  combined with an  $SL(2, \mathbb{Z})$  transformation  $T^r : (H, F) \mapsto (H, F + rH)$ ,  $r \in \mathbb{Z}$ , that leaves the pair of flux vectors invariant.

Consider a choice of fluxes and moduli values that solves the F-flatness conditions, has an unbroken shift symmetry, and has  $W_{\text{pert}} = 0$ , all at the level of the perturbative prepotential  $\mathcal{F}_{\text{pert}}(U)$ . We call such a configuration a *perturbatively flat vacuum*. Here is a sufficient condition for the existence of such a vacuum.

**Lemma:** *Suppose there exists a pair  $(\vec{M}, \vec{K}) \in \mathbb{Z}^n \times \mathbb{Z}^n$  satisfying  $-\frac{1}{2}\vec{M} \cdot \vec{K} \leq Q_{\text{D3}}$  such that  $N_{ab} \equiv \mathcal{K}_{abc}M^c$  is invertible, and  $\vec{K}^T \mathbf{N}^{-1} \vec{K} = 0$ , and  $\vec{p} \equiv \mathbf{N}^{-1} \vec{K}$  lies in the Kähler cone of the mirror CY, and such that  $\mathbf{a} \cdot \vec{M}$  and  $\vec{b} \cdot \vec{M}$  are integer-valued. Then there exists a choice of fluxes, compatible with the tadpole bound set by  $Q_{\text{D3}}$ , for which a perturbatively flat vacuum exists. The perturbative F-flatness conditions obtained from (4.6) are then satisfied along the one-dimensional locus  $\vec{U} = \tau \vec{p}$  along which  $W_{\text{pert}}$  vanishes.*

To verify the Lemma, one considers the fluxes

$$F = (\vec{M} \cdot \vec{b}, \vec{M}^T \cdot \mathbf{a}, 0, \vec{M}^T), \quad H = (0, \vec{K}^T, 0, 0), \quad (4.9)$$

which can be shown to be the most general ones leading to a perturbative superpotential  $W_{\text{pert}}$  that is homogeneous of degree two in the  $n+1$  moduli. The monodromy transformation  $M_\infty^{\vec{\nu}}$  combined with an appropriate  $SL(2, \mathbb{Z})$  transformation leaves (4.9) invariant, so a discrete shift symmetry remains unbroken.

Because  $W_{\text{pert}}$  is homogeneous, there is a perturbatively-massless modulus cor-

responding to an overall rescaling of the moduli. This modulus can be stabilized by the nonperturbative terms in  $\mathcal{F}$ . Given  $(\vec{M}, \vec{K})$  for which stabilization of the rescaling mode occurs at weak coupling,  $W_{\text{inst}}$  will be exponentially small. One finds the effective superpotential

$$\frac{W_{\text{eff}}(\tau)}{\sqrt{2/\pi}} = M^a \partial_a \mathcal{F}_{\text{inst}} = \sum_{\vec{q}} \frac{A_{\vec{q}} \vec{M} \cdot \vec{q}}{(2\pi i)^2} e^{2\pi i \tau \vec{p} \cdot \vec{q}}, \quad (4.10)$$

where we have chosen the axiodilaton  $\tau$  as a coordinate along the flat valley. As the inner product  $\vec{p} \cdot \vec{q}$  need not be integer, it is possible to find flux quanta such that  $\tau$  can be stabilized at weak coupling, by realizing a racetrack.<sup>6</sup> This works efficiently if the two most relevant instantons, which we label as  $\vec{q}_1$  and  $\vec{q}_2$ , satisfy  $\vec{p} \cdot \vec{q}_1 \approx \vec{p} \cdot \vec{q}_2$ .

### 4.3 An example

We now illustrate our method in an explicit example, with  $n = 2$ . We consider the degree 18 hypersurface in weighted projective space  $\mathbb{CP}_{[1,1,1,6,9]}$  studied in [69]. This is a CY with 272 complex structure moduli, but as explained in [155], it is useful to study a particular locus in moduli space where the CY becomes invariant under a  $G = \mathbb{Z}_6 \times \mathbb{Z}_{18}$  discrete symmetry.<sup>7</sup> By turning on only flux quanta invariant under  $G$ , we are guaranteed to find solutions of the full set of F-term equations, by solving only those corresponding to the directions tangent to the invariant subspace. Conveniently, the periods in these directions are identical to the periods of the mirror CY, and are obtained from an effective two-moduli prepotential as

---

<sup>6</sup>Achieving racetrack stabilization within our class of models could aid in the search for large axion decay constants via alignment, as in [228]. See [188, 54] for approaches using unbroken shift symmetries, and [183] for Kähler moduli stabilization in this context.

<sup>7</sup>If we were to orbifold by this symmetry group and resolve the singularities we would obtain the mirror CY [166]. We will *not* proceed in this direction, but instead stay with the original CY.

in (4.6) with the data

$$\begin{aligned} \mathcal{K}_{111} &= 9, \quad \mathcal{K}_{112} = 3, \quad \mathcal{K}_{122} = 1, \\ \mathbf{a} &= \frac{1}{2} \begin{pmatrix} 9 & 3 \\ 3 & 0 \end{pmatrix}, \quad \vec{b} = \frac{1}{4} \begin{pmatrix} 17 \\ 6 \end{pmatrix}. \end{aligned} \quad (4.11)$$

The instanton corrections take the form [69]

$$(2\pi i)^3 \mathcal{F}_{\text{inst}} = \mathcal{F}_1 + \mathcal{F}_2 + \cdots, \quad (4.12)$$

$$\mathcal{F}_1 = -540q_1 - 3q_2, \quad (4.13)$$

$$\mathcal{F}_2 = -\frac{1215}{2}q_1^2 + 1080q_1q_2 + \frac{45}{8}q_2^2, \quad (4.14)$$

where  $q_i = \exp(2\pi i U^i)$  with  $i \in \{1, 2\}$ . Note the  $\mathcal{O}(10^{-2})$  hierarchy in the coefficients of the one-instanton terms. We consider an orientifold involution described in [248], with two O7-planes, each with four D7-branes, and in which we find  $Q_{\text{D3}} = 138$ . The D7-brane tadpole cancels automatically.

We will now use the Lemma to find a pair  $(\vec{M}, \vec{K}) \in \mathbb{Z}^2 \times \mathbb{Z}^2$  yielding a perturbatively flat vacuum. Using (4.11), the condition  $\vec{K}^T \mathbf{N}^{-1} \vec{K} = 0$  becomes

$$M_1 = \frac{M_2 K_2 (2K_1 - 3K_2)}{(K_1 - 3K_2)^2}, \quad (4.15)$$

and the flat direction is given by

$$\vec{U} = \tau \begin{pmatrix} p_1 \\ p_2 \end{pmatrix} = \frac{\tau(K_1 - 3K_2)}{M_2} \begin{pmatrix} -K_2/K_1 \\ 1 \end{pmatrix}. \quad (4.16)$$

Once the nonperturbative corrections (4.12) are included, the effective superpotential along the flat direction reads

$$W_{\text{eff}}(\tau) = c \left( e^{2\pi i p_1 \tau} + A e^{2\pi i p_2 \tau} \right) + \cdots, \quad (4.17)$$

where  $c$  and  $A$  depend on the pair  $(\vec{M}, \vec{K})$ , but not on  $\tau$ . A racetrack potential is realized when the two terms in (4.17) are of comparable magnitude, which requires

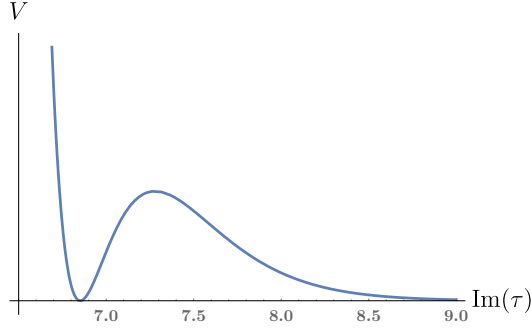


Figure 4.1: The scalar potential on the positive  $\text{Im } \tau$  axis.

$|p_1 - p_2| \ll p_2$ . We are thus looking for  $\vec{M}$  and  $\vec{K}$  obeying (4.15) for which  $Q_{\text{D3}}^{\text{flux}} \equiv -\frac{1}{2}\vec{M} \cdot \vec{K} \leq 138$  and  $|K_1 + K_2| \ll |K_2|$ . A suitable choice is

$$\vec{M} = \begin{pmatrix} -16 \\ 50 \end{pmatrix}, \quad \vec{K} = \begin{pmatrix} 3 \\ -4 \end{pmatrix}, \quad (4.18)$$

which gives  $Q_{\text{D3}}^{\text{flux}} = 124$ ,  $A = -\frac{5}{288}$ , and  $c = -\sqrt{\frac{2}{\pi}} \frac{8640}{(2\pi i)^3}$ . The resulting racetrack potential is depicted in Figure 1. The moduli are stabilized at

$$\langle \tau \rangle = 6.856i, \quad \langle U_1 \rangle = 2.742i, \quad \langle U_2 \rangle = 2.057i, \quad (4.19)$$

and we find

$$|W_0| = 2.037 \times 10^{-8}. \quad (4.20)$$

The instanton expansion is under excellent control: the two-instanton terms (4.14) are a factor  $\mathcal{O}(10^{-5})$  smaller than the one-instanton terms (4.13), and the three-instanton terms are smaller by a further factor  $\mathcal{O}(10^{-5})$ .

#### 4.4 Statistics of small $W_0$

A systematic understanding of statistical predictions of the flux landscape was developed in [21, 98, 99, 128, 129], in part by approximating the integer fluxes

by continuous variables. Let us compare our result (4.20) with the statistical prediction for the smallest possible  $W_0$  in our orientifold.

We write  $\mathcal{N}(\lambda_*, Q_{\text{D3}})$  for the expected number of vacua with D3-brane charge in fluxes less than  $Q_{\text{D3}}$  and with  $|W_0|^2 \leq \lambda_* \ll 1$ . According to [98],  $\mathcal{N}(\lambda_*, Q_{\text{D3}})$  is given for  $n = 2$  by

$$\mathcal{N}(\lambda_*, Q_{\text{D3}}) = \frac{2\pi^4(2Q_{\text{D3}})^5}{5!} \lambda_* \int_{\mathcal{M}} \star e^{2\mathcal{K}} \mathcal{F}_{abc} \overline{\mathcal{F}}^{abc}, \quad (4.21)$$

where  $\mathcal{M}$  is the axiodilaton and complex structure moduli space,  $\star$  is the Hodge star on  $\mathcal{M}$ , and  $\mathcal{F}_{abc} \equiv \partial_{abc}^3 \mathcal{F}$ . Taking  $Q_{\text{D3}} = 138$  and numerically integrating over the LCS region  $1 < \text{Im}(U)$ , we find that  $\mathcal{N}(\lambda_*, 138) < 1$  for  $\sqrt{\lambda_*} \lesssim 6 \times 10^{-7}$ . The prediction of [98] is thus that the smallest value of  $|W_0|$  expected to exist is of order  $6 \times 10^{-7}$ , which agrees reasonably well with (4.20).

## 4.5 Toward stabilizing all moduli

Thus far we have found a class of no-scale vacua in which the complex structure moduli and axiodilaton F-terms vanish, and  $W_0$  is exponentially small. To achieve stabilization of the Kähler moduli from this promising starting point, two issues must be addressed: the masses of the complex structure moduli and axiodilaton, and the nonperturbative superpotential for the Kähler moduli.

For the example of §4.3, we have computed the mass matrix along the  $G$ -symmetric locus. Two of the moduli are heavy, but the third, corresponding to the perturbatively-flat direction  $\tau$ , has a mass proportional to  $|W_0|$ . We are not aware of a reason why any of the  $G$ -breaking combinations should be comparably light, but checking this directly will be important, and rather challenging. Assuming

that the  $G$ -breaking moduli are indeed heavy, the low energy theory describing Kähler moduli stabilization will include  $\tau$  and the Kähler moduli  $T_1, T_2$ .

Provided that the configuration of seven-branes (with vanishing D7-brane tadpole) wraps divisors that are either rigid [346], or else are rigidified by the introduction of fluxes [224, 222, 47], we expect a nonperturbative superpotential of the form

$$W_{\text{eff}}(\tau, T_1, T_2) = c \left( e^{2\pi i \frac{2}{5}\tau} + A e^{2\pi i \frac{3}{10}\tau} \right) + B e^{-\frac{2\pi}{c_1}T_1} + C e^{-\frac{2\pi}{c_2}T_2}. \quad (4.22)$$

Here  $A$  and  $c$  are known coefficients, cf. (4.17),  $c_1$  and  $c_2$  are the dual Coxeter numbers of the confining seven-brane gauge groups, and  $\text{Re}(T_i)$  are the volumes of the corresponding divisors.

The unbroken discrete shift symmetry implies that the Pfaffian prefactors  $B$  and  $C$  are independent of  $\tau$ , up to nonperturbatively-small corrections, and so can be treated as unknown constants.

To exhibit vacua with all moduli stabilized in this setting, one should establish (4.22) and compute  $B$  and  $C$  for a seven-brane configuration in which  $c_1$  and  $c_2$  are sufficiently large to ensure control of the  $\alpha'$  expansion. This worthy goal is beyond the scope of the present work.

## 4.6 Conclusions

We have described a method for constructing flux vacua with exponentially small Gukov-Vafa-Witten superpotential in compactifications of type IIB string theory on Calabi-Yau orientifolds, at weak string coupling and large complex structure.

The first step is to neglect nonperturbative terms in the prepotential expanded around large complex structure, and find quantized fluxes that at this level yield vanishing F-terms and vanishing superpotential along a flat direction in the complex structure and axiodilaton moduli space. We provided simple and constructive sufficient conditions for the existence of such solutions, and we determined the flat direction analytically, vastly simplifying the search for vacua. Upon restoring the nonperturbative corrections, one can find full solutions in which the flat direction is lifted, although it remains anomalously light, and the flux superpotential is exponentially small.

We gave an explicit example with  $|W_0| \approx 2 \times 10^{-8}$  in an orientifold of the Calabi-Yau hypersurface in  $\mathbb{CP}_{[1,1,1,6,9]}$ . This value of  $|W_0|$  accords well with the statistical expectation derived from the work of Denef and Douglas [98]. Stabilizing the Kähler moduli in this class of vacua, and then pursuing more explicit de Sitter solutions, are important tasks for the future.

## CHAPTER 5

### CONIFOLD VACUA WITH SMALL FLUX SUPERPOTENTIAL

#### Abstract<sup>1</sup>

We introduce a method for finding flux vacua of type IIB string theory in which the flux superpotential is exponentially small and at the same time one or more complex structure moduli are stabilized exponentially near to conifold points.

---

<sup>1</sup>This chapter is published as M. Demirtas, M. Kim, L. McAllister, J. Moritz, “Conifold Vacua with Small Flux Superpotential,” *Fortschritte der Physik*, Volume 68, Issue 11-12 2000085 [arxiv:2009.03312 [hep-th]].



## 5.1 Introduction

In order to understand the cosmologies that are possible in quantum gravity, one can search for de Sitter solutions in compactifications of string theory. Kachru, Kallosh, Linde, and Trivedi (KKLT) famously proposed that orientifold compactifications of type IIB string theory that contain specific ‘components’ in the right proportions will admit parametrically controlled de Sitter vacua [215].

These components — a small classical flux superpotential [21, 98, 100, 92], a warped throat region [233, 151, 152, 127, 54, 262], a potential for the Kähler moduli from Euclidean D3-branes or strong gauge dynamics [346, 240, 53, 167, 47, 48, 178, 179, 71, 148, 37, 217], and a supersymmetry-breaking sector from anti-D3-branes [219, 36, 134, 32, 20, 55, 297, 130] — are by now rather well understood *separately*. A remaining challenge in the pursuit of explicit examples of KKLT de Sitter vacua is to exhibit Calabi-Yau orientifolds that contain all these components at once, through calculations in which corrections to the leading approximations are demonstrably well-controlled.

In this work we present a method for finding flux vacua that contain *both* a warped throat region and an exponentially small classical flux superpotential,  $|W_0| \ll 1$ . We do so by building on our recent work [92], where we showed how to find flux vacua with  $|W_0| \ll 1$ . In [92] we took all complex structure moduli to be near large complex structure (LCS). Warped throats, on the other hand, occur in flux vacua in which one or more complex structure moduli are stabilized near conifold singularities — we refer to such vacua as *conifold vacua*.

If the quantized fluxes threading the A-cycle and B-cycle of a conifold in such a vacuum are sufficiently large, then the conifold region is accurately described by the

warped deformed conifold supergravity solution found by Klebanov and Strassler [233], and can serve as a setting for metastable supersymmetry breaking by anti-D3-branes [219]. In the opposite regime of small 't Hooft coupling, the conifold region is accurately described by a cascading gauge theory that potentially has a metastable supersymmetry-breaking state — gauge theory vacua of this sort have been analyzed in [15, 299, 18, 17, 16].

In order to generalize the mechanism of [92] to include conifolds one has to overcome the following obstacle. Introducing fluxes on the conifold cycles generates a conifold superpotential  $W_{\text{cf}}$  that by itself cannot be tuned to be small. Thus, the total flux superpotential will be small in string units only if the large conifold superpotential is efficiently canceled by a comparably large contribution  $W_{\text{bulk}}$  generated by fluxes on other cycles, i.e. if

$$|W_0| := |\langle W_{\text{flux}} \rangle| = |\langle W_{\text{cf}} \rangle + \langle W_{\text{bulk}} \rangle| \ll 1. \quad (5.1)$$

To achieve such a cancellation, one must first accurately compute the conifold superpotential  $W_{\text{cf}}$  in the vicinity of a conifold singularity.

In the first part of this work, we compute  $W_{\text{cf}}$  analytically in the case where the shrinking  $S^3$  of the conifold is mirror dual to a shrinking curve. In such a case  $W_{\text{cf}}$  is obtained by resumming the instanton corrections from string worldsheets wrapping the shrinking curve in the mirror threefold. We then show, along the same lines as [92], that one can choose quantized fluxes leading to an exponentially precise cancellation of the form shown in eq. (5.1). Finally, we present explicit examples of conifold vacua in an O3/O7 orientifold of a Calabi-Yau hypersurface  $\tilde{X}$  with  $h^{1,1}(\tilde{X}) = 99$  and  $h^{2,1}(\tilde{X}) = 3$ .

Let us be clear in advance about the scope of this work. We will present a mechanism for constructing classical flux vacua in which  $|W_0| \ll 1$  and at least

one complex structure modulus is stabilized near a conifold, and we will illustrate the mechanism with flux vacua of an explicit orientifold. Although a long-term goal is to combine such results with Kähler moduli stabilization and a metastable uplift to a de Sitter solution,<sup>2</sup> we will not take these latter steps here. Exhibiting ensembles of flux vacua that can be lifted to metastable de Sitter solutions is an ambitious task for the future.

The organization of this paper is as follows. In §5.2 we set our notation (§5.2.1), recall a few results about the large complex structure limit in Calabi-Yau moduli space (§5.2.2), and review the mechanism of [92] for constructing vacua with small flux superpotential (§5.2.3). In §5.3 we present a mechanism for constructing conifold vacua with small flux superpotential. To illustrate this, in §5.4 we examine a Calabi-Yau threefold  $X$  with  $h^{1,1}(X) = 3$  and  $h^{2,1}(X) = 99$  (§5.4.1); construct its mirror  $\tilde{X}$ , and an orientifold thereof (§5.4.2); and exhibit conifold vacua with  $|W_0| \ll 1$  in the orientifold of  $\tilde{X}$  (§5.4.3). We conclude in §5.5. The appendix contains two independent computations of the D3-brane tadpole in the orientifold of §5.4.2.

## 5.2 Vacua with small flux superpotential

### 5.2.1 Setup

We will work in the landscape of four-dimensional  $\mathcal{N} = 1$  supergravity solutions obtained from compactifications of type IIB string theory on O3/O7 orientifolds of Calabi-Yau threefolds. While we are ultimately interested in analyzing the full

---

<sup>2</sup>See e.g. [248] for an analysis of a de Sitter solution arising from an explicit flux vacuum.

vacuum structure of such models, arising in particular from the non-perturbative potential for the Kähler moduli, in this paper we will neglect the Kähler moduli altogether. That is, we consider the classical no-scale solutions of [151]. Throughout this paper, unless noted otherwise, we will work in ten-dimensional Einstein frame in units where  $\ell_s^2 \equiv (2\pi)^2 \alpha' = 1$ , and use our freedom to Weyl-rescale the four-dimensional metric to set the four-dimensional reduced Planck mass to one. These conventions match those of [92].

To begin, we consider a Calabi-Yau threefold  $\tilde{X}$  and a holomorphic and isometric involution  $\tilde{\mathcal{I}} : \tilde{X} \rightarrow \tilde{X}$ , with induced action on the holomorphic three-form  $\Omega \mapsto -\Omega$ . After the orientifolding, the fixed locus of  $\tilde{\mathcal{I}}$  hosts O3-planes and O7-planes.

Let  $Q$  be the total D3-brane charge of the O3-planes and seven-brane stacks. If  $Q < 0$  then its contribution to the D3-brane tadpole can be canceled by  $N_{D3}$  mobile D3-branes as well as three-form fluxes  $F_3$  and  $H_3$  such that<sup>3</sup>

$$Q_{D3}^{\text{total}} = N_{D3} + \frac{1}{2} \int_{\tilde{X}} F_3 \wedge H_3 + Q = 0. \quad (5.2)$$

Let  $\{\Sigma_{(3)a}, \Sigma_{(3)}^a\}$  be a symplectic basis of  $H_3(\tilde{X}, \mathbb{Z})$  and  $\{\alpha^a, \beta_a\}$  their Poincaré dual forms,

$$\int_{\tilde{X}} \alpha^a \wedge \beta_b = \delta^a_b, \quad \int_{\tilde{X}} \alpha^a \wedge \alpha^b = \int_{\tilde{X}} \beta_a \wedge \beta_b = 0, \quad a, b = 0, \dots, h^{2,1}(\tilde{X}). \quad (5.3)$$

The *periods*

$$z^a = \int_{\Sigma_{(3)a}} \Omega = \int_{\tilde{X}} \Omega \wedge \alpha^a, \quad \mathcal{F}_a = \int_{\Sigma_{(3)}^a} \Omega = \int_{\tilde{X}} \Omega \wedge \beta_a \quad (5.4)$$

form an overcomplete set of coordinates on complex structure moduli space: locally we have  $\mathcal{F}_a = \mathcal{F}_a(z)$  and the  $z^a$  are a set of projective coordinates. Similarly, the

---

<sup>3</sup>In our conventions a mobile D3-brane has a single unit of D3-brane charge, while a D3-brane frozen onto the orientifold fixed locus has charge 1/2.

fluxes  $F_3$  and  $H_3$  are characterized by the Dirac-quantized flux vectors

$$f^a = \int_{\Sigma_{(3)a}} F_3, \quad f_a = \int_{\Sigma_{(3)}^a} F_3, \quad h^a = \int_{\Sigma_{(3)a}} H_3, \quad h_a = \int_{\Sigma_{(3)}^a} H_3, \quad (5.5)$$

and we will write  $\vec{f} = (f_a, f^a)$ ,  $\vec{h} = (h_a, h^a)$ .

Prior to orientifolding, the complex structure moduli come in  $\mathcal{N} = 2$  vector multiplets, and the periods  $\mathcal{F}_a(z)$  derive from a prepotential  $\mathcal{F}(z)$  via  $\mathcal{F}_a(z) = \partial_a \mathcal{F}(z)$ . The tree-level exact Weil-Petersson metric on complex structure moduli space is obtained from the Kähler potential

$$K_{cs} = -\ln \left( -i \int_{\tilde{X}} \Omega \wedge \bar{\Omega} \right) = -\ln(-i \vec{\Pi}^\dagger \Sigma \vec{\Pi}), \quad (5.6)$$

with period vector  $\vec{\Pi} = (\partial_a \mathcal{F}, z^a)^t$  and symplectic pairing  $\Sigma := \begin{pmatrix} 0 & \mathbb{I} \\ -\mathbb{I} & 0 \end{pmatrix}$ .

The orientifold involution induces a splitting of the cohomology groups,

$$H^{p,q}(\tilde{X}, \mathbb{Q}) = H_+^{p,q}(\tilde{X}, \mathbb{Q}) \oplus H_-^{p,q}(\tilde{X}, \mathbb{Q}) \quad (5.7)$$

into even and odd eigenspaces, and the complex structure moduli that survive the projection are counted by  $h_-^{2,1}(\tilde{X}, \tilde{\mathcal{I}}) := \dim H_-^{2,1}(\tilde{X}, \mathbb{Q})$  and come in  $\mathcal{N} = 1$  chiral multiplets. We will denote these surviving complex structure moduli by  $z^a$ ,  $a = 1, \dots, h_-^{2,1}(\tilde{X}, \tilde{\mathcal{I}})$ . Likewise,  $h_+^{1,1}(\tilde{X}, \tilde{\mathcal{I}})$  counts the number of surviving Kähler moduli  $T^\alpha$ . Finally,  $h_-^{1,1}(\tilde{X}, \tilde{\mathcal{I}})$  and  $h_+^{2,1}(\tilde{X}, \tilde{\mathcal{I}})$  are the number of axionic chiral multiplets and  $U(1)$  vector multiplets, respectively, but will play no role in this paper. The full tree-level effective action has been worked out in [170].

After orientifolding, the Kähler potential of eq. (5.6) will in general receive corrections from fluxes and orientifold planes, but these are subleading at sufficiently large volume where fluxes are dilute and warping is negligible. The superpotential, however, is exact up to non-perturbative corrections in the Kähler moduli and

D(-1) instantons and is given by [176, 151]

$$W(z, \tau, T) = W_{\text{flux}}(z, \tau) + W_{\text{np}}(z, \tau, T), \quad \text{with} \quad (5.8)$$

$$\sqrt{\frac{\pi}{2}} W_{\text{flux}}(z, \tau) = \int_{\tilde{X}} (F_3 - \tau H_3) \wedge \Omega(z) = (\vec{f} - \tau \vec{h})^t \Sigma \vec{\Pi}(z), \quad (5.9)$$

where  $W_{\text{np}}(z, \tau, T)$  parameterizes non-perturbative corrections in the Kähler moduli  $T$  and the dilaton  $\tau$ , which are typically difficult to compute.<sup>4</sup> We will neglect these corrections self-consistently. Moreover, even when flux backreaction is severe, the vacuum solutions  $D_\tau W = D_{z^a} W = 0$  obtained using the classical Kähler potential (5.6) are reliable as long as the ten-dimensional geometry is in the supergravity regime, even though the scalar potential away from the supersymmetric minimum can no longer be computed from it [151].

This fact will be particularly important for the purposes of this paper because we will stabilize complex structure moduli near a conifold point in moduli space. In this case, for moderate values of the overall volume modulus, in the vicinity of the (deformed) conifold regions in the Calabi-Yau the fluxes are no longer dilute and their backreaction produces the famous Klebanov-Strassler throats [233]. These produce an exponentially strong gravitational redshift (warping) that is not appropriately captured by eq. (5.6) and (5.8). Nevertheless, the Klebanov-Strassler solution falls into the class of imaginary-self-dual (ISD) solutions of [151], and the F-term equations arising from (5.6) and (5.8) can be used as a tool to find points in Calabi-Yau moduli space where the fluxes are indeed ISD.

---

<sup>4</sup>The leading order contributions come from D(-1) instantons  $\sim e^{2\pi i \tau}$  as well as Euclidean D3-branes and gaugino condensation effects on seven-branes  $\sim e^{-2\pi T/c}$ ,  $c \in \mathbb{N}$ .

### 5.2.2 The large complex structure patch

In the following, we will be interested in the large complex structure (LCS) patch of complex structure moduli space of  $\tilde{X}$ , which is mirror dual to the large volume region of the mirror threefold  $X$ .<sup>5</sup> Let  $\{\Sigma_{(2)a}\}$  be a basis of  $H_2(X, \mathbb{Z})$  and  $\{\Sigma_{(4)}^a\}$  a dual basis of  $H_4(X, \mathbb{Z})$ , i.e.  $\Sigma_{(2)a} \cdot \Sigma_{(4)}^b = \delta_a^b$ . Curve classes  $[\mathcal{C}] \in H_2(X, \mathbb{Z})$  are represented by integer vectors  $\beta_a^{\mathcal{C}}$ ,

$$[\mathcal{C}] = \sum_{a=1}^{h^{1,1}(X)} \beta_a^{\mathcal{C}} [\Sigma_{(2)a}], \quad \beta_a^{\mathcal{C}} \in \mathbb{Z}. \quad (5.10)$$

The complexified (string frame) curve volumes  $z^a = \int_{\Sigma_{(2)a}} (B + iJ)$ ,  $a = 1, \dots, h^{1,1}(X)$ , serve as local coordinates on moduli space and are identified with the type IIB complex structure moduli  $z^a$  in a gauge where  $z^0 = 1$ . Henceforth, we will work in this gauge and let  $a, b = 1, \dots, h^{1,1}(X)$ .

The prepotential enjoys the expansion [197]

$$\mathcal{F}(z) = \mathcal{F}_{\text{poly}}(z) + \mathcal{F}_{\text{inst}}(z), \quad (5.11)$$

$$\text{with } \mathcal{F}_{\text{poly}}(z) = -\frac{1}{3!} \mathcal{K}_{abc} z^a z^b z^c + \frac{1}{2} a_{ab} z^a z^b + b_a z^a + \frac{\chi \zeta(3)}{2(2\pi i)^3}. \quad (5.12)$$

Here,  $\mathcal{K}_{abc}$  are the triple intersection numbers of  $X$ , and the quadratic term can be taken to be

$$a_{ab} = \frac{1}{2} \begin{cases} \mathcal{K}_{aab} & a \geq b \\ \mathcal{K}_{abb} & a < b \end{cases}, \quad (5.13)$$

where  $b_a = \frac{1}{24} \int_{\Sigma_{(4)}^a} c_2(X)$ ,  $\chi = \int_X c_3(X)$ , and  $\zeta(3)$  is Apéry's constant. Moreover,

$$\mathcal{F}_{\text{inst}}(z) = -\frac{1}{(2\pi i)^3} \sum_{[\mathcal{C}]} n_{\mathcal{C}}^0 \text{Li}_3(q^{\mathcal{C}}), \quad q^{\mathcal{C}} := \exp(2\pi i \beta_a^{\mathcal{C}} z^a), \quad (5.14)$$

---

<sup>5</sup>For a recent study of scalar potentials from fluxes in asymptotic limits such as the LCS region, see [169].

where the sum runs over all *effective* curve classes  $[\mathcal{C}]$ ,  $n_{\mathcal{C}}^0 \in \mathbb{Z}$  are the genus zero Gopakumar-Vafa (GV) invariants [158, 159], and  $\text{Li}_k(q) := \sum_{n=1}^{\infty} q^n/n^k$  is the polylogarithm. When all effective curves in  $X$  are large,  $\mathcal{F}_{\text{inst}}$  parameterizes type IIA worldsheet instanton corrections to the derivatives of the prepotential as

$$\mathcal{F}_a(z) = \partial_a \mathcal{F}_{\text{poly}} - \frac{1}{(2\pi i)^2} \sum_{[\mathcal{C}]} n_{\mathcal{C}}^0 \beta_a^{\mathcal{C}} \text{Li}_2(q^{\mathcal{C}}). \quad (5.15)$$

### 5.2.3 Small flux superpotentials at large complex structure

As demonstrated in [92], one can find weakly coupled flux vacua at LCS with exponentially small flux superpotential by making a restricted choice of fluxes. Near LCS, the flux superpotential splits as

$$W_{\text{flux}}(z^a, \tau) \equiv W_{\text{poly}}(z^a, \tau) + W_{\text{inst}}(z^a, \tau), \quad (5.16)$$

where  $W_{\text{poly}}(z, \tau)$  is the flux superpotential that arises from the approximation  $\mathcal{F}(z) \approx \mathcal{F}_{\text{poly}}(z)$ , and  $W_{\text{inst}}(z, \tau)$  parameterizes the instanton corrections,

$$-\sqrt{\frac{\pi}{2}} W_{\text{inst}}(z, \tau) := (f^a - \tau h^a) \partial_a \mathcal{F}_{\text{inst}}(z) + (f^0 - \tau h^0) \left( 2\mathcal{F}_{\text{inst}}(z) - z^a \partial_a \mathcal{F}_{\text{inst}}(z) \right). \quad (5.17)$$

We choose fluxes

$$\vec{f} = (b_a M^a, a_{ab} M^b, 0, M^a)^t, \quad \vec{h} = (0, K_a, 0, 0)^t, \quad (5.18)$$

parameterized by a pair  $\vec{M}, \vec{K} \in \mathbb{Z}^{h^{2,1}(\tilde{X}, \tilde{\mathcal{I}})}$  that satisfies

$$K_a p^a = 0, \quad 0 \leq -M^a K_a \leq -2Q, \quad \text{with} \quad p^a := (\mathcal{K}_{abc} M^c)^{-1} K_b, \quad (5.19)$$

such that  $\vec{p}$  is in the Kähler cone of  $X$ . For such a choice of fluxes the polynomial part of the superpotential takes the form

$$W_{\text{poly}}(z, \tau) \propto \frac{1}{2} \mathcal{K}_{abc} M^a z^b z^c - \tau K_a z^a, \quad (5.20)$$



and has a supersymmetric valley  $\partial_{z^a} W_{\text{poly}} = W_{\text{poly}} = 0$  along the one-dimensional locus where  $z^a = p^a \tau$ . Generically, the orthogonal directions to the flat valley are heavy and can be integrated out — we will verify this in explicit examples in §5.4.3.

As the polynomial part of the superpotential vanishes along the flat valley, the instanton corrections to the superpotential become relevant, and serve to stabilize  $\tau$ . The effective superpotential is

$$W_{\text{eff}}(\tau) := W_{\text{inst}}(p^a \tau, \tau) = \sqrt{\frac{2}{\pi}} \frac{1}{(2\pi i)^2} \sum_{[c]} n_c^0 M^a \beta_a^c \text{Li}_2 \left( e^{2\pi i \beta_a^c p^a \tau} \right) + \mathcal{O}(e^{2\pi i \tau}, e^{-2\pi T}). \quad (5.21)$$

In the regime where D(-1) instanton effects can be consistently neglected, one should only retain terms in the sum with  $\beta_a^c p^a < 1$ . For appropriately aligned  $p^a$  and suitably hierarchical GV invariants the above structure leads to a *racetrack* stabilization of  $\tau$  at weak coupling and near LCS.

### 5.3 Stabilizing near the conifold

We will now extend the construction of [92] to operate in a regime where one or more of the moduli are away from their LCS region, and are instead exponentially close to developing a conifold singularity.

At a conifold singularity in complex structure moduli space a collection of  $n_{\text{cf}}$  three-cycles shrink to zero size [67, 70]. Let us assume that these all lie in the same homology class, corresponding to one of the basis elements  $\Sigma_{(3)a}$ , with corresponding modulus  $z_{\text{cf}}$ . We denote the remaining moduli by  $z_i$ , i.e.  $\{z^a\} =$

$\{z_{\text{cf}}, z^i\}$ . Then the dual period, which we will denote by  $\mathcal{F}_{\text{cf}}$ , takes the form

$$\mathcal{F}_{\text{cf}}(z^a) = \mathcal{F}_{\text{cf}}(z^i, z_{\text{cf}}) = \frac{n_{\text{cf}}}{2\pi i} z_{\text{cf}} \ln(z_{\text{cf}}) + f(z^i, z_{\text{cf}}), \quad (5.22)$$

where  $f(z^i, z_{\text{cf}})$  is a model-dependent function. Although  $f(z^i, z_{\text{cf}})$  is holomorphic around  $z_{\text{cf}} = 0$ , it will play an important role in our discussion, because generically  $f(z^i, 0) \neq 0$ .

Then, with  $-M$  units of  $F_3$  flux on the shrinking cycle and  $K$  units of  $H_3$  flux on the dual cycle, the flux superpotential splits as [151]

$$W_{\text{flux}} = W_{\text{cf}}(z^a) + W_{\text{bulk}}(z^a) \quad (5.23)$$

$$\sqrt{\frac{\pi}{2}} W_{\text{cf}}(z^a) := M \left( \frac{n_{\text{cf}}}{2\pi i} z_{\text{cf}} \ln(z_{\text{cf}}) + f(z^a) \right) - \tau K z_{\text{cf}}, \quad (5.24)$$

where  $W_{\text{bulk}}(z^a)$  is holomorphic around  $z_{\text{cf}} = 0$  and parameterizes the contribution to the superpotential from other cycles. Provided that  $|K| > g_s |M|$  and that  $K$  and  $M$  have the same sign, this stabilizes the conifold modulus exponentially close to the singularity,

$$|z_{\text{cf}}| \sim \exp\left(-\frac{2\pi K}{n_{\text{cf}} g_s M}\right). \quad (5.25)$$

Upon stabilizing in this regime, one is left with codimension-three defects hosting confining Klebanov-Strassler gauge theories if  $g_s M \ll 1$ , or with warped throats with a controlled ten-dimensional supergravity description in the regime  $g_s M \gg 1$  [233]. In the former case,  $|z_{\text{cf}}|^{1/3}$  is identified with the confining scale of the gauge theory, while in the latter case it is the gravitationally redshifted Randall-Sundrum-type [298] warp factor<sup>6</sup>  $e^A|_{\text{tip}} \sim |z_{\text{cf}}|^{1/3}$ .

For generating uplifts to de Sitter vacua by including anti-D3-branes it is natural to consider the regime  $g_s M \gtrsim 1$  where the infrared region of the throat supports

---

<sup>6</sup>Here we assume only a moderately large Calabi-Yau volume  $\mathcal{V}$ , i.e.  $|z_{\text{cf}}| \ll 1$  and also  $\mathcal{V}|z_{\text{cf}}|^2 \ll 1$ . In the opposite regime of parametrically large volume such that  $\mathcal{V}|z_{\text{cf}}|^2 \gg 1$ , there is neither a throat nor a gauge theory but simply an everywhere weakly curved conifold region with dilute fluxes. For results on moduli stabilization in this opposing regime, see [54].

metastable supersymmetry-breaking anti-D3-brane configurations that contribute to the vacuum energy [215]. However, this restriction might well be unnecessary due to the plausible existence of a supersymmetry-breaking vacuum in the Klebanov-Strassler gauge theory, see e.g. [15, 299, 18, 17, 16]. In any event, in this paper we will study classical conifold vacua in both regimes of  $g_s M$ , and defer metastable supersymmetry breaking to future work.

After stabilizing exponentially close to the conifold singularity, the flux superpotential reads

$$W_{\text{flux}}(z^i, z_{\text{cf}}) = \sqrt{\frac{2}{\pi}} M f(z^i, 0) + W_{\text{bulk}}(z^i, 0) + \mathcal{O}(z_{\text{cf}}). \quad (5.26)$$

In particular, the holomorphic piece  $f(z^a)$  in the conifold period (5.22) gives an  $\mathcal{O}(1)$  contribution to the superpotential that has to be canceled against the bulk superpotential  $W_{\text{bulk}}$  to give a small flux superpotential, as alluded to in the introduction. We will now explain how this cancellation is achieved.

### 5.3.1 The conifold prepotential from a shrinking curve

In this section we will compute the periods of  $\tilde{X}$  analytically near certain types of conifold points. The idea is to analytically continue the periods computed at LCS into the regime where one of the moduli,  $z_{\text{cf}}$ , is small and close to a conifold singularity, while the other moduli  $z^i$  stay large. Our result will take the form of a double expansion in the conifold modulus  $z_{\text{cf}} \ll 1$  and in type IIA worldsheet instantons wrapping curves in  $X$  that are not mirror-dual to the A-cycle of the conifold.

Performing an analytic continuation from the LCS region to the conifold region generally requires knowing the instanton expansion of the prepotential in eq. (5.14)

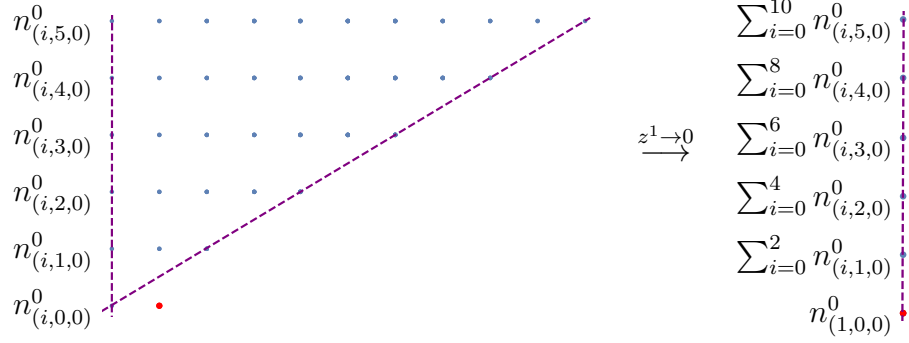


Figure 5.1: The slice  $\beta_3^C = 0$  in the Mori cone of the Calabi-Yau  $X$  described in §5.4. Blue lattice points are populated by nonvanishing GV invariants  $n_{(i,j,0)}^0$ . The red lattice point is GV-nilpotent of order one, and lies outside the closure of the interior cone (bounded by dashed purple lines). Near the origin of the Coulomb branch  $z^1 \rightarrow 0$ , one retains a controlled expansion in  $e^{2\pi iz^{2,3}}$  with coefficients  $\sum_i n_{(i,j,k)}^0$ . These are the GV invariants on the Higgs branch, and are computable because the sum over  $i$  terminates: each row in the figure has finite length.

to all orders. After all, the conifold branch cut can at best arise at the radius of convergence of the LCS expansion. Lacking such all-orders information, one might instead determine the prepotential to high order in the instanton expansion, and compute the Taylor coefficients of  $f(z^a)$  in (5.22) numerically by comparing in an overlapping region where both expansions converge, as in [54]. However, in order to demonstrate an accurate cancellation between the bulk and conifold superpotential (5.1) by this approach, one has to reach high numerical precision. For this reason we opt instead for an analytic approach, and now lay out a set of conditions under which we can obtain the required all-orders information.

First, let us introduce some terminology. We write  $\mathcal{M}(X)$  for the Mori cone of  $X$ , and we call a curve class  $[\mathcal{C}] \in \mathcal{M}(X)$  *GV-nilpotent of order  $k_0$*  if the genus zero GV invariants of  $k[\mathcal{C}]$  vanish for all  $k > k_0$ . A class that is not GV-nilpotent of order  $k_0$  for any finite  $k_0$  we call *GV-potent*. We define the *interior cone* as the closure of the real cone generated by all GV-potent curve classes in  $\mathcal{M}(X)$ .

Comparing to eq. (5.14), one sees that the infinite tower of instanton corrections from worldsheet instantons wrapping a GV-nilpotent curve class  $[\mathcal{C}]$  an arbitrary number of times are simply determined by a *finite* sum over polylogarithms. Therefore, if we can find a slice in moduli space where *only* GV-nilpotent curve classes shrink, we only need to analytically continue the well-known polylogarithms. The following condition (which we will establish in the example of §5.4) guarantees this.

We suppose that there exists a curve  $\mathcal{C}_v \in \mathcal{M}(X)$  in the mirror threefold  $X$  that is GV-nilpotent of order one and lies outside the closure of the cone generated by all other curve classes in  $\mathcal{M}(X)$  with non-vanishing GV invariants: see Figure 5.1. (In particular,  $\mathcal{C}_v$  lies outside the interior cone.) In this case, there exists a wall  $\mathcal{W}_{\mathcal{C}_v}$  of the Kähler cone of  $X$  where the volume of  $\mathcal{C}_v$  vanishes. The wall  $\mathcal{W}_{\mathcal{C}_v}$  is a cone itself, and asymptotically far out in this cone the volumes of all other curves with non-vanishing GV invariants tend to infinity. For ease of exposition we will assume that  $\mathcal{C}_v$  is an element of our basis of curves, so without loss of generality we can choose  $\mathcal{C}_v = \Sigma_{(2)1}$ . We will denote the corresponding Kähler modulus of  $X$  by  $z_{\text{cf}} := z^1$ . The other Kähler moduli of  $X$  will be denoted by  $z^i$  with  $i = 2, \dots, h^{1,1}(X)$ . Then, we have

$$\mathcal{F}_i(z_{\text{cf}}, z^i) := \partial_{z^i} \mathcal{F}(z_{\text{cf}}, z^i) = -\frac{1}{2} \mathcal{K}_{iab} z^a z^b + a_{ia} z^a + b_i - \frac{1}{(2\pi i)^2} \sum_{[\mathcal{C}] \neq [\mathcal{C}_v]} n_{\mathcal{C}}^0 \beta_i^{\mathcal{C}} \text{Li}_2(q^{\mathcal{C}}). \quad (5.27)$$

Since the vanishing class  $[\mathcal{C}_v]$  does not appear in the instanton sum, the arguments of the polylogarithm remain small as in the LCS regime even for small  $z_{\text{cf}}$ . This is not quite enough for a sensible expansion: for two curve classes  $[\mathcal{C}]$  and  $[\mathcal{C}']$  with  $[\mathcal{C}] - [\mathcal{C}'] \propto [\mathcal{C}_v]$  the corresponding arguments of the polylogarithms become identical in the limit  $z_{\text{cf}} \rightarrow 0$ , so the GV invariants of curve classes differing by the vanishing class are effectively summed up in that limit.<sup>7</sup> For the instanton expansion to

---

<sup>7</sup>Note that if there is a Higgs branch meeting the origin of the Coulomb branch at  $z_{\text{cf}} = 0$ ,

remain controlled, we need that these sums of GV invariants terminate. But this is guaranteed because our vanishing curve class lies *outside* the interior cone (see Figure 5.1). Thus, any ray parallel to  $[\mathcal{C}_v]$  intersects finitely many lattice points in the interior cone.

The remaining task is to compute  $\mathcal{F}_1(z_{\text{cf}}, z^i) := \partial_{z_{\text{cf}}} \mathcal{F}(z_{\text{cf}}, z^i)$ . The crucial difference compared to the  $\mathcal{F}_i(z_{\text{cf}}, z^i)$  is that the vanishing curve *does* contribute to the instanton sum, so we need to evaluate the polylogarithm near  $q = 1$ . This is most easily done using Euler's reflection formula<sup>8</sup>

$$-\frac{\text{Li}_2(e^{2\pi iz})}{(2\pi i)^2} = \frac{1}{24} + \frac{z}{2\pi i} \ln(1 - e^{2\pi iz}) + \frac{\text{Li}_2(1 - e^{2\pi iz})}{(2\pi i)^2} = \frac{1}{24} + \frac{z}{2\pi i} (\ln(-2\pi iz) - 1) + \mathcal{O}(z^2). \quad (5.28)$$

Thus, finally, we arrive at

$$\begin{aligned} \mathcal{F}_1(z_{\text{cf}}, z^i) &:= \partial_{z_{\text{cf}}} \mathcal{F}(z_{\text{cf}}, z^i) = n_{\text{cf}} \frac{z_{\text{cf}}}{2\pi i} \ln(1 - e^{2\pi i z_{\text{cf}}}) \\ &- \frac{1}{2} \mathcal{K}_{1ab} z^a z^b + a_{1a} z^a + b_1 + n_{\text{cf}} \left( \frac{1}{24} + \frac{\text{Li}_2(1 - e^{2\pi i z_{\text{cf}}})}{(2\pi i)^2} \right) - \frac{1}{(2\pi i)^2} \sum_{[\mathcal{C}] \neq [\mathcal{C}_v]} n_{\mathcal{C}}^0 \beta_1^{\mathcal{C}} \text{Li}_2(q^{\mathcal{C}}). \end{aligned} \quad (5.29)$$

Provided that the singular locus  $z_{\text{cf}} \rightarrow 0$  is in fact a conifold singularity in  $\tilde{X}$ , we may identify  $\mathcal{F}_{\text{cf}}(z_{\text{cf}}, z^i) \equiv \mathcal{F}_1(z_{\text{cf}}, z^i)$ . The first term in (5.29) contains the universal logarithm of the general conifold period of eq. (5.22), as well as an infinite series of holomorphic corrections. These corrections, together with the entire second line of eq. (5.29), constitute the holomorphic term  $f(z^a)$  in (5.22). We can therefore compute  $f(z^a)$  to any desired accuracy by computing the GV invariants  $n_{\mathcal{C}}^0$  of curve classes  $[\mathcal{C}]$  up to a sufficiently high degree.

In summary, we have gained the much needed analytical control over the period

---

such a summation yields the GV invariants of the Higgs branch.

<sup>8</sup>The corresponding series of instanton corrections to the period vector is thus resummed into the perturbative one-loop correction from integrating out light hypermultiplets from wrapped D2-branes/M2-branes near the origin of the Coulomb branch [312, 165, 158, 159].

vector near a special class of conifolds.<sup>9</sup> For this special class the shrinking  $S^3$  of the conifold is mirror dual to a shrinking *curve*. This is a nontrivial restriction because a conifold singularity in  $\tilde{X}$  may be mirror dual to a shrinking curve, divisor or entire threefold  $X$ .<sup>10</sup>

### 5.3.2 Moduli stabilization in three steps

We will turn on the following subset of three-form fluxes:

$$\vec{f} = (P_0, P_a, 0, M^a)^t, \quad \vec{h} = (0, K_a, 0, 0)^t. \quad (5.30)$$

Instead of splitting the superpotential into contributions from the conifold fluxes and the bulk, we expand in the conifold modulus  $z_{\text{cf}}$ ,

$$\sqrt{\frac{\pi}{2}} W_{\text{flux}}(z_{\text{cf}}, z^i, \tau) = W^{(0)}(z^i, \tau) + W^{(1)}(z^i, \tau, z_{\text{cf}}) z_{\text{cf}} + \mathcal{O}(z_{\text{cf}}^2). \quad (5.31)$$

The  $\mathcal{O}(z_{\text{cf}}^0)$  term takes a form akin to the LCS expansion (5.16), but only in the bulk moduli  $z^i$ , i.e.

$$W^{(0)}(z^i, \tau) = W_{\text{poly}}^{(0)}(z^i, \tau) + W_{\text{inst}}^{(0)}(z^i), \quad (5.32)$$

with

$$W_{\text{poly}}^{(0)}(z^i, \tau) = M^a \left( \frac{1}{2} K_{aij} z^i z^j - a_{ai} z^i - \tilde{b}_a \right) + P_i z^i + P_0 - \tau K_i z^i, \quad (5.33)$$

$$W_{\text{inst}}^{(0)}(z^i) = \frac{1}{(2\pi i)^2} \sum_{[C] \neq [C_v]} n_C^0 M^a \beta_a^C \text{Li}_2(q^C)|_{z_{\text{cf}}=0}, \quad (5.34)$$

and with shifted  $\tilde{b}_a := b_a + n_{\text{cf}} \delta_{a1}/24$ . Note that by expanding in  $z_{\text{cf}}$  we have absorbed all contributions to the flux superpotential that survive in the conifold

---

<sup>9</sup>Note that we have left out the remaining period  $\mathcal{F}_0$ , which receives a nontrivial correction from resumming instanton corrections on  $\mathcal{C}_v$ . These are holomorphic in  $z_{\text{cf}}$ . We will not turn on fluxes on the dual cycle, so we can omit this period.

<sup>10</sup>For instance the famous conifold point in the mirror quintic is mirror dual to a shrinking Calabi-Yau threefold [68]. For more examples, see [168, 52].

limit  $z_{\text{cf}} \rightarrow 0$  into the expression  $W^{(0)}(z^i, \tau)$  containing both bulk and conifold contributions. Provided that we can stabilize the bulk moduli and the dilaton such that  $|\langle W^{(0)}(z^i, \tau) \rangle| \ll 1$ , and also stabilize  $z_{\text{cf}}$  near the conifold, a small *overall* flux superpotential as in eq. (5.1) will result.

The next-to-leading order term in the expansion (5.32) contains the conifold logarithm

$$W^{(1)}(z^i, \tau) = M \frac{n_{\text{cf}}}{2\pi i} \left( \ln(-2\pi i z_{\text{cf}}) - 1 \right) - \tau K + \mathcal{K}_{1ai} M^a z^i + P - a_{1a} M^a + \mathcal{O}\left(e^{2\pi i z^i}\right), \quad (5.35)$$

where

$$M := -M^1, \quad P := P_1, \quad \text{and} \quad K := K_1. \quad (5.36)$$

Given this structure, we may stabilize moduli in three essentially independent steps. First, we use  $W_{\text{poly}}^{(0)}$  to stabilize all but one combination of the bulk moduli and dilaton as in [92] in a vacuum with  $W_{\text{poly}}^{(0)} = 0$ . For that we choose integer fluxes such that

$$P_i = a_{ia} M^a, \quad P_0 = \tilde{b}_a M^a, \quad (5.37)$$

and

$$K_i p^i = 0, \quad 0 \leq -M^a K_a \leq 2Q, \quad \text{with} \quad p^i := (\mathcal{K}_{ija} M^a)^{-1} K_j, \quad (5.38)$$

such that  $p^i$  is interior to the wall of the Kähler cone of  $X$  specified by  $z_{\text{cf}} = 0$ . In analogy to the previous section, this stabilizes the *bulk* moduli along the valley  $z^i = p^i \tau$  and indeed  $W_{\text{poly}}^{(0)}(z^i = p^i \tau, \tau) = 0$ . At this stage the leading contributions to the superpotential from the bulk and the conifold have been canceled against each other perfectly. The neglected contributions from  $W_{\text{inst}}^{(0)}$  and  $z_{\text{cf}} W^{(1)}$  to the F-term conditions of the directions orthogonal to the flat valley  $z^i = p^i \tau$  are negligible if  $\text{Im}(\tau)$  is large and the conifold modulus  $z_{\text{cf}}$  is small.



We note that the above corresponds to a Wilsonian integrating out of heavy degrees of freedom (the orthogonal moduli), so we can stabilize the light degrees of freedom  $(\tau, z_{\text{cf}})$  using the low energy effective field theory. Below the mass scale of the heavy orthogonal moduli, the effective superpotential reads

$$\sqrt{\frac{\pi}{2}} W_{\text{eff}}(\tau, z_{\text{cf}}) = W_{\text{inst}}^{(0)}(z^i = p^i \tau, \tau) + z_{\text{cf}} W^{(1)}(z^i = p^i \tau, \tau, z_{\text{cf}}). \quad (5.39)$$

Next, we may solve the F-term equation of the conifold modulus  $z_{\text{cf}}$ , giving

$$|z_{\text{cf}}| = \frac{1}{2\pi} \exp\left(-\frac{2\pi K'}{n_{\text{cf}} g_s M}\right) + \mathcal{O}\left(z_{\text{cf}}^2, z_{\text{cf}} e^{2\pi i p^i \tau}\right), \quad (5.40)$$

in terms of the string coupling  $1/g_s = \text{Im}(\tau)$ , and with  $K' := K_1 - M^a \mathcal{K}_{1ai} p^i$ .<sup>11</sup> The phase of  $z_{\text{cf}}$  is similarly stabilized in terms of  $C_0 = \text{Re}(\tau)$ . As long as  $z_{\text{cf}} \ll 1$  the stabilization of  $z_{\text{cf}}$  does not affect the stabilization of the previously integrated-out heavy moduli.

The remaining light direction  $\tau$  can be stabilized as in [92] using the instanton corrections  $W_{\text{inst}}^{(0)}$  in a regime where  $\text{Im}(\tau)$  is indeed large.<sup>12</sup> If we stabilize in a regime where the resulting vev  $\langle W_{\text{inst}}^{(0)} \rangle$  is much larger than  $z_{\text{cf}} W^{(1)}$  then it is consistent to neglect the contribution of  $z_{\text{cf}} W^{(1)}$  to the F-term of  $\tau$ . The vacuum value of the full flux superpotential is then given, up to corrections of  $\mathcal{O}(z_{\text{cf}})$ , by

$$W_0 \approx \sqrt{\frac{2}{\pi}} \left\langle W_{\text{inst}}^{(0)}(p^i \tau, \tau) \right\rangle. \quad (5.41)$$

We have therefore extended the mechanism of [92] to conifold vacua.

<sup>11</sup>The combination  $K'/n_{\text{cf}}$  appearing in eq. (5.40) is naturally interpreted as the integrated (but not necessarily quantized) three-form field strength residing in a single throat. The presence of more than one throat that share the same B-cycle may lead to the presence of light degrees of freedom (*thractions*) that control the relative distribution of fluxes [187] and would threaten the stability of a warped uplift. In our example of §5.4 we will have  $n_{\text{cf}} = 2$ , but the two throats are identified in the orientifold so the thraction is projected out.

<sup>12</sup>We are primarily interested in the regime  $|z_{\text{cf}}|^{2/3} \sim |W_0| \ll 1$  where  $\tau$  is much lighter than the conifold modulus, i.e.  $m_\tau \sim |W_0| \sim |z_{\text{cf}}|^{2/3} \ll |z_{\text{cf}}|^{1/3} \sim m_{z_{\text{cf}}}$ . In the opposite regime  $|z_{\text{cf}}|^{1/3} \ll |W_0|$  it is more natural in the Wilsonian sense to first integrate out  $\tau$  and finally stabilize the light conifold modulus  $z_{\text{cf}}$ , but our formulas are valid in both regimes.

### 5.3.3 Comments on the supergravity approximation

In the regime of small string coupling  $g_s < 1$ , the curvature of the infrared region of the throat is large in string units unless one chooses sufficiently large  $M$  to ensure that  $g_s M > 1$ . Furthermore, obtaining a substantial throat hierarchy  $|z_{\text{cf}}| \ll 1$  requires choosing  $K > n_{\text{cf}} g_s M > 1$ , and thus the contribution to the D3-brane tadpole from the throats is generically substantial,  $KM \gg 1$ . This leaves little room to choose appropriate bulk fluxes that would give rise to a small flux superpotential. Given a flux tadpole  $Q$  the maximum possible value of  $g_s M$  is obtained by saturating the above inequalities, which gives

$$g_s M|_{\text{max}} \lesssim \sqrt{|Q|}. \quad (5.42)$$

In §5.4 we will work with an orientifold that has  $Q = -52$ , so that the maximum possible  $g_s M$  is of order 7. In this orientifold we will be able to find fluxes giving  $g_s M \sim 3$ . Whether this is enough for the anti-D3-brane stability analysis of [219] to apply will be left for future work to decide.

We note that it has been argued in [32] that the restriction (5.42) generally prevents one from obtaining well-controlled warped throats in weakly-coupled type IIB compactifications. While it is clear that parametrically large  $g_s M$  is impossible, we see no reason why finding numerically large values should be impossible.

## 5.4 An example

In this section we will construct explicit flux vacua with small flux superpotential, exponentially close to a conifold singularity, along the lines discussed in the previous section.

We start with a certain Calabi-Yau hypersurface  $X$  in a toric fourfold  $Y$ , with Hodge numbers  $h^{1,1}(X) = 3$  and  $h^{2,1}(X) = 99$ , and specify an O3/O7 orientifold involution  $\mathcal{I} : X \rightarrow X$  such that  $h_-^{1,1}(X, \mathcal{I}) = h_+^{2,1}(X, \mathcal{I}) = 0$ . Using the Greene-Plesser description [166] of the mirror threefold  $\tilde{X}$  as the resolution of an orbifold  $X/G$  for a particular abelian group  $G$ , we show that the induced action of  $\mathcal{I}$  on  $\tilde{X}$ , denoted  $\tilde{\mathcal{I}} : \tilde{X} \rightarrow \tilde{X}$ , specifies an O3/O7 orientifold involution in  $\tilde{X}$  with  $h_-^{1,1}(\tilde{X}, \tilde{\mathcal{I}}) = h_+^{2,1}(\tilde{X}, \tilde{\mathcal{I}}) = 0$ . For the orientifold of  $\tilde{X}$  specified by  $\tilde{\mathcal{I}}$  we will find conifold vacua with small flux superpotential.<sup>13</sup>

For simplicity, we choose to cancel the D7-brane tadpole locally by placing four D7-branes on top of each O7-plane, with trivial gauge bundle. More precisely, we choose diagonal worldvolume fluxes  $F_{D_I} = -\frac{1}{2}c_1(D_I)$  on the worldvolumes of the  $\mathfrak{so}(8)$  seven-brane stacks on the fixed divisors  $D_I$  to cancel potential Freed-Witten anomalies [142]. Furthermore, we turn on a half-integral orientifold-even NSNS two-form,

$$B_2 = \sum_I \frac{1}{2}[D_I]. \quad (5.43)$$

Since  $c_1(D_I) = -i^*[D_I]$ , where  $i^*$  is the pull-back of the two-form  $[D_I]$  to the divisor  $D_I$ , the gauge-invariant field-strengths  $\mathcal{F}_{D_I} := F_{D_I} - i^*B_2$  are proportional to the Poincaré duals of the two-cycles in  $D_I$  obtained by intersecting with  $\sum_{J \neq I}[D_J]$ . Because the orientifold-invariant Calabi-Yau will be smooth, the O7-planes do not intersect each other. Therefore, the field-strengths  $\mathcal{F}_{D_I}$  are trivial in  $H^2(D_I, \mathbb{Z})$  and so do not contribute to the D3-brane and D5-brane tadpoles. In this configuration the total D3-brane charge  $Q$  of the seven-brane stacks and O3-planes is given by

$$Q = -\frac{\chi(\mathfrak{F}_{\mathcal{I}})}{4}, \quad (5.44)$$

where  $\chi(\mathfrak{F}_{\mathcal{I}})$  is the Euler characteristic of the fixed locus  $\mathfrak{F}_{\mathcal{I}}$  of  $\mathcal{I}$  [78].

---

<sup>13</sup>Alternatively, one can search for vacua along the  $G$ -symmetric locus in the complex structure moduli space of the orientifold of  $X$ , as in [155]. This would require an analysis of the action of  $G$  on the three-cycles in  $X$ , which we would like to avoid in this paper.

### 5.4.1 A Calabi-Yau threefold and an orientifold

Let  $\Delta^\circ \subset N \simeq \mathbb{Z}^4$  be the favorable reflexive polytope whose points not interior to facets are the columns of

$$\begin{pmatrix} -1 & 1 & -1 & -1 & -1 & -1 & -1 \\ 3 & -1 & 0 & 0 & 0 & 0 & 0 \\ -2 & 0 & 0 & 0 & 1 & 2 & 1 \\ -1 & 0 & 1 & 0 & 1 & 0 & 0 \end{pmatrix}. \quad (5.45)$$

The first six of these points are vertices. A fine, regular, star triangulation (FRST) of the points in (5.45) defines a complete, simplicial fan. The toric fourfold  $Y$  defined by this fan contains a smooth anticanonical hypersurface  $X$  that is Calabi-Yau. The linear relations among these points define the rows of a gauged linear sigma model (GLSM) charge matrix

$$Q = \begin{pmatrix} 0 & 0 & 1 & -1 & -1 & 0 & 1 \\ 1 & 3 & -1 & 1 & 2 & 0 & 0 \\ 0 & 0 & 0 & 1 & 0 & 1 & -2 \end{pmatrix}. \quad (5.46)$$

Each of the points in (5.45) corresponds to a prime effective divisor  $\widehat{D}_i \subset Y$  defined by  $x_i = 0$ , that intersects  $X$  transversely. The polytope  $\Delta^\circ$  has three FRSTs, each giving rise to a smooth Calabi-Yau threefold with favorable embedding in  $Y$ , i.e. the divisors  $D_i := \widehat{D}_i \cap X$  generate  $H_4(X, \mathbb{Z})$  [25]. Denoting the FI parameters by  $\xi^a$ , we find that the corresponding Kähler cones are<sup>14</sup>

$$\text{CY}_1 : \quad \xi^1 > 0, \quad \xi^2 > 0, \quad \xi^3 > 0, \quad (5.47)$$

$$\text{CY}_2 : \quad -\xi^1 > 0, \quad \xi^2 + 2\xi^1 > 0, \quad \xi^3 + \xi^1 > 0, \quad (5.48)$$

$$\text{CY}_3 : \quad \xi^3 > 0, \quad \xi^2 + 2\xi^1 > 0, \quad -\xi^3 - \xi^1 > 0. \quad (5.49)$$

---

<sup>14</sup>We have computed the Kähler cone and intersection numbers using the software package `CYTools` [93].

One can show that the triple intersection numbers and the second Chern class of the three phases agree with each other in a suitable basis. Thus, it follows from Wall's theorem [334] that the three Calabi-Yau manifolds are all diffeomorphic to each other. Without loss of generality we will focus on the phase  $\text{CY}_1$ .

In general, computing the Kähler cone (or its dual, the Mori cone) of a Calabi Yau hypersurface is difficult. However, in the present example the Mori cone of the ambient fourfold  $Y$ ,  $\mathcal{M}(Y)$ , is equivalent to the Mori cone of the Calabi-Yau hypersurface  $\mathcal{M}(X)$ . This can be shown as follows. We have  $\mathcal{M}(Y) \supseteq \mathcal{M}(X)$  as  $X$  is a holomorphic submanifold of  $Y$ . The GV invariants of the generators of  $\mathcal{M}(Y)$  are non-trivial (see (5.54)), so  $\mathcal{M}(X) \supseteq \mathcal{M}(Y)$ .

The Stanley-Reisner (SR) ideal of this phase is<sup>15</sup>

$$SR = \{x_3x_6, x_4x_6, x_3x_7, x_1x_2x_4x_5, x_1x_2x_5x_7\}. \quad (5.50)$$

We choose to work in a basis of divisor classes  $H^a \in H_2(X, \mathbb{Z})$  dual to the generators  $\mathcal{C}_a \equiv [\Sigma_{2,a}]$  of  $\mathcal{M}(X)$ , i.e.

$$H^1 = [D_1] + [D_3], \quad H^2 = [D_1], \quad H^3 = [D_6]. \quad (5.51)$$

In this basis, the non-vanishing triple intersection numbers are

$$\mathcal{K}_{111} = \mathcal{K}_{112} = \mathcal{K}_{122} = 4, \quad \mathcal{K}_{113} = \mathcal{K}_{123} = \mathcal{K}_{223} = 2, \quad \mathcal{K}_{222} = 3, \quad (5.52)$$

and the second Chern class is

$$\int_{\vec{H}} c_2(X) = \begin{pmatrix} 52 \\ 42 \\ 24 \end{pmatrix}. \quad (5.53)$$

In the limit  $\xi^1 \rightarrow 0$ , keeping  $\xi^{2,3} > 0$ , one approaches the wall in the Kähler cone that separates  $\text{CY}_1$  from  $\text{CY}_2$ . The holomorphic curve class represented by  $(1, 0, 0)$

---

<sup>15</sup>We have used **Sage** to determine this [321].

is GV-nilpotent of order one, and lies outside the interior cone. Because this class is a generator of the Mori cone, it also lies outside the cone generated by all other curves with non-vanishing GV invariants. Thus, as we approach the wall of the Kähler cone only the instanton corrections in (5.14) from the curve class  $(1, 0, 0)$  become unsuppressed and have to be resummed using (5.28). Only the period  $\mathcal{F}_1$  develops a logarithmic singularity, indicating a conifold singularity in the mirror dual  $\tilde{X}$ .

For later reference (using the methods developed in [198, 199]) we compute all the non-vanishing GV invariants  $n_{(i,j,k)}^0$  with  $j + k \leq 2$  and arbitrary  $i$ ,

$n_{(i,0,0)}^0$	$n_{(i,1,0)}^0$	$n_{(i,0,1)}^0$	$n_{(i,2,0)}^0$	$n_{(i,1,1)}^0$
$n_{(1,0,0)}^0 = 2$	$n_{(0,1,0)}^0 = 252$	$n_{(0,0,1)}^0 = 2$	$n_{(0,2,0)}^0 = -9252$	$n_{(1,1,1)}^0 = 2376$
	$n_{(1,1,0)}^0 = 2376$	$n_{(1,0,1)}^0 = 2$	$n_{(1,2,0)}^0 = 10260$	$n_{(2,1,1)}^0 = 2376$
	$n_{(2,1,0)}^0 = 252$		$n_{(2,2,0)}^0 = 206712$	
			$n_{(3,2,0)}^0 = 10260$	
			$n_{(4,2,0)}^0 = -9252$	

(5.54)

Since  $n_{(1,0,0)}^0 = 2$ , we expect to find two conifold singularities in the corresponding limit in complex structure moduli space of  $\tilde{X}$ . We will confirm this in the next section.

We now choose an orientifold using the involution

$$\mathcal{I} : x_2 \mapsto -x_2 . \quad (5.55)$$

The fixed locus in the ambient variety is

$$\mathfrak{F}_{\mathcal{I}} = \{x_2 = 0\} \cup \{x_1 = x_3 = x_4 = 0\} \cup \{x_1 = x_5 = x_7 = 0\} . \quad (5.56)$$

The generic  $\mathbb{Z}_2$ -even anticanonical polynomial is non-vanishing along these loci. The third locus does not intersect  $X$ , while the first two intersect  $X$  transversally.

The first locus gives rise to an O7-plane on the divisor  $D_2$ , and the second gives rise to a single O3-plane. Using the adjunction formula one computes  $\chi_{D_2} = 207$ . Placing four D7-branes on top of the O7-plane, the D7-brane tadpole is canceled and the total induced D3-brane charge on the O7-plane plus the D3-brane charge of the O3-plane is

$$Q = -\frac{\chi_{D_2}}{4} - \frac{1}{4} = -\frac{207}{4} - \frac{1}{4} = -52. \quad (5.57)$$

Therefore, we can turn on three-form fluxes  $(F_3, H_3)$  with

$$Q_{D3}^{\text{flux}} := \frac{1}{2} \int_X F_3 \wedge H_3 \leq 52. \quad (5.58)$$

We have  $h_-^{1,1}(X, \mathcal{I}) = 0$  because the toric divisors generate  $H_4(X, \mathbb{Z})$  and they are invariant under the orientifold action. From the Lefschetz fixed point theorem one computes

$$h_-^{2,1}(X, \mathcal{I}) = h_-^{1,1}(X, \mathcal{I}) - Q - \frac{\chi_{CY}}{4} - 1 = 0 + 52 - (-48) - 1 = 99 = h^{2,1}(X). \quad (5.59)$$

Thus we have  $h_-^{1,1}(X, \mathcal{I}) = h_+^{2,1}(X, \mathcal{I}) = 0$ . As a consequence, none of the moduli are projected out. In the following we will use the involution  $\mathcal{I}$  to define an involution  $\tilde{\mathcal{I}}$  in the mirror threefold  $\tilde{X}$ .

### 5.4.2 The Greene-Plesser mirror dual

Next, we construct the orbifold  $X/G$ . We start by computing the dual polytope  $\Delta := (\Delta^\circ)^\circ$ ,  $\Delta \subset M \simeq \mathbb{Z}^4$ . Its vertices are the columns of

$$\begin{pmatrix} 1 & 1 & -5 & -11 & 1 & 1 \\ 2 & 0 & -4 & -10 & 2 & 2 \\ 0 & 0 & 0 & -6 & 3 & 0 \\ 0 & 0 & -6 & -6 & 0 & 6 \end{pmatrix}. \quad (5.60)$$

We have an embedding

$$\iota : N \hookrightarrow M, \quad n \mapsto \Lambda n, \quad \Lambda = \begin{pmatrix} 11 & 10 & 6 & 6 \\ 10 & 10 & 6 & 6 \\ 6 & 6 & 3 & 6 \\ 6 & 6 & 6 & 0 \end{pmatrix}, \quad (5.61)$$

which is a group homomorphism that maps the vertices of  $\Delta^\circ$  to the vertices of  $\Delta$ . The Greene-Plesser group is the group coset  $G := N/\iota(M) \simeq \mathbb{Z}_6 \times \mathbb{Z}_6$ . The two  $\mathbb{Z}_6$  factors can be chosen to act on the toric coordinates with charges

$$\vec{w}_1 = (0, 3, 0, 0, 1, 1, 1), \quad \vec{w}_2 = (0, 0, 0, 0, 5, 0, 1). \quad (5.62)$$

The points in  $\Delta^\circ$  not interior to facets are mapped to the vertices of  $\Delta$ , and to the further point  $(-5, -4, -3, 0)^t$ . These seven points correspond to seven  $G$ -invariant monomials of the anticanonical line bundle of our toric fourfold  $Y$ ,

$$f(\vec{x}) = \psi_0 \prod_{i=1}^7 x_i - \psi_1 x_1^6 - \psi_2 x_2^2 - \psi_3 x_4^6 x_6^6 x_7^6 - \psi_4 x_3^6 x_4^{12} x_7^6 - \psi_5 x_5^3 x_6^6 x_7^3 - \psi_6 x_3^6 x_5^6 - \psi_7 x_3^6 x_4^6 x_5^3 x_7^3. \quad (5.63)$$

This represents the *generic* anticanonical polynomial defining  $X/G$ , or equivalently the generic  $G$ -invariant polynomial defining a symmetric Calabi-Yau  $X$ . There exists a special locus in moduli space where the  $G$ -symmetric  $X$  develops a set of 18 conifold singularities. To see this one considers the patch where  $x_{3,5,7} \neq 0$ , where we can gauge fix (part of) the toric scaling relations by setting  $x_3 = x_5 = x_7 = 1$ . Note that this leaves a residual scaling equivalence  $(x_4, x_6) \sim (-x_4, -x_6)$ , because the toric scaling relation associated with the third row of the GLSM charge matrix in (5.46) preserves our gauge fixing condition for scaling parameters  $\pm 1$ . Furthermore, we use up the action of the algebraic torus on  $X$  and the freedom to rescale  $f$  to set  $\psi_{0,2,3,4,5} = 1$ . Then, along a codimension-one locus in moduli space specified by

$$\psi_7 = 1 + \psi_6, \quad (5.64)$$



one finds that  $f = df = 0$  at the following set of points in  $X$ ,

$$x_1 = x_2 = 0, \quad x_4^6 = -1, \quad x_6^6 = 1 - \psi_6. \quad (5.65)$$

Naïvely this is a set of  $6 \times 6 = 36$  conifold singularities, but we need to account for the residual scaling equivalence  $(x_4, x_6) \sim (-x_4, -x_6)$  which implies that there are only 18 inequivalent conifolds. One can show that these 18 conifolds can be resolved to give the anticanonical hypersurface in the toric fourfold specified by the GLSM charge matrix

$$\begin{pmatrix} 0 & -1 & 0 & 0 & 0 & 1 & 1 & 0 \\ 0 & 0 & 1 & -1 & 0 & 0 & -1 & 1 \\ 1 & 3 & -1 & 1 & 0 & 0 & -1 & 0 \\ 0 & 0 & 0 & 1 & 1 & 0 & 0 & -2 \end{pmatrix} \quad (5.66)$$

with positive FI parameters. The first row corresponds to the resolution  $\mathbb{P}^1$  and indeed has GV invariant equal to 18.

The gauge-invariant coordinates adapted to the LCS patch are  $\tilde{\psi}_a = \prod_{i=1}^7 (\psi_i)^{Q_i^a}$ , i.e. in our gauge we have

$$\tilde{\psi}_1 = \psi_7, \quad \tilde{\psi}_2 = \psi_1, \quad \tilde{\psi}_3 = \frac{\psi_6}{\psi_7^2}, \quad (5.67)$$

and the flat LCS coordinates mirror-dual to curve volumes are

$$z^a = \frac{\ln(\tilde{\psi}_a)}{2\pi i} + \sum_{\vec{n} \in \mathbb{N}_0^3} \alpha_{\vec{n}}^a \prod_{b=1}^3 \tilde{\psi}_b^{n_b}, \quad (5.68)$$

with coefficients  $\alpha_{\vec{n}}^a$  that can be computed systematically as in [199]. Let us define

$$\Psi(\tilde{\psi}_3) := \frac{1 - \sqrt{1 - 4\tilde{\psi}_3}}{2\tilde{\psi}_3} = 1 + \tilde{\psi}_3 + \mathcal{O}(\tilde{\psi}_3^2). \quad (5.69)$$

In terms of the  $\tilde{\psi}_a$ , the conifold locus (5.64) occurs when  $\tilde{\psi}_1 = \Psi(\tilde{\psi}_3)$ . In terms of the flat coordinates  $z^a$  this simply corresponds to the locus  $z^1 = 0$ , as follows from

the identity

$$\ln\left(\Psi(\tilde{\psi}_3)\right) + 2\pi i \sum_{\vec{n} \in \mathbb{N}_0^3} \alpha_{\vec{n}}^1 \Psi(\tilde{\psi}_3)^{n_1} \tilde{\psi}_2^{n_2} \tilde{\psi}_3^{n_3} = 0, \quad (5.70)$$

which one may verify order by order in  $\tilde{\psi}_2, \tilde{\psi}_3$ .<sup>16</sup> Thus, we see that keeping  $\text{Im}(z_{2,3}) > 1$  while sending  $z_1 \rightarrow 0$  produces the 18 conifold singularities that we just analyzed.

Next, we take  $\tilde{X}$  at its orbifold point in Kähler moduli space, and consider the induced action of  $\mathcal{I} : X \rightarrow X, [x_1 : \dots : x_7] \mapsto [x_1 : -x_2 : x_3 : \dots : x_7]$  on  $\tilde{X}$ ,

$$\tilde{\mathcal{I}} : \tilde{X} \rightarrow \tilde{X}, \quad \pi([x_1 : \dots : x_7]) \mapsto \pi([x_1 : -x_2 : x_3 : \dots : x_7]), \quad (5.71)$$

defined to act on representatives  $[x_1 : \dots : x_7]$  as  $\pi \circ \mathcal{I}$ . Here,  $\pi : X \rightarrow X/G$  is the projection mod  $G$ . Since  $G$  commutes with  $\mathcal{I}$ , the involution  $\tilde{\mathcal{I}}$  is well-defined. Clearly, no complex structure moduli are projected out by the orientifolding, i.e.  $h_+^{2,1}(\tilde{X}, \tilde{\mathcal{I}}) = 0$ . This is simply because none of the complex structure moduli of  $X$  were projected out by orientifolding by  $\mathcal{I}$ . Furthermore, we can extend the action of  $\tilde{\mathcal{I}}$  to the resolution of the orbifold in such a way that  $h_-^{1,1}(\tilde{X}, \tilde{\mathcal{I}}) = 0$ . This is done by letting all toric coordinates associated with the resolution divisors transform trivially under the involution  $\tilde{\mathcal{I}}$ . This leaves the inherited divisor classes invariant, and one can show that in fact all divisor classes are invariant under the involution — see Appendix C.1.1. Using this and the Lefschetz fixed point theorem one computes the D3-brane tadpole for  $\mathfrak{so}(8)$  stacks as

$$-Q = \frac{\chi(\mathfrak{F}_{\tilde{\mathcal{I}}})}{4} = \frac{1}{2} \left( h_-^{1,1}(\tilde{X}) + h_+^{2,1}(\tilde{X}) \right) - \left( h_-^{1,1}(\tilde{X}, \tilde{\mathcal{I}}) + h_+^{2,1}(\tilde{X}, \tilde{\mathcal{I}}) \right) + 1 = 52, \quad (5.72)$$

where  $\chi(\mathfrak{F}_{\tilde{\mathcal{I}}})$  denotes the Euler characteristic of the fixed locus  $\mathfrak{F}_{\tilde{\mathcal{I}}}$  of the involution  $\tilde{\mathcal{I}}$ . Alternatively, one can directly compute the Euler characteristic of the fixed locus in the orbifold limit (see Appendix C.1.2), which agrees with (5.72).

---

<sup>16</sup>We have verified this to order 42 in  $\tilde{\psi}_{2,3}$ .

Since  $h_+^{1,1}(\tilde{X}, \tilde{\mathcal{I}}) = h^{1,1}(\tilde{X}, \tilde{\mathcal{I}})$  we may go away from the orbifold point in Kähler moduli space without affecting the periods. As a consequence, we have defined an orientifold of the *resolved* orbifold  $\tilde{X}$ .

It remains to show that the conifolds in  $X$  correspond to conifolds in  $\tilde{X}$ , and to determine how many conifold singularities arise in the singular limit  $z_1 \rightarrow 0$ . To do so, we will need to slightly change the gauge of the defining polynomial  $f(\vec{x})$ . In eq. (5.63) we have used the continuous  $G$ -compatible ambient space automorphisms

$$x_2 \mapsto x_2 + \lambda x_1 x_3 x_4 x_5 x_6 x_7, \quad \lambda \in \mathbb{C}, \quad (5.73)$$

in order to eliminate the monomial  $x_1^2 x_3^2 x_4^2 x_5^2 x_6^2 x_7^2$ . In order to analyze the orientifold, instead we would like to restrict to a manifestly orientifold-invariant polynomial  $f$ . Starting from (5.63) in our gauge  $\psi_0 = \psi_2 = 1$ , and using (5.73) with  $\lambda = -1/2$  amounts to replacing

$$\prod_i x_i \mapsto -\frac{1}{4} x_1^2 x_3^2 x_4^2 x_5^2 x_6^2 x_7^2, \quad (5.74)$$

which makes the defining polynomial  $f$  manifestly invariant under  $\tilde{\mathcal{I}}$ .

Since (5.73) acts trivially on the locus  $x_1 = x_2 = 0$  where the conifolds reside, their position is not altered by (5.74). In  $X$ , the curve  $x_1 = x_2 = 0$  can be shown (see Appendix C.1) to be a fixed curve of a  $\mathbb{Z}_2$  subgroup of the Greene-Plesser group  $G = \mathbb{Z}_6 \times \mathbb{Z}_6$ . The coset  $G/\mathbb{Z}_2$  acts transitively on the 18 conifolds, so after modding out by  $G/\mathbb{Z}_2$  we retain only a single conifold singularity. Finally, we have to mod out by the remaining  $\mathbb{Z}_2$  symmetry that maps the curve  $x_1 = x_2 = 0$  to itself pointwise. Locally, around a solution of (5.65), we may embed the conifold in  $\mathbb{C}^4 \ni (x, y, u, v)$  via the vanishing of the polynomial

$$P(x, y, u, v) = x^2 + y^2 + u^2 + v^2 - \epsilon + \dots = 0, \quad (5.75)$$

with deformation parameter  $\epsilon$  such that we have  $dP = P = 0$  on the locus  $x = y = u = v = 0$  in the singular limit  $\epsilon \rightarrow 0$ . Here,

$$x := \frac{x_6^0}{2}x_1, \quad y := ix_2, \quad \begin{pmatrix} u \\ v \end{pmatrix} := \begin{pmatrix} -6i & 3i(1 - \psi_6) \\ 0 & 3(1 - \psi_6) \end{pmatrix} \begin{pmatrix} \frac{x_4}{x_4^0} - 1 \\ \frac{x_6}{x_6^0} - 1 \end{pmatrix}, \quad (5.76)$$

and  $(x_4^0, x_6^0)$  is a solution to eq. (5.65). Here,  $\epsilon := 1 + \psi_6 - \psi_7$ , and we neglect higher-order corrections in  $(x, y, u, v)$  as well as non-constant terms that vanish in the limit  $\epsilon \rightarrow 0$ .

Locally, the  $\mathbb{Z}_2$ -orbifold action is given by

$$\mathbb{Z}_2 : (x, y) \mapsto (-x, -y), \quad (5.77)$$

and the local action of the orientifold involution is

$$\tilde{\mathcal{I}} : (x, y) \mapsto (x, -y) \stackrel{\mathbb{Z}_2}{\sim} (-x, y), \quad (5.78)$$

so there is an O7-plane on the divisor  $x = 0$  as well as on  $y = 0$ .

Orbifolding by (5.77) produces an  $A_1$  singularity in the ambient  $\mathbb{C}^2 \subset \mathbb{C}^4$  parameterized by  $(x, y)$ , and both orientifold planes and the conifold intersect at the singular locus (see Figure 5.2). As usual, we can resolve this singularity using toric geometry by introducing a blowup coordinate  $\alpha$  (see Figure 5.3 for the toric fan), and a  $\mathbb{C}^*$ -scaling relation

$$(x, \alpha, y) \sim (\lambda x, \lambda^{-2}\alpha, \lambda y), \quad \lambda \in \mathbb{C}^*. \quad (5.79)$$

The locus  $x = y = 0$  is removed (it is in the SR ideal of the toric fourfold) and replaced by the exceptional divisor  $\alpha = 0$ . The polynomial  $P$  is replaced by

$$\hat{P}(\alpha, x, y, u, v) = \alpha(x^2 + y^2) + u^2 + v^2 - \epsilon = 0, \quad (5.80)$$

In the limit  $\epsilon \rightarrow 0$  we get not one but two conifold singularities. To see this, consider the exceptional divisor  $\{\alpha = 0\} \simeq \mathbb{P}^1 \times \mathbb{C}^2$  parameterized by homogeneous

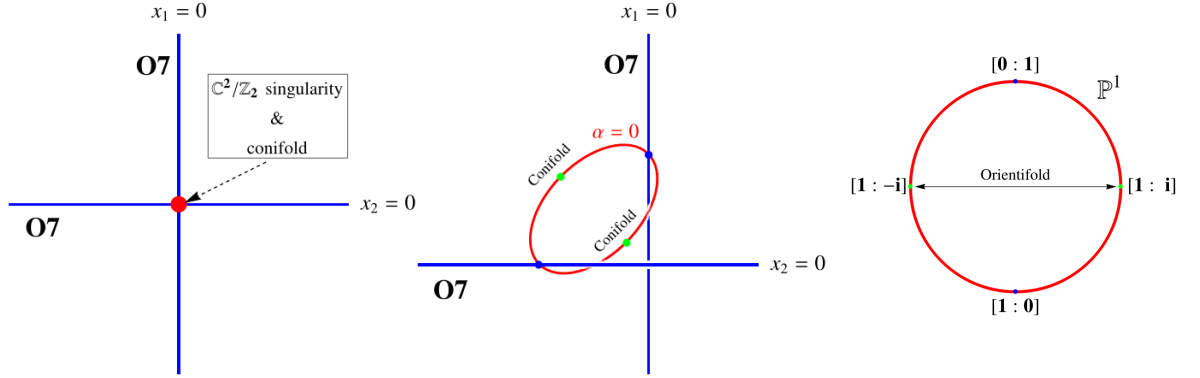


Figure 5.2: Left: the slice  $\{u = v = 0\} = \mathbb{C}^2/\mathbb{Z}_2$  and the position of the orientifold planes  $x_1 = 0$  and  $x_2 = 0$ . Two O7-planes intersect at the orbifold singularity  $x_1 = x_2 = 0$  which also contains the conifold singularity. Middle and right: the same slice after the resolution of the orbifold singularity and a closeup of the exceptional divisor. The O7-planes intersect the exceptional divisor  $\alpha = 0$  at antipodal points  $[1 : 0]$  and  $[0 : 1]$ . The conifold singularities reside at  $[1 : i]$  and  $[1 : -i]$  and are mapped into each other by the orientifold involution.

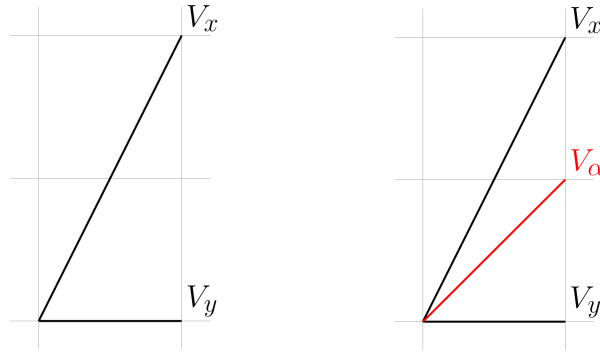


Figure 5.3: Left: the toric fan of the singular surface  $\mathbb{C}^2/\mathbb{Z}_2$  with with two vertices  $v_x = (1, 2)$  and  $v_y = (1, 0)$ . Right: the toric fan of the resolution of  $\mathbb{C}^2/\mathbb{Z}_2$  by a resolution divisor  $\alpha = 0$  associated with the vertex  $v_\alpha = \frac{1}{2}(v_x + v_y) = (1, 1)$ .

coordinates  $[x : y] \in \mathbb{P}^1$  and  $(u, v) \in \mathbb{C}^2$ . For  $\epsilon = 0$  we have  $\hat{P} = d\hat{P} = 0$  at the two points

$$\alpha = u = v = 0, \quad [x : y] = [1 : \pm i]. \quad (5.81)$$

Indeed, the GV invariant of the curve class  $(1, 0, 0)$  that is mirror dual to the conifold  $S^3$  has  $n_{(1,0,0)}^0 = 2$ , see eq. (5.54). Finally, the O7-planes at  $x = 0$  and  $y = 0$  intersect the exceptional divisor  $\alpha = 0$  at  $[x : y] = [0 : 1]$  and  $[x : y] = [1 : 0]$ , respectively, so the two orientifold planes no longer intersect each other and the two conifold singularities are also separated from the O7-planes at finite blowup volume. The conifolds are moreover mapped into each other by the involution in eq. (5.78) and are therefore identified in the orientifold. We conclude that in the limit  $z^1 \rightarrow 0$  there appears a single conifold at generic position in the orientifold of  $\tilde{X}$ .

### 5.4.3 Explicit flux vacua

Now we are ready to find explicit conifold vacua with small flux superpotential in the complex structure moduli space of the Calabi-Yau orientifold discussed in the previous section. We have  $h_+^{1,1}(\tilde{X}, \tilde{\mathcal{I}}) = h^{1,1}(\tilde{X}) = 99$ , and  $h_-^{2,1}(\tilde{X}, \tilde{\mathcal{I}}) = h^{2,1}(\tilde{X}) = 3$ . Thus, all three-form classes are orientifold-odd and we can turn on generic three-form fluxes  $\vec{f}, \vec{h} \in \mathbb{Z}^8$  on the three-cycles in  $\tilde{X}$ , compatible with the D3-brane tadpole bound

$$\frac{1}{2} \int_{\tilde{X}} F_3 \wedge H_3 = \frac{1}{2} \vec{f}^t \Sigma \vec{h} \leq 52. \quad (5.82)$$

We will search for appropriate flux quanta systematically as follows. As a first step, we compile a list of restricted candidate flux integers in a box:

$$V_M := \left\{ \vec{M} \in \mathbb{Z}^3 \left| \begin{array}{l} 0 \neq M^a \in \{-200, 200\} \ \forall a = 1, 2, 3, \quad M^3 > 0, \quad \det \left( \sum_{a=1}^3 \mathcal{K}_{ija} M^a \right) \neq 0, \\ \sum_{a=1}^3 M^a \tilde{b}_a \in \mathbb{Z}, \quad \sum_{a=1}^3 a_{ia} M^a \in \mathbb{Z} \ \forall i = 2, 3 \end{array} \right. \right\}, \quad (5.83)$$

with

$$a_{ia} = \begin{pmatrix} 2 & \frac{3}{2} & 0 \\ 0 & 0 & 0 \end{pmatrix}_{ia}, \quad \tilde{b}_a = \frac{1}{24} \left( \begin{pmatrix} 52 \\ 42 \\ 24 \end{pmatrix} + \begin{pmatrix} 2 \\ 0 \\ 0 \end{pmatrix} \right)_a = \begin{pmatrix} \frac{9}{4} \\ \frac{7}{4} \\ 1 \end{pmatrix}_a. \quad (5.84)$$

Such choices of  $\vec{M}$  give rise to integer RR fluxes as in eq. (5.30) that satisfy eq. (5.37), and we have gauge-fixed the center of  $SL(2, \mathbb{Z})$  by enforcing that  $M^3 > 0$ .

For each element  $\vec{M} \in V_M$ , let  $V_K^{(\vec{M})}$  be the set of integers  $\vec{K} \in \mathbb{Z}^3$  that satisfy eq. (5.38) for the given choice of  $\vec{M}$ . Enumerating these involves solving a homogeneous Diophantine equation of degree *two* in the variables  $(K_2, K_3) \in \mathbb{Z}^2$  subject to the constraints  $0 \leq -\vec{M}^t \vec{K} \leq 104$  and  $0 < p^i < 1$  with  $p^i := (\mathcal{K}_{ija} M^a)^{-1} K_j$ . This can be done efficiently using **Mathematica**.<sup>17</sup> The resulting set of flux integers in

$$V := \left\{ (\vec{M}, \vec{K}) \in V_M \times V_K^{(\vec{M})} \right\} \quad (5.85)$$

give rise to perturbatively flat vacua of the superpotential  $W_{\text{poly}}^{(0)}(z^i, \tau)$ , i.e.  $W_{\text{poly}}^{(0)}(z^i, \tau) = dW_{\text{poly}}^{(0)}(z^i, \tau) = 0$  along the loci where  $z^i = p^i \tau$ , compatible with the tadpole bound.

For each element of  $V$ , we stabilize the remaining light direction using the truncation of  $W_{\text{inst}}^{(0)}$  in (5.31) to leading order in the instanton expansion, i.e. we

---

<sup>17</sup>Note that quadratic Diophantine equations are solvable, in contrast to the generic case [307, 284].

approximate

$$W_{\text{inst}}^{(0)}(\tau) \approx A_{(1,0)} e^{2\pi i p^2 \tau} + A_{(0,1)} e^{2\pi i p^3 \tau}, \quad (5.86)$$

with

$$A_{(1,0)} := \frac{1}{(2\pi i)^2} \sum_j (jM^1 + M^2) n_{(i,1,0)}^0 = \frac{2880(M^1 + M^2)}{(2\pi i)^2}, \quad (5.87)$$

$$A_{(0,1)} := \frac{1}{(2\pi i)^2} \sum_j (jM^1 + M^3) n_{(i,0,1)}^0 = \frac{2(M^1 + 2M^3)}{(2\pi i)^2}. \quad (5.88)$$

The above superpotential has  $\partial_\tau W_{\text{inst}}^{(0)} = 0$  for

$$e^{2\pi i \tau} = \left( -\frac{A_{(0,1)} p^3}{A_{(1,0)} p^2} \right)^{\frac{1}{p^2 - p^3}}. \quad (5.89)$$

Generically, we have  $A_{(1,0)} \gg A_{(0,1)}$ , so one stabilizes at weak coupling,  $\text{Im}(\tau) > 1$ , if  $p^2 > p^3$ . If furthermore  $p^2 \approx p^3$ , then  $e^{2\pi i \tau}$  is in fact exponentially small.

Of course, the true F-term equations also contain the Kähler covariantization of the partial derivative  $\partial_\tau \rightarrow D_\tau = \partial_\tau + \partial_\tau K_{\text{eff}}$ , with effective Kähler potential obtained by evaluating (5.6) along the flat valley, i.e.

$$K_{\text{eff}}(\tau, \bar{\tau}) = -4 \ln \left( -i(\tau - \bar{\tau}) \right) + \mathcal{O} \left( \text{Im}(\tau)^{-3} \right) + \text{constant}. \quad (5.90)$$

For large  $\text{Im}(\tau)$  this gives a small correction to eq. (5.89), and even for relatively small values one still finds nearby vacua of the actual F-term equation.

We will consider only those fluxes in  $V$  for which the next-to-leading corrections to  $W_{\text{inst}}^{(0)}$  are suppressed at least at the 10% level relative to the leading terms in (5.86), and for which  $|z_{\text{cf}}| \ll |W_0| \ll 1$ . This leaves us with 696 vacua, for which we show the values of  $|W_0|$  and  $|z_{\text{cf}}|$  in Figure 5.4.<sup>18</sup> For most of these the Klebanov-

---

<sup>18</sup>Strictly speaking, each of these vacua again comes as a family because we have not specified the flux integer  $P$  which can be freely chosen in a fundamental domain of the conifold monodromy  $0 \leq P < |M|$ . Since it only affects the phase of the conifold modulus, and does not contribute to the D3-brane charge its value is of no relevance to us.



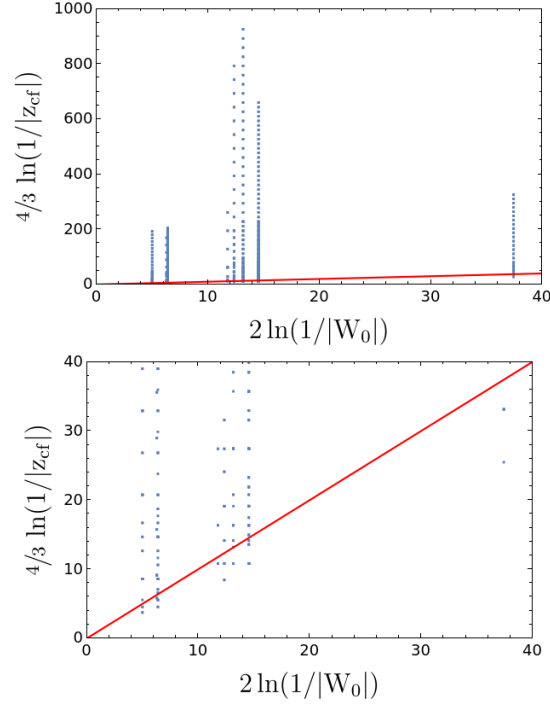


Figure 5.4: Scatter plots showing the values of  $2 \ln(1/|W_0|)$  and  $\frac{4}{3} \ln(1/|z_{cf}|)$  with diagonal in red indicating the critical region where the uplift potential of an anti-D3-brane would compete efficiently with KKL bulk moduli stabilization. Left: All vacua. Right: Only vacua that live close to the critical line.

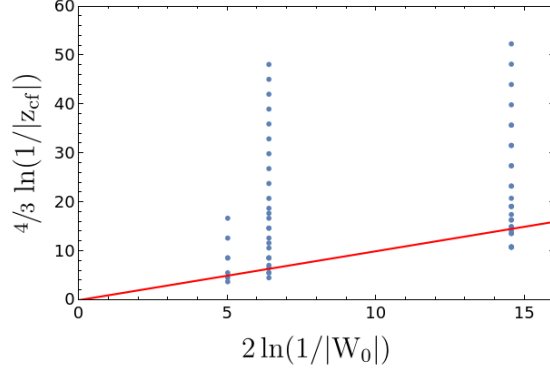


Figure 5.5: A scatter plot as in Figure 5.4 but showing only vacua with  $g_s M > 1$ .

Strassler sector has small 't Hooft coupling  $|g_s M| < 1$ , and the smallest value of  $W_0$  that we find is given by (see Table 5.1)

$$\min |W_0| \approx 7.4 \times 10^{-9}. \quad (5.91)$$

However, there are also 63 vacua with  $|g_s M| > 1$  that may somewhat marginally live in the ten-dimensional supergravity regime.<sup>19</sup> We find a maximum value (see Table 5.1)

$$\max |g_s M| \approx 2.8. \quad (5.92)$$

The 63 vacua with potential supergravity throats come in three families with flux superpotentials  $|W_0| \approx \{6.9 \times 10^{-4}, 4.1 \times 10^{-2}, 8.1 \times 10^{-2}\}$ , but with vastly different values of  $|z_{cf}|$ . We have checked that the neglected two-instanton corrections are suppressed by a relative factor of order  $|W_0|$  and the three-instanton corrections are suppressed by further such factors. We show the values of  $|W_0|$  and  $|z_{cf}|$  in Figure 5.5.

Let us walk through the stabilization steps for one of these vacua. We consider  $\vec{M} = (4, -8, 8)$  and  $\vec{K} = (-8, 3, -6)$ . These correspond to the family of flux

<sup>19</sup>Although it is well-known that  $g_s M \gg 1$  is sufficient for the infrared region of the throat to be weakly curved in string units, we are not aware of a specific numerical threshold  $(g_s M)_{\min}$  that demarcates the region below which the supergravity approximation fails. Determining such a threshold would be worthwhile.

vectors

$$\vec{f} = (3, P, -4, 0, 0, 4, -8, 8)^t, \quad \vec{h} = (0, -8, 3, -6, 0, 0, 0, 0)^t, \quad (5.93)$$

and we may choose  $P = 0$ . We have

$$Q_{\text{flux}}^{D3} = \frac{1}{2} \vec{f}^t \Sigma \vec{h} = -\frac{1}{2} \vec{M}^t \vec{K} = 52, \quad (5.94)$$

so we exactly saturate the tadpole bound. Furthermore,

$$N_{ij} := \sum_a \mathcal{K}_{ija} M^a = 8 \begin{pmatrix} 1 & -1 \\ -1 & 0 \end{pmatrix}_{ij}, \quad p^i := (N^{-1})^{ij} K_j = \frac{3}{8} \begin{pmatrix} 2 \\ 1 \end{pmatrix}^i, \quad p^i K_i = 0. \quad (5.95)$$

Thus, we stabilize the two bulk moduli  $z^{2,3}$  and the dilaton along the flat valley

$$z^i = \frac{3}{8} \tau \begin{pmatrix} 2 \\ 1 \end{pmatrix}^i. \quad (5.96)$$

In the basis  $(\tau, z^2, z^3)$ , the matrix of second derivatives of the superpotential  $W_{\text{poly}}^{(0)}(\tau, z^i)$  reads

$$\partial^2 W_{\text{poly}}^{(0)}(\tau, z^i) = \begin{pmatrix} 0 & -K_j \\ -K_i & N_{ij} \end{pmatrix} = \begin{pmatrix} 0 & -3 & 6 \\ -3 & 8 & -8 \\ 6 & -8 & 0 \end{pmatrix}, \quad (5.97)$$

which has eigenvalues  $(0, 4 \pm 5\sqrt{5})$ . Thus, we may indeed integrate out the field directions away from the flat valley, and consider the effective theory along the valley in the next step. The effective superpotential  $W_{\text{inst}}^{(0)}$  takes the form

$$W_{\text{inst}}^{(0)}(\tau) \approx A_{(1,0)} e^{2\pi i \frac{3}{4} \tau} + A_{(0,1)} e^{2\pi i \frac{3}{8} \tau}, \quad (5.98)$$

with

$$A_{(1,0)} = \frac{2880(M^1 + M^2)}{(2\pi i)^2} = \frac{-11520}{(2\pi i)^2}, \quad A_{(0,1)} = \frac{2(M^1 + 2M^3)}{(2\pi i)^2} = \frac{40}{(2\pi i)^2}, \quad (5.99)$$

so we stabilize  $\tau$  near

$$e^{2\pi i\tau_0} = \left( \frac{40 \cdot 3/8}{11520 \cdot 3/4} \right)^{\frac{8}{3}} \approx 4.4 \times 10^{-8}. \quad (5.100)$$

Replacing  $\partial_\tau \rightarrow D_\tau$  shifts this slightly to  $g_s \approx 0.38$ . Furthermore, the vacuum value of the superpotential is

$$|W_0| \approx \sqrt{\frac{2}{\pi}} \left| W_{\text{inst}}^{(0)}(\tau_0) \right| \approx 6.9 \times 10^{-4}, \quad (5.101)$$

neglecting the contribution from  $W^{(1)}_{z_{\text{cf}}}$ . The neglected two-instanton corrections are suppressed by a relative  $\mathcal{O}(10^{-3})$  factor and the three-instanton corrections are suppressed by a further  $\mathcal{O}(10^{-3})$  factor, so the value of  $|W_0|$  is a good measure of control of the instanton expansion.

In the final step, we stabilize the conifold modulus  $z_{\text{cf}}$  with the superpotential  $W_{\text{cf}}(z_{\text{cf}})$ . The conifold fluxes are

$$K' := K_1 - M^a \mathcal{K}_{1ai} p^i = -5, \quad M := -M^1 = -4, \quad (5.102)$$

so we stabilize the conifold modulus at

$$|z_{\text{cf}}| = \frac{1}{2\pi} e^{-2\pi \frac{K'}{2g_s M}} \approx 5 \times 10^{-6}. \quad (5.103)$$

The Klebanov-Strassler theory is (marginally) in its supergravity regime with somewhat large 't Hooft coupling  $g_s M \approx 1.5$ , and the infrared warp factor is of order

$$e^{2A}|_{\text{min}} \sim |z_{\text{cf}}|^{\frac{2}{3}} \approx 2.9 \times 10^{-4}. \quad (5.104)$$

We note that  $e^{2A}|_{\text{min}}$  and  $|W_0|$  are of the same order, as one would want for a KKLT uplift from including an anti-D3-brane in the warped region. In Table 5.1 we list some interesting flux vacua.

$\vec{M}$	$\vec{K}$	$ W_0 $	$ z_{\text{cf}} $	$\frac{ z_{\text{cf}} ^{2/3} -  W_0 }{ W_0 }$	$g_s M$	$\varepsilon$
(4, -8, 10)	(-6, 3, -4)	$7.4 \times 10^{-9}$	$5.4 \times 10^{-14}$	-0.8	0.6	$\sim 10^{-7}$
(8, -12, 6)	(-5, 1, -2)	$6.9 \times 10^{-4}$	$1.4 \times 10^{-5}$	-0.2	1.0	$\sim 10^{-3}$
(-8, 4, 12)	(5, 1, -4)	$4.1 \times 10^{-2}$	$5.2 \times 10^{-3}$	-0.3	2.8	$4 \times 10^{-2}$
(-14, 6, 27)	(4, 1, -2)	$1.4 \times 10^{-3}$	$5.3 \times 10^{-5}$	0.03	0.9	$\sim 10^{-3}$

Table 5.1: Some interesting vacua. First line: smallest  $W_0$ . Second line: smallest  $W_0$  with  $g_s M > 1$ . Third line: largest  $g_s M$ . Fourth line: best alignment between  $z_{\text{cf}}^{2/3}$  and  $W_0$ . The parameter  $\varepsilon$  is the magnitude of the neglected two-instanton contributions to the superpotential relative to the retained one-instanton terms.

## 5.5 Discussion

In this work we have demonstrated that the mechanism of [92] for constructing flux vacua of type IIB string theory with exponentially small values of the flux superpotential can be applied not just at large complex structure, as in [92], but also near conifold points in moduli space. We laid out a procedure for finding *conifold vacua* in which the flux superpotential is small.

The key challenge was to compute, and then to cancel, an order-one contribution to the superpotential coming from flux on the conifold cycles. To accomplish this we considered the case in which the shrinking three-cycle of the conifold in a Calabi-Yau  $\tilde{X}$  is mirror to a shrinking curve in the mirror threefold  $X$ . Computing the prepotential for the complex structure moduli space of  $\tilde{X}$ , and then resumming the terms corresponding to type IIA worldsheet instantons wrapping the shrinking curve in  $X$ , we obtained the flux superpotential for type IIB compactification on  $\tilde{X}$ , including the term resulting from fluxes on the shrinking three-cycle of the conifold. We then applied the mechanism of [92] to find fluxes for which the total flux superpotential, including the conifold term, is exponentially small.

We illustrated our approach in flux compactification of type IIB string theory on an orientifold of a Calabi-Yau threefold  $\tilde{X}$  with  $h^{1,1}(\tilde{X}) = 99$  and  $h^{2,1}(\tilde{X}) = 3$ . To

analyze  $\tilde{X}$  and its orientifold we made heavy use of the Greene-Plesser construction:  $\tilde{X}$  is the resolution of the orbifold  $X/G$ , with  $X$  the mirror of  $\tilde{X}$ , and  $G \simeq \mathbb{Z}_6 \times \mathbb{Z}_6$  the Greene-Plesser group of  $X$ . We found an O3/O7 orientifold involution  $\tilde{\mathcal{I}}$  of  $\tilde{X}$  leading to a D3-brane tadpole  $-Q = 52$ , allowing reasonable freedom in choosing fluxes. We found many flux vacua and laid out in detail a flux choice for which  $|W_0| \approx 7 \times 10^{-4}$ , the conifold modulus  $z_{\text{cf}}$  is stabilized at  $|z_{\text{cf}}| \approx 5 \times 10^{-6}$ , and the Klebanov-Strassler throat has  $g_s M \approx 1.5$ .

As classical flux vacua, our examples are rather well-controlled. However, they are just a first step toward finding parametrically large Klebanov-Strassler throats in vacua with small values of the flux superpotential, and subsequently achieving Kähler moduli stabilization and a metastable uplift to de Sitter space. Indeed, in our examples ten-dimensional supergravity is at best marginally valid near the tip of the throat, and at the same time the significant number of Kähler moduli makes stabilization computationally challenging. We believe that these limitations have no deep relationship to our mechanism, but are instead accidental properties of the examples. After all, we would expect to have to search through many candidate geometries to find one in which the flux superpotential is exponentially small, a throat region is parametrically large, and the numbers of moduli are small enough for simultaneous computational control of the geometry and its mirror. Here we have examined one particularly tractable orientifold with  $h^{2,1}(\tilde{X}) = 3$ , and already finding therein a foundation for a parametrically controlled KKLT de Sitter vacuum would have been surprising to us.

One further limitation, however, is intrinsic to our mechanism, and will hold in all examples: at least one linear combination of the string coupling and the complex structure moduli remains rather light, with a mass of the same order as that of the

Kähler moduli. As noted in [92], this is a departure from the original scenario of [215]. In the present context of conifold vacua, an important consequence is that the warp factor at the tip of the Klebanov-Strassler throat is set by the vev of a relatively light field.<sup>20</sup> Metastable supersymmetry breaking in the presence of such light moduli will require further analysis.

Systematically enumerating conifold vacua in a much larger class of geometries will be very informative, but we leave this for future work.

---

<sup>20</sup>Qualitatively similar results have been emphasized in [55, 32], though the details and the causes are very different here.

CHAPTER 6

ENTANGLEMENT ENTROPY AND EDGE MODES IN  
TOPOLOGICAL STRING THEORY: I

**Abstract**<sup>1</sup>

Progress in identifying the bulk microstate interpretation of the Ryu-Takayanagi formula requires understanding how to define entanglement entropy in the bulk closed string theory. Unfortunately, entanglement and Hilbert space factorization remains poorly understood in string theory. As a toy model for AdS/CFT, we study the entanglement entropy of closed strings in the topological A-model in the context of Gopakumar-Vafa duality. We will present our results in two separate papers. In this work, we consider the bulk closed string theory on the resolved conifold and give a self-consistent factorization of the closed string Hilbert space using extended TQFT methods. We incorporate our factorization map into a Frobenius algebra describing the fusion and splitting of Calabi-Yau manifolds, and find string edge modes transforming under a  $q$ -deformed surface symmetry group. We define a string theory analogue of the Hartle-Hawking state and give a canonical calculation of its entanglement entropy from the reduced density matrix. Our result matches with the geometrical replica trick calculation on the resolved conifold, as well as a dual Chern-Simons theory calculation which will appear in our next paper [117]. We find a realization of the Susskind-Uglum proposal identifying the entanglement entropy of closed strings with the thermal entropy of open strings ending on entanglement branes. We also comment on the BPS microstate counting of the entanglement entropy. Finally we relate the nonlocal

---

<sup>1</sup>This chapter is published as W. Donnelly, Y. Jiang, M. Kim, G. Wong, “Entanglement entropy and edge modes in topological string theory: I,” [arxiv:2010.15737 [hep-th]].



aspects of our factorization map to analogous phenomenon recently found in JT gravity.

## 6.1 Introduction

The holographic principle states that the number of degrees of freedom in a spacetime region scales with the area of its boundary, and is exemplified by the Bekenstein-Hawking (BH) entropy formula. In the context of the AdS/CFT correspondence [252, 174, 348], the Ryu-Takayanagi (RT) formula [303] generalizes BH entropy to extremal surfaces in AdS which are anchored to the asymptotic boundary, and identifies the leading area term with the leading  $\mathcal{O}(N^2)$  contribution to the entanglement entropy of the boundary CFT [253, 138]. Given a factorization of the CFT Hilbert space<sup>2</sup>, this implies that the bulk extremal area is capturing the degrees of freedom for quantum states of a boundary subregion. However, the bulk micro-state interpretation of the entropy remains mysterious. One aspect of this puzzle is that the bulk supergravity only contains  $\mathcal{O}(1)$  number of fields, while the classical area term is of  $\mathcal{O}(N^2)$  [246, 317]. Where does this large number of degrees of freedom come from?

We want to understand this question directly in the bulk from the microscopic string theory. In the case of BH entropy, Susskind and Uglum [315] proposed that the horizon area measures the entanglement entropy of closed strings across the horizon. In the tree level replica trick calculation, the entanglement entropy is due to a sphere diagram which intersects the entangling surface, representing

---

<sup>2</sup>Even though it is quite plausible, such a factorization has never been carefully worked out. However for rational CFT's, the question of Hilbert space factorization and edge modes was recently addressed in [204].

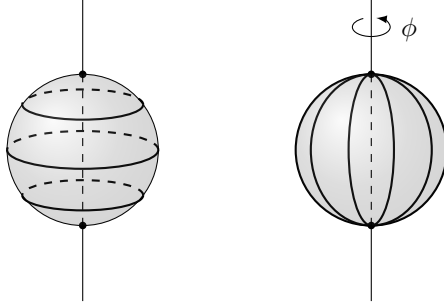


Figure 6.1: The partition function of the  $A$ -model on a line bundle over  $S^2$  has two interpretations. In the closed string channel (left), it represents the overlap  $\langle HH^* | HH \rangle$  between the Hartle-Hawking state and its orientation reversal. In the open string channel (right), it represents a trace in the Hilbert space of open strings. Figure borrowed from Ref. [122].

closed strings which are cut into open strings as depicted in figure 6.1. What distinguishes string theory from quantum field theory (QFT) is that this tree level closed string diagram has a one-loop open string interpretation, suggesting a trace over a quantum Hilbert space. This led Susskind and Uglum to conclude that the BH entropy counts microstates of open string endpoints anchored on the horizon. In the language of Ref. [122] the horizon is wrapped by *entanglement branes*, which gives rise to entanglement edge modes responsible for the large  $\mathcal{O}(1/g_{\text{string}}^2) = \mathcal{O}(1/G_{\text{Newton}})$  entropy. Given the analogy between RT formula and BH entropy, it is tempting to apply this proposal to give a canonical interpretation of the RT entropy from the bulk string theory.

While the seminal work [313] succeeded in reproducing the BH entropy for five dimensional extremal Reissner-Nordstrom black holes via counting BPS microstates in string theory, little is known about how to compute entanglement entropy and the associated Hilbert space factorization in string theory. In field theory, the replica trick as computed by the Euclidean path integral offers a shortcut that circumvents the factorization problem. However a naive application to string theory requires putting an  $n$ -sheeted cover in the target space, which requires an

off-shell formulation of string theory that is not well understood.<sup>3</sup> Since string theory is well-defined in the presence of conical deficits, the references [84, 182, 351] attempted worldsheet calculations of entanglement entropy using an “orbifold” replica trick. However these calculations do not capture the sphere contribution to the entanglement entropy and the associated edge modes.<sup>4</sup> An attempt at an off-shell calculation was made in [24] via Witten’s open string field theory. They showed that the symplectic structure of the string field theory in a subregion implies that pure gauge (BRST) modes become dynamical edge modes at the entanglement cut, but did not go beyond this classical analysis.

Edge modes are boundary degrees of freedom introduced to give a self consistent description of a subsystem. In string theory they appear due to the need to cut strings at the point where the string worldsheet intersects the entangling surface, leaving configurations where the strings end at the entangling surface. A similar phenomenon occurs in Maxwell theory, where the edge modes can be thought of as configurations of “electric strings” with their endpoints anchored to the entangling surface [64]. As in string field theory, the presence of edge modes can be deduced from the symplectic structure of a subregion [116]. These edge modes give an important contribution to the entanglement entropy [120, 121], in particular reproducing the contact interaction of [213] which may be viewed as a field theory limit of a string worldsheet intersecting the entangling surface. However, these field theory calculations can only capture the one-loop correction to the entropy, corresponding to toroidal worldsheets.

In this work, we initiate a program to realize the Susskind-Uglum proposal

---

<sup>3</sup>For the closed bosonic string, such an off-shell formulation was proposed by Tseytlin [322] and applied by Susskind and Uglum in their proposal.

<sup>4</sup>The sphere contribution vanishes at the orbifold point, and hence remains zero when analytically continued in the replica number.

for the topological A-model string in the context of Gopakumar-Vafa duality (GV duality) [158, 159, 161, 160, 285, 6, 91], which can be viewed as a topological version of AdS/CFT. The role of the bulk string theory is played by the topological A-model closed string on a resolved conifold geometry [67]. This is a six-dimensional Calabi-Yau manifold which is a rank-2 bundle over a sphere of complexified area  $t$ . The boundary CFT is replaced by the large- $N$  limit of  $U(N)$  Chern-Simons theory, with gauge coupling  $g_{cs} = \frac{2\pi}{k+N}$  and 't Hooft parameter  $ig_{cs}N$ . The closed string coupling  $g_s$  and the target space modulus  $t$  in the bulk are related to the parameters of the CS theory by

$$\begin{aligned} g_s &= g_{cs} = \frac{2\pi}{k+N}, \\ t &= \frac{2\pi i N}{N+k}. \end{aligned} \tag{6.1}$$

The advantage of studying the A-model string is that it provides a setting similar to AdS/CFT where we can give precise accounting of edge modes and their entanglement entropy on both sides of the duality. In this paper, we will focus on the closed string theory and define its Hilbert space via the categorical description of the A-model as a topological quantum field theory (TQFT) [62, 8, 63]. This allows us to apply the framework developed in [122] to define the factorization of the string theory Hilbert space purely in terms of the categorical data of an open-closed TQFT. For the A-model, the relevant TQFT can be viewed as coming from a large  $N$ , chiral limit of  $q$ -deformed 2D Yang-Mills theory (2DYM)[9].<sup>5</sup> Using the TQFT description, we propose a factorization of the closed string Hilbert space that is consistent with the entanglement entropy as computed by the replica trick. For the Hartle-Hawking state of the closed string theory, we find that the

---

<sup>5</sup>The  $q$ -deformed 2D Yang-Mills theory has been proposed as a non-chiral UV completion for the closed topological string theory, and in the discussion section we will discuss the implications of this completion and its connection to wormholes and baby universes.

entanglement entropy can be interpreted as the thermal entropy of open strings, with the aforementioned  $\mathcal{O}(1/g_s^2)$  scaling arising from the counting of Chan-Paton factors.

As in [122], these Chan-Paton factors are the entanglement edge modes of the closed string theory, which we will interpret as coming from the stacks of entanglement branes at the entangling surface. Interestingly, the coupling of these branes to the string endpoints endows them with nontrivial braiding statistics. The corresponding edge modes thus behave like anyons and transform under a quantum group symmetry, which plays the role of the surface symmetry group (c.f. [116]) for the topological string theory.

In the follow-up paper [117], we will give a dual Chern-Simons gauge theory description of the entanglement entropy and the corresponding edge modes, thus giving an independent check of our closed string calculations. In the closed string theory, we will define a Hartle-Hawking state obtained by summing over worldsheets ending on a stack of D-branes. By applying GV duality, we will show that there is a *local* mapping between these worldsheets and unknotted Wilson loops in the Chern-Simons theory, so that cutting the worldsheets correspond to cutting the Wilson loops. In gauge theory, the entanglement entropy  $\delta S$  due to cutting a Wilson loop  $W_R$  in a representation  $R$  is [244]

$$\delta S = (1 - n\partial_n) \log \langle W_R \rangle = \langle H_{\text{mod}} \rangle_{W_R} + \log \langle W_R \rangle. \quad (6.2)$$

This is the entanglement entropy relative to the vacuum state, also referred to as the defect entropy [209, 210]. Here  $\langle H_{\text{mod}} \rangle_{W_R}$  is the expectation value of the modular Hamiltonian in the presence of the Wilson loop, which vanishes in Chern-Simons theory. Thus, the defect entanglement entropy associated with the Wilson loop is just  $\log \langle W_R \rangle$ . For the unknot,  $\langle W_R \rangle$  is precisely the quantum dimension

which captures the topological degeneracy associated with the fusion Hilbert space of an anyon. By superposing such Wilson loops in all possible representations, we will reproduce the string theory Hartle-Hawking state as well as its entanglement entropy in an appropriate large- $N$  limit of the quantum dimensions. This limit gives a precise relation between the closed string edge modes and the anyons of Chern-Simons theory.

Our description of the relation between string worldsheets and Wilson loops has a direct analogue in AdS/CFT [285, 156, 133]. A Wilson loop in the CFT in the fundamental representation is dual to a probe string worldsheet in the bulk geometry, and equation (6.2) was used in [244] to compute its entanglement entropy. In this calculation the entanglement entropy is  $\mathcal{O}(\log(1/g_s))$ , which is large at weak coupling but still much smaller than the  $\mathcal{O}(1/g_s^2)$  RT entropy.

A similar phenomenon was noted in Refs. [122] for the string dual to 2DYM — any state with  $\mathcal{O}(1)$  number of strings has an entanglement entropy of  $\mathcal{O}(\log(1/g_s))$ . However, for the Hartle-Hawking state, competition between the Chan-Paton factors and the string action leads to a saddle point with  $\mathcal{O}(1/g_s^2)$  strings. The counting of Chan-Paton factors at this saddle point leads to an  $\mathcal{O}(1/g_s^2)$  entanglement entropy that is reminiscent of the scaling of “spacetime” entropy [119].

Similarly, in AdS/CFT, in the presence of Wilson loops corresponding to “large representations” with order  $\mathcal{O}(N^2) = \mathcal{O}(1/g_s^2)$  number of boxes, the dual branes backreact on the geometry. In this case the defect entropy can be computed using the RT formula in the new background, and the  $\mathcal{O}(N^2) = \mathcal{O}(1/g_s^2)$  entropy is recovered [10, 149]. In our computation, the resolved conifold itself is an emergent geometry arising from the superposition of a large number of fundamental strings,

dual to a large number of Wilson loops in the dual gauge theory. By accounting for the contributions from the entire superposition of states, our entropy calculation captures the entanglement which “makes up the spacetime” itself.

Finally, we comment on how our work differs from the recent work [202] which also studied entanglement in the A-model string theory. The essential difference is twofold: first our choice of state cuts through the base manifold  $S^2$  where the closed string worldsheets wrap, whereas the state defined in [202] does not. As a result, our entanglement cut will directly probe the string edge modes that were not revealed by their computation. Second, rather than relying solely on the dual Chern-Simons field theory, we give a self-consistent Hilbert space factorization and entropy calculation on the closed string side.

## 6.2 Summary, overview of GV duality and the Hartle-Hawking state

Here we give a summary of our paper, starting with an overview of the GV duality and a description of the closed string state whose factorization and entanglement entropy we will be studying.

### 6.2.1 Summary of the GV duality

Like AdS/CFT, the Gopakumar-Vafa duality is an open-closed string duality. Figure 6.2 shows the 6D target space geometries for the closed and open strings. These can be conveniently presented as two different ways to resolve the singularity of

the conifold geometry, which is a cone over  $S^3 \times S^2$ . The closed strings live on the resolved conifold where the conical tip is resolved into an  $S^2$ , whereas the open strings live on the deformed conifold, where the tip is deformed into an  $S^3$ . The defining equations and details of the geometries are summarized in §D.2.

An intuitive way to understand the GV duality is via ‘t Hooft’s argument for the emergence of string theory from gauge theory [316]. ‘t Hooft observed that in the large  $N$  limit, the Feynman diagrams of a  $U(N)$  gauge theory can be represented by ribbon graphs which should be viewed as Riemann surfaces with holes. These are open string worldsheets, corresponding to a free energy expansion in which the gauge coupling  $g_{\text{YM}}^2$  plays the role of the string coupling  $g_s$ :

$$F = \sum_{g=0}^{\infty} \sum_{h=1}^{\infty} (g_{\text{YM}}^2)^{2g-2+h} N^h F_{g,h}. \quad (6.3)$$

Here  $g$  is the genus of the worldsheet,  $h$  is the number of holes, and  $N$  accounts for Chan-Paton factors of  $U(N)$ . The dual closed string theory is obtained by summing over holes, giving

$$\begin{aligned} F &= \sum_{g=0}^{\infty} (g_{\text{YM}}^2)^{2g-2} F_g(t), \\ F_g(t) &= \sum_{h=1}^{\infty} F_{g,h} t^h, \quad t = g_{\text{YM}}^2 N. \end{aligned} \quad (6.4)$$

Here  $t$  is the ‘t Hooft coupling of the gauge theory, which plays the role of a target space modulus for the closed string.

In the ‘t Hooft paradigm, the gauge theory which is relevant to GV duality is  $U(N)$  Chern-Simons theory on  $S^3$ . A direct  $1/N$  expansion of the Chern-Simons partition function leads to the connected amplitudes  $F_{g,h}$  of the open topological string on the deformed conifold, which is the same as the cotangent bundle  $T^*S^3$  [161]. In this geometry the open string degenerates into a pointlike object and



is restricted to live on the base  $S^3$ . These degenerate Riemann surfaces of zero area correspond precisely to the ribbon graphs of the gauge theory. Chern-Simons theory is thus the string field theory of these open strings [343]. Closed topological strings wrap minimal volume representative among homologous 2-cycles [340, 349]; in the resolved conifold, the only such 2-cycle is the  $S^2$  at the tip. Open topological strings end on Lagrangian 3-cycles, and in the GV duality, they end on the base  $S^3$  of the deformed conifold. Similar to AdS/CFT, the open string theory with a large  $N$  number of branes on  $S^3$  is dual to a closed string theory where the branes have been dissolved and replaced by a nontrivial flux  $t = ig_S N$  of the  $B$  field through the  $S^2$ .

The dual closed string theory was derived from the worldsheet by directly summing over the holes in [285]. The resulting theory is the A-model closed string on the resolved conifold, which should be viewed as the gravitational dual of Chern-Simons theory on  $S^3$ . While the resolved conifold is locally a direct product, globally it has a nontrivial fiber bundle structure over the base  $S^2$ . Denote by  $\mathcal{O}(n)$  the complex line bundle over  $S^2$  with Chern class  $n$ . The resolved conifold can then be identified with the rank-2 vector bundle:

$$\mathcal{O}(-1) \oplus \mathcal{O}(-1) \rightarrow S^2. \quad (6.5)$$

More generally we can consider A-model closed strings on geometries of the form

$$X = L_1 \oplus L_2 \rightarrow \mathcal{S}, \quad (6.6)$$

where  $\mathcal{S}$  is a general Riemann surface, and  $L_1, L_2$  are line bundles with Chern classes  $(k_1, k_2)$ .<sup>6</sup> It was shown in [63] that the all genus amplitudes on such vector

---

<sup>6</sup>Strictly speaking, when  $\mathcal{S}$  is contractible, the Chern class  $c_1 \in H^2(\mathcal{S})$  is always trivial. Hence, the Chern class cannot keep track of the bundle data required for the gluing. For a manifold with boundary, such as a disk, we instead use the euler class  $e(L) \in H_2(\mathcal{S}, \partial\mathcal{S})$  which equals to the Chern class upon gluing.

bundles satisfy the gluing rules of a TQFT, which can be viewed as the string field theory for the A-model. Formally, the A-model TQFT is a functor from the category  $2\text{Cob}^{L_1, L_2}$  of 2-dimensional cobordisms with line bundles to the category of vector spaces. Physically, it can be interpreted as an appropriate large  $N$  limit of  $q$ -deformed 2D Yang Mills on the base manifold  $\mathcal{S}$ . Figure 6.2 gives a summary of the geometries and target space theories on both sides of the duality.


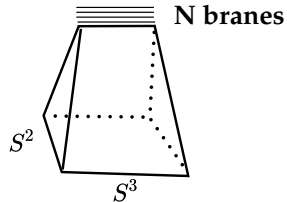
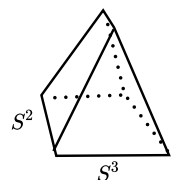
	<b>Geometric transition</b> 	
	<b>Open A model string</b> $(g_s, N)$	<b>Closed A model string</b> $(g_s, t)$
<b>Target space geometry</b>	<b>Deformed Conifold</b> 	<b>Resolved Conifold</b> 
<b>Target space theory</b>	<b>U(N) Chern Simons theory</b> <b>on <math>S^3</math></b>	<b>A Model TQFT</b>

Figure 6.2: Gopakumar duality relates closed A-model string on the resolved conifold to the open A-model string on the deformed conifold

### 6.2.2 The Hartle Hawking state in string theory

In QFT, quantum states live on a codimension-1 time slice  $\Sigma$ . Geometric states are defined by the Euclidean path integral on a manifold  $\mathcal{M}$  with  $\partial\mathcal{M} = \Sigma$ . In particular, the Hartle-Hawking state  $|HH\rangle$  is defined cutting the spacetime geometry at a moment of time reflection symmetry[181]. Thus the QFT partition

function can be expressed as the overlap<sup>7</sup>

$$Z_{QFT} = \langle HH|HH \rangle. \quad (6.7)$$

However, in closed string theories the fundamental degrees of freedoms are closed loops, so the field theory construction of geometric states doesn't strictly apply. In the first quantized theory, a single string state is a wavefunctional on the space of loops

$$\Psi[X^\mu(\sigma)], \quad X^\mu(\sigma) \in \mathcal{F}. \quad (6.8)$$

Here, elements of  $\mathcal{F}$  are closed string configurations specified by the embedding map  $X^\mu(\sigma)$ , with  $\sigma \in S^1$ . By direct analogy with QFT, the operators of the second quantized theory are obtained by promoting  $\Psi$  to a string field

$$\hat{\Psi} = \hat{\Psi}[X^\mu(\sigma)], \quad (6.9)$$

which is an operator-valued function on the loop space  $\mathcal{F}$  of the target manifold. This is in contrast to QFT where the second-quantized field operators are functions of spacetime points  $X^\mu$ . Thus the degrees of freedom in string theory are labelled by elements of the loop space  $\mathcal{F}$ , and the specification of time slices refers to subsets of  $\mathcal{F}$ .

Similarly, the second quantized string Hilbert space is defined on a time slice of  $\mathcal{F}$  rather than on a time slice  $\Sigma$  of spacetime [338, 337, 355]. Nevertheless, we can associate a string Hilbert space  $\mathcal{H}_\Sigma$  with  $\Sigma$  by a choice of mapping between time slices

$$\Sigma \rightarrow \mathcal{F}_\Sigma \subset \mathcal{F}. \quad (6.10)$$

---

<sup>7</sup>Following conventions in TQFT, the geometric dual  $\langle M|$  denotes the amplitude on the manifold  $M$  with orientation reversed. The bracket is then just a gluing of manifolds, viewed as a natural pairing. In particular a TQFT does not assume a Hermitian inner product.

For example, if  $\Sigma$  is given by  $X^0 = 0$ , we could define a time slice in the loop space by

$$\mathcal{F}_\Sigma = \{X^\mu(\sigma) : X^0(\sigma) = 0, \sigma \in S^1\}. \quad (6.11)$$

However, as noted in [24], the mapping between  $\Sigma$  and  $\mathcal{F}_\Sigma$  is not unique; for example, we can restrict only the center of mass of the string to live in  $\Sigma$ .

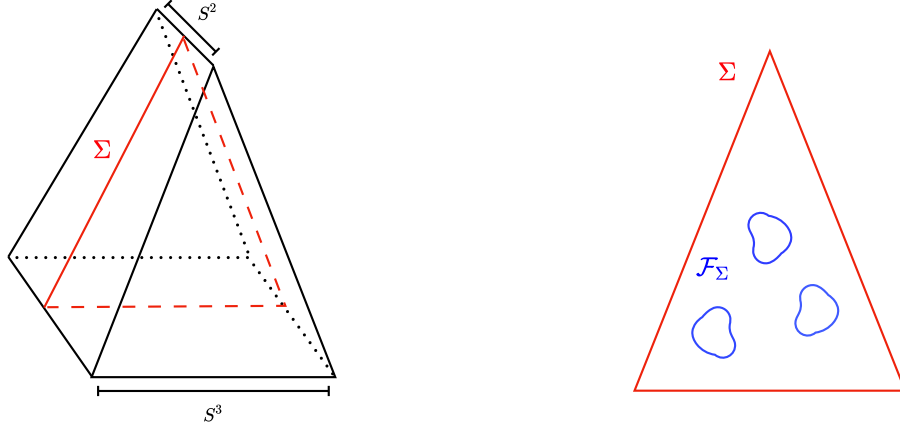


Figure 6.3: The left figure shows the codimension-1 slice  $\Sigma$  of the resolved conifold where a QFT state would be defined. In the closed string theory, the analogue of a time slice is a set  $\mathcal{F}_\Sigma$  of loops configurations associated with  $\Sigma$ . For the A-model string, we will restrict these loop configurations to lie in a Lagrangian submanifold  $\mathcal{L} \subset \Sigma$ . The string wavefunctional assigns an amplitude to each configuration of such loops.

To define the A-model Hilbert space, we choose  $\Sigma$  to be the 5-dimensional region of the resolved conifold which intersects the base  $S^2$  along the equator  $C$ . This represents a symmetric cut through the target space geometry, and we would like to define the string theory analog of the Hartle-Hawking state on  $\Sigma$ . We choose  $\mathcal{F}_\Sigma$  to consist of noncontractible string loops living on a Lagrangian submanifold  $\mathcal{L} \subset \Sigma$ . As shown in figure 6.3, this is a three-dimensional manifold with topology  $\mathbb{C} \times S^1$  and its defining equation is given in (D.26) of appendix D.2. The topological vertex formalism [4, 263] can then be applied to define a string wavefunctional on  $\mathcal{F}_\Sigma$  which gives a string theory analog of the Hartle-Hawking state.

The topological vertex encodes the A-model amplitude on  $\mathbb{C}^3$  with three stacks of D-branes. It is a basic building block for partition functions on toric Calabi-Yau manifolds, such as the resolved conifold. To compute the partition functions of more complicated geometries, one can glue the topological vertices by brane-antibrane annihilation. This gluing procedure allows us to cut and sew target space geometries as in Euclidean path integrals. In particular, we will define the Hartle-Hawking state  $|HH\rangle$  using the topological vertex with a single stack of nontrivial D-branes on  $\mathcal{L}$ . Denoting by  $\langle HH^*|$  the opposite vertex with antibranes inserted and opposite orientation, it can be shown that

$$Z = \langle HH^* | HH \rangle, \quad (6.12)$$

where  $Z$  is the partition function on the resolved conifold. Note that that  $Z$  is not a real norm of a state as in the QFT definition (6.7). This is due to the holomorphic nature of the A model partition function, which is analogous to a chiral half of a conformal block. From the point of view of  $2\text{Cob}^{L_1, L_2}$ , the HH state is given by a hemisphere with  $(0, -1)$  Chern class, while  $\langle HH^*|$  is the oppositely oriented hemisphere with  $(-1, 0)$  Chern class:

$$|HH\rangle = \begin{matrix} (0, -1) \\ \text{hemisphere} \end{matrix}, \quad \langle HH^*| = \begin{matrix} (-1, 0) \\ \text{hemisphere} \end{matrix}. \quad (6.13)$$

In our next paper we will derive the Chern-Simons dual of the HH state, which lives on the surface of a torus containing a specific superposition of Wilson loops inside.

### 6.2.3 Outline of the paper

Our paper is organized as follows. We start with closed topological A model in section 3 and give a chiral boson description of the Hilbert space. Using the

topological vertex formalism, we obtain the Hartle-Hawking state of topological A model on the resolved conifold and compute its entanglement entropy using the geometric replica trick preserving the Calabi-Yau condition. We will also introduce the entanglement brane boundary state as a coherent state of chiral bosons.

In sections 4-5, we define a factorization of the closed string Hilbert space following the framework introduced in [123]. We first review the relation between extended Hilbert space factorization and extensions of closed TQFT. We then present the A-model closed TQFT [63] and propose an extension compatible with the entanglement brane axiom introduced in [123]. The essential new ingredient in this factorization is the presence of an emergent quantum group symmetry which acts on the string edge modes. Compatibility with this symmetry leads us to modify the usual definition of Von Neumann entropy to:

$$S = -\mathrm{tr}_q(\rho \log \rho) = -\mathrm{tr}(D\rho \log \rho), \quad (6.14)$$

where the quantum trace  $\mathrm{tr}_q$  is defined with the insertion of the operator  $D$ , the Drinfeld element of a quantum group. We find that this definition of the entropy in the factorized Hilbert space agrees with the replica trick calculation in section 3. This  $q$ -deformed notion of entropy has been studied previously in the context of quantum group invariant spin chains and non-unitary quantum systems [81, 295].  $D$  is also the direct analogue of the defect operator introduced in [208]<sup>8</sup> to factorize the Hilbert space of JT gravity and in our case it is completely determined by the surface symmetry group. In the end of section 5 we will revisit the geometric calculation of the replica trick and show how the preservation of the Calabi-Yau condition is enforced by the quantum trace. We will also show that the entanglement entropy has a natural interpretation in terms of the BPS microstate counting.

---

<sup>8</sup> $\rho$  is equivalent to  $\tilde{\rho}$  in [208].

Finally, in the discussion section, we will comment on the relation between our work and factorization in JT gravity, particularly as it relates to the quantum group symmetry.

### **6.3 The closed string Hilbert space and entanglement entropy from the replica trick**

Topological string theory is a broad subject, so we will not try to give an extensive review in this paper. Nevertheless we give a short review on topological sigma model in Appendix D.1. In a similar spirit, we give a very short review on geometric transition between the deformed conifold and the resolved conifold in Appendix D.2. Curious readers may refer to [195, 280, 258, 200, 257, 333].

#### **6.3.1 The Hartle-Hawking state from the all-genus amplitude**

Worldsheet topological string theory comes from applying topological twists to the  $N = (2, 2)$  supersymmetric sigma models, and the two inequivalent twisting procedures give the topological A-model and the topological B-model [340]. In this paper, we will consider the A-model, whose target space is a six real dimensional Calabi-Yau manifold  $X$ . The theory only depends on the Kahler modulus of the target space and is invariant under area preserving diffeomorphisms in the target space. The free energy for the A model is a sum over all worldsheet instanton sectors corresponding to holomorphic worldsheets. Let  $[S_i]$  be a basis of  $H_2(X, \mathbb{Z})$ ,

so that a generic element  $\beta \in H_2(X, \mathbb{Z})$  can be expressed as  $\beta = \sum_i n_i [S_i]$ . Let  $t_i = \int_{S_i} \omega$  be the complexified Kahler parameters and denote  $Q^\beta = \prod_i e^{-n_i t_i}$ . The free energy of the A-model on  $X$  then takes the form of a sum over all worldsheet instanton sectors:

$$F = \sum_g g_s^{2g-2} F_g(t_i) = \sum_{g, \beta} g_s^{2g-2} N_{g, \beta} Q^\beta. \quad (6.15)$$

$N_{g, \beta}$  is the genus- $g$  Gromov-Witten invariant that “counts” the number of holomorphic curves of genus  $g$  in the two-homology class  $\beta$  in an appropriate sense.

A remarkable fact about the closed A-model string is that we can compute the all-genus amplitude using localization, connection to M-theory, mirror symmetry, and many other techniques [235, 4, 343, 161, 108, 2, 326, 263]. The free energy of the A-model can be resummed to be expressed in terms of the BPS index, Gopakumar-Vafa invariants  $n_\beta^g$  for a curve  $\beta$ ,

$$F = \sum_{g, \beta, k} n_\beta^g \frac{1}{k} \left( 2 \sin \frac{k g_s}{2} \right)^{2g-2} Q^{k\beta}. \quad (6.16)$$

In particular the partition function  $Z = e^F$  on the resolved conifold is

$$Z(\mathcal{O}(-1) \oplus \mathcal{O}(-1) \rightarrow S^2) = \exp \left( \sum_{n=1}^{\infty} \frac{1}{n (2 \sin(\frac{n g_s}{2}))^2} e^{-nt} \right), \quad (6.17)$$

because  $n_{S^2}^g = 0$  for all  $g > 0$  but  $n_{S^2}^0 = 1$ . In (6.17), we have already summed over all genera. Note that although the partition function on the resolved conifold is well-defined for both weak and strong coupling, we presented an asymptotic form (6.17) which is valid for large values of the string coupling  $g_s$ . By expanding (6.17) in  $g_s$ , one can recover the free energy expression (6.15) in terms of Gromov-Witten invariants, which is valid at weak string coupling. The  $e^{-nt}$  factors correspond to holomorphic worldsheet instantons that wrap  $n > 0$  times the base manifold  $S^2$ .

As discussed in section 6.2, we want to define a Hartle-Hawking state for the resolved conifold as a wavefunctional of string loops inside the Lagrangian manifold



$\mathcal{L}$ . To do this we apply the topological vertex formalism [326] which express the string partition function (6.17) in terms of the overlap in (6.12) by inserting branes and antibranes on  $\mathcal{L}$ . These branes cut through the worldsheets along the equator while extending into the fiber directions as shown in figure 6.4.

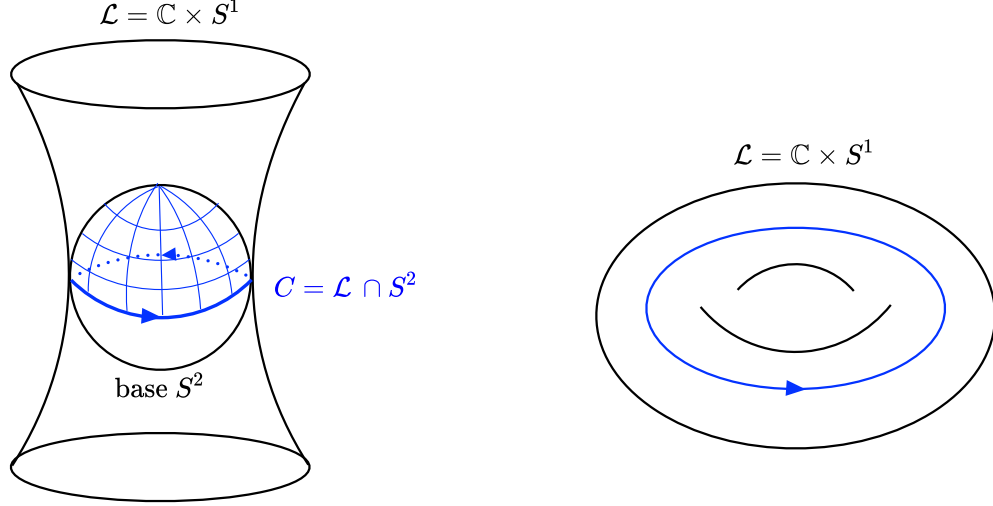


Figure 6.4: The left figure shows a D-brane on  $\mathcal{L} \subset \Sigma$  which intersects the base  $S^2$  along the equator and extends in to the fiber directions along a hyperbola. In the right figure, we show the string loops in the time slice  $\mathcal{F}_\Sigma$  which lives in  $\mathcal{L}$ . The state  $|HH\rangle$  state is defined via worldsheets which end on these loops and wrap the upper hemisphere, as shown in the left figure. Similarly  $\langle HH^*|$  describes worldsheets on the southern hemisphere which end on anti-branes.

Due to the coupling between the string endpoints and the branes, the A-model amplitude depends on the holonomy  $U$  of the world volume gauge field. For the worldsheets ending on the branes and wrapping the upper hemisphere  $D_+$ , the amplitude is

$$Z_+(\mathcal{O}(0) \oplus \mathcal{O}(-1) \rightarrow D_+^2, U), \quad U = P \exp \oint_C A. \quad (6.18)$$

For  $N$  branes the worldvolume gauge theory is  $U(N)$  Chern-Simons theory, and in the large  $N$  limit the amplitude (6.18) corresponds to the topological vertex with a single nontrivial stack of branes. Similarly we can define another vertex via the amplitude  $Z_-$  for the oppositely oriented worldsheets which wrap the lower

hemisphere and end on antibranes. By annihilating the brane-antibrane pairs, these vertices can be glued together to recover the partition function of the resolved conifold:

$$Z(\mathcal{O}(-1) \oplus \mathcal{O}(-1) \rightarrow S^2) = \int dU Z_+(U) Z_-(U^{-1}). \quad (6.19)$$

Here the gluing is implemented by integration over the gauge group  $U(N)$  using the Haar Measure.

The vertex  $Z_+$  can be interpreted as a closed string wavefunctional for the Hartle-Hawking state:

$$\langle U | HH \rangle = Z_+(U). \quad (6.20)$$

$|HH\rangle$  is a state in the second-quantized string theory, and the path integral  $Z_+$  includes all disconnected worldsheet configurations winding an arbitrary number of times in one orientation. Each closed string configuration is defined by the occupation numbers  $k_j$  which enumerate how many closed strings wind  $j$  times around  $C$ , which should be identified with the non-contractible cycle of  $\mathcal{L}$ .

In terms of  $k_j$ , the wavefunctional is of the form

$$\begin{aligned} \langle U | HH \rangle &= \sum_{\vec{k}} C_{00\vec{k}}(g_s, t) \prod_{i=1} \frac{(\text{tr} U^i)^{k_i}}{z_{\vec{k}}}, \quad k_i > 0 \\ z_{\vec{k}} &= \prod_{j=1}^{\infty} j^{k_j} k_j!, \end{aligned} \quad (6.21)$$

where  $C_{00\vec{k}}(g_s, t)$  are the vertex coefficients derived in [4, 263], and the normalization  $z_{\vec{k}}$  is a combinatorial factor associated with redundancy in labelling by  $\vec{k}$ . (6.21) can be also derived by calculating the open Gromov-Witten invariants from the worldsheet theory [227, 263]. In the large  $N$  limit the multi-trace factors form a linearly independent set called the winding basis  $|\vec{k}\rangle$

$$\lim_{N \rightarrow \infty} \prod_{i=1} \text{tr}(U^i)^{k_i} = \langle U | \vec{k} \rangle, \quad k_j > 0. \quad (6.22)$$

The overlap between the states  $|\vec{k}\rangle$  is defined via the Haar measure  $dU$ :

$$\langle \vec{k} | \vec{k}' \rangle = \int dU \operatorname{tr}_{\vec{k}}(U) \operatorname{tr}_{\vec{k}'}(U^{-1}) = \delta_{\vec{k}, \vec{k}'} z_{\vec{k}}. \quad (6.23)$$

This basis defines the chiral closed string Hilbert space  $\mathcal{H}_\Sigma$  associated with strings winding around the equator.<sup>9</sup>

So far we have expressed the closed strings states as functions of the holonomies  $U$ . Let us interpret these explicitly as wavefunctionals of loops in  $\mathcal{F}_\Sigma$ . Due to the topological invariance of the A-model, elements of  $\mathcal{F}_\Sigma$  fall into equivalence classes labelled by their winding numbers around  $C$ . If  $X_n(\sigma)$  is a string loop winding  $n$  times, then each single trace factor in (6.22) should be treated as a single string functional:

$$\Psi[X_n(\sigma)] = \operatorname{tr}(U^n) = \operatorname{tr} P \left( \exp \oint X_n^* A \right). \quad (6.24)$$

Similarly, the Hartle-Hawking state is a multi-string functional obtained by treating multi loop configuration in  $\mathcal{F}_\Sigma$  as boundary conditions for the string path integral.

### 6.3.2 The chiral boson description of $\mathcal{H}_\Sigma$ and D branes

The Hilbert space  $\mathcal{H}_\Sigma$  has a second quantized description in terms of a chiral boson which can be viewed as a string field theory for the A-model.<sup>10</sup> This is obtained by defining string creation/annihilation operators  $\alpha_{\mp n}, n > 0$  which create and

---

<sup>9</sup>This Hilbert space can be viewed as a “chiral half” of the space of functions on  $U(N)$  in the large  $N$  limit in the following sense. In the large  $N$  limit, the Hilbert space of functions on  $U(N)$  factorizes into two sectors consisting of positively oriented strings represented by wavefunctions  $\operatorname{tr}(U^k)$  and negatively oriented strings represented by wavefunctions  $\operatorname{tr}(U^{\dagger k})$  [172]. The Hilbert space we consider consists only of the positively-oriented strings.

<sup>10</sup>This is the Hilbert space associated with the representations of  $U(\infty)$ . Strictly speaking, this is the string field theory for the topological B-model on the mirror manifold [4, 45, 2].

annihilate closed strings winding  $n$  times with positive orientation [45, 2, 4]:

$$\langle U | \prod_n \alpha_{-n}^{k_n} | 0 \rangle = \prod_n \text{tr}(U^n)^{k_n}. \quad (6.25)$$

In terms of these oscillators, the D-branes  $|U\rangle$  are coherent states

$$|U\rangle = \exp\left(\sum_{n=1}^{\infty} \frac{\text{tr}(U^n)}{n} \alpha_{-n}\right) |0\rangle. \quad (6.26)$$

This gives a more precise definition of  $|U\rangle$  in the large  $N$  limit, as we can apply the mapping

$$|U\rangle \rightarrow |t\rangle = \exp\left(\sum_{n=1}^{\infty} \frac{t_n}{n} \alpha_{-n}\right) |0\rangle, \quad t_n = \text{tr} U^n. \quad (6.27)$$

In the large  $N$  limit,  $t_n$  can be viewed as formal variables without reference to the matrix  $U$ . In particular, the HH state is given by evolution of such a coherent state [4]

$$|HH\rangle = e^{-t\hat{H}/2} \exp\left(\sum_{n=1}^{\infty} \frac{1}{n(q^{n/2} - q^{-n/2})} \alpha_{-n}\right) |0\rangle, \quad (6.28)$$

$$\hat{H} = \sum_{n=1}^{\infty} \alpha_{-n} \alpha_n, \quad q = \exp(ig_s), \quad (6.29)$$

where  $\hat{H}$  is the Hamiltonian of the closed string field theory and  $e^{-\frac{t}{2}\hat{H}}$  is a string field propagator which evolves the geometry from an infinitesimal disk to a finite hemisphere of area  $t/2$ . The dual state defined by the amplitude  $Z_-$  with antibranes inserted is given by<sup>11</sup>

$$\langle HH^* | = \langle 0 | \exp\left(\sum_{n=1}^{\infty} \alpha_n \frac{-1}{n(q^{n/2} - q^{-n/2})}\right) e^{-t\hat{H}/2}. \quad (6.30)$$

---

<sup>11</sup>This is a nontrivial adjoint operation which corresponds to changing the Chern class in addition to changing the orientation of the hemisphere[4, 45, 325]. When  $t$  is real, this is equal to the complex conjugation. When  $t$  is complex, due to the holomorphicity of the A-model, we shall not use the complex conjugation and our formula for the dual is correct for a generical complex  $t$ .

It can be verified directly from (6.28),(6.30),and (6.17), that

$$Z = \langle HH^* | HH \rangle . \quad (6.31)$$

**The entanglement brane boundary state** It is useful to identify the holonomy  $D \in U(\infty)$  corresponding to the state on the infinitesimal disk :

$$|U = D\rangle = \exp \left( \sum_{n=1} \frac{1}{n(q^{n/2} - q^{-n/2})} \alpha_{-n} \right) |0\rangle . \quad (6.32)$$

From (6.27), we know  $D$  must satisfy

$$\text{tr} D^n = \frac{1}{(q^{n/2} - q^{-n/2})} = \frac{1}{[n]_q}, \quad (6.33)$$

where we have introduced the  $q$ -deformed integer  $[n]_q$ . A diagonal matrix that satisfies this equation in the  $N \rightarrow \infty$  limit has components:

$$D_{jj} = q^{-j+\frac{1}{2}}, \quad j = 1, \dots, N. \quad (6.34)$$

Deriving this holonomy requires a regularization of the trace. Note that

$$\text{tr} D^n = \sum_{j=1}^N q^{n(-j+\frac{1}{2})} = q^{-n/2} \sum_{j=0} (q^{-n})^j = \frac{1 - q^{-n(N+1)}}{q^{n/2} - q^{-n/2}}, \quad (6.35)$$

so we need to give  $g_s = -i \log q$  a small imaginary part for the sum to converge. This analytic continuation is possible because in topological string theory  $g_s$  is a formal expansion variable rather than a physical coupling. In terms of  $|D\rangle$  we can write  $Z$  as a propagation amplitude

$$Z = \langle D^* | e^{-\hat{H}t} | D \rangle . \quad (6.36)$$

We will show in section 6.5 that the state  $|D\rangle$  is the analogue of the “entanglement brane” boundary state described in [122], and the holonomy  $D$  determines the

corresponding entanglement boundary condition. We can compute the amplitude (6.36) in the winding basis using the overlaps:

$$\langle \vec{k} | D \rangle = \prod_{n=1} (\text{tr} D^n)^{k_n} = \prod_{n=1} \left( \frac{1}{e^{ig_s n/2} - e^{-ig_s n/2}} \right)^{k_n}, \quad (6.37)$$

which gives another expression for the partition function:

$$Z = \sum_{\vec{k}} (d_q(\vec{k}, g_s))^2 e^{-l(\vec{k})t}, \quad l(\vec{k}) = \sum_j j k_j, \\ (d_q(\vec{k}, g_s))^2 = \frac{1}{z_{\vec{k}}} |\langle \vec{k} | D \rangle|^2 = \prod_{n=1} \frac{1}{z_{\vec{k}}} (|[n]_q^{-1}|)^{2k_n}. \quad (6.38)$$

If we interpret  $Z$  as a statistical partition function with Boltzmann factor  $e^{-l(\vec{k})t}$ , this expression suggests that  $(d_q(\vec{k}, g_s))^2$  is a degeneracy factor. A small  $g_s$  expansion of (6.37) then shows that

$$(d_q(\vec{k}, g_s))^2 \sim \prod_n \left( \frac{1}{g_s} \right)^{2k_n}. \quad (6.39)$$

We will see that this factor leads to a large  $O(\frac{1}{g_s})$  number of microstates per open string endpoint, as alluded to in the introduction. The appearance of the quantum integers  $[n]_q$  indicates an emergent quantum group symmetry in the target space. In the next subsection we will see additional evidence of this symmetry in the structure of the entanglement entropy as computed by the replica trick.

**Boson representation of the topological vertex** As a final remark, we note that in the chiral boson language, the topological vertex can be viewed as a highly nontrivial choice of the “pair of pants” amplitude. This is a state  $|\mathcal{V}\rangle \in \mathcal{H}_\Sigma \otimes \mathcal{H}_\Sigma \otimes \mathcal{H}_\Sigma$ . Its wavefunction in the coherent state basis is defined by

$$\langle U_1, U_2, U_3 | \mathcal{V} \rangle = Z_{\mathbb{C}^3}, \quad (6.40)$$

where  $Z_{\mathbb{C}^3}$  is the A-model amplitude on  $\mathbb{C}^3$  with 3 stacks of D-branes with holonomies  $U_i, i = 1, 2, 3$ . It is in this sense that the states  $|U\rangle$  corresponds to

degrees of freedom on A-branes. In terms of the vertex, the Hartle-Hawking state in (6.21) is

$$\langle U|HH\rangle = \langle U| \otimes \langle 0| \otimes \langle 0| |\mathcal{V}\rangle, \quad (6.41)$$

where  $|0\rangle$  corresponds to the state with no strings.

### 6.3.3 Entanglement entropy from the replica trick

In string field theories, an entanglement partition corresponds to a cut in the space  $\mathcal{F}_\Sigma$  of field configurations. Given a spatial partition  $\Sigma = \Sigma_A \cup \Sigma_B$ , one can consider string configurations  $\mathcal{F}_{\Sigma_A}$  and  $\mathcal{F}_{\Sigma_B}$ , define the respective string Hilbert spaces  $\mathcal{H}_{\Sigma_A}$ ,  $\mathcal{H}_{\Sigma_B}$ , and define the factorization map

$$\mathcal{H}_\Sigma \rightarrow \mathcal{H}_{\Sigma_A} \otimes \mathcal{H}_{\Sigma_B}. \quad (6.42)$$

However, here we will bypass this procedure and apply the replica trick as suggested by Susskind and Uglum [315]. We choose  $\Sigma_A$  to be the subregion fibered over an arc  $A \subset C$  of the equator, and  $\Sigma_B$  to be region over the complementary arc  $B$ . The entangling surface is a codimension-2 surface fibered over two points on  $C$  and separates the Lagrangian manifold  $\mathcal{L}$  into two pieces, cutting the closed strings winding around the equator into two open strings.

To apply the replica trick we have to compute the A-model partition function  $Z(\alpha)$  on the  $\alpha$ -fold replicated geometry with opening angle  $2\pi\alpha$  around  $\partial\Sigma_A$ . As we will show later, the replication can be applied in a way that preserves the bundle structure and the Calabi-Yau condition. As the topological A-model is invariant under area preserving diffeomorphisms, the replicated manifold thus remains  $\mathcal{O}(-1) \oplus \mathcal{O}(-1) \rightarrow S^2$  with the volume rescaled by a factor of  $\alpha$ . The replica

partition function is thus:

$$Z(\alpha) = \sum_k (d_q(\vec{k}, g_s))^2 e^{-\alpha l(k)t}, \quad (6.43)$$

which gives the entanglement entropy:

$$\begin{aligned} S_{\text{replica}} &= (1 - \alpha \partial_\alpha)|_{\alpha=1} \log Z(\alpha) = \sum_k p(k) (-\ln p(k) + 2 \ln d_q(\vec{k}, g_s)), \\ p(k) &= \frac{(d_q(\vec{k}, g_s))^2 e^{-tl(k)}}{Z}. \end{aligned} \quad (6.44)$$

This formula is reminiscent of entanglement entropy in gauge theories. To make this analogy more precise, we compute the amplitude expression (6.36) for  $Z(\alpha = 1)$  in the representation basis. At finite  $N$ , these basis elements  $|R\rangle$  are defined by characters of  $U(N)$ .

$$\begin{aligned} \langle U | R \rangle &= \text{tr}_R(U), \\ \langle R' | R \rangle &= \int dU \text{tr}_{R'}(U^{-1}) \text{tr}_R(U) = \delta_{RR'}, \end{aligned} \quad (6.45)$$

where  $R$  labels irreducible representations(irreps) of  $U(N)$ . They are related to the winding basis by the Frobenius relation

$$|R\rangle = \sum_{\vec{k} \in S_n} \frac{\chi_R(\vec{k})}{z_{\vec{k}}} |\vec{k}\rangle. \quad (6.46)$$

Here each  $R$  is identified with a Young diagram with  $n$  boxes, and  $\chi_R(\vec{k})$  is the character of the symmetric group  $S_n$  associated with the diagram. In the  $N \rightarrow \infty$  limit we take the expression on the RHS (which is independent of  $N$ ) as a definition of  $|R\rangle$ . This limit captures states  $|R\rangle$  whose diagrams have columns of arbitrary length.<sup>12</sup>

---

<sup>12</sup>This only captures a chiral half of the Hilbert space because it misses the representations obtained by tensoring anti-fundamental representations of  $U(N)$ .



In the representation basis we have

$$\langle R|D\rangle = \text{tr}_R(D) = (-i)^{l(R)} d_q(R) q^{\kappa_R/4}. \quad (6.47)$$

where  $l(R)$  is the number of boxes in the Young diagram. The quantity  $d_q(R)$  is the quantum dimensions of the symmetric group representation  $R$ . In term of the Young diagram,  $d_q(R)$  is given by

$$d_q(R) = \prod_{\square \in R} \frac{i}{q^{h(\square)/2} - q^{-h(\square)/2}} = \prod_{\square \in R} \frac{1}{2 \sin(\frac{h(\square)g_s}{2})}, \quad (6.48)$$

with  $h(\square)$  being the hook length, and the phase  $q^{\kappa_R/4}$  is given by

$$\kappa_R = 2 \sum_{\square \in R} (i(\square) - j(\square)), \quad (6.49)$$

here  $i(\square), j(\square)$  are the row and column numbers of the box.

It will be useful to view these quantities as arising from a particular large  $N$  limit of the quantum dimensions  $\text{dim}_q(R)$  for  $U(N)_q$ :

$$\lim_{N \rightarrow \infty} q^{-Nl(R)/2} \text{dim}_q(R) = (-i)^{l(R)} d_q(R) q^{\kappa_R/4}, \quad (6.50)$$

where the prefactor  $q^{-Nl(R)/2}$  renormalizes the quantum dimension for  $U(N)_q$ , rendering it finite in the large  $N$  limit. As we will show later, this is the same regularization used to determine the matrix  $D$  in (6.34).

In the representation basis, the Hartle-Hawking state (6.28) can be written as

$$|HH\rangle = \sum_R e^{-t\hat{H}/2} |R\rangle \langle R|D\rangle = \sum_R d_q(R) (-i)^{l(R)} q^{\kappa_R/4} e^{-tl(R)/2} |R\rangle, \quad (6.51)$$

and the partition function on the resolved conifold is

$$Z = \sum_R (d_q(R))^2 e^{-tl(R)}. \quad (6.52)$$

Equations (6.51) and (6.52) are direct analogues of formulas for the Hartle-Hawking state in two dimensional gauge theories as well as in JT gravity. Together with

(6.50), they suggest that  $(d_q(R))^2$  is a degeneracy factor due to a quantum group symmetry associated with the large  $N$  limit of  $U(N)_q$ .

Applying the replica trick to (6.52) gives another expression for the entropy (6.44):

$$\begin{aligned} S_{\text{replica}} &= (1 - \alpha \partial_\alpha)|_{\alpha=1} \log Z(\alpha), \\ &= \sum_R p(R) (-\ln p(R) + 2 \ln d_q(R)), \quad p(R) = \frac{(d_q(R))^2 e^{-t\ell(R)}}{Z}. \end{aligned} \quad (6.53)$$

This is a direct analogue of the entropy in 2D nonabelian gauge theories [114, 171, 115] with  $R$  playing the role of representation labels for a surface symmetry,  $p(R)$  a probability factor, and  $d_q(R)$  the dimension of each representation. Indeed it can be shown [117] that the Hartle-Hawking state and its entropy is a large  $N$  limit of

$$\begin{aligned} |HH\rangle &= \sum_R \dim_q(R) e^{-t\ell(R)} |R\rangle, \\ S_{\text{replica}}(N) &= \sum_R p(R) (-\ln p(R) + 2 \ln \dim_q(R)), \quad p(R) = \frac{(\dim_q(R))^2 e^{-t\ell(R)}}{Z}, \end{aligned} \quad (6.54)$$

which are the Hartle-Hawking state and entropy for  $q$ -deformed 2DYM. In the context of the  $q$ -deformed 2d Yang-Mills, the limit (6.50) has a very natural explanation. Rather than removing the  $N$  dependence of  $\dim_q(R)$  by hand, we should view this as a renormalization procedure in which the divergent term  $q^{N\ell(R)/2}$  is absorbed into the Boltzmann factor  $e^{-t\ell(R)}$ . The divergence arises due to the analytic continuation of  $q$ , and has precisely the right form so that it can be absorbed into a redefinition of the “coupling”  $t$ . In our next paper [117], we will explain this renormalization from the point of view of the geometric transition.

Given this limit, we expect that  $2 \log d_q(R)$  has a state counting interpretation in terms of edge modes transforming in an irrep of a surface symmetry group. This

symmetry group has been  $q$ -deformed, leading to quantum dimensions which do not have to be integers.

## 6.4 The A-model closed TQFT and representation category of quantum groups

### 6.4.1 General comments about factorization, E-brane axiom, and cobordisms

In the following two sections, we give a canonical interpretation of the replica trick entropy in (6.53) by defining a factorization of the closed string Hilbert space  $\mathcal{H}_\Sigma$  associated with the decomposition  $\Sigma = \Sigma_A \cup \Sigma_B$  into the subregions. The intersection of these subregions with  $\mathcal{L}$  are shown in the right of figure 6.5. We start by defining the spaces  $\mathcal{F}_{\Sigma_A}, \mathcal{F}_{\Sigma_B}$  of string configurations associated to these subregions. These spaces contain open string configurations  $X_{ij}(\sigma)$  inside  $\mathcal{L} \cap \Sigma_A$  which are stretched between entanglement branes (E-branes) which cut  $\mathcal{L}$  in two disconnected slices. The E-branes wrap a submanifold <sup>13</sup>  $\mathcal{L}'$  that intersects the base  $S^2$  along a circle orthogonal to  $C$ . The indices  $i, j$  are Chan-Paton factors labelling the  $N \gg 1$  E-branes, which can be identified with the entanglement edge modes of the closed string. We will give an explicit description of the open string Hilbert space  $\mathcal{H}_{\Sigma_A}, \mathcal{H}_{\Sigma_B}$  and the factorization map

$$\mathcal{H}_\Sigma \rightarrow \mathcal{H}_{\Sigma_A} \otimes \mathcal{H}_{\Sigma_B}. \quad (6.55)$$

---

<sup>13</sup>We expect  $\mathcal{L}'$  to be a Lagrangian submanifold. see comments in the discussion section .

This mapping embeds the Hilbert space of closed strings into an extended Hilbert space of open strings.

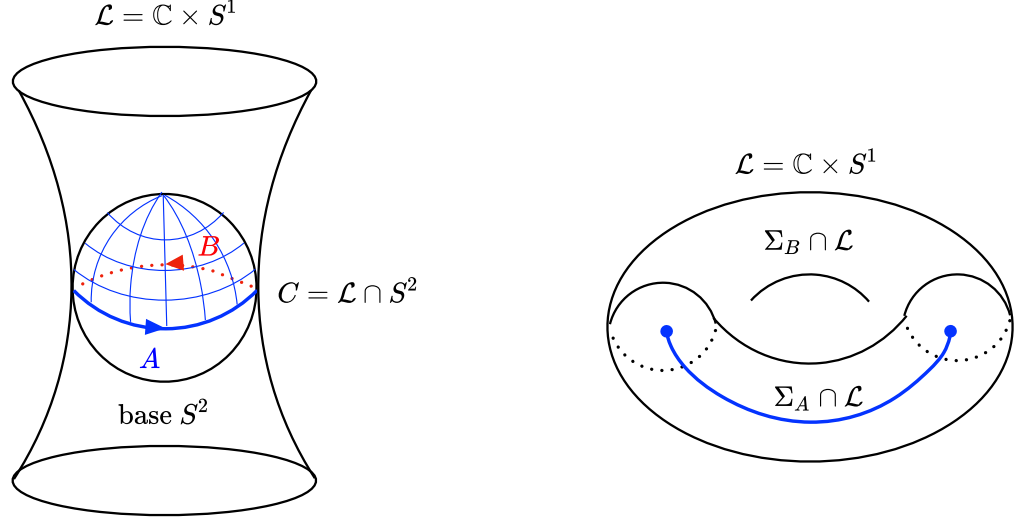


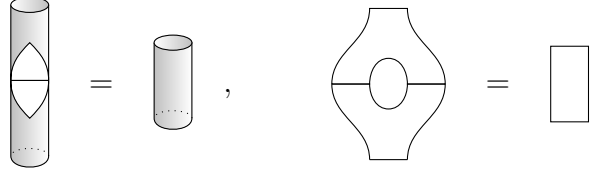
Figure 6.5: On the left, we show the splitting of the worldsheet boundary into  $A$  and  $B$ . On the right, the brane  $\mathcal{L}$  on which the closed string configurations  $X(\sigma)$  live is split into subregions by the entanglement branes. We show an open string configuration  $X_{ij}(\sigma) \in \mathcal{F}_{\Sigma_A}$ . These end on the entanglement branes intersecting  $\mathcal{L}$  along two open disks.

Just as in QFT, the factorization problem is strongly ambiguous in the absence of locality constraints. For example, as noted in [208], we can always map the physical states into a maximally entangled state of some arbitrary extended Hilbert space, leading to an arbitrarily large entanglement entropy. When the locality constraints are available, the strongest form of such constraints come from using the Euclidean path integral to split a time slice into subregions. In 2 dimensions, such a factorization of a circle or an interval is obtained from the Euclidean evolution (read from top to bottom)

$$\begin{array}{c} \text{Cylinder} \end{array} : \mathcal{H}_{\text{circle}} \rightarrow \mathcal{H}_{\text{interval}} \quad \begin{array}{c} \text{Y-shape} \end{array} : \mathcal{H}_{\text{interval}} \rightarrow \mathcal{H}_{\text{interval}} \otimes \mathcal{H}_{\text{interval}} \quad (6.56)$$

with some appropriate choice of boundary conditions at the entangling surface. In the previous work [123], we introduced a constraint on these factorization maps

called the entanglement-brane (E-brane) axiom (6.57), which ensures that the factorized state preserves all the correlations of the original state. This requires that *all* holes traced out by the entangling surface can be closed up. For example, we require that the cobordisms<sup>14</sup> in (6.56) satisfy



$$\text{Cylinder with vertical line} = \text{Cylinder}, \quad \text{Cylinder with horizontal line} = \text{Rectangle}. \quad (6.57)$$

This ensures that splitting the state does not change its correlations, since we can fuse it back and obtain the identity map by allowing the hole to contract.

The E-brane axiom, generally requires that the factorization involves a sum over edge modes at the entangling surface. It axiomatizes the state counting interpretation of the replica trick entropy. The replica trick, in both gravity and QFT, involves a path integral  $Z(\alpha)$  on a background with a contractible circle around the entangling surface. However a thermal interpretation

$$Z(\alpha) = \text{tr}_V e^{-\alpha H} \quad (6.58)$$

requires a path integral in a background with a *non-contractible* circle. The E-brane axiom enforces the non-trivial requirement that these two are equal:



$$\text{Sphere with horizontal line} = \text{Circle with inner circle and horizontal line}. \quad (6.59)$$


Previous works in gauge theory have shown that this can be satisfied provided we introduce appropriate edge modes into the Hilbert space of the subregion  $V$  [123].

Unfortunately, demanding a path integral formulation of the target space physics is an overly restrictive requirement; in particular it is not generally a

---


<sup>14</sup>The right diagram of (6.57) was referred to as isometry condition and employed to study factorization in JT gravity in [208]. It is one of the axioms of a “special” Frobenius algebra.

useful assumption in CFT's or in string theory. However there is a categorical reformulation of the path integral in terms of cobordisms which does not presume a notion of path integration over local fields. From the categorical point of view, a path integral for a  $D$ -dimensional Euclidean theory is a rule which assigns a number (the partition function) to a  $D$ -dimensional manifold, a Hilbert space to  $D - 1$  manifolds, and linear maps to cobordisms, which are  $D$ -dimensional manifolds with “initial” and “final” boundaries. Gluing of cobordisms along initial and final boundaries corresponds to composition of linear maps. The standard example of such a cobordism theory is a *closed* 2D TQFT in which a Hilbert space  $V^{\otimes n}$  is assigned to a disjoint union of  $n$  circles, and linear maps are assigned to cobordisms interpolating between collections of circles. The theory on an arbitrary closed Riemann surface can then be constructed by gluing the basic cobordisms [237, 22]:

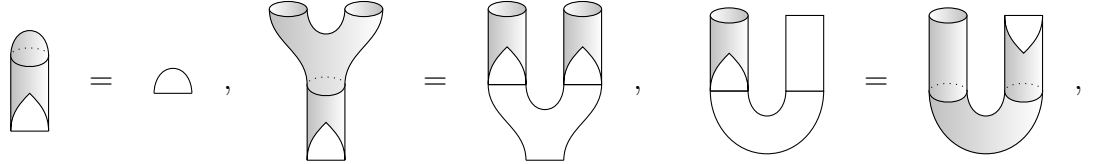

(6.60)

Consistency of different gluings for the same manifold is enforced by a set of sewing axioms which provide strong constraints on the cobordism data (6.60). For a 2D TQFT, the resulting structure is a Frobenius algebra with multiplication defined by the pair of pants cobordism. A similar formulation can be applied to 2D gauge theories and 2D conformal field theories [204].

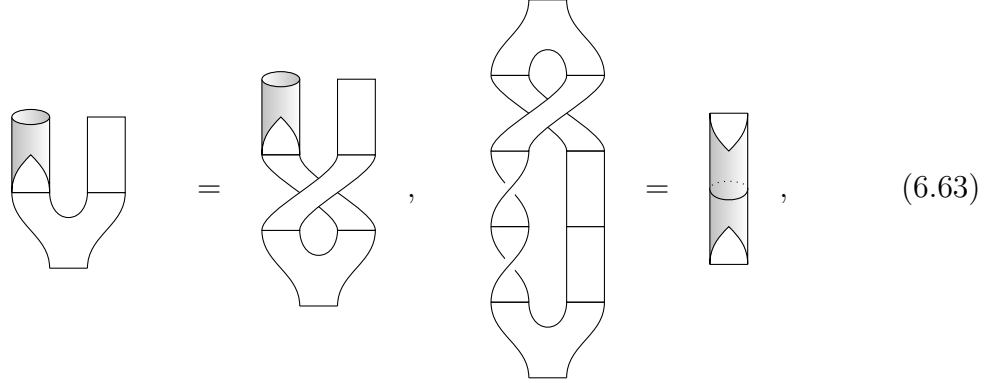
In the categorical framework [123], the path integral factorization maps (6.56) are viewed as additional cobordism data that defines an open *extension* of the closed TQFT. This extension introduces Hilbert spaces associated with codimension-one manifolds with boundaries (i.e. intervals) and additional set of cobordisms


(6.61)

which must be compatible with (6.60) according to the sewing relations



$$(6.62)$$



$$(6.63)$$

that defines an open-closed TQFT [242, 278].

It was shown in [123] that the sewing axioms for an open-closed TQFT can be consistently combined with the E-brane axiom:



$$(6.64)$$

to give a complete set of locality constraints that a consistent factorization should satisfy. As explained in [123], when combined with (6.62) equation (6.64) is powerful enough to ensure that *all* holes traced out by the entangling surface can be closed. A solution to all of these constraints was given for 2DYM and its string theory dual, and led to a factorization consistent with the replica trick entropy.

In the next 2 sections, we will apply the approach described above to define the factorization of the A-model string theory. It was shown in [8, 63] that the closed string amplitudes on direct sums of line bundles

$$X = L_1 \oplus L_2 \rightarrow \mathcal{S}, \quad (6.65)$$

over a Riemann surface  $\mathcal{S}$  can be determined by a closed TQFT on  $2\text{Cob}^{L_1, L_2}$ . This means that the A-model amplitudes on  $X$  can be broken up into open string amplitudes by inserting brane-antibrane pairs as in our construction of the Hartle-Hawking state, and the gluing of these open string amplitudes satisfies the same rules as the category  $2\text{Cob}^{L_1, L_2}$  of 2-cobordisms with line bundles. The A-model TQFT [63] is a generalization of 2D TQFT, with the information about the higher-dimensional geometry captured by Chern classes  $(k_1, k_2)$  of the line bundles  $L_1, L_2$ . It is generated by cobordisms in (6.60) with  $(0, 0)$  Chern class, together with the following four cobordisms

$$\begin{array}{c} (-1, 0) \\ \text{---} \end{array} , \quad \begin{array}{c} (0, -1) \\ \text{---} \end{array} , \quad \begin{array}{c} (1, 0) \\ \text{---} \end{array} , \quad \begin{array}{c} (0, 1) \\ \text{---} \end{array} . \quad (6.66)$$

Note that this generates a much larger category than the set  $2\text{Cob}$  of two-dimensional cobordisms, and the A-model TQFT has a more complicated set of sewing relations than an ordinary Frobenius algebra. However, in formulating the factorization of the A-model Hilbert space, we will restrict to target spaces which are Calabi-Yau manifolds. This requires the Chern classes to satisfy

$$k_1 + k_2 = -\chi(\mathcal{S}), \quad (6.67)$$

where  $\chi(\mathcal{S})$  is the Euler characteristic of the base manifold. This is an important restriction that determines the form of the factorization map which we will propose.

### 6.4.2 A model TQFT on Calabi Yau manifolds

The subcategory of  $2\text{Cob}^{L_1, L_2}$  corresponding to Calabi-Yau manifolds defines a symmetric Frobenius algebra just like a 2D TQFT. The basic building blocks for this category are the same as the generators in (6.60), except they are now decorated by Chern class labellings satisfying (6.67). Since both the Chern classes



and the Euler characteristic of the base manifolds are additive under gluing, the Calabi-Yau condition (6.67) is preserved under gluing. The A-model TQFT is a functor which assigns a linear map to each generators [8] :

$$\begin{array}{c} (0,-1) \\ \text{---} \end{array} = \sum_R (-i)^{l(R)} d_q(R) q^{\kappa_R/4} e^{-tl(R)} |R\rangle \quad (6.68)$$

$$\begin{array}{c} (-1,0) \\ \text{---} \end{array} = \sum_R i^{l(R)} d_q(R) q^{-\kappa_R/4} e^{-tl(R)} \langle R| \quad (6.69)$$

$$\begin{array}{c} (0,1) \\ \text{---} \end{array} = \sum_R \frac{i^{l(R)}}{d_q(R)} q^{-\kappa_R/4} e^{-tl(R)} |R\rangle \langle R| \langle R| \quad (6.70)$$

$$\begin{array}{c} (1,0) \\ \text{---} \end{array} = \sum_R \frac{(-i)^{l(R)}}{d_q(R)} q^{\kappa_R/4} e^{-tl(R)} |R\rangle |R\rangle \langle R| \quad (6.71)$$

$$\begin{array}{c} (0,0) \\ \text{---} \end{array} = e^{-t\hat{H}} = \sum_R e^{-tl(R)} |R\rangle \langle R| \quad (6.72)$$

Note that each of the cobordisms describes a Riemann surface  $\mathcal{S}$  with boundaries in the *target* space. Each (oriented) circle intersects a stack of Lagrangian branes on which worldsheets wrapping  $\mathcal{S}$  ends. Due to the area-dependent Boltzmann factors  $e^{-tl(R)}$ , the A-model TQFT is not exactly a Frobenius algebra. However the Frobenius algebra gluing rules are satisfied provided we keep track of the Kahler modulus  $t$ , which just adds upon gluing [302].

**Gluing rules** To see the effect of introducing the Chern classes, we present some of the gluing rules here in detail. The pair of pants <sup>15</sup> (6.70) defines a multiplication on closed string states and the Hartle Hawking state (6.68), also known as the

---

<sup>15</sup>Note that the pair of pants amplitude here differs from the one defined by the topological vertex, because the location of the branes is different in the two cases.

“Calabi Yau cap” is the unit element. These satisfy

$$\begin{array}{c} (0,-1) \\ (0,1) \end{array} \text{Y-shape} = \text{Cylinder} \begin{array}{c} (0,0) \end{array} \quad (6.73)$$

with the  $(0,0)$  cylinder treated as the identity of the algebra. Gluing the counit (6.69) to the product (6.70) we obtain a bilinear form we call the closed pairing:

$$\begin{array}{c} (-1,1) \\ \text{Cup} \end{array} := \begin{array}{c} (0,1) \\ \text{Y-shape} \\ (-1,0) \end{array} = \sum_R (-1)^{l(R)} q^{-2\kappa_R/4} \langle R | \langle R |. \quad (6.74)$$

Note that the closed pairing has a different Chern class than the cylinder even though both have the same Euler characteristic. This is required by the Chern class assignments of the counit and unit, together with the fact that they are adjoint with respect to each other under the closed pairing.

Applying the closed pairing to the unit gives the counit:

$$\begin{array}{c} (0,-1) \\ \text{Cup} \end{array} = \begin{array}{c} \text{Cup} \\ (-1,0) \end{array}. \quad (6.75)$$

This equation implements the mapping<sup>16</sup>

$$|HH\rangle \rightarrow \langle HH^*| \quad (6.76)$$

taking the Hartle-Hawking state to its adjoint as defined in section 6.3.

The pairing has an inverse, called the copairing, which is obtained by gluing

---

<sup>16</sup>In general the mapping  $*$  which changes orientation while mapping branes to anti branes is given in the representation basis by  $|R\rangle \rightarrow (-1)^{l(R)} \langle R^t|$ . This agrees with the adjoint operation defined by (6.74) when acting on the unit (6.68) and counit (6.69).

the unit to the coproduct

$$\begin{aligned}
 & \text{Cap}^{(1,-1)} := \text{Cup}^{(0,-1)/(1,0)} \\
 & \text{Cup}^{(1,-1)/(-1,1)} = \text{Cylinder}^{(0,0)}
 \end{aligned} \tag{6.77}$$

The resolved conifold partition function is obtained by gluing the unit to the counit:

$$Z = \text{Cap}^{(0,-1)/(-1,0)} = \sum_R (d_q(R))^2 e^{-tl(R)}. \tag{6.78}$$

More generally, by gluing the generators, we can obtain the closed string partition function for a local Calabi-Yau manifold with base manifold  $\mathcal{S}$  of genus  $g$  and Chern classes  $(2g - 2 + p, p)$ :

$$Z = \sum_R \left( \frac{1}{d_q(R)} \right)^{2g-2} q^{(g-1)\kappa_R/2} e^{-tl(R)} \tag{6.79}$$

where  $t$  is the complexified area of  $\mathcal{S}$ .

### 6.4.3 Quantum traces and q-deformation of the A model

#### TQFT

Following [8], we have expressed the linear maps (6.68) to (6.72) in an orthonormal basis  $|R\rangle$  labelled by representations of  $U(\infty)$ . These linear maps should be viewed as string amplitudes. This becomes manifest when we express the basis  $|R\rangle$  as

wavefunctions on the group

$$\langle U|R \rangle = \text{tr}_R(U), \quad (6.80)$$

where  $U = \exp \oint A$  gives the usual coupling of the worldsheet boundary to the worldvolume gauge field.

This gives a consistent closed TQFT so long as we restrict to gluing of cobordisms along circles. However, it was observed in [88] that for finite  $N$  the use of the classical trace in (6.80) leads to inconsistencies when gluing along *open* edges. This is precisely the type of gluing which was needed to compute the replica trick entropy (6.44), since this requires opening the base  $S^2$  into a disk  $D^2$  and then gluing a sequence of such disks along half of their boundary  $\partial D^2$ . The same inconsistency appears if we apply the 2DYM factorization in [122] to the closed string wavefunction  $\text{tr}_R(U)$ . This was defined by splitting the Wilson loop  $U = U_A U_B$  into the product of Wilson lines in region  $A$  and  $B$ , and then taking the classical trace:

$$\text{tr}_R(U) \rightarrow \text{tr}_R(U_A U_B) = \sum_{i,j=1}^{\dim R} R_{ij}(U_A) R_{ji}(U_B), \quad (6.81)$$

where  $R_{ij}(U_{A,B})$  are matrix elements in the  $R$  representation, viewed as wavefunctions in the subregion  $A, B$ . The indices  $i, j$  label entanglement edge modes transforming under the gauge group  $U(\infty)$ , and in the case of undeformed 2DYM, led to an entropy consistent with the replica trick. However, for the A-model, this naive counting of edge modes would lead to degeneracy factors of  $\dim R$ , which are incompatible with the quantum dimensions in the replica trick entropy (6.53). In terms of the sewing relations, the  $U(\infty)$  edge modes fail to satisfy the E-brane axiom.

This problem arises because the A-model TQFT restricted to Calabi-Yau manifolds is really a functor which maps  $2\text{Cob}^{L_1, L_2}$  to the representation category of

a *quantum* group. This is suggested by the presence of the  $q$ -deformed dimension factor  $d_q(R)$ , which implies that the surface symmetry acting on the endpoints of the open strings, is  $q$ -deformed. However, the classical trace employed in the wavefunction (6.80) is not invariant under this quantum group symmetry. We will explain what this quantum group symmetry is in subsequent sections. For now we note that [88] observed that gauge invariance under the quantum group symmetry can be achieved by replacing the classical trace with the quantum trace:

$$\langle U | R \rangle = \text{tr}_{q,R}(U) := \text{tr}_R(uU), \quad (6.82)$$

where  $u$  is the Drinfeld element of the quantum group. This element is defined abstractly from quantum group data, and its classical trace gives the associated quantum dimension.

Thus for  $U(N)_q$  we have

$$\text{tr}_{q,R}(1) = \text{tr}_R(u) = \dim_q(R). \quad (6.83)$$

This equation remains valid for a general quantum group, with  $\dim_q(R)$  the quantum dimension defined from its representation category data. For the A-model string, the role of the Drinfeld element is played by the matrix  $D$  defined in (6.34), which may be viewed as a renormalized version of the Drinfeld element  $u$  for  $U(N)_q$ :

$$D = q^{-N/2}u, \quad \lim_{N \rightarrow \infty} \text{tr}_R(D) = (-i)^{l(R)} d_q(R) q^{\kappa_R/4}. \quad (6.84)$$

This is the analogue of equation (6.50) and will be useful in relating the quantum group symmetry for the A-model string to  $U(N)_q$ . Finally note that the wavefunctions (6.82) are orthonormal

$$\int dU \text{tr}_{q,R}(U) \text{tr}_{q,R'}(U) = \delta_{R,R'}, \quad (6.85)$$

and span the Hilbert space of class functions on the quantum group, which is isomorphic to  $\mathcal{H}_\Sigma$  defined previously in section 6.3. For this reason, the use of classical traces in [8] was adequate for the purposes of computing A-model partition functions by sewing along circles. However, as we will see, the quantum trace and the  $q$ -deformed nature of the holonomy  $U$  becomes essential when we perform operations that effectively cut open the closed string loops.

#### 6.4.4 String theory origin of the $q$ -deformation

In the previous discussion, we explained the necessity for quantum traces and the associated  $q$ -deformation of the closed string Hilbert space from consistency requirements of the TQFT. Here we would like to explain how the quantum group symmetry emerges from the viewpoint of the worldvolume gauge theory on the D-branes.

**$q$ -deformed connection in the worldvolume gauge theory** Replacing classical traces with quantum traces means that the coupling of the worldsheet boundary to the worldvolume gauge fields have been changed to

$$\mathrm{tr}(uP \exp \oint A). \quad (6.86)$$

This is because the *classical* gauge field should be viewed as a  $q$ -connection, whose components  $A_\mu^a(X)$  ( $a$  is a group index) are noncommutative functions on the brane. This  $q$ -deformation is a known property of the worldvolume  $U(N)$  Chern Simons theory on a stack of  $N$  branes, and we will give a brief review here. Usually, the gauge fields components  $A_\mu(X)$  are taken to be commutative functions of  $X$ . However one can see how a  $q$ -deformed gauge field arises by considering the Gauss

law constraint. This is a constraint applied in canonical quantization along a constant time slice  $M$  (see figure 6.6), which we can take to be a surface at fixed angle along the non-contractible  $S^1$  on the Lagrangian manifold  $\mathcal{L}$  (D.26). In the

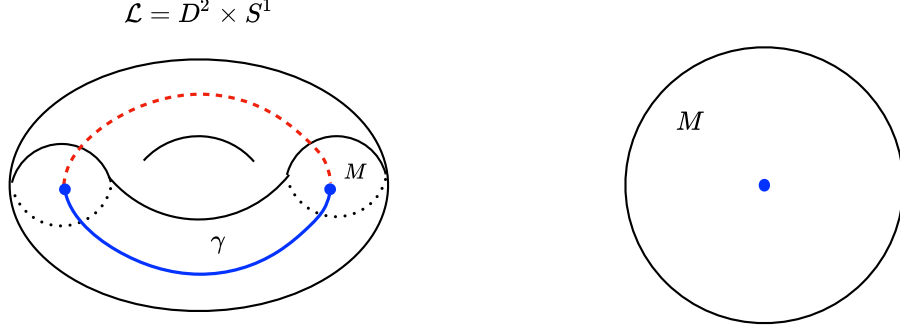


Figure 6.6: Quantizing the worldvolume gauge theory with time running around the non-contractible cycle of  $\mathcal{L}$ , we have to impose Gauss’s law on  $M$ . The puncture on  $M$  corresponds to the anyon charge on the Wilson loop which sources Gauss Law.

presence of a Wilson loop around this cycle, corresponding to boundary  $\gamma$  of the string worldsheet ending on the brane, Gauss law reads

$$\frac{k}{8\pi} \epsilon^{ij} F_{ij}^a(X) = \delta^2(X - P) T^a, \quad (6.87)$$

where  $i, j$  are spatial indices on  $M$ ,  $P$  is the location of the puncture where  $M$  cuts the Wilson loop,  $T^a$ ,  $a = 1 \cdots \dim \text{U}(N)$  are generators of  $\text{U}(N)$ . It was noted in [341] that this equation cannot be solved for an ordinary gauge field because  $F_{ij}^a$  is a number while  $T^a$  is a non commuting matrix. This mismatch occurs because the Wilson loop is a non-dynamical defect operator; there is no “matter field” on the loop  $\gamma$  that couples to  $A$ . One solution is to “integrate in” dynamical degrees of freedom on the loop, which will couple to  $A$  and render the objects on both sides of (6.87) commutative[341, 136]. However to see the quantum group symmetry, we should apply the alternative prescription suggested in [341], and  $q$ -deform the gauge field  $A_\mu^a$  into a non-commutative object, i.e. a matrix in the lie algebra

of  $U(N)$ . This idea was carried out in [173], where an explicit solution to (6.87) was derived, giving a noncommutative connection that can be identified with the Knizhnik–Zamolodchikov connection in conformal field theory. In appendix D, we give a string sigma model argument for noncommutative world volume gauge fields following [305]

## 6.5 Extension of the A-model closed TQFT

Having formulated the A-model closed TQFT in terms of representation categories of quantum groups, we now describe its extension to the open sector. We begin by defining the open string Hilbert space associated to an interval on which the operators of the open sector act. We give an explicit action of the quantum group symmetry on this Hilbert space and the associated decomposition into irreducible representations. Next, we derive the open-closed cobordisms which include diagrams describing the factorization of the closed string Hilbert space. We then compute the  $q$ -deformed entropy from the reduced density matrix of the Hartle–Hawking state and show that it matches the geometric replica trick calculation in section 6.3.3. Finally we will revisit the geometric replica trick calculation and show that the preservation of the Calabi Yau condition requires the insertion of a “defect” operator at the entangling surface, which plays the role of the (inverse) Drinfeld element of the quantum group.



### 6.5.1 The open string Hilbert space as the coordinate algebra $\mathcal{A}(\mathrm{U}(\infty)_q)$

The  $q$ -deformation of the spacetime gauge field  $A$  means that its holonomy  $U = P \exp \oint A$  is an element of the quantum group  $\mathrm{U}(N)_q$ . This can be defined by  $q$ -deforming the algebra  $\mathcal{A}(\mathrm{U}(N))$  of functions on  $\mathrm{U}(N)$ , referred to as its *coordinate algebra*.  $\mathcal{A}(\mathrm{U}(N))$  is generated by matrix elements  $U_{ij}$  satisfying the unitary constraint

$$\sum_k U_{ik} U_{jk}^* = \sum_k U_{ki}^* U_{kj} = \delta_{ij}. \quad (6.88)$$

As a vector space,  $\mathcal{A}(\mathrm{U}(N))$  is defined over the complex numbers and spanned by the basis

$$U_{i_1 j_1} U_{i_2 j_2} \cdots U_{i_n j_n}, \quad n = 1, \dots, \infty. \quad (6.89)$$

In the undeformed algebra, the matrix elements themselves commute:

$$U_{ij} U_{kl} = U_{kl} U_{ij}. \quad (6.90)$$

However, in the quantum group  $\mathrm{U}(N)_q$  this multiplication law (distinct from the matrix multiplication rule) becomes noncommutative. There exists a conjugate linear involution  $*$  of the coordinate algebra  $\mathcal{A}(\mathrm{U}(N)_q)$  for which the unitary constraint (6.88) still holds. However, due to the noncommutativity, the placement of the  $*$  is now crucial in (6.88). In particular, it should be noted that for  $U_{ij} \in \mathcal{A}(\mathrm{U}(N)_q)$

$$\sum_k U_{ik}^* U_{jk} \neq \delta_{ij}. \quad (6.91)$$

It is customary to abuse language and refer to both the “quantum space”  $\mathrm{U}(N)_q$  and the algebra of functions  $\mathcal{A}(\mathrm{U}(N)_q)$  as a quantum group. This is done in

the spirit of noncommutative geometry, where the geometry of a noncommutative space  $X$  is defined by the algebra of noncommutative functions on  $X$  [79, 126].

The precise nature of the noncommutative product in  $U(N)_q$  is determined by the R-matrix of the quantum group. To express the product rule it is useful to consider an element  $U \in U(N)_q$  as a matrix acting in the fundamental representation. Thus it acts on a vector space  $V$  according to

$$U : V \rightarrow V,$$

$$v_i \mapsto \sum_j U_{ij} \otimes v_j, \quad (6.92)$$

where the tensor product  $\otimes$  symbol has been used to distinguish this product from the noncommutative product we wish to define. In the same fashion, the R-matrix  $\mathcal{R} \in U(N)_q \otimes U(N)_q$  can be regarded as an element  $\mathcal{R} \in \text{End}(V \otimes V)$ , i.e. a matrix operator acting on two copies of  $V$ . If we define matrices

$$U_1 = U \otimes \mathbf{1},$$

$$U_2 = \mathbf{1} \otimes U. \quad (6.93)$$

Then the multiplication rule for the coordinate algebra on  $U(N)_q$  is

$$\mathcal{R}U_1U_2 = U_2U_1\mathcal{R}, \quad (6.94)$$

where the composition of the operators above is defined with ordinary matrix multiplication. An explicit example of the R-matrix,  $*$  structure, and other quantum group properties of  $\mathbf{SL}_q(2)$  is presented in appendix D.3.

**Definition of the open string Hilbert space** We now define the open string Hilbert space  $\mathcal{H}_{\Sigma_A}$  assigned to the subregion string configurations in  $\mathcal{F}_{\Sigma_A}$  as the

large  $N$  limit of the coordinate algebra on  $U(N)_q$ :

$$\begin{aligned}\mathcal{H}_{\Sigma_A} &= \mathcal{A}(U(\infty)_q), \\ q &= e^{ig_s}.\end{aligned}\tag{6.95}$$

This a  $q$ -deformation of the open string Hilbert space defined in [122] for the string theory dual to 2DYM. In particular the subspace of  $n$  open strings is spanned by the states  $|IJ\rangle$  with wavefunctions

$$\begin{aligned}\langle U|I, J\rangle &= U_{i_1 j_1} U_{i_2 j_2} \cdots U_{i_n j_n}, \\ U_{i_a j_a} &= P \exp \int X_{i_a j_a}^* A,\end{aligned}\tag{6.96}$$

where in the second equation we have emphasized that these wavefunctions live on the space of subregion open string configurations  $X_{ij}(\sigma) \in \mathcal{F}_{\Sigma_A}$ . Due to the topological invariance, they are completely specified by the multi-index Chan-Paton factors  $I, J$  labeling the entanglement branes. In the undeformed case where  $q = 1$ , the commutativity of the matrix elements  $U_{ij}$  implies these open string are bosonic [122], so that the  $n$  string Hilbert space is

$$\mathcal{H}_n = (V \otimes V^*)^{\otimes n} / S_n.\tag{6.97}$$

Here  $V^*$  denotes the dual of the fundamental representation, giving the strings an orientation. Open string indistinguishability is enforced by the quotient of the permutations group  $S_n$ , which permutes the open strings by acting simultaneously on both endpoints  $|I, J\rangle \rightarrow |\sigma(I), \sigma(J)\rangle$  for  $\sigma \in S_n$ . In the presence of nontrivial string interactions,  $g_s > 0, q \neq 1$ , the open string endpoints become anyons [156]. This change in statistics is implemented by the equivalence relation (6.94), which tells us that the exchange of open strings must be accompanied by an  $R$  matrix transformation. The operation of permutating strings is therefore replaced by

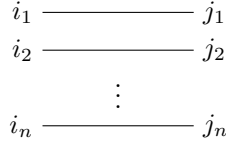


Figure 6.7: The state  $|IJ\rangle$  represents a configuration of  $n$  open strings with Chan-Paton factors  $(i_1, j_1) \dots (i_n, j_n)$ .

braiding, and the open string Hilbert space is

$$\mathcal{H}_{\Sigma_A} = \bigoplus_{n=1}^{\infty} \mathcal{H}_n(q),$$

$$\mathcal{H}_n(q) = (V^* \otimes V)^{\otimes n} / (\mathcal{R}U_1U_2 \sim U_2U_1\mathcal{R}). \quad (6.98)$$

For  $q \in \mathbb{R}$ , the inner product on  $\mathcal{H}_{\Sigma_A}$  is defined by the quantum group Haar measure and is given in terms of the representation basis in (6.112).

### 6.5.2 Quantum group symmetry on the open string Hilbert space

Each open string in the state  $|I, J\rangle$  transforms in the adjoint representation of the quantum group symmetry, which is the surface symmetry of the A-model string.

To describe the action of this symmetry and the associated decomposition of  $\mathcal{A}(\mathrm{U}(\infty)_q)$ , we need to introduce an operation called the antipode. A more thorough presentation of the algebraic structure of a quantum group is given in appendix D.3. Below we will work with  $\mathcal{A}(\mathrm{U}(N)_q)$  and then consider the  $N \rightarrow \infty$  limit later.

$$\begin{aligned}
U_{ij}^1 U_{kl}^2 - U_{il}^1 U_{kj}^2 &= \begin{array}{c} i \bullet \text{---} j \\ k \bullet \text{---} l \end{array} - \begin{array}{c} i \bullet \text{---} j \\ k \bullet \text{---} l \end{array} \quad \text{with crossing} \\
U_{ij}^1 U_{kl}^2 - U_{kj}^1 U_{il}^2 &= \begin{array}{c} i \bullet \text{---} j \\ k \bullet \text{---} l \end{array} - \begin{array}{c} i \bullet \text{---} j \\ k \bullet \text{---} l \end{array} \quad \text{with crossing}
\end{aligned}$$

Figure 6.8: The figure shows a state of two open strings. Antisymmetrization of the right and left indices can be expressed by fixing the Chan-Paton factors while changing the pattern of connection between them. In the figure we have put string number 1 on top of string number 2. When the open strings have bosonic statistics as imposed by the  $S_n$  quotient in (6.97), the antisymmetrization of the left or the right endpoints give the same state, since the two operations are relating by commuting string number 1 and 2. However, the A-model open string has anyonic statistics, so the two orderings are not equal. This corresponds a nontrivial braiding structure in the diagrams above.

**The antipode and the conjugate representation** Given a quantum group  $\mathcal{A}$  the antipode is an anti-homomorphism

$$S : \mathcal{A} \rightarrow \mathcal{A}, \quad (6.99)$$

$$S(UV) = S(V)S(U), \quad U, V \in \mathcal{A}. \quad (6.100)$$

It acts on *single* string elements  $f_{ij}(U) = U_{ij} \in \mathcal{A}(U(N)_q)$  by giving the analogue of the matrix inverse:

$$\sum_j U_{ij} S(U)_{jk} = S(U)_{ij} U_{jk} = \delta_{ik}. \quad (6.101)$$

Note that due to the noncommutativity of  $U_{ij}$ ,  $S(U)_{ij}$  is different from the usual inverse  $U_{ij}^{-1}$ , which is defined with respect to a commutative multiplication rule. The definition of  $S$  can be extended to the rest of the algebra recursively using the property (6.100).

Given a representation  $R$  of  $\mathcal{A}$ , the antipode defines the conjugate (“anti-particle”) representation  $\bar{R}$  by

$$\bar{R}(U) = (R \circ S(U))^t, \quad (6.102)$$

where  $t$  denotes the transpose.

**The adjoint action, Drinfeld element, and the quantum trace** We can now define how the quantum group acts on the open string Hilbert space via the adjoint action of the quantum group on itself. For an element  $g \in \mathcal{A}(U(N)_q)$ , the adjoint action is defined using a combination of the coproduct and antipode:

$$U_{ij} \rightarrow (\text{Ad}_g(U))_{ij} = \sum_{k,l} U_{kl} \otimes g_{ik} S(g)_{lj}, \quad (6.103)$$

where we have used  $\otimes$  in the same manner (6.92) to distinguish the objects  $U_{ij}$  in the representation space  $V^* \otimes V$  with the quantum group elements acting on that space. It is important to note that  $U_{ij}$  commutes with  $g_{ik}$  and  $S(g)_{lj}$  but  $g_{ik}$  and  $S(g)_{lj}$  do not commute among themselves.

As observed earlier, the ordinary trace  $\text{tr}_R(U)$  in any representation  $R$  is not invariant under this transformation law. However, there exists an invariant “quantum” trace function which can be defined purely in terms of quantum group data. One first defines the “Drinfeld” element  $u$  in terms of the  $\mathcal{R}$  matrix

$$\mathcal{R} = \sum_i a_i \otimes b_i \in \mathcal{A} \otimes \mathcal{A}, \quad (6.104)$$

and the antipode  $S$  according to

$$u = \sum_i S(b_i) a_i. \quad (6.105)$$

The quantum trace of an element  $U \in \mathcal{A}$  in any representation  $R$  can then be defined as:

$$\text{tr}_{q,R}(U) = \sum_{ij} u_{ij}^R R_{ji}(U), \quad (6.106)$$

where  $R_{ij}(U)$  are the representation matrices for  $U$  and we defined  $u_{ij}^R = R_{ij}(u)$ . The properties

$$\begin{aligned} S^2(V) &= uVu^{-1} \\ S(UV) &= S(V)S(U), \quad U, V \in \mathcal{A}, \end{aligned} \tag{6.107}$$

of  $u$  and  $S$  then imply that the quantum trace is invariant under the adjoint action (6.103) of the quantum group. An explicit proof is given in eq.(5.8) of [88], and it gives a nice illustration of subtleties arising from the  $q$  deformed multiplication rule. For  $U(N)_q$  the Drinfeld element is a diagonal matrix of complex phases<sup>17</sup> given explicitly by [285, 88]

$$u_{ii} = q^{\frac{N}{2}} q^{-i+\frac{1}{2}}. \tag{6.108}$$

Finally, we note that the quantum trace is multiplicative under tensor products:

$$\mathrm{tr}_q(A \otimes B) = \mathrm{tr}_q(A) \mathrm{tr}_q(B). \tag{6.109}$$

**The representation basis and Schur-Weyl duality** Let us now consider how the open string Hilbert space is organized into irreducible representations of the quantum group symmetry. Compact quantum groups such as  $U(N)_q$  satisfy a Peter-Weyl theorem [353], which states that its space of functions is spanned by the matrix elements in all irreducible representations<sup>18</sup> of the quantum group. These (noncommutative) matrix elements form an un-normalized basis of wavefunctions on  $\mathcal{A}(U(N)_q)$ :

$$\langle U | Rij \rangle = R_{ij}(U) \quad i, j = 1, \dots, \dim R, \quad U \in U(N)_q, \tag{6.110}$$

---

<sup>17</sup>The quantum group is an associative algebra over the complex numbers, so  $u$  is a nongeneric element that consists of scalar elements of the algebra.

<sup>18</sup>A precise description of the representation theory for quantum groups is described in chapter 11 of [236].

where  $\dim R$ , distinct from  $\dim_q(R)$ , is the *integer* dimension of the representation  $R$ . Note that  $|Rij\rangle$  labels a basis in  $V_R \otimes V_R^*$ , which is a vector space with an integer dimension. There is also a  $q$ -analogue of the translation-invariant Haar measure,

$$h : \mathcal{A} \rightarrow \mathbb{C}, \quad (6.111)$$

which can be used to define the inner product on  $\mathcal{A}(U(N)_q)$

$$(R_{ij}(U), R'_{kl}(U)) := h(R_{ij}^*(U), R'_{kl}(U)) = \delta_{RR'} \frac{(u^R)^{-1}_{jk} \delta_{il}}{\dim_q R}. \quad (6.112)$$

We now relate the representation (6.110) and the open string basis (6.96) by applying a  $q$ -deformed version of Schur-Weyl duality to the  $n$ -open string states  $\mathcal{H}_n(q)$ . This relation will be necessary to define the representation basis in the  $N \rightarrow \infty$  limit. We first recall the undeformed Schur-Weyl duality. The vector space  $V^{\otimes n}$  carries a representation of  $S_n$  which permutes the factors as well as a diagonal action of  $U(N)$ . The Schur-Weyl duality states that  $V^{\otimes n}$  decomposes into irreducible representations of these two groups as:

$$V^{\otimes n} = \bigoplus_{R \in Y_n} V_R^{U(N)} \otimes V_R^{S_n}, \quad (6.113)$$

where  $Y_n$  denotes the set of Young diagrams with  $n$  boxes which label irreducible representations of both  $U(N)$  and  $S_n$ . Equation (6.113) is the formal way of saying that irreducible representations of  $U(N)$  are obtained by symmetrizing/antisymmetrizing fundamental representations according to a Young diagram  $R$ . To obtain the decomposition of the Hilbert space of  $n$  strings, we apply the Schur-Weyl duality twice:

$$\begin{aligned} \mathcal{H}_n &= (V^n \otimes V^{*n})/S_n, \\ &= \left( \bigoplus_{R \in Y_n} V_R^{U(N)} \otimes V_R^{S_n} \right) \otimes \left( \bigoplus_{R' \in Y_n} V_{R'}^{U(N)} \otimes V_{R'}^{S_n} \right)^* / S_n, \\ &= \bigoplus_{R \in Y_n} V_R \otimes V_R^*, \end{aligned} \quad (6.114)$$

$$V_R := V_R^{U(N)} \otimes V_R^{S_n}, \quad (6.115)$$



where the vector space  $V_R \otimes V_R^*$  is spanned by the representation basis  $|Rij\rangle$   $i, j = 1, \dots, \dim R$ . We can thus interpret  $|Rij\rangle$  as symmetrized/antisymmetrized linear combinations of  $|I, J\rangle$ . As a simple example, the projection on to the antisymmetric representation  $R$  for  $n = 2$  is given by:

$$U_{ij}^1 U_{kl}^2 \rightarrow R_{ab}(U) = U_{ij}^1 U_{kl}^2 - U_{il}^1 U_{kj}^2 \in V_R \otimes V_R^*,$$

$$a, b = 1, \dots, \dim R, \quad (6.116)$$

where the superscripts label the strings. This decomposition (6.114) holds in the large  $N$  limit, and leads to a dimension formula

$$\dim \mathcal{H}_n = \sum_{R \in Y_n} (\dim R)^2, \quad (6.117)$$

which relates the counting of Chan-Paton factors to degeneracy factors of  $U(N)$ .

In the  $q$ -deformed case, the vector space  $V^{\otimes n}$  is a tensor product of  $U(N)_q$  fundamentals, so it can be organized into quantum group representations in a similar way. The operations which commute with the action of  $U(N)_q$  belong to a  $q$ -deformed version of the symmetric group called the Hecke algebra  $S_n^q$ , which combines the permutation of the tensor factors with applications of the  $R$  matrix. Given a transposition  $\tau_{12} \in S_n$  which acts on a basis of  $V_1 \otimes V_2$  by

$$\tau(\mathbf{e}_1 \otimes \mathbf{e}_2) = \mathbf{e}_2 \otimes \mathbf{e}_1. \quad (6.118)$$

We define an element  $h(\tau) \in S_n^q$  in the Hecke algebra by

$$h(\tau) = \tau \circ R. \quad (6.119)$$

The  $q$ -deformed Schur-Weyl duality states that the space  $V^{\otimes n}$  decomposes under the commuting action of  $(U(N)_q)^{\otimes n}$  and  $S_n^q$  as:[88]

$$V^{\otimes n} = \oplus_{R \in Y_n} V_R^{U(N)_q} \otimes V_R^{S_n^q}. \quad (6.120)$$

The  $q$ -deformed Hilbert space for  $n$  strings decomposes into

$$\begin{aligned}
\mathcal{H}_n(q) &= (V^n \otimes V^{*n}) / \sim, \\
&= \left( \oplus_{R \in Y_n} V_R^{U(N)_q} \otimes V_R^{S_n^q} \right) \otimes \left( \oplus_{R' \in Y_n} V_{R'}^{U(N)_q} \otimes V_{R'}^{S_n^q} \right)^* / \sim, \\
&= \oplus_{R \in Y_n} V_R^q \otimes V_R^{q*},
\end{aligned} \tag{6.121}$$

$$V_R^q := V_R^{U(N)_q} \otimes V_R^{S_n^q}, \tag{6.122}$$

where  $\sim$  refers to the equivalence relation

$$\mathcal{R}U_1U_2 = U_2U_1\mathcal{R}, \tag{6.123}$$

which determines the braiding structure of the open strings. In direct analogy with the undeformed case, we should view  $|Rij\rangle$  as a basis for the subspace  $V_R^q \otimes V_R^{q*}$ , obtained by symmetrizing/antisymmetrizing the Chan-Paton factors  $|IJ\rangle$  using the Hecke algebra elements. The corresponding projectors labelled by Young diagrams  $R \in Y_n$  were constructed in [88]. In contrast to the permutation group, the action of the Hecke algebra provides a representation of the braid group. This is because the endpoints of the open strings behave as anyons due to their coupling to the worldvolume Chern-Simons theory of the A-model branes [156]. The quantum dimension of  $\mathcal{H}_n(q)$  is computed from the trace of the Drinfeld element in the representations given in the Hilbert space decompositions of Eq. (6.121):

$$\dim_q \mathcal{H}_n(q) := \text{tr}_{\mathcal{H}_n}(u) = \sum_{R \in Y_n} (\dim_q R)^2, \tag{6.124}$$

which is the  $q$ -deformed version of equation (6.117). In the large  $N$  limit, this formula will give a canonical interpretation to the total degeneracy factors in the resolved conifold partition function (6.52) and the replica trick entanglement entropy (6.53).

**The large  $N$  limit of Schur-Weyl duality and the Drinfeld element** Schur-Weyl duality continues to hold in the large  $N$  limit of  $U(N)$ . As  $N \rightarrow \infty$ , we con-

tinue to identify the representation basis  $|Rij\rangle$  with Young diagrams describing the (anti)symmetrizations of Chan-Paton factors of the open string states  $|IJ\rangle$ . This basis spans the extended Hilbert space for the string theory dual to 2DYM with gauge group  $U(\infty)$  [122]. At large  $N$  the 2DYM partition function is determined by symmetric group data, which captures the wrapping of string worldsheets on the target space.

In a similar fashion, the  $q$ -deformed Schur-Weyl duality also survives the large  $N$  limit of  $U(N)_q$  and the corresponding basis  $|Rij\rangle$  is once again determined by the symmetrization of the Chan-Paton factors by elements of the Hecke algebra [88]. This basis spans the extended Hilbert space of  $q$ -deformed 2DYM with gauge group  $U(\infty)_q$ . As in the undeformed case, we wish to identify these states with the extended Hilbert space of the A-model TQFT, which is also determined by  $q$ -deformed symmetric group data.

Moreover in order for the counting of states in q2DYM to match with the A-model, we must identify the correct large  $N$  limit of the Drinfeld element  $u$  given in (6.108). Since  $u$  determines the trace function (6.106) on the extended Hilbert space, it can be viewed as determining the choice of measure on the open string states.

We will define the large  $N$  limit of  $u$  according to (6.84) in terms of the holonomy matrix  $D$  of (6.34). As explained in the derivation of (6.34) this limit requires an analytic continuation of  $q$  which regularizes the trace over the large  $N$  Hilbert space. As a result, even though the dimension

$$\mathrm{tr}_R(u) = \mathrm{tr}_R(u^{-1}) = \dim_q R, \quad (6.125)$$

is always a real quantity, in the large  $N$  limit  $D$  has a complex trace:

$$\begin{aligned}\mathrm{tr}_R(D) &= (-i)^{l(R)} d_q(R) q^{\kappa_R/4} \in \mathbf{C}, \\ \mathrm{tr}_R(D^{-1}) &= (\mathrm{tr}_R(D))^* = i^{l(R)} d_q(R) q^{-\kappa_R/4}.\end{aligned}\tag{6.126}$$

Accordingly, we define the quantum trace for the large  $N$  limit

$$\mathrm{tr}_q(U) = \mathrm{tr}(DU).\tag{6.127}$$

This feature is related to the holomorphic nature of the A model and essential to the emergence of the line bundle structure of the Calabi-Yau manifold.

With this definition of the large  $N$  Drinfeld element, the quantum dimension of the  $n$ -string Hilbert space becomes

$$\begin{aligned}\dim_q \mathcal{H}_n &:= \mathrm{tr}_{\mathcal{H}_n}(D) = \sum_{R \in Y_n} \mathrm{tr}_{R \otimes \bar{R}}(D) \\ &= \sum_{R \in Y_n} \mathrm{tr}_R(D) (\mathrm{tr}_R(D))^* = \sum_{R \in Y_n} (d_q(R))^2,\end{aligned}\tag{6.128}$$

where in the second to last equality we have used the multiplicative property of the quantum trace (6.109) and the unitarity of the representations.

### 6.5.3 A-model open-closed TQFT and factorization maps

We have now assembled all the ingredients necessary to describe the extension of the A-model TQFT into a  $q$ -deformed open-closed theory which incorporates the factorization of the closed and open string states.

We begin by defining the factorization maps in (6.56) and then extend these into an interwoven set of open-closed cobordisms.

**Factorization maps** The factorization map which embeds closed string states into open string states in the extended Hilbert space as shown in the left of figure (6.56) is called the zipper  $i_*$ . Our definition of the closed string wavefunction  $\langle U|R\rangle$  as a quantum trace suggests that

$$i_* = \text{cylinder with a wedge removed} : |R\rangle \rightarrow \sum_{i,j} (D^{-1})_{ji}^R |Rij\rangle . \quad (6.129)$$

Compatibility with the E-brane axiom then requires the co-zipper to be

$$i^* = \text{cylinder with a wedge added} : |Rij\rangle \rightarrow (-i)^{l(R)} \frac{\delta_{ij}}{d_q(R) q^{-\kappa_R/4}} |R\rangle , \quad (6.130)$$

so that

$$\text{cylinder with a wedge removed and added} = \text{cylinder} : |R\rangle \rightarrow |R\rangle , \quad (6.131)$$

as can be shown by noting that  $\sum_i (D^{-1})_{ii}^R = i^{l(R)} d_q(R) q^{-\kappa_R/4}$ .

Next we consider the cobordism on the right of figure (6.56), which embeds open string states of one subregion into the open string Hilbert space of two subregions.<sup>19</sup> We identify this factorization map with the coproduct in the open sector of the A-model TQFT:

$$\Delta = \text{pair of pants} : |Rij\rangle \rightarrow \sum_k |Rik\rangle |Rkj\rangle . \quad (6.132)$$

To see that this satisfies the E-brane axiom, we have to first define the open product

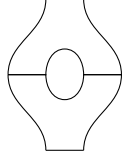

$$\mu_O = \text{Y-shape} , \quad (6.133)$$

which fuses two subregions together. This is the A-model version of the “entangling product” [116], and we propose that it is given by

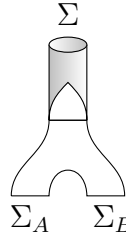
$$\mu_O = \text{Y-shape} : |Rij\rangle |R'kl\rangle \rightarrow (i)^{l(R)} \frac{D_{jk}^R}{d_q(R) q^{\kappa_R/4}} |Ril\rangle . \quad (6.134)$$

<sup>19</sup>The intervals in the cobordism diagrams really correspond to subregions of a time slice  $\mathcal{F}_\Sigma$  in the space of string loops.

This satisfies the E-brane axiom which requires that splitting followed by fusion gives the identity map:

$$
= 

: |Rij\rangle \rightarrow |Rij\rangle, \quad (6.135)$$

which follows from  $\sum_i D_{ii}^R = (-i)^{l(R)} d_q(R) q^{\kappa_R/4}$ . Finally, combining the zipper and coproduct gives the factorization map as promised in (6.55):

$$
: \mathcal{H}_\Sigma \rightarrow \mathcal{H}_{\Sigma_A} \otimes \mathcal{H}_{\Sigma_B}, \quad (6.136)$$

$$|R\rangle \rightarrow \sum_{ij} (D^{-1})_{ij}^R |Rji\rangle \rightarrow \sum_{ijk} (D^{-1})_{ij}^R |Rjk\rangle |Rki\rangle.$$

We have seen from previous sections that open string Hilbert spaces  $\mathcal{H}_{\Sigma_A}, \mathcal{H}_{\Sigma_B}$  transform nontrivially under the quantum group symmetry  $U(\infty)_q$ . However, by the invariance of the quantum trace, we know that the factorized state for  $|R\rangle$  is invariant. Thus the factorization map (6.136) into the extended Hilbert space respects the quantum group symmetry as promised.

Notice that even though we have imposed the hole-closing conditions (6.135), (6.131), this does not uniquely determine the factorization map. In particular these conditions would have been satisfied with a factorization with respect to an undeformed surface symmetry group<sup>20</sup>, which does not involve the Drinfeld element. As we show in section 6.5.5, the necessity for the q-deformed edge mode symmetry and the insertion of the Drinfeld element can only be seen when we enforce the E-brane axiom with a choice of a *geometric* state such as the closed unit (6.68).

---

<sup>20</sup>In this case, the more natural undeformed surface symmetry group would be  $S_n$  in each sector with  $n$  strings, since the A model partition function depends on dimensions of the symmetry group

### 6.5.4 The open A-model TQFT and sewing relations

As discussed in the beginning of section 6.4, our choice of factorization maps (6.129), (6.132) satisfies a set of sewing relations in addition to the E-brane axiom. Here we work out some of these relations explicitly in the open sector. As in 2D extended TQFT, we find that the A-model open TQFT forms a Frobenius algebra under the product  $\mu_O$ . We will taking the generating set for this algebra to be

$$\begin{array}{c} \text{Y-shape} \end{array}, \quad \begin{array}{c} \text{A-shape} \end{array}, \quad \begin{array}{c} \text{D-shape} \end{array}, \quad \begin{array}{c} \text{U-shape} \end{array}, \quad \begin{array}{c} \text{X-shape} \end{array}. \quad (6.137)$$

We have already defined the product and coproduct, which satisfy the Frobenius condition:

$$\begin{array}{c} \text{X-shape} \end{array} = \begin{array}{c} \text{A-shape with vertical lines} \end{array} = \begin{array}{c} \text{A-shape with vertical lines} \end{array}, \quad (6.138)$$

and are associative and co-associative. Next we can determine the open unit  $1_O$  and counit  $\epsilon$  from the product and coproduct using the defining relations

$$\begin{array}{c} \text{Y-shape with top line} \end{array} = \begin{array}{c} \text{A-shape with top line} \end{array} = \begin{array}{c} \text{Vertical line} \end{array}. \quad (6.139)$$

We find that

$$\begin{aligned} 1_O &= \begin{array}{c} \text{D-shape} \end{array} = \sum_{R,i,j} (-i)^{l(R)} d_q(R) q^{\kappa_R/4} (D^{-1})_{ij}^R |Rji\rangle, \\ \epsilon &= \begin{array}{c} \text{U-shape} \end{array} : |Rij\rangle \rightarrow \delta_{ij}. \end{aligned} \quad (6.140)$$

**The open pairing, adjoint operation and the quantum trace** Our open string Frobenius algebra also possesses a nondegenerate bilinear form (the Frobenius form)  $\xi$ , which defines an adjoint operation on the open string Hilbert space. This is called the open pairing and can be obtained by gluing the counit  $\epsilon$  to the

product  $\mu_O$

$$\xi = \text{cup} = \text{Y-shape} : |Rij\rangle |R'kl\rangle \rightarrow (i)^{l(R)} \delta_{RR'} \frac{D_{jk}^R \delta_{il}}{d_q(R) q^{\kappa_R/4}}. \quad (6.141)$$

Notice that our definition of  $\xi$  coincides precisely with the large  $N$  limit of the bilinear form (6.112) and should therefore be related to the large  $N$  limit of the  $q$ -deformed Haar measure. Its inverse, called the copairing, can be obtained by gluing the unit to the product,

$$\xi^{-1} = \text{X-shape} = \text{arc} : 1 \rightarrow \sum_{R,i,j,k} (-i)^{l(R)} d_q(R) q^{\kappa_R/4} (D^{-1})_{ij}^R |Rik\rangle |Rkj\rangle. \quad (6.142)$$

and satisfies the zigzag identity

$$\text{zigzag} = \text{zigzag} = \text{rectangle} : |Rij\rangle \rightarrow |Rij\rangle. \quad (6.143)$$

The pairing and copairing define an adjoint operation by turning the input Hilbert space to output Hilbert space and vice versa. For example they relate the unit and product to the counit and coproduct:

$$\text{Y-shape} = \text{X-shape with vertical lines}, \quad \text{cup} = \text{arc}. \quad (6.144)$$

They also define a canonical trace operation on open cobordisms by connecting the input Hilbert spaces to output Hilbert space:

$$\text{trace diagram 1}, \quad \text{trace diagram 2}. \quad (6.145)$$

Notice that we have drawn the partial trace to avoid braiding, so the trace on the left/right side has to closed on the left/right side. If we violate this rule, we would



have to account for the nontrivial braiding that occurs when the strips cross. Most importantly, this categorical definition of the trace coincides with the quantum trace  $\mathcal{A}(\mathrm{U}(\infty)_q)$  as defined in (6.127), (6.128).

Using the pairing and copairing we can calculate the annulus:

$$\begin{aligned}
\text{Annulus} &= \sum_R \mathrm{tr}_R(D) \mathrm{tr}_R(D^{-1}), \\
&= \sum_R \mathrm{tr}_{R \otimes \bar{R}}(D) = \mathrm{tr}_q(1),
\end{aligned} \tag{6.146}$$

where we used the multiplicative property of the trace and unitarity of the representations. The final expression above is just the quantum trace of the identity operator on the total open string Hilbert space.

The final generator of our open Frobenius algebra is the braiding operator

$$\mathcal{B} = \tau \circ \mathcal{R}_{\text{string}} = \text{X} : \mathcal{A} \otimes \mathcal{A} \rightarrow \mathcal{A} \otimes \mathcal{A}, \tag{6.147}$$

where  $\tau$  is the operation that exchanges two copies of the open string Hilbert space. The operation  $\mathcal{R}_{\text{string}}$  refers to the  $R$  matrix which describes the braiding of the open strings. This is nontrivial, in contrast with the usual 2D open-closed TQFT [278], since the left/right string endpoints themselves have nontrivial braiding. However, since we will not require the braiding operation in our calculation of entanglement entropy, we will leave this for future work.

### 6.5.5 The open closed sewing axioms and factorization of the Hartle-Hawking state

We have seen that the factorization map  $\Delta$  extends consistently to a Frobenius algebra describing the open sector of the A-model TQFT. We now consider the

open-closed sewing axioms [278] which enforce the compatibility of the open string algebra with the closed string algebra defined by (6.68)-(6.72). We will pay particularly close attention to the consistency of the Chern class labelings, which places additional constraints on the factorization. This is because one could obtain factorization maps that satisfy (6.131) and (6.135), and extend to a consistent open Frobenius algebra, but is nevertheless incompatible with the A-model TQFT restricted to Calabi-Yau manifolds<sup>21</sup>. As an application of this machinery, we give a simple factorization of the Hartle-Hawking state.

The relation between the closed and open sector is given by the zipper and co-zipper, which are algebra/coalgebra homomorphisms between the respective Frobenius algebras. Keeping track of the Chern class on the closed cobordisms, the homomorphism property is equivalent to the sewing relations

$$\begin{array}{c} (0,-1) \\ \text{zipper} \end{array} = \text{cap} \quad , \quad \begin{array}{c} (0,1) \\ \text{co-zipper} \end{array} = \text{cup} \quad , \quad (6.148)$$

$$\begin{array}{c} \text{zipper} \\ (0,-1) \end{array} = \text{cap} \quad , \quad \begin{array}{c} \text{co-zipper} \\ (1,0) \end{array} = \text{cup} \quad , \quad (6.149)$$

which is satisfied by our open-closed cobordisms. The left diagrams above express the fact that the unit/counit is preserved by the zipper/cozipper.

<sup>21</sup>For example, since the  $(0,0)$  sector of the A model TQFT is a closed algebra which is isomorphic to the Frobenius algebra of an ordinary 2D TQFT, we could simply use the factorization maps with respect to an undeformed  $S_n$  surface symmetry. The E-brane condition would then be defined with the  $(0,0)$  cap, giving a factorization that is compatible with the  $(0,0)$  sector of the A-model TQFT, but incompatible with the Calabi-Yau condition.



**Factorization of the HH state** We now apply our factorization map to the Hartle-Hawking state and its dual at  $t = 0$ :

$$\begin{aligned}
|HH\rangle &\rightarrow \begin{array}{c} (0,-1) \\ \text{[Diagram: A vertical cylinder with a horizontal cut, shaded top and bottom, and a central horizontal line.]} \end{array} = \begin{array}{c} \text{[Diagram: A Y-shaped surface with a horizontal cut.]} \end{array} = \begin{array}{c} \text{[Diagram: A semi-circular arc.]} \end{array} = \sum_{R,i,j,k} (-i)^{l(R)} d_q(R) q^{\kappa_R/4} (D^{-1})_{ij}^R |Rik\rangle |R \\
\langle HH^*| &\rightarrow \begin{array}{c} \text{[Diagram: A vertical cylinder with a horizontal cut, shaded top and bottom, and a central horizontal line.]} \\ (-1,0) \end{array} = \begin{array}{c} \text{[Diagram: A Y-shaped surface with a horizontal cut.]} \end{array} = \begin{array}{c} \text{[Diagram: A semi-circular arc.]} \end{array} : |Rij\rangle |R'kl\rangle \rightarrow (i)^{l(R)} \delta_{RR'} \frac{D_{jk}^R \delta_{il}}{d_q(R) q^{\kappa_R/4}}.
\end{aligned}
\tag{6.152}$$

Using this factorization map the A-model partition function on the resolved conifold can be given a canonical open string interpretation:

$$\begin{aligned}
Z = \langle HH^* | HH \rangle &\rightarrow \begin{array}{c} \text{[Diagram: A circle with a smaller circle inside, connected by a horizontal line.]} \end{array} = \text{tr}_q(e^{-tH_{\text{open}}}), \\
&= \sum_R (d_q(R))^2 e^{-tl(R)} = \begin{array}{c} (0,-1) \\ \text{[Diagram: A sphere with a horizontal cut, shaded top and bottom, and a central horizontal line.]} \\ (-1,0) \end{array}.
\end{aligned}
\tag{6.153}$$

where we have defined the open string modular Hamiltonian

$$H_{\text{open}} |Rij\rangle = l(R) |Rij\rangle. \tag{6.154}$$

Even though we have drawn the same diagram as in the  $t = 0$  case, we have included an open string propagator  $e^{-tH_{\text{open}}}$  which introduces an explicit  $t$  dependence. Equation (6.153) gives an explicit realization of the Susskind-Uglum proposal to interpret the closed string amplitude as a trace over an open strings which end on the entangling surface.

**Compatibility of open and closed string pairings** The closed pairing (6.74) defines the adjoint operation in our closed string TQFT which maps the Hartle-Hawking state to its dual. Having defined an extension to the open TQFT with an adjoint operation given by the open pairing (6.141), we should check that these two adjoint operations are compatible. This is a consequence of the E-brane axiom together with the right diagrams in (6.148) (6.149), which states that zipper/cozipper respects the multiplication/comultiplication. Explicitly, we can glue the counit to both sides of the right diagram in (6.148) :

$$\begin{array}{c} (0,1) \\ \text{Diagram: A vertical cylinder with a Y-shaped opening at the top and a small cup at the bottom.} \end{array} = \begin{array}{c} \text{Diagram: A vertical cylinder with two separate openings at the top and a small cup at the bottom.} \end{array} . \quad (6.155)$$

On the left diagram, we apply the E-brane axiom in the form:

$$\begin{array}{c} \text{Diagram: A vertical cylinder with a small cup at the bottom.} \end{array} = \begin{array}{c} (-1,0) \\ \text{Diagram: A small cup.} \end{array} , \quad (6.156)$$

which then implies

$$\begin{array}{c} (-1,1) \\ \text{Diagram: A vertical cylinder with a U-shaped opening at the top and a small cup at the bottom.} \end{array} = \begin{array}{c} \text{Diagram: A vertical cylinder with two separate openings at the top and a small cup at the bottom.} \end{array} . \quad (6.157)$$

This expresses the compatibility of the open and closed pairing, with analogous relations holding for the copairing. Note that in both (6.156) and (6.157), the E-brane axiom is satisfied only for a specific Chern class labelling compatible with the Calabi-Yau constraint defining our closed string algebra.

Finally note that the zipper and cozipper are adjoint operations, which is im-

plied by the third sewing axiom in (6.62):

$$\begin{array}{c} \text{Diagram 1} \end{array} = \begin{array}{c} \text{Diagram 2} \\ (-1,1) \end{array} . \quad (6.158)$$

By gluing the copairing to the right input of this relation and applying the zigzag identity, we find that the cozipper is the adjoint of the zipper

$$\begin{array}{c} \text{Diagram 1} \end{array} = \begin{array}{c} \text{Diagram 2} \end{array} . \quad (6.159)$$

### 6.5.6 The reduced density matrix for the Hartle-Hawking state and a canonical calculation of entanglement entropy

The reduced density matrix for the Hartle-Hawking state is easily derived from the factorization map (6.152). First note that unnormalized density matrix<sup>22</sup>  $\tilde{\rho}$  for the Hartle Hawking state factorizes as

$$\tilde{\rho} = |HH\rangle \langle HH^*| = \begin{array}{c} (-1,0) \\ \text{Diagram 1} \\ (0,-1) \\ \text{Diagram 2} \end{array} \rightarrow \begin{array}{c} \text{Diagram 3} \\ \text{Diagram 4} \end{array} . \quad (6.160)$$

The corresponding reduced density matrix is given by the (quantum) partial

---

<sup>22</sup> $\tilde{\rho}$  is defined by  $\text{tr}(\tilde{\rho}O) = \langle HH^*|O|HH\rangle$  for any operator  $O$  with the trace defined by the closed pairing/copairing. This has the same structure as density matrices in non-Hermitian systems[81].

trace, which is defined by (6.145), over the subregion  $\Sigma_B$  :

$$\tilde{\rho}_A = \text{tr}_B \tilde{\rho} = \begin{array}{c} \text{Diagram: A vertical strip with two horizontal lines, each having a semi-circular loop extending to the left.} \end{array} = \begin{array}{c} \text{Diagram: A simple vertical strip with two horizontal lines.} \end{array} = \sum_R e^{-tl(R)} \mathbf{1}_R = \sum_{R,i,j} e^{-tl(R)} |Rij\rangle \langle Rij|. \quad (6.161)$$

where we have applied the zigzag identity and absorbed the area dependence into the propagator represented by the strip. Note that we have applied a quantum partial trace defined by the pairing and copairing. This operation cancels the insertions of  $D$  and  $D^{-1}$  in the density matrix which would have led to non local boundary conditions for the modular Hamiltonian. We will comment more on this in the next section.

As in the case of undeformed gauge theory, the form of the reduced density matrix (6.161) is dictated by symmetry. The action of  $U(\infty)_q$  must commute with  $\tilde{\rho}_A$ , since our factorization map (6.136) respects the quantum group symmetry. Schur's lemma then requires the reduced density matrix to act as the identity in each irreducible representation  $R$ , leading to the block-diagonal form of (6.161). Note that while the degeneracy associated with each irreducible representation  $R$  is generic (it holds for any gauge-invariant state in the theory), the modular Hamiltonian (6.154) actually has a much larger degeneracy, since all representations with the same number of boxes has the same modular energy.

Tracing over  $\Sigma_A$  gives the expected normalization

$$Z = \text{tr}_A(\tilde{\rho}_A) = \sum_R (d_q(R))^2 e^{-tl(R)}. \quad (6.162)$$

It is useful to express the normalized reduced density density matrix  $\rho_A = \tilde{\rho}_A/Z$

as a direct sum over normalized<sup>23</sup> operators  $\frac{\mathbf{1}_R}{(d_q R)^2}$  in each superselection sector labelled by  $R$ :

$$\begin{aligned}\rho_A &= \oplus_R p(R) \frac{\mathbf{1}_R}{(d_q R)^2}, \\ p(R) &= \frac{(d_q(R))^2 e^{-\ell(R)}}{Z}.\end{aligned}\tag{6.163}$$

The  $q$ -deformed entanglement entropy can be directly evaluated from

$$S = -\mathrm{tr}_q(\rho_A \log \rho_A) = -\mathrm{tr}(D\rho_A \log \rho_A).\tag{6.164}$$

This type of  $q$ -deformed entropy has been studied previously in the context of quantum group invariant spin chains [81, 295]. Here we have seen that the use of the quantum trace arises naturally from the requirement of quantum group symmetry as dictated by the cobordisms of the open-closed TQFT.

Since the spectrum of the  $\rho_A$  can be read off from (6.163), we can compute the entanglement entropy without appealing to the replica trick:

$$\begin{aligned}S &= -\sum_R \mathrm{tr}_q \left( \frac{p(R)\mathbf{1}_R}{(d_q R)^2} \log \frac{p(R)\mathbf{1}_R}{(d_q R)^2} \right) = -\sum_R \mathrm{tr}_q(\mathbf{1}_R) \frac{p(R)}{(d_q R)^2} \log \frac{p(R)}{(d_q R)^2}, \\ &= \sum_R (-p(R) \log p(R) + 2p(R) \log d_q R).\end{aligned}\tag{6.165}$$

This gives the sought after canonical calculation of entanglement entropy which agrees with the replica trick answer in section 6.3.3

### 6.5.7 Revisiting the replica trick on the resolved conifold

As discussed previously, the resolved conifold is a nontrivial vector bundle  $\mathcal{O}(-1) \oplus \mathcal{O}(-1) \rightarrow S^2$ . In section 6.3.3 we gave a prescription for the replication of this

---

<sup>23</sup>Normalized according to the quantum trace.



geometry in which the volume of the base manifold is replicated without affecting the bundle structure. Here we explain this prescription, first in terms of the our categorical formulation of the reduced density matrix, and then by appealing to a direct geometric construction of the replica manifold.

**Replica trick in terms of cobordisms** Using the reduced density matrix (6.161) for  $|HH\rangle$ , we can apply the replica trick in the form

$$S = \partial_n \text{tr}_q(\rho_A^n)|_{n=1} = \partial_n \text{tr}(D\rho_A^n)|_{n=1}. \quad (6.166)$$

Note that we did not replicate  $D$  because it is merely part of the definition of the quantum trace. In terms of cobordisms, the  $n$ th power of  $\rho_A$  is simply a long strip, and  $\text{tr}_q(\rho_A^n)$  is a large annulus with one insertion of  $D$  and  $D^{-1}$  as in the  $n = 1$  case.

$$\begin{aligned} \rho_A^n &= \oplus_R \frac{d_q(R)^2 e^{-ntH_{\text{open}}}}{Z_1^n} \frac{\mathbf{1}_R}{d_q(R)^2}, \\ \text{tr}_q \rho_A^n &= \frac{\sum_R d_q(R)^2 e^{-ntH_{\text{open}}}}{Z_1^n}, \end{aligned} \quad (6.167)$$

and the only effect of the replication is to rescale the area factor  $t$  by a factor of  $n$ . This replicated partition function agrees with the prescription given in (6.43) and is proportional to the resolved conifold partition function, indicating that Calabi-Yau condition is preserved.

The main reason that the Calabi-Yau condition is preserved is the use of the quantum partial trace in (6.161). To see this, consider an alternative replication in which we use a naive trace, corresponding to simply gluing the Hartle-Hawking state and its dual along region  $\Sigma_B$  without the application of state-channel map

as in (6.161).

$$\rho_A^C = \text{[Diagram: A vertical strip with a C-shaped cutout on the left side]} : |Rij\rangle \rightarrow D_{lj}^R (D^{-1})_{ik}^R e^{-tl(R)} |Rkl\rangle. \quad (6.168)$$

As shown in figure 6.9,  $\rho_A^C$  differs from  $\rho_A$  because of the nontrivial braiding of the open string, so that when we “straighten” the cobordism for  $\rho_A^C$  we get a nontrivial double twist diagram instead of a strip.  $\rho_A^C$  also does not commute with the quantum group symmetry that permutes the edge modes. When we replicate  $\rho_A^C$ , the Wilson lines  $D$  and  $D^{-1}$  do not cancel. As a result we find that

$$\text{tr}(\rho_A^{Cn}) = \sum_R \text{tr}_R(D^n) \text{tr}_R(D^{-n}), \quad (6.169)$$

which does not satisfy the Calabi-Yau condition and gives an entropy inconsistent with the replica prescription of section 6.3.3. The problem is that the entanglement boundary condition is violated each time we replicate this density matrix. A simple

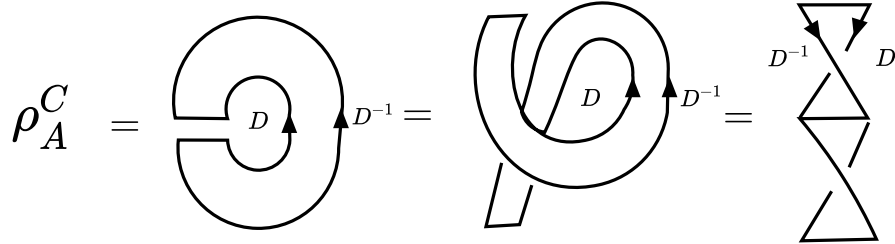


Figure 6.9: The reduced density matrix  $\rho_A^C$  defined using a noncanonical trace operation fails to satisfy the E-brane axiom when it is replicated. It also does not commute with the edge mode symmetry group

way to compensate for this is to insert a factor of  $D^{-1}$  each time we replicate  $\rho_A^C$ .

The replica entropy (6.166) can then be expressed as

$$S = \partial_n \text{tr}(D \rho_A^n) |_{n=1} = \partial_n \log \text{tr}(D^{1-n} (\rho_A^C)^n) |_{n=1}, \quad (6.170)$$

where we have introduced the log to account for normalization. These are the direct analogue of the replica entropy in [208], with  $D$  playing the role of the “defect” operator.

**Geometric replication of the resolved conifold geometry** Rather than appealing to the categorical formulation of the density matrix, we can also try to replicate the resolved conifold geometry directly by appealing to the usual multi-sheeted construction of the replica manifold. This will show more explicitly the geometrical role played by the defect operator as a topological twisting.

In [8, 63], it was shown that one can compute topological A-model partition function on  $L_1 \oplus L_2 \rightarrow \Sigma_g$ , for a 2 dimensional surface  $\Sigma_g$  with genus  $g$ . It was then further shown that one can glue  $L_1 \oplus L_2 \rightarrow \Sigma_1$  and  $L'_1 \oplus L'_2 \rightarrow \Sigma_2$ , given a gluing map  $i : \partial\Sigma_1 \rightarrow \partial\Sigma_2$ , to compute the topological A-model partition function on  $(L_1 + L'_1) \oplus (L_2 + L'_2) \rightarrow \Sigma_1 \cup \Sigma_2$ .

We define the Hartle-Hawking state to be the topological A-model partition function on  $\mathcal{O}_1 \oplus \mathcal{O}_2(-1) \rightarrow D_1^2$

$$|HH\rangle = \quad A_1 \quad \bigcirc \quad B_1 \quad , \quad (6.171)$$

where the black dot in (6.171) represents a pole of a local section in  $\mathcal{O}_2(-1)$ . For later use, we split  $\partial D_1^2 = A_1 \cup B_1$ . In the similar way, we define a dual of the Hartle-Hawking state to be topological A-model partition function on  $\mathcal{O}_1(-1) \oplus \mathcal{O}_2 \rightarrow D_2^2$

$$\langle HH^*| = \quad B_2 \quad \left( \text{---} \bigcirc \text{---} \right) \quad A_2 \quad , \quad (6.172)$$

where the blue dot in (6.172) represents a pole of a local section in  $\mathcal{O}_1(-1)$ .

To construct  $|HH\rangle\langle HH^*|$ , we prepare  $\mathcal{O}_1 \oplus \mathcal{O}(-1) \rightarrow D_1^2$  and  $\mathcal{O}_1(-1) \oplus \mathcal{O}_2 \rightarrow D_2^2$ .

$$|HH\rangle\langle HH^*| = A_1 \left( \text{circle with solid boundary and black dot} \right) B_1 \otimes B_2 \left( \text{circle with dashed boundary and blue dot} \right) A_2 \quad . \quad (6.173)$$

Now we can obtain a reduced density matrix  $\rho_{red} = \text{tr}_{B_1 \sim B_2}(|HH\rangle\langle HH^*|)$  by identifying  $B_1 \in \partial D_1^2$  and  $B_2 \in \partial D_2^2$ . We expect that  $\rho_{red}$  is equivalent to  $\rho_A$ , but we have not explicitly verified this claim.

$$\rho_{red} = A_1 \left( \text{circle with solid boundary and two dots: black and blue} \right) A_2 \quad . \quad (6.174)$$

One can check, under the identification  $A_1 \sim A_2$ ,  $\text{tr}_{A_1 \sim A_2}(\rho_{red})$  computes topological A-model partition function of  $\mathcal{O}_1(-1) \oplus \mathcal{O}_2(-1) \rightarrow S^2$ .

Let us consider a replicated geometry of (6.174). First we prepare two copies of (6.174)

$$\rho_{red} \otimes \rho_{red} = A_1 \left( \text{circle with solid boundary and two dots: black and blue} \right) A_2 \otimes A_3 \left( \text{circle with dashed boundary and two dots: blue and black} \right) A_4 \quad . \quad (6.175)$$

In order to compute  $\rho_{red}^2$ , we then identify  $A_2 \sim A_3$

$$\rho_{red}^2 = A_1 \left( \text{circle with solid boundary and four dots: two black and two blue} \right) A_4 \quad . \quad (6.176)$$

Note that as a result of the replication, volume of the base manifold is doubled. This naïve replica trick (6.176) has a problem. To illustrate the problem, let us compute  $\text{tr}_{A_1 \sim A_4}(\rho_{red}^2)$ . Because there are two poles for each section of line bundles  $L_1$  and  $L_2$ , one can deduce that  $L_1 = \mathcal{O}(-2)$  and  $L_2 = \mathcal{O}(-2)$  whereas topology of the base manifold is still of  $S^2$ . Then the manifest problem occurs as



It is very interesting to observe that (6.183) is proportional to the number of BPS states, including the multi-particle states. In fact, the linear dependence of the EE on the BPS index is not a special feature of the resolved conifold. For a general non-compact Calabi-Yau of the form

$$L_1 \oplus L_2 \rightarrow \mathcal{S}, \quad (6.184)$$

the linear dependence continues to hold

$$S = \sum_{\beta, g, k} n_{\beta}^g \left( \frac{1}{k} + t_{\beta} \right) \left( 2 \sin \frac{kg_s}{2} \right)^{2g-2} Q^{k\beta}, \quad (6.185)$$

if one replicates the geometry while fixing the topology of the replicated Calabi-Yau.

## 6.6 Discussion

In this work we have given a factorization of the A-model closed string Hilbert space and a canonical calculation of the entanglement entropy for the Hartle-Hawking state on the resolved conifold. The factorization maps (6.135), (6.131) and associated string edge modes are determined by solving the sewing relations of the A-model extended TQFT. These sewing relations, particularly the E-brane axiom, were chosen to be compatible with the Calabi-Yau condition. This constraint imposes a nontrivial holonomy  $D$  (6.34) along the entangling surface, which is captured by the entanglement boundary state  $|D\rangle$ . This boundary condition is local in the sense that it can be introduced without affecting the state, but is nonlocal with respect to the “modular time” going around the entangling surface. We then interpret this as an E-brane boundary state by showing that in the open string channel it corresponds to the insertion of a large  $N$  number of E-branes at the entangling

surface. We view this as a realization of Susskind and Uglum’s proposal [315] in the target space of the A-model string theory. Finally we found that the compatibility of the E-brane axiom with the Calabi-Yau condition requires edge modes to transform in a  $q$ -deformed edge mode symmetry group. This  $q$ -deformation changes the statistics of the open strings: they are no longer bosonic strings but obey anyonic statistics. Invariance under the quantum group symmetry requires the introduction of the Drinfeld element into the factorization map, and leads to the appearance of quantum dimensions in the entanglement entropy. In a follow-up paper, we will relate this calculation to the dual Chern-Simons description of the A-model, where quantum dimensions also appear.

The use of extended TQFT techniques was crucial in making our closed string factorization maps self-consistent. However our proposed extension of the A-model TQFT is not yet complete, since we did not consider sewing relations which involve the braiding operator (6.147). We also worked entirely in the target space theory, whereas D-branes are usually formulated in the first-quantized, worldsheet point of view and we do not know how to formulate the E-brane boundary condition on the worldsheet. A direct check along this direction would be to quantize open strings stretched between intersecting D-branes on  $\mathcal{L}$  and  $\mathcal{L}'$  as shown in figure 10 and check whether this description agrees with the E-brane calculation we present in this paper. We leave these problems to future work.

**Analogy to JT gravity** The Drinfeld element  $D$  can be viewed as an operator on the open string Hilbert space. It is incorporated into the definition of the quantum trace (6.82), which agrees with the categorical trace defined by elements of the open string Frobenius Algebra. However, as shown in section 6.5.6, we can also interpret  $D$  as a “defect” operator whose insertion at the entangling surface

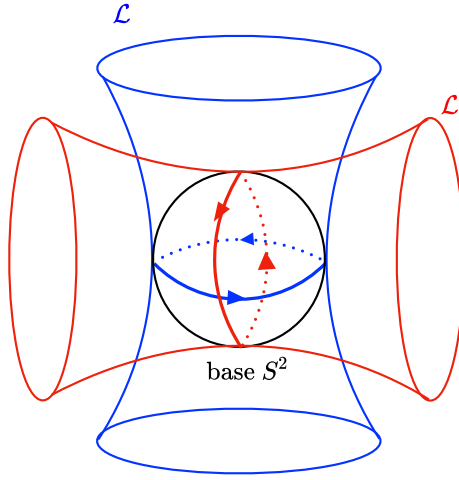


Figure 6.10: D-branes on  $\mathcal{L}'$  intersect with D-branes on  $\mathcal{L}$ .

enforces a topological constraint, which is equivalent to filling in the hole with a Calabi-Yau cap.

An analogous defect operator was found in the factorization of JT gravity [208]<sup>24</sup>. In that work, the topological constraint analogous to the Calabi Yau condition in the A-model is the gravitational constraint imposed on the BF gauge theory description of JT gravity. This constraint is needed because while the variables of JT gravity can be mapped to the BF gauge theory, there are gauge theory configurations such as those with trivial Chern class which are not allowed in the JT gravity path integral. In particular, the analogue of the E-brane condition for JT gravity requires that the hole can be filled in such a way to reproduce the Einstein-Hilbert term on a disk, which is a topological invariant that can only be captured with nontrivial holonomy of the BF gauge field around the hole. The defect operator in JT gravity implements this nontrivial holonomy around the entangling surface, just like the Drinfeld element in the A-model. These similarities suggest that the defect operator in JT gravity might also be viewed as a limit of

<sup>24</sup>[231] considered a statistical mechanical model for JT gravity which also gave rise to the analogue of this defect operator when attempting to write the partition function on the disk as a trace over a Hilbert space.



the Drinfeld element of a quantum group surface symmetry.

There are other indications that quantum groups play an important role in JT gravity as well. In [51], it was proposed that the edge mode symmetry of JT gravity is given by the semi-group  $SL^+(2, \mathbb{R})$  as a  $q \rightarrow 1$  limit of  $SL_q^+(2, \mathbb{R})$ , based on the fact that JT gravity can be obtained from the extremal limit of the dimensional reduction of 3D gravity, whose dynamics is connected to the representation theory of the quantum group  $SL_q^+(2, \mathbb{R})$  [339, 320, 272, 132, 51, 276]. In [272], it was also observed that the Bekenstein-Hawking entropy for 3d BTZ black holes can be reproduced in the large charge limit by the topological entanglement entropy related to the quantum dimensions in Liouville theory. It will be very interesting to see if there is a canonical way to directly justify the origin of the above observation.

One way to see quantum group symmetry appearing in JT gravity is via the Sachdev-Ye-Kitaev model, for which JT gravity can be viewed as an infrared effective theory. Specifically, Ref. [44] studied correlation functions in a “double-scaling” limit of SYK and found evidence of quantum group symmetry such as  $q$ -deformed  $6j$  symbols. This suggests that the bulk dual of the double-scaled SYK model could be identified as a TQFT with quantum group symmetry like the one described here for the A-model string. Such a TQFT would be a  $q$ -deformation of JT gravity which might elucidate the appearance of  $q \rightarrow 1$  limits of quantum group structures in JT gravity.

In this work, we have calculated entanglement entropy of topological A-model on a fixed geometry: the resolved conifold. We have made use of a TQFT formalism in which the topology of spacetime is fixed rather than summed over. This is analogous to the entanglement entropy on the hyperbolic disk in JT gravity [247, 208, 51]. However, JT gravity can be UV completed by a random matrix

model by summing over all different topologies, which is interpreted as being dual to an ensemble average of theories [304]. Recently, it has also been shown in the context of models related to JT gravity that topology-changing processes play an important role in understanding the black hole information paradox when we calculate the entropy using the replica trick [290, 13]. There is an analogue UV completion of topological string theory by including topology-changing processes via nonperturbative effects in the context of  $q$ -deformed 2d Yang-Mills theory [327, 9]. In [106, 7], it was further shown that the inclusion of baby universes doesn't lead to naive loss of quantum coherence, in accordance with earlier arguments from [77, 153, 154]. On the other hand, the ensemble average interpretation and the lack of factorization in JT gravity is clearly in tension with the standard AdS/CFT correspondence. In [207, 260], another perspective is given, interpreting the ensemble average as coming from gravitational constraints and different superselection sectors of the baby universe Hilbert space. Based on this observation, it was further conjectured in [275] based on [274] that the constraint is so strong in  $d > 3$  that the baby universe Hilbert space is always one-dimensional in a consistent theory of quantum gravity, thus resolving the contradiction. As we have a UV completion for a theory of quantum gravity involving topology changes [327, 9, 106, 7], we find it appealing that we might be able to test all these ideas in this context, and may directly identify an “information paradox” in string theory where calculations of entropy without the inclusion of topology-changing procedures leads to violation of unitarity.

**Comment on the BPS formula for the EE** At strong string coupling, fundamental degrees of freedom are no longer string states rather D-brane particle states. Furthermore, the degeneracy of the BPS states is typically expected to

be exponential in the number of the BPS states [324]. This exponential scaling of the degeneracy equates well with (6.185) as is proportional to the BPS index  $n_\beta^g$ . Hence, (6.185) implies that the entanglement entropy counts how many BPS states (including the multi particle states) there are across the entangling surface. Interestingly enough, in [313] the Bekenstein-Hawking entropy computed via the BPS microstate counting is also polynomial in the BPS index due to the exponential scaling of the degeneracy. It will be therefore interesting to explicitly show that the degeneracy of the Calabi-Yau manifold is exponential in the number of the M2-brane BPS states in M-theory on  $\text{CY}_3 \times S^1$ .

CHAPTER 7

ENTANGLEMENT ENTROPY AND EDGE MODES IN  
TOPOLOGICAL STRING THEORY II: THE DUAL GAUGE  
THEORY STORY

**Abstract**<sup>1</sup>

This is the second in a two-part paper devoted to studying entanglement entropy and edge modes in the A model topological string theory. This theory enjoys a gauge-string (Gopakumar-Vafa) duality which is a topological analogue of AdS/CFT. In part 1, we defined a notion of generalized entropy for the topological closed string theory on the resolved conifold. We provided a canonical interpretation of the generalized entropy in terms of the  $q$ -deformed entanglement entropy of the Hartle-Hawking state. We found string edge modes transforming under a quantum group symmetry and interpreted them as entanglement branes. In this work, we provide the dual Chern-Simons gauge theory description. Using Gopakumar-Vafa duality, we map the closed string theory Hartle-Hawking state to a Chern-Simons theory state containing a superposition of Wilson loops. These Wilson loops are dual to closed string worldsheets that determine the partition function of the resolved conifold. We show that the *undeformed* entanglement entropy due to cutting these Wilson loops reproduces the bulk generalized entropy and therefore captures the entanglement underlying the bulk spacetime. Finally, we show that under the Gopakumar-Vafa duality, the bulk entanglement branes are mapped to a configuration of topological D-branes, and the non-local entanglement boundary condition in the bulk is mapped to a local boundary condition in

---

<sup>1</sup>This chapter is published as Y. Jiang, M. Kim, G. Wong, “Entanglement entropy and edge modes in topological string theory II: The dual gauge theory story,” [arxiv:2012.13397 [hep-th]].

the gauge theory dual. This suggests that the geometric transition underlying the gauge-string duality may also be responsible for the emergence of entanglement branes.

## 7.1 Introduction

In the context of the AdS/CFT correspondence [252, 174, 348], the HRRT/generalized entropy [303, 203, 139, 137] formula provides the basis for our understanding of how spacetime emerges from quantum entanglement. It states that entanglement entropy of a boundary subregion in the strongly coupled regime is given by the generalized entropy of the semi-classical bulk theory:

$$S_{\text{CFT}} = S_{\text{gen}} = \frac{\langle A \rangle}{4G} + S_{\text{bulk}} + \cdots \quad (7.1)$$

The generalized entropy  $S_{\text{gen}}$  is defined via the Euclidean gravity path integral  $Z(\beta)$  on geometries for which the asymptotic boundary has a circle<sup>2</sup> of length  $\beta$  [243] (see Fig. 7.1). One then defines the generalized entropy as

$$S_{\text{gen}} = (1 - \beta \partial_\beta)_{\beta=2\pi} \log Z(\beta) \quad (7.2)$$

$$Z(\beta) \sim e^{-I_{\text{classical}}} Z_{\text{fluctuations}}, \quad (7.3)$$

where  $Z(\beta)$  is evaluated on a saddle point and  $-I_{\text{classical}}$  is the on-shell action. In order to interpret  $S_{\text{gen}}$  in terms of a statistical mechanical entropy we must treat

---

<sup>2</sup>This circle is non-contractible at asymptotic infinity but can shrink smoothly in the bulk.

$Z(\beta)$  as a thermal partition function:

$$Z(\beta) = \text{tr} e^{-\beta H}. \quad (7.4)$$

However, we do not have a general understanding of the bulk quantum gravity Hilbert space on which this trace would be defined. As first discussed in [150] and emphasized recently in [180], the leading area term in (7.1) only arises from saddles in which the circle shrinks smoothly in the interior, which gives the cigar geometry in the left of Fig. 7.1. This represents an apparent obstruction to the trace interpretation (7.4) from the viewpoint of effective field theory and obscures the bulk quantum mechanical origin of area term. This is an important puzzle to address because the area term, which is the analogue of Bekenstein-Hawking entropy, is expected to capture the entropy of the spacetime itself [331].

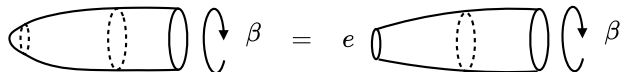


Figure 7.1: The left figure shows the cigar geometry which is the saddle point that contributes the area term in the generalized entropy. On the right we have removed a cap at the tip of the cigar and inserted a shrinkable boundary condition  $e$ .

We can view equation (7.4) as a constraint on the quantum gravity microstates, determined by the path integral that governs the low energy effective theory.

The idea is illustrated on the right of Fig. 7.1. To interpret  $Z(\beta)$  on a cigar geometry as a trace we excise a small cap from the tip of the cigar and impose a “shrinkable” boundary condition. This boundary condition is defined so that the path integral on the excised geometry is the same as  $Z(\beta)$ . It corresponds to inserting a boundary state given by the path integral on the small cap. If the shrinkable boundary condition were local, we can immediately interpret  $Z(\beta)$  as a thermal partition function by quantizing with respect to time variable around

the circle. Fig. 7.2 suggests that the corresponding thermal density matrix can be viewed as the reduced density matrix  $\rho_V$  on a subregion  $V$  of a spatial slice<sup>3</sup>. If we could identify

$$Z(\beta = 2\pi n) = \text{tr}_V \rho_V^n, \quad (7.5)$$

then the generalized entropy (7.2) would give the replica trick entanglement entropy of the subregion  $V$ . Since string theory provides the UV completion of the

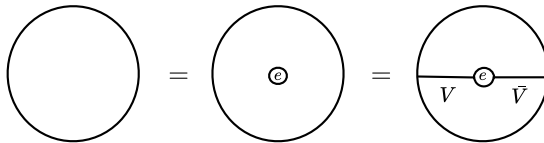


Figure 7.2: In this figure we have flattened out the cigar geometry into a disk. On the right figure, we can view the lower half of the annulus as a path integral preparation of a factorized state with a shrinkable boundary condition at the entangling surface. Quantizing  $Z(\beta)$  with respect to the time variable around the origin shows that it can be viewed as the trace of a reduced density matrix on  $V$ .

bulk gravity theory in AdS/CFT, this suggest that the generalized entropy can be viewed as entanglement entropy of closed strings making up the spacetime. A worldsheet version of this proposal was first discussed by Susskind and Uglum [315]. As shown in Fig. 7.3, from the worldsheet point of view, the quantization with respect to the modular time and the shrinkable boundary condition is equivalent to a form of open-closed string duality.

In [123], an explicit realization of these ideas was first obtained in two dimensional Yang Mills and its string theory dual, using the framework of *extended* topological quantum field theory (TQFT)<sup>4</sup>. Extended TQFT is a categorical re-

<sup>3</sup>In gravitational path integral, there will be an extra complication due to the fact that we cannot fix the location of the “stretched horizon” where we removed the small cap. However we expect this construction remains valid provided that we sum over the location of the shrinkable boundary.

<sup>4</sup>TQFT’s have finite dimensional Hilbert spaces, where as area dependent QFT’s such as 2D Yang Mills have infinite dimensional Hilbert spaces. Nevertheless, they obey very similar sewing rules so we will use extended TQFT to refer to both types of theories in this paper.

formulation of the path integral as a cobordism theory constrained by sewing relations. In [123], the shrinkable boundary condition was interpreted as an additional sewing relation called the “entanglement brane axiom.” In that theory, the shrinkable boundary condition is local and provides a constraint on the consistent factorization of the Hilbert space which requires the presence of edge modes localized to the entangling surface. It was shown that the analogue of generalized entropy can indeed be interpreted as entanglement entropy of a subregion, and has a dominant edge mode contribution which plays the role of the area term. In the string theory dual, these edge modes correspond to a large  $N$  number of entanglement branes<sup>5</sup>.

Unfortunately, in gravitational theories, the shrinkable boundary condition is non-local due to a *topological* feature of the gravity path integral on the small cap. As explain in [208], this is because the Gauss Bonnet theorem implies that reproducing the Einstein Hilbert action inside the cap requires a non trivial holonomy around the shrinkable boundary. This seems to create an additional obstacle to interpreting generalized entropy as a statistical entropy.

In [118], we addressed these questions in the A model topological string theory using the extended TQFT framework developed in [123]. We defined an analogue of generalized entropy for closed strings on the resolved conifold geometry (see left of Fig. 7.4) and showed that it has a canonical Hilbert space interpretation despite the presence of a non-local shrinkable boundary condition. The analogue of the topological constraint in gravity is given by the Calabi-Yau condition<sup>6</sup>,

---

<sup>5</sup>Interestingly, the entanglement brane axiom requires the number of branes in that theory to be related to the closed string coupling as [122, 123]:  $N = \frac{1}{g_s}$ . This is a direct example of how the entanglement brane axiom relates parameters of the low energy theory, i.e. the closed string coupling  $g_s$ , to high energy microstates given by the entanglement branes.

<sup>6</sup>The A model string theory is well defined on any Kahler manifolds, so the Calabi Yau condition is a strong restriction. The shrinkable boundary condition we obtained is specific to this sub-category of the target spaces for the topological string theory.



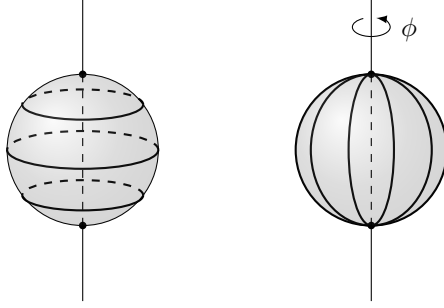


Figure 7.3: Susskind and Uglum considered the generalized entropy of perturbative closed strings in flat space, viewed as a limit of the cigar geometry. Using off shell arguments, they computed generalized entropy by inserting a conical singularity in the background, corresponding to the tip of the cigar geometry. In perturbative string theory, the area term comes from the sphere diagram which intersects the conical singularity. Viewed in the open string channel, this is a one-loop open string diagram. This interpretation amounts to an open-closed string duality which identifies Bekenstein-Hawking entropy as thermal entropy of open strings that end on the conical singularity. Figure borrowed from Ref. [122].

which we imposed on the replica manifold so that the topology of the resolved conifold geometry is preserved as  $\beta$  is varied in (7.2). The resulting boundary state corresponds to a “Calabi-Yau” cap [63, 8], and leads to string edge modes that obey anyonic statistics and transform under the quantum group  $U(\infty)_q$ . As in [122, 123], these edge modes correspond to a large  $N$  number of entanglement branes which implements the entanglement cut on the closed strings. Using a  $q$ -deformed version of the extended TQFT sewing relations, we determined the factorization of the closed string Hilbert space and showed that the generalized entropy has a quantum mechanical description as a  $q$ -deformed entanglement entropy:

$$S = -\text{tr}_q \rho \log \rho = -\text{tr}(D\rho \log \rho). \quad (7.6)$$

Here  $D$  is an operator called the Drinfeld element of  $U(\infty)_q$ , whose insertion makes the quantum trace  $\text{tr}_q$  invariant under the quantum group symmetry. It can also be interpreted as a defect operator which creates the nontrivial bundle structure of the Calabi-Yau cap. The analogue of the area term in the generalized entropy is once again given by the edge mode contribution to the  $q$ -deformed entropy. Note

that in [208]. the same formula (7.6) was obtained for the gravitational generalized entropy in JT gravity, with  $D$  given by a defect operator which implements the topological constraint associated to the “Einstein Hilbert” cap.

In this work we apply Gopakumar-Vafa (GV) duality [161] to the A model topological string and give a dual calculation of the q-deformed entanglement entropy (7.6) from Chern-Simons gauge theory<sup>7</sup> The GV duality is a topological analogue of AdS/CFT. It is an open-closed string duality that relates bulk closed strings on the resolved conifold geometry to open strings on the deformed conifold geometry. This is illustrated in Fig. 7.4. Like AdS/CFT, the GV duality involves a geometric transition in which a large  $N$  number of branes dissolve into fluxes. On the deformed conifold, the branes wrap the Lagrangian submanifold  $S^3$  at the tip and are replaced by flux passing through an  $S^2$  on the resolved conifold across the geometric transition.

The role of the boundary CFT is played by the large- $N$  limit of  $U(N)$  Chern-Simons (CS) theory. It is the worldvolume theory of the branes wrapping  $S^3$  on the deformed conifold. Remarkably, this is also the exact string field theory for open strings on the deformed conifold [343]. The gauge coupling  $g_{cs} = \frac{2\pi}{k+N}$  and ‘t Hooft parameter  $ig_{cs}N$  of the CS theory are related to the closed string coupling  $g_s$  and the Kahler modulus  $t$  of the resolved conifold by

$$\begin{aligned} g_s &= g_{cs} = \frac{2\pi}{k+N} \\ t &= ig_s N \end{aligned} \tag{7.7}$$

Using the string field theory description, we can obtain the exact shrinkable bound-

---

<sup>7</sup>Reference [202] also studied entanglement entropy in topological string theory using the dual Chern Simons gauge theory. The idea of using the factorization map in Chern Simons theory to probe the entanglement structure in topological string theory via Gopakumar Vafa duality was originally suggested in [352].


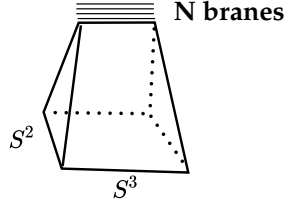
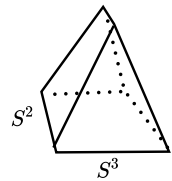
	<b>Geometric transition</b> 	
	<b>Open A model string</b> $(g_s, N)$	<b>Closed A model string</b> $(g_s, t)$
<b>Target space geometry</b>	<b>Deformed Conifold</b> 	<b>Resolved Conifold</b> 
<b>Target space theory</b>	<b>U(N) Chern Simons theory</b> <b>on <math>S^3</math></b>	<b>A Model TQFT</b>

Figure 7.4: Gopakumar-Vafa duality relates closed A-model string on the resolved conifold to the open A-model string on the deformed conifold

ary condition, edge modes, and entanglement entropy on both sides of the duality.

As in AdS/CFT [251, 300], there is a local mapping between Wilson loops in the dual Chern-Simons gauge theory and worldsheets in the bulk closed string theory [285, 156]. This is illustrated in Fig. 7.20, 7.21. The entanglement cut of the closed string worldsheets is therefore mapped to the entanglement cut of the Wilson loops. We will reproduce the  $q$ -deformed entanglement entropy of the bulk closed string theory via a canonical calculation of the “defect entropy” [209, 210, 244] associated to Wilson loops. The defect entropy is obtained from the *undeformed* entanglement entropy by subtracting the entanglement entropy of the vacuum, thus capturing the entanglement due to the Wilson loops alone. An analogous relation between the defect entropy of Wilson loops in the boundary gauge theory and bulk entropy of probe string worldsheets also holds in AdS/CFT [244]. However, our gauge theory calculation computes the entanglement entropy

of a large superposition of Wilson loops. These are dual to the worldsheets that determine the resolved conifold partition function, so our calculation captures the entropy that makes up the spacetime itself.

One important issue we will address using the GV duality is the nature of the entanglement branes, which were defined previously using the categorical language of extended TQFT. While this provides a precise mathematical definition of a brane, its relation to the usual worldsheet definition as boundary conditions for the string sigma model is rather obscure. Here we will show that the GV duality maps the entanglement branes to a configuration of D branes, which corresponds to Lagrangian boundary conditions for the topological string. In the string field theory description, the dual brane configuration correspond to the CFT edge modes of the  $U(N)$  Chern-Simons theory. The shrinkable boundary condition is *local* in the Chern-Simons theory, and the quantum group edge mode symmetry is replaced by the large  $N$  Kac-Moody symmetry of the WZW model edge modes. This is a manifestation of the fact that quantum groups arise as a hidden symmetry in conformal field theories [341, 173, 310].

As shown in Fig. 7.3, the shrinkable boundary condition on the worldsheet implies a type of open-closed string duality. This was manifest in the canonical calculation of generalized entropy in [118], in which a trace over the open string Hilbert space (i.e. RHS of (7.4)) reproduces *closed* string amplitudes that determine the generalized entropy. However the worldsheet mechanism behind this open-closed duality was not explained. In this work we will find strong evidence that the open-closed duality responsible for the shrinkable boundary condition and the entanglement brane edge modes is related to the GV duality itself. Remarkably the worldsheet mechanism behind GV duality is well understood and can be

interpreted as a phase transition on the worldsheet corresponding to the condensation of vortices that represent the D branes [286]. Our work seems to suggest that a similar worldsheet mechanism might be responsible for the emergence of entanglement branes.

Our paper is organized as follows. In section 2, we give an extended review of relevant results in our previous work on the generalized entropy of the A model closed string theory. In particular we will review our construction of the closed string Hartle-Hawking state on the resolved conifold using the topological vertex formalism [3]. We explain the construction of the string edge modes and the Drinfeld element, paying particular attention to the large  $N$  limit and regularization which is needed to define the shrinkable boundary condition. In section 3, we will give the dual Chern-Simons gauge theory calculation of the bulk generalized entropy, starting with a dual replica trick calculation. The dual Hartle-Hawking state is given by a state on a torus containing a superposition of Wilson loops. We explain the large  $N$  limit which maps the entanglement edge modes of this state to the entanglement branes in string theory. In section 4, we will explain the duality between Wilson loops in Chern-Simons theory and worldsheets in topological string theory. Moreover we will re-visit our discussion of Chern-Simons edge modes of the Hartle-Hawking state from the point of view of worldsheets on the deformed conifold. We show that these edge mode correspond to a configuration of D branes that include dynamical branes on wrapping 3-spheres in the deformed geometry. We will explain the precise sense in which GV duality relates these branes to the entanglement branes on the resolved conifold.

## 7.2 Review of part 1

### 7.2.1 Generalized entropy for A model closed strings

**A model closed strings on the resolved conifold** The topological A model closed string theory is defined on target spaces which are six real dimensional Kahler manifolds [340]. The perturbative string amplitudes can in principle be computed to all orders in the genus expansion and depend only on the Kahler modulus of the target space [343, 6, 4, 235, 108, 2, 80, 201]. The simplicity of this string theory is due to the localization of the worldsheet path integral to holomorphic instantons which wrap minimal-volume two cycles on the target space.

In our previous work we considered the A model closed string theory on the resolved conifold geometry. As depicted in the right of Fig. 7.4, this geometry is obtained from a resolution of a cone over a  $S^2 \times S^3$  base. The only minimal volume two-cycle is the  $S^2$  at the tip whose (complexified) area determines the Kahler modulus, and the closed string instantons are arbitrary coverings of this sphere with winding number  $n > 0$ . The exact resolved conifold partition function is given by<sup>8</sup>

$$\begin{aligned} Z_{\text{res}} &= \exp \left( \sum_{n=1}^{\infty} \frac{1}{n(2 \sin(\frac{ng_s}{2}))^2} e^{-nt} \right) \\ &= \sum_R (d_q(R))^2 e^{-t\ell(R)}. \end{aligned} \tag{7.8}$$

The first formula comes directly from the exponentiation of the free energy, corresponding to a sum over all connected string diagrams.  $e^{-nt}$  is the exponential of the worldsheet action for instantons wrapping the  $S^2$   $n$  times, and the worldsheet

---

<sup>8</sup>The free energy can also get contributions from constant maps, which are finite polynomials in  $t$ . For non-compact Calabi-Yau manifolds, they are ambiguous and not well-defined, and we naturally set them to zero [4].

genus has already been summed over [235, 4, 343, 161, 108, 2, 326, 263]. The second formula can be obtained from the gluing of topological vertices [3], which are basic building blocks for A model amplitudes that satisfy gluing rules reminiscent of a cubic field theory in spacetime.

For the purposes of studying entanglement and edge modes, it will prove convenient to work with the second formula. Here  $R$  labels Young tableaux with an arbitrary number of boxes denoted by  $l(R)$ . The quantity  $d_q(R)$  is the quantum dimensions of the symmetric group representation  $R$ . In term of the Young diagram,  $d_q(R)$  is given by

$$d_q(R) = \prod_{\square \in R} \frac{i}{q^{h(\square)/2} - q^{-h(\square)/2}} = \prod_{\square \in R} \frac{1}{2 \sin(\frac{h(\square)g_s}{2})}, \quad (7.9)$$

with  $h(\square)$  being the hook length.

**Generalized entropy in topological string theory** We would like to define an analogue of generalized entropy for the A model by replicating the partiton function  $Z_{\text{res}}$ . The analogue of the cigar geometry is given by the minimal volume two-sphere where the string worldsheets wrap. We will define the replica manifold by making an opening angle of  $\beta = 2\pi n$  around two antipodal points as shown in Fig. 7.6.

In defining the replica manifold, it is important to note that global geometry of the resolved conifold is not a that of a direct product with a  $S^2$  factor. Instead it is a nontrivial rank 2 bundle over the sphere:

$$\mathcal{O}(-1) \oplus \mathcal{O}(-1) \rightarrow S^2 \quad (7.10)$$

Here  $\mathcal{O}(-1)$  denotes the complex line bundle over the sphere with chern class  $-1$ . Moreover, the resolved conifold is a Calabi Yau manifold. For rank 2 bundles of

the form

$$\mathcal{O}(k_1) \oplus \mathcal{O}(k_2) \rightarrow \mathcal{S} \quad (7.11)$$

over a Riemann surface  $\mathcal{S}$ , the Calabi Yau condition translates into the relation

$$k_1 + k_2 = -\chi(\mathcal{S}) \quad (7.12)$$

between the Chern classes and the Euler characteristics of  $\mathcal{S}$ .

Since the bundle structure over the minimal  $S^2$  is nontrivial, we need to specify what happens to the fiber directions when we replicate around the two antipodal points. As discussed in [118], a naive cyclic gluing of the resolved conifold replicas would lead to a vector bundle of the form

$$\mathcal{O}(-n) \oplus \mathcal{O}(-n) \rightarrow S^2 \quad (7.13)$$

While there is nothing apriori incorrect about this replica manifold, it does not provide a good candidate for the definition of generalized entropy [243]. This is because it violates the Calabi-Yau (CY) condition and changes the topology of the resolved conifold. This implies that when analytically continuing to non-integer  $n$ , the replica partition function no longer has a geometric interpretation in terms of a target space where string worldsheets can propagate, since we can not define a bundle with non-integer Chern classes<sup>9</sup>.

However, if we impose the CY condition (7.12) as a topological constraint on the replica manifold, we obtain a replica partition function which does have a geometric interpretation at all values of  $n$ , even when it is non integer. This is because the Euler characteristic of the base sphere is invariant under replication,

---

<sup>9</sup>Another reason for imposing the CY condition comes from mirror symmetry [195, 349]. In contrast to the A-model, the B-model is only well defined on Calabi-Yau manifolds. In order for the replica trick to commute with mirror symmetry, the replica manifold must preserve the Calabi Yau condition. More comments related to the B-model are in the discussion section



so the CY condition forces the bundle structure to stay fixed as well. This implies that the only effect of the replication is to rescale the area  $t$  of the sphere<sup>10</sup>. Since the A model is only sensitive to the Kahler modulus given by this area, the replica partition function is simply given by rescaling  $t$ :

$$Z(n)_{\text{res}} = \sum_R (d_q(R))^2 e^{-ntl(R)}. \quad (7.14)$$

From this we can obtain the generalized entropy on the resolved conifold geometry by applying eq. (7.2)

$$\begin{aligned} S_{\text{gen}} &= (1 - n\partial_n)_{n=1} \log Z_{\text{res}}(n) \\ &= \sum_R p(R) (-\ln p(R) + 2 \ln d_q(R)), \quad p(R) = \frac{(d_q(R))^2 e^{-tl(R)}}{Z_{\text{res}}}. \end{aligned} \quad (7.15)$$

This formula has exactly the same structure as the entanglement entropy of two dimensional non abelian gauge theory, with  $R$  playing the role of a representation label,  $d_q(R)$  the associated dimension, and  $p(R)$  a probability factor. As in 2DYM, the  $\sum_R 2p(R) \log d_q(R)$  term plays the role of the area term. The factor of 2 counts the number of putative entangling surfaces given by branch points of the replica manifold.

## 7.2.2 The closed string Hilbert space, A model TQFT, and the Hartle-Hawking state

As noted in the introduction, the A model string theory has an exactly solvable string field theory, so we can apply the usual formulation of entanglement entropy

---

<sup>10</sup>Note that the area  $t$  is complex and includes the  $B$  field flux, so we are replicating the flux as well. Also, when we increase the number of entangling points or consider other Riemann surfaces  $\mathcal{S}$ , the Euler characteristic of the base manifold will no longer be invariant under replication. Nevertheless we can consistently impose the condition (7.12) even though the geometric interpretation at non integer  $n$  is obscured or may not exist.

in terms of a second quantized theory of strings. For target space geometries which take the form of vector bundles like (7.11), the string field theory is given by a topological quantum field theory, which we will simply refer to as the A model TQFT [63, 8]. We will use the TQFT formalism to define the closed string Hilbert space.

The A model TQFT is a map<sup>11</sup> that assigns multi-string amplitudes to basic building blocks of spacetime that are represented as 2-cobordisms with line bundles. These are target spaces of the form (7.11) in which the Riemann surface  $\mathcal{S}$  is viewed as Euclidean evolution from initial and final boundaries. We represent such a cobordism by a decorated two-dimensional diagram (evolution from top to bottom)

$$(k_1, k_2) \quad , \quad (k_1, k_2) \quad , \dots \quad (7.16)$$

In order to cut up the closed string amplitudes into these basic building blocks, we have to insert brane/anti branes at the in/out boundaries where the worldsheets can end. The gluing of these cobordisms should then be viewed as the annihilation of these branes and anti branes.

The D branes of the A model wrap three dimensional Lagrangian submanifolds. Each diagram in eq.(7.16) represent open string amplitudes consisting of worldsheets that end on these Lagrangians, which intersect  $\mathcal{S}$  along its boundary circles. The coupling of the worldsheet to the branes is given by multi-trace factors

$$\prod_{i=1} \text{tr}(U^i)^{k_i}, \quad k_j > 0, \\ U \in U(N) \quad (7.17)$$

---

<sup>11</sup>The precise statement is that it is a functor from the category of 2-cobordisms with line bundles to the category of vector spaces

where  $U = P \exp \oint A$  is the holonomy on the brane, and  $k_j$  labels the number of strings the wind  $j$  times<sup>12</sup>.

In the large  $N$  limit, we identify the multi-trace factors (7.17) with the winding basis of wavefunctions

$$\langle U | \vec{k} \rangle = \prod_{i=1} \text{tr}(U^i)^{k_i} \quad (7.18)$$

that span a closed string Hilbert space  $\mathcal{H}_{\text{closed}}$  assigned to each boundary of  $\mathcal{S}$ , with  $U$  playing the role of a configuration space variable. The Hilbert space is thus identified with class functions on  $U(\infty)$ . Note that when the holonomy  $U$  is pulled back to the worldsheet, the wavefunctions (7.17) are *functionals* of the string loops that make up the worldsheet boundary.

We will also make use of the representation basis, related to (7.17) by the Frobenius relation

$$\langle U | R \rangle = \text{tr}_R(U) = \sum_{\vec{k} \subset S_n} \frac{\chi_R(\vec{k})}{z_{\vec{k}}} \langle U | \vec{k} \rangle, \quad (7.19)$$

where  $R$  is a representation of  $U(\infty)$  associated with Young diagram of  $n$  boxes, and  $\chi_R(\vec{k})$  is the symmetric group character for  $\vec{k}$ , viewed as a conjugacy class in  $S_n$ . In the large  $N$  limit we can include states with an arbitrary number of boxes  $n$ .

Formally the A model TQFT assigns a tensor product of  $\mathcal{H}_{\text{closed}}$  to the disjoint union of in or out circles, and linear maps to cobordisms that join these circles. The gluing of the cobordisms corresponds to the composition of linear maps, and is implemented by the haar integral on the closed string Hilbert space:

$$\int dU \text{tr}_R(U) \text{tr}_{R'}(U^{-1}) = \delta_{RR'} \quad (7.20)$$

---

<sup>12</sup> $k_j > 0$  reflects the fact that the A model is a chiral theory so the strings wind in a single direction, and around the boundary circles of  $\mathcal{S}$ .

**Hartle-Hawking state** Since our replica trick preserves the Calabi-Yau condition, we can also consistently restrict to this subset of vector bundles satisfying (7.12). The resulting TQFT forms a Frobenius Algebra [8, 63, 118], and is generated by four basic cobordisms.

$$\begin{array}{ccccccc}
 (0,-1) & , & (-1,0) & , & (0,1) & , & (1,0) \\
 \text{[Diagram: Sphere with dashed line]} & & \text{[Diagram: Bowl]} & & \text{[Diagram: Y-shape]} & & \text{[Diagram: Inverted Y-shape]}
 \end{array} \tag{7.21}$$

The resolved conifold is given by the overlap

$$Z = \begin{array}{c} (0,-1) \\ \text{[Diagram: Sphere with dashed line]} \\ (-1,0) \end{array} = \sum_R (d_q(R))^2 e^{-tl(R)}. \tag{7.22}$$

We define the Hartle-Hawking state to be the string amplitude on “half” of the resolved conifold geometry:

$$\begin{aligned}
 |HH(t)\rangle &= \begin{array}{c} (0,-1) \\ \text{[Diagram: Sphere with dashed line]} \end{array} = \sum_R (-i)^{l(R)} d_q(R) q^{\kappa_R/4} e^{-tl(R)} |R\rangle \\
 \kappa_R &= C_2(R) - Nl(R)
 \end{aligned} \tag{7.23}$$

where  $C_2(R)$  is the eigenvalue of the quadratic Casimir operator in the representation  $R$ . The other half of the resolve conifold geometry is given by the linear functional<sup>13</sup>

$$\langle HH^*(t)| = \begin{array}{c} (-1,0) \\ \text{[Diagram: Bowl]} \end{array} = \sum_R i^{l(R)} d_q(R) q^{-\kappa_R/4} e^{-tl(R)} \langle R| \tag{7.24}$$

which is the string amplitude in the presence of anti branes on the Lagrangian that intersect  $\mathcal{S}$ .

Fig. 7.5 shows the worldsheet instantons for the wavefunction  $\langle U|HH\rangle$  which end on branes that extend into the fiber directions as a hyperbola. The topology

<sup>13</sup>Note that the bra and ket states denote dual basis elements which are not related by a *Hermitian* inner product. Instead they are related by an adjoint operation on the string amplitudes which maps branes to anti-branes [325, 3].

of the corresponding Lagrangian submanifold is that of a non-compact solid torus  $\mathbb{C} \times S^1$ , and the winding basis (7.18) describe string loops winding around the non contractible  $S^1$ . The worldvolume theory on the branes is  $U(\infty)$  Chern-Simons theory.

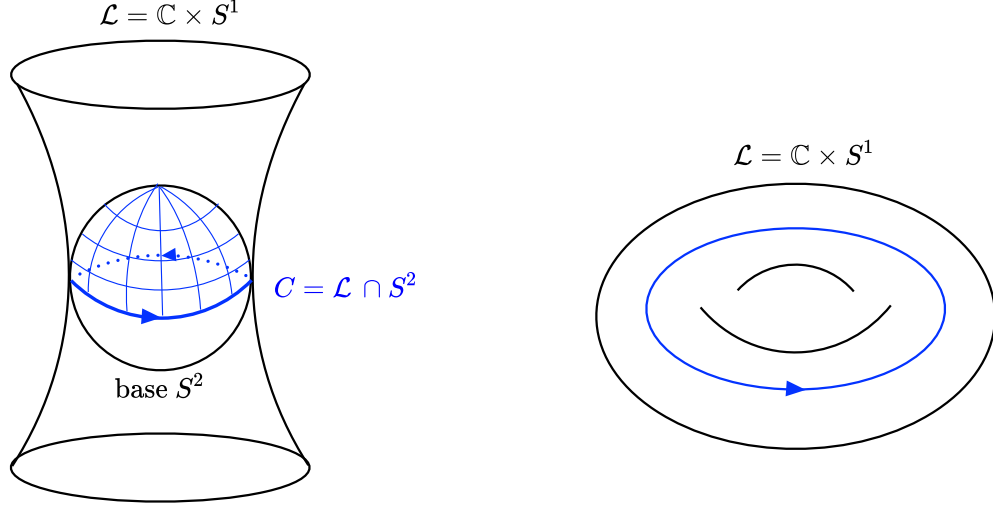


Figure 7.5: The left figure shows worldsheet instantons ending on D-branes which cut the minimal volume  $S^2$  of the resolved conifold along the equator. The branes extend into the non compact fiber directions and wrap a Lagrangian submanifold with the topology  $\mathbb{C} \times S^1$

### 7.2.3 Shrinkable boundary condition and the Calabi Yau Cap

Having defined the closed string Hilbert space we can give a closed string channel description of the entanglement boundary state and shrinkable boundary condition. Consider the partition function on the resolved conifold, viewed as a closed string amplitude between the entanglement boundary states:

$$Z_{\text{res}}(t) = \langle D^* | e^{-H_{\text{closed}}} | D \rangle$$

$$H_{\text{closed}} = tl(R) \tag{7.25}$$

Here  $H_{\text{closed}}$  is the string field Hamiltonian. As shown in Fig. 7.6, this corresponds to a decomposition of the base manifold into a cylinder and two small caps near the antipodal branch points associated with the entangling surfaces. To satisfy the CY condition, the cylinder must have Chern class  $(0,0)$ , so the non trivial topology is carried by the two “Calabi Yau” caps [63, 8]. These caps represent A model amplitudes with branes/anti branes and define a boundary states we call  $|D\rangle$  and  $\langle D^*|$ . They are simply given by the states  $|HH\rangle$  and  $\langle HH^*|$  with zero area  $t = 0$ , and the corresponding wave functions are

$$\begin{aligned}\langle U|D\rangle &= \sum_R (-i)^{l(R)} d_q(R) q^{\kappa_R/4} \text{tr}_R(U) \\ \langle D^*|U\rangle &= \sum_R i^{l(R)} d_q(R) q^{-\kappa_R/4} \text{tr}_R(U^{-1})\end{aligned}\tag{7.26}$$

As discuss in the introduction, these boundary states determine the shrinkable boundary condition (see right of Fig. 7.6). The amplitudes of these wave functions capture the degeneracy factors in the partition function, which indicates the presence of q-deformed string edge modes.

To understand this point it is useful to consider the analogous entanglement boundary state  $|\Omega\rangle$ , obtained from the large  $N$  limit of  $U(N)$  2DYM on a two dimensional cap [122]. This is a state in  $\mathcal{H}_{\text{closed}}$  with wavefunction

$$\begin{aligned}\langle U|\Omega\rangle &= \sum_R \dim R \text{tr}_R(U) \\ &= \delta(U, 1)\end{aligned}\tag{7.27}$$

In the second expression, we observed that the wavefunction for  $|\Omega\rangle$  is a group theory Fourier transform of a delta function which forces  $U = 1$ . The triviality of this holonomy implies a local shrinkable boundary condition, corresponding to setting the gauge field component around the entangling surface to zero.

Figure 7.6: The closed string channel description of entanglement branes on the resolved conifold geometry. The total space is a six dimensional Calabi Yau manifold fibered over a sphere. We have shown only the base manifold and indicated the bundle structure with the Chern class labelling.

In the large  $N$  limit it was shown in [122] that the dimension factor  $\dim R$  arises in the open string channel from edge modes transforming in the  $R$  representation of  $U(N)$ , which were identified with the Chan-Paton factors labelling entanglement branes.

We can apply a similar analysis to the boundary state  $|D\rangle$ , keeping in mind that  $U$  is now interpreted as a worldvolume holonomy on a three dimensional brane embedded inside a six dimensional Calabi-Yau manifold. The wave function (7.26) again gives a delta function on the group, but it now sets  $U$  to a nontrivial group element

$$\begin{aligned} \langle U|D\rangle &= \sum_R (-i)^{l(R)} d_q(R) q^{\kappa_R/4} \text{tr}_R(U) \\ &= \delta(U, D) \end{aligned} \tag{7.28}$$

where  $D$  is a diagonal  $U(N)$  matrix of phases

$$\begin{aligned} D_{ij} &= \delta_{ij} q^{-i+\frac{1}{2}} \in U(N) \\ q &= e^{igs} \end{aligned} \tag{7.29}$$

The non-triviality of holonomy  $D$  implies that there is no way to enforce it as a *local* boundary condition on the worldvolume gauge field. Thus the shrinkable boundary condition for the A model is non-local, just as in Einstein-Hilbert gravity.

If we analytically continue the string coupling  $g_s$  to give it an imaginary part, we can identify the overlap  $\langle R|D\rangle$  as a suitably regularized trace:

$$\langle R|D\rangle = \lim_{N \rightarrow \infty} \text{tr}_R(D) = (-i)^{l(R)} d_q(R) q^{\kappa_R/4} \quad (7.30)$$

Note that in addition to the degeneracy factor  $d_q(R)$ , this overlap contains phases with nontrivial information about the fiber bundles structure in the transverse directions.

A similar formula holds for the coupling to the boundary state  $\langle D^*|$ <sup>14</sup>

$$\langle D^*|R\rangle = \lim_{N \rightarrow \infty} \text{tr}_R(D^{-1}) = (i)^{l(R)} d_q(R) q^{-\kappa_R/4} \quad (7.31)$$

We can thus write

$$\begin{aligned} Z_{\text{res}} &= \sum_R \langle D^*|R\rangle e^{-tl(R)} \langle R|D\rangle \\ &= \sum_R \text{tr}_R(D) \text{tr}_R(D^*) e^{-tl(R)} = \sum_R d_q(R)^2 e^{-tl(R)} \end{aligned} \quad (7.32)$$

We see that the degeneracy factor  $d_q(R)^2$  arises from the coupling of the closed string states  $|R\rangle$  to the entanglement boundary state  $|D\rangle$  [4]. Notice that the phases in (7.30) have cancelled out to give a real, positive degeneracy factor.

Equation (7.32) suggests that we can obtain a thermal interpretation of  $Z_{\text{res}}$  if we associate a degenerate edge mode Hilbert space  $V_R \times V_{\bar{R}}$  with the superselection label  $R$ , so that

$$Z_{\text{res}} = \sum_R \text{tr}_R(D) \text{tr}_{\bar{R}}(D) e^{-tl(R)} = \sum_R \text{tr}_{R \times \bar{R}}(D e^{-H_{\text{open}}}) \quad (7.33)$$

where  $H_{\text{open}}$  is an open string Hamiltonian with the same eigenvalues as  $H_{\text{closed}}$ , and  $D$  should be viewed as a choice of measure on the degenerate open string

---

<sup>14</sup>The fact that this happens to be the complex conjugate of  $\langle R|D\rangle$  is an accidental feature of the state when  $t$  is real. We emphasize once again that we are not applying a Hermitian adjoint to obtain  $\langle D^*|$  from  $|D\rangle$ , but are instead using the branes to anti brane mapping defined in [4] [325].



microstates<sup>15</sup>. Notice that this measure is quite nontrivial<sup>16</sup>, since tracing over  $U(N)$  indices of  $D_{ij}$  gives *symmetric* group dimensions.

$$\lim_{N \rightarrow \infty} \text{tr}_{R \otimes \bar{R}}(D) = d_q(R)^2 \quad (7.34)$$

As we explain below,  $D$  is the Drinfeld element of a quantum group and should be absorbed into the trace to define the *quantum* trace. This is a modification of the trace which makes it invariant under the adjoint action of the quantum group symmetry on the open string microstates.

#### 7.2.4 Factorization and the q-deformed entanglement entropy

In this section we identify the open string microstates whose thermal partition function is given by  $Z_{\text{res}}$  and provide the statistical interpretation for its generalized entropy. More precisely we determine a factorization map

$$\begin{array}{c} \text{Diagram: A cylinder with a handle. The top boundary is a circle labeled } e. \text{ The bottom boundary is a circle labeled } e. \end{array} : \mathcal{H}_{\text{closed}} \rightarrow \mathcal{H}_{\text{open}} \otimes \mathcal{H}_{\text{open}} \quad (7.35)$$

from the the closed string Hilbert space into an extended Hilbert space of open strings. We apply the factorization map to the Hartle-Hawking state and obtain its reduced density matrix

$$\rho = e^{-H_{\text{open}}} \quad (7.36)$$

---

<sup>15</sup>We thank Laurent Freidel for suggesting this interpretation.

<sup>16</sup>It is also a complex measure, as indicated in equation (7.30)

by doing a quantum partial trace over half of the closed string. The corresponding q-deformed entanglement entropy

$$S = -\text{tr}(D\rho \log \rho) \quad (7.37)$$

agrees with the generalized entropy (7.15) and provides the statistical interpretation we were after.

**Factorization as an extension of the TQFT** In terms of elementary cobordisms, equation (7.35) is the composition of two elementary factorization maps

$$\begin{array}{c} \text{cylinder with a wedge-shaped hole at the bottom labeled } e \end{array}, \quad \begin{array}{c} \text{pair of pants cobordism with a wedge-shaped hole at the bottom labeled } e \end{array} \quad (7.38)$$

which describe the *extension* of the closed TQFT into an open-closed TQFT that includes cobordisms with corners. These corners are the boundaries of the initial and final slice and carry labels which specify objects in the category of  $D$  branes. The extended TQFT assigns an open string Hilbert space to such labelled intervals and linear maps to cobordisms that connect them. These cobordisms satisfy sewing relations which provide local constraints on the factorization maps.

In our setup, corners correspond to *entanglement* branes that represent string edge modes satisfying the shrinkability condition. Denoting these branes by the label  $e$ , the shrinkability condition is formulated as the sewing relation

$$(0,-1) \quad = \quad \begin{array}{c} \text{cylinder with a wedge-shaped hole at the top labeled } e \end{array}, \quad (7.39)$$

called the entanglement brane axiom [123].

When combined with the sewing relations of the open-closed TQFT, it can be shown that the entanglement brane axiom implies all holes labelled by  $e$  can be

closed.

$$\begin{array}{c} \text{cylinder with } e \end{array} = \begin{array}{c} \text{cylinder} \end{array}, \quad \begin{array}{c} \text{pair of pants with } e \end{array} = \begin{array}{c} \text{rectangle} \end{array}, \quad \begin{array}{c} (0,-1) \\ \text{pair of pants} \\ (-1,0) \end{array} = \begin{array}{c} e \\ \text{circle with } e \end{array}, \dots \quad (7.40)$$

The first two relation implies that the factorization maps do not change the state. The third is the cobordism description of eq.(7.33) which identifies the resolved conifold partition function as a thermal partition function.

In fact, this partition function is precisely the *categorical* trace of the unnormalized reduced density matrix for the Hartle-Hawking state (7.23), obtained by tracing out half of the closed string. To see how this works in the cobordism language, we first factorize  $|HH\rangle$  using (7.46):

$$\begin{array}{l} |HH\rangle \rightarrow \begin{array}{c} (0,-1) \\ \text{cylinder with } e \end{array} = \begin{array}{c} \text{pair of pants} \end{array} = \begin{array}{c} \text{arc} \end{array} \\ \langle HH^*| \rightarrow \begin{array}{c} \text{pair of pants} \\ (-1,0) \end{array} = \begin{array}{c} \text{Y-shape} \end{array} = \begin{array}{c} \text{arc} \end{array} \end{array} \quad (7.41)$$

$$\tilde{\rho} = |HH\rangle \langle HH^*| = \begin{array}{c} (-1,0) \\ \text{pair of pants} \\ (0,-1) \end{array} \rightarrow \begin{array}{c} \text{arc} \\ \text{arc} \end{array}. \quad (7.42)$$

The corresponding reduced density matrix is given by the categorical partial

trace

$$\tilde{\rho}_A = \text{tr}_B \tilde{\rho} = \begin{array}{c} \text{---} \\ \text{---} \\ \text{---} \\ \text{---} \end{array} = \begin{array}{c} \text{---} \\ \text{---} \end{array} = e^{-H_{\text{open}}}. \quad (7.43)$$

This partial trace operation is defined by the half annuli which turns input into output intervals and glues them together. Such a trace operation can be defined abstractly from the cobordism theory; we will see that for the A model, it coincides with the *quantum* partial trace. In a purely topological theory where the Hamiltonian is strictly zero, the resulting strip in (7.124) is a trivial evolution operator which is equal to the identity operator. However, the A model has a non-trivial Hamiltonian due to its dependence on the Kahler modulus of the target space, so the strip is an open string propagator which that depends on the complexified area and modular energies.

Applying the categorical partial trace on the remaining subregion  $A$  gives the quantum trace of the reduced denstiy matrix.

$$\text{tr}_{q,A}(\tilde{\rho}_A) = \begin{array}{c} (0,-1) \\ \text{---} \\ (-1,0) \end{array} = \begin{array}{c} e \\ \text{---} \\ e \end{array}, \quad (7.44)$$

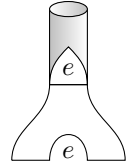
where we have applied the entanglement brane axiom in the last line.

**The Open string Hilbert space and the factorization map** In [118], we defined the open string Hilbert space  $\mathcal{H}_{\text{open}}$  in terms of a noncommutative algebra of functions on the quantum group  $U(\infty)_q$ . This Hilbert space is spanned by a basis

of open string wavefunctions given by representation matrix elements of  $U(\infty)_q$ :

$$\begin{aligned}\mathcal{H}_{\text{open}} &= \lim_{N \rightarrow \infty} \text{span}\{R_{ij}(U) = \langle U | R_{ij} \rangle, U \in U(N)_q, i, j = 1, \dots, \dim R\} \\ &= \otimes_R V_R \otimes V_{\bar{R}}\end{aligned}\tag{7.45}$$

The matrix indices of  $R_{ij}$  correspond to edge mode degrees of freedom which transform under the quantum group as a representation space  $V_R \otimes V_{\bar{R}}$ . Given this definition of  $\mathcal{H}_{\text{open}}$ , the embedding (7.35) of the closed string Hilbert space into the extended Hilbert space of open strings is given by



$$: |R\rangle \rightarrow \sum_{ijk} (D^{-1})_{ij}^R |Rjk\rangle |Rki\rangle\tag{7.46}$$

We showed previously that this satisfies the entanglement brane axiom. Here  $D_R$  is the quantum group representation of the Drinfeld element  $D$ , which we will explain below.

We can understand the mapping (7.46) intuitively as follows. Fig. 7.7 shows the closed string loops in the Lagrangian submanifold  $\mathcal{L}$  where the closed string states are defined as a function of the worldvolume holonomy  $U$ . To cut the closed string loops into open strings, we introduce a large  $N$  number of entanglement branes which intersect  $\mathcal{L}$  as shown along two open disks. This introduces new sectors of open strings inside complementary subregions of  $\mathcal{L}$  that end on the entanglement branes. We denote these open strings configurations by

$$X_{ij}^A, X_{ij}^{\bar{A}}, \quad i, j = 1, \dots, N \gg 1\tag{7.47}$$

where  $i, j$  labels the branes and define corresponding Wilson lines

$$\begin{aligned} U_{ij}^A &= P \left( \exp \oint X_{ij}^{A*} A \right) \\ U_{ij}^{\bar{A}} &= P \left( \exp \oint X_{ij}^{\bar{A}*} A \right) \end{aligned} \quad (7.48)$$

The factorization of the closed string states would naively follow by splitting the configuration space holonomy  $U$  into the subregion Wilson lines

$$U = U^A U^{\bar{A}} \quad (7.49)$$

This would give the factorization map

$$\begin{aligned} \text{tr}_R(U) &\rightarrow \text{tr}_R(U^A U^{\bar{A}}) = \sum_{ij} R(U^A)_{ij} R(U^{\bar{A}})_{ji} \\ |R\rangle &\rightarrow \sum_{ij} |Rij\rangle |Rji\rangle \end{aligned} \quad (7.50)$$

where  $R_{ij}(U^A)$  is a representation matrix element, viewed as a wavefunction in a subregion Hilbert space. This factorization map preserves a diagonal part of the  $U(N) \times U(N)$  edge mode symmetry which acts on the subregion wavefunctions by conjugation

$$\begin{aligned} U^A &\rightarrow g U^A g^{-1} \\ U^{\bar{A}} &\rightarrow g U^{\bar{A}} g^{-1} \end{aligned} \quad (7.51)$$

Unfortunately, this fails to satisfy the entanglement brane axiom for the A model. This is because the factorization map gives a reduced density matrix in the  $R$  sector of the form

$$\rho_R = \sum_{i,j} |Rij\rangle \langle Rij| \quad (7.52)$$

which has a  $(\dim R)^2$  degeneracy due to the  $U(N)$  edge mode symmetry. We can view this as a choice of measure on the edge mode Hilbert space which is

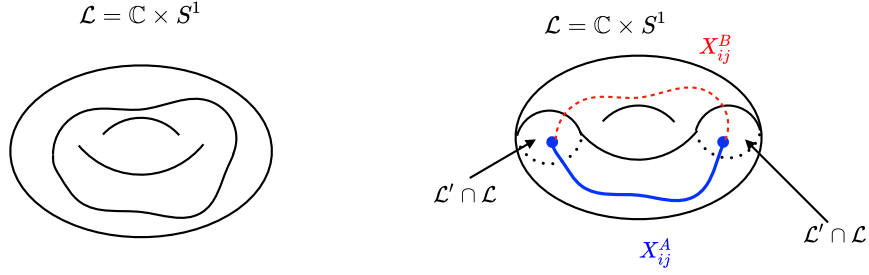


Figure 7.7: On the left, we show a closed string loop  $X(\sigma)$  inside the non-compact Lagrangian manifold  $\mathcal{L} = \mathbb{C} \times S^1$  where we put probe D branes. On the right  $\mathcal{L}$  is split into subregions by the entanglement branes on  $\mathcal{L}'$ . The factorization map embeds the closed string  $X(\sigma)$  into open string configuration  $X_{ij}^A(\sigma), X_{ij}^B(\sigma)$  which are glued together along the entanglement branes

compatible with the degeneracy factors of 2DYM (7.27), but incompatible with the  $q$ -deformed symmetric group dimensions (7.30) of the A model.

The symmetry viewpoint naturally suggests a modification of (7.50), which does give the correct factorization. The presence of the  $q$ -deformed dimension factors implies that the edge mode symmetry is also  $q$ -deformed. Thus we should treat the holonomies  $U, U^A, U^{\bar{A}}$  as elements of the quantum group  $U(N)_q$ . The trace function which is invariant under the adjoint action of the quantum group is given by the *quantum* trace:

$$\begin{aligned} \text{tr}_{q,R}(U) &= \text{tr}_R(uU) \\ u &= \delta_{ij} q^{-i+(N+1)/2} \end{aligned} \quad (7.53)$$

where  $u$  is the Drinfeld element of  $U(N)_q$ . This is an object defined purely from quantum group data and reproduces the quantum dimension of a  $U(N)_q$  rep:

$$\text{tr}_{q,R}(1) = \text{tr}_R(u) = \dim_q(R) \quad (7.54)$$

This defines a  $q$ -deformed measure on the edge mode Hilbert space. To get the precise edge mode measure for the A model partition function we need to define a large  $N$  limit of  $u$  which captures symmetry group quantum dimensions and the

phases in (7.30).

**The most important formula of this paper** The key to finding this limit is to observe that the shrinkable holonomy  $D$  is a renormalized version of the  $U(N)_q$  Drinfeld element. According to equation (7.28), it gives the correct edge mode measure for the A model provided we use a suitable regularization of the trace as  $N \rightarrow \infty$ . Explicitly we have

$$D = q^{-N/2}u$$

$$\lim_{N \rightarrow \infty} \text{tr}_R(D) = (-i)^{l(R)} d_q(R) q^{\kappa_R/4} \quad (7.55)$$

Moreover, the proportionality of  $D$  and  $u$  implies that the quantum trace defined with  $D$  or  $D^{-1}$  is also invariant under the conjugation action of the quantum group  $U(\infty)_q$ .

Equation (7.55) can also be interpreted as a particular large  $N$  limit (7.82) of the  $U(N)$  quantum dimension  $\dim_q R$ , which was previously applied to derive the topological vertex from Chern-Simons link invariants [6, 4]. In section 3, we discuss this limit from the point of view of the Chern-Simons dual, and in section 4 we give a string theory interpretation in terms of the geometric transition. The upshot is that equation (7.55) is a form of open-closed string duality that intimately related to GV duality itself.

The above discussion suggests the correct factorization map can be obtained by promoting the closed string wavefunctions to *quantum* characters[89, 118]

$$\text{tr}_R(U) \rightarrow \text{tr}_R(DU) \quad (7.56)$$



and then applying the splitting  $U = U^A U^{\bar{A}}$

$$\mathrm{tr}_R(DU) \rightarrow \mathrm{tr}_R(DU^A U^{\bar{A}}) = \sum_{ijk} D_{ij}^R R_{jk}(U^A) R_{ki}(U^{\bar{A}}), \quad (7.57)$$

The open string wavefunctions  $R_{jk}(U^A)$  now transform under a the  $U(\infty)_q$  version of the edge mode symmetry (7.51). It was shown in [118] that this factorization map satisfies the entanglement brane axiom and sewing relations of a properly q-deformed extended TQFT. By applying this factorization map to the Hartle-Hawking state, we can compute the reduced density matrix on the open string Hilbert space and compute its entanglement entropy. In the cobordism computation, the partial trace operations on each subregion as defined by the half annulus diagrams are automatically quantum traces which preserve the edge mode symmetry. As a result the entanglement entropy is q-deformed [82, 295]:

$$S = -\mathrm{tr}_q(\rho \log \rho) = -\mathrm{tr}(D\rho \log \rho) \quad (7.58)$$

An explicit computation shows that the q-deformed entropy matches precisely with the generalized entropy (7.15), with the leading “area term” arising from the entropy of edge modes.

### 7.2.5 Quantum group symmetry, defect operator and non-local boundary conditions

Since the quantum group  $U(N)_q$  is the symmetry of anyons, its presence implies that the string edge modes are anyons with nontrivial braiding. This can be understood via the large  $N$  duality with Chern-Simons gauge theory, since the string worldsheets are mapped to Wilson lines representing worldlines of anyons. We will present this mapping in section 4.

Here we give an heuristic explanation in the bulk closed string theory for why quantum group symmetry emerges from the non local shrinkable boundary condition. We noted earlier that the boundary state  $|D\rangle$  defined by the Calabi Yau cap produces the shrinkable boundary condition which sets the worldvolume holonomy to  $U = D$  along the stretched entangling surface.

We could define a new holonomy basis

$$|U\rangle \rightarrow |U\rangle' = \sum_R \text{tr}_R(DU) |R\rangle \quad (7.59)$$

so that

$$|D\rangle = |U = 1\rangle' \quad (7.60)$$

In terms of this new holonomy variable for the configuration space, it would seem that the boundary condition is local as in the 2DYM example. However the new wavefunction  $\text{tr}_R(DU)$  is no longer invariant under

$$U \rightarrow gUg^{-1}, \quad g \in U(N) \quad (7.61)$$

because  $D$  is not in the center of  $U(N)$  so it doesn't commute with a general group element  $g$ . However, the new wavefunction  $\text{tr}_R(DU)$  is invariant under the adjoint action of *quantum group* elements  $g \in U(N)_q$ . Thus by insisting on quantizing in the open string channel with a local boundary condition, we see the emergence of a q-deformed edge mode symmetry !

**Defect operator and the Calabi Yau cap** As noted earlier, the Drinfeld element  $D$  also has an interpretation as a defect operator which is associated with the nontrivial topology of the Calabi Yau cap. Naively, the operator associated with the boundary state  $|D\rangle$  for this cap is just the identity. However as in the

discussion above, if we compare the Calabi Yau cap with  $(0, -1)$  Chern classes to a trivial cap with  $(0, 0)$  Chern classes, we find that the difference can be accounted for by the insertion of a defect operator (see figure 7.8). This operator creates poles in the local sections of the bundles which leads to a nontrivial Chern class, and was shown to be equivalent to insertions of the Drinfeld element of the quantum group in the trace over the open string Hilbert space[118]. We thus have the equivalences

$$\text{Defect operator} \leftrightarrow \text{Non-local shrinkable boundary condition} \leftrightarrow \text{Quantum group symmetry} \quad (7.62)$$

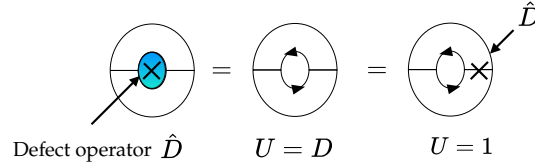


Figure 7.8: On the left, the blue disk corresponds to a  $(0, 0)$  cap with trivial bundle structure. To obtain the Calabi Yau cap, a defect operator is inserted to implement the nontrivial topology. In the first equality, we have integrated over the cap to obtain a non local shrinkable boundary condition  $U = D$ . An equivalent A model amplitude on the disk can be obtained by moving the defect operator outside the hole and putting a local boundary condition on its boundary.

### 7.3 Chern-Simons dual of the Hartle-Hawking state and the entanglement entropy

In the previous section, we defined a factorization of the closed string Hilbert space  $\mathcal{H}_{\text{closed}}$  in terms of an extension of the A-model closed TQFT. We formulated the closed TQFT in terms of the representation category of quantum groups, and derived an extension compatible with the quantum group symmetry as well as the

E-brane axiom. This naturally led to a  $q$ -deformed notion of entanglement entropy consistent with the presence of edge modes transforming under the quantum group  $U(\infty)_q$ . In this section, we provide additional evidence supporting this definition of closed string entanglement entropy by appealing to the dual Chern-Simons theory.

As shown in Fig. (7.4), the dual Chern-Simons description can be obtained by first applying a geometric transition which maps closed strings on the resolved conifold to open strings on the deformed conifold  $T^*S^3$ , with a large  $N$  number of branes wrapping  $S^3$  [161]. The string field theory for these open strings is then given by  $U(N)$  Chern-Simons theory on  $S^3$ . The equivalence between Chern-Simons theory on  $S^3$  and open topological string theory on  $T^*S^3$  holds even at finite  $N$  and can be understood as follows [343]. The A model open string theory contains only zero mode degrees of freedom and localizes to holomorphic instantons that must wrap a minimal volume two dimensional manifold with boundaries ending on  $S^3$ . In the deformed conifold geometry, the only such minimal volume manifolds are points on  $S^3$ . These point-like worldsheets are degenerate instantons and act like particles charged under  $U(N)$ . We thus expect that this theory should be a topological field theory on the  $S^3$ , which can be shown to be Chern-Simons gauge theory. From the point of view of the original closed string theory on the resolved conifold, the Chern-Simons gauge theory can be thought of as living on the  $S^3$  at infinity. [318, 285, 156] This is reminiscent of AdS/CFT.

The relation between Chern-Simons theory and the gravitational dual closed string theory extends to more general geometries with multiple  $S^2$  resolutions and to backgrounds with branes wrapped on Lagrangian manifolds [285, 156]. The duality provides a local mapping between branes on the resolved conifold and Wilson loops in Chern-Simons theory. It is essential for obtaining the gauge

theory dual of the Hartle-Hawking state and relates the entanglement cuts on the two sides.

We will give a full derivation of this duality in section 4. In this section, our immediate goal is to present the Chern-Simons dual of Hartle-Hawking state (7.23) and compute its standard and undeformed entanglement entropy using the extended Hilbert space factorization into left and right moving WZW model edge modes [336, 352, 85]. We will find a precise matching between the vacuum subtracted defect entropy [209, 210, 244] in Chern-Simons theory and the  $q$ -deformed entanglement entropy we calculated above in the dual string theory. We also present a Chern-Simons dual to the replica trick calculation of generalized entropy [112, 141] and explain the construction of the generating functional for Wilson loops which plays an essential role in the duality map on the branes.

### 7.3.1 Review of Chern-Simons theory

We begin by summarizing some important well-known results from Chern-Simons theory. More details can be found for example in [341, 136, 258]. Consider Chern-Simons theory with gauge group  $G$  on a manifold  $M$  with a boundary  $\Sigma = \partial M$ . The action is given by

$$S_{CS,M}(A) = \frac{ik}{4\pi} \int_M \text{Tr} \left( A \wedge dA + \frac{2}{3} A \wedge A \wedge A \right). \quad (7.63)$$

where the integer  $k$  is the level determining the central extension of the lie algebra.

**The Chern-Simons Hilbert space on a Torus** The path integral on  $M$  defines a state in the Hilbert space  $\mathcal{H}(\Sigma)$  on  $\Sigma$ . This is given by the wave functional

$$\Psi_M(A_\Sigma) = \langle A_\Sigma | \Psi \rangle = \int_{A|_\Sigma = A_\Sigma} \mathcal{D}A e^{iS}, \quad (7.64)$$

where  $A_\Sigma$  is the boundary value of the gauge field.

In [341], it was shown that  $\mathcal{H}(\Sigma)$  is isomorphic to the space of conformal blocks of a WZW model on  $\Sigma$  with gauge group  $G$ . In particular,  $\mathcal{H}(S^2)$  is one dimensional and  $\mathcal{H}(T^2)$  is spanned by irreducible representations of the affine Kac-Moody algebra. We will focus on the torus since the Chern-Simons dual of the Hartle-Hawking state  $|HH\rangle$  belongs to  $\mathcal{H}(T^2)$ .

The basis elements  $|R\rangle_{CS}$  for  $\mathcal{H}(T^2)$  are obtained by performing the Chern-Simons path integral on a solid torus  $D^2 \times S^1$  with an insertion of the Wilson loop operator

$$W_R = \text{tr}_R P \exp \oint_C A, \quad (7.65)$$

where  $R$  labels the representation and  $C$  is the non-contractible cycle of the solid torus. This is shown in figure 7.9. The trivial representation corresponds to the vacuum state  $|0\rangle \in \mathcal{H}(T^2)$  with no Wilson loops inserted.

We can superpose the states  $|R\rangle_{CS}$ . Since no local operator can connect states with different representation labels, each representation labels a superselection sector corresponding to an anyon of type  $R$ .

**Chern-Simons partition functions from Heegaard splitting** Now we can consider partition functions of Chern-Simons theory on a manifold  $M$  without a boundary by gluing the aforementioned building blocks. Consider a Heegaard

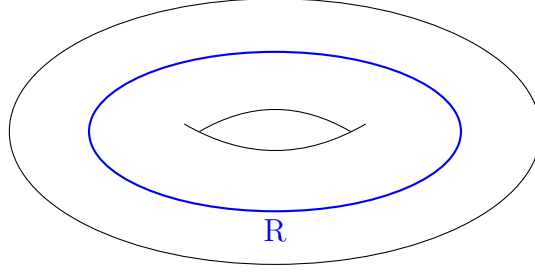


Figure 7.9: The state  $|R_{CS}\rangle$  is defined by the path integral on a solid torus with a Wilson loop operator inserted.

splitting of  $M$  into two manifolds with boundaries  $M_1$  and  $M_2$  that are glued together by a nontrivial diffeomorphism  $f : \partial M_1 \rightarrow \partial M_2$ . Then there is a linear map  $U_f$  such that

$$Z(M) = \langle \Psi_{M_2} | U_f | \Psi_{M_1} \rangle, \quad (7.66)$$

where  $\Psi_{M_1}$  and  $\Psi_{M_2}$  are states assigned to  $M_1$  and  $M_2$  via (7.64), and  $U_f$  forms a representation of the diffeomorphisms that define the gluing.

In particular, under the Heegard splitting,  $S^3$  is decomposed into two solid tori  $\mathbb{T}_i^3 = D_i^2 \times S_i^1$  for  $i = 1, 2$ , which are glued together with an  $S$  transformation that exchanges the A and B cycles. Thus we have

$$Z(S^3) = \langle 0 | S | 0 \rangle \quad (7.67)$$

The value of the matrix element (7.67) is fixed by a normalization for the vacuum state  $|0\rangle$ , which we choose to be

$$\langle 0 | 0 \rangle = Z(S^2 \times S^1) = 1. \quad (7.68)$$

Notice that this normalization is equivalent to a choice of path integral measure. This defines the S matrix element

$$Z(S^3) = S_{00} \quad (7.69)$$

The same Heegard splitting can be applied to compute expectation values of Wilson loops  $S^3$ . By gluing the state  $|R\rangle_{CS} \in \mathcal{H}(T^2)$  to the vacuum state  $|0\rangle \in \mathcal{H}(T^2)$  with an S transformation, we find

$$\begin{aligned}\langle \text{tr}_R(U) \rangle_{S^3} &= \langle 0|S|R \rangle_{CS} = S_{0R} \\ &= S_{00} \dim_q(R)\end{aligned}\tag{7.70}$$

In the second equality we introduced the quantum dimension  $\dim_q(R)$  of  $U(N)$ . It is the *normalized* expectation value of the unknot in  $S^3$  and give the effective dimension of the topological Hilbert space for the anyon labelled by  $R$ .

### 7.3.2 Generating functional for Wilson loops and the $\Omega$ state

Here we define the generating functional for Wilson loop operators in Chern-Simons theory [285], which plays an essential role in the duality between Wilson loops and worldsheets in topological string theory.

This can be obtained from the Ooguri-Vafa operator [285]

$$\exp\left(\sum_{n=1}^{\infty} \frac{1}{n} \text{tr} U^n \text{tr} V^n\right) = \sum_R \text{tr}_R(U) \text{tr}_R(V)\tag{7.71}$$

where  $U = \exp(\oint_{\gamma} A)$ , and  $\gamma$  is an unknot in  $S^3$ . This can be derived from integrating out a massless bi-fundamental field which couples to both the source and dynamical gauge fields [285]. Treating  $V$  as a source, we insert this operator into the path integral to obtain the generating functional

$$Z(V) = \int \mathcal{D}A e^{iS_{CS}(A) + \sum_n \frac{1}{n} \text{tr} U^n \text{tr} V^n} = \sum_R \langle \text{tr}_R(U) \rangle_{S^3} \text{tr}_R(V)\tag{7.72}$$



for Wilson loops in an arbitrary representation  $R$ .

It will be useful to view the generating functional (7.72) as a wavefunction for a state  $|\Omega\rangle$  on the torus Hilbert space, defined by

$$\begin{aligned} |\Omega\rangle &= \sum_R S_{0R} |R\rangle_{CS} \\ &= S_{00} \sum_R \dim_q(R) |R\rangle_{CS} \end{aligned} \quad (7.73)$$

If we introduce the coherent state basis  $|V\rangle \in \mathcal{H}(T^2)$  with wavefunctionals

$$\langle V|R\rangle = \text{tr}_R V, \quad (7.74)$$

then the wave function of  $|\Omega\rangle$  in this basis can be identified with the generating functional  $Z(V)$

$$Z(V) = \sum_R S_{00} \dim_q(R) \text{tr}_R(V) = \langle V|\Omega\rangle \quad (7.75)$$

### 7.3.3 Hartle-Hawking state in Chern-Simons theory

Consider Chern-Simons theory at level  $k$  with gauge group  $U(N)$ , which corresponds to the  $q$  parameter

$$q = \exp\left(\frac{2\pi i}{k+N}\right). \quad (7.76)$$

For any  $t \in \mathbb{C}$ , define the following state on the torus

$$|\Omega(t)\rangle = S_{00} \sum_R \dim_q(R) e^{-\frac{t}{2}l(R)} |R\rangle_{CS}, \quad (7.77)$$

which consists of a superposition of Wilson loops, and reduces to the state  $|\Omega\rangle$  at  $t = 0$ . We claim that the Hartle-Hawking state  $|HH(t)\rangle$  for string theory on the

resolved conifold is dual to a suitable large  $N$  limit of  $|\Omega(t)\rangle$ . In the coherent state basis, the wavefunction for this state is

$$\langle V|\Omega(t)\rangle = \langle e^{-t/2}V|\Omega\rangle = S_{00} \sum_R \dim_q(R) e^{-\frac{t}{2}l(R)} \text{tr}_R(V) \quad (7.78)$$

As in the case of  $t = 0$  we can identify this expression as a generating wavefunctional obtained by a path integral on  $S^3$ :

$$\begin{aligned} \langle V|\Omega(t)\rangle &= Z(V, t) := \int \mathcal{D}A e^{iS_{CS}(A) + \sum_n \frac{e^{-nt/2}}{n} \text{tr} U^n \text{tr} V^n} \\ &= \sum_R \langle \text{tr}_R(U) \rangle_{S^3} e^{-l(R)t/2} \text{tr}_R(V) \end{aligned} \quad (7.79)$$

where we have applied a generalization of (7.71) by replacing  $V \rightarrow e^{-t/2}V$ .  $Z(V, t)$  can again be obtained from integrating out a massive bi-fundamental field coupling the source and dynamical gauge fields [285, 5, 4].

To obtain the appropriate large  $N$  limit of eq (7.77), we need to specify the large  $N$  limit of the states  $|R_{CS}\rangle$ . To do this, first define the states  $|k_{CS}\rangle$  whose wavefunctions are obtained by inserting Wilson loops in the winding basis (7.18)

$$\begin{aligned} \langle A_{T^2} | \vec{k}_{CS} \rangle &= \int_{A|_{T^2} = A_{T^2}} \mathcal{D}A e^{iS} \prod_{n=1}^{\infty} \text{tr}(U^n)^{k_n} \\ U &= \exp\left(\oint_{S^1} A\right) \end{aligned} \quad (7.80)$$

$|k_{CS}\rangle$  is well defined in the large  $N$  limit, and  $|R_{CS}\rangle$  is defined by it's relation to  $|k_{CS}\rangle$  via the Frobenius relation (7.19) In this limit  $R$  is a representation label for  $U(\infty)$  corresponding to a Young tableaux.

The large  $N$  limit of the amplitudes  $\langle R|\Omega(t)\rangle$  is more subtle. Following [3, 258], we first take the large  $N$  limit while fixing the 't Hooft coupling  $t'$

$$\begin{aligned} N &\rightarrow \infty \\ t' &= \frac{2\pi i N}{k + N} = \text{constant}, \end{aligned} \quad (7.81)$$

which is the same as holding the ratio  $\frac{k}{N}$  constant. We then analytically continue  $t'$  to a real number and then take  $t' \rightarrow \infty$ . In this limit we can expand the quantum dimensions as

$$\dim_q(R) = (-i)^{l(R)} d_q(R) q^{Nl(R)/2} q^{\kappa(R)/4} + \mathcal{O}(q^{-l(R)N/2}), \quad (7.82)$$

where  $d_q(R)$  is defines as in (7.9) with

$$g_s = \frac{2\pi}{k + N} \quad (7.83)$$

Notice that we needed to analytically continue  $t'$  so that  $q^{Nl(R)/2} = e^{\frac{t'}{2}l(R)}$  has a divergent norm  $t' \rightarrow \infty$ ; the first term of (7.82) can then be considered large relative to the rest. Remarkably, we can absorb this divergence into the Boltzman factor  $e^{-\frac{t}{2}l(R)}$  because they both have the same exponent dependence on  $l(R)$ . More precisely, we will apply a shift to the “coupling”  $t$  in the Boltzman factor

$$e^{-\frac{t}{2}l(R)} \rightarrow e^{-\frac{t+t'}{2}l(R)} \quad (7.84)$$

and identify the leading dependence of  $\dim_q(R)$  on  $N$  as

$$q^{Nl(R)/2} = e^{t'l(R)/2} \quad (7.85)$$

The state

$$|HH_{CS}(t)\rangle := \lim_{t' \rightarrow \infty} \lim_{N \rightarrow \infty} |\Omega(t + t')\rangle = \lim_{t' \rightarrow \infty} \lim_{N \rightarrow \infty} S_{00} \sum_R \dim_q(R) e^{-\frac{t+t'}{2}l(R)} |R\rangle_{CS} \quad (7.86)$$

is then well defined since the divergent term (7.85) has been cancelled. Note that  $S_{00}(t')$  diverges as  $t' \rightarrow \infty$ , but this just gives the usual infinite normalization which arises from the path integral measure. Using (7.82), we find that the putative Chern-Simons dual of the Hartle-Hawking state  $|HH(t)\rangle$  is:

$$|HH_{CS}(t)\rangle = S_{00} \sum_R (-i)^{l(R)} d_q(R) q^{\kappa(R)/4} e^{-\frac{t}{2}l(R)} |R_{CS}\rangle \quad (7.87)$$

In the dual closed string theory on the resolved conifold, the shift  $t \rightarrow t + t'$  in (7.84) is performed to correctly parametrize the Kähler cone in the presence of the B-flux on the  $S^2$  on which the worldsheet ends [105]. Notice that the this shift by  $t'$  is equivalent the introducing the relative factor between the Drinfeld elements  $D$  and  $u$ :

$$D = q^{-N/2}u \tag{7.88}$$

In the large  $N$  limit, this choice of  $D$  effectively absorbs the divergence in the quantum dimension as defined by  $u$  and assigns a finite dimension to the edge mode Hilbert space in the  $R$  sector.

To see that we have obtained the correct dual to the Hartle-Hawking state, we must show that the identification

$$|R_{CS}\rangle \rightarrow |R\rangle \tag{7.89}$$

preserves locality in some sense. Otherwise equation (7.89) is just a linear map between basis elements which is rather trivial, since all vector spaces of the same dimensionality are isomorphic. The preservation of locality is captured most precisely by showing that local Hilbert space factorization of CS theory is mapped to the factorization in the string theory. The sharpest expression of the local nature of this mapping between  $|HH(t)\rangle$  and  $|HH_{CS}(t)\rangle$  is obtained by identifying the Wilson loops in CS theory to the boundaries of worldsheets in the string theory: we will explain this duality in the next section [251, 300, 285, 156]. We will also show the preservation of locality by checking that the entanglement entropy computed with either factorization agrees.

### 7.3.4 Matching with the dual partition function and emergence of the bulk geometry

Consider the density matrix for  $|HH_{CS}\rangle$ . In the following it is important to observe that a TQFT is not endowed with a canonical choice of a Hermitian inner product. Indeed, the sesquilinear property of such an inner product is incompatible with the holomorphic nature of the A model. Therefore in the dual Chern-Simons theory, we will define the density matrix and the partial trace without reference to a Hermitian inner product. While this departs from the conventions of [336, 352, 112, 141], this is consistent with the usual representation of the reduced density matrix as a Euclidean path integral with a cut along the subregion. It also agrees with conventions in defining entanglement entropy in non Hermitian systems where a positive definite Hermitian inner product is not readily available.

We define the density matrix for the Hartle-Hawking state by

$$\rho = |HH_{CS}\rangle \langle HH_{CS}^*|$$

$$\langle HH_{CS}^*| := \sum_R (i)^{l(R)} d_q(R) q^{-\kappa_R/4} e^{-l(R)(t)/2} \langle R_{CS}| \quad (7.90)$$

where we denote by  $\langle R_{CS}|$  the basis dependent dual of  $|R_{CS}\rangle$ , obtained by doing the path integral on a torus of opposite orientation with the insertion of the Wilson loop in the conjugate representation  $\bar{R}$ . By definition the dual basis satisfies

$$\langle R_{CS}|R'_{CS}\rangle = \delta_{RR'}, \quad (7.91)$$

but note that this makes no reference a Hermitian inner product<sup>17</sup>. Instead equation (7.91) arises from evaluating the Wilson loops expectation values in the  $S^2 \times S^1$

---

<sup>17</sup>The usual Hermitian inner product agrees with (7.91) on a basis. However its sesquilinear property is not consistent with the holomorphic nature of the A model and its Chern-Simons dual.

geometry obtained from gluing the two tori with opposite orientation. In particular  $\langle HH_{CS}^*|$  is not related to  $|HH_{CS}\rangle$  by an anti-linear map.

In the string theory,  $\langle HH_{CS}^*|$  corresponds to the linear functional that is related to the geometric state  $|HH_{CS}\rangle$  by flipping orientation and mapping branes to anti-branes [325, 3]. In the Chern-Simons theory, we will take  $\langle HH_{CS}^*|$  as part of the choice of a density matrix  $\rho$  which determines the expectation value of operators via

$$\langle O \rangle = \text{tr}(\rho O) \quad (7.92)$$

The trace of the density matrix agrees with the A model partition function on the resolved conifold:

$$Z = \text{tr}(\rho) = \sum_R (d_q(R))^2 e^{-t\ell(R)} = Z_{\text{top}} \quad (7.93)$$

Just like the A model, this is a holomorphic quantity and is not a real norm. It is important to note that from the point of view of the Chern-Simons theory, the parameters  $t$  carry no geometric interpretation; it merely specifies a particular superposition of Wilson loops. Remarkably, in the dual closed string theory, a geometry has emerged in which  $t$  becomes the Kahler modulus of the target space. Note that this Kahler modulus is not the one that arise from applying a geometric transition to branes wrapping  $S^3$  in Chern-Simons theory. Instead it arises from a particular superposition of Wilson loops.

### 7.3.5 Entropy from geometrical replica trick in Chern-Simons theory

Here we perform the replica trick calculation of entanglement entropy for the putative Chern-Simons dual (7.87) to the Hartle-Hawking state and show that they match on the two sides of the duality. More precisely, we show that the q-deformed entanglement entropy in the closed string theory coincides with the undeformed defect entropy in Chern-Simons theory in the large N-limit. The defect entropy is the difference between the entanglement entropy and the state independent ground state entanglement entropy, and it measures the entanglement entropy due to cutting the Wilson loops [209, 210, 244]. We will sidestep the question of how to factorize of the Chern-Simons Hilbert space by applying the geometric replica trick via surgery methods as in [112].

As pointed out earlier, our calculation of the entanglement entropy of a generic state

$$|\psi\rangle = \sum_R \psi(R) |R\rangle \quad (7.94)$$

differs from [112] in the choice of inner product: since reference [112] uses a Hermitian inner product which defines an anti-linear adjoint operation, their density will involve complex conjugation of the amplitudes  $\psi(R)$ , whereas ours do not.

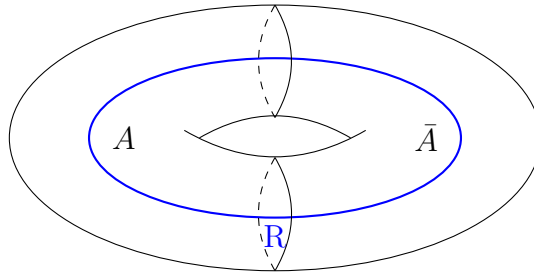


Figure 7.10: Separated solid torus with a Wilson loop operator inserted.

However apart from determining the coefficients in the density matrix  $\rho$ , the choice of inner product has no bearing on the construction of the replica manifold which computes the replica partition functions

$$Z(n) = \text{tr}_A \rho_A^n, \quad (7.95)$$

since neither the partial trace nor matrix multiplication implicit in the replica trick uses the inner product. This point was recently emphasised in [131]. As a result, we can borrow the results of [112] directly. First note that in when computing  $Z(n)$  there are no “cross term” corresponding to replica manifolds with insertions of Wilson loop  $R$  and  $R'$  which are not conjugate to each other.

The reduced density matrix defined by the replica manifold will therefore decompose into superselection sectors labelled by  $R$ . This means we can apply the result of [112] for each state  $|R_{CS}\rangle$  separately and sum up the results. For each  $R$ , we partition the torus in Fig. 7.10 defining  $|R_{CS}\rangle$  as well as the dual torus corresponding to  $\langle R_{CS}|$ . We glue together the  $\bar{A}$  to obtain a reduced density matrix, and then construct the replica manifold by the usual cyclic gluing. The reference [112] showed that the partition function for the  $n$ th replica is

$$Z(n) = \text{tr}_{\rho_A}(R)^n = Z(S; R_i)^{1-n} Z(S; \bar{R}_i)^{1-n}. \quad (7.96)$$

The normalization factor is

$$Z(1) = \text{tr}_{\rho_A}(R) = \langle R_i | R_i \rangle = \frac{Z(S^3; R_i)^2 Z(S^3; \bar{R}_i)^2}{Z(S^3; R_i)^2 Z(S^3; \bar{R}_i)^2} = 1. \quad (7.97)$$

Using the large N identity

$$\lim_{N \rightarrow \infty} Z(S^3; R) Z(S^3; \bar{R}) = S_{00}^2 d_q(R)^2. \quad (7.98)$$

we obtain the replica trick entropy

$$S_R = -\frac{\partial}{\partial n} \frac{Z_n}{Z_1^n} \Big|_{n=1} = 2 \log S_{00} d_q(R). \quad (7.99)$$



Now we apply the replica trick the putative dual to the Hartle-Hawking state  
(7.87)

$$|HH_{CS}(t)\rangle = S_{00} \sum_R (-i)^{l(R)} d_q(R) q^{\kappa(R)/4} e^{-\frac{i}{2}l(R)} |R_{CS}\rangle. \quad (7.100)$$

As noted earlier, the reduced density matrix

$$\rho_A = \text{tr}_{\bar{A}} |HH_{CS}(t)\rangle \langle HH_{CS}(t)^*|, \quad (7.101)$$

breaks into superselection sectors labelled by  $R$ , so the replica partition function is just

$$\begin{aligned} Z_n &= \text{tr}_A(\rho_A^n) = \sum_R (S_{00} d_q(R))^{2-2n} (S_{00} d_q(R) e^{-\frac{i}{2}l(R)})^{2n} \\ &= \sum_R S_{00}^2 d_q(R)^2 e^{-ntl(R)}. \end{aligned} \quad (7.102)$$

It is very interesting to note that the only effect of the replication is the replication of the complexified area  $t$ . This means that from the string theory point of view, the topology of the target space is not changed, and the Calabi-Yau condition is preserved. This was precisely the topological constraint we imposed in our definition of generalized entropy on the resolved conifold [118]. We can thus view our Chern-Simons replica manifold as the in gauge theory dual to the replica manifold we constructed for the resolved conifold in [118].

Given (7.102), we find that

$$\frac{Z_n}{Z_1^n} = \frac{\text{tr}_A \rho_A^n}{(\text{tr}_A \rho_A)^n} = S_{00}^{2-2n} \sum_R d_q(R)^2 e^{-ntl(R)}, \quad (7.103)$$

where we defined  $Z \equiv \sum_R d_q(R)^2 e^{-tl(R)}$ . The total entanglement entropy is

$$S_{tot} = -\frac{\partial}{\partial n} \frac{Z_n}{Z_1^n} \Big|_{n=1} = \sum_R p(R) (-\ln p(R) + 2 \ln d_q(R)) + 2 \ln(S_{00}) \quad (7.104)$$

where  $p(R) = \frac{d_q(R)^2 e^{-tl(R)}}{Z}$

As noted earlier, we will only be interested in the entropy due to cutting the Wilson loops, since these are dual to the closed string worldsheets. This is captured by the defect entropy which subtracts the state independent contribution

$$S_0 = 2 \ln(S_{00}) \quad (7.105)$$

which is the analogue of the background extremal entropy in [208, 247, 209, 210, 244]. The defect entropy is therefore

$$S = S_{tot} - S_0 = \sum_R p(R) (-\ln p(R) + 2 \ln d_q R). \quad (7.106)$$

which matches with the generalized entropy computed in the closed string theory.

### 7.3.6 Factorization and edge modes in the dual Chern-Simons theory

In this section we give the Chern-Simons dual of the factorization map (7.46) and edge modes for the closed string theory on the resolved conifold. These can be obtained from a suitable large N limit of the factorization map developed in [336, 352], where an explicit description of the extended Hilbert space for Chern-Simons theory was given in terms of CFT edge modes. We will apply this factorization map to the state  $|\Omega(t)\rangle$  and give a canonical calculation of entanglement entropy which agrees with the results of the previous section. We find that the quantum group edge mode symmetry of the closed string theory is described in the dual gauge theory by the large N limit of Kac-Moody symmetry of the CFT edge modes.

**Entanglement cut and the factorization map at finite N** The entanglement cut which we apply to the state  $|\Omega(t)\rangle$  is shown in Fig. 7.11. The surface

of the torus is partitioned into two disconnected subregions  $A$  and  $\bar{A}$ , separated by a cylindrical region of size  $\epsilon$ . This is a UV regulator which we will send to zero at the end of the calculation. To define the subregion Hilbert space  $\mathcal{H}_A, \mathcal{H}_{\bar{A}}$ , we choose a “shrinkable” entanglement boundary condition which breaks the topological invariance<sup>18</sup> and introduces CFT edge modes along  $\partial A$  and  $\partial \bar{A}$  [336, 352]. This shrinkable boundary condition is *local* and corresponds to setting the component of the gauge field in the angular direction around the entangling surface to zero. For  $U(N)_k$  Chern-Simons theory, the edge modes correspond to chiral  $U(N)_k$  WZW models at the boundaries of  $A$  with opposite chiralities.

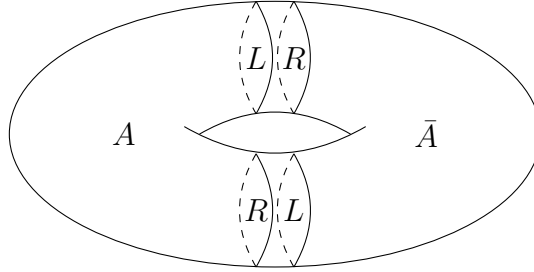


Figure 7.11: Geometric entanglement entropy in Chern-Simons theory is equivalent to left-right entanglement entropy in the WZW model. L and R in the diagram represents left and right moving chiralities for the WZW models.

The subregion Hilbert space can be expressed as

$$\begin{aligned}\mathcal{H}_A &= \mathcal{H}_{WZW}^L \otimes \mathcal{H}_{WZW}^R \\ \mathcal{H}_{\bar{A}} &= \mathcal{H}_{WZW}^R \otimes \mathcal{H}_{WZW}^L\end{aligned}\tag{7.107}$$

Due to the Gauss Law constraint, the Chern-Simons Hilbert space  $\mathcal{H}(T^2)$  on the torus does not naively factorize into a tensor product of subregion Hilbert spaces. Instead, the factorization should be viewed as a mapping

$$\mathcal{H}(T^2) \rightarrow \mathcal{H}_A \otimes \mathcal{H}_{\bar{A}}\tag{7.108}$$

---

<sup>18</sup>More specifically, the boundary condition introduces a choice of complex structure which defines the chiral edge modes [141].

that embeds the physical Hilbert space into the extended Hilbert space<sup>19</sup>; due to the holographic nature of Chern-Simons theory, the extended Hilbert space consists entirely of edge modes. The factorization map on each basis element is given by

$$|R_{CS}\rangle \rightarrow |R\rangle_1 |R\rangle_2$$

$$|R\rangle_1 = \frac{e^{\frac{-8\pi\epsilon}{l}(\bar{L}_0 - \frac{c}{24})}}{\sqrt{n_R}} \sum_{N=0}^{\infty} \sum_{j=1}^{d_R(N)} |R, N, j\rangle_L \overline{|R, N, j\rangle_R}, \quad (7.110)$$

where 1, 2 labells the two entangling surfaces, and  $|R\rangle$  is a normalized Ishibashi state that satisfy the Gauss law constraint across the entangling surface. The integers  $N, j$  label descendents, and  $d_R(N)$  is a degeneracy for each level  $N$ . As explained in [352], the factorization map is implemented by the Euclidean path integral with a “brick wall” regularization. If we flip a ket into a bra in (7.110) using a CPT conjugation<sup>20</sup>, the normalized Ishibashi state becomes the modular operator which implements the “half modular flow” from  $\mathcal{H}_A$  to  $\mathcal{H}_{\bar{A}}$ . Finally the normalization factor

$$n(R) = \chi_R(e^{\frac{-8\pi\epsilon}{l}}) = \text{tr}_R e^{\frac{-8\pi\epsilon}{l}(\bar{L}_0 - \frac{c}{24})} \quad (7.111)$$

is the charactor of the integrable representation  $R$  of the Kacs Moody algebra for  $U(N)$  at level  $k$ , and  $l$  is the length of entangling surface. Observe that the brick wall regulator  $\epsilon$  is needed to render the normalization finite, as  $\epsilon \rightarrow 0$  corresponds to an infinite temperature limit.

For fixed  $|R_{CS}\rangle$ , the reduced density matrix is obtained by factorizing the density matrix (7.90) and tracing over  $\bar{A}$ . This corresponds to tracing out a chiral

---

<sup>19</sup>Equivalently, we can view the physical Hilbert space as a fusion product

$$\mathcal{H}(T^2) = \mathcal{H}_A \otimes_G \mathcal{H}_{\bar{A}} \quad (7.109)$$

in which we impose quotient relation determined by a quantum gluing condition.

<sup>20</sup>This is referred to as the state-channel duality

half of the left-right entangled Ishibashi states  $|R\rangle\rangle$ , which gives the reduced density matrix

$$\rho^R = \rho_1^R \otimes \rho_2^{\bar{R}}, \quad (7.112)$$

with

$$\begin{aligned} \rho_1^R &= \frac{1}{\bar{n}_R} \sum_{N_1, j_1} e^{\frac{-8\pi\epsilon}{l}(\bar{L}_0 - \frac{c}{24})} |R, N_1, j_1\rangle_L \langle R, N_1, j_1|_L, \\ \rho_2^{\bar{R}} &= \frac{1}{n_R} \sum_{N_2, j_2} e^{\frac{-8\pi\epsilon}{l}(L_0 - \frac{c}{24})} |\bar{R}, N_2, j_2\rangle_R \langle \bar{R}, N_2, j_2|_R \end{aligned} \quad (7.113)$$

Note that edge modes at the two boundaries of a subregion have opposite chiralities, and combine to form a diagonal CFT. The entanglement Hamiltonian<sup>21</sup> is identified with the non-chiral WZW Hamiltonian:

$$H_A = \frac{-8\pi\epsilon}{l}(L_0 + \bar{L}_0 - \frac{c}{12}) \quad (7.114)$$

$$\rho_A = \frac{e^{-H_A}}{Z_A} \quad (7.115)$$

where  $Z_A = \bar{n}_R n_R$  is the partition function of the CFT edge modes.

The entanglement entropy can be obtained directly without appealing to the replica trick:

$$S = -\text{tr} \rho_A \log \rho_A = \text{tr}_A(\rho_A H_A) + \log Z_A \quad (7.116)$$

As  $\epsilon \rightarrow 0$ , the “modular energy term” vanishes and the entropy is identified with the free energy. For a fixed  $R$  sector we have

$$S_R = \log Z_A = \log \chi_R(e^{\frac{-8\pi\epsilon}{l}}) \chi_{\bar{R}}(e^{\frac{-8\pi\epsilon}{l}}) \quad (7.117)$$

---

<sup>21</sup>Our entanglement Hamiltonian is slightly different the usual definition of the modular Hamiltonian since it doesn't contained the constant term due to  $Z_A$  in the denominator

In the  $\epsilon \rightarrow 0$  limit, the reduced density becomes maximally mixed, so the entropy is the logarithm of the number of states in a suitable sense. In fact this interpretation becomes sharper when we consider only the entropy due to cutting the Wilson loop. This is obtained by subtracting the vacuum entropy for  $R = 0$ , which gives the defect entropy  $S_{\text{defect}}(R)$ . This gives a counting of the degeneracy according to

$$e^{S_{\text{defect}}(R)+S_{\text{defect}}(\bar{R})} = \left( \lim_{\epsilon \rightarrow 0} \frac{\text{tr}_R e^{-2\pi\epsilon H_{\text{CFT}}}}{\text{tr}_{R=0} e^{-2\pi\epsilon H_{\text{CFT}}}} \right) \left( \lim_{\epsilon \rightarrow 0} \frac{\text{tr}_{\bar{R}} e^{-2\pi\epsilon \bar{H}_{\text{CFT}}}}{\text{tr}_{\bar{R}=0} e^{-2\pi\epsilon \bar{H}_{\text{CFT}}}} \right) = \dim_q(R) \dim_q(\bar{R}) \quad (7.118)$$

The ratio of CFT partition functions define the “regularized dimension” of a representations  $R/\bar{R}$  of the chiral algebra, which is one way to *define* the quantum dimensions. In practice the  $\epsilon \rightarrow 0$  limit is computed by first applying a modular transformation to  $\chi_R$

$$\chi_R(e^{-\frac{8\pi\epsilon}{l}}) = \sum_{R'} S_{RR'} \chi_{R'}(e^{-\frac{\pi l}{2\pi\epsilon}}) \rightarrow S_{R0} e^{\frac{\pi cl}{48\epsilon}} = S_{00} \dim_q(R) e^{\frac{\pi cl}{48\epsilon}} \quad (7.119)$$

At finite  $N$  we have  $\dim_q(\bar{R}) = \dim_q(R)$ , so from the point of view of the defect entropy, we have an effective degeneracy of  $\dim_q(R)^2$  for each superselection sector labelled by  $R$ .

In the section 2, we observed that the quantum dimensions  $\dim_q(R)$  can be viewed as a choice of measure determined by the Drinfeld element of  $U(N)_q$  and the corresponding quantum trace (7.44). Here we see an alternative definition of this measure via the ratio of CFT partition functions. We will see below that in the large  $N$  limit, these correspond to the two alternative descriptions of the edge modes in the string theory and the Chern-Simons dual.

By linearity, we can apply the factorization map (7.113) to the state  $|\Omega(t)\rangle$

$$|\Omega(t)\rangle = S_{00} \sum_R \dim_q(R) e^{-l(R)t/2} |R\rangle_{CS} \quad (7.120)$$

which gives

$$|\Omega(t)\rangle = S_{00} \sum_R \dim_q(R) e^{-l(R)t/2} |R\rangle_1 |R\rangle_2, \quad (7.121)$$

The (normalized) reduced density matrix now consists of a sum over superselection sectors labelled by  $R$

$$\begin{aligned} \rho_A &= \sum_R P(R) \rho_1^R \otimes \rho_2^{\bar{R}} \\ P(R) &= \frac{\dim_q(R)^2 e^{-tl(R)}}{Z} \end{aligned} \quad (7.122)$$

This takes the form of a “thermo-mixed double” state [332] in which the two edge modes CFT’s are classically correlated due to the Wilson loop threading the torus.

This reduced density matrix takes a form which is directly analogous to that of a nonabelian gauge theory. We can make this manifest by writing the normalized density matrices  $\rho_i^R$  explicitly as a maximally mixed state in the  $R$  sector.

$$\rho_1^R = \frac{e^{\frac{-8\pi\epsilon}{l}(L_0 - \frac{c}{24})}}{\chi_R(e^{\frac{-8\pi\epsilon}{l}})} \rightarrow \frac{\mathbf{1}_R}{\dim_q R S_{00} e^{\frac{\pi cl}{48\epsilon}}} \quad (7.123)$$

and similarly for  $\rho_2^{\bar{R}}$ . Then we have

$$\rho_A = \sum_R P(R) \frac{\mathbf{1}_{R \otimes \bar{R}}}{|\dim_q R|^2 |S_{00} e^{\frac{\pi cl}{48\epsilon}}|^2} \quad (7.124)$$

so we can identify  $P(R)$  as a probability factor for being in the  $R \otimes \bar{R}$  sector, where the density matrix is just proportional to the identity. The analogy become exact when we subtract off the vacuum entropy which gets rid of the contribution from  $S_{00} e^{\frac{\pi cl}{48\epsilon}}$ . Written in this form, we see that the entanglement Hamiltonian should be identified (up to a state independent constant) with the operator

$$H_A = tl(R) \quad (7.125)$$

The CFT edge modes Hamiltonian (7.115) merely plays an intermediary role in regularizing the trace, in order to determine a finite degeneracy factor for fixed  $R$ .

We now repeat the edge mode calculation of defect entropy in the large  $N$  limit, and show that it matches with string edge mode calculation involving entanglement branes. In particular we want to identify the entanglement spectrum and degeneracy on both sides. In the string theory, the edge mode Hilbert space breaks up into superselection sectors  $R \otimes \bar{R}$  labelled by a young tableaux. In the large  $N$  limit, each sector has an infinite number of states with modular eigenvalue  $tl(R)$ . The degeneracy in each sector is obtained by applying a regularized trace

$$\text{tr}_{R \otimes \bar{R}}(D) = \text{tr}_R(D) \text{tr}_{\bar{R}}(D) = (d_q(R))^2 \quad (7.126)$$

where  $D$  is related to the Drinfeld element  $u$  of  $U(N)_q$  by

$$D_{ij} = q^{-N/2} u_{ij} = \delta_{ij} q^{-i+\frac{1}{2}} \quad (7.127)$$

The regularization involves a continuation

$$q \rightarrow q e^{\epsilon_{\text{string}}} \quad (7.128)$$

which makes the trace converge. We interpret the trace as a sum over entanglement branes.

In the Chern-Simons dual, we find a similar structure from the large  $N$  limit of the WZW model edge mode CFT [230]. The primary states of the  $U(N)_k$  WZW model are labelled by a finite number of integrable representations. However in the large  $N$  limit, the truncation is lifted and we can associate each a chiral/antichiral primary to each Young Tableaux. The conformal dimensions for these chiral primaries are given by

$$\Delta(R) = \frac{C_2(R)}{2(k+N)}, \quad (7.129)$$

where  $C_2(R)$  is the quadratic Casimir. The large  $N$  limit at fixed  $t'$  gives

$$\Delta_R(t') = \frac{1}{4\pi i} l(R) t' + \mathcal{O}\left(\frac{1}{N}\right). \quad (7.130)$$



This determines the large  $N$  spectrum which defines the WZW model propagator, and the associated normalized Ishibashi state (7.110). Notice that we had to introduce  $UV$  regulator  $\epsilon$  to define this propagator, which regularizes the trace over the CFT edge modes. This is the CFT analogue of the string theory regulator  $\epsilon_{\text{string}}$ .

Given these definitions we can factorize each state  $|R_{CS}\rangle$  as in (7.110) for the finite  $N$  case. Applying this factorization to  $|HH_{CS}(t)\rangle$  and  $\langle HH_{CS}(t)^*|$  and doing the partial trace gives the reduced density matrix

$$\begin{aligned} \rho_A &= \sum_R p(R) \rho_1^R \otimes \rho_2^{\bar{R}}, \quad p(R) = \frac{d_q(R)^2 e^{-tl(R)}}{Z} \\ \rho_1^R &= \frac{e^{\frac{-8\pi\epsilon}{l}(L_0 - \frac{c}{24})}}{\chi_R(e^{\frac{-8\pi\epsilon}{l}})}, \quad \rho_2^{\bar{R}} = \frac{e^{\frac{-8\pi\epsilon}{l}(\bar{L}_0 - \frac{c}{24})}}{\chi_{\bar{R}}(e^{\frac{-8\pi\epsilon}{l}})} \end{aligned} \quad (7.131)$$

where  $Z$  is the resolved conifold partition function. As in the finite  $N$  case the density matrix in the fixed  $R$  sector is maximally mixed when we take  $\epsilon \rightarrow 0$ , and the entanglement entropy in each sector just computes the log of the degeneracy. The entanglement Hamiltonian is then given by

$$H_A = tl(R) \quad (7.132)$$

which is the same as in the string theory

We can obtain this degeneracy factor for fixed  $R$  by first keeping  $N$  and  $t'$  finite and taking the  $\epsilon \rightarrow 0$ . In this limit, we can formally write

$$\rho_A = \sum_R p(R) \frac{e^{\frac{-8\pi\epsilon}{l}(L_0 + \bar{L}_0 - \frac{c}{12})}}{|\chi_R(e^{\frac{-8\pi\epsilon}{l}})|^2} \sim \sum_R p(R) \frac{\mathbf{1}_{R \otimes \bar{R}}}{|\dim_q R|^2 |S_{00} e^{\frac{\pi c l}{48\epsilon}}|^2} \quad (7.133)$$

If we now take the large  $N$  limit of the quantum dimensions using (7.82), then

$$\rho_A \sim \sum_R p(R) \frac{\mathbf{1}_{R \otimes \bar{R}}}{d_q(R)^2 |S_{00} e^{\frac{\pi c l}{48\epsilon}}|^2} \quad (7.134)$$

which shows that after the vacuum subtraction there is an effective degeneracy  $d_q(R)^2$  just as in the string theory. Note that in obtaining this degeneracy, it was crucial to take into account the opposite chiralities of the two edges, which have complex conjugate characters. Explicitly, using this order of limits the entanglement entropy of  $|HH_{CS}\rangle$  is given by

$$\begin{aligned} S &= \lim_{t' \rightarrow \infty} \lim_{N \rightarrow \infty} \sum_R (-p(R) \ln p(R)) + p(R) \ln |\dim_q R|^2 + \frac{\pi cl}{12\epsilon} + 2 \ln S_{00} \\ &= \sum_R (-p(R) \ln p(R)) + p(R) \ln (d_q(R))^2 + \frac{\pi cl}{12\epsilon} + 2 \ln S_{00} \end{aligned} \quad (7.135)$$

If we subtract the “extremal entropy”, which is the ground state entanglement entropy in the absence of Wilson loops:

$$S_{ext} = \frac{\pi cl}{12\epsilon} + 2 \ln S_{00} \quad (7.136)$$

we obtain the defect entropy

$$S_{\text{defect}} = S - S_{ext} = \sum_R (-p(R) \ln p(R)) + p(R) \ln (d_q(R))^2 \quad (7.137)$$

which again agrees with the q-deformed entropy of the closed string theory.

In Chern-Simons theory, the area term in (7.136) originates from UV divergences in field theories, which can also be obtained from careful treatment of the replica trick calculation [141]. The area term is important when applying CS theory as a low energy effective field theory, since it is required for the positivity of the entanglement entropy. However, our definition of generalized entropy in string theory does not include this term, since we are only capturing the entanglement purely due to cutting the worldsheets, which is dual to cutting the Wilson loops. As a result we obtain a manifestly positive entropy without including the area term.

## 7.4 Large $N$ expansion of Wilson loops and dual string worldsheets

In the previous section we applied a large  $N$  limit to the state (7.87) in Chern-Simons theory, and showed that its factorization leads to an entanglement entropy consistent with the  $q$ -deformed entropy of the Hartle-Hawking state in the closed string theory. This bolsters our claim that the  $q$ -deformed entropy should be viewed as the topological string analogue of generalized entropy in AdS/CFT. Here we will explain the matching of the states and the dual entropy calculations from the point of view of the large  $N$  duality between Wilson loops and string worldsheets [285, 156].

**Toric diagrams and geometric transitions.** Toric diagrams provide a useful representation for topological string amplitudes which gives a precise description of the geometric transition between the resolved and deformed conifold. They capture the duality in the presence of branes in a simple graphical language. We give a very brief description here and defer a more detailed explanation to the Appendix.

Toric manifolds such as the resolved and deformed conifold can be characterized as a  $T^2 \times \mathbb{R}$  fibration over  $\mathbb{R}^3$ . The toric diagrams specify the degeneracy locus of this fibration where a cycle of  $T^2$  shrinks. It turns out this locus lives in a  $R^2$  subspace of the base, and we can specify this locus by edges on a graph. The orientation of the edges determines which cycle degenerates on  $T^2$ .

For example  $\mathbb{C}^3$  is given by a trivalent graph with a single vertex as shown as the third diagram in Fig. 7.16. The topological vertex is given by adding branes on

this graph, labelled by arrows. In particular, the Hartle-Hawking state corresponds to adding one stack of branes along an edge, as shown in the right of figure 7.16.

Gluing two topological vertices with branes and anti branes inserted gives the resolved conifold geometry as shown in the right of Fig. (7.138). Note that the inner edge describes a sphere with Kahler modulus  $t'$ , which can be described by a cycle which expands from a point and then shrinks. The deformed conifold geometry  $T^*S^3$  is given by the left diagram in figure (7.138). The dotted line describes the base  $S^3$ ; this can be understood via the Heegaard splitting in which  $S^3$  is described as two solid torus glued together with an  $S$  transformation. The dotted line captures this geometry as a foliation of 2- tori  $T^2$  which begins with a pinched  $A$  cycle and ends with a pinched  $B$  cycle.

In terms of toric diagrams, the geometric transition is captured precisely by the equality in (7.138), in which the dotted line representing the three-sphere wrapped by a large  $N$  number of branes is replaced by a two sphere with flux  $t' = ig_s N$

$$\begin{array}{c}
 \begin{array}{c}
 \text{(0,1)} \\
 | \\
 \text{---} \text{z=-a} \quad \text{---} \text{z=0} \quad \text{---} \text{(1,0)} \\
 | \\
 \text{---} \text{S}^3 \text{---}
 \end{array}
 =
 \begin{array}{c}
 \text{(0,1)} \\
 | \\
 \text{---} \text{(-1,0)} \quad \text{---} \text{(1,0)} \text{---} \\
 | \quad \text{t}' \\
 \text{---} \text{(0,-1)}
 \end{array}
 . \quad (7.138)
 \end{array}$$

### 7.4.1 Mapping Wilson loops to worldsheets on the deformed conifold

**Worldsheet description at finite  $N$**  We first consider the worldsheet description of  $|\Omega(t)\rangle$  from the point of view of the open string theory on the deformed conifold geometry. This is valid even at finite  $N$ , since Chern-Simons theory is the exact string field theory for strings on the deformed conifold. We start with the case  $t = 0$ . Note that while  $|\Omega(0)\rangle$  is defined on the torus, its wavefunction in the coherent state basis is given by the generating functional (7.72) for Wilson loops on  $S^3$ .

To obtain a worldsheet description of the Wilson loops, we use the Frobenius relation to change to the winding basis.

$$W_{\vec{k}}(U) := \prod_n (\text{tr} U^n)^{k_n} \quad (7.139)$$

In this basis,  $|\Omega\rangle$  is given by

$$|\Omega\rangle = S_{00} \sum_{\vec{k}} \frac{\text{dim}_q(\vec{k})}{z_{\vec{k}}} |\vec{k}\rangle$$

$$\text{dim}_q(\vec{k}) = \frac{1}{S_{00}} \langle W_{\vec{k}} \rangle_{S^3}, \quad (7.140)$$

where

$$\langle \vec{k} | \vec{k}' \rangle = \delta_{\vec{k}, \vec{k}'} z_{\vec{k}}$$

$$z_{\vec{k}} = \prod_j k_j! j^{k_j} \quad (7.141)$$

The combinatorial factor  $z_{\vec{k}}$  reflects the different ways to glue together the Wilson loops in the bra and ket state.

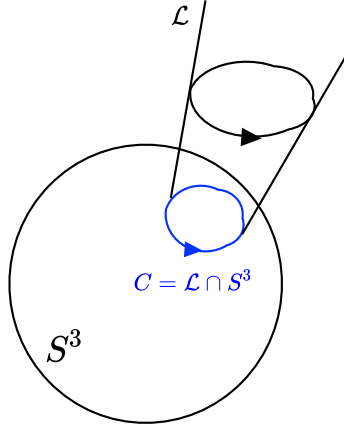


Figure 7.12: The generating functional for Wilson loops can be viewed as the open string amplitude on the deformed conifold with dynamical branes wrapping  $S^3$  and probe branes wrapping  $\mathcal{L}$ . They intersect along a knot  $C$  on  $S^3$ , colored in blue.

The generating functional (7.72) is given by

$$\begin{aligned} Z(V) &= \int \mathcal{D}A e^{iS_{CS}(A) + \sum_n \frac{1}{n} \text{tr} U^n \text{tr} V^n} \\ &= \sum_{\vec{k}} \frac{1}{z_{\vec{k}}} \langle W_{\vec{k}}(U) \rangle_{S^3} \langle V | \vec{k} \rangle, \end{aligned} \quad (7.142)$$

where we applied the identity

$$\exp \left( \sum_{n=1}^{\infty} \frac{1}{n} \text{tr} U^n \text{tr} V^n \right) = 1 + \sum_{\vec{k}} \frac{1}{z_{\vec{k}}} W_{\vec{k}}(U) W_{\vec{k}}(V), \quad (7.143)$$

used  $U$  to denote the holonomy of the dynamical gauge field  $A$ , and  $V$  to denote the holonomy of the source. We used the notation  $\langle V | \vec{k} \rangle$  instead of  $W_{\vec{k}}(V)$  in (7.142) to distinguish the source Wilson loop, which should be viewed as a state in  $\mathcal{H}(T^2)$ .

As we have noted earlier,  $Z(V) = \langle V | \Omega \rangle$  is the coherent state wavefunction for  $|\Omega\rangle$ . When expressed in the winding basis, each term in (7.142) labelled by  $\vec{k}$  has a string theory interpretation on the deformed conifold in terms of open string worldsheets ending on a configuration of intersecting D branes. As shown in Fig.

7.12, this configuration consists of non-compact, probe branes on a Lagrangian submanifold  $\mathcal{L}$  which intersects a large  $N$  number of *dynamical* branes on  $S^3$  along the knot  $C$  [285]. It was shown in [285] that  $Z(V)$  is the spacetime effective field theory obtained by integrating out the strings ending on the intersection of these branes. More precisely, each term in (7.142) labeled by  $\vec{k}$  corresponds to open string worldsheets that end on the intersection of the D branes, with one set of boundaries on dynamical branes coupled to the holonomy  $U$ , and the other set of boundaries on probe branes with holonomy  $V$ . The winding pattern  $\vec{k}$  of the Wilson loop variables is identified with the winding of the open string endpoint around the knot  $C$ . The toric diagram for  $Z(V, t)$  is given in Fig. 7.13.

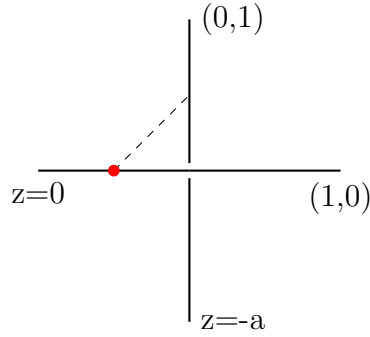


Figure 7.13: Toric diagram for the deformed conifold with probe D-branes on  $\mathcal{L}$  intersecting the  $S^3$ . For the simplicity, we have not specified the frame of the D-brane and the probe brane is depicted as a red dot.

The worldsheets stretched between the two sets of branes with winding numbers  $\vec{k}$  should be viewed as worldsheet instantons, i.e. a classical backgrounds in the string path integral [156]. When quantizing strings around these backgrounds there is a sector of open string worldsheets living on  $S^3$  which ends on the winding boundary of the worldsheet instanton. These can be identified with the ribbon diagrams of the Chern-Simons path integral which produces the expectation value  $\langle W_{\vec{k}}(U) \rangle_{S^3} = S_{00} \dim_q(\vec{k})$ . These ribbon diagrams can be seen explicitly by

expanding  $\dim_q(k)$  in small string coupling

$$g_s = \frac{2\pi}{k + N}. \quad (7.144)$$

This gives

$$\begin{aligned} \dim_q(\vec{k}) &= \prod_j \left( \frac{\sin((jNg_s/2))}{\sin(jg_s/2)} \right)^{k_j} = \prod_j \left( \frac{q^{jN/2} - q^{-jN/2}}{q^{j/2} - q^{-j/2}} \right)^{k_j} \\ &\rightarrow \prod_j \left( N + \frac{j^2 g_s^2}{24} (N - N^3) + \mathcal{O}(g_s^4) \right)^{k_j} \end{aligned} \quad (7.145)$$

At zero string coupling, there are no interactions between the instanton worldsheets and the ribbon diagrams, so we just get a factor of  $N$  per boundary due to the Chan Paton factors running in a loop. However turning on the string coupling introduces corrections where the fatgraphs interact with the winding boundary of the instanton. For example, the first subleading term proportional to  $N - N^3$  comes from the well known “theta” diagrams. Remarkably the all order corrections sum up into a  $q^j$  deformed number:

$$[N]_{q^j} = \frac{q^{jN/2} - q^{-jN/2}}{q^{j/2} - q^{-j/2}} \quad (7.146)$$

This shows explicitly how the open string interactions obey a hidden quantum group symmetry which dictates the final form of the target space amplitude. We have performed a series expansion in  $g_s$  to make this open string interactions explicit, but it is important to observe that the series has to be summed to obtain the quantum group symmetry.

The factor  $\langle V|\vec{k} \rangle$  in (7.142) arises from the opposite boundaries of the worldsheet instantons that end on the probe branes on  $\mathcal{L}$ . Since these branes are non-compact, the worldvolume gauge field is non-dynamical and  $\langle V|\vec{k} \rangle$  comes from the coupling of the worldsheet boundary to the background gauge field. These are identified with the coherent state wavefunctionals of the Chern-Simons theory.



The worldsheet description given above generalizes to the state  $|\Omega(t)\rangle$ . Making  $t$  non zero corresponds to displacing the probe branes away from  $S^3$ , so that the stretched worldsheet instantons now have (complexified) area  $t$ . In terms of the winding basis, the wavefunctional for  $|\Omega(t)\rangle$  is

$$\begin{aligned}\langle V|\Omega(t)\rangle &= Z(V, t) \\ &= S_{00} \sum_{\vec{k}} \dim_q(\vec{k}) e^{-t l(\vec{k})/2} \prod_n \text{tr}(V^n)^{k_n},\end{aligned}\quad (7.147)$$

where the Boltzman factors  $e^{-t l(\vec{k})/2}$  originates from the exponential of the worldsheet action for the stretched worldsheets. Fig. 7.14 shows the toric diagram for  $\langle V|\Omega(t)\rangle$ .

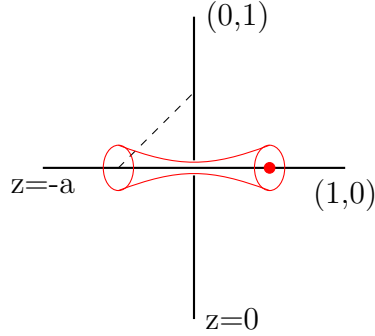


Figure 7.14: Toric diagram for the deformed conifold with  $M$  D-branes on  $\mathcal{M}$ . Note that we have not specified the frame of the probe D-brane on  $\mathcal{M}$ .

**The large  $N$ ,  $t'$  limit and shift of the the worldsheet area** Just as in the representation basis, the large  $N$  and  $t'$  limit of  $\dim_q(k)$  has a divergent factor

$$\dim_q(\vec{k}) \rightarrow q^{N l(\vec{k})/2} (-i)^{\sum_j k_j} d_q(\vec{k}) + \mathcal{O}(q^{-N l(\vec{k})/2}) \quad (7.148)$$

which should be absorbed into a shift of the coupling  $t$

$$e^{-t l(\vec{k})/2} \rightarrow e^{-(t+t') l(\vec{k})/2} \quad (7.149)$$

In terms of the string theory, the shift is interpreted as a modification of the worldsheet area of the stretched instantons to account for a nontrivial  $B$  field flux. Applying this limit, we can write

$$\begin{aligned} \lim_{t' \rightarrow \infty} \lim_{N \rightarrow \infty} \langle V | \Omega(t + t') \rangle &= S_{00} \sum_{\vec{k}} q^{Nl(\vec{k})/2} (-i)^{\sum_j k_j} d_q(\vec{k}) e^{-(t+t')l(\vec{k})/2} \langle V | k_{CS} \rangle \\ &= S_{00} \sum_{\vec{k}} (-i)^{\sum_j k_j} d_q(\vec{k}) e^{-tl(\vec{k})/2} \langle V | k_{CS} \rangle \end{aligned} \quad (7.150)$$

The worldsheet description of each Wilson loop insertion in this wavefunction is given in Fig. 7.15.

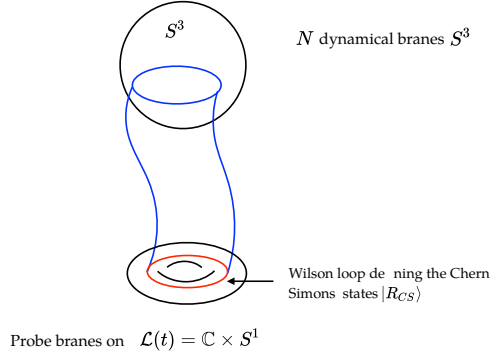


Figure 7.15: Displacing the probe branes away from  $S^3$  gives rise to open string instantons of finite area, stretched between the branes.

## 7.4.2 Applying the geometric transition to the resolved conifold geometry

Having described the large  $N$  limit of the Chern-Simons state  $|\Omega(t)\rangle$  in terms of string theory on the deformed conifold, we now apply the geometric transition to show that it is mapped to the Hartle-Hawking state  $|HH(t)\rangle$ . We have to consider the geometric transition of the brane configuration in Fig. 7.15. This is illustrated

in Fig. 7.17; In the large  $N$  limit,

$$\lim_{N \rightarrow \infty} |\Omega(t + t')\rangle \quad (7.151)$$

the geometric transition replace the branes wrapping a three-sphere into B field flux  $t' = ig_s N$  threading a two sphere of size  $t'$ . The area of the two-sphere is then “sent to infinity” by taking the limit  $t' \rightarrow \infty$ . A precise geometric description of this limit is described in terms of toric diagrams in Fig. 7.16.

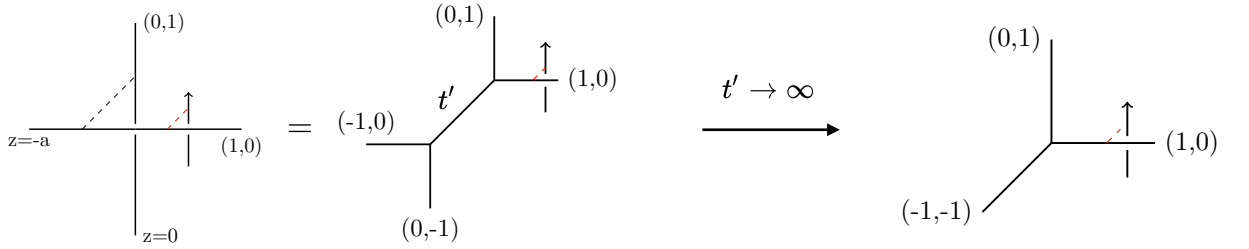


Figure 7.16: The toric diagrams show the result of the geometric transition applied to the deformed reosolved with probe branes displaced from  $S^3$ . Under the transition the  $S^3$  is replaced by a sphere of size  $t'$ . On the right, we show the  $t'$  limit in which that sphere  $t'$  is sent to infinity. This results in “half” the resolved conifold geometry with probe branes inserted, which defines the Hartle-Hawking state. It is important to note that we have specified the framing for the probe D-brane for the HH state, which is determined by the direction of the arrow [4].

As shown in Fig. 7.17, under the geometric transition, the worldsheet boundaries ending on the  $S^3$  closes up. On the other hand, the displaced probe branes  $\mathcal{L}$  on the deformed conifold are mapped to probe branes  $\mathcal{L}'$  on the resolved conifold, which cut through the equator of the base  $S^2$ . These are precisely the probe branes which defines the Hartle-Hawking state on the resolved conifold. We can therefore identify the Chern-Simons wavefunction

$$\langle V | HH_{CS}(t) \rangle = \lim_{t' \rightarrow \infty} \lim_{N \rightarrow \infty} |\Omega(t + t')\rangle = S_{00} \sum_{\vec{k}} (-i)^{\sum_j k_j} d_q(\vec{k}) e^{t l(\vec{k})/2} \prod_n \text{tr}(V^n)^{k_n} \quad (7.152)$$

with the string amplitude that defines the Hartle-Hawking state (neglecting an overall normalization).

Similarly, the overlap  $\langle HH_{CS}(t)^* | HH_{CS}(t) \rangle$  can be identified with the resolved conifold partition function by applying the geometric transition as shown in Fig. 7.18, and then taking the  $t' \rightarrow \infty$  limit. As stated earlier, notice that the geometric transition is being applied to the spheres with Kahler Modulus  $t'$ , rather than the inner sphere with Kahlar modulus  $t$ .

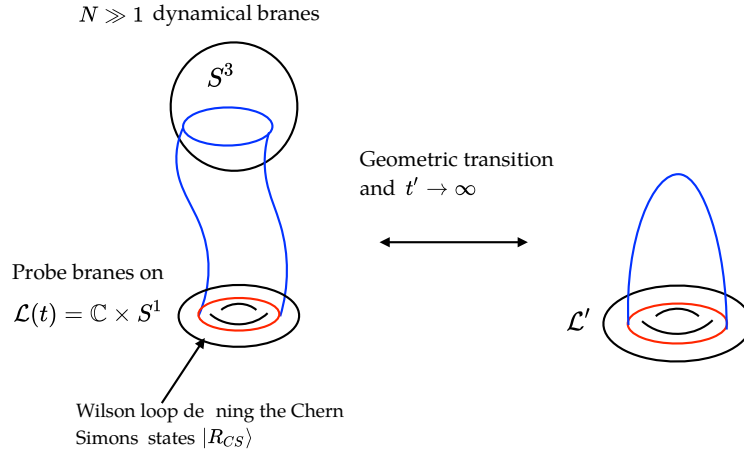


Figure 7.17: The geometric transition, combined with the  $t' \rightarrow \infty$  limit maps the state on the deformed conifold (left figure) to the Hartle-Hawking state on the resolved conifold.

### 7.4.3 Dual description of the entanglement brane

In section 2, we observed that the entanglement brane boundary state  $|D\rangle$  in the closed string theory can be identified with the Hartle-Hawking state  $|HH(t=0)\rangle$  when the Kahler modulus is set to zero. Geometrically, this boundary state describes a “Calabi Yau cap”, which corresponds to a non-local boundary condition that leads to a q-deformation of the edge mode symmetry. Since we have identified the dual description of  $|HH(t=0)\rangle$  on the deformed conifold, we can also identify

the dual of the entanglement brane boundary state; this is given by configuration of *dynamical* D branes wrapping the  $S^3$  and probe branes on a deformed conifold geometry.

**E-brane boundary state and the shrinkable boundary condition on the deformed conifold geometry** We want to give a dual thermal description of the E brane boundary state  $|D\rangle$  in terms of a shrinkable boundary condition on the deformed conifold geometry. This is obtained essentially by running the duality transformation described in the previous section backwards. We begin with a closed string channel interpretation of two stacks of E branes on the resolved conifold geometry:

$$\begin{aligned} Z_{\text{resolved}}(t) &= \langle D^* | e^{-H_{\text{closed}}} | D \rangle \\ &= \langle HH^*(t=0) | e^{-H_{\text{closed}}} | HH(t=0) \rangle \\ H_{\text{closed}} &= l(R)t \end{aligned} \tag{7.153}$$

This is an amplitude between two E brane boundary states on the resolved conifold. To obtain a dual thermal interpretation, we have to first introduce two  $S^2$ 's with Kahler parameter  $t' = ig_s N$  as shown in the left diagram of Fig. 7.18. For large  $t'$  this effectively introduces a constant factor of  $S_{00}(t')^2$  into  $Z_{\text{resolved}}(t)$ . We then apply a geometric transition to obtain a deformed geometry where the fluxes are replaced by a large  $N$  number of branes wrapping two  $S^3$ 's. In terms of the overlap (7.153), this corresponds to mapping:

$$\begin{aligned} S_{00} |HH(t=0)\rangle &= |HH_{CS}(t=0)\rangle \rightarrow \lim_{N \rightarrow \infty} |\Omega(t')\rangle \\ \langle HH^*(t=0) | S_{00} &= \langle HH_{CS}^*(t=0) | \rightarrow \lim_{N \rightarrow \infty} \langle \Omega(t')^* | \end{aligned} \tag{7.154}$$

while keeping the same string theory Hamiltonian.

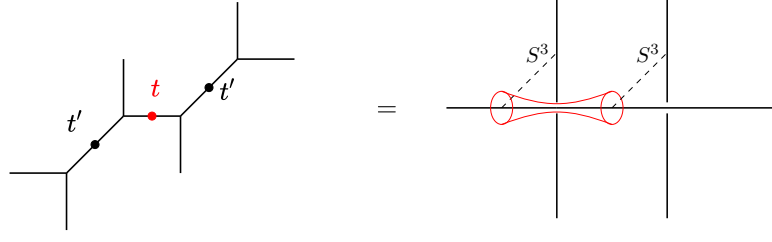


Figure 7.18: The dual thermal interpretation of the resolved conifold partition function is obtained by first introducing two  $S^2$  with Kahler parameter  $t'$  (left figure) and then applying a geometric transition to the deformed geometry on the right with branes on two  $S^3$ . The worldsheets stretched between these branes describe open string loop diagrams .

In the previous section, we developed a string worldsheet description of  $|\Omega(t')\rangle$  in terms of configurations of D branes wrapping  $S^3$  and probe branes on a Lagrangian  $\mathcal{L}$ . The linear functional  $\langle\Omega(t')^*|$  corresponds a similar D brane configuration where we change probe branes on  $\mathcal{L}$  to anti branes. The overlap then corresponds to annihilation of the probe branes, giving the the string theory partition function on a deformed geometry with dynamical branes on two  $S^3$ 's:

$$\begin{aligned}
Z_{\text{deformed}}(t, t') &= \lim_{N \rightarrow \infty} \langle\Omega(t')^*| e^{-H_{\text{closed}}} |\Omega(t')\rangle \\
&= \lim_{N \rightarrow \infty} \sum_{\vec{k}} \frac{1}{z_{\vec{k}}} \langle\Omega(t')^*| e^{-t l(\vec{k})/2} |\vec{k}\rangle \langle\vec{k}| e^{-t l(\vec{k})/2} |\Omega(t')\rangle \\
&= \lim_{N \rightarrow \infty} (S_{00}(t'))^2 \sum_{\vec{k}} \frac{1}{z_{\vec{k}}} \dim_q(\vec{k}) \overline{\dim_q(\vec{k})} e^{-t l(\vec{k})} \quad (7.155)
\end{aligned}$$

Here we have identified the coupling of the closed strings to the entanglement boundary state to be  $\langle\vec{k}|\Omega(t')\rangle = S_{00} \dim_q(\vec{k})$ . As shown in Fig. 7.19 each term labelled by  $\vec{k}$  describes nondegenerate worldsheet instantons stretched between dynamical branes on the two  $S^3$ . In the open string channel, these are viewed as loop diagrams describing a thermal ensemble of open strings. Thus, in the large  $N$  limit, the D-branes on  $S^3$ 's give the shrinkable boundary condition in the dual geometry. Note that the shrinkable boundary condition in the deformed

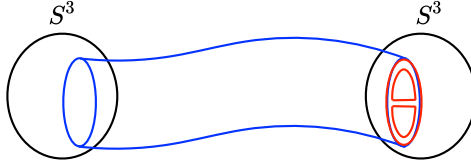


Figure 7.19: Annihilation of the probe branes gives rise to the partition function  $Z_{\text{deformed}}(t, t')$ , which describes world worldsheet instantons stretched between D branes on the two  $S^3$ 's. The quantum dimensions which lead to the q-deformation of the edge modes arise from the ribbon diagrams (red) interacting with the boundary of the instanton worldsheets. We have shown one term in the ribbon diagram expansion corresponding to the “theta” diagram.

geometry is *local* in the sense that D-branes define local boundary conditions on the worldsheet BCFT.

Let's consider in more detail what these worldsheets look like at finite  $N$  in order to understand the worldsheet description of the shrinkable boundary condition. We thus consider the overlap

$$\sum_{\vec{k}} \frac{1}{z_{\vec{k}}} \langle \Omega^*(t') | e^{-t\ell(\vec{k})/2} | \vec{k} \rangle \langle \vec{k} | e^{-t\ell(\vec{k})/2} | \Omega(t') \rangle = (S_{00})^2 \sum_{\vec{k}} \frac{1}{z_{\vec{k}}} \dim_q(\vec{k}) \overline{\dim_q(\vec{k})} e^{-t\ell(\vec{k})}, \quad (7.156)$$

where the quantum dimensions should be viewed as a function of the open string parameters:

$$\dim_q(\vec{k}) = \dim_q(\vec{k})(N, g_s) \quad (7.157)$$

As we saw in eq (7.145), by expanding  $\dim_q(k)$  in small  $g_s$ , we obtain the ribbon diagrams of the worldvolume Chern-Simons theory on the D branes which arise from the quantization of the open strings in the background of the instantons. Thus, the thermal open string partition function describes a modification of the usual one-loop diagrams in which the boundary of the winding worldsheet instantons interact with ribbon diagrams living on the  $D$  branes (see Figure 7.19 ). These

interactions on the branes are crucial to the shrinkability of the D brane boundary condition, since it is the full summation over these ribbon diagrams which leads to a q-deformation of the usual  $N^2$  degeneracy factor for one-loop open strings

$$N^2 \rightarrow ([N]_{q_j})^2. \quad (7.158)$$

Here  $j$  is the winding number of the worldsheet instanton around the thermal circle. This q-deformation is needed to reproduce wavefunctions of the E brane boundary state, and is therefore essential to the shrinkability condition.

As we noted earlier, applying the large  $N$  geometric transition and sending  $t' \rightarrow \infty$  closes up the holes on the open string worldsheets due to the D branes, recovering the closed string worldsheets on the resolved conifold. The sigma model description of this transition is well known. The novelty of this set up is that these D branes are related to the entanglement branes which are inserted to define an entanglement cut in the string theory.

**Replica trick and the thermal partition function for open strings** An open string Hilbert space description of  $Z_{\text{deformed}}(t, t')$  can be given explicitly in term of the unnormalized reduced density matrix of the large  $N$  Chern-Simons theory (7.133):

$$\begin{aligned} Z_{\text{deformed}}(t, t') &= \text{tr}_A \tilde{\rho}_A \\ \tilde{\rho}_A &= \lim_{\epsilon \rightarrow 0} \sum_R (S_{00}(t'))^2 d_q(R)^2 e^{-tl(R)} \frac{e^{\frac{-8\pi\epsilon}{l}(L_0 + \bar{L}_0 - \frac{c}{12})}}{|\chi_R(e^{\frac{-8\pi\epsilon}{l}})|^2} \\ &\sim \sum_R e^{-tl(R)} 1_{R \otimes \bar{R}} \end{aligned} \quad (7.159)$$

In the last expression, have denoted by  $1_{R \otimes \bar{R}}$  a maximally mixed state in the sector  $R \otimes \bar{R}$ , which has a degeneracy factor of

$$\chi_{R\chi\bar{R}} \rightarrow (d_q(R))^2 S_{00}^2(t') e^{\frac{cl}{\epsilon}} \quad (7.160)$$



as  $\epsilon \rightarrow 0$ . Notice also that  $\tilde{\rho}_A$  can be identified with the reduced density of open strings on the deformed conifold, obtained from cutting the stretched open string instantons defining  $|\Omega\rangle$ . This is because we have previously identified the worldsheet instanton description of the wavefunction  $\langle V|\Omega\rangle = Z(V)$ , so we can lift the entanglement cut of Wilson loops in  $|\Omega\rangle$  directly to the entanglement cut of the worldsheet instantons.

**The  $S_{00}^2$  factor** In the Chern-Simons theory description  $Z_{\text{deformed}}$ , the  $S_{00}(t')^2$  factor arises from the measure in the path integral, and  $t'$  is viewed as the 't Hooft parameter. This constant sets the normalization of the partition functions<sup>22</sup>. In the string theory description, this constant has a geometric origin. It comes from the two  $S^3$ 's in the deformed conifold geometry, and two  $S^2$  in the resolved geometry after the transition.

It should be noted that multiplying the partition function or the reduced density matrix by a constant has no physical consequences and does not change the entanglement entropy. We see this explicitly in the replica trick, which computes the ratio

$$\frac{Z(n)}{Z(1)^n} = \frac{\text{tr}_A \tilde{\rho}_A^n}{(\text{tr}_A \tilde{\rho}_A)^n} \quad (7.161)$$

so any rescaling of the un-normalized reduced density matrix  $\tilde{\rho}_A$  would cancel. However, a change in the measure for the path integral does change the entanglement entropy, because the measure is *not* replicated in  $Z(n)$ . This is why we obtain an extra  $\log S_{00}(t')^2$  in the entanglement entropy computed in Chern Simons.

In the string theory we can understand the distinction between an overall constant and a choice of measure geometrically. When we replicate the deformed

---

<sup>22</sup>Interestingly, this choice matches the normalization chosen for the q-deformed Yang Mills theory [9]

geometry in figure 7.6, we do *not* duplicate the  $S^3$ 's. Instead the replica manifold is obtained simply by rescaling the Kahler modulus  $t$  by a factor of  $n$ , which rescales area of the stretched worldsheet instantons by the same factor. This is the string theory analogue of treating  $S_{00}(t')^2$  as a measure rather than an overall constant, and leads to the  $\log S_{00}(t')^2$  term in the entanglement entropy. Notice that not duplicating the  $S^3$ 's also manifestly preserves the Calabi Yau condition, consistent with the constraint imposed on the dual replica manifold for the resolved conifold geometry.

Now, we explain why we added an additional layer to the story by including and subtracting the contributions from  $S^3$ . In the original closed string calculation, we computed the generalized entropy due to cutting non-degenerate worldsheet instantons with finite area. For the Hartle Hawking state corresponding to "half" of the resolved conifold, these instantons wrap half of the minimal volume  $S^2$  and end on probe branes intersecting the equator. However there is no way to cut the deformed conifold  $T^*S^3$  in half and also obtain non-degenerate instantons. To obtain a dual description on a deformed geometry with non-degenerate instantons, we had to first introduce the  $S^3$  to allow strings that stretch between them and then subtract the contribution from ribbon diagrams that do not connect to the instantons. These give precisely the  $S_{00}(t')^2$  we subtracted.

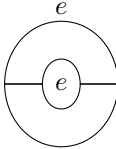
## 7.5 Discussion

In this work we provided a dual gauge theory description of generalized entropy for closed topological strings on the resolved conifold. This was obtained by applying a geometric transition to the brane configurations for Hartle Hawking state, as

shown 7.21. The duality map on the branes has a direct analogue in AdS/CFT, where the anyons are replaced by heavy quarks( see figure 7.20 ) .

We showed that the non-local shrinkable boundary condition in the bulk geometry and the associated quantum group edge mode symmetry are mapped to a local boundary condition in the gauge theory and CFT edge modes that transform under a large  $N$  Kacs-Moody symmetry. In the same spirit, the q-deformed entropy that arises from cutting the bulk string worldsheets is mapped to the un-deformed defect entropy of Wilson loops in the boundary gauge theory.

We can summarize these results by saying that Gopakumar-Vafa duality provides a geometric interpretation of the *measure* on the entanglement brane edge modes as defined by the Drinfeld element via equation (7.55). This is captured most concisely by the toric diagrams in figure 7.18, in which the quantum trace

$$Z_{\text{res}} = \text{tr}(De^{-H}) = \text{tr}(e^{-H}) = \text{tr}(e^{-H}) \quad (7.162)$$


over entanglement branes on the resolved conifold is reproduced by introducing fluxes on the resolved geometry and turning them into branes on a deformed geometry. The open strings instantons stretched between these branes determines a thermal partition function which agrees with the partition sum in (7.162). This provides a relation between the categorical description of entanglement brane edge modes defined in [118] and the worldsheet description of topological D branes of the A model string theory.

Our ultimate motivation for studying entanglement in topological string theory was to understand entanglement in bulk quantum gravity in AdS/CFT. It is thus natural to ask what features of entanglement in topological string theory is expected to generalize to the physical string. The general picture of string entan-

glement which we have developed in this two-part paper (as well as in [122, 123]) suggest that winding modes play a crucial role in determining the entanglement entropy of closed strings. Indeed it is the sum over the winding patterns of the string around the stretched entangling surface that allows it to be closed up.

We have also provided further evidence that open-closed string duality plays an important role in characterising the entanglement structure of closed strings, as originally proposed by Susskind and Uglum. As in [122, 123], we show that this involves the introduction of entanglement branes which provide the entanglement cut for the closed strings. It should be emphasized that while these branes seem to be rigid in the perturbative worldsheet description, we expect them to fluctuate dynamically in the low energy effective gravitational theory just like ordinary D branes. Indeed, it has been shown from the analysis of the symplectic structure of classical gravity that gravitational edge modes contains degrees of freedom associated with the fluctuations of a co-dimension two brane [116]. It would be interesting to see if this can be related to the entanglement branes, similar to the way that string theory D branes are related to black branes in supergravity.

**Entanglement in Topoogical M-theory** Just like in superstring theory where different consistent formulations are expected to be unified by M-theory [345, 196], it was proposed that topological string theories can be reduced from topological M-theory [107]. It would be interesting to see if our formalism can be generalized to calculate entanglement entropy in topological M-theory. Interestingly, the simplest state we can consider on a six-dimensional time slice would be the A model partition function deformed conifold geometry in figure 7.22, viewed as a wavefunction

for topological M-theory in one higher dimension<sup>23</sup>. Figures 7.22 and 7.23 suggest a parallel between the conifold geometry and the thermal field double state associated with the AdS-Schwarzschild geometry<sup>24</sup>. In AdS/CFT, the entanglement between the two boundary CFT's in the TFD state is captured holographically by a spatial wormhole which connects the two boundaries through the eternal black hole geometry [253]. This is an example of the "ER=EPR" [250] slogan, which relates quantum entanglement and geometric connections. For strings propagating on the conifold geometry in figure 7.22, it would seem that "ER=EPR" manifests itself through worldsheets connecting entangled subsystems corresponding to the two  $S^3$ 's.

**Duality web and the B model** Finally, we want to point out that almost all corners of the duality web for the topological string are well understood. This is summarized in Fig. 7.24 and warrants further study. One particularly interesting corner is the proposed UV completion of the A model via q-deformed 2D Yang Mills at large  $N$ . This theory has non perturbative corrections (of order  $e^{-N}$ ) which describes baby universes corresponding to topology changing processes in string theory [327, 9, 106, 7, 260, 275]. It would also be interesting to consider how entanglement entropy behaves under mirror symmetry, which maps the A model to the B model. Although the  $B$  model has the same closed string Hilbert space as the  $A$  model, they have different local properties. The chiral boson theory which describes the  $B$  model has a "pair of pants" amplitude which differs from the one which defines the  $A$  model TQFT. We thus expect that the associated cobordism theory would define a different notion of factorization.

---

<sup>23</sup>Historically, the wavefunction behavior of the topological string partition function [45, 342, 288] was observed first and led to the conjecture of the existence of topological M-theory.

<sup>24</sup>We thank Tom Hartman for the discussion on this observation.

Another motivation for studying the  $B$  model comes from an interesting connection with JT gravity. It was shown in the seminal paper that open topological B models are equivalent to matrix models on Calabi-Yau manifolds that can be written as a fibration over the spectral curve of the matrix model [109]. For example, the JT matrix model [304], whose spectral curve is

$$F(x, y) = y^2 - \sin(\sqrt{x})^2 \tag{7.163}$$

can be realized as topological B-model on Calabi-Yau[304, 275]

$$y^2 - \sin(\sqrt{x})^2 + u^2 + v^2 = 0. \tag{7.164}$$

It would be interesting to compare how local properties of the topological string and JT gravity emerges from the matrix model and see if the  $B$  model offers further insight into JT gravity. In particular, the B model admits a Nekrasov deformation [281, 206, 282] that is related to q-deformations. Perhaps this can be related to q-deformations of JT gravity. <sup>25</sup>.

---

<sup>25</sup>We thank Cumrun Vafa for pointing this possible connection to us.

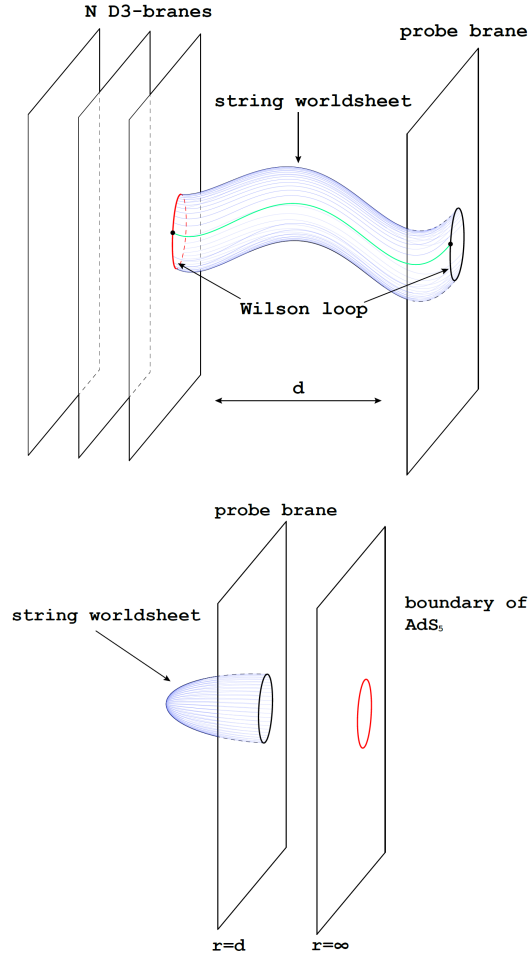


Figure 7.20: Duality between Wilson loop and worldsheet in AdS/CFT. On the left figure, we showed the open string frame, where displacing a probe brane away from a stack of D branes leads to stretched worldsheets ending on Wilson loops. On the right we applied a geometric transition to obtain the closed string  $AdS \times S^5$  geometry where the worldsheet has only one boundary ending on the probe brane. This is a direct analogue of the duality between Wilson loops and worldsheets in topological string theory

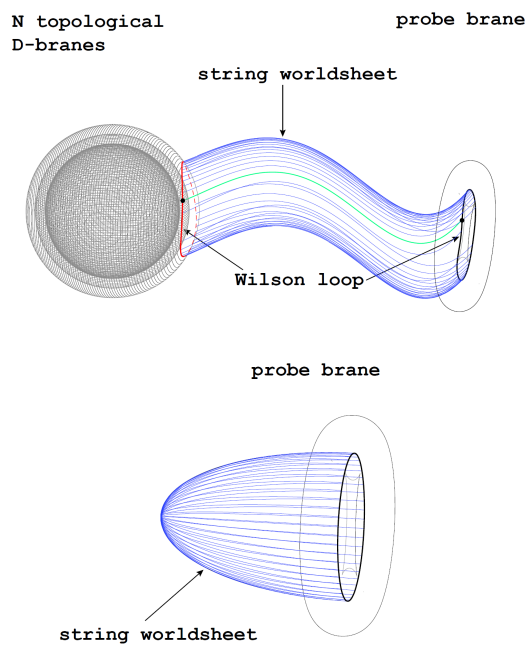


Figure 7.21: Duality between Wilson loop and worldsheet in topological string. There is an  $S^3$  at asymptotic infinity that has been omitted from the picture. [156]

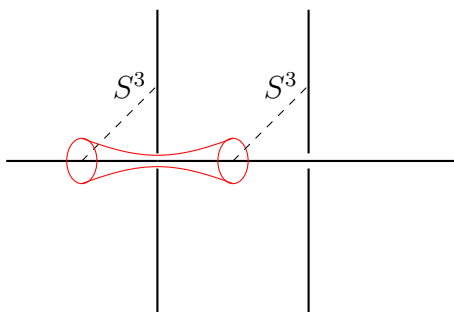


Figure 7.22: Toric diagram for the conifold geometry



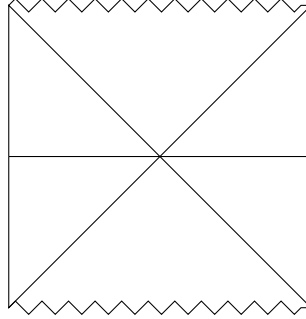


Figure 7.23: Thermo-field double state and the Penrose diagram for the dual AdS-Schwarzschild geometry. The horizontal line in the middle represents the  $t = 0$  time slice.

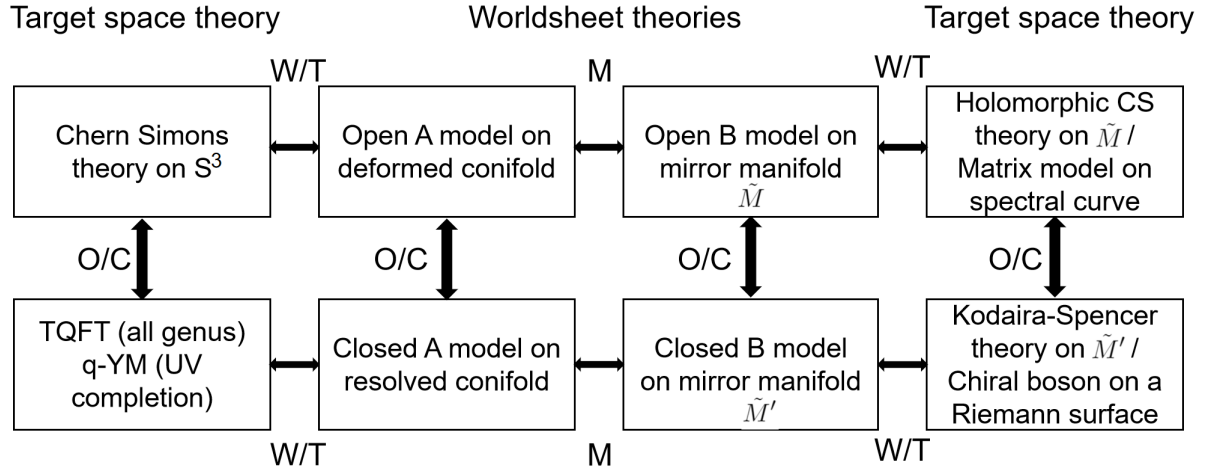


Figure 7.24: Web of dualities for topological string theory. W/T: worldsheet/target space duality. O/C: open/closed duality (large N duality); M : mirror symmetry.

## APPENDIX A

### APPENDIX FOR CHAPTER 2

#### A.1 Conventions for Differential Forms

The orientations of D7-branes, and the self-duality properties of two-form fluxes on them, are crucial in D7-brane monodromy models. We therefore devote this Appendix to laying out our conventions for differential forms, orientation, and the Hodge star operator.

Consider an orientable Riemannian manifold  $X$  of real dimension  $2d$ . Given an orientation on  $X$ , and equipped with the natural inner product  $\langle -, - \rangle$  such that

$$\langle -, - \rangle : \Lambda^p T X^* \times \Lambda^p T X^* \rightarrow \mathbb{C}, \quad (\omega, \nu) \mapsto \langle \omega, \nu \rangle, \quad (\text{A.1})$$

we define the Hodge star map for differential  $p$ -forms  $\omega$  and  $\nu$  as a map

$$\star_{2d} : \Lambda^p T X^* \rightarrow \Lambda^{2d-p} T X^*, \quad (\text{A.2})$$

such that

$$\omega \wedge \star_{2d} \nu = \langle \omega, \nu \rangle \text{Vol}_{2d}, \quad (\text{A.3})$$

where  $\text{Vol}_{2d}$  is the volume form of  $X$  with the given orientation. There is a natural generalization of the Hodge star (A.2) in the case that  $X$  is a complex manifold of complex dimension  $d$ . Taking  $\omega, \nu$  to be elements of  $\Lambda^p T X^* \wedge \Lambda^q \overline{T X}^*$ , the Hodge star map is a linear map

$$\star_d : \Lambda^p T X^* \wedge \Lambda^q \overline{T X}^* \rightarrow \Lambda^{d-q} T X^* \wedge \Lambda^{d-p} \overline{T X}^*, \quad (\text{A.4})$$

such that

$$\omega \wedge \star_d \bar{\nu} = \langle \omega, \bar{\nu} \rangle \text{Vol}_d. \quad (\text{A.5})$$

The definitions (A.2), (A.4) agree on real differential forms and there is no ambiguity regarding the definition of the Levi-Civita symbol.

Under a change of the orientation, the volume form changes sign, and hence so do the eigenvalues of the Hodge star. Taking  $d = 3$ , a fixed three-form flux that is ISD for one orientation of  $X$  is IASD for the opposite orientation. Likewise, taking  $X$  to be a divisor of a threefold ( $d = 2$ ), a fixed two-form flux that is SD in one orientation is ASD for the opposite orientation. Thus, to give a correct description of D-branes in a flux compactification on a threefold  $X$ , we must specify a set of internally consistent conventions for the orientation of  $X$ , the orientation of divisors  $D \subset X$ , and the definitions of  $\star_6$  and  $\star_4$ . We will now work out the relations among these definitions.

We begin with a canonical choice of orientation, and show which other choices are logically possible. For  $X$  a Kähler manifold, we write the Kähler form  $J$  in local coordinates as

$$J = ig_{a\bar{b}}dz^a \wedge d\bar{z}^{\bar{b}}. \quad (\text{A.6})$$

It is natural to define the volume form, and thus the orientation of the manifold, as

$$\text{Vol}_d = \frac{1}{d!} J^d, \quad (\text{A.7})$$

where in local coordinates with diagonalized metric the volume form is written as

$$\text{Vol}_d = i^d \det(g_{a\bar{b}}) dz^1 \wedge d\bar{z}^{\bar{1}} \cdots dz^d \wedge d\bar{z}^{\bar{d}}. \quad (\text{A.8})$$

We then call the orientation constructed above the *canonical orientation*. For example, the canonical orientation of the volume form on a manifold  $X$  with  $d = 3$  is

$$-idz^1 \wedge d\bar{z}^{\bar{1}} \wedge dz^2 \wedge d\bar{z}^{\bar{2}} \wedge dz^3 \wedge d\bar{z}^{\bar{3}}. \quad (\text{A.9})$$

Correspondingly, if  $D \subset X$  is a submanifold of complex dimension two, and is dual to a curve of positive volume, then the orientation on  $D$  is

$$-dz^1 \wedge d\bar{z}^1 \wedge dz^2 \wedge d\bar{z}^2. \quad (\text{A.10})$$

From the definition of the Hodge star map, an SD real two-form  $\mathcal{S}$  and an ASD real two-form  $\mathcal{A}$  satisfy the following relations:

$$\mathcal{S} \wedge \mathcal{S} = \mathcal{S} \wedge \star \mathcal{S} = \langle \mathcal{S}, \mathcal{S} \rangle \text{Vol}, \quad (\text{A.11})$$

$$\mathcal{S} \wedge \mathcal{A} = 0, \quad (\text{A.12})$$

$$\mathcal{A} \wedge \mathcal{A} = -\mathcal{A} \wedge \star \mathcal{A} = -\langle \mathcal{A}, \mathcal{A} \rangle \text{Vol}. \quad (\text{A.13})$$

The Kähler form in a manifold with  $d = 2$  is SD in the canonical orientation, as  $\langle J, J \rangle = 2$ .

Taking the definition of the Hodge star to be (A.4), one finds that a flux of Hodge type  $(2, 1)_{\text{primitive}} + (0, 3)$  is ISD — a relation that is ubiquitous in the literature on flux compactifications — and similarly a flux of Hodge type  $(2, 0) + (0, 2)$  on  $D \subset X$  is SD. These results confirm that our conventions (A.6), (A.7), and (A.4) for orientation and for the Hodge star in Kähler manifolds are compatible with the literature.

For completeness let us nevertheless explore other possible choices of consistent conventions: see Table A.1. We will impose a few requirements, which imply conditions on the numbers  $a, b \in \{\pm 1\}$  appearing in Table A.1. The first requirement is that the integral of the volume form over a positively-oriented manifold must be positive. We will also require that forms of Hodge type  $(2, 1)_{\text{primitive}} + (0, 3)$  are ISD rather than IASD, which implies  $ab = 1$ . A final requirement is that the bulk Chern-Simons coupling  $\propto \frac{1}{i} \int G \wedge \bar{G}$  for forms of type  $(2, 1)_{\text{primitive}} + (0, 3)$  should correspond to positive D3-brane charge whose sign is  $b$ . Given these physics

	+	-
Choice of Hodge star (a)	$\omega \wedge \star \bar{\nu} = \langle \omega, \bar{\nu} \rangle \text{Vol}$	$\star \omega \wedge \bar{\nu} = \langle \omega, \bar{\nu} \rangle \text{Vol}$
Choice of Kähler form (b)	$ig_{z_i \bar{z}_j} dz^i \wedge d\bar{z}^j$	$-ig_{z_i \bar{z}_j} dz^i \wedge d\bar{z}^j$

Table A.1: Possible conventions. The first column denotes the quantity whose definition can be chosen. The variables  $a$  and  $b$  in parentheses equal  $+1$  if the choice corresponds to the second column and  $-1$  if the choice corresponds to the third column. We have taken  $a = b = 1$  throughout this work.

inputs, the following describe self-consistent conventions. First, spacetime-filling Dp-brane actions are of the form

$$- \mu_p \int \text{Im } \tau \text{Vol}_{p+1} + b \mu_p \int C_{p+1}. \quad (\text{A.14})$$

The Bianchi identity for the RR 4-form field is

$$d\tilde{F}_5 = H \wedge F - b \rho^{D3}, \quad (\text{A.15})$$

where  $\rho^{D3}$  is the D3-brane charge density. If  $G$  is ISD, then

$$H \wedge F = - \frac{G \wedge \bar{G}}{2i \text{Im } \tau} = -b \frac{|G|^2 \text{Vol}}{2 \text{Im } \tau}. \quad (\text{A.16})$$

In an ISD background, the following quantity vanishes:

$$\Phi_{-1,b} = h^{-1} - b\alpha, \quad (\text{A.17})$$

where  $h$  is the warp factor and  $C_4 = \alpha dx^0 \wedge dx^1 \wedge dx^2 \wedge dx^3$ . In this paper, we have taken  $a = b = 1$ .

For *any* choice of  $a$  and  $b$ , the orientation on an effective divisor  $D$  is  $\frac{1}{2}J \wedge J$ , and a form of type  $(2,0) + (0,2)$  on  $D$  is self-dual on  $D$ , and so induces D3-brane charge, rather than anti-D3-brane charge, on a D7-brane wrapping  $D$ .

## A.2 Green's Function on a Toroidal Orientifold

In this section, we provide the Green's function on a simple toroidal orientifold. The Green's function on  $T^2$  is very well known — see e.g. [291]. Here we will provide modular invariant Green's functions on orbifolds and orientifolds of  $T^2$  and  $T^6$ .

Finding a Green's function on a compact manifold of real dimension greater than two by the method of images can be challenging, as the sum diverges in general. In order to deal with this divergence, we regulate the Green's function on a torus. Given this regularized Green's function, we extend it to a Green's function on an orbifold and an orientifold.

We begin with a  $T^6$  obtained by identification of the opposite faces of the six-cube of side length  $L$ . We then define a toroidal Green's function to be a function that satisfies

$$\nabla^2 G_{(6)}(x; x') = \delta_{(6)}(x - x') - \frac{1}{\int_{T^6} \text{Vol}_6}. \quad (\text{A.18})$$

The Green's function for the torus is then written as

$$G_{(6)}(x; 0) = - \sum_{n \in \mathbb{Z}^6} (1 - \delta_{n,0}) \frac{e^{2\pi i \vec{n} \cdot \vec{x}/L}}{4\pi^2 n^2 L^4}. \quad (\text{A.19})$$

As we anticipated above, this sum diverges. We follow a prescription given in [306] to regularize the Green's function:

$$G_{(6)}(x; 0) = L^{-4} \int_0^\infty \sum_{n \in \mathbb{Z}^6} (1 - \delta_{n,0}) e^{2\pi i \vec{n} \cdot \vec{x}/L - 4\pi^2 n^2 s} ds \quad (\text{A.20})$$

$$= L^{-4} \int_0^\infty \left( 1 - \prod_{j=1}^6 \sum_{n \in \mathbb{Z}} e^{2\pi i n_j x_j / L - 4\pi^2 n_j^2 s} \right) ds \quad (\text{A.21})$$

$$= L^{-4} \int_0^\infty \left( 1 - \prod_{j=1}^6 \vartheta_3 \left( \frac{x_j}{L} \middle| 4\pi i s \right) \right) ds. \quad (\text{A.22})$$

We used the identity

$$\vartheta_3(\nu|\tau) = \sum_n e^{2\pi i(\nu n + \tau n^2/2)} \quad (\text{A.23})$$

for the last equality.

In order to obtain lower-dimensional toroidal Green's functions, we dimensionally reduce the six-dimensional Green's function (A.20). It is then clear that the Green's function satisfies the identity

$$\int d^d x G_{(6)}(x; x') = G_{(6-d)}(x; x'). \quad (\text{A.24})$$

We choose  $G_{(0)}(x; x') = 0$ . We expect that  $G_{(2)}(z; z')$  would correspond to the well known toroidal Green's function

$$G^{(2)}(z; z') = \frac{1}{2\pi} \log \left| \vartheta_1 \left( \frac{z - z'}{L} \middle| \tau \right) \right| - \frac{(\text{Im}(z - z'))^2}{2L^2 \text{Im} \tau} + C(\tau), \quad (\text{A.25})$$

where  $\tau$  is the complex structure modulus, and  $C(\tau)$  is a function of  $\tau$  [245] that must obey

$$C(\tau + 1) = C(\tau), \quad (\text{A.26})$$

$$C(-1/\tau) = C(\tau) - \frac{1}{4\pi} \log |\tau|, \quad (\text{A.27})$$

in order for the Green's function to be invariant under modular transformations.

These modular transformation properties suggest that  $C(\tau)$  is given by

$$C(\tau) = -\frac{1}{2\pi} \log |\eta(\tau)| + C_0, \quad (\text{A.28})$$

where  $\eta(\tau)$  is the Dedekind eta function and  $C_0$  is undetermined constant. We determined  $C_0 = 0$  numerically by demanding that the integral of the Green's function (A.25) over the torus vanishes.

Given the toroidal Green's function (A.20), it is natural to extend it to the Green's function defined on a toroidal orbifold or a toroidal orientifold. Let us

work with an example for simplicity. For a finite group  $\mathbb{Z}_N$ , let there be a group action  $\theta$  on a complex coordinate  $z$ . Then we denote a Green's function defined on the toroidal orbifold/orientifold  $T^6/\mathbb{Z}_N$  as

$$G_{T^6/\mathbb{Z}_N}(z; z') = \sum_i^N G_{(6)}(z; \theta^i z'). \quad (\text{A.29})$$

Similarly, a Green's function on  $T^2/\mathbb{Z}_N$  is determined as

$$G_{T^2/\mathbb{Z}_N}(z; z') = \sum_i^N G_{(2)}(z; \theta^i z'). \quad (\text{A.30})$$

Here  $z$  and  $z'$  are understood to be in the fundamental domain. We frequently omit the subscript  $T^2/\mathbb{Z}_N$ .

Finally, we will make use of the identity

$$\int d^d x' \nabla G_{(d)}(x; x') \cdot \nabla G_{(d)}(x'; x_0) = - \int d^d x' G_{(d)}(x; x') \nabla^2 G_{(d)}(x'; x_0) \quad (\text{A.31})$$

$$= - G_{(d)}(x; x_0). \quad (\text{A.32})$$



APPENDIX B  
APPENDIX FOR CHAPTER 3

## B.1 Dimensional Reduction

In this appendix we first obtain, in §B.1.1 and §B.1.2, the couplings of D7-brane gauginos that are required for our analysis. Then, in §B.1.3 and §B.1.5 we give details of the superpotential and Kähler potential, respectively, in the four-dimensional theory. Our conventions are as in [292], augmented by  $(2\pi)^2\alpha' = 1$ .

### B.1.1 D7-brane gaugino action

We first compactify type I superstring theory on  $T^2$  and T-dualize to find the action on type IIB D7-branes. As the ten-dimensional  $\mathcal{N} = 1$  supergravity action with a vector multiplet, including the four-gaugino action, is well known, we can determine with precision the D7-brane gaugino action including four-gaugino terms.

One minor complication is that some fields, such as the NS-NS two-form  $B$ , are projected out in type I superstring theory. We will therefore first arrive at a D7-brane action containing all terms that do not involve such fields, but this will not yet be the full D7-brane action. To obtain the proper gaugino-flux coupling, one can then  $SL(2, \mathbb{Z})$  covariantize the gaugino-flux coupling, following [238, 135].

The type I supergravity action in ten-dimensional Einstein frame is [110, 42,

221]

$$S = \frac{1}{2\kappa_{10}^2} \int \sqrt{-G} \left[ \mathcal{R}_{10} - \frac{1}{2} \partial_A \phi \partial^A \phi - \frac{e^\phi}{12} \left( F_{ABC} - \frac{1}{4} e^{-\phi/2} \text{tr } \bar{\chi} \Gamma_{ABC} \chi \right)^2 \right. \\ \left. - \frac{e^{\phi/2}}{16\sqrt{2}\pi^2} \text{tr } F_{AB} F^{AB} - \text{tr } \bar{\chi} \Gamma^A D_A \chi \right], \quad (\text{B.1})$$

where  $\chi$  is a 32-component Majorana-Weyl spinor. Traces here are taken in the vector representation of  $SO(32)$ . In order to simplify T-duality, we first rescale to string frame, using  $G \mapsto e^{-\phi/2} G$ . Compactifying on a  $T^2$  with volume  $1/2t$ , we find

$$S = \frac{1/2t}{2\kappa_{10}^2} \int \sqrt{-G_8} \left[ e^{-2\phi} \mathcal{R}_8 + \dots \right]. \quad (\text{B.2})$$

Next, we T-dualize; since we are in type I string theory, this replaces the  $T^2$  by a  $T^2/\mathbb{Z}_2$  with volume  $t$ , and re-defines  $e^{-2\phi} \mapsto 2t^2 e^{-2\phi}$ , yielding the eight-dimensional action

$$S = \frac{t}{2\kappa_{10}^2} \int \sqrt{-G_8} \left[ e^{-2\phi} \mathcal{R}_8 + \dots \right]. \quad (\text{B.3})$$

Finally, we rescale back to ten-dimensional Einstein frame, using  $G \mapsto e^{\phi/2} G$ .

This procedure yields the new Yang-Mills term

$$\frac{1}{2\kappa_{10}^2} \cdot \frac{1}{8\pi^2} \int \sqrt{-G_8} \left[ -\frac{1}{4} \text{tr } F_{ab} F^{ab} \right]. \quad (\text{B.4})$$

Here  $a, b \in \{0, \dots, 7\}$ , and we will later use  $i, j \in \{8, 9\}$ . The action (B.4) is consistent with the Einstein-frame D7-brane Dirac-Born-Infeld action

$$- \frac{\mu_7}{2} \int \text{tr} \left\{ e^\phi \sqrt{-\det(G + e^{-\phi/2} F/2\pi)} \right\}. \quad (\text{B.5})$$

The factor of  $1/2$  is due to the fact that the gauge group is  $SO(2n)$ ; Higgsing to  $U(n)$  by moving away from an O7-plane eliminates this factor (cf. [292]).

It is now convenient to take the  $T^2$  in the type I frame to have the coordinate range  $[0, 1]^2$ , and to use the same coordinates for the double cover of the type IIB

$T^2/\mathbb{Z}_2$ . For simplicity, we also take the type I torus to be a square torus with string frame metric  $g_{ij} = \frac{1}{2t}\delta_{ij}$ . This means that the string frame metric transforms via  $G_2 \mapsto G_2/(2t)^2$ .

We can now study the fermionic action of the D7-brane in Einstein frame. Since we are interested in studying D7-branes on a holomorphic divisor, we will eventually take  $\text{tr } \bar{\chi}\Gamma_{ABC}\chi$  to be a linear combination of the (pullback of the) holomorphic three-form and its complex conjugate, and we can therefore retain only functions of  $\text{tr } \bar{\chi}\Gamma_{abi}\chi$ . Other contractions do not contribute to the terms of interest.

With that restriction, after T-dualizing we find the string-frame D7-brane gaugino action

$$S_{\text{ferm}} = \mu_7 \int \sqrt{-G_8} \left[ -e^{-\phi} \text{tr } \bar{\chi}\Gamma^a D_a \chi + \frac{1}{8} F_{abi} \text{tr } \bar{\chi}\Gamma^{abi} \chi - \frac{1}{64t} (\text{tr } \bar{\chi}\Gamma_{abi} \chi)^2 \right], \quad (\text{B.6})$$

and the corresponding Einstein-frame D7-brane gaugino action

$$S_{\text{ferm}} = \mu_7 \int \sqrt{-G_8} \left[ -\text{tr } \bar{\chi}\Gamma^a D_a \chi + \frac{1}{8} e^{\phi/2} F_{abi} \text{tr } \bar{\chi}\Gamma^{abi} \chi - \frac{1}{64t_E} (\text{tr } \bar{\chi}\Gamma_{abi} \chi)^2 \right], \quad (\text{B.7})$$

where we have introduced the Einstein frame volume  $t_E := te^{-\phi/2}$ .

We remark in passing that the gaugino quartic term has a prefactor  $1/t$  that depends not just on fields localized to the D7-brane, but also on the volume  $t$  of the space transverse to the D7-branes. One could wonder how such a coupling arises in a local action (we thank the referee for comments on this point). To understand this, we consider the T-dual configuration of a stack of D3-branes transverse to  $T^6/\mathbb{Z}_2$ . The four-dimensional supergravity resulting upon compactification contains a quartic gaugino term whose coefficient is proportional to  $M_{\text{pl}}^{-2}$ , or in ten-dimensional terms is proportional to  $1/\text{Vol}_{T^6/\mathbb{Z}_2}$ . Upon T-dualizing four

times,  $1/\text{Vol}_{T^6/\mathbb{Z}_2}$  is replaced by  $1/t$ . Thus, the D7-brane gaugino quartic term is a Planck-suppressed interaction that is T-dual to a local coupling required by four-dimensional  $\mathcal{N} = 1$  supergravity coupled to vector multiplets.

Leaving implicit henceforth that  $ABC$  is a permutation of  $abi$ , the D7-brane gaugino action can be written in the more symmetric form

$$S_{\text{ferm}} = -\mu_7 \int \sqrt{-G_8} \left[ \text{tr} \bar{\chi} \Gamma^A D_A \chi - \frac{e^{\phi/2}}{24} F_{ABC} \text{tr} \bar{\chi} \Gamma^{ABC} \chi + \frac{1}{192t_E} \left( \text{tr} \bar{\chi} \Gamma^{ABC} \chi \right)^2 \right]. \quad (\text{B.8})$$

In (B.8) we have obtained the part of the action that survived the type I projections. The full D7-brane action is then given by  $SL(2, \mathbb{Z})$ -covariantizing. As doing so would involve studying the transformation properties of the D7-brane fields under  $SL(2, \mathbb{Z})$ , which would take us too far from our main aims, and the full set of two-gaugino terms in the  $\kappa$ -symmetric D7-brane action was found in [238, 135], we simply  $SL(2, \mathbb{Z})$ -covariantize the action by including the missing terms found by [238, 135], leading to

$$S_{\text{ferm}} = \mu_7 \int \sqrt{-G_8} \left[ -\text{tr} \bar{\chi} \Gamma^A D_A \chi - \frac{e^{\phi/2}}{24} \text{tr} \bar{\chi} \Gamma^{ABC} \left( i\tilde{F}_{ABC} \sigma_1 - i e^{-\phi} H_{ABC} \sigma_3 \right) \chi - \frac{1}{192t_E} \left( \text{tr} \bar{\chi} \Gamma_{ABC} \sigma_1 \chi \right)^2 \right], \quad (\text{B.9})$$

where the  $\sigma$  matrix notation will be explained below.

### B.1.2 Reduction of the D7-brane action on a divisor

Equipped with the gaugino action (B.9), we now consider wrapping D7-branes on a divisor  $D$  in an orientifold  $M$  of a Calabi-Yau threefold. We assume that there is a single Kähler modulus  $T$ , with the Kähler form written as

$$J = t\omega, \quad (\text{B.10})$$

and the volume

$$\mathcal{V}e^{6u} = \frac{1}{3!}t^3, \quad (\text{B.11})$$

where we have normalized  $\omega \in H_+^2(M, \mathbb{Z})$  such that  $\int_M \omega \wedge \omega \wedge \omega = 1$ , and we have normalized  $e^{-4A}$  such that  $\int_M e^{-4A} \omega \wedge \omega \wedge \omega = 1$ . We take the volume of  $D$  to be

$$\int_D \sqrt{g} e^{-4A+4u} = \text{Re}(T) = t^2/2, \quad (\text{B.12})$$

while the volume of the curve dual to  $D$  is  $t$ , and corresponds to  $t_E$  in (B.9). The divisor  $D$  is assumed to be rigid, and so the D7-branes will not explore the transverse space, and therefore the geometry of the latter is unimportant. However, for later use we record that the volume of the transverse space is

$$\mathcal{V}_\perp e^{2u} = \frac{1}{3}t. \quad (\text{B.13})$$

We note that wrapping on  $D$  topologically twists the D-brane worldvolume theory, so that scalars become sections of the normal bundle  $N$  of  $D$  and fermions become spinors on the total space of this normal bundle [46]. For notational convenience, we implement the topological twist via a background  $U(1)$  R-symmetry gauge field, rather than by re-defining the local Lorentz group. Since, locally, the Calabi-Yau manifold looks like the total space of the normal bundle, there is no topological obstruction to relating these fermions to the covariantly constant spinor on the Calabi-Yau.

### Internal spinors

As our ansatz for the geometry of the internal space  $M$ , we take  $M$  to have an  $SU(2)$  structure. This can be encoded in terms of two globally-defined orthonormal spinors,  $\eta_+$  and  $\chi_+$ , and an invariant one-form  $v_a dy^a$ , that are related by

$$\chi_+ = \frac{1}{2}v^a \gamma_a \eta_+^*, \quad (\text{B.14})$$

where  $|v|^2 = 2$ . Using  $\chi_+$  and  $\eta_+$  one can construct invariant forms with the components

$$v^a = \eta_+^T \gamma^a \chi_+, \quad J_2^{mn} = i\eta_+^\dagger \gamma^{mn} \eta_+ - i\chi_+^\dagger \gamma^{mn} \chi_+, \quad \Omega_2^{mn} = -i\chi_+^\dagger \gamma^{mn} \eta_+, \quad (\text{B.15})$$

$$J^{mn} = i\eta_+^\dagger \gamma^{mn} \eta_+, \quad \Omega^{mnp} = -i\eta_+^T \gamma^{mnp} \eta_+. \quad (\text{B.16})$$

The invariant forms satisfy

$$J_2 \wedge \Omega_2 = \Omega_2 \wedge \Omega_2 = 0, \quad v_a \Omega_2^{ab} = v_a J_2^{ab} = 0, \quad J_2 \wedge J_2 = \frac{1}{2} \Omega \wedge \bar{\Omega}_2, \quad (\text{B.17})$$

$$J = J_2 + \frac{i}{2} v \wedge \bar{v}, \quad \Omega = \Omega_2 \wedge v. \quad (\text{B.18})$$

We now construct the linear combinations

$$\eta_1 := ie^{A/2+i\vartheta/2} \left( \cos \frac{\varphi}{2} \eta_+ + \sin \frac{\varphi}{2} \chi_+ \right), \quad (\text{B.19})$$

$$\eta_2 := e^{A/2-i\vartheta/2} \left( \cos \frac{\varphi}{2} \eta_+ - \sin \frac{\varphi}{2} \chi_+ \right), \quad (\text{B.20})$$

which are normalized as

$$\eta_1^\dagger \eta_1 = \eta_2^\dagger \eta_2 = e^A. \quad (\text{B.21})$$

The parameters  $\varphi$  and  $\vartheta$  represent the angles between  $\eta_1$  and  $\eta_2$ : from (B.19) and (B.20) one has

$$\eta_2^\dagger \eta_1 = ie^{i\vartheta+A} \cos \varphi. \quad (\text{B.22})$$

The spinors  $\eta_1$  and  $\eta_2$  can be repackaged into a pair of bispinors:

$$\Phi_1 := -8ie^{-A} \eta_1 \otimes \eta_2^\dagger, \quad (\text{B.23})$$

$$\Phi_2 := -8ie^{-A} \eta_1 \otimes \eta_2^T. \quad (\text{B.24})$$

Using the Clifford map,  $\Phi_1$  and  $\Phi_2$  are polyforms: specifically, they can be written in terms of invariant forms as

$$\Phi_1 = e^{i\vartheta} e^{\frac{1}{2} v \wedge \bar{v}} \left[ \cos \varphi \left( 1 - \frac{1}{2} J_2 \wedge J_2 \right) - iJ_2 + \sin \varphi \operatorname{Im} \Omega_2 \right], \quad (\text{B.25})$$

$$\Phi_2 = v \wedge \left[ i \operatorname{Re} \Omega_2 - \cos \varphi \operatorname{Im} \Omega_2 + \sin \varphi \left( 1 - \frac{1}{2} J_2 \wedge J_2 \right) \right]. \quad (\text{B.26})$$

The ansatz we have just described corresponds to a generic  $\text{SU}(2)$  structure. If  $M$  is a Calabi-Yau orientifold then in fact  $e^{i\vartheta} = 1$  and  $\varphi = 0$ . However, once gaugino condensation is incorporated and  $M$  becomes a generalized complex geometry,  $\varphi$  will vary non-trivially along  $M$ ; the  $\text{SU}(2)$  structure is then said to be dynamic.

We now expand to first order in the small quantity  $\langle \lambda \lambda \rangle$ , using the fact that  $\varphi = \mathcal{O}(\langle \lambda \lambda \rangle)$ . We find

$$\Phi_1 = e^{-iJ} \left( 1 + \varphi \operatorname{Im} \Omega_2 \right) + \mathcal{O}(\langle \lambda \lambda \rangle^2), \quad (\text{B.27})$$

$$\Phi_2 = i\Omega + \varphi v \wedge \left( 1 - \frac{1}{2} J_2 \wedge J_2 \right) + \mathcal{O}(\langle \lambda \lambda \rangle^2), \quad (\text{B.28})$$

while the two-form component of  $\mathfrak{t}$  is

$$\mathfrak{t} = +e^{-\phi/2-2A} \varphi \operatorname{Im} \Omega_2 + \mathcal{O}(\langle \lambda \lambda \rangle^2). \quad (\text{B.29})$$

On neglecting the terms of order  $\langle \lambda \lambda \rangle^2$ ,  $\Phi_1$  and  $\Phi_2$  reduce to the  $\beta$ -deformed pure spinors found in [135].

## Ten-dimensional spinor ansatz

Equipped with the six-dimensional spinors  $\eta_1$  and  $\eta_2$ , we can now give our ansatz for the ten-dimensional spinors. The  $SL(2, \mathbb{Z})$ -covariant  $\kappa$ -symmetric D7-brane action is usefully written in a redundant notation, involving two copies of the ten-dimensional fermion [249, 189], which we now adopt. We consider a doublet  $\chi = (\chi_1, \chi_2)$  of 32-component ten-dimensional Majorana-Weyl spinors, and decompose these spinors under  $\text{Spin}(10) \rightarrow \text{Spin}(4) \times \text{Spin}(6)$ . The ten-dimensional gamma matrices decompose as

$$\Gamma^\mu = e^{-A+3u} \gamma^\mu \otimes 1, \quad \Gamma^i = e^{A-u} \gamma^5 \otimes \gamma^i. \quad (\text{B.30})$$

For gamma matrices and spinor manipulations, we use the conventions of [330],

$$\gamma_0 = \begin{pmatrix} 0 & i \\ i & 0 \end{pmatrix}, \gamma_i = \begin{pmatrix} 0 & -i\sigma_i \\ i\sigma_i & 0 \end{pmatrix}, \gamma_5 = \begin{pmatrix} 1 & 0 \\ 0 & -1 \end{pmatrix}, \mathcal{C} = \begin{pmatrix} \epsilon & 0 \\ 0 & -\epsilon \end{pmatrix}, \epsilon = \begin{pmatrix} 0 & 1 \\ -1 & 0 \end{pmatrix}. \quad (\text{B.31})$$

Under this decomposition, a ten-dimensional Weyl spinor decomposes as  $\mathbf{16}_+ \mapsto (\mathbf{2}_+ \otimes \mathbf{4}_+) \oplus (\mathbf{2}_- \otimes \mathbf{4}_-)$ , where subscripts denote chirality. We can thus write the ten-dimensional Majorana-Weyl spinors as

$$\chi_1 = \frac{1}{4\pi} e^{-2A+9u/2} \lambda_D \otimes \eta_1 + c.c. \quad (\text{B.32})$$

and

$$\chi_2 = -\frac{1}{4\pi} e^{-2A+9u/2} \lambda_D \otimes \eta_2 + c.c. \quad (\text{B.33})$$

where *c.c.* refers to charge conjugation, and  $\lambda_D$  is the embedding of a four-dimensional Weyl spinor  $\lambda$  into a Dirac spinor via

$$\lambda_D = \begin{pmatrix} 0 \\ \bar{\lambda}^{\dot{\alpha}} \end{pmatrix}. \quad (\text{B.34})$$

## Decomposition of D7-brane action

We can now expand the D7-brane action (B.9) in terms of the spinors in (B.32) and (B.33). We will henceforth leave traces implicit, writing

$$\text{tr } \chi \chi = \frac{1}{2} \chi^a \chi_a = \frac{1}{2} \chi \chi, \quad (\text{B.35})$$

with the normalization

$$\text{tr } T^a T^b = \frac{1}{2} \delta^{ab} \quad (\text{B.36})$$

for Lie algebra generators. We likewise leave implicit pullbacks to the divisor  $D$ .



The gaugino kinetic term can be decomposed as

$$S_{\text{kin}} = -\mu_7 \int_{X \times D} \sqrt{-G} \text{tr} \bar{\chi} \Gamma^A D_A \chi = \int_{X \times D} \sqrt{-G} \left( \mathcal{L}_{\text{kin},X} + \mathcal{L}_{\text{kin},D} \right), \quad (\text{B.37})$$

with

$$\int_{X \times D} \sqrt{-G} \mathcal{L}_{\text{kin},X} = -2\pi \int_{X \times D} \sqrt{-G} \text{tr} \bar{\chi} \Gamma^\mu D_\mu \chi \quad (\text{B.38})$$

$$= -\frac{i}{4\pi} \int_{X \times D} \sqrt{-g} e^{-4A+4u} \bar{\lambda} \bar{\sigma}^\mu D_\mu \lambda \quad (\text{B.39})$$

$$= -\frac{i}{4\pi} \int_X \sqrt{-g} \text{Re}(T) \bar{\lambda} \bar{\sigma}^\mu D_\mu \lambda, \quad (\text{B.40})$$

and

$$\mathcal{L}_{\text{kin},D} = -2\pi \text{tr} \bar{\chi} \Gamma^a D_a \chi \quad (\text{B.41})$$

$$= \frac{1}{16\pi} \bar{\lambda}_D^c \lambda_D \left( \eta_1^T D_a (e^{-3A} \gamma^a \eta_1) + \eta_2^T D_a (e^{-3A} \gamma^a \eta_2) \right) + c.c. \quad (\text{B.42})$$

$$= -\frac{1}{16\pi} \bar{\lambda} \bar{\lambda} \left( \eta_1^T D_a (e^{-3A} \gamma^a \eta_1) + \eta_2^T D_a (e^{-3A} \gamma^a \eta_2) \right) + c.c. \quad (\text{B.43})$$

$$= -\frac{1}{128\pi} \bar{\lambda} \bar{\lambda} \left( (e^{-A} \eta_1^T \gamma_{123} \eta_2) \eta_2^\dagger \gamma^{123} D_a (e^{-3A} \gamma^a \eta_1) + (\eta_1 \leftrightarrow \eta_2) \right) + c.c. \quad (\text{B.44})$$

$$= \frac{i}{32\pi} e^{-2u+\phi/2} \bar{\lambda} \bar{\lambda} i d_2 \mathbf{t} \cdot \Omega + c.c. \quad (\text{B.45})$$

where we have defined  $d_2 \mathbf{t} = \partial_a \mathbf{t} dz^a + \partial_{\bar{a}} \mathbf{t} d\bar{z}^{\bar{a}}$ . Here  $a \in \{1, 2\}$ , where  $z_1$  and  $z_2$  are complex coordinates along the D7-brane divisor  $D$ , and we stress that  $\mathbf{t}$  in (B.45) must be understood as the pullback onto  $D$  of the form  $\mathbf{t}$  defined in  $M$ .

In (B.45) we have omitted terms that are higher order in  $\langle \lambda \lambda \rangle$ , in particular the terms of order  $\langle \lambda \lambda \rangle^2$  in (B.27), (B.28), and (B.29). We make the same approximation in the computations below.

For the gaugino-flux couplings, we find

$$\mathcal{L}_{F\lambda\lambda} = i \frac{e^{\phi/2-2u-A}}{384\pi} \left( \bar{\lambda}_D \otimes \eta_1^\dagger + \bar{\lambda}_D^c \otimes \eta_1^T \right) \tilde{F}_{ABC} \gamma^{ABC} \gamma^5 (\lambda_D \otimes \eta_2 + \lambda_D^c \otimes \eta_2^*) + (\eta_1 \leftrightarrow \eta_2) \quad (\text{B.46})$$

$$= -i \frac{e^{\phi/2-2u-A}}{384\pi} (\bar{\lambda}_D^c \lambda_D \eta_1^T \gamma^{ABC} \eta_2 + c.c.) \tilde{F}_{ABC} + (\eta_1 \leftrightarrow \eta_2) \quad (\text{B.47})$$

$$= \frac{ie^{\phi/2-2u}}{32\pi} \bar{\lambda} \tilde{F} \cdot \Omega + c.c. \quad (\text{B.48})$$

$$\mathcal{L}_{H\lambda\lambda} = i \frac{e^{-\phi/2-2u-A}}{384\pi} \left( \bar{\lambda}_D \otimes \eta_1^\dagger + \bar{\lambda}_D^c \otimes \eta_1^T \right) H_{ABC} \gamma^{ABC} \gamma^5 (\lambda_D \otimes \eta_1 + \lambda_D^c \otimes \eta_1^*) + (\eta_1 \leftrightarrow \eta_2), \quad (\text{B.49})$$

$$= -i \frac{e^{-\phi/2-2u-A}}{384\pi} (\bar{\lambda}_D^c \lambda_D \eta_1^T \gamma^{ABC} \eta_1 + c.c.) H_{ABC} + (\eta_1 \leftrightarrow \eta_2) \quad (\text{B.50})$$

$$= \frac{e^{-\phi/2-2u}}{32\pi} \bar{\lambda} H \cdot \Omega + c.c. \quad (\text{B.51})$$

We should point out that in (B.48) and (B.51) only the three-form fluxes appear, in contrast to the democratic formulation of generalized complex geometry in which three-forms and seven-forms enter on equal footing. One might then worry that the deformation of the background due to gaugino condensation could introduce corrections to the action of the Hodge star on internal forms, and in turn to the effective action. (We thank the referee for raising this issue.) However, from (B.28) one finds that the three-form component of  $\Phi_2$  is not corrected at order  $\mathcal{O}(\langle\lambda\lambda\rangle)$ . Thus, the Hodge star acting on internal three-forms is not corrected at order  $\mathcal{O}(\langle\lambda\lambda\rangle)$ , and the resulting corrections to the effective action are smaller than order  $\mathcal{O}(\langle\lambda\lambda\rangle^2)$ , and can therefore be neglected in our analysis.

Combining (B.48) and (B.51), we obtain the coupling

$$S_{G\lambda\lambda} = \frac{i}{32\pi} \int_{X \times D} \sqrt{-g} e^{-2u+\phi/2} \bar{\lambda} \lambda G \cdot \Omega + c.c. \quad (\text{B.52})$$

Thus, combining (B.52) and (B.45), the total gaugino-flux coupling is

$$S_{\mathfrak{G}\lambda\lambda} = \frac{i}{32\pi} \int_{X \times D} \sqrt{-g} e^{-2u+\phi/2} \bar{\lambda}\bar{\lambda} \mathfrak{G}^{[2]} \cdot \Omega + c.c. \quad (\text{B.53})$$

The result (B.53) precisely agrees with that of [135] once one accounts for the difference in normalization of the gaugino kinetic term there and here.

Similarly, we find the four-gaugino couplings

$$\mathcal{L}_{\lambda\lambda\lambda\lambda} = -\frac{e^{10u-6A}}{3 \cdot 2^{15}\pi^3 t} \left[ (\bar{\lambda}_D \otimes \eta_1^\dagger + c.c.) \gamma^{abc} (\lambda_D \otimes \eta_2 + c.c.) + (\eta_1 \leftrightarrow \eta_2) \right]^2 \quad (\text{B.54})$$

$$= -\frac{e^{10u-6A}}{3 \cdot 2^{15}\pi^3 t} \left[ \bar{\lambda}_D^c \lambda_D \eta_1^T \gamma^{abc} \eta_2 + c.c. + (\eta_1 \leftrightarrow \eta_2) \right]^2 \quad (\text{B.55})$$

$$= -\frac{e^{10u-4A}}{3 \cdot 2^{15}\pi^3 t} \left[ 2i \bar{\lambda}\bar{\lambda} \Omega^{abc} - 2i \lambda\lambda \bar{\Omega}^{abc} \right]^2 \quad (\text{B.56})$$

$$= -\frac{\nu e^{8u-4A}}{6144\pi^3} \Omega \cdot \bar{\Omega} \lambda\lambda \bar{\lambda}\bar{\lambda}, \quad (\text{B.57})$$

where  $\nu$  was defined below (3.51).

We have thus obtained the Lagrangian density for D7-brane gauginos, up to and including  $|\lambda\lambda|^2$  terms:

$$\mathcal{L}_{\text{gaugino}} = -\frac{i}{4\pi} e^{-4A+4u} \bar{\lambda} \bar{\sigma}^\mu \partial_\mu \lambda + \frac{i}{32\pi} e^{-2u+\phi/2} \mathfrak{G}^{[2]} \cdot \Omega \bar{\lambda}\bar{\lambda} + c.c. - \frac{\nu}{6144\pi^3} e^{8u-4A} \Omega \cdot \bar{\Omega} |\lambda\lambda|^2$$

(B.58)

### B.1.3 Killing spinor equations and the superpotential

The overall goal of this work has been to determine whether the ten-dimensional field configuration that results when gaugino condensation is taken as a source in the ten-dimensional equations of motion ultimately leads to a four-dimensional scalar potential that exactly matches that computed in the four-dimensional supergravity theory of [216]. In order to perform this comparison, we must *translate* the

data of the ten-dimensional fields into four-dimensional expressions. Specifically, we need to express the gaugino-flux coupling (3.47) in terms of the superpotential  $W$ , by relating the generalized flux  $\mathfrak{G}$  to  $W$ . In this section we carefully explain the correspondence between ten-dimensional and four-dimensional data.

## Outline

As a guide through the computations ahead, we first outline our logic. First, building on [240, 37], we write down the ten-dimensional Killing spinor equations whose solutions are supersymmetric configurations. The classical Killing spinor equations are well-known, and the difficulty lies in modifying them to account for the effect of gaugino condensation. To determine the correct modification, we demand the following consistency conditions:

1. The three-form fluxes  $G_{0,3}$ ,  $G_{3,0}$ , and  $G_{1,2}$  obtained from the Killing spinor equations must be compatible with the solution of the Bianchi identities.
2. The IASD three-form flux  $G_{3,0}$  obtained from the Killing spinor equations must vanish in the vacuum configuration: nonvanishing  $G_{3,0}$  would give mass to the gaugino on a probe D3-brane, and so is incompatible with supersymmetry.<sup>1</sup>

We write down a very general modification of the classical Killing spinor equations, involving three a priori independent terms proportional to  $\langle \lambda \lambda \rangle$ , with initially undetermined coefficients, and show that the above conditions uniquely determine the values of all three coefficients. As we explain in detail below, the resulting Killing spinor equations (B.93)-(B.95) are *not* exactly those of [240], which contain

---

<sup>1</sup>We thank Jakob Moritz for suggesting this condition.

only a single term proportional to  $\langle\lambda\lambda\rangle$ . We believe that the consistency conditions above are compulsory, independent of any attempt to argue for or against a ten-dimensional description of the de Sitter vacua of [216], and so we claim that our modified Killing spinor equations (B.93)-(B.95) are the correct ones in this setting.

We then turn to the superpotential  $W_{\text{GCG}}$  (B.96) that has been argued to govern a general type IIB string compactification on a generalized complex geometry [163, 38, 277, 240, 249]. Computing the expectation value  $\langle W_{\text{GCG}} \rangle$  on the solution of the Killing spinor equations, we find that  $\langle W_{\text{GCG}} \rangle$  equals the full superpotential  $W$  when the Killing spinor equations are the corrected ones that we justified above, but that  $\langle W_{\text{GCG}} \rangle \neq W$  when the Killing spinor equations are those given in [240, 37]. Correspondingly, we demonstrate that *using the corrected Killing spinor equations (B.93)-(B.95) we exactly recover the scalar potential of [216] from ten dimensions.*

## Gaugino condensation and the Killing spinor equations

We begin with a rather general form of the Killing spinor equations,

$$d_H \left( e^{(\phi/4-A)\hat{p}} e^{3A-\phi/4} \Phi_2 \right) = 2i\mu e^{(\phi/4-A)\hat{p}} e^{2A-\phi/2} \text{Im } \Phi_1 + 2\alpha \langle S \rangle \delta^{(2)}, \quad (\text{B.59})$$

$$d_H \left( e^{(\phi/4-A)\hat{p}} e^{2A-\phi/2} \text{Im } \Phi_1 \right) = 0, \quad (\text{B.60})$$

$$\begin{aligned} d_H \left( e^{(\phi/4-A)\hat{p}} e^{4A} \text{Re } \Phi_1 \right) &= 3e^{(\phi/4-A)\hat{p}} e^{3A-\phi/4} \text{Re } (\bar{\mu} \Phi_2) + e^{(2A-\phi/2)(3-\hat{p})} e^{4A+\phi} \tilde{F} \\ &\quad + \frac{e^{\phi/2}}{2} \text{Re } (\langle S \rangle \bar{\Omega}) \left( \beta \delta^{(0)} + \frac{\xi}{\mathcal{V}_\perp} \right). \end{aligned} \quad (\text{B.61})$$

We define  $d_H := d - H \wedge$  and  $\tilde{F} = (-1)^{\hat{p}(\hat{p}-1)/2} \star_6 F$ . We have written (B.59)-(B.61) in Einstein frame, and with the notational simplification  $\langle S \rangle \equiv \langle \lambda\lambda \rangle / 32\pi^2$ .

The parameter  $\mu = -ie^{\phi/2} \kappa_4^2 W$  is determined by the full superpotential  $W$ ,<sup>2</sup> and

---

<sup>2</sup>Throughout this work,  $W$  always denotes the full superpotential, as opposed to a single term in the superpotential, such as the flux superpotential term  $W_{\text{flux}}$ .

so is related to the cosmological constant  $\Lambda$  at the supersymmetric minimum by  $e^{\kappa_4^2 K/2} e^{-\phi/2} |\mu| = \sqrt{-\Lambda/3}$ .

In the Killing spinor equations given in [240, 37], the constants  $\beta$  and  $\xi$  are zero, and  $\alpha = 1$ . We will demonstrate below that consistency actually requires  $\alpha = 1$ ,  $\beta = 2$ , and  $\xi = 0$ .<sup>3</sup>

### Fluxes and the Bianchi identities

We now compute various fields from the Killing spinor equations. To obtain the three-form flux, we compute  $\langle (B.61), e^{(\phi/4-A)\hat{p}} e^{3A-\phi/4} \Phi_2 \rangle$ . We first examine the left-hand side of (B.61) and use (B.59) to obtain

$$\left\langle d_H(e^{(\phi/4-A)\hat{p}} e^{4A} \text{Re } \Phi_1), e^{(\phi/4-A)\hat{p}} e^{3A-\phi/4} \Phi_2 \right\rangle = \mu e^\phi \langle \bar{\Phi}_2, \Phi_2 \rangle + i \frac{\alpha e^\phi}{4} \langle S \rangle \langle \bar{\Phi}_2, \Phi_2 \rangle \delta^{(0)}, \quad (B.62)$$

where  $\langle, \rangle$  denotes the Mukai pairing, and we have used the relations  $\langle \text{Re } \Phi_1, \text{Im } \Phi_1 \rangle = i \langle \Phi_1, \bar{\Phi}_1 \rangle / 2 = -i \langle \bar{\Phi}_2, \Phi_2 \rangle / 2$  and  $\langle \text{Re } \Phi_1, \delta^{(2)} \rangle = \frac{i}{8} \langle \bar{\Phi}_2, \Phi_2 \rangle \delta^{(0)}$ .

We have taken the normalization

$$\langle \Phi_1, \bar{\Phi}_1 \rangle = \langle \Phi_2, \bar{\Phi}_2 \rangle = 8iJ^3/3! + \mathcal{O}(\lambda\lambda), \quad (B.63)$$

cf. (B.27) and §B.1.5. Using the right-hand side of (B.61), we find

$$\begin{aligned} \left\langle d_H(e^{(\phi/4-A)\hat{p}} e^{4A} \text{Re } \Phi_1), e^{(\phi/4-A)\hat{p}} e^{3A-\phi/4} \Phi_2 \right\rangle &= \frac{3}{2} \mu e^\phi \langle \bar{\Phi}_2, \Phi_2 \rangle + e^{4A+3\phi/2} \langle \tilde{F}, \Phi_2 \rangle \\ &\quad + \frac{1}{4} e^\phi \langle S \rangle \langle \bar{\Omega}, \Phi_2 \rangle \left( \beta \delta^{(0)} + \frac{\xi}{\mathcal{V}_\perp} \right). \end{aligned} \quad (B.64)$$

---

<sup>3</sup>We could also have added a nonsingular term  $2\gamma \langle S \rangle / \mathcal{V}_\perp$  to the right-hand side of (B.59), but from the analysis below it will be easily seen that in fact  $\gamma$  must vanish. To reduce the complexity of the expressions that follow, we set  $\gamma = 0$  at the outset.

We therefore compute:

$$\tilde{F}|_{(0,3)} = \frac{i}{2}\mu e^{-4A-\phi/2}\overline{\Omega} + \frac{1}{4}e^{-4A-\phi/2}\langle S\rangle\overline{\Omega}\left((\alpha-\beta)\delta^{(0)} - \frac{\xi}{\mathcal{V}_\perp}\right), \quad (\text{B.65})$$

$$\mathfrak{G}|_{(0,3)} = i\left(\tilde{F} + e^{-4A-\phi}d_H(e^{\phi/2+2A}\text{Re}\Phi_1^{(2)})\right)\Big|_{(0,3)} \quad (\text{B.66})$$

$$= \frac{1}{2}e^{-4A-\phi/2}\mu\overline{\Omega} + \frac{i}{4}e^{-4A-\phi/2}\langle S\rangle\overline{\Omega}\left((2\alpha-\beta)\delta^{(0)} - \frac{\xi}{\mathcal{V}_\perp}\right), \quad (\text{B.67})$$

$$\overline{\mathfrak{G}}|_{(0,3)} = -\frac{3}{2}\mu e^{-4A-\phi/2}\overline{\Omega} - \frac{i}{4}\langle S\rangle e^{-4A-\phi/2}\overline{\Omega}\left(\beta\delta^{(0)} + \frac{\xi}{\mathcal{V}_\perp}\right), \quad (\text{B.68})$$

$$id\mathfrak{t} := ie^{-4A-\phi}d(e^{\phi/2+2A}\text{Re}\Phi_1^{(2)}), \quad (\text{B.69})$$

$$id\mathfrak{t}_{(0,3)} = +\frac{i\alpha}{2}e^{-4A-\phi/2}\langle S\rangle\overline{\Omega}\left(\delta^{(0)} - \frac{1}{\mathcal{V}_\perp}\right), \quad (\text{B.70})$$

$$G_{(1,2)} = -id\mathfrak{t}_{(1,2)} = -2i\alpha e^{-4A-\phi/2}\langle S\rangle\partial_z^2 G_{(2)}(z; z_{D7})v \wedge \overline{\Omega}_2, \quad (\text{B.71})$$

$$G_{(0,3)} = \frac{1}{2}e^{-4A-\phi/2}\mu\overline{\Omega} - \frac{i}{4}e^{-4A-\phi/2}\langle S\rangle\left(\beta\delta^{(0)} + \frac{\xi-2\alpha}{\mathcal{V}_\perp}\right), \quad (\text{B.72})$$

$$G_{(3,0)} = -\frac{3}{2}e^{-4A-\phi/2}\bar{\mu}\Omega - \frac{i}{4}e^{-4A-\phi/2}\langle\bar{S}\rangle\Omega\left((2\alpha-\beta)\delta^{(0)} - \frac{\xi+2\alpha}{\mathcal{V}_\perp}\right). \quad (\text{B.73})$$

Next we find the solutions of the Bianchi identities. To simplify the problem, we will assume that  $d\tau = 0$ . The Bianchi identities are

$$dG_+ = dG_-, \quad (\text{B.74})$$

and

$$d\Lambda = dX, \quad (\text{B.75})$$

with

$$\Lambda = e^{4A}\star_6 G_3 - i\alpha G_3, \quad (\text{B.76})$$

and, as we shall show,

$$X = \frac{e^{-\phi/2}}{32\pi^2}\lambda\lambda\overline{\Omega}\delta^{(0)}. \quad (\text{B.77})$$

Let us first establish (B.77). Starting from the action

$$S_{G\lambda\lambda} = \frac{1}{32\pi} \int_{X \times D} \sqrt{-g} e^{\phi/2} \bar{\lambda} \bar{\lambda} G \wedge \Omega + c.c. , \quad (\text{B.78})$$

we compute

$$\frac{\partial \mathcal{L}_{G\lambda\lambda}}{\partial dC_2} = \frac{e^{\phi/2}}{32\pi} d^4x \wedge (\bar{\lambda} \bar{\lambda} \Omega + \lambda \lambda \bar{\Omega}) \delta^{(0)} , \quad (\text{B.79})$$

and

$$\frac{\partial \mathcal{L}_{G\lambda\lambda}}{\partial dB_2} = \frac{e^{\phi/2}}{32\pi} d^4x \wedge (-\tau \bar{\lambda} \bar{\lambda} \Omega - \bar{\tau} \lambda \lambda \bar{\Omega}) \delta^{(0)} , \quad (\text{B.80})$$

so that

$$\tau d \left( \frac{\partial \mathcal{L}_{G\lambda\lambda}}{\partial dC_2} \right) + d \left( \frac{\partial \mathcal{L}_{G\lambda\lambda}}{\partial dB_2} \right) = \frac{ie^{-\phi/2}}{16\pi} d^4x \wedge d(\lambda \lambda \bar{\Omega} \delta^{(0)}) , \quad (\text{B.81})$$

confirming (B.77).

At lowest order in  $\mathcal{O}(\lambda\lambda)$ ,  $\Lambda = 2e^{4A}G_-$ , and so

$$G_- = -\frac{e^{-4A-\phi/2}}{32\pi^2} \lambda \lambda \partial_a \partial_b G_{(2)}(z; z_{D7}) g^{b\bar{b}} \bar{\Omega}_{\bar{b}\bar{c}\bar{d}} , \quad (\text{B.82})$$

and

$$G_+ = \frac{e^{-4A}}{2} X = \frac{e^{-4A-\phi/2}}{64\pi^2} \lambda \lambda \bar{\Omega} \delta^{(0)} , \quad (\text{B.83})$$

so that the *singular* terms in the flux are

$$G_{(1,2)} = iG_-|_{(1,2)} = -i \frac{e^{-4A-\phi/2}}{32\pi^2} \lambda \lambda \partial_a \partial_b G_{(2)}(z; z_{D7}) g^{b\bar{b}} \bar{\Omega}_{\bar{b}\bar{c}\bar{d}} , \quad (\text{B.84})$$

and

$$G_{(0,3)} = -iG_+|_{(0,3)} = -i \frac{e^{-4A-\phi/2}}{64\pi^2} \lambda \lambda \bar{\Omega} \delta^{(0)} , \quad (\text{B.85})$$

whereas

$$G_{(3,0)} = \text{nonsingular} . \quad (\text{B.86})$$



## Consistency conditions

As explained above, we must enforce that the Killing spinor equations are compatible with the Bianchi identities:

1. The three-form flux  $G_{1,2}$  obtained from the Killing spinor equations must be compatible with the solution of the Bianchi identities. Comparing (B.71) and (B.84), this implies that  $\alpha = 1$ .
2. The three-form flux  $G_{0,3}$  obtained from the Killing spinor equations must be compatible with the solution of the Bianchi identities. Comparing (B.72) and (B.85), this implies that  $\beta = 2$ .
3. The three-form flux  $G_{3,0}$  obtained from the Killing spinor equations must be compatible with the solution of the Bianchi identities. Comparing (B.73) and (B.86), this implies that  $\beta = 2\alpha$ .

We conclude that  $\alpha = 1$  and  $\beta = 2$ . The normalization  $\alpha = 1$  agrees with [240, 37]. However,  $\beta = 0$  in [240, 37], so we find that consistency with the Bianchi identities requires that we include a new term in the Killing spinor equations.

The coefficient  $\xi$  has not yet been fixed, but we have another consistency condition to impose:

4. The IASD three-form flux  $G_{3,0}$  obtained from the Killing spinor equations must vanish in a supersymmetric vacuum. Using  $\alpha = 1$  and  $\beta = 2$  in (B.73) gives

$$e^{4A+\phi/2}G_{(3,0)} = -\frac{3}{2}\bar{\mu}\Omega + \frac{i(\xi + 2\alpha)}{4\mathcal{V}_\perp}\langle\bar{S}\rangle\Omega. \quad (\text{B.87})$$

Using the relations  $\mu = -ie^{\phi/2}W/(4\pi\mathcal{V})$ ,  $\langle S \rangle = \frac{1}{2\pi}e^{\kappa_4^2 K/2}\partial_T W_{\text{np}}$ , and  $\mathcal{V} = \mathcal{V}_\perp \text{Re } T$ , we find

$$-4\pi i \mathcal{V}_\perp e^{4A+\phi/2} G_{(3,0)} = \left\{ \left( \frac{2\alpha+\xi}{2} \right) \overline{\partial_T W} + \overline{K_T W} \right\} \Omega. \quad (\text{B.88})$$

The D3-brane gaugino mass is<sup>4</sup>

$$m_{\lambda\lambda} \propto \int e^{4A} G \wedge \overline{\Omega} \delta^{(0)}(z - z_{D3}). \quad (\text{B.89})$$

Comparing (B.88) and (B.89), we see that the D3-brane gaugino mass can vanish in a supersymmetric vacuum, where  $F_T = 0$ , only if  $2\alpha + \xi = 2$ . We found above that  $\alpha = 1$ , so we conclude that  $\xi = 0$ .

In sum, we obtain

$$\alpha = 1, \quad \beta = 2, \quad \text{and} \quad \xi = 0. \quad (\text{B.90})$$

There are two other conditions that we have *not* used, but that serve as further consistency checks of the above system of equations:

5. We will show below in (B.100) that  $\langle W_{\text{GCG}} \rangle = W - \frac{1}{\pi} \text{Re } T \partial_T W_{\text{np}} (2\alpha - \beta - \xi)$ .

Hence, if we were to require  $\langle W_{\text{GCG}} \rangle = W$ , as explained in §B.1.3, then we would obtain the condition  $2\alpha - \beta - \xi = 0$ , which is fulfilled by (B.90).

6. The integrability condition obtained from (B.59) is<sup>5</sup>

$$-6i\mu\mathcal{V}_\perp + 2\alpha\langle S \rangle = 0, \quad (\text{B.91})$$

---

<sup>4</sup>We have omitted a term proportional to  $dt$  in the D3-brane gaugino mass, because  $t$  only varies along the coordinates of the internal manifold, and so  $dt$  has no components parallel to the D3-brane worldvolume.

<sup>5</sup>In the interest of complete generality, one could have added a smeared correction  $2\gamma\langle S \rangle/\mathcal{V}_\perp$  to the right-hand side of (B.59). However, the integrability condition then requires  $\alpha + \gamma = 1$ , whereas the consistency condition from  $G_{(1,2)}$  requires  $\alpha = 1$ , and so  $\gamma = 0$ . We have therefore not included such a term in (B.59).

where we used  $t = 3\mathcal{V}_\perp$ . We use the relation  $\mu = -ie^{\phi/2}W/(4\pi\mathcal{V})$  to rewrite the integrability condition as

$$\alpha\partial_TW_{\text{np}} + \kappa_4^2 K_TW = 0. \quad (\text{B.92})$$

Hence, we obtain  $\alpha = 1$ , which accords with the above.

In summary, we find that the Killing spinor equations that consistently incorporate the effects of gaugino condensation are:

$$d_H\left(e^{(\phi/4-A)\hat{p}}e^{3A-\phi/4}\Phi_2\right) = 2i\mu e^{(\phi/4-A)\hat{p}}e^{2A-\phi/2}\text{Im}\Phi_1 + 2\langle S\rangle\delta^{(2)}, \quad (\text{B.93})$$

$$d_H\left(e^{(\phi/4-A)\hat{p}}e^{2A-\phi/2}\text{Im}\Phi_1\right) = 0, \quad (\text{B.94})$$

$$\begin{aligned} d_H\left(e^{(\phi/4-A)\hat{p}}e^{4A}\text{Re}\Phi_1\right) &= 3e^{(\phi/4-A)\hat{p}}e^{3A-\phi/4}\text{Re}(\bar{\mu}\Phi_2) + e^{(2A-\phi/2)(3-\hat{p})}e^{4A+\phi}\tilde{F} \\ &\quad + e^{\phi/2}\text{Re}(\langle S\rangle\bar{\Omega})\delta^{(0)}. \end{aligned} \quad (\text{B.95})$$

These equations, which differ from those of [240, 37]<sup>6</sup> by the presence of the final term<sup>7</sup> in (B.95), constitute one of the main results of this Appendix.

## The superpotential

In a general type IIB string compactification on a generalized complex geometry, the superpotential is [163, 38, 277, 240, 249]

$$W_{\text{GCG}} = \pi \int \left\langle \Phi_2, \tilde{F} + e^{-4A-\phi}d_H\left(e^{4A+(\phi/4-A)\hat{p}}\text{Re}\Phi_1\right) \right\rangle, \quad (\text{B.96})$$

---

<sup>6</sup>The findings in §6 of [240] were arrived at using (B.61) rather than (B.95), but in many (though not all) respects appear consistent with ours, even though we have used (B.95). The reason for the near-match is that in [240] a nonperturbative superpotential term was *added* to the generalized complex geometry superpotential. According to our analysis, (B.95) should be used, and then no addition is needed, nor indeed would one be consistent.

<sup>7</sup>This term can also be derived from the results of [135] (for related approaches, see [43, 190]). The fluxes we find from (B.95), but not those following from the unmodified (B.61), agree with the fluxes obtained in [135], after accounting for a difference in normalization.

We will now explain how to evaluate (B.96) in our solution.

In the dynamic  $SU(2)$  structure background sourced by gaugino condensation, the one-form and five-form components of  $e^{4A+\phi}\tilde{F} + d_H(e^{-\phi+(\phi/4-A)\hat{p}}\text{Re}\Phi_1)$  and  $\Phi_2$ , and the  $(0,3)$  component of  $e^{4A+\phi}\tilde{F} + d_H(e^{-\phi+(\phi/4-A)\hat{p}}\text{Re}\Phi_1)$ , are  $\mathcal{O}(\langle\lambda\lambda\rangle)$ . However, the three-form component of  $\Phi_2$  is  $\Omega + \mathcal{O}(\langle\lambda\lambda\rangle^2)$ . Hence, collecting the terms in (B.96) up to order  $\mathcal{O}(\langle\lambda\lambda\rangle)$ , we obtain the generalized Gukov-Vafa-Witten flux superpotential,

$$W_{\text{GCG}} = \pi \int \mathfrak{G} \wedge \Omega. \quad (\text{B.97})$$

with

$$\mathfrak{G} := G_3 + i d\mathfrak{t}. \quad (\text{B.98})$$

For the computations of §3.3 — in particular, to arrive at (3.50) — we need to compute  $\mathfrak{G}_{0,3}$ . Let us temporarily work with expressions that follow from the general Killing spinor equations (B.59)-(B.61) rather than from the particular form (B.93)-(B.95) that results from imposing (B.90). One can then write (B.66) as

$$\mathfrak{G}_{0,3} = -\frac{e^{-4A}\overline{\Omega}}{\pi \int_M e^{-4A}\Omega \wedge \overline{\Omega}} W + i \frac{e^{-4A-\phi/2}}{4} \langle S \rangle \overline{\Omega} \left( (2\alpha - \beta)\delta^{(0)} - \frac{\xi}{\mathcal{V}_\perp} \right). \quad (\text{B.99})$$

Thus, the vev of the generalized complex geometry superpotential  $W_{\text{GCG}}$  on the solution of the ten-dimensional Killing spinor equations is given by

$$\langle W_{\text{GCG}} \rangle = W - \frac{1}{\pi} \text{Re} T \partial_T W_{\text{np}} (2\alpha - \beta - \xi), \quad (\text{B.100})$$

so that  $\langle W_{\text{GCG}} \rangle = W$  if and only if  $2\alpha - \beta - \xi = 0$ . On imposing (B.90) we conclude that

$$\langle W_{\text{GCG}} \rangle = W. \quad (\text{B.101})$$

Using (B.98), we can now combine (B.99) and (B.70) to compute  $G_{(0,3)}$ :

$$G_{(0,3)} = \underbrace{-\frac{e^{-4A}\overline{\Omega}}{\pi \int_M e^{-4A}\Omega \wedge \overline{\Omega}} W}_{=:G_W} - \underbrace{\frac{i}{64\pi^2} e^{-4A-\phi/2} \langle \lambda\lambda \rangle \overline{\Omega}}_{=:G_{\lambda\lambda}} \left( \delta^{(0)} - \frac{1}{\mathcal{V}_\perp} \right). \quad (\text{B.102})$$

Our result accords with [279], where it was shown that in the presence of gaugino condensation (and upon converting to our normalizations), one has

$$G_{(0,3)} = -\frac{i}{64\pi^2} e^{-4A-\phi/2} \langle \lambda\lambda \rangle \overline{\Omega} \delta^{(0)} + G_0, \quad (\text{B.103})$$

for some  $G_0$  with  $dG_0 = 0$ . Thus we find agreement between [279] and the singular term in (B.102), and moreover we learn that  $G_0$  is given by the nonsingular terms in (B.102).

#### B.1.4 Dimensional reduction and translation to four-dimensional terms

We will now use the results of §B.1.3 to compute the four-dimensional potential terms that result from dimensional reduction of the gaugino-flux coupling (B.53) and the four-gaugino term (B.57), upon assigning the gaugino bilinear vev (3.34).

In our specific setup,  $\mathbf{t}$  is sourced only by gaugino condensation on  $D$ , and is given by (B.29). Writing  $\text{Re } \Omega_2 = \frac{1}{2} (\Omega_{12} dz^1 \wedge dz^2 + \overline{\Omega}_{\bar{1}\bar{2}} d\bar{z}^{\bar{1}} \wedge d\bar{z}^{\bar{2}})$ , we have

$$d_2 \mathbf{t} = -\frac{1}{2} \partial_a (e^{\phi/2-2A} \varphi \overline{\Omega}_{\bar{1}\bar{2}}) d\bar{z}^{\bar{1}} \wedge d\bar{z}^{\bar{2}} \wedge dz^a - \frac{1}{2} \partial_{\bar{a}} (e^{\phi/2-2A} \varphi \Omega_{12}) dz^1 \wedge dz^2 \wedge d\bar{z}^{\bar{a}}. \quad (\text{B.104})$$

It follows from the index structure of (B.104) that  $d_2 \mathbf{t} \cdot \Omega = 0$ . Thus we arrive at

$$\int_{X \times D} \sqrt{-g} d_2 \mathbf{t} \cdot \Omega = 0. \quad (\text{B.105})$$

Assigning the gaugino bilinear vev (3.34) and using (B.105) and (B.102), the coupling (B.53) dimensionally reduces to

$$S_{\mathfrak{G}\lambda\lambda} = - \int_{X \times M} \sqrt{-g} e^{\phi/2-6u} \frac{i e^{-4A+4u} \Omega \cdot \bar{\Omega}}{\pi \int_M e^{-4A} \Omega \wedge \bar{\Omega}} \frac{\langle \bar{\lambda} \lambda \rangle}{32\pi} W \delta^{(0)} + c.c. + S_{\lambda\lambda}^{\text{sing}}, \quad (\text{B.106})$$

$$= \int_X \sqrt{-g_4} e^{\phi/2-6u+\kappa_4^2 K/2} \frac{\text{Re}(T)}{2\pi\mathcal{V}} \partial_{\bar{T}} \bar{W} W + c.c. + S_{\lambda\lambda}^{\text{sing}}, \quad (\text{B.107})$$

$$= - \kappa_4^2 \int_X \sqrt{-g_4} e^{\kappa_4^2 K} K^{T\bar{T}} \partial_{\bar{T}} \bar{W} K_T W + c.c. + S_{\lambda\lambda}^{\text{sing}}, \quad (\text{B.108})$$

where the singular term

$$S_{\lambda\lambda}^{\text{sing}} = \frac{i}{32\pi} \int \sqrt{-g} e^{\phi/2-2u} G_{\lambda\lambda} \cdot \Omega \bar{\lambda} \bar{\lambda} \delta^{(0)} + c.c., \quad (\text{B.109})$$

with  $G_{\lambda\lambda}$  given in (B.102), is analyzed in Appendix B.3. We used the identity  $\kappa_4^2 K^{T\bar{T}} K_T = -\text{Re}(T)/(2\pi\mathcal{V})$ , which follows from (3.38) and (B.11).

Similarly, assigning the gaugino bilinear vev (3.34), the integral of the four-gaugino term (B.57) dimensionally reduces to

$$S_{\lambda\lambda\lambda\lambda} = - \int_X \int_M \sqrt{-g} e^{\kappa_4^2 K+4u} \frac{e^{-4A+4u} \Omega \cdot \bar{\Omega}}{24\pi\mathcal{V}_{\perp}} \partial_T W_{\text{np}} \partial_{\bar{T}} \bar{W}_{\text{np}} \delta^{(0)} \quad (\text{B.110})$$

$$= - \int_X \sqrt{-g_4} e^{\kappa_4^2 K} \frac{\text{Re}(T)^2}{3\pi\mathcal{V}} \partial_T W \partial_{\bar{T}} \bar{W} \quad (\text{B.111})$$

$$= - \int_X \sqrt{-g_4} e^{\kappa_4^2 K} K^{T\bar{T}} \partial_T W \partial_{\bar{T}} \bar{W}. \quad (\text{B.112})$$

We used the identity  $K^{T\bar{T}} = \text{Re}(T)^2/(3\pi\mathcal{V})$ .

The *modified* Killing spinor equations (B.93)-(B.95) were crucial in the above: if instead of (B.101) one had  $\langle W_{\text{GCG}} \rangle \stackrel{!}{=} W_{\text{flux}}$  then in (B.108) the factor  $K_T W$  would instead read  $K_T W_{\text{flux}}$ , and the scalar potential obtained from ten dimensions would disagree with that obtained in four-dimensional supergravity. However, we reiterate that the form (B.93)-(B.95) of the Killing spinor equations was not derived by requiring that they should lead to (B.101); instead, the logically independent

consistency conditions of §B.1.3 were imposed to derive (B.93)-(B.95), and (B.101) was then a consequence.<sup>8</sup>

### B.1.5 Normalization of the Kähler potential

We temporarily normalize the flux superpotential as

$$W_{\text{flux}} = a \int_M G \wedge \Omega, \quad (\text{B.113})$$

and the Kähler potential as

$$\kappa_4^2 K = -3 \log(T + \bar{T}) - \log \left( i \int_M e^{-4A} \Omega \wedge \bar{\Omega} \right) - \log(-i(\tau - \bar{\tau})) - \log b. \quad (\text{B.114})$$

Given a complex structure, we normalize

$$i \int_M e^{-4A} \Omega \wedge \bar{\Omega} = c. \quad (\text{B.115})$$

We now fix  $a$ ,  $b$ , and  $c$  by dimensional reduction of the ten-dimensional supergravity action.

The first constraint is given by matching the F-term potential for the complex structure moduli and axiodilaton. Matching the gravitino mass does not provide an additional constraint. The potential

$$V_\tau = \frac{1}{2\kappa_{10}^2} \int_M \sqrt{g_6} e^{4A-12u+\phi} |G_{3,0}|^2 \quad (\text{B.116})$$

$$= \frac{1}{2\kappa_{10}^2} \int_M e^{4A-12u+\phi} \left( \frac{\int_M G \wedge \bar{\Omega}}{\int_M e^{-4A} \Omega \wedge \bar{\Omega}} e^{-4A} \Omega \right) \wedge \star_6 \left( -\frac{\int_M \bar{G} \wedge \Omega}{\int_M e^{-4A} \Omega \wedge \bar{\Omega}} e^{-4A} \bar{\Omega} \right) \quad (\text{B.117})$$

$$= \frac{1}{2\kappa_{10}^2} e^{-12u+\phi} \frac{\int_M G \wedge \bar{\Omega} \int_M \bar{G} \wedge \Omega}{i \int_M e^{-4A} \Omega \wedge \bar{\Omega}} \quad (\text{B.118})$$

---

<sup>8</sup>Although (B.101) is essential to our derivation of the correct finite four-dimensional potential (3.61) from a ten-dimensional configuration, the cancellation of divergences exhibited in Appendix B.3 does *not* rely on (B.101).

must match

$$V_\tau = e^{\kappa_4^2 K} K^{\tau\bar{\tau}} D_\tau W D_{\bar{\tau}} \bar{W} = \kappa_4^2 e^{\kappa_4^2 K} a^2 \int_M G \wedge \bar{\Omega} \int_M \bar{G} \wedge \Omega, \quad (\text{B.119})$$

which requires

$$\frac{a^2}{b} = 2^7 \pi^2 \mathcal{V}^3. \quad (\text{B.120})$$

Another constraint is given by matching the F-term potential for D3-brane moduli. Matching the F-term potential for the Kähler modulus does not provide an additional constraint. From (B.200) with the undetermined coefficient  $c$  we have

$$\Phi_- = c \frac{e^{\kappa_4^2 K}}{8\mu_3 \mathcal{V}} K^{a\bar{b}} D_a W D_{\bar{b}} \bar{W}. \quad (\text{B.121})$$

Hence we fix

$$i \int_M e^{-4A} \Omega \wedge \bar{\Omega} = 8\mathcal{V}. \quad (\text{B.122})$$

There remains the freedom to choose  $a$  and  $b$ , corresponding to Kähler invariance. All such choices are physically equivalent; for the sake of simplicity we normalize the superpotential as

$$\pi \int_M G \wedge \Omega, \quad (\text{B.123})$$

and the Kähler potential as

$$\kappa_4^2 K = -3 \log(T + \bar{T}) - \log \left( i \int_M e^{-4A} \Omega \wedge \bar{\Omega} \right) - \log(-i(\tau - \bar{\tau})) + \log(2^7 \mathcal{V}^3). \quad (\text{B.124})$$

## B.2 Spectroscopy of Interactions

In this appendix we show that the interactions of anti-D3-branes with a gaugino condensate that are mediated by Kaluza-Klein excitations of a Klebanov-Strassler



throat can be safely neglected, in the sense defined in §3.4.

### B.2.1 Kaluza-Klein modes on $T^{1,1}$

We will use the conventions of [27] for denoting fields on the conifold and operators in the Klebanov-Witten theory. We use labels  $L \equiv (j_1, j_2, R)$  and  $M \equiv (m_1, m_2)$  for the quantum numbers under the  $SU(2) \times SU(2) \times U(1)_R$  isometries of  $T^{1,1}$ , and write a solution to the Laplace equation on the conifold,  $\nabla^2 f = 0$ , as

$$f(r, \Psi) = \sum_{L, M} f_{LM} \left( \frac{r}{r_{\text{UV}}} \right)^{\Delta_s(L)} Y_{LM}(\Psi), \quad (\text{B.125})$$

with the eigenvalues<sup>9</sup>

$$\Delta_s(L) = -2 + \sqrt{6[j_1(j_1 + 1) + j_2(j_2 + 1) - R^2/8]} + 4. \quad (\text{B.126})$$

The singlet  $j_1 = j_2 = R = 0$  has  $\Delta_s = 0$ , and the next-lowest eigenvalue, for  $j_1 = j_2 = 1/2, R = 1$ , is  $\Delta_s = 3/2$ .

### Perturbations sourced by D3-branes and anti-D3-branes

We now consider in turn the perturbations sourced by D3-branes or anti-D3-branes in the infrared or ultraviolet regions of a Klebanov-Strassler throat. Recall that the Dirac-Born-Infeld + Chern-Simons action of a probe D3-brane is  $S_{D3} = \mu_3 \Phi_-$ , and a D3-brane is a localized source for the scalar  $\Phi_+$ , whereas the Dirac-Born-Infeld + Chern-Simons action of a probe anti-D3-brane is  $S_{\overline{D3}} = \mu_3 \Phi_+$ , and an anti-D3-brane is a localized source for the scalar  $\Phi_-$ . As explained in [26], see also

---

<sup>9</sup>The eigenvalues  $\Delta_s(L)$  were denoted by  $\Delta(L)$  in [26], by  $\Delta_f(L)$  in [27], and by  $\Delta(I_s) - 4$  in [145].

[145], it is useful to define the fields  $\varphi_+ := r^4 \Phi_+^{-1}$  and  $\varphi_- := r^{-4} \Phi_-$ , which have canonical kinetic terms and so have solutions of the usual form

$$\varphi_{\pm} = \alpha r^{-\Delta_{\pm}} + \beta r^{\Delta_{\pm}-4}. \quad (\text{B.127})$$

with  $\alpha, \beta$  independent of  $r$ .

- Anti-D3-brane in the infrared:

The leading perturbation of  $\Phi_-$  is a normalizable profile,

$$\delta(r^{-4} \Phi_-) \sim r^{-8-\Delta_s(L)}. \quad (\text{B.128})$$

The leading (singlet) mode scales as  $r^{-8}$ , and corresponds in the dual field theory to an expectation value for the dimension-eight operator [218, 26, 134]

$$\mathcal{O}_8 = \int d^2\theta d^2\bar{\theta} \text{Tr}[W_+^2 \bar{W}_+^2]. \quad (\text{B.129})$$

Higher multipoles in the linear solution result from operators such as (but not limited to, cf. [26, 27])

$$\mathcal{O}_{8+3k/2} = \int d^2\theta d^2\bar{\theta} \text{Tr}[W_+^2 \bar{W}_+^2 (AB)^k], \quad (\text{B.130})$$

for  $k \in \mathbb{Z}_+$ . The first non-singlet mode is  $\mathcal{O}_{19/2}$ , and scales as  $r^{-19/2}$ . See [26, 27, 145] for extensive analysis of this system.

- D3-brane in the infrared:

The leading perturbation of  $\Phi_+$  is a normalizable profile,

$$\delta(r^4 \Phi_+^{-1}) \sim r^{-\Delta_s(L)}. \quad (\text{B.131})$$

The singlet is a constant, while higher multipoles correspond to expectation values for operators such as (but not limited to, cf. [26])

$$\mathcal{O}_{3k/2} = \text{Tr}[(AB)^k] \Big|_b, \quad (\text{B.132})$$

for  $k \in \mathbb{Z}_+$ , with  $|_b$  denoting the bottom ( $\theta = \bar{\theta} = 0$ ) component of a supermultiplet, as in [27]. The leading non-singlet mode scales as  $r^{-3/2}$  [28, 26, 27, 145], and is dual to an expectation value for

$$\mathcal{O}_{3/2} = \text{Tr}[AB]|_b. \quad (\text{B.133})$$

Higher multipoles can be found in [26, 27, 145].

- D3-brane in the ultraviolet:

The leading perturbation of  $\Phi_+$  is a non-normalizable profile [26]

$$\delta\left(r^4\Phi_+^{-1}\right) \sim r^{\Delta_s(L)+4}. \quad (\text{B.134})$$

The singlet mode scales as  $r^4$ , and is dual to a source for the operator  $\mathcal{O}_8$  in (B.129) whose expectation value arose in the anti-D3-brane solution (B.128).

Higher multipoles are dual to sources for operators such as  $\mathcal{O}_{8+3k/2}$  in (B.130).

The leading non-singlet mode scales as  $r^{11/2}$ , and is dual to  $\mathcal{O}_{19/2}$  [26, 27, 145].

## B.2.2 Effect of anti-D3-branes on gaugino condensate

We would like to examine the long-distance solution sourced by  $p$  anti-D3-branes smeared<sup>10</sup> around the tip of a Klebanov-Strassler throat. To start out, we will linearize in the strength of the anti-D3-brane backreaction, and then discuss nonlinear effects.

---

<sup>10</sup>At different stages of the evolution of a collection of anti-D3-branes interacting with flux, as described in [219], the anti-D3-branes may be localized at a point on the  $S^3$  at the tip, or puffed up into a nontrivial configuration, and in such a case the supergravity equations of motion become difficult partial differential equations. Fortunately (cf. [134]), in any of these cases the leading long-distance solution linearized around  $AdS_5 \times T^{1,1}$  can be obtained from the  $SU(2) \times SU(2)$  invariant part of the linearized solution, i.e. from the linearized solution obtained from considering anti-D3-branes smeared around the  $S^3$ . This latter problem requires solving only ordinary differential equations.

## Coulomb interaction with a D3-brane

The  $SU(2) \times SU(2)$  invariant part of the linearized long-distance solution sourced by  $p$  anti-D3-branes at the tip of a noncompact Klebanov-Strassler throat has been studied in [103, 36, 33, 34, 134, 35]. The leading perturbation of  $\Phi_-$  corresponds to the normalizable profile (B.128), up to logarithmic corrections.

A strong consistency check of this solution comes from considering a D3-brane in the ultraviolet region of the throat. The potential for motion of such a D3-brane can be computed either by treating the D3-brane as a probe in the solution (B.128) sourced by the anti-D3-branes, or by treating the anti-D3-branes as probes in the solution sourced by the backreaction of a D3-brane in a Klebanov-Strassler throat. The former approach amounts to evaluating the action of a probe D3-brane in the solution of [36, 33, 34, 134, 35].

The latter approach, which was used to compute the D3-brane Coulomb potential in [214], is even simpler, because the D3-brane and the Klebanov-Strassler background preserve the same supersymmetry, and so the perturbation due to the D3-brane enjoys harmonic superposition. One finds [26] that the leading perturbation of  $\Phi_+$  sourced by D3-brane in the ultraviolet is the non-normalizable profile (B.134).

The Coulomb potential between an anti-D3-brane in the infrared and a D3-brane in the ultraviolet can be computed either from (B.128) [26, 33] or from (B.134) [214], with exact agreement.

We can understand this match in the language of the dual field theory (see §3.3 of [26]). A D3-brane in the ultraviolet creates a potential by sourcing a

non-normalizable<sup>11</sup> profile  $\delta\Phi_+$ , corresponding to a *source* (in the field theory Lagrangian) for operators such as  $\mathcal{O}_8$ . An anti-D3-brane in the infrared creates a potential by sourcing a normalizable profile  $\delta\Phi_-$ , corresponding to an *expectation value* for operators such as  $\mathcal{O}_8$ . Either way, the mediation occurs by a high-dimension operator, and leads to a very feeble interaction at long distances.

The above arguments give several conceptually different — but precisely compatible — perspectives on a single fact, which is that the Coulomb interaction of a D3-brane with an anti-D3-brane in a warped region is suppressed by eight powers of the warp factor, and so is extremely weak [214].

### D3-brane perturbation to gauge coupling

Thus far, as a first step, we have used a D3-brane in the ultraviolet as a probe of the solution generated by anti-D3-branes in the infrared. Our actual interest is in the effect of anti-D3-branes in the infrared on D7-branes in the ultraviolet.

Now, as a further warm-up, we recall the effect of D3-branes (not yet anti-D3-branes) in the infrared on gaugino condensation on D7-branes in the ultraviolet.<sup>12</sup> The effect of the perturbation (B.131) on a gaugino condensate was computed in [28]. Upon summing over all the chiral and non-chiral operators of the Klebanov-Witten theory [234], and applying highly nontrivial identities to collapse the sum, the result for  $\delta T$  took the form of a logarithm of the embedding function of the D7-branes, expressed in local coordinates [28]. The perturbation (B.131) is thus the effect responsible for the dependence of the gaugino condensate on the D3-brane

---

<sup>11</sup>In the sense of footnote 8 of [26].

<sup>12</sup>Corrections to gaugino condensation on D7-branes due to interactions with distant branes have been extensively studied in the context of D3-brane inflation, both from the open string worldsheet [40, 39] and in supergravity [28]: see [30] for a review.

position [40, 28], which is of central importance in D3-brane inflation [214].

This result was exactly reproduced by an entirely different computation in [27], as reviewed in Appendix B.3 below: the  $G_-$  flux sourced by the gaugino-flux couplings on the D7-branes leads to a solution for  $\Phi_-$ , and a D3-brane probing this solution experiences the potential implied by the perturbation  $\delta T$  computed in [28].

For completeness, we now explain an asymmetry between the effects of D3-branes and of anti-D3-branes. As will be explained in §B.2.2 below, one finds from (B.128) that an anti-D3-brane in the infrared has only extremely small effects on D3-branes or D7-branes in the ultraviolet (except through couplings via the zero-mode  $e^u$ ). In contrast, a D3-brane in the infrared *does* have a detectable effect at long distances. Adding a D3-brane increases the total D3-brane charge of the throat by one unit,  $N \rightarrow N + 1$ , and this change is reflected in the solution by a non-normalizable correction relative to the throat with  $N$  units of flux and no D3-brane.

Simply adding an anti-D3-brane would likewise change the net tadpole and the flux, and so have a detectable effect at long distances. However, this is not the relevant comparison for our purposes. The anti-D3-brane configuration of [219] is a metastable state in a throat with less flux and some wandering D3-branes, but the *same* total tadpole. The anti-D3-branes thus source small normalizable corrections to the solution that is dual to the supersymmetric ground state.

### Anti-D3-brane perturbation to gauge coupling

To compute the effect on the gaugino condensate of the perturbation (B.128) due to anti-D3-branes in the infrared, we follow the same logic used in [28] and reviewed in §B.2.2. We evaluate the D7-brane gauge coupling function (3.33),

$$T = e^{4u} \int_D \sqrt{g_6} e^{-4A} + i \int_D C_4, \quad (\text{B.135})$$

in the perturbed solution, and use (3.36). Examining (B.135), we see that it suffices to know the breathing mode  $e^u$ , as well as the leading perturbations to  $\Phi_{\pm}$  and to the metric  $g_{ab}$  at the location of the D7-brane. Because  $e^u$  is a six-dimensional zero-mode, we will treat it separately: at this stage we seek to check that any influences of the anti-D3-branes on the condensate, *except* via the breathing mode, can be neglected.

Because  $\Phi_- = 0$  in the Klebanov-Strassler background, we write (see Appendix D of [267])

$$\delta \text{Re } T \approx e^{4u} \int_D \sqrt{g_{(0)}} \left( -2(\Phi_+^{(0)})^{-2} (\delta\Phi_+ + \delta\Phi_-) + (\Phi_+^{(0)})^{-1} g_{(0)}^{ab} \delta g_{ab} \right), \quad (\text{B.136})$$

where for a field  $\phi$ , the background profile in the Klebanov-Strassler solution is denoted  $\phi^{(0)}$ .

Our consideration above of a D3-brane probe in the ultraviolet showed that  $\delta\Phi_-$  is mediated by  $\mathcal{O}_8$  (with subleading corrections from operators of even higher dimension) and is negligible at the D7-brane location. Perturbations  $\delta\Phi_+$  (or more usefully,  $\delta\varphi_+$ ) are mediated by operators such as  $\mathcal{O}_{3/2}$ , and can be sizable *if strongly sourced*, e.g. by the presence of a D3-brane. However, in [145] it was shown that the leading profile  $\delta\varphi_+$  that arises in the full nonlinear solution due to an anti-D3-brane scales as  $\delta\varphi_+ \sim r^{-8}$ , just like the profile  $\delta\varphi_-$  in (B.128) that is directly

sourced by the anti-D3-brane: see §5 of [145]. Likewise, in Appendix D of [267] it was shown that the leading non-singlet metric perturbation scales as  $r^{-19/2}$  (see [145, 267] for definitions of the associated tensor harmonics on  $T^{1,1}$ ).

In summary, in the linearized background (B.128) sourced by anti-D3-branes in the infrared, the leading corrections to  $\text{Re } T$  are mediated by operators of dimension  $\Delta \geq 8$ , resulting in extremely small corrections to the D7-brane gaugino condensate when the hierarchy of scales in the Klebanov-Strassler throat is large. Thus, the only influence of the anti-D3-branes on the gaugino condensate that is non-negligible for our purposes occurs via the breathing mode  $e^u$ , and was already included in the four-dimensional analysis of [216]. We have therefore established (3.72).

### B.2.3 Effect of gaugino condensate on anti-D3-branes

For the avoidance of doubt, we now reverse the roles of source and probe relative to §B.2.2, and examine the influence of gaugino condensation in the ultraviolet on anti-D3-branes in the infrared. As in §B.2.2, we treat the breathing mode separately.

#### Leading effect of flux

The anti-D3-brane probe action is  $S_{\overline{D3}} = \mu_3 \Phi_+$ , so we seek the leading perturbations of  $\Phi_+$  in the infrared. Gaugino condensation on D7-branes directly sources flux perturbations  $\delta G_-$  and  $\delta G_+$  via the gaugino-flux coupling (3.45), as shown in [27] and reviewed in §3.3. Expanding in Kaluza-Klein modes on  $T^{1,1}$ , the lowest



mode of  $\delta G_+$  is dual to the operator

$$\mathcal{O}_{5/2} = \int d^2\theta \operatorname{Tr}[AB], \quad (\text{B.137})$$

of dimension  $\Delta = 5/2$  [27]. The coefficient  $c_{5/2}$  of this mode in the ultraviolet is at most of order  $\langle\lambda\lambda\rangle$ , because it is incompatible with the no-scale symmetry of the Klebanov-Strassler background, and so is present only once it is sourced by the gaugino condensate [27, 145]. We stress, however, that  $c_{5/2}$  might well be parametrically smaller than  $\langle\lambda\lambda\rangle$ : the operator  $\mathcal{O}_{5/2}$  is easily forbidden by (approximate) symmetries, corresponding in the bulk to symmetries of the D7-brane configuration.<sup>13</sup> Our estimates of the anti-D3-brane potential will therefore be upper bounds.

The equation of motion for the scalar  $\Phi_+$  is

$$\nabla^2\Phi_+ = \frac{e^{8A}}{\operatorname{Im}\tau}|G_+|^2 + \dots \quad (\text{B.138})$$

where the omitted terms (cf. §3.2) can be neglected for the present purpose. In the Klebanov-Strassler background, the three-form flux has a nonvanishing profile  $G_+^{(0)}$  [233]. With one insertion of the background flux and one insertion of the perturbation  $\delta G_+$ , we have

$$\nabla^2\Phi_+ = \frac{e^{8A}}{\operatorname{Im}\tau} \left( G_+^{(0)} \cdot \delta G_+ + c.c. \right), \quad (\text{B.139})$$

from which one finds

$$\delta\Phi_+ \sim e^{\frac{5}{2}A_{\text{tip}}} \times \langle\lambda\lambda\rangle, \quad (\text{B.140})$$

with  $e^{A_{\text{tip}}}$  the warp factor at the tip. Since

$$\langle\lambda\lambda\rangle \sim \mathcal{O}(e^{2A_{\text{tip}}}), \quad (\text{B.141})$$

---

<sup>13</sup>See e.g. [220] for related work.

we conclude that

$$\delta V_{\overline{D3}} \lesssim \mu_3 e^{\frac{9}{2}A_{\text{tip}}} , \quad (\text{B.142})$$

which is smaller, by a power  $e^{\frac{1}{2}A_{\text{tip}}}$ , than the anti-D3-brane potential (3.64) in the Klebanov-Strassler background. Thus, the influence of the gaugino condensate on the anti-D3-brane, via the linearized perturbation  $\delta G_+$ , is a parametrically small correction.

### Spurion analysis

Thus far we have considered only the linearized perturbation  $\delta G_+$  dual to  $\mathcal{O}_{5/2}$ , leading to the small correction (B.142) to the anti-D3-brane potential. If the D7-brane configuration enjoys no additional symmetries that enforce  $c_{5/2} \ll \langle \lambda \lambda \rangle$ , then (B.142) is indeed the parametrically dominant correction to the anti-D3-brane potential from gaugino condensation [144]. However, establishing this requires extending the treatment of §B.2.3 to incorporate more general perturbations, such as perturbations of the metric, and also requires working at nonlinear order in these perturbations. A complete analysis of this system is carried out in [144]; here we review the strategy and summarize the main findings.

To find the general form of the infrared solution created by a partially-known ultraviolet source, one can perform a *spurion analysis*, in which the parametric size of the ultraviolet coefficient  $c_\Delta$  of a given mode  $\delta\phi_\Delta$  dual to a source for an operator  $\mathcal{O}_\Delta$  is determined by the symmetries preserved by  $\mathcal{O}_\Delta$ .

Specifically, perturbations allowed in a no-scale compactification of the Klebanov-Strassler throat, as in [151], have  $c_\Delta \sim \mathcal{O}(1)$ . Perturbations that are allowed only after (a single) insertion of the gaugino condensate expectation value

$\langle\lambda\lambda\rangle$  have  $c_\Delta \sim \mathcal{O}(\langle\lambda\lambda\rangle)$ , while perturbations that are allowed only after inserting  $|\langle\lambda\lambda\rangle|^2$  have  $c_\Delta \sim \mathcal{O}(\langle\lambda\lambda\rangle^2)$ .

To determine the spurion assignment for a given operator, we examine couplings of the field theory dual to the throat to the D7-brane field theory. Consider, for example,

$$\int d^2\theta \operatorname{Tr}[AB] \operatorname{Tr}[W_\alpha W^\alpha]_{\text{D7}}, \quad (\text{B.143})$$

where<sup>14</sup>

$$\left\langle \operatorname{Tr}[W_\alpha W^\alpha]_{\text{D7}} \right\rangle_b = \frac{1}{2} \langle\lambda\lambda\rangle. \quad (\text{B.144})$$

From (B.143) we find the coupling

$$\delta W = \frac{1}{2} \langle\lambda\lambda\rangle \int d^2\theta \operatorname{Tr}[AB], \quad (\text{B.145})$$

which can be interpreted as a perturbation to the superpotential of the Klebanov-Witten theory, with the exponentially small spurion coefficient  $\langle\lambda\lambda\rangle$ .

Evidently, to carry out such a spurion analysis one needs to know which perturbations of the supergravity fields are allowed in the background, versus requiring either one or two factors of  $\langle\lambda\lambda\rangle$  as spurion coefficients. This information can be read off from an assignment of the operators of the dual field theory to supermultiplets, as in [73, 72]. A systematic treatment along these lines appears in [27, 145, 144].

Examining (B.138), one sees that the leading linearized perturbations to the anti-D3-brane potential are modes of the flux  $G_+$ , the axiodilaton  $\tau$ , and the metric  $g$ . At this stage we need to know, from Kaluza-Klein spectroscopy and from spurion analysis, the dimensions  $\Delta_{\min}$  of the lowest-dimension non-singlet modes of  $G_+$ ,  $\tau$ ,

---

<sup>14</sup>The D7-brane gauge field strength superfield  $W^\alpha|_{\text{D7}}$  should not be confused with  $W_+$  appearing in (B.129), which is the gauge field strength superfield of the D3-brane fields of the Klebanov-Witten theory.

and  $g$ , as well as their spurion coefficients  $c_\Delta$ . For the flux, one finds [144]

$$\Delta_{\min}(G_+) = 5/2 \quad \text{with} \quad c_{5/2} \sim \langle \lambda \lambda \rangle, \quad (\text{B.146})$$

corresponding to  $\mathcal{O}_{5/2}$  in (B.137), as explained above. Another mode of flux gives a slightly smaller contribution:

$$\Delta(G_+) = 3 \quad \text{with} \quad c_3 \sim \langle \lambda \lambda \rangle, \quad (\text{B.147})$$

corresponding to the operator  $\mathcal{O}_{3,+} = \text{Tr}[W_+^2] \big|_b$ . For the dilaton, one finds [144]

$$\Delta_{\min}(\tau) = 11/2 \quad \text{with} \quad c_{11/2} \sim \mathcal{O}(1), \quad (\text{B.148})$$

corresponding to

$$\mathcal{O}_{11/2} = \int d^2\theta \text{Tr}[W_+^2(AB)], \quad (\text{B.149})$$

which is allowed in the background of [151]. (There is also a  $\Delta = 4$  mode of  $\tau$ , but we can absorb this into the background value of the dilaton.) For the metric, one finds the leading contribution [144, 279]

$$\Delta_{\min}(g) = 3 \quad \text{with} \quad c_3 \sim \langle \lambda \lambda \rangle, \quad (\text{B.150})$$

corresponding to

$$\mathcal{O}_{3,-} = \text{Tr}[W_-^2] \big|_b. \quad (\text{B.151})$$

The first subleading correction from a metric mode has

$$\Delta(g) = \sqrt{28} \approx 5.29 \quad \text{with} \quad c_{\sqrt{28}} \sim \mathcal{O}(1), \quad (\text{B.152})$$

corresponding to

$$\mathcal{O}_{\sqrt{28}} = \int d^2\theta d^2\bar{\theta} \text{Tr}[f(A, B, \bar{A}, \bar{B})], \quad (\text{B.153})$$

where  $f$  is a harmonic, but not holomorphic, function of the chiral superfields  $A$  and  $B$ . The perturbation dual to  $\mathcal{O}_{\sqrt{28}}$  is allowed in the background of [151].

Using (B.141), we find from the linearized perturbations (B.146), (B.147), (B.148), (B.150), (B.152), that the anti-D3-brane potential receives corrections of the parametric form

$$\delta V_{\overline{D3}} \lesssim \mu_3 e^{4A_{\text{tip}}} \left( e^{\frac{1}{2}A_{\text{tip}}} + e^{A_{\text{tip}}} + e^{(\sqrt{28}-4)A_{\text{tip}}} + e^{\frac{3}{2}A_{\text{tip}}} + \dots \right). \quad (\text{B.154})$$

For completeness, we remark that upon applying the methods of [145] to study the nonlinear solution, one finds [144] that a specific nonlinear perturbation, corresponding to two insertions of (B.146), gives a correction to the potential of the form

$$\delta V_{\overline{D3}} \lesssim \mu_3 e^{4A_{\text{tip}}} \times e^{A_{\text{tip}}}, \quad (\text{B.155})$$

which can be more important than some of the modes in (B.154), but less important than the linearized flux perturbation (B.146).

Let us summarize. To compute the influence of a gaugino condensate in the ultraviolet on anti-D3-branes in the infrared, one can allow perturbations of all of the supergravity fields, grading these modes via a spurion analysis, and examine the resulting solution for  $\Phi_+$  in the infrared. We have collected here, in (B.154), the leading contributions of the fields that appear in (B.138), at linear order in perturbations. Results for all fields, to all orders, appear in [145, 144], and the only nonlinear correction competitive with any of the terms in (B.154) is the quadratic flux perturbation (B.155).

The final result is that the largest correction to the anti-D3-brane potential mediated by excitations of the throat solution is suppressed by at least a factor  $e^{\frac{1}{2}A_{\text{tip}}} \ll 1$  compared to the anti-D3-brane potential in the background solution, and so can be neglected. This finding is compatible with that of §B.2.2, and constitutes strong evidence for (3.72).

## B.3 Cancellation of Divergences, and the D3-brane Potential

In this appendix we give details of the computation of the four-dimensional curvature  $\mathcal{R}_4$ . First, in §B.3.1 we show that the singular terms contributing to the master equation (3.22) cancel each other, and the finite remainder is the scalar potential (3.61) for the Kähler modulus  $T$ , in exact agreement with the four-dimensional analysis: see (B.157).

Then, in §B.3.2 we repeat this calculation for a compactification containing a D3-brane. In this case the result expected from the four-dimensional theory is the F-term potential (B.196) for the D3-brane moduli and the Kähler modulus. We recover this result as well from ten dimensions in (B.200).

In summary, the ten-dimensional computations of this appendix yield finite answers for the four-dimensional curvature, in compactifications with or without D3-branes. These results precisely agree with the corresponding expressions obtained in the associated four-dimensional effective theories.

### B.3.1 Cancellation of divergences

We begin by adapting the master equation (3.22). The term in (3.22) involving  $\partial_a \Phi_- \partial^a \Phi_-$  is smaller than  $\mathcal{O}(\langle \lambda \lambda \rangle^2)$ , and can be neglected for present purposes. We likewise omit the kinetic terms for the moduli  $u$  and  $\tau$ . Following (3.60), the trace of the stress-energy tensor  $T_{\mu\nu}^{D7}$  of the D7-brane can be written  $T_{\mu\nu}^{D7} g^{\mu\nu} =$

$T_{\mu\nu}^{\lambda\lambda}g^{\mu\nu} + T_{\mu\nu}^{\lambda\lambda\lambda\lambda}g^{\mu\nu} \equiv T^{\lambda\lambda} + T^{\lambda\lambda\lambda\lambda}$ . We thus have

$$\begin{aligned} M_{\text{pl}}^2 \mathcal{R}_4[g] = & - \int_M \sqrt{g_6} e^{-4A} T^{\lambda\lambda} - \int_M \sqrt{g_6} e^{-4A} T^{\lambda\lambda\lambda\lambda} \\ & + 16\pi \int_M \sqrt{g_6} e^{-12u+4A} \rho_{\overline{D3}} - 8\pi e^{-8u} \int_M \sqrt{g_6} \mathcal{R}_6[g], \end{aligned} \quad (\text{B.156})$$

where we have applied our convention that  $(2\pi)^2 \alpha' = 1$ .

Three of the four contributions on the right-hand side of (B.156) include singular terms. In the presence of the localized ISD flux (B.103) sourced by the gaugino condensate, the soft mass term (3.47) has a singular stress-energy that enters  $T_{\mu\nu}^{\lambda\lambda}$ . In the presence of the IASD flux (3.62) sourced by the gaugino condensate, the IASD flux kinetic term, proportional to  $|G_-|^2$ , is likewise singular, and contributes to  $\rho_{\overline{D3}}$  via (B.158). Finally, the internal curvature  $\mathcal{R}_6$  is singular in the presence of singular sources.<sup>15</sup> Our goal is now to show that *these three singularities cancel*, and the finite remainder is the F-term potential (3.61): that is,

$$\boxed{\frac{1}{4} \int_M \sqrt{g_6} \left( -e^{-4A} T^{\lambda\lambda} - e^{-4A} T^{\lambda\lambda\lambda\lambda} + 16\pi e^{4A} \rho_{\overline{D3}} - 8\pi \mathcal{R}_6[g] \right) = V}, \quad (\text{B.157})$$

up to corrections smaller than  $\mathcal{O}(\langle\lambda\lambda\rangle^2)$ .

Let us first set our notation. We will expand in powers of  $\langle\lambda\lambda\rangle$ , with superscripts  $(i)$  denoting quantities of order  $\mathcal{O}(\langle\lambda\lambda\rangle^i)$ . We take  $G_{(0,3)}$  to be of order  $\mathcal{O}(\langle\lambda\lambda\rangle)$ . Capital indices  $M, N$  run from 1 to 6, while indices  $a, b$  run from 1 to 3, and we adopt the convention  $g^{MN} v_M v_N = 2g^{a\bar{b}} v_a \bar{v}_{\bar{b}}$ . To simplify our expressions, we denote  $g_{MN}^{(1)}$  as  $h_{MN}$ ,  $g^{(0)MN} g_{MN}^{(1)}$  as  $h$ ,  $\det(g^{(0)})$  as  $\bar{g}$ ,  $G_{+ab\bar{c}}^{(0)}$  as  $\chi_{ab\bar{c}}$ , and  $G_{-a\bar{b}\bar{c}}^{(1)}$  by  $\eta_{a\bar{b}\bar{c}}$ . We have  $\mathcal{R}_6^{(0)} = 0$ , and we fix the gauge  $\partial^M h_{MN} = 0$ . The D3-brane and anti-D3-brane charge densities are

$$\rho_{D3} = \frac{1}{2 \text{Im } \tau} |G_+|^2 + \rho_{D3}^{\text{loc}}, \quad \rho_{\overline{D3}} = \frac{1}{2 \text{Im } \tau} |G_-|^2 + \rho_{\overline{D3}}^{\text{loc}}, \quad (\text{B.158})$$

---

<sup>15</sup>We thank the referee for useful remarks about these contributions.

where  $\rho_{D3}^{\text{loc}}$  and  $\rho_{\overline{D3}}^{\text{loc}}$  are the charge densities due to localized D3-branes and anti-D3-branes, respectively. For now (in contrast to §B.3.2) we are assuming that there are no localized D3-branes or anti-D3-branes, and so we have  $\rho_{D3} = \frac{1}{4\text{Im}\tau}\chi_{abc}\bar{\chi}^{abc}$  and  $\rho_{\overline{D3}} = \frac{1}{4\text{Im}\tau}\eta_{a\bar{b}\bar{c}}\bar{\eta}^{a\bar{b}\bar{c}}$ . In a local coordinate patch, we fix the gauge  $\Omega_{abc} = \epsilon_{abc}$  and  $\chi_{ab}{}^c = \xi\sqrt{\rho_{D3}}\epsilon_{ab}$ , for  $c \in \{1, 2, 3\}$ , and with  $\xi$  a constant. The equations of motion for this system are well-known, and can be found in, for example, §3.1 of [229].

Discarding total derivatives and retaining terms up to  $\mathcal{O}(\langle\lambda\lambda\rangle^2)$ , we have

$$\int_M \sqrt{g_6} \mathcal{R}_6[g] = -\frac{1}{4} \int_M \sqrt{\bar{g}} \left( \partial_M h \partial^M h - \partial_M h^{NP} \partial^M h_{NP} \right). \quad (\text{B.159})$$

The equation of motion for  $h_{MN}$  is

$$\nabla^2 h_{MN} + \nabla_M \nabla_N h = \frac{e^{4A}}{2\text{Im}\tau} \left( \chi_{(M}{}^{PQ} \bar{\eta}_{N)PQ} + c.c. \right), \quad (\text{B.160})$$

where [27]

$$\eta_{a\bar{b}\bar{c}} = -i \frac{e^{-4A-\phi/2} \lambda \lambda}{32\pi^2} \partial_a \partial^{\bar{d}} G_{(2)}(z; z_{D7}) \bar{\Omega}_{\bar{b}\bar{c}\bar{d}}. \quad (\text{B.161})$$

Because  $\chi_{abc}$  is a (2,1) form and  $\eta_{a\bar{b}\bar{c}}$  is a (1,2) form, (B.160) implies that  $\nabla^2 h = 0$ .

We will thus take  $h = 0$ , so that (B.160) takes the form

$$\nabla^2 h_{ab} = \frac{e^{4A}}{\text{Im}\tau} \chi_{(a}{}^{\bar{c}d} \bar{\eta}_{b)\bar{c}d}, \quad \nabla^2 h_{\bar{a}\bar{b}} = \frac{e^{4A}}{\text{Im}\tau} \bar{\chi}_{(\bar{a}}{}^{cd} \eta_{\bar{b})cd}. \quad (\text{B.162})$$

Solving in terms of the six-dimensional and two-dimensional Green's functions  $G_{(6)}$

and  $G_{(2)}$ , we find

$$h_{ab} = \zeta \int_M d^6 x' G_{(6)}(x; x') \chi_{acd} \partial^c \partial^e G_{(2)}(x'; x_{D7}) \Omega_{be}{}^{\bar{d}} + (a \leftrightarrow b), \quad (\text{B.163})$$

and  $h_{\bar{a}\bar{b}} = \bar{h}_{ab}$ , where

$$\zeta = -i \frac{e^{\phi/2}}{2^6 \pi^2} \langle \lambda \lambda \rangle. \quad (\text{B.164})$$

We thus find that to  $\mathcal{O}(\langle\lambda\lambda\rangle)^2$ ,

$$2 \int_M \sqrt{g_6} \mathcal{R}_6[g] = \int_M \sqrt{\bar{g}} \left( -h^{ab} \nabla^2 h_{ab} \right). \quad (\text{B.165})$$



We now use an identity that is applicable in the local coordinate chart,

$$\partial_z \partial_{\bar{z}} G_{(2)}(z; 0) = \frac{1}{2} g_{z\bar{z}} \left( \delta^{(2)}(z) - \frac{k}{\mathcal{V}_\perp} \right), \quad (\text{B.166})$$

where  $z$  is the complex coordinate for the space transverse to the D7-brane stack.

We can then simplify  $-h^{ab} \nabla^2 h_{ab}$  as follows:

$$-h^{ab} \nabla^2 h_{ab} = -\zeta h^{ab}(x) \left( \chi_{acd} \partial^c \partial^e G_{(2)}(z; z_{D7}) \Omega_{be}^{\bar{d}} + (a \leftrightarrow b) \right) \quad (\text{B.167})$$

$$= \frac{|\zeta|^2}{2} \left( \bar{\chi}^{acd'} \partial_{e'} G_{(2)}(z; z_{D7}) \bar{\Omega}_{d'}^{be'} + (a \leftrightarrow b) \right) \left( \chi_{acd} \partial^e G_{(2)}(z; z_{D7}) \Omega_{be}^{\bar{d}} + (a \leftrightarrow b) \right) \quad (\text{B.168})$$

$$= 2^5 |\zeta|^2 e^{-\phi} \rho_{D3} \partial_e G_{(2)} \partial^e G_{(2)}. \quad (\text{B.169})$$

To arrive at the sign in (B.168) we used  $\partial_{x'} G_{(6)}(x; x') = -\partial_x G_{(6)}(x; x')$ .

We next compute  $\int_M \sqrt{g_6} e^{4A} \rho_{D3}$ :

$$\int_M \sqrt{g} e^{4A} \rho_{D3} = \int_M \sqrt{g} \frac{e^{4A}}{\text{Im } \tau} \frac{1}{4} \eta_{ab\bar{c}} \bar{\eta}^{a\bar{b}c} \quad (\text{B.170})$$

$$= |\zeta|^2 \int_M \sqrt{g} e^{-4A} e^{-\phi} \partial_a \partial^{\bar{d}} G_{(2)} \epsilon_{\bar{b}c\bar{d}} \partial^a \partial^d G_{(2)} \epsilon_{bcd} g^{\bar{b}b} g^{c\bar{c}} \quad (\text{B.171})$$

$$= 2^4 |\zeta|^2 \int_M \sqrt{g} e^{-4A} e^{-\phi} \partial_a \partial_d G_{(2)} \partial^a \partial^d G_{(2)} \quad (\text{B.172})$$

$$= -2^3 |\zeta|^2 \int_M \sqrt{g} \rho_{D3} e^{-\phi} \partial_a G_{(2)} \partial^a G_{(2)}, \quad (\text{B.173})$$

where we used  $2\partial_a \partial^a e^{-4A} = -\rho_{D3}$ , which holds to lowest order.

The final singular contribution comes from the D7-brane action. From (3.54) and (B.108) we have

$$-\frac{1}{4} \int_M \sqrt{g_6} e^{-4A} T^{\lambda\lambda} = \kappa_4^2 \int_X \sqrt{-g_4} e^{\kappa_4^2 K} K^{T\bar{T}} \partial_{\bar{T}} \bar{W} K_T W + c.c. - S_{\lambda\lambda}^{\text{sing}}, \quad (\text{B.174})$$

with

$$-S_{\lambda\lambda}^{\text{sing}} = -2\pi \bar{\zeta} \int_M G_{\lambda\lambda} \cdot \Omega \delta^{(0)} + c.c., \quad (\text{B.175})$$

where  $G_{\lambda\lambda}$  is given in (B.102).

To manipulate  $S_{\lambda\lambda}^{\text{sing}}$ , we derive an identity involving the two-dimensional Green's function. Taking the internal space transverse to the D7-branes to be compact, with volume  $\mathcal{V}_\perp$ , Green's equation takes the form

$$2g^{a\bar{b}}\partial_a\partial_{\bar{b}}G_{(2)}(z;0) = \delta_{(2)}(z) - \frac{1}{\mathcal{V}_\perp}. \quad (\text{B.176})$$

It follows that

$$\int_M e^{-4A} \left( \delta^{(0)} - \frac{1}{\mathcal{V}_\perp} \right)^2 = \left( \int_M e^{-4A} \delta^{(0)^2} \right) - \frac{2e^{4u} \text{Re}(T)}{\mathcal{V}_\perp} + \frac{\mathcal{V}}{\mathcal{V}_\perp^2} \quad (\text{B.177})$$

$$= \left( \int_M e^{-4A} \delta^{(0)^2} \right) - \frac{e^{4u} \text{Re}(T)}{\mathcal{V}_\perp} \quad (\text{B.178})$$

$$= \int_M e^{-4A} \left( \delta^{(0)} - \frac{1}{\mathcal{V}_\perp} \right) \delta^{(0)}, \quad (\text{B.179})$$

which implies that

$$\int_M e^{-4A} \partial_a \partial^a G_{(2)}(z; z_{D7}) \delta^{(0)} = \int_M 2e^{-4A} \partial_a \partial^a G_{(2)}(z; z_{D7}) \partial_b \partial^b G_{(2)}(z; z_{D7}). \quad (\text{B.180})$$

Using (B.102) in (B.109) and using (B.180), we find

$$-S_{\lambda\lambda}^{\text{sing}} = - \int_M 2^7 \pi |\zeta|^2 e^{-4A} e^{-\phi} \partial_a \partial^a G_{(2)}(z; z_{D7}) \partial_b \partial^b G_{(2)}(z; z_{D7}) \quad (\text{B.181})$$

$$= \int_M 2^6 \pi |\zeta|^2 e^{-\phi} \rho_{D3} \partial_a G_{(2)}(z; z_{D7}) \partial^a G_{(2)}(z; z_{D7}). \quad (\text{B.182})$$

Combining (B.169), (B.173), and (B.182), we find that

$$\frac{1}{4} \int_M \sqrt{g_6} \left( -e^{-4A} T^{\lambda\lambda} + 16\pi e^{4A} \rho_{D3} - 8\pi \mathcal{R}_6[g] \right) = V_{\lambda\lambda}, \quad (\text{B.183})$$

where the finite term  $V_{\lambda\lambda}$  was given in (3.56). Including also the finite term resulting from  $T_{\mu\nu}^{\lambda\lambda\lambda\lambda}$ , see (3.58), we arrive at (B.157), completing the proof.

### B.3.2 D3-brane potential from flux

We now turn to the case in which a spacetime-filling D3-brane is present. The potential for motion of a D3-brane in a nonperturbatively-stabilized flux com-

pactification, such as [216], is well understood from the perspective of the four-dimensional effective supergravity theory [214, 28, 241, 29], with the Kähler potential obtained in [102] (see also [261, 83, 262]) and with the nonperturbative superpotential computed in [40, 28]. Showing that this potential is reproduced by the Dirac-Born-Infeld + Chern-Simons action of a probe D3-brane in a candidate ten-dimensional solution sourced by gaugino condensation serves as a quantitative check of the ten-dimensional configuration [240, 27, 135]. An exact match was demonstrated in [27] in the limit that four-dimensional gravity decouples.

In this appendix we compute the potential of such a D3-brane probe. Through a consistent treatment of the Green's functions on the compact space, we extend the match found in [27] to include terms proportional to  $\kappa_4^2$ .

Within this appendix we take the Kähler potential (3.38) to include D3-brane moduli,

$$\kappa_4^2 K = -3 \log(T + \bar{T} - \gamma k) - \log(-i(\tau - \bar{\tau})) - \log\left(i \int_M e^{-4A} \Omega \wedge \bar{\Omega}\right) + \log(2^7 \mathcal{V}^3), \quad (\text{B.184})$$

with (cf. [102, 29, 83])<sup>16</sup>

$$\gamma = \frac{2}{3} \mu_3 \kappa_4^2 \text{Re}(T) e^{-4u} = \frac{1}{3\mathcal{V}_\perp}. \quad (\text{B.185})$$

Here  $k$  is the Kähler potential of  $M$ , obeying  $k_{a\bar{b}} = g_{a\bar{b}}$ , where  $a$  and  $\bar{b}$  are holomorphic and anti-holomorphic indices for D3-brane moduli. We use the convention  $ds^2 = 2g_{a\bar{b}} dz^a d\bar{z}^{\bar{b}}$  for the line element.

The  $G_-$  flux sourced by gaugino condensation [27] is given by (3.62), where  $G_{(2)}$  is the Green's function on the internal space transverse to the D7-branes. If

---

<sup>16</sup>As explained in [29], the relation (B.185) should be understood to hold exactly at a reference location in field space. Deviations from (B.185) at other locations lead to corrections of order  $\frac{\gamma k}{T + \bar{T}}$  in (B.198) and (B.199) below, which we will neglect.

this space is taken to be noncompact, we have

$$G_{(2)}(z; 0) = \frac{1}{2\pi} \log |z|, \quad (\text{B.186})$$

in terms of a local coordinate  $z$ .

The flux (3.62) is a source for the scalar  $\Phi_-$ , leading to a potential for D3-brane motion. The equation of motion for  $\Phi_-$  is

$$\nabla^2 \Phi_- = \frac{e^{8A}}{\text{Im } \tau} |G_-|^2 + \dots \quad (\text{B.187})$$

where the omitted terms are not important for the present computation. Solving (B.187) and taking the D7-brane location to be given by an equation  $h(z) = 0$  in local coordinates, one finds<sup>17</sup>

$$\Phi_- = \int_M d^6 y G_{(6)}(z; z') \frac{e^{8A}}{\text{Im } \tau} |G_-|^2 \quad (\text{B.188})$$

$$= \frac{e^{\kappa_4^2 K} e^{16u}}{4\pi^2 N_c^2} g^{a\bar{b}} \frac{\partial_a h \partial_{\bar{b}} \bar{h}}{h \bar{h}} |W_{\text{np}}|^2, \quad (\text{B.189})$$

so that

$$\mu_3 \Phi_- = e^{12u} e^{\kappa_4^2 K} K^{a\bar{b}} \partial_a W \partial_{\bar{b}} \bar{W}. \quad (\text{B.190})$$

Thus, the flux (3.62) sourced by gaugino condensation gives rise to a profile for  $\Phi_-$  that matches the *rigid part* of the F-term potential.

At this point, the Kähler connection terms in the F-term potential are not evident in the ten-dimensional computation. The result of this appendix, which we will now establish, is that the Kähler connection terms arise once one consistently incorporates finite volume effects in the Green's function.

If the space transverse to the D7-branes is compact, with volume  $\mathcal{V}_\perp$ , then the

---

<sup>17</sup>Throughout this appendix, we write only the contribution to  $\Phi_-$  sourced by  $G_-$  flux via (B.187). Further contributions are present in general [27].

Green's function reads

$$G_{(2)}(z; 0) = \frac{1}{2\pi} \log |z| - \frac{k}{6\mathcal{V}_\perp}. \quad (\text{B.191})$$

Using (B.191) to solve (B.187), one finds

$$\Phi_- = \int_M G_{(6)}(z; z') \partial_a \partial_b G_{(2)}(z'; z_{D7}) \partial_{\bar{a}} \partial_{\bar{b}} G_{(2)}(z'; z_{D7}) g^{a\bar{a}} g^{b\bar{b}} e^{16u} \left| \frac{\lambda\lambda}{32\pi^2} \right|^2 \Omega \cdot \bar{\Omega} \quad (\text{B.192})$$

$$= \frac{1}{2} \int_M \delta_{(6)}(z; z') \partial_a G_{(2)}(z'; z_{D7}) \partial_{\bar{b}} G_{(2)}(z'; z_{D7}) g^{a\bar{b}} e^{16u} \left| \frac{\lambda\lambda}{32\pi^2} \right|^2 \Omega \cdot \bar{\Omega} \quad (\text{B.193})$$

$$= 2^4 |\zeta|^2 e^{-\phi} \partial_a G_{(2)}(z; z_{D7}) \partial^a G_{(2)}(z; z_{D7}) \quad (\text{B.194})$$

$$= \frac{1}{4N_c^2 \pi^2} \left( \frac{\partial_a h(z)}{h(z)} - \frac{2\pi k_a}{3\mathcal{V}_\perp} \right) \left( \frac{\partial_{\bar{b}} \bar{h}(\bar{z})}{\bar{h}(\bar{z})} - \frac{2\pi k_{\bar{b}}}{3\mathcal{V}_\perp} \right) g^{a\bar{b}} e^{\kappa_4^2 K} e^{16u} |W_{\text{np}}|^2. \quad (\text{B.195})$$

The F-term potential that we wish to compare to (B.195) is given by

$$V_F = e^{\kappa_4^2 K} \left( K^{\Delta\bar{\Gamma}} D_\Delta W D_{\bar{\Gamma}} \bar{W} - 3\kappa_4^2 W \bar{W} \right), \quad (\text{B.196})$$

where  $K^{\Delta\bar{\Gamma}}$  is the inverse Kähler metric derived from the DeWolfe-Giddings Kähler potential [102, 65],

$$K^{\Delta\bar{\Gamma}} = \frac{\kappa_4^2 (T + \bar{T} - \gamma k)}{3\gamma} \left( \frac{\gamma(T + \bar{T} - \gamma k) + \gamma^2 k_a k^{a\bar{b}} k_{\bar{b}}}{\gamma k^{a\bar{b}} k_{\bar{b}}} \middle| \frac{\gamma k_a k^{a\bar{b}}}{k^{a\bar{b}}} \right), \quad (\text{B.197})$$

and the index  $\Delta$  runs over  $T$  and the D3-brane moduli  $y_a$ . Using (B.185), we can rewrite (B.195) as

$$\Phi_- = \frac{e^{\kappa_4^2 K} e^{16u}}{4\pi^2} g^{a\bar{b}} (D_a W + \gamma k_a D_T W) (D_{\bar{b}} \bar{W} + \gamma k_{\bar{b}} D_{\bar{T}} \bar{W}) + \dots \quad (\text{B.198})$$

$$= e^{\kappa_4^2 K} e^{12u} \frac{\kappa_4^2 \text{Re}(T)}{3\pi\gamma} \begin{pmatrix} D_T W & D_a W \end{pmatrix} \left( \frac{\gamma^2 k_a k^{a\bar{b}} k_{\bar{b}}}{\gamma k^{a\bar{b}} k_{\bar{b}}} \middle| \frac{\gamma k_a k^{a\bar{b}}}{k^{a\bar{b}}} \right) \begin{pmatrix} D_{\bar{T}} \bar{W} \\ D_{\bar{b}} \bar{W} \end{pmatrix} + \dots, \quad (\text{B.199})$$

where the omitted terms are of higher order in  $\frac{\gamma k}{T + \bar{T}}$ .

Combining (3.61) and (B.199), we conclude that in a compact space, the flux (3.62) sourced by gaugino condensation leads to a  $\Phi_-$  profile that agrees with the F-term potential (B.196):

$$\mu_3 e^{-12u} \Phi_-(z) + V_{\lambda\lambda} + V_{\lambda\lambda\lambda\lambda} = e^{\kappa_4^2 K} \left( K^{\Delta\bar{\Gamma}} D_{\Delta} W D_{\bar{\Gamma}} \bar{W} - 3\kappa_4^2 W \bar{W} \right) + \dots, \quad (\text{B.200})$$

where again the omitted terms are subleading in  $\frac{\gamma^k}{T+\bar{T}}$ .

Finally, we will show that (B.200) also follows from (3.22) upon adapting the calculation of §B.3.1 to account for the presence of localized D3-branes. From (B.160) we see that the metric at order  $\mathcal{O}(\langle\lambda\lambda\rangle)$  is only sourced by the fluxes  $\chi$  and  $\eta$ , and so (B.169) is altered to

$$2 \int_M \sqrt{g_6} \mathcal{R}_6[g] = \int_M 2^5 |\zeta|^2 e^{-\phi} (\rho_{D3} - \rho_{D3}^{\text{loc}}) \partial_e G_{(2)} \partial^e G_{(2)}. \quad (\text{B.201})$$

On the other hand, the warp factor  $e^{-4A}$  is sourced by the full D3-brane charge density  $\rho_{D3}$ , i.e. by both localized and distributed sources, and obeys  $2\partial_a \partial^a e^{-4A} = -\rho_{D3}$ . As a result, equations (B.173) and (B.182) continue to hold.

Combining (B.201), (B.173), and (B.182) we find

$$\frac{1}{4} \int_M \sqrt{g_6} \left( -e^{-4A} T^{\lambda\lambda} + 16\pi e^{4A} \rho_{D3} - 8\pi \mathcal{R}_6[g] \right) = V_{\lambda\lambda} + 2\pi \int_M \sqrt{g_6} \rho_{D3}^{\text{loc}} \Phi_-. \quad (\text{B.202})$$

When  $-\frac{1}{4} \int_M \sqrt{g_6} e^{-4A} T^{\lambda\lambda\lambda\lambda}$  is added to (B.202), we recover the full F-term potential (B.200).

## APPENDIX C

### APPENDIX FOR CHAPTER 5

#### C.1 The D3-brane tadpole in the orbifold

In this appendix we will compute the Euler characteristic  $\chi(\mathfrak{F}_{\tilde{\mathcal{I}}})$  of the fixed locus  $\mathfrak{F}_{\tilde{\mathcal{I}}}$  of the orientifold involution  $\tilde{\mathcal{I}}$ , as promised in eq. (5.72), in two different ways. First, in §C.1.1 we will show directly that  $h_{-}^{1,1}(\tilde{X}, \tilde{\mathcal{I}}) = h_{+}^{2,1}(\tilde{X}, \tilde{\mathcal{I}}) = 0$  for the involution  $\tilde{\mathcal{I}} : \tilde{X} \rightarrow \tilde{X}$ , by using the description of  $\tilde{X}$  as a smooth Calabi-Yau hypersurface in a toric fourfold  $\tilde{Y}$ . We then use the Lefschetz fixed point theorem to compute the Euler characteristic. Then, in §C.1.2 we go to the orbifold limit  $\tilde{X} \rightarrow X/G$  and compute the Euler characteristic directly. The two computations agree.

##### C.1.1 Computation in the resolved orbifold

In this section, we verify that  $h_{-}^{1,1}(\tilde{X}, \tilde{\mathcal{I}}) = 0$  and  $h_{-}^{2,1}(\tilde{X}, \tilde{\mathcal{I}}) = 3$  under the orientifold involution  $\tilde{\mathcal{I}}$  in the resolved orbifold.

First, let us briefly review how the anticanonical monomials and the automorphism group of the ambient fourfold  $\tilde{Y}$  are determined from polytope data. Let  $\Delta^{\circ} \in M$  be the Newton polyhedron for the anticanonical class of  $Y$  and let  $\Delta \in N$  be the dual polytope of  $\Delta^{\circ}$ . A point  $\rho \in \Delta \cap N$  corresponds to an edge of the toric fan of  $Y$  and thus corresponds to a homogeneous coordinate  $x_{\rho}$ . Similarly, each point  $v \in \Delta^{\circ} \cap M$  determines a monomial  $x^v$ ,

$$x^v = \prod_{\rho \in \Delta \cap N} x_{\rho}^{\langle v, \rho \rangle + 1}. \quad (\text{C.1})$$

As was shown in [25], a point  $m \in \Delta^\circ \cap M$  strictly interior to a facet corresponds to a non-trivial so-called *root automorphism*. Because  $m$  is in a facet, there is a point  $\rho_m \in \Delta \cap N$  such that  $\langle m, \rho_m \rangle = -1$  and  $\langle m, \rho \rangle > -1$ ,  $\forall \rho \neq \rho_m$ . Then the action of the automorphism of the group element  $m$  is

$$x_{\rho_m} \mapsto x_{\rho_m} + \lambda_m \prod_{\rho' \neq \rho_m} x_{\rho'}^{\langle m, \rho' \rangle}, \quad \lambda_m \in \mathbb{C}. \quad (\text{C.2})$$

Let  $\mathcal{A}$  be the automorphism group of  $\tilde{Y}$ . Then, its connected component containing the identity is generated by the root automorphisms, as well as the action of the algebraic torus  $(\mathbb{C}^*)^4 \times \tilde{Y} \rightarrow \tilde{Y}$ . Thus, the dimension of the automorphism group  $\mathcal{A}$  is given by

$$\dim \mathcal{A} = 4 + \sum_{\text{codim} \Theta^\circ = 1} \ell^*(\Theta^\circ), \quad (\text{C.3})$$

where for a face  $\Theta^\circ \subset \Delta^\circ$ ,  $\ell^*(\Theta^\circ)$  denotes the number of points in the interior of  $\Theta^\circ$ .

Given the anticanonical monomials and the automorphisms of  $Y$ , we can compute the number of Kähler moduli  $h^{1,1}(\tilde{X})$  and the number of complex structure moduli  $h^{2,1}(\tilde{X})$  of the Calabi-Yau hypersurface  $\tilde{X}$ . If a Kähler modulus is inherited from the ambient variety, then we call that Kähler modulus toric. We define  $h_{\text{toric}}^{1,1}(\tilde{X})$  to be the number of toric Kähler moduli. Similarly, we define toric complex structure deformations to be deformations of the coefficients of the anticanonical monomials modulo the deformations that can be undone by elements of  $\mathcal{A}$ , and modulo the overall scale. Likewise, we define  $h_{\text{toric}}^{2,1}(\tilde{X})$  as the number of toric complex structure moduli. We have

$$h_{\text{toric}}^{2,1}(\tilde{X}) = \#(\text{monomials}) - \dim \mathcal{A} - 1 = \sum_{\text{codim} \Theta^\circ \geq 2} \ell^*(\Theta^\circ) - 4. \quad (\text{C.4})$$

To determine  $h_{\text{toric}}^{1,1}(\tilde{X})$ , we recall that each point on  $\Delta$  gives rise to a homogeneous



coordinate.<sup>1</sup> Hence, naïvely there are  $\sum_{\text{codim}\Theta \geq 1} \ell^*(\Theta)$  toric divisors. However, points interior to facets correspond to ambient divisors that do not intersect the Calabi-Yau. Furthermore, there are in total four linear relations among the toric divisors. As a result, we obtain

$$h_{\text{toric}}^{1,1}(\tilde{X}) = \sum_{\text{codim}\Theta \geq 2} \ell^*(\Theta) - 4. \quad (\text{C.5})$$

The Calabi-Yau  $\tilde{X}$  considered in §5.4 has  $h^{2,1}(\tilde{X}) = 3$  and  $h^{1,1}(\tilde{X}) = 99$ , and from the corresponding pair of dual polytopes  $\Delta, \Delta^\circ$  one finds  $h_{\text{toric}}^{2,1}(\tilde{X}) = 3$  and  $h_{\text{toric}}^{1,1}(\tilde{X}) = 97$ . Thus all complex structure moduli of  $\tilde{X}$  are toric, but two generators of the Picard group are non-toric. In order to determine the orientifold action on  $H_4(\tilde{X}, \mathbb{Z})$  we must therefore consider the non-toric divisors in more detail. Consider a point  $\rho \in \Theta$ , with  $\text{codim}\Theta = 2$ . Then  $\{x_\rho = 0\} \cap \tilde{X}$  is a reducible variety in  $\tilde{X}$  and there are  $1 + \ell^*(\Theta^\circ)$  irreducible components [25, 61]. Hence, there are in total  $\sum_{\text{codim}\Theta=2} \ell^*(\Theta)\ell^*(\Theta^\circ)$  non-toric divisors. As a result, we obtain

$$h^{1,1}(\tilde{X}) = h_{\text{toric}}^{1,1}(\tilde{X}) + \sum_{\text{codim}\Theta=2} \ell^*(\Theta)\ell^*(\Theta^\circ). \quad (\text{C.6})$$

For a point  $\rho$ , we call the divisor  $\{x_\rho = 0\}$  *strictly favorable* if either  $\rho$  is not interior to any two-face or it is interior to a two-face  $\Theta$  but  $\ell^*(\Theta^\circ) = 0$ .

Given isomorphisms  $i^\circ : M \rightarrow \mathbb{Z}^4$  and  $i : N \rightarrow \mathbb{Z}^4$ , we can assign coordinates to points in  $\Delta^\circ \cap M$  and  $\Delta \cap N$ . Including the origin, the points in  $\Delta^\circ \cap \mathbb{Z}^4$  are

$$\Delta^\circ \cap \mathbb{Z}^4 = \begin{pmatrix} 0 & -1 & 1 & -1 & -1 & -1 & -1 & -1 & -1 \\ 0 & 3 & -1 & 0 & 0 & 0 & 0 & 0 & 1 \\ 0 & -2 & 0 & 0 & 0 & 1 & 2 & 1 & 0 \\ 0 & -1 & 0 & 1 & 0 & 1 & 0 & 0 & 0 \end{pmatrix}, \quad (\text{C.7})$$

---

<sup>1</sup>We defined  $\Delta^\circ$  as the dual (i.e.,  $N$ -lattice) polytope for  $X$ , but are now studying the mirror  $\tilde{X}$ , for which  $\Delta$  is the dual polytope.

where each column corresponds to a point. The last point  $(-1, 1, 0, 0)$  is strictly interior to a facet.

We also record points of importance in the dual polytope  $\Delta \cap \mathbb{Z}^4$ :

$$(\Delta \cap \mathbb{Z}^4) \supset \begin{pmatrix} 1 & 1 & -5 & -11 & 1 & 1 & -5 & -4 & -3 \\ 2 & 0 & -4 & -10 & 2 & 2 & -4 & -4 & -3 \\ 0 & 0 & 0 & -6 & 3 & 0 & -3 & -2 & -1 \\ 0 & 0 & -6 & -6 & 0 & 6 & 0 & -3 & -3 \end{pmatrix} \quad (\text{C.8})$$

The first six points in (C.8) are the vertices of  $\Delta \cap \mathbb{Z}^4$ . There is only one two-face  $\check{\Theta} \in \Delta$  such that  $\ell^*(\check{\Theta}^\circ) \neq 0$ , and for this face  $\ell^*(\check{\Theta}^\circ) = 1$ . The last two points in (C.8) are strictly interior to  $\check{\Theta}$ , and hence each of those two points yields the union of two distinct divisors in  $\tilde{X}$ . For notational simplicity we will suppress the dependence of the monomials on all the homogeneous coordinates except those that are explicitly presented in (C.8). We will denote by  $x_i$  the coordinate given by the  $i^{\text{th}}$  column.

The most general polynomial  $f$  is

$$\begin{aligned} f(\vec{x}) = & \psi_0 x_1 x_2 x_3 x_4 x_5 x_6 x_7 x_8 x_9 - \psi_1 x_1^6 - \psi_2 x_2^2 x_8 x_9 - \psi_3 x_4^6 x_6^6 x_7^6 x_8^2 x_9 - \psi_4 x_3^6 x_4^{12} x_7^6 x_8^5 x_9^4 \\ & - \psi_5 x_5^3 x_6^6 x_7^3 - \psi_6 x_3^6 x_5^6 x_8 x_9^2 - \psi_7 x_3^6 x_4^6 x_5^3 x_7^3 x_8^3 x_9^3 - \psi_8 x_1^2 x_3^2 x_4^2 x_5^2 x_6^2 x_7^2 x_8 x_9. \end{aligned} \quad (\text{C.9})$$

The action of the root automorphism is

$$x_2 \mapsto x_2 + \lambda x_1 x_3 x_4 x_5 x_6 x_7. \quad (\text{C.10})$$

Hence, we confirm that  $h^{2,1}(\tilde{X}) = 9 - 5 - 1 = 3$ .

Now consider an orientifold action  $\tilde{\mathcal{I}} : x_2 \mapsto -x_2$ . The most general  $\tilde{\mathcal{I}}$ -invariant

polynomial  $f_{\tilde{\mathcal{I}}}$  contains 8 monomials,

$$\begin{aligned} f_{\tilde{\mathcal{I}}}(\vec{x}) = & -\psi_1 x_1^6 - \psi_2 x_2^2 x_8 x_9 - \psi_3 x_4^6 x_6^6 x_7^2 x_8^2 x_9 - \psi_4 x_3^6 x_4^{12} x_7^6 x_8^5 x_9^4 \\ & - \psi_5 x_5^3 x_6^6 x_7^3 - \psi_6 x_3^6 x_5^6 x_8 x_9^2 - \psi_7 x_3^6 x_4^6 x_5^3 x_7^3 x_8^3 x_9^3 - \psi_8 x_1^2 x_3^2 x_4^2 x_5^2 x_6^2 x_7^2 x_8 x_9. \end{aligned} \quad (\text{C.11})$$

Because the nontrivial root automorphism of eq. (C.10) does not commute with  $\tilde{\mathcal{I}}$  we have  $\dim \mathcal{A}_{\tilde{\mathcal{I}}} = 4$ , where  $\mathcal{A}_{\tilde{\mathcal{I}}}$  is the subgroup of  $\mathcal{A}$  that commutes with the orientifold involution. As a result, there are in total three independent complex structure moduli, i.e.  $h_-^{2,1}(\tilde{X}, \tilde{\mathcal{I}}) = 8 - 4 - 1 = 3$ .

Next, we consider the structure of the non-toric divisors. To simplify the computation, we will blow down all of the blowup divisors whose blowup coordinates are implicit in eq. (C.8). First, we consider the locus  $x_8 = f = 0$ . We have

$$f|_{x_8=0} = -\psi_1 x_1^6 - \psi_5 x_5^3 x_6^6 x_7^3. \quad (\text{C.12})$$

We verified that  $x_1 = x_8 = 0$  does not intersect  $X$  by confirming that the intersection numbers of  $\{x_1 = 0\}$ ,  $\{x_8 = 0\}$ , and  $\{x_\rho = 0\}$  are trivial for any  $\rho$ , i.e.  $x_1 x_8$  is in the SR ideal. Hence, for  $f|_{x_8=0}$  to have a solution,  $x_5 x_6 x_7$  must not vanish. Using the toric rescaling, we set  $\psi_1 = -1$  and  $\psi_5 = 1$ . Then naïvely we obtain six disconnected solutions

$$x_1^2 = \omega_3^i x_5 x_6^2 x_7, \quad (\text{C.13})$$

for  $i = 0, 1, 2$ , where  $\omega_3$  is a third root of unity. However, there is a  $\mathbb{Z}_3$  subgroup of the Greene-Plesser group  $G$ , (5.62), with the charge

$$\vec{\lambda}_{\mathbb{Z}_3} = (0, 0, 0, 0, 1, 1, 1). \quad (\text{C.14})$$

This subgroup acts non-trivially on  $x_5 x_6^2 x_7$ ,

$$\mathbb{Z}_3 : x_5 x_6^2 x_7 \mapsto \omega_3 x_5 x_6^2 x_7. \quad (\text{C.15})$$

One can verify that  $G/\mathbb{Z}_3$  acts trivially on  $(x_5 x_6^2 x_7)^{1/2}$ . As a result, there are two solutions to  $x_8 = f = 0$ :

$$x_1 = \pm (x_5 x_6^2 x_7)^{1/2}. \quad (\text{C.16})$$

Likewise, the surface  $x_9 = f = 0$  splits into the two solutions of eq. (C.16).

Using this we proceed to compute  $h_-^{1,1}(\tilde{X}, \tilde{\mathcal{I}})$ . Clearly,  $\tilde{\mathcal{I}}$  acts trivially on the strictly favorable divisors  $\{x_\rho = 0\}$ . Hence, we only need to check how  $\tilde{\mathcal{I}}$  acts on the solutions of  $x_8 = f = 0$  and  $x_9 = f = 0$ . As (C.16) does not explicitly depend on  $x_2$ , the orientifold involution acts trivially on the solutions of (C.16). Thus, the orientifold action on  $H_4(\tilde{X}, \mathbb{Z})$  is trivial, and so  $h_-^{1,1}(\tilde{X}, \tilde{\mathcal{I}}) = 0$ .

Finally, we can compute the Euler characteristic  $\chi(\mathfrak{F}_{\tilde{\mathcal{I}}})$  of the fixed locus  $\mathfrak{F}_{\tilde{\mathcal{I}}}$  of  $\tilde{\mathcal{I}}$  using the Lefschetz fixed point theorem,

$$-Q = \frac{\chi(\mathfrak{F}_{\tilde{\mathcal{I}}})}{4} = \frac{\chi(\tilde{X})}{4} + 1 + \left( h_-^{2,1}(\tilde{X}, \tilde{\mathcal{I}}) - h_-^{1,1}(\tilde{X}, \tilde{\mathcal{I}}) \right) = 52. \quad (\text{C.17})$$

This corresponds to the D3-brane tadpole.

### C.1.2 Computation in the orbifold limit

The orientifold fixed locus in the orbifold  $X/G$  contains the  $G$ -orbifold of the orientifold-fixed locus in  $X$ , but also further loci whose lifts in  $X$  are the sets of points mapped by the orientifold to distinct points in the same  $G$ -orbit. It is straightforward to show that the full fixed locus  $\mathfrak{F}_{\tilde{\mathcal{I}}}$  in  $X/G$  is

$$\mathfrak{F}_{\tilde{\mathcal{I}}} \equiv \mathfrak{F}/G = (D_1 \cup D_2 \cup D_3 \cup D_4 \cup D_6)/G. \quad (\text{C.18})$$

We can compute the Euler characteristic of an orbifold as in [166, 68]. We partition  $\mathfrak{F}$  as  $\mathfrak{F} = \cup_I \mathfrak{F}_{H_I}^f$  where the  $\mathfrak{F}_{H_I}^f$  are the sets of points in  $\mathfrak{F}$  that are fixed pointwise

by subgroups  $H_I \subset G$ . Then, we have

$$\chi(\mathfrak{F}/G) = \sum_I \frac{\chi(\mathfrak{F}_{H_I}^f)|H_I|}{|F_I|}, \quad (\text{C.19})$$

where  $F_I$  are the subgroups of  $G/H_I$  that act freely (i.e. without fixed points) on  $\mathfrak{F}_{H_I}^f$ . As our group  $G$  acts via multiplication by phases on the toric coordinates, the  $\mathfrak{F}_{H_I}^f$  are the loci where a subset of the toric coordinates are set to zero, with subloci removed where further toric coordinates vanish. Such loci are mapped to themselves by all of  $G$ , so we have  $F_I = G/H_I$ . First, let us define toric divisors  $D_i$ , curves  $\mathcal{C}_{ij}$  and sets of points  $\mathcal{P}_{ijk}$  as

$$D_i = \{x_i = 0\}, \quad \mathcal{C}_{ij} = \{x_i = x_j = 0\}, \quad \mathcal{P}_{ijk} = \{x_i = x_j = x_k = 0\}, \quad (\text{C.20})$$

with pairwise distinct indices. The  $\mathfrak{F}_{H_I}^f$  can be chosen to be the above with lower-dimensional loci removed, i.e.

$$\hat{D}_i = D_i \setminus \left( \bigcup_{j \neq i} \mathcal{C}_{ij} \bigcup \bigcup_{j \neq k \neq i} \mathcal{P}_{ijk} \right), \quad \hat{\mathcal{C}}_{ij} = \mathcal{C}_{ij} \setminus \bigcup_{k \neq i \neq j} \mathcal{P}_{ijk}, \quad \hat{\mathcal{P}}_{ijk} = \mathcal{P}_{ijk}. \quad (\text{C.21})$$

Along the dense subset  $\hat{D}_1 \cup \hat{D}_2 \cup \hat{D}_3 \cup \hat{D}_4 \cup \hat{D}_6$  in  $X$ , the full group  $G$  acts without fixed points. The Euler characteristics of the  $D_i$  are  $\chi_i = (45, 207, 11, 13, 24)$ .

The curves  $\hat{\mathcal{C}}_{ij}$  are invariant under certain subgroups recorded on the left in Table C.1. The points  $\mathcal{P}_{ijk}$  are invariant under the subgroups listed on the right in Table C.1. The Euler characteristics of the non-compact curves  $\hat{\mathcal{C}}_{ij}$  are obtained from those of  $\mathcal{C}_{ij}$  by subtracting the Euler characteristics of the points  $\mathcal{P}_{ijk} \subset \mathcal{C}_{ij}$ , which we also record in Table C.1. The Euler characteristics  $\hat{\chi}_i$  of the non-compact divisors  $\hat{D}_i$ ,  $i = 1, 2, 3, 5, 6$  are likewise given by subtracting the Euler characteristics of the curves  $\hat{\mathcal{C}}_{ij} \subset D_i$  and points  $\mathcal{P}_{ijk} \subset D_i$ . The result is

$$\hat{\chi}_i = (108, 324, 36, 36, 72). \quad (\text{C.22})$$

$(i, j)$	$ H $	$\chi$	$\hat{\chi}$	$(i, j, k)$	$ H $	$\chi$
$(1, 2)$	2	-36	-54	$(1, 2, 3)$	12	3
$(1, 3)$	6	0	-6	$(1, 2, 4)$	12	3
$(1, 4)$	6	0	-6	$(1, 2, 5)$	6	6
$(1, 5)$	3	-2	-12	$(1, 2, 6)$	12	6
$(1, 6)$	6	-2	-12	$(1, 2, 7)$	6	0
$(1, 7)$	3	4	0	$(1, 3, 4)$	36	1
$(2, 3)$	2	-6	-18	$(1, 3, 5)$	18	2
$(2, 4)$	2	-6	-18	$(1, 4, 5)$	18	0
$(2, 5)$	1	-18	-36	$(1, 4, 7)$	18	2
$(2, 6)$	2	-18	-36	$(1, 5, 6)$	18	2
$(2, 7)$	1	12	0	$(1, 5, 7)$	6	0
$(3, 4)$	6	0	-6	$(1, 6, 7)$	18	2
$(3, 5)$	3	-2	-12	$(2, 3, 4)$	12	3
$(4, 5)$	3	4	0	$(2, 3, 5)$	6	6
$(4, 7)$	3	-2	-12	$(2, 4, 5)$	6	0
$(5, 6)$	3	-2	-12	$(2, 4, 7)$	6	6
$(6, 7)$	3	-2	-12	$(2, 5, 6)$	6	6
				$(2, 5, 7)$	6	0
				$(2, 6, 7)$	6	6
				$(3, 4, 5)$	18	2
				$(4, 5, 7)$	18	2
				$(5, 6, 7)$	18	2

Table C.1: Left: The curves  $\mathcal{C}_{ij}$  invariant under subgroups  $H_{ij} \subset G$ , their Euler characteristics  $\chi$ , and the Euler characteristics  $\hat{\chi}$  of the curves  $\hat{\mathcal{C}}_{ij}$  obtained by removing toric points. Right: Analogous table for toric points.

Thus, finally, we obtain

$$\chi(\mathfrak{F}_{\tilde{\mathcal{I}}}) = \frac{1}{36} \sum_I \chi(\mathfrak{F}_{H_I}^f) |H_I|^2 = 208, \quad (\text{C.23})$$

where the index  $I$  collectively runs over the  $\hat{D}_i$ ,  $\hat{C}_{ij}$  and  $\hat{P}_{ijk}$ .

Thus, we confirm that

$$-Q = \frac{\chi(\mathfrak{F}_{\tilde{\mathcal{I}}})}{4} = 52, \quad (\text{C.24})$$

in agreement with eq. (C.17).

## APPENDIX D

### APPENDIX FOR CHAPTER 6

#### D.1 Topological twist and topological sigma model on the worldsheet

Let us briefly review  $N = 2$  supersymmetric non-linear sigma model defined on a Riemann surface  $\Sigma$  with a Kahler manifold  $X$  as a target space. This theory consists of the following data: holomorphic map/coordinate function  $\Phi : \Sigma \rightarrow TX$ , superpartners of  $\Phi$ . Because of the complex structure of  $X$ , the complexified tangent bundle  $TX$  decomposes into holomorphic and anti-holomorphic tangent bundle

$$TX = T^{1,0}X \oplus T^{0,1}X. \quad (\text{D.1})$$

Respective to the decomposition of the complexified tangent bundle, we denote the holomorphic components of  $\Phi$  by  $\phi^i \in T^{1,0}X$  and similarly for the anti-holomorphic components. With this holomorphic decomposition, we can think of  $\phi^i$  as a holomorphic tangent vector, of the target space, valued scalar field on the worldsheet. A superpartner of such field then should live in holomorphic tangent vector valued *spin* bundle, which reads

$$\sqrt{K_\Sigma} \otimes (\mathcal{O}_\Sigma \oplus \Omega_\Sigma^{0,1}) \otimes \Phi^*(TX^{1,0}), \quad (\text{D.2})$$

where  $\sqrt{K_\Sigma}$  is an algebraic square root of canonical bundle of  $\Sigma$ ,  $\mathcal{O}_\Sigma$  is structure sheaf of  $\Sigma$ , and  $\Omega_\Sigma^{0,1} \equiv \overline{K_\Sigma}$  is anti-holomorphic cotangent bundle of  $\Sigma$ . As anti-holomorphic canonical bundle is dual of canonical bundle, the corresponding spinor bundle can be written as

$$(K_\Sigma^{1/2} \oplus \overline{K_\Sigma}^{1/2}) \otimes \Phi^*(TX^{1,0}). \quad (\text{D.3})$$



We will then denote the fermions living in  $K_\Sigma^{1/2} \otimes \Phi^*(TX^{1,0})$  and  $\overline{K}_\Sigma^{1/2} \otimes \Phi^*(TX^{1,0})$  by  $\psi_+^i$  and  $\psi_-^i$ , respectively. We will use the similar convention for  $\psi_+^{\bar{i}}$  and  $\psi_-^{\bar{i}}$ . Given the field contents, the worldsheet action is

$$S = 2t \int_\Sigma \left( \frac{1}{2} g_{IJ} \partial_z \phi^I \partial_{\bar{z}} \phi^J + i g_{i\bar{i}} \psi_-^{\bar{i}} D_z \psi_-^i + i g_{i\bar{i}} \psi_+^{\bar{i}} D_{\bar{z}} \psi_+^i + R_{i\bar{i}j\bar{j}} \psi_+^i \psi_+^{\bar{i}} \psi_-^j \psi_-^{\bar{j}} \right), \quad (\text{D.4})$$

where  $g$  is the hermitian metric of the target space.

Topological string model is then obtained by a topological twist to the bundle [349], in which fermionic fields live in, that preserves the form of kinetic terms of fermionic fields. The topological twist of A model can be understood as moving the non-trivial bundle  $\sqrt{K_\Sigma}$  from  $K_\Sigma^{1/2} \otimes \Phi^*(TX^{1,0})$  to  $K_\Sigma^{1/2} \otimes \Phi^*(TX^{0,1})$  and similarly for  $\overline{K}_\Sigma^{1/2}$ . As a result of this topological twist,  $\psi_+^i$  and  $\psi_-^i$  becomes (anti)-holomorphic tangent vector valued scalar field on the worldsheet. Then we can focus on transformation that transforms  $\phi^i$  into  $\psi_+^i$  and  $\phi^{\bar{i}}$  into  $\psi_-^{\bar{i}}$ , as those transformations can be represented by a globally well defined functions and others not in general.

Given the topological twist, let us rename the fermionic fields as  $\chi^i = \psi_+^i$  and  $\chi^{\bar{i}} = \psi_-^{\bar{i}}$ . Supersymmetry transformation is concisely repackaged as

$$\begin{aligned} \{Q, \Phi\} &= \chi, \\ \{Q, \chi\} &= 0, \\ \{Q, \psi_-^I\} &= i \partial_{\bar{z}} \Phi^I - \chi^J \Gamma_{JK}^I \psi_-^K, \\ \{Q, \psi_+^{\bar{I}}\} &= i \partial_z \Phi^{\bar{I}} - \chi^{\bar{J}} \Gamma_{\bar{J}\bar{K}}^{\bar{I}} \psi_+^{\bar{K}}, \end{aligned} \quad (\text{D.5})$$

where  $Q^2 = 0$  on-shell thus supersymmetry becomes BRST symmetry. The action

is

$$S = 2t \int_{\Sigma} \left( \frac{1}{2} g_{IJ} \partial_z \phi^I \partial_{\bar{z}} \phi^J + i g_{i\bar{i}} \psi_-^i D_z \chi_-^{\bar{i}} + i g_{i\bar{i}} \psi_+^{\bar{i}} D_{\bar{z}} \chi^i - R_{i\bar{i}j\bar{j}} \psi_-^i \psi_+^{\bar{i}} \chi^j \chi^{\bar{j}} \right). \quad (\text{D.6})$$

A very important observation is that this action is a sum of a Q-exact term and a topological term

$$S = it \int_{\Sigma} d^2 z \{Q, V\} + t \int_{\Sigma} \Phi^*(J), \quad (\text{D.7})$$

where  $V = g_{i\bar{j}} (\psi_+^{\bar{i}} \partial_z \phi^j + \partial_z \phi^{\bar{i}} \psi_-^j)$  and  $\Phi^*(J)$  is pullback of the Kähler form defined on  $X$ . One can add pullback of two-form tensor  $B$  to the action to complexfy the Kähler form.

We have not specified yet if  $\Sigma$  has boundaries or not. If  $\Sigma$  does not attain a boundary, then the worldsheet theory is a closed string theory. Similarly, if  $\Sigma$  has boundaries, then the worldsheet theory is an open string theory.

Topological strings wrap volume minimizer, which is energetically stable, among homologous 2 cycles in  $X$ . This means that for closed string theory, worldsheet instanton is classfied by homology class

$$\Phi_*([\Sigma]) \in H_2(X, \mathbb{Z}). \quad (\text{D.8})$$

This classification can be generalized to open string theory directly. Open string worlsheet can be regarded as a Riemann surface with  $h$  holes due to the conformal invariance. As there are  $h$  boundaries of the Riemann surface, one should impose boundary conditions. Let us denote  $h$  boundaries of  $\Sigma$  by  $C_i$ , where  $i = 1, \dots, h$ . In [343], Witten showed that the physical boundary condition is given by

$$\Phi(C_i) \subset \mathcal{L} \quad (\text{D.9})$$

for some  $\mathcal{L}$  which is a Lagrangian submanifold of  $X$ . Note that a submanifold  $\mathcal{L}$  is Lagrangian if  $J|_{\mathcal{L}} = 0$ . This condition implies that supersymmetric D-branes in

topological A model wrap Lagrangian three-cycles in  $X$ .<sup>1</sup> Therefore, open string worldsheet instanton is naturally classified by relative homology class

$$\Phi_*(\Sigma) \in H_2(X, \mathcal{L}). \quad (\text{D.10})$$

One important class of observable in closed A model is a three points function which has various interpretations in physical string theory. Let us consider a non-trivial 2 form  $[D_i] \in H^2(X)$ . Then one can consider an operator

$$\mathcal{O}_{D_i} = (D_i)_{i_1, i_2} \chi^{i_1} \chi^{i_2}. \quad (\text{D.11})$$

If we assume that  $X$  is a Calabi-Yau threefolds, when computed on string worksheet  $\mathbb{P}^1$ , the three points function of  $\mathcal{O}(D_i)$  is [68]

$$\langle \mathcal{O}_{D_1} \mathcal{O}_{D_2} \mathcal{O}_{D_3} \rangle = \mathcal{K}_{D_1 D_2 D_3} + \sum_{\beta} N_{0, \beta}(D_1, D_2, D_3) \prod_i \int_{\beta} [D_i] Q^{\beta}, \quad (\text{D.12})$$

where  $\mathcal{K}_{D_1 D_2 D_3}$  is an intersection number and  $N_{0, \beta}(D_1, D_2, D_3)$  is a genus 0 Gromov-Witten invariant for an integral curve  $\beta \in H_2(X)$ , and  $Q = e^{-\int_{\beta} J}$ . Note that this three points function can be obtained from the third derivative of the genus 0 prepotential, which is free energy of genus 0 worldsheet theory,

$$\partial_{t_1} \partial_{t_2} \partial_{t_3} F_0(t) = \langle \mathcal{O}_{D_1} \mathcal{O}_{D_2} \mathcal{O}_{D_3} \rangle, \quad (\text{D.13})$$

where  $t_i = \int_{D_i} J$ . Genus 0 prepotential receives classical and instanton contributions

$$F_0 = F_0^{cl} + F_0^{inst}, \quad (\text{D.14})$$

where (to add prepotential at LCS). Coupling to gravity [343], genus g free energy can be computed as well which reads

$$F_g(t) = \sum_{\beta} N_{g, \beta} Q^{\beta}, \quad (\text{D.15})$$

---

<sup>1</sup>In this work, we do not focus on torsion one or five cycles.

where  $N_{g,\beta}$  is a genus  $g$  Gromov-Witten invariant. Combining all genera prepotential, we get a generating functional the all genera free energy

$$F(g_s, t) = \sum_g F_g(t) g_s^{2g-2}. \quad (\text{D.16})$$

## D.2 Topological String on Conifolds and Geometric Transition

In this appendix, we briefly the geometric transition of interest. Let us consider A-model open topological string theory on the deformed conifold  $T^*S^3$ . We wrap  $N$  D-branes on  $S^3$ , whose low energy effective theory is  $U(N)$  Chern-Simons theory [343]. Wilson lines can be introduced, if  $M$  D-branes wrap on a lagrangian submanifold<sup>2</sup>  $\mathcal{L}$  of  $T^*S^3$  which intersects  $S^3$  at  $S^1$ . This corresponds to  $U(N)$  Chern-Simons theory on  $S^3$  with  $M$  knots on  $S^1$ . Under the geometric transition at large  $N$ , we obtain A-model topological string theory on the resolved conifold  $\mathcal{O}(-1) \oplus \mathcal{O}(-1) \rightarrow \mathbb{P}^1$ , in which the  $N$  D-branes are desolved into B-flux and  $M$  D-branes are still wrapped on the same special lagrangian  $\mathcal{L}$  [285].

Let us first study the deformed conifold. Cotangent bundle of  $S^3$  can be embedded into  $\mathbb{C}^4$  by an equation

$$y_1^2 + y_2^2 + y_3^2 + y_4^2 = a^2, \quad (\text{D.17})$$

$y_i$ 's  $\in \mathbb{C}$ . We assume that  $a$  is a real number. The bundle structure is more vivid when we write  $y_i = x_i + ip_i$ , then the embedding equation is written as

$$\sum_i x_i^2 = a^2 + \sum_i p_i^2, \quad \sum_i x_i p_i = 0. \quad (\text{D.18})$$

---

<sup>2</sup>In topological string theory. Unlike physical string theory, Lagrangian is good enough to ensure supersymmetry. Note that in the conifold, Lagrangian submanifolds we consider are in fact special Lagrangian.

It is then clear when  $p_i = 0$ , for all  $i$ , then the equations are reduced to

$$\sum_i x_i^2 = a^2. \quad (\text{D.19})$$

Thus  $a$  describes radius of  $S^3$ . When  $a$  is sent to 0, the deformed conifold in the limit described by

$$y_1^2 + y_2^2 + y_3^2 + y_4^2 = 0. \quad (\text{D.20})$$

As Jacobian of the defining equation vanishes at the origin  $y_1 = y_2 = y_3 = y_4 = 0$ , the conifold at the origin is singular.

### D.2.1 Blow up of the resolved conifold

To fix the singularity at the origin, we blow up the origin such that  $y_1 = y_2 = y_3 = y_4 = 0$  is replaced with a smooth manifold. If we reparametrize the coordinates as

$$z_{ij} = \sum_n \sigma_{ij}^n y_n, \quad (\text{D.21})$$

then (D.20) is written as

$$\det z_{ij} = 0. \quad (\text{D.22})$$

In this presentation, the singularity occurs when the matrix coordinates  $z_{ij}$  are trivial. It is important to note that we can view (E.22) as a condition for the following equation to have a non-trivial solution

$$\begin{pmatrix} z_{11} & z_{12} \\ z_{21} & z_{22} \end{pmatrix} \begin{pmatrix} \lambda_1 \\ \lambda_2 \end{pmatrix} = 0, \quad (\text{D.23})$$

for some complex variable  $\lambda_1$  and  $\lambda_2$  which cannot be simultaneously zero, because  $\lambda_1 = \lambda_2 = 0$  results in no constraints on  $z_{ij}$  matrix. Furthermore, (D.23) provides a resolution of the singularity because when  $z_{ij}$  is non trivial  $\lambda_1$  and  $\lambda_2$  are fixed

up to rescaling and  $z_{ij} = 0$  is replaced with coordinates  $(\lambda_1, \lambda_2)$ . This implies that equation (D.23) is an embedding of the resolved conifold into  $\mathbb{C}^4 \times \mathbb{P}^1$  in which  $z_{ij}$  is a coordinate of  $\mathbb{C}^4$  and  $[\lambda_1, \lambda_2]$  is a homogeneous coordinate of  $\mathbb{P}^1$ . Note that, when  $\det(z_{ij}) = 0$  the non-homogeneous coordinate  $z$  of  $\mathbb{P}^1$  is related to the rest of the coordinates by

$$z := \frac{\lambda_1}{\lambda_2} = \frac{-y_1 + iy_2}{y_3 + y_4} = \frac{y_3 - y_4}{y_1 + iy_2}. \quad (\text{D.24})$$

### D.2.2 Lagrangian Submanifolds

Lagrangian submanifolds can be easily found by finding symmetric locus of an anti-holomorphic involution. We consider an anti-holomorphic involution

$$y_{1,2} = \bar{y}_{1,2}, \quad y_{3,4} = -\bar{y}_{3,4}. \quad (\text{D.25})$$

In the deformed conifold, the invariant locus of (D.25), a lagrangian submanifold  $\mathcal{L}$ , is

$$p_{1,2} = 0, \quad x_{3,4} = 0. \quad (\text{D.26})$$

At the symmetric locus of (D.25), the embedding equation becomes

$$x_1^2 + x_2^2 = a^2 + p_3^2 + p_4^2. \quad (\text{D.27})$$

Hence  $\mathcal{L}$  intersects  $S^3$  at

$$x_1^2 + x_2^2 = a^2, \quad (\text{D.28})$$

which is a  $S^1$ .

Similarly, in the resolved conifold, the lagrangian submanifold is defined by

$$\begin{pmatrix} ip_3 + ip_4 & x_1 - ix_2 \\ x_1 + ix_2 & ip_4 - ip_3 \end{pmatrix} \begin{pmatrix} \lambda_1 \\ \lambda_2 \end{pmatrix} = 0. \quad (\text{D.29})$$

## D.3 Quantum groups and their representations

### D.3.1 Hopf algebra structure

The quantum group  $\mathcal{A}(U(N)_q)$  is a quasi-triangular Hopf algebra. To explain what this is, we start with the simpler structure of a bi-algebra  $\mathcal{A}$ , which is an algebra endowed with 4 operations

$$\begin{aligned}
&\text{product} \quad \nabla : \mathcal{A} \otimes \mathcal{A} \rightarrow \mathcal{A} \\
&\text{unit} \quad \eta : \mathbb{C} \rightarrow \mathcal{A} \\
&\text{coproduct} \quad \Delta : \mathcal{A} \rightarrow \mathcal{A} \otimes \mathcal{A} \\
&\text{counit} \quad \epsilon : \mathcal{A} \rightarrow \mathbb{C}
\end{aligned} \tag{D.30}$$

These operations satisfy various sewing relations [236]; in particular the product and coproduct are associative and co-associative respectively. A basic example is the set of  $\mathcal{A}(G)$  of  $\mathbb{C}$  valued-functions on a group  $G$ , where  $\nabla$  is pointwise multiplication,  $\eta = 1$ , and the coproduct and counit are defined to act on  $f \in \mathcal{A}(G)$  as

$$\begin{aligned}
\Delta(f)(U, V) &= f(UV), \quad U, V \in G \\
\epsilon(f) &= f(1_G)
\end{aligned} \tag{D.31}$$

Here  $UV$  denotes the group multiplication of  $U$  and  $V$ , and  $1_G$  is the identity element of  $G$ . The formulas (D.31) show that the coproduct and counit are dual to the product and unit on the group  $G$ . For  $G = U(N)$ , this describes the algebraic structure of the Hilbert space for 2DYM and its string theory dual.

In the coordinate algebra  $\mathcal{A}(U(N)_q)$ ,  $\nabla$  is  $q$ -deformed into a non-commutative product, while  $UV$  remains the same as the ordinary matrix multiplication and  $1_G$

is still the identity matrix. In particular, the actions of the coproduct and counit on single string wavefunctions  $f_{ij}(U) = U_{ij}$  are given by

$$\begin{aligned}\Delta(U_{ij}) &= \sum_k U_{ik} \otimes U_{kj} \\ \epsilon(U_{ij}) &= \delta_{ij}\end{aligned}\tag{D.32}$$

Meanwhile the counit defines the trivial, or “vacuum” representation.

This bi-algebra structure is upgraded into a Hopf algebra by the introduction of a mapping called the antipode

$$\text{antipode } S : \mathcal{A} \rightarrow \mathcal{A}\tag{D.33}$$

which acts as an inverse on the quantum group:

$$\sum_k S(U)_{ik} U_{kj} = \sum_k U_{ik} S(U)_{kj} = \delta_{ij}\tag{D.34}$$

The final element that makes a Hopf Algebra into a quantum group is the  $R$  matrix, which makes it a quasi-triangular Hopf algebra. This can be viewed as an element

$$\begin{aligned}\mathcal{R} &\in \mathcal{A} \otimes \mathcal{A} \\ \mathcal{R} &= \sum_i a_i \otimes b_i\end{aligned}\tag{D.35}$$

We can also interpret this as a linear operator on  $V \otimes V$ . It satisfies the Yang-Baxter equation.



### D.3.2 R matrix and antipode for $SL_q(2)$

To illustrate this definition, consider the quantum group  $SL_q(2)$ . Its coordinate algebra is generated by 4 elements (a,b,c,d) of a matrix

$$U = \begin{pmatrix} a & b \\ c & d \end{pmatrix} \quad (\text{D.36})$$

and the  $R$  matrix is

$$\mathcal{R} = \begin{pmatrix} q^{1/2} & 0 & 0 & 0 \\ 0 & q^{-1/2} & 0 & 0 \\ 0 & q^{1/2} - q^{-3/2} & 1 & 0 \\ 0 & 0 & 0 & q^{1/2} \end{pmatrix} \quad (\text{D.37})$$

Then the multiplication rule (6.94) is equivalent to

$$\begin{aligned} ab &= qba, & ac &= qca, & bd &= qdb, & cd &= qdc \\ cb &= bc, & ad - da &= (q - q^{-1})bc \\ ad - qbc &= 1 \end{aligned} \quad (\text{D.38})$$

The antipode is given by

$$S(a) = d, \quad S(c) = -qc, \quad S(b) = -q^{-1}b, \quad S(d) = a \quad (\text{D.39})$$

### D.3.3 \* structure and unitary representations

**\* on the coordinate algebra** we define an involution of the  $SL(2)_q$  algebra which plays the role of complex conjugation by

$$a^* = d, \quad b^* = -qc, \quad c^* = -q^{-1}b, \quad d^* = a \quad (\text{D.40})$$

From the antipode (D.39) we find the relation

$$U^{t*} = S(U) \quad (\text{D.41})$$

where  $t$  stands for transpose.  $SU(2)_q$  refers to  $SL(2)_q$  equipped with the above star structure.

## D.4 Spacetime non-commutativity from B fields

Here we show how a non commutative worldvolume gauge field arises from the string sigma model due to the coupling to a nontrivial  $B$  field flux in the base  $S^2$ . For the physical string, it is known [305] that the presence of the  $B$  field alters the boundary conditions for the open string, and leads to an anti-symmetric part to the worldsheet propagator. This in turn leads to nontrivial commutation relations of the open string endpoint, resulting in a non-commutative worldvolume gauge theory on the D branes.

For the A model, we can see how this phenomenon arises from the bosonic part of the sigma model action in the presence of the  $B$  field:

$$S = \int_W \frac{1}{2} g_{IJ} \delta^{ab} \partial_a X^I \partial_b X^J + i B_{IJ} \epsilon^{ab} \partial_a X^I \partial_b X^J d^2 \sigma \quad (\text{D.42})$$

where  $W$  denotes the 2 dimensional worldsheet. For a constant B field  $B_{IJ} = B \epsilon_{IJ}$ , the second term is a total derivative that can be written as a boundary term:

$$S = \int_W \frac{1}{2} g_{IJ} \delta^{ab} \partial_a X^I \partial_b X^J + i \int_{\partial W} B \epsilon_{IJ} X^I \epsilon^{ab} \partial_s X^J ds \quad (\text{D.43})$$

where  $s$  is the "time" coordinate along the boundary. We can treat the boundary term as the integral of the canonical one-form  $\int p dq$  for a quantum mechanical particle corresponding to the open string endpoint. This implies that the  $B \epsilon_{IJ} X^I$

is the canonical momentum conjugate to  $X^J$ , and therefore the equal time commutation relations in  $g_{ij} \rightarrow 0$  limit are

$$[X^I, X^J] = i \frac{\epsilon^{IJ}}{B} \quad (\text{D.44})$$

for the open string endpoints.

APPENDIX E  
APPENDIX FOR CHAPTER 7

## E.1 Topological twist and topological sigma model on the worldsheet

Before we move on to the topological sigma model, let us briefly review  $N = 2$  supersymmetric non-linear sigma model defined on a Riemann surface  $\Sigma$  with a Kahler manifold  $X$  as a target space. This theory consists of the following data: holomorphic map/coordinate function  $\Phi : \Sigma \rightarrow TX$ , superpartners of  $\Phi$ . Because of the complex structure of  $X$ , the complexified tangent bundle  $TX$  decomposes into holomorphic and anti-holomorphic tangent bundle

$$TX = T^{1,0}X \oplus T^{0,1}X. \quad (\text{E.1})$$

Respective to the decomposition of the complexified tangent bundle, we denote the holomorphic components of  $\Phi$  by  $\phi^i \in T^{1,0}X$  and similarly for the anti-holomorphic components. With this holomorphic decomposition, we can think of  $\phi^i$  as a holomorphic tangent vector, of the target space, valued scalar field on the worldsheet. A superpartner of such field then should live in holomorphic tangent vector valued *spin* bundle, which reads

$$\sqrt{K_\Sigma} \otimes (\mathcal{O}_\Sigma \oplus \Omega_\Sigma^{0,1}) \otimes \Phi^*(TX^{1,0}), \quad (\text{E.2})$$

where  $\sqrt{K_\Sigma}$  is an algebraic square root of canonical bundle of  $\Sigma$ ,  $\mathcal{O}_\Sigma$  is structure sheaf of  $\Sigma$ , and  $\Omega_\Sigma^{0,1} \equiv \overline{K_\Sigma}$  is anti-holomorphic cotangent bundle of  $\Sigma$ . As anti-holomorphic canonical bundle is dual of canonical bundle, the corresponding spinor bundle can be written as

$$(K_\Sigma^{1/2} \oplus \overline{K_\Sigma}^{1/2}) \otimes \Phi^*(TX^{1,0}). \quad (\text{E.3})$$

We will then denote the fermions living in  $K_\Sigma^{1/2} \otimes \Phi^*(TX^{1,0})$  and  $\overline{K}_\Sigma^{1/2} \otimes \Phi^*(TX^{1,0})$  by  $\psi_+^i$  and  $\psi_-^i$ , respectively. We will use the similar convention for  $\psi_+^{\bar{i}}$  and  $\psi_-^{\bar{i}}$ . Given the field contents, the worldsheet action is

$$S = 2t \int_\Sigma \left( \frac{1}{2} g_{IJ} \partial_z \phi^I \partial_{\bar{z}} \phi^J + i g_{i\bar{i}} \psi_-^{\bar{i}} D_z \psi_-^i + i g_{i\bar{i}} \psi_+^{\bar{i}} D_{\bar{z}} \psi_+^i + R_{i\bar{i}j\bar{j}} \psi_+^i \psi_+^{\bar{i}} \psi_-^j \psi_-^{\bar{j}} \right), \quad (\text{E.4})$$

where  $g$  is the hermitian metric of the target space.

Topological string model is then obtained by a topological twist to the bundle [349], in which fermionic fields live in, that preserves the form of kinetic terms of fermionic fields. The topological twist of A model can be understood as moving the non-trivial bundle  $\sqrt{K_\Sigma}$  from  $K_\Sigma^{1/2} \otimes \Phi^*(TX^{1,0})$  to  $K_\Sigma^{1/2} \otimes \Phi^*(TX^{0,1})$  and similarly for  $\overline{K}_\Sigma^{1/2}$ . As a result of this topological twist,  $\psi_+^i$  and  $\psi_-^i$  becomes (anti)-holomorphic tangent vector valued scalar field on the worldsheet. Then we can focus on transformation that transforms  $\phi^i$  into  $\psi_+^i$  and  $\phi^{\bar{i}}$  into  $\psi_-^{\bar{i}}$ , as those transformations can be represented by a globally well defined functions and others not in general<sup>1</sup>.

Given the topological twist, let us rename the fermionic fields as  $\chi^i = \psi_+^i$  and  $\chi^{\bar{i}} = \psi_-^{\bar{i}}$ . Supersymmetry transformation is concisely repackaged as

$$\begin{aligned} \{Q, \Phi\} &= \chi, \\ \{Q, \chi\} &= 0, \\ \{Q, \psi_-^I\} &= i \partial_{\bar{z}} \Phi^I - \chi^J \Gamma_{JK}^I \psi_-^K, \\ \{Q, \psi_+^{\bar{I}}\} &= i \partial_z \Phi^{\bar{I}} - \chi^{\bar{J}} \Gamma_{\bar{J}\bar{K}}^{\bar{I}} \psi_+^{\bar{K}}, \end{aligned} \quad (\text{E.5})$$

where  $Q^2 = 0$  on-shell thus supersymmetry becomes BRST symmetry. The action

---

<sup>1</sup>For high genus curves, there are still more non-trivial supersymmetry transformations. But, I have no idea what will happen if I take those non-trivial transformations into account. Perhaps, BRST operator will just go away

is

$$S = 2t \int_{\Sigma} \left( \frac{1}{2} g_{IJ} \partial_z \phi^I \partial_{\bar{z}} \phi^J + i g_{i\bar{i}} \psi_-^i D_z \chi_-^{\bar{i}} + i g_{i\bar{i}} \psi_+^{\bar{i}} D_{\bar{z}} \chi^i - R_{i\bar{i}j\bar{j}} \psi_-^i \psi_+^{\bar{i}} \chi_-^j \chi_{\bar{j}}^{\bar{j}} \right). \quad (\text{E.6})$$

A very important observation is that this action is a sum of a Q-exact term and a topological term

$$S = it \int_{\Sigma} d^2 z \{Q, V\} + t \int_{\Sigma} \Phi^*(J), \quad (\text{E.7})$$

where  $V = g_{i\bar{j}} (\psi_+^{\bar{i}} \partial_z \phi^j + \partial_z \phi^{\bar{i}} \psi_-^j)$  and  $\Phi^*(J)$  is pullback of the Kähler form defined on  $X$ . One can add pullback of two-form tensor  $B$  to the action to complexfy the Kähler form.

We have not specified yet if  $\Sigma$  has boundaries or not. If  $\Sigma$  does not attain a boundary, then the worldsheet theory is a closed string theory. Similarly, if  $\Sigma$  has boundaries, then the worldsheet theory is an open string theory.

Topological strings wrap “volume minimizer,” which is energetically stable, among homologous 2 cycles in  $X$ . Which means that for closed string theory, worldsheet instanton is classified by homology class

$$\Phi_*([\Sigma]) \in H_2(X, \mathbb{Z}). \quad (\text{E.8})$$

This classification can be generalized to open string theory directly. Open string worksheet can be regarded as a Riemann surface with  $h$  holes due to the conformal invariance. As there are  $h$  boundaries of the Riemann surface, one should impose boundary conditions. Let us denote  $h$  boundaries of  $\Sigma$  by  $C_i$ , where  $i = 1, \dots, h$ . In [343], Witten showed that the physical boundary condition is given by

$$\Phi(C_i) \subset \mathcal{L} \quad (\text{E.9})$$

for some  $\mathcal{L}$  which is a Lagrangian submanifold of  $X$ . Note that a submanifold  $\mathcal{L}$  is Lagrangian if  $J|_{\mathcal{L}} = 0$ . This condition implies that supersymmetric D-branes in

topological A model wrap Lagrangian three-cycles in  $X^2$ . Therefore, open string worldsheet instanton is naturally classified by relative homology class

$$\Phi_*(\Sigma) \in H_2(X, \mathcal{L}). \quad (\text{E.10})$$

One important class of observable in closed A model is a three points function which has various interpretations in physical string theory. Let us consider a non-trivial 2 form  $[D_i] \in H^2(X)$ . Then one can consider an operator

$$\mathcal{O}_{D_i} = (D_i)_{i_1, i_2} \chi^{i_1} \chi^{i_2}. \quad (\text{E.11})$$

If we assume that  $X$  is a Calabi-Yau threefolds, when computed on string worksheet  $\mathbb{P}^1$ , the three points function of  $\mathcal{O}(D_i)$  is [68]

$$\langle \mathcal{O}_{D_1} \mathcal{O}_{D_2} \mathcal{O}_{D_3} \rangle = \mathcal{K}_{D_1 D_2 D_3} + \sum_{\beta} N_{0, \beta}(D_1, D_2, D_3) \prod_i \int_{\beta} [D_i] Q^{\beta}, \quad (\text{E.12})$$

where  $\mathcal{K}_{D_1 D_2 D_3}$  is an intersection number and  $N_{0, \beta}(D_1, D_2, D_3)$  is a genus 0 Gromov-Witten invariant for an integral curve  $\beta \in H_2(X)$ , and  $Q = e^{-\int_{\beta} J}$ . Note that this three points function can be obtained from the third derivative of the genus 0 prepotential, which is free energy of genus 0 worldsheet theory,

$$\partial_{t_1} \partial_{t_2} \partial_{t_3} F_0(t) = \langle \mathcal{O}_{D_1} \mathcal{O}_{D_2} \mathcal{O}_{D_3} \rangle, \quad (\text{E.13})$$

where  $t_i = \int_{D_i} J$ . Genus 0 prepotential receives classical and instanton contributions

$$F_0 = F_0^{cl} + F_0^{inst}, \quad (\text{E.14})$$

where (to add prepotential at LCS). Coupling to gravity [343], genus g free energy can be computed as well which reads

$$F_g(t) = \sum_{\beta} N_{g, \beta} Q^{\beta}, \quad (\text{E.15})$$

---

<sup>2</sup>In this work, we do not focus on torsion one or five cycles.

where  $N_{g,\beta}$  is a genus  $g$  Gromov-Witten invariant. Combining all genera prepotential, we get a generating functional the all genera free energy

$$F(g_s, t) = \sum_g F_g(t) g_s^{2g-2}, \quad (\text{E.16})$$

which will prove to be useful.

## E.2 Topological String on Conifolds and Geometric Transition

Let us review briefly the geometric transition from open string to closed string theory of interest. Let us consider A-model open topological string theory on the deformed conifold  $T^*S^3$ . We wrap  $N$  D-branes on  $S^3$ , whose low energy effective theory is  $SU(N)$  Chern-Simons theory [343]. Wilson lines can be introduced, if  $M$  D-branes wrap on a lagrangian submanifold<sup>3</sup>  $\mathcal{L}$  of  $T^*S^3$  which intersects  $S^3$  at  $S^1$ . This corresponds to  $U(N)$  Chern-Simons theory on  $S^3$  with  $M$  knots on  $S^1$ . Under the geometric transition at large  $N$ , we obtain A-model topological string theory on the resolved conifold  $\mathcal{O}(-1) \oplus \mathcal{O}(-1) \rightarrow \mathbb{P}^1$ , in which the  $N$  D-branes are desolved into B-flux and  $M$  D-branes are still wrapped on the same special lagrangian  $\mathcal{L}$  and intersect  $S^2$  at  $S^1$  [285].

Using the topological vertex formalism, one can obtain partition function on  $\mathcal{O}(-1) \oplus \mathcal{O}(-1) \rightarrow D^2$ , where  $\partial D^2 = S^1$  which implies that the partition function can be understood as a wave function of topological string theory on  $S^1$  with the fiber. Now, we need to subdivide  $S^1$  into two line segments to compute the

---

<sup>3</sup>In topological string theory, Lagrangian is good enough to ensure supersymmetry whereas in physical string theory special Lagrangian is required. Note that in the conifold, Lagrangian submanifolds we consider are special Lagrangian actually.



entanglement entropy<sup>4</sup>. In order to subdivide  $S^1$ , one needs D-brane/anti-D-brane pair intersecting  $S^1$  at two points. The D-brane/anti-D-brane pair cannot wrap any submanifold of the resolved conifold rather the D-brane/anti-D-brane pair should wrap a special lagrangian submanifold. Previously, we have said that there is a special lagrangian submanifold, on which a flavour D-brane can wrap to generate Wilson loop in the dual Chern-Simons theory. Hence, it is natural to conjecture that D-brane/anti-D-brane pair needed to cut  $S^1$  to two line segments is dual to flavour D-brane/anti-D-brane pair in the dual open string theory.

The conjecture implies that the local degrees of freedom counted in closed string theory should result from open strings extended between the intersecting D-branes. Furthermore, cutting through  $S^1$ , which is wrapped by the flavour D-brane/anti-D-brane pair, corresponds to cutting through the Wilson line/anti-Wilson-line pair, so we obtain nice interpretation in open string theory as well.

Let us first study the deformed conifold. Cotangent bundle of  $S^3$  can be embedded into  $\mathbb{C}^4$  by an equation

$$y_1^2 + y_2^2 + y_3^2 + y_4^2 = a^2, \quad (\text{E.17})$$

$y_i$ 's  $\in \mathbb{C}$ . We assume that  $a$  is a real number. The bundle structure is more vivid when we write  $y_i = x_i + ip_i$ , then the embedding equation is written as

$$\sum_i x_i^2 = a^2 + \sum_i p_i^2, \quad \sum_i x_i p_i = 0. \quad (\text{E.18})$$

It is then clear when  $p_i = 0$ , for all  $i$ , then the equations are reduced to

$$\sum_i x_i^2 = a^2. \quad (\text{E.19})$$

---

<sup>4</sup>For replica trick, this subdivision is not needed. But still, understanding on the Wilson line dual to the cutting is absolutely necessary.

Thus  $a$  describes radius of  $S^3$ . When  $a$  is sent to 0, the deformed conifold in the limit described by

$$y_1^2 + y_2^2 + y_3^2 + y_4^2 = 0. \quad (\text{E.20})$$

As Jacobian of the defining equation vanishes at the origin  $y_1 = y_2 = y_3 = y_4 = 0$ , the conifold at the origin is singular.

To fix the singularity at the origin, one can blow up/resolve the origin such that  $y_1 = y_2 = y_3 = y_4 = 0$  is replaced with a smooth manifold. If we reparametrize the coordinates by

$$z_{ij} = \sum_n \sigma_{ij}^n y_n, \quad (\text{E.21})$$

then (E.20) is written as

$$\det z_{ij} = 0. \quad (\text{E.22})$$

In this presentation, the singularity occurs when the matrix coordinate  $z_{ij}$  is trivial. It is important to note that we can view (E.22) as a condition for the following equation to have a non-trivial solution

$$\begin{pmatrix} z_{11} & z_{12} \\ z_{21} & z_{22} \end{pmatrix} \begin{pmatrix} \lambda_1 \\ \lambda_2 \end{pmatrix} = 0, \quad (\text{E.23})$$

for some complex variable  $\lambda_1$  and  $\lambda_2$  which cannot be simultaneously zero, because  $\lambda_1 = \lambda_2 = 0$  results in no constraints on  $z_{ij}$  matrix. Furthermore, (E.23) provides a resolution of the singularity because when  $z_{ij}$  is non trivial  $\lambda_1$  and  $\lambda_2$  are fixed up to rescaling and  $z_{ij} = 0$  is replaced with coordinates  $(\lambda_1, \lambda_2)$ . This implies that equation (E.23) is an embedding of the resolved conifold into  $\mathbb{C}^4 \times \mathbb{P}^1$  in which  $z_{ij}$  is a coordinate of  $\mathbb{C}^4$  and  $[\lambda_1, \lambda_2]$  is a homogeneous coordinate of  $\mathbb{P}^1$ . Note that, when  $z_{ij}$  is generic, the non-homogeneous coordinate  $z$  of  $\mathbb{P}^1$  is related to the rest of the coordinates by

$$z := \frac{\lambda_1}{\lambda_2} = \frac{y_1 + iy_2}{y_3 - iy_4} = \frac{y_3 + iy_4}{iy_2 - y_1}. \quad (\text{E.24})$$

Lagrangian submanifolds can easily be found by finding symmetric locus of an anti-holomorphic involution. We consider an anti-holomorphic involution

$$y_{1,2} = \bar{y}_{1,2}, \quad y_{3,4} = -\bar{y}_{3,4}. \quad (\text{E.25})$$

There are more anti-holomorphic involutions, but it will be clear that one can choose (E.25) without loss of generality to find a special lagrangian intersecting  $S^3$  at  $S^1$ . In the deformed conifolde, for example, the invariant locus of (E.25), a lagrangian submanifold  $\mathcal{L}$ , is

$$p_{1,2} = 0, \quad x_{3,4} = 0. \quad (\text{E.26})$$

At the symmetric locus of (E.25), the embedding equation becomes

$$x_1^2 + x_2^2 = a^2 + p_3^2 + p_4^2. \quad (\text{E.27})$$

Hence  $\mathcal{L}$  intersects  $S^3$  at

$$x_1^2 + x_2^2 = a^2, \quad (\text{E.28})$$

which is a  $S^1$ .

The Wilson loop or knot on  $S^3$  is  $S^1$  which is described by

$$x_1^2 + x_2^2 = a^2, x_3 = x_4 = p_1 = p_2 = p_3 = p_4 = 0. \quad (\text{E.29})$$

We now want to show that (E.29) is homologous to  $S^1$  on  $S^2$ . We will use homotopy equivalence, with an understanding that two homotopically equivalent cycles are homologous. First let us consider a parametrization  $C_a(t)$  for  $t \in [0, 1]$ ,

$$(x_1(t), x_2(t)) = a(\cos(2\pi t), \sin(2\pi t)). \quad (\text{E.30})$$

Let us then consider a homotopy  $\gamma_a(t, l)$  for  $t, l \in [0, 1]$ ,

$$(x_1(t), x_2(t), p_3(t), p_4(t)) = (\sqrt{a^2 + l^2} \cos(2\pi t), \sqrt{a^2 + l^2} \sin(2\pi t), l \cos(-4\pi t), l \sin(-4\pi t)). \quad (\text{E.31})$$

From this homotopy equivalence, we have checked that the curve (E.29) is homotopic to a curve  $\gamma_a(t, 1)$

$$(x_1(t), x_2(t), p_3(t), p_4(t)) = (\sqrt{a^2 + 1} \cos(2\pi t), \sqrt{a^2 + 1} \sin(2\pi t), \cos(-4\pi t), \sin(-4\pi t)). \quad (\text{E.32})$$

Let us take the singular limit  $a \rightarrow 0$ , and blow up the singular point. Under this geometric transition,  $\gamma_a(t, 1)$  becomes  $\gamma_0(t, 1)$

$$(x_1(t), x_2(t), p_3(t), p_4(t)) = (\cos(2\pi t), \sin(2\pi t), \cos(-4\pi t), \sin(-4\pi t)). \quad (\text{E.33})$$

What is left for us to check is if  $\mathcal{L}$  intersects  $S^2$  of the blow up, and if  $\mathcal{L}$  and  $S^2$  intersect whether or not the intersection is  $\gamma_0(t, 1)$ . Let us first check if  $\mathcal{L}$  intersects  $S^2$ . In the resolved conifold,  $\mathcal{L}$  is given by

$$x_1^2 + x_2^2 = p_3^2 + p_4^2, \quad p_{1,2} = x_{3,4} = 0. \quad (\text{E.34})$$

As  $(y_1 + iy_2)/(y_3 - iy_4) = (y_3 + iy_4)/(iy_2 - y_1)$  at  $\mathcal{L}$  it is manifest that  $\mathcal{L}$  intersects  $S^2$ . To study if  $\gamma_a(t, 1)$  intersects  $S^2$ , let us parametrize  $z = (y_1 + iy_2)/(y_3 - iy_4)$

$$z = -i(\cos(-2\pi t) + i \sin(-2\pi t)). \quad (\text{E.35})$$

Hence, we have shown that  $\gamma_0(t, 1)$  is an equator of  $S^2$  thus proved the claim<sup>5</sup>.

### E.3 $\mathbb{C}^3$ as a toric variety

$\mathbb{C}^3$  can be regarded as a Calabi-Yau manifold in a sense that the first chern class of  $\mathbb{C}^3$  is trivial. We want to find a  $T^2 \times \mathbb{R}$  fiber hiding in  $\mathbb{C}^3$ . Let  $z_i$  be complex

---

<sup>5</sup>It still remains ambiguous what other choices of homotopy equivalences mean. For example, if I choose a homotopy equivalence  $(x_1(t), x_2(t), p_3(t), p_4(t)) = (\cos(2\pi t), \sin(2\pi t), \cos(-2\pi t), \sin(-2\pi t))$  then I could send  $S^1$  on  $S^3$  in the deformed conifold to a point on  $S^2$  in the resolved conifold. This shows that there could be many distinct choices, which partially results from the fact that  $S^1$  in  $S^2$  is trivial in homology, or more precisely  $H_1(S^2, \mathbb{Z}) = 0$ .

coordinates of  $\mathbb{C}^3$ , for  $i = 1, 2, 3$ . We first introduce three Hamiltonians, which encode the fibration structure,

$$r_\alpha(z) = |z_1|^2 - |z_3|^2, \quad (\text{E.36})$$

$$r_\beta(z) = |z_2|^2 - |z_3|^2, \quad (\text{E.37})$$

$$r_\gamma(z) = \text{Im}(z_1 z_2 z_3). \quad (\text{E.38})$$

Given the symplectic form  $\omega$

$$\omega = dz_i \wedge d\bar{z}_i, \quad (\text{E.39})$$

the Hamiltonians, which can be understood as base coordinates, uniquely determine the fiber coordinates through Poisson bracket

$$\partial_v z_i = \{r_v, z_i\}_\omega. \quad (\text{E.40})$$

More explicitly, let  $\alpha$  be a coordinate of an  $\alpha$ -cycle, which is generated by  $r_\alpha$ , and  $\beta$  be a coordinate of a  $\beta$ -cycle of  $T^2$ , both of which parametrize phases of the complex coordinates of  $\mathbb{C}^3$  by following group action

$$r_\alpha \otimes r_\beta : (z_1, z_2, z_3) \mapsto (e^{i\alpha} z_1, e^{i\beta} z_2, e^{-i(\alpha+\beta)} z_3). \quad (\text{E.41})$$

In a similar way, translation along the remaining fiber direction  $\mathbb{R}$  induces

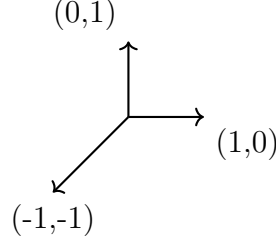
$$(z_1, z_2, z_3) \mapsto (z_1 + \gamma \bar{z}_2 \bar{z}_3, z_2 + \gamma \bar{z}_1 \bar{z}_3, z_3 + \gamma \bar{z}_1 \bar{z}_2). \quad (\text{E.42})$$

As we have identified the fiber  $T^2 \times \mathbb{R}$ , let us now study at which places in the base manifold the fiber degenerates, meaning that some cycles in  $T^2$  shrink to a point. An easy way to see if some cycle shrinks to a point is to check if the flow generated by a Hamiltonian is trivial. For example,  $r_\alpha$  generates trivial flow if  $z_1 = z_3 = 0$ . In a similar way,  $r_\beta$  generates trivial flow if  $z_2 = z_3 = 0$ . Now consider a cycle generated by  $r_\alpha - r_\beta$ . The flow generated by  $r_\alpha - r_\beta$  is

$$(z_1, z_2, z_3) \mapsto (e^{i\theta} z_1, e^{-i\theta} z_2, z_3). \quad (\text{E.43})$$

Which shows that the cycle generated by  $r_\alpha - r_\beta$  degenerates at  $z_1 = z_2 = 0$ . More generally, one can consider a cycle generated by  $pr_\alpha + qr_\beta$ , which degenerates  $z_1 = z_2 = z_3 = 0$ .

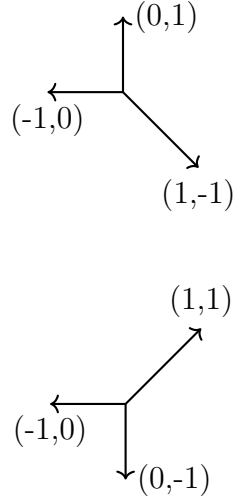
Now let us analyze the degeneration loci in the base manifold  $\mathbb{R}^3$ .  $\alpha$  cycle degenerates at  $z_1 = z_3 = 0$ , which then implies that the degeneration locus in the base manifold for  $\alpha$  cycle is  $r_\alpha = r_\gamma = 0$ . One can show that  $\beta$  cycle degenerates at  $r_\beta = r_\gamma = 0$  in the base manifold. For a generic cycle generated by  $pr_\alpha + qr_\beta$ , the degeneration locus in the base manifold is simply  $pr_\alpha + qr_\beta = r_\gamma = 0$ . Thus it is manifest that the degeneration loci in the base manifold can be compactly encoded in the two dimensional space, at  $r_\gamma = 0$ , which is parametrized by  $(r_\alpha, r_\beta)$ . We denote a cycle generated by  $(pr_\alpha + qr_\beta)$  as  $(-q, p)$  cycle. With the understanding on the degeneration loci of  $T^2$  cycles, we represent  $\mathbb{C}^3$  by



Note that equivalent graph can be obtained by applying a  $SL(2, Z)$  transformation on all the vectors. For example, upon acting

$$\begin{pmatrix} 1 & 0 \\ -1 & 1 \end{pmatrix}, \quad (\text{E.44})$$

we obtain equivalent toric diagrams



## E.4 Replica trick in Chern-Simons theory

We first introduce an identity that provides the basis for the surgery method. For a manifold  $M$  which is the connected sum of two manifolds  $M_1$  and  $M_2$  glued along a boundary  $S^2$ , Chern-Simons theory partition function obeys an identity [112, 341].

$$Z(M) = \frac{Z(M_1)Z(M_2)}{Z(S^3)}. \quad (\text{E.45})$$

(E.45) can be generalized to a manifold  $M$  which is glued along  $n$   $S^2$ 's

$$Z(M) = \frac{Z(M_1)Z(M_2)}{Z(S^3)^n}. \quad (\text{E.46})$$

A straightforward generalization of the surgery formula (E.45) for  $M_1$  and  $M_2$  with unknots of representations  $R_1 \in M_1$  and  $R_2 \in M_2$  is [112]

$$Z(M; R_1, R_2) = \frac{Z(M_1; R_1)Z(M_2; R_2)}{Z(S^3, R_{S^3})}, \quad (\text{E.47})$$

where  $R_{S^3}$  is the representation of the Wilson line going through the gluing boundary  $S^2$ . An important identity we will use at various steps in the large  $N$ -limit is

$$\lim_{N \rightarrow \infty} Z(S^3; R)Z(S^3; \bar{R}) = S_{00}(t')^2 d_q(R)^2. \quad (\text{E.48})$$

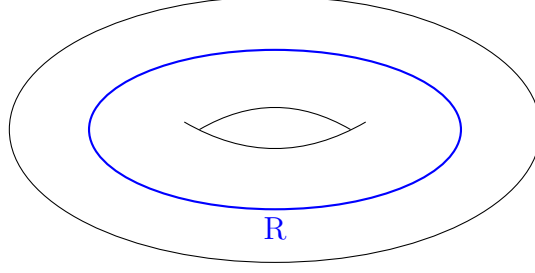


Figure E.1: Solid torus with a Wilson loop operator inserted.

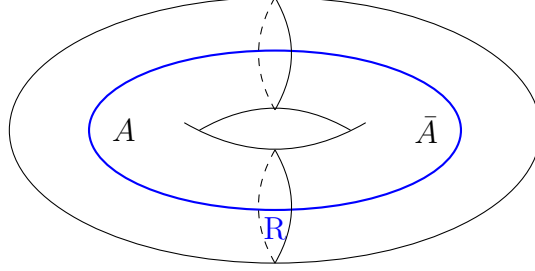


Figure E.2: Separated solid torus with a Wilson loop operator inserted.

Let us consider a single state without superposition  $|R\rangle_{CS} \in \mathcal{H}(T^2)$ , see Fig. E.1. We separate the solid torus into two regions  $A$  and  $\bar{A}$ , see Fig. E.2. An overlap  $\langle R_i | R_j \rangle$  is equivalent to a path integral on  $S^2 \times S^1$  with insertions of Wilson loops with representations  $R_j$  and  $\bar{R}_i$  along  $S^1$ .

To gain intuition on the replicated geometry, let us deform Fig. E.2 and compute  $\langle R_i | R_j \rangle$  performing the surgery [341]. One can understand  $A$  or  $\bar{A}$  as two three-dimensional half solid-balls,  $\mathbb{H}B_l^3$  and  $\mathbb{H}B_r^3$ , that are connected by a three-dimensional solid cylinder  $D^2 \times I$ . It is useful to note that the boundary of  $\mathbb{H}B^3$  consists of two two-dimensional disks glued along  $S^1$ ,  $\partial(\mathbb{H}B^3) = D_u^2 \cup D_d^2$ . To prepare a reduced density matrix, we prepare two copies of Fig. E.2 and glue  $\bar{A}_1$  and  $\bar{A}_2$  as follows. First, we glue  $\mathbb{H}B_{1,l}^3 \in \bar{A}_1$  and  $\mathbb{H}B_{2,l}^3 \in \bar{A}_2$  along  $D_{1,d}^2 \in \mathbb{H}B_{1,l}^3$  and  $D_{2,d}^2 \in \mathbb{H}B_{2,l}^3$ . As a result of this gluing, we again obtain a three dimensional half solid-ball whose boundary is  $S^2 = D_{1,u}^2 \cup D_{2,u}^2$ . Similarly, we can glue  $\mathbb{H}B_{1,r}^3 \in \bar{A}_1$  and  $\mathbb{H}B_{2,r}^3$  following the same procedure to obtain one more three dimensional half



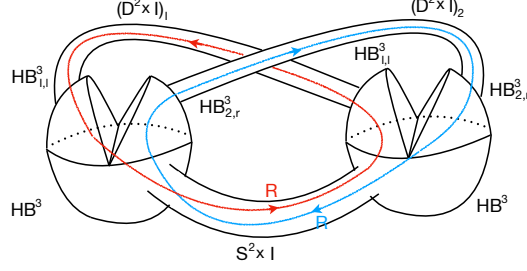


Figure E.3: Geometric representation of the reduced density matrix

solid ball. Finally, we glue two solid cylinders along  $S^1 \times I$  to produce  $S^2 \times I$ . As a result, we obtain the reduced density matrix  $\rho_A$ , c.f. Fig. E.3. By repeating the surgery for the region  $A$ ,  $\text{tr}_A(\rho_A)$  can be obtained similarly, c.f. Fig. E.4.

The geometric representation of  $\langle R_i | R_i \rangle$  constitutes of two large  $S^3$ 's, two thin  $S^3$ 's hosting the Wilson loops [112]. Note that one can pinch the end points of  $S^2 \times I$  to deform the tube into  $S^3$  glued to the large  $S^3$ 's.

Because each one of the small large  $S^3$ 's is glued along two  $S^2$ , from (E.46) we obtain

$$\text{tr} \rho_A(R) = \langle R_i | R_i \rangle = \frac{Z(S^3; R_i)^2 Z(S^3; \bar{R}_i)^2}{Z(S^3; R_i)^2 Z(S^3; \bar{R}_i)^2} = 1. \quad (\text{E.49})$$

An  $n$ -sheeted copy of E.4 can be similarly obtained by the surgery operation. Each replication adds two Wilson loops,  $R_i$  and  $\bar{R}_i$ , each of which is going through two thin  $S^3$ 's successively. As a result, the  $n$ -sheeted copy contains  $2 + 2n$   $S^3$ 's and the large  $S^3$ 's are connected to the thin  $S^3$ 's via gluing along  $4n$   $S^2$ 's. Hence,

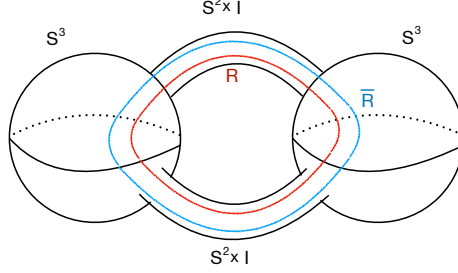


Figure E.4: Geometric representation of  $Z_1$ .

we obtain

$$\text{tr} \rho_A(R)^n = Z(S; R_i)^{1-n} Z(S; \bar{R}_i)^{1-n}. \quad (\text{E.50})$$

## E.5 Wilson loops in AdS/CFT

In this section, we want to further explain that the open/closed duality between the Hartle-Hawking states in each duality frame exhibited in the previous sections is not special to topological string theory. In fact, it has striking similarity to the AdS/CFT correspondence [251, 300]. We first review the holographic dictionary between Wilson loops in four-dimensional  $\mathcal{N} = 4$   $SU(N)$  super Yang-Mills theory (SYM<sub>4</sub>) and worldsheets in  $AdS_5$ . Then we argue that the duality between the Wilson loops and the worldsheets is the AdS/CFT analogue of the duality between the HH states in closed/open topological string theories.

Let's begin with the Wilson lines in  $\mathcal{N} = 4$   $SU(N)$  SYM<sub>4</sub>, in particular in the

fundamental representation. The Wilson lines in the fundamental representation are interpreted as world lines of heavy quarks in  $\text{SYM}_4$  as follows. The Wilson lines can be introduced to  $\text{SYM}_4$ , in string theory, by first placing  $N + 1$  D3-branes to get a  $SU(N + 1)$  SYM and then displacing one of the D3-branes. The separated D3-brane at distance  $d$  probes the background generated by the  $N$  D3-branes. The open string connecting  $N$  D3-brane stack and the probe brane breaks the gauge symmetry from  $SU(N + 1)$  to  $SU(N) \times U(1)$ . The boundary of the worldsheet in the  $N$  D-branes stack can be naturally understood as a Wilson loop in the fundamental representation. On a similar note, the end point of the open string in the  $N$  D-brane stack can be understood as a heavy quark in the  $SU(N)$   $\text{SYM}_4$ . Thus, the worldline of the heavy quark in the  $\text{SYM}_4$  corresponds to a Wilson loop in the fundamental representation.

We can ask for the closed string dual by invoking the geometric transition to replace the  $N$  D-branes with the non-trivial background  $AdS_5 \times S^5$ . The string worldsheet connecting the stack  $N$  D-branes and the probe D-brane, after the geometric transition, remains to be a string worldsheet ending on the probe D-brane. Once we identify the boundary of  $AdS_5$  with where the  $\text{SYM}_4$  is, these two different point of views provide us the Wilson loop/worldsheet duality in AdS/CFT. Later, the duality was generalized by [157] beyond the fundamental representation to all representations.

It was suggested in [161] and later shown by [285, 156, 318] that the duality between the worldsheet and the Wilson loops continues to hold in topological string theory under geometric transitions. The similarity and differences of the dualities in these two cases can be seen directly by comparing Fig. 7.20 and Fig. 7.21, and summarized in the table below.

	Type IIB Superstring	Topological string
Open string geometry	$\mathbb{R}^{1,9}$	Deformed conifold
Dynamical brane topology	$\mathbb{R}^{1,3}$	$S^3$
Target space field theory	$\text{SYM}_4(\text{worldvolume EFT})$	Chern-Simons theory(exact)
Closed string geometry	$AdS_5 \times S^5(\text{decoupling limit})$	Resolved conifold
Probe brane topology	$\mathbb{R}^{1,3}$	$\mathbb{C} \times S^1$
External heavy particles	Heavy quarks	Anyons
Where probe brane ends	$\mathbb{R}^{1,3}$ at infinity of $AdS_5$	$S^3$ at infinity of resolved conifold

So the correspondence between the entanglement entropy from the Wilson loop/worldsheet duality is in the same spirit as [244]. However, we are not looking at the extra entanglement entropy from a single probe Wilson loop, we are instead calculating the entanglement entropy from a superposition of Wilson loops that build up a geometrical dual spacetime!

## BIBLIOGRAPHY

- [1] Lars Aalsma, Magnus Tournoy, Jan Pieter Van Der Schaar, and Bert Ver-cnocke. Supersymmetric embedding of antibrane polarization. *Phys. Rev.*, D98(8):086019, 2018.
- [2] Mina Aganagic, Robbert Dijkgraaf, Albrecht Klemm, Marcos Marino, and Cumrun Vafa. Topological strings and integrable hierarchies. *Commun. Math. Phys.*, 261:451–516, 2006.
- [3] Mina Aganagic, Albrecht Klemm, Marcos Mariño, and Cumrun Vafa. The Topological Vertex. *Communications in Mathematical Physics*, 254(2):425–478, March 2005.
- [4] Mina Aganagic, Albrecht Klemm, Marcos Marino, and Cumrun Vafa. The Topological vertex. *Commun. Math. Phys.*, 254:425–478, 2005.
- [5] Mina Aganagic, Marcos Mariño, and Cumrun Vafa. All Loop Topological String Amplitudes from Chern-Simons Theory. *Communications in Mathematical Physics*, 247(2):467–512, January 2004.
- [6] Mina Aganagic, Marcos Marino, and Cumrun Vafa. All loop topological string amplitudes from Chern-Simons theory. *Commun. Math. Phys.*, 247:467–512, 2004.
- [7] Mina Aganagic, Takuya Okuda, and Hiroshi Ooguri. Quantum entanglement of baby universes. *Nuclear Physics B*, 778(1-2):36–68, August 2007.
- [8] Mina Aganagic, Hiroshi Ooguri, Natalia Saulina, and Cumrun Vafa. Black holes, q-deformed 2d Yang-Mills, and non-perturbative topological strings. *Nucl. Phys.*, B715:304–348, 2005.
- [9] Mina Aganagic, Hiroshi Ooguri, Natalia Saulina, and Cumrun Vafa. Black holes, q-deformed 2d Yang Mills, and non-perturbative topological strings. *Nuclear Physics B*, 715(1):304–348, May 2005.
- [10] Jeremías Aguilera-Damia, Diego H. Correa, Francesco Fucito, Victor I. Giraldo-Rivera, Jose F. Morales, and Leopoldo A. Pando Zayas. Strings in Bubbling Geometries and Dual Wilson Loop Correlators. *JHEP*, 12:109, 2017.

- [11] Ofer Aharony, Yaron E. Antebi, and Micha Berkooz. Open string moduli in KKLT compactifications. *Phys. Rev.*, D72:106009, 2005.
- [12] Y. Akrami et al. Planck 2018 results. X. Constraints on inflation. 2018.
- [13] Ahmed Almheiri, Thomas Hartman, Juan Maldacena, Edgar Shaghoulian, and Amirhossein Tajdini. Replica wormholes and the entropy of Hawking radiation. *Journal of High Energy Physics*, 2020(5):13, May 2020.
- [14] Maximilian Arends, Arthur Hebecker, Konrad Heimpel, Sebastian C. Kraus, Dieter Lust, Christoph Mayrhofer, Christoph Schick, and Timo Weigand. D7-Brane Moduli Space in Axion Monodromy and Fluxbrane Inflation. *Fortsch. Phys.*, 62:647–702, 2014.
- [15] Riccardo Argurio, Matteo Bertolini, Sebastian Franco, and Shamit Kachru. Gauge/gravity duality and meta-stable dynamical supersymmetry breaking. *JHEP*, 01:083, 2007.
- [16] Riccardo Argurio, Matteo Bertolini, Sebastián Franco, Eduardo García-Valdecasas, Shani Meynet, Antoine Pasternak, and Valdo Tatitscheff. Dimers, Orientifolds and Stability of Supersymmetry Breaking Vacua. 7 2020.
- [17] Riccardo Argurio, Matteo Bertolini, Sebastián Franco, Eduardo García-Valdecasas, Shani Meynet, Antoine Pasternak, and Valdo Tatitscheff. The Octagon and the Non-Supersymmetric String Landscape. 5 2020.
- [18] Riccardo Argurio, Matteo Bertolini, Shani Meynet, and Antoine Pasternak. On supersymmetry breaking vacua from D-branes at orientifold singularities. *JHEP*, 12:145, 2019.
- [19] Nima Arkani-Hamed, Lubos Motl, Alberto Nicolis, and Cumrun Vafa. The String landscape, black holes and gravity as the weakest force. *JHEP*, 06:060, 2007.
- [20] Jay Armas, Nam Nguyen, Vasilis Niarchos, Niels A. Obers, and Thomas Van Riet. Meta-stable non-extremal anti-branes. *Phys. Rev. Lett.*, 122(18):181601, 2019.
- [21] Sujay Ashok and Michael R. Douglas. Counting flux vacua. *JHEP*, 01:060, 2004.

- [22] Michael F Atiyah. Topological quantum field theory. *Publications Mathématiques de l'IHÉS*, 68:175–186, 1988.
- [23] Vijay Balasubramanian, Per Berglund, Joseph P. Conlon, and Fernando Quevedo. Systematics of moduli stabilisation in Calabi-Yau flux compactifications. *JHEP*, 03:007, 2005.
- [24] Vijay Balasubramanian and Onkar Parrikar. Remarks on entanglement entropy in string theory. *Phys. Rev. D*, 97:066025, Mar 2018.
- [25] Victor V. Batyrev. Dual polyhedra and mirror symmetry for Calabi-Yau hypersurfaces in toric varieties. *J. Alg. Geom.*, 3:493–545, 1994.
- [26] Daniel Baumann, Anatoly Dymarsky, Shamit Kachru, Igor R. Klebanov, and Liam McAllister. Holographic Systematics of D-brane Inflation. *JHEP*, 03:093, 2009.
- [27] Daniel Baumann, Anatoly Dymarsky, Shamit Kachru, Igor R. Klebanov, and Liam McAllister. D3-brane Potentials from Fluxes in AdS/CFT. *JHEP*, 06:072, 2010.
- [28] Daniel Baumann, Anatoly Dymarsky, Igor R. Klebanov, Juan Martin Maldacena, Liam P. McAllister, and Arvind Murugan. On D3-brane Potentials in Compactifications with Fluxes and Wrapped D-branes. *JHEP*, 11:031, 2006.
- [29] Daniel Baumann, Anatoly Dymarsky, Igor R. Klebanov, and Liam McAllister. Towards an Explicit Model of D-brane Inflation. *JCAP*, 0801:024, 2008.
- [30] Daniel Baumann and Liam McAllister. *Inflation and String Theory*. Cambridge University Press, 2014.
- [31] Florent Baume and Eran Palti. Backreacted Axion Field Ranges in String Theory. *JHEP*, 08:043, 2016.
- [32] Iosif Bena, Emilian Dudas, Mariana Graña, and Severin Lust. Uplifting Runaways. *Fortsch. Phys.*, 67(1-2):1800100, 2019.
- [33] Iosif Bena, Gregory Giecold, Mariana Grana, and Nick Halmagyi. On The Inflaton Potential From Antibranes in Warped Throats. *JHEP*, 07:140, 2012.

- [34] Iosif Bena, Gregory Giecold, Mariana Grana, Nick Halmagyi, and Stefano Massai. On Metastable Vacua and the Warped Deformed Conifold: Analytic Results. *Class. Quant. Grav.*, 30:015003, 2013.
- [35] Iosif Bena, Gregory Giecold, Mariana Grana, Nick Halmagyi, and Stefano Massai. The backreaction of anti-D3 branes on the Klebanov-Strassler geometry. *JHEP*, 06:060, 2013.
- [36] Iosif Bena, Mariana Grana, and Nick Halmagyi. On the Existence of Metastable Vacua in Klebanov-Strassler. *JHEP*, 09:087, 2010.
- [37] Iosif Bena, Mariana Graña, Nicolas Kovensky, and Ander Retolaza. Kähler moduli stabilization from ten dimensions. *JHEP*, 10:200, 2019.
- [38] Iman Benmachiche and Thomas W. Grimm. Generalized N=1 orientifold compactifications and the Hitchin functionals. *Nucl. Phys.*, B748:200–252, 2006.
- [39] Marcus Berg, Michael Haack, and Boris Kors. On the moduli dependence of nonperturbative superpotentials in brane inflation. 2004.
- [40] Marcus Berg, Michael Haack, and Boris Kors. Loop corrections to volume moduli and inflation in string theory. *Phys. Rev.*, D71:026005, 2005.
- [41] Marcus Berg, David Marsh, Liam McAllister, and Enrico Pajer. Sequestering in String Compactifications. *JHEP*, 06:134, 2011.
- [42] E. Bergshoeff, M. de Roo, B. de Wit, and P. van Nieuwenhuizen. Ten-Dimensional Maxwell-Einstein Supergravity, its Currents, and the Issue of its Auxiliary Fields. *Nucl. Phys.*, B195:97, 1982.
- [43] Eric Bergshoeff, Renata Kallosh, Tomas Ortin, Diederik Roest, and Antoine Van Proeyen. New formulations of D = 10 supersymmetry and D8 - O8 domain walls. *Class. Quant. Grav.*, 18:3359–3382, 2001.
- [44] Micha Berkooz, Mikhail Isachenkov, Vladimir Narovlansky, and Genis Torrents. Towards a full solution of the large N double-scaled SYK model. *JHEP*, 03:079, 2019.
- [45] M. Bershadsky, S. Cecotti, H. Ooguri, and C. Vafa. Kodaira-Spencer theory of gravity and exact results for quantum string amplitudes. *Commun. Math. Phys.*, 165:311–428, 1994.



- [46] M. Bershadsky, V. Sadov, and C. Vafa. D-Branes and Topological Field Theories. *Nucl. Phys.*, B463:420–434, 1996.
- [47] Massimo Bianchi, Andres Collinucci, and Luca Martucci. Magnetized E3-brane instantons in F-theory. *JHEP*, 12:045, 2011.
- [48] Massimo Bianchi, Gianluca Inverso, and Luca Martucci. Brane instantons and fluxes in F-theory. *JHEP*, 07:037, 2013.
- [49] S. Bielleman, L. E. Ibanez, F. G. Pedro, and I. Valenzuela. Multifield Dynamics in Higgs-otic Inflation. *JHEP*, 01:128, 2016.
- [50] Sjoerd Bielleman, Luis E. Ibanez, Francisco G. Pedro, Irene Valenzuela, and Clemens Wieck. Higgs-otic Inflation and Moduli Stabilization. *JHEP*, 02:073, 2017.
- [51] Andreas Blommaert, Thomas G. Mertens, and Henri Verschelde. Fine structure of Jackiw-Teitelboim quantum gravity. *Journal of High Energy Physics*, 2019(9):66, September 2019.
- [52] Ralph Blumenhagen, Volker Braun, Thomas W. Grimm, and Timo Weigand. GUTs in Type IIB Orientifold Compactifications. *Nucl. Phys. B*, 815:1–94, 2009.
- [53] Ralph Blumenhagen, Mirjam Cvetič, Shamit Kachru, and Timo Weigand. D-Brane Instantons in Type II Orientifolds. *Ann. Rev. Nucl. Part. Sci.*, 59:269–296, 2009.
- [54] Ralph Blumenhagen, Daniela Herschmann, and Florian Wolf. String Moduli Stabilization at the Conifold. *JHEP*, 08:110, 2016.
- [55] Ralph Blumenhagen, Daniel Kläwer, and Lorenz Schlechter. Swampland Variations on a Theme by KKLT. *JHEP*, 05:152, 2019.
- [56] Ralph Blumenhagen, Boris Kors, Dieter Lust, and Stephan Stieberger. Four-dimensional String Compactifications with D-Branes, Orientifolds and Fluxes. *Phys. Rept.*, 445:1–193, 2007.
- [57] Ralph Blumenhagen, Irene Valenzuela, and Florian Wolf. The Swampland Conjecture and F-term Axion Monodromy Inflation. *JHEP*, 07:145, 2017.

- [58] Konstantin Bobkov, Volker Braun, Piyush Kumar, and Stuart Raby. Stabilizing All Kahler Moduli in Type IIB Orientifolds. *JHEP*, 12:056, 2010.
- [59] R. Bousso and J. Polchinski. Quantization of Four-form Fluxes and Dynamical Neutralization of the Cosmological Constant. *JHEP*, 06:006, 2000.
- [60] Raphael Bousso and Joseph Polchinski. Quantization of four form fluxes and dynamical neutralization of the cosmological constant. *JHEP*, 06:006, 2000.
- [61] Andreas P. Braun, Cody Long, Liam McAllister, Michael Stillman, and Benjamin Sung. The Hodge Numbers of Divisors of Calabi-Yau Threefold Hypersurfaces. 12 2017.
- [62] Jim Bryan and Rahul Pandharipande. Curves in Calabi-Yau 3 folds and topological quantum field theory. 6 2003.
- [63] Jim Bryan and Rahul Pandharipande. The Local Gromov-Witten theory of curves. *J. Am. Math. Soc.*, 21:101–136, 2008.
- [64] P.V. Buividovich and M.I. Polikarpov. Entanglement entropy in gauge theories and the holographic principle for electric strings. *Phys. Lett. B*, 670:141–145, 2008.
- [65] Cliff P. Burgess, James M. Cline, Keshav Dasgupta, and Hassan Firouzjahi. Uplifting and Inflation with D3 Branes. *JHEP*, 03:027, 2007.
- [66] Pablo G. Camara, L. E. Ibanez, and A. M. Uranga. Flux-induced SUSY-breaking soft terms on D7-D3 brane systems. *Nucl. Phys.*, B708:268–316, 2005.
- [67] Philip Candelas and Xenia C. de la Ossa. Comments on Conifolds. *Nucl. Phys. B*, 342:246–268, 1990.
- [68] Philip Candelas, Xenia C. De La Ossa, Paul S. Green, and Linda Parkes. A Pair of Calabi-Yau manifolds as an exactly soluble superconformal theory. *AMS/IP Stud. Adv. Math.*, 9:31–95, 1998.
- [69] Philip Candelas, Anamaria Font, Sheldon H. Katz, and David R. Morrison. Mirror symmetry for two parameter models. 2. *Nucl. Phys.*, B429:626–674, 1994.

- [70] Philip Candelas, Paul S. Green, and Tristan Hubsch. Rolling Among Calabi-Yau Vacua. *Nucl. Phys. B*, 330:49, 1990.
- [71] Federico Carta, Jakob Moritz, and Alexander Westphal. Gaugino condensation and small uplifts in KKLT. *JHEP*, 08:141, 2019.
- [72] Anna Ceresole, Gianguido Dall’Agata, and Riccardo D’Auria. K K spectroscopy of type IIB supergravity on  $\text{AdS}(5) \times T^{**}11$ . *JHEP*, 11:009, 1999.
- [73] Anna Ceresole, Gianguido Dall’Agata, Riccardo D’Auria, and Sergio Ferrara. Spectrum of type IIB supergravity on  $\text{AdS}(5) \times T^{**}11$ : Predictions on  $N=1$  SCFT’s. *Phys. Rev.*, D61:066001, 2000.
- [74] Michele Cicoli, Joseph P. Conlon, Anshuman Maharana, and Fernando Quevedo. A Note on the Magnitude of the Flux Superpotential. *JHEP*, 01:027, 2014.
- [75] Diego Cohen-Maldonado, Juan Diaz, Thomas van Riet, and Bert Vercnocke. Observations on fluxes near anti-branes. *JHEP*, 01:126, 2016.
- [76] Alex Cole, Andreas Schachner, and Gary Shiu. Searching the Landscape of Flux Vacua with Genetic Algorithms. *JHEP*, 11:045, 2019.
- [77] Sidney R. Coleman. Black Holes as Red Herrings: Topological Fluctuations and the Loss of Quantum Coherence. *Nucl. Phys. B*, 307:867–882, 1988.
- [78] Andres Collinucci, Frederik Denef, and Mboyo Esole. D-brane Deconstructions in IIB Orientifolds. *JHEP*, 02:005, 2009.
- [79] A. Connes. *Noncommutative Geometry*. Elsevier Science, 1995.
- [80] Cesar Fierro Cota, Albrecht Klemm, and Thorsten Schimannek. Topological strings on genus one fibered Calabi-Yau 3-folds and string dualities. *JHEP*, 11:170, 2019.
- [81] Romain Couvreur, Jesper Lykke Jacobsen, and Hubert Saleur. Entanglement in nonunitary quantum critical spin chains. *Phys. Rev. Lett.*, 119(4):040601, 2017.
- [82] Romain Couvreur, Jesper Lykke Jacobsen, and Hubert Saleur. Entanglement in nonunitary quantum critical spin chains. *Physical Review Letters*, 119(4), Jul 2017.

- [83] Brad Cownden, Andrew R. Frey, M. C. David Marsh, and Bret Underwood. Dimensional Reduction for D3-brane Moduli. *JHEP*, 12:139, 2016.
- [84] Atish Dabholkar. Strings on a cone and black hole entropy. *Nuclear Physics B*, 439:650–664, Feb 1995.
- [85] Diptarka Das and Shouvik Datta. Universal features of left-right entanglement entropy. *Phys. Rev. Lett.*, 115(13):131602, 2015.
- [86] Keshav Dasgupta, Carlos Herdeiro, Shinji Hirano, and Renata Kallosh. D3 / D7 inflationary model and M theory. *Phys. Rev.*, D65:126002, 2002.
- [87] Keshav Dasgupta, Jonathan P. Hsu, Renata Kallosh, Andrei D. Linde, and Marco Zagermann. D3/D7 brane inflation and semilocal strings. *JHEP*, 08:030, 2004.
- [88] Sebastian de Haro, Sanjaye Ramgoolam, and Alessandro Torrielli. Large N expansion of q-deformed two-dimensional Yang-Mills theory and Hecke algebras. *Commun. Math. Phys.*, 273:317–355, 2007.
- [89] Sebastian de Haro, Sanjaye Ramgoolam, and Alessandro Torrielli. Large n expansion of q-deformed two-dimensional yang-mills theory and hecke algebras. *Communications in Mathematical Physics*, 273(2):317–355, May 2007.
- [90] B. De Wit, D. J. Smit, and N. D. Hari Dass. Residual supersymmetry of compactified  $d = 10$  supergravity. *Nuclear Physics B*, 283:165–191, 1987.
- [91] Mykola Dedushenko and Edward Witten. Some Details On The Gopakumar-Vafa and Ooguri-Vafa Formulas. *Adv. Theor. Math. Phys.*, 20:1–133, 2016.
- [92] Mehmet Demirtas, Manki Kim, Liam McAllister, and Jakob Moritz. Vacua with Small Flux Superpotential. *Phys. Rev. Lett.*, 124(21):211603, 2020.
- [93] Mehmet Demirtas, Liam McAllister, and Andres Rios-Tascon. *CYTools: A Software Package for Analyzing Calabi-Yau Hypersurfaces in Toric Varieties*, to appear.
- [94] F. Denef, M. R. Douglas, B. Florea, A. Grassi, and S. Kachru. Fixing All Moduli in a Simple F-Theory Compactification. *Adv. Theor. Math. Phys.*, 9:861–929, 2005.

- [95] F. Denef, M. R. Douglas, and S. Kachru. Physics of String Flux Compactifications. *Ann. Rev. Nucl. Part. Sci.*, 57:119–144, 2007.
- [96] Frederik Denef. Les Houches Lectures on Constructing String Vacua. *Les Houches*, 87:483–610, 2008.
- [97] Frederik Denef and Michael R. Douglas. Distributions of flux vacua. *JHEP*, 05:72, 2004.
- [98] Frederik Denef and Michael R. Douglas. Distributions of flux vacua. *JHEP*, 05:072, 2004.
- [99] Frederik Denef and Michael R. Douglas. Distributions of nonsupersymmetric flux vacua. *JHEP*, 03:061, 2005.
- [100] Frederik Denef, Michael R. Douglas, and Bogdan Florea. Building a better racetrack. *JHEP*, 06:034, 2004.
- [101] Frederik Denef, Michael R. Douglas, Bogdan Florea, Antonella Grassi, and Shamit Kachru. Fixing all moduli in a simple f-theory compactification. *Adv. Theor. Math. Phys.*, 9(6):861–929, 2005.
- [102] Oliver DeWolfe and Steven B. Giddings. Scales and hierarchies in warped compactifications and brane worlds. *Phys. Rev.*, D67:066008, 2003.
- [103] Oliver DeWolfe, Shamit Kachru, and Michael Mulligan. A Gravity Dual of Metastable Dynamical Supersymmetry Breaking. *Phys. Rev.*, D77:065011, 2008.
- [104] Oliver DeWolfe, Liam McAllister, Gary Shiu, and Bret Underwood. D3-brane Vacua in Stabilized Compactifications. *JHEP*, 09:121, 2007.
- [105] Duiliu-Emanuel Diaconescu, Bogdan Florea, and Antonella Grassi. Geometric transitions and open string instantons. *Adv. Theor. Math. Phys.*, 6:619–642, 2003.
- [106] Robbert Dijkgraaf, Rajesh Gopakumar, Hiroshi Ooguri, and Cumrun Vafa. Baby universes in string theory. *Phys. Rev. D*, 73(6):066002, March 2006.
- [107] Robbert Dijkgraaf, Sergei Gukov, Andrew Neitzke, and Cumrun Vafa. Topological M-theory as unification of form theories of gravity. *Adv. Theor. Math. Phys.*, 9(4):603–665, 2005.

- [108] Robbert Dijkgraaf and Cumrun Vafa. Matrix models, topological strings, and supersymmetric gauge theories. *Nucl. Phys. B*, 644:3–20, 2002.
- [109] Robbert Dijkgraaf and Cumrun Vafa. Matrix models, topological strings, and supersymmetric gauge theories. *Nuclear Physics B*, 644(1):3–20, November 2002.
- [110] Michael Dine, R. Rohm, N. Seiberg, and Edward Witten. Gluino Condensation in Superstring Models. *Phys. Lett.*, 156B:55–60, 1985.
- [111] Michael Dine and Nathan Seiberg. Is the Superstring Weakly Coupled? *Phys. Lett. B*, 162:299–302, 1985.
- [112] Shiyong Dong, Eduardo Fradkin, Robert G. Leigh, and Sean Nowling. Topological Entanglement Entropy in Chern-Simons Theories and Quantum Hall Fluids. *JHEP*, 05:016, 2008.
- [113] Xi Dong, Bart Horn, Eva Silverstein, and Alexander Westphal. Simple exercises to flatten your potential. *Phys. Rev.*, D84:026011, 2011.
- [114] William Donnelly. Decomposition of entanglement entropy in lattice gauge theory. *Phys. Rev. D*, 85:085004, 2012.
- [115] William Donnelly. Entanglement entropy and nonabelian gauge symmetry. *Class. Quant. Grav.*, 31(21):214003, 2014.
- [116] William Donnelly and Laurent Freidel. Local subsystems in gauge theory and gravity. *JHEP*, 09:102, 2016.
- [117] William Donnelly, Yikun Jiang, Manki Kim, and Gabriel Wong. Entanglement entropy and edge modes in topological string theory: II.
- [118] William Donnelly, Yikun Jiang, Manki Kim, and Gabriel Wong. Entanglement entropy and edge modes in topological string theory: I. *arXiv e-prints*, page arXiv:2010.15737, October 2020.
- [119] William Donnelly, Sydney Timmerman, and Nicolás Valdés-Meller. Entanglement entropy and the large  $N$  expansion of two-dimensional Yang-Mills theory. *JHEP*, 04:182, 2020.
- [120] William Donnelly and Aron C. Wall. Entanglement entropy of electromagnetic edge modes. *Phys. Rev. Lett.*, 114(11):111603, 2015.

- [121] William Donnelly and Aron C. Wall. Geometric entropy and edge modes of the electromagnetic field. *Phys. Rev. D*, 94(10):104053, 2016.
- [122] William Donnelly and Gabriel Wong. Entanglement branes in a two-dimensional string theory. *JHEP*, 09:097, 2017.
- [123] William Donnelly and Gabriel Wong. Entanglement branes, modular flow, and extended topological quantum field theory. *JHEP*, 10:016, 2019.
- [124] Michael R. Douglas and Shamit Kachru. Flux Compactification. *Rev. Mod. Phys.*, 79:733–796, 2007.
- [125] Michael R. Douglas and Shamit Kachru. Flux compactification. *Rev. Mod. Phys.*, 79:733–796, 2007.
- [126] Michael R. Douglas and Nikita A. Nekrasov. Noncommutative field theory. *Reviews of Modern Physics*, 73(4):977–1029, October 2001.
- [127] Michael R. Douglas, Jessie Shelton, and Gonzalo Torroba. Warping and supersymmetry breaking. 4 2007.
- [128] Michael R. Douglas, Bernard Shiffman, and Steve Zelditch. Critical points and supersymmetric vacua. *Commun. Math. Phys.*, 252:325–358, 2004.
- [129] Michael R. Douglas, Bernard Shiffman, and Steve Zelditch. Critical points and supersymmetric vacua, II: Asymptotics and extremal metrics. *J. Diff. Geom.*, 72(3):381–427, 2006.
- [130] Emilian Dudas and Severin Lüst. An update on moduli stabilization with antibrane uplift. 12 2019.
- [131] Thomas Dupic, Benoit Estienne, and Yacine Ikhlef. Entanglement entropies of minimal models from null-vectors. *SciPost Physics*, 4(6), Jun 2018.
- [132] Maïté Dupuis, Laurent Freidel, Florian Girelli, Abdulmajid Osumanu, and Julian Rennert. On the origin of the quantum group symmetry in 3d quantum gravity. *arXiv e-prints*, page arXiv:2006.10105, June 2020.
- [133] A. Dymarsky, Steven S. Gubser, Z. Guralnik, and Juan Martin Maldacena. Calibrated surfaces and supersymmetric Wilson loops. *JHEP*, 09:057, 2006.

- [134] Anatoly Dymarsky. On gravity dual of a metastable vacuum in Klebanov-Strassler theory. *JHEP*, 05:053, 2011.
- [135] Anatoly Dymarsky and Luca Martucci. D-brane non-perturbative effects and geometric deformations. *JHEP*, 04:061, 2011.
- [136] Shmuel Elitzur, Gregory W. Moore, Adam Schwimmer, and Nathan Seiberg. Remarks on the Canonical Quantization of the Chern-Simons-Witten Theory. *Nucl. Phys. B*, 326:108–134, 1989.
- [137] Netta Engelhardt and Aron C. Wall. Quantum extremal surfaces: holographic entanglement entropy beyond the classical regime. *Journal of High Energy Physics*, 2015:73, January 2015.
- [138] Thomas Faulkner, Aitor Lewkowycz, and Juan Maldacena. Quantum corrections to holographic entanglement entropy. *JHEP*, 11:074, 2013.
- [139] Thomas Faulkner, Aitor Lewkowycz, and Juan Maldacena. Quantum corrections to holographic entanglement entropy. *Journal of High Energy Physics*, 2013:74, November 2013.
- [140] Raphael Flauger, Liam McAllister, Enrico Pajer, Alexander Westphal, and Gang Xu. Oscillations in the CMB from Axion Monodromy Inflation. *JCAP*, 1006:009, 2010.
- [141] Jackson R. Fliss and Robert G. Leigh. Interfaces and the extended Hilbert space of Chern-Simons theory. 4 2020.
- [142] Daniel S. Freed and Edward Witten. Anomalies in string theory with D-branes. *Asian J. Math.*, 3:819, 1999.
- [143] Katherine Freese, Joshua A. Frieman, and Angela V. Olinto. Natural inflation with pseudo - Nambu-Goldstone bosons. *Phys. Rev. Lett.*, 65:3233–3236, 1990.
- [144] Sohang Gandhi, Liam McAllister, and Stefan Sjors. *to appear*.
- [145] Sohang Gandhi, Liam McAllister, and Stefan Sjors. A Toolkit for Perturbing Flux Compactifications. *JHEP*, 12:053, 2011.
- [146] Ori J. Ganor. A Note on zeros of superpotentials in F theory. *Nucl. Phys.*, B499:55–66, 1997.



- [147] F. F. Gautason, V. Van Hemelryck, and T. Van Riet. The Tension between 10D Supergravity and dS Uplifts. *Fortsch. Phys.*, 67(1-2):1800091, 2019.
- [148] F.F. Gautason, V. Van Hemelryck, T. Van Riet, and G. Venken. A 10d view on the KKLT AdS vacuum and uplifting. *JHEP*, 06:074, 2020.
- [149] Simon A. Gentle and Michael Gutperle. Entanglement entropy of wilson loops: Holography and matrix models. *Physical Review D*, 90(6), Sep 2014.
- [150] G. W. Gibbons and S. W. Hawking. Action integrals and partition functions in quantum gravity. *Phys. Rev. D*, 15:2752–2756, May 1977.
- [151] Steven B. Giddings, Shamit Kachru, and Joseph Polchinski. Hierarchies from fluxes in string compactifications. *Phys. Rev.*, D66:106006, 2002.
- [152] Steven B. Giddings and Anshuman Maharana. Dynamics of warped compactifications and the shape of the warped landscape. *Phys. Rev. D*, 73:126003, 2006.
- [153] Steven B. Giddings and Andrew Strominger. Loss of Incoherence and Determination of Coupling Constants in Quantum Gravity. *Nucl. Phys. B*, 307:854–866, 1988.
- [154] Steven B. Giddings and Andrew Strominger. Baby Universes, Third Quantization and the Cosmological Constant. *Nucl. Phys. B*, 321:481–508, 1989.
- [155] Alexander Giriyavets, Shamit Kachru, Prasanta K. Tripathy, and Sandip P. Trivedi. Flux compactifications on Calabi-Yau threefolds. *JHEP*, 04:003, 2004.
- [156] Jaume Gomis and Takuya Okuda. Wilson loops, geometric transitions and bubbling Calabi-Yau’s. *JHEP*, 02:083, 2007.
- [157] Jaume Gomis and Filippo Passerini. Holographic Wilson loops. *Journal of High Energy Physics*, 2006(8):074, August 2006.
- [158] Rajesh Gopakumar and Cumrun Vafa. M theory and topological strings. 1. 9 1998.
- [159] Rajesh Gopakumar and Cumrun Vafa. M theory and topological strings. 2. 12 1998.

- [160] Rajesh Gopakumar and Cumrun Vafa. Topological gravity as large N topological gauge theory. *Adv. Theor. Math. Phys.*, 2:413–442, 1998.
- [161] Rajesh Gopakumar and Cumrun Vafa. On the gauge theory / geometry correspondence. *AMS/IP Stud. Adv. Math.*, 23:45–63, 2001.
- [162] Mariana Grana. Flux compactifications in string theory: A comprehensive review. *Phys. Rept.*, 423:91–158, 2006.
- [163] Mariana Grana, Jan Louis, and Daniel Waldram. Hitchin functionals in N=2 supergravity. *JHEP*, 01:008, 2006.
- [164] Mariana Grana, Ruben Minasian, Michela Petrini, and Alessandro Tomasiello. Generalized structures of N=1 vacua. *JHEP*, 11:020, 2005.
- [165] Brian R. Greene, David R. Morrison, and Andrew Strominger. Black hole condensation and the unification of string vacua. *Nucl. Phys. B*, 451:109–120, 1995.
- [166] Brian R. Greene and M. R. Plesser. Duality in Calabi-Yau Moduli Space. *Nucl. Phys.*, B338:15–37, 1990.
- [167] Thomas W. Grimm, Max Kerstan, Eran Palti, and Timo Weigand. On Fluxed Instantons and Moduli Stabilisation in IIB Orientifolds and F-theory. *Phys. Rev. D*, 84:066001, 2011.
- [168] Thomas W. Grimm and Albrecht Klemm. U(1) Mediation of Flux Supersymmetry Breaking. *JHEP*, 10:077, 2008.
- [169] Thomas W. Grimm, Chongchuo Li, and Irene Valenzuela. Asymptotic Flux Compactifications and the Swampland. 2019.
- [170] Thomas W. Grimm and Jan Louis. The Effective action of N = 1 Calabi-Yau orientifolds. *Nucl. Phys. B*, 699:387–426, 2004.
- [171] Andrey Gromov and Raul A. Santos. Entanglement Entropy in 2D Non-abelian Pure Gauge Theory. *Phys. Lett. B*, 737:60–64, 2014.
- [172] David J. Gross and Washington Taylor. Two-dimensional QCD is a string theory. *Nucl. Phys. B*, 400:181–208, 1993.

- [173] E. Guadagnini, M. Martellini, and M. Mintchev. Braids and Quantum Group Symmetry in Chern-Simons Theory. *Nucl. Phys. B*, 336:581–609, 1990.
- [174] S. S. Gubser, I. R. Klebanov, and A. M. Polyakov. Gauge theory correlators from non-critical string theory. *Physics Letters B*, 428(1-2):105–114, May 1998.
- [175] Steven S. Gubser. Einstein manifolds and conformal field theories. *Phys. Rev.*, D59:025006, 1999.
- [176] Sergei Gukov, Cumrun Vafa, and Edward Witten. CFT’s from Calabi-Yau four folds. *Nucl. Phys.*, B584:69–108, 2000. [Erratum: Nucl. Phys.B608,477(2001)].
- [177] Michael Haack, Renata Kallosh, Axel Krause, Andrei D. Linde, Dieter Lust, and Marco Zagermann. Update of D3/D7-Brane Inflation on  $K3 \times T^{**2}/Z(2)$ . *Nucl. Phys.*, B806:103–177, 2009.
- [178] Yuta Hamada, Arthur Hebecker, Gary Shiu, and Pablo Soler. On brane gaugino condensates in 10d. *JHEP*, 04:008, 2019.
- [179] Yuta Hamada, Arthur Hebecker, Gary Shiu, and Pablo Soler. Understanding KKLT from a 10d perspective. *JHEP*, 06:019, 2019.
- [180] Daniel Harlow and Edgar Shaghoulian. Global symmetry, Euclidean gravity, and the black hole information problem. *arXiv e-prints*, page arXiv:2010.10539, October 2020.
- [181] J. B. Hartle and S. W. Hawking. Wave function of the universe. *Phys. Rev. D*, 28:2960–2975, Dec 1983.
- [182] Song He, Tokiro Numasawa, Tadashi Takayanagi, and Kento Watanabe. Notes on entanglement entropy in string theory. *Journal of High Energy Physics*, 2015:106, May 2015.
- [183] Arthur Hebecker, Daniel Junghans, and Andreas Schachner. Large Field Ranges from Aligned and Misaligned Winding. *JHEP*, 03:192, 2019.
- [184] Arthur Hebecker, Sebastian C. Kraus, Moritz Kuntzler, Dieter Lust, and Timo Weigand. Fluxbranes: Moduli Stabilisation and Inflation. *JHEP*, 01:095, 2013.

- [185] Arthur Hebecker, Sebastian C. Kraus, Dieter Lust, Stephan Steinfurt, and Timo Weigand. Fluxbrane Inflation. *Nucl. Phys.*, B854:509–551, 2012.
- [186] Arthur Hebecker, Sebastian C. Kraus, and Lukas T. Witkowski. D7-Brane Chaotic Inflation. *Phys. Lett.*, B737:16–22, 2014.
- [187] Arthur Hebecker, Sascha Leonhardt, Jakob Moritz, and Alexander Westphal. Thraxions: Ultralight Throat Axions. *JHEP*, 04:158, 2019.
- [188] Arthur Hebecker, Patrick Mangat, Fabrizio Rompineve, and Lukas T. Witkowski. Winding out of the Swamp: Evading the Weak Gravity Conjecture with F-term Winding Inflation? *Phys. Lett.*, B748:455–462, 2015.
- [189] Ben Heidenreich, Liam McAllister, and Gonzalo Torroba. Dynamic SU(2) Structure from Seven-branes. *JHEP*, 05:110, 2011.
- [190] Johannes Held, Dieter Lust, Fernando Marchesano, and Luca Martucci. DWSB in heterotic flux compactifications. *JHEP*, 06:090, 2010.
- [191] Mark P. Hertzberg, Shamit Kachru, Washington Taylor, and Max Tegmark. Inflationary Constraints on Type IIA String Theory. *JHEP*, 12:095, 2007.
- [192] Yoshinori Honma and Hajime Otsuka. On the Flux Vacua in F-theory Compactifications. *Phys. Lett.*, B774:225–228, 2017.
- [193] Yoshinori Honma and Hajime Otsuka. F-theory Flux Vacua and Attractor Equations. 2019.
- [194] Petr Horava and Edward Witten. Heterotic and type I string dynamics from eleven-dimensions. *Nucl. Phys. B*, 460:506–524, 1996.
- [195] Kentaro Hori, Richard Thomas, Sheldon Katz, Cumrun Vafa, Rahul Pandharipande, Albrecht Klemm, Ravi Vakil, and Eric Zaslow. *Mirror symmetry*, volume 1. American Mathematical Soc., 2003.
- [196] Petr Horava and Edward Witten. Heterotic and Type I string dynamics from eleven dimensions. *Nuclear Physics B*, 460(3):506–524, February 1996.
- [197] S. Hosono, A. Klemm, and S. Theisen. Lectures on mirror symmetry. *Lect. Notes Phys.*, 436:235–280, 1994.

- [198] S. Hosono, A. Klemm, S. Theisen, and Shing-Tung Yau. Mirror symmetry, mirror map and applications to Calabi-Yau hypersurfaces. *Commun. Math. Phys.*, 167:301–350, 1995.
- [199] S. Hosono, A. Klemm, S. Theisen, and Shing-Tung Yau. Mirror symmetry, mirror map and applications to complete intersection Calabi-Yau spaces. *AMS/IP Stud. Adv. Math.*, 1:545–606, 1996.
- [200] Min-Xin Huang. Recent Developments in Topological String Theory. *Sci. China Phys. Mech. Astron.*, 62(9):990001, 2019.
- [201] Min-xin Huang, Sheldon Katz, and Albrecht Klemm. Topological String on elliptic CY 3-folds and the ring of Jacobi forms. *JHEP*, 10:125, 2015.
- [202] Veronika E. Hubeny, Roji Pius, and Mukund Rangamani. Topological string entanglement. *JHEP*, 10:239, 2019.
- [203] Veronika E. Hubeny, Mukund Rangamani, and Tadashi Takayanagi. A covariant holographic entanglement entropy proposal. *Journal of High Energy Physics*, 2007(7):062, July 2007.
- [204] Ling Yan Hung and Gabriel Wong. Entanglement branes and factorization in conformal field theory. *arXiv e-prints*, page arXiv:1912.11201, December 2019.
- [205] Luis E. Ibanez, Fernando Marchesano, and Irene Valenzuela. Higgs-otic Inflation and String Theory. *JHEP*, 01:128, 2015.
- [206] Amer Iqbal, Can Kozçaz, and Cumrun Vafa. The refined topological vertex. *Journal of High Energy Physics*, 2009(10):069, October 2009.
- [207] Daniel Louis Jafferis. Bulk reconstruction and the Hartle-Hawking wavefunction. *arXiv e-prints*, page arXiv:1703.01519, March 2017.
- [208] Daniel Louis Jafferis and David K. Kolchmeyer. Entanglement Entropy in Jackiw-Teitelboim Gravity. 2019.
- [209] Kristan Jensen and Andreas Karch. The holographic dual of an EPR pair has a wormhole. *arXiv e-prints*, page arXiv:1307.1132, July 2013.
- [210] Kristan Jensen and Andy O’Bannon. Holography, entanglement entropy,

- and conformal field theories with boundaries or defects. *Phys. Rev. D*, 88(10):106006, November 2013.
- [211] Hans Jockers and Jan Louis. D-terms and F-terms from D7-brane fluxes. *Nucl. Phys.*, B718:203–246, 2005.
  - [212] Hans Jockers and Jan Louis. The Effective action of D7-branes in  $N = 1$  Calabi-Yau orientifolds. *Nucl. Phys.*, B705:167–211, 2005.
  - [213] Daniel N. Kabat. Black hole entropy and entropy of entanglement. *Nucl. Phys. B*, 453:281–299, 1995.
  - [214] Shamit Kachru, Renata Kallosh, Andrei D. Linde, Juan Martin Maldacena, Liam P. McAllister, and Sandip P. Trivedi. Towards inflation in string theory. *JCAP*, 0310:013, 2003.
  - [215] Shamit Kachru, Renata Kallosh, Andrei D. Linde, and Sandip P. Trivedi. De Sitter vacua in string theory. *Phys. Rev.*, D68:046005, 2003.
  - [216] Shamit Kachru, Renata Kallosh, Andrei D. Linde, and Sandip P. Trivedi. De Sitter vacua in string theory. *Phys. Rev.*, D68:046005, 2003.
  - [217] Shamit Kachru, Manki Kim, Liam McAllister, and Max Zimet. de Sitter Vacua from Ten Dimensions. 8 2019.
  - [218] Shamit Kachru, Liam McAllister, and Raman Sundrum. Sequestering in String Theory. *JHEP*, 10:013, 2007.
  - [219] Shamit Kachru, John Pearson, and Herman L. Verlinde. Brane / flux annihilation and the string dual of a nonsupersymmetric field theory. *JHEP*, 06:021, 2002.
  - [220] Shamit Kachru, Dusan Simic, and Sandip P. Trivedi. Stable Non-Supersymmetric Throats in String Theory. *JHEP*, 05:067, 2010.
  - [221] Renata Kallosh. Gaugino Condensation and Geometry of the Perfect Square. *Phys. Rev.*, D99(6):066003, 2019.
  - [222] Renata Kallosh, Amir-Kian Kashani-Poor, and Alessandro Tomasiello. Counting fermionic zero modes on M5 with fluxes. *JHEP*, 06:069, 2005.

- [223] Renata Kallosh, Lev Kofman, Andrei D. Linde, and Antoine Van Proeyen. Superconformal symmetry, supergravity and cosmology. *Class. Quant. Grav.*, 17:4269–4338, 2000. [Erratum: *Class. Quant. Grav.*21,5017(2004)].
- [224] Renata Kallosh and Dmitri Sorokin. Dirac action on M5 and M2 branes with bulk fluxes. *JHEP*, 05:005, 2005.
- [225] Nemanja Kaloper and Lorenzo Sorbo. A Natural Framework for Chaotic Inflation. *Phys. Rev. Lett.*, 102:121301, 2009.
- [226] Vadim Kaplunovsky and Jan Louis. Field dependent gauge couplings in locally supersymmetric effective quantum field theories. *Nucl. Phys.*, B422:57–124, 1994.
- [227] Sheldon Katz and Chiu-Chu Melissa Liu. Enumerative geometry of stable maps with Lagrangian boundary conditions and multiple covers of the disc. *arXiv Mathematics e-prints*, page math/0103074, March 2001.
- [228] Jihn E. Kim, Hans Peter Nilles, and Marco Peloso. Completing natural inflation. *JCAP*, 0501:005, 2005.
- [229] Manki Kim and Liam McAllister. Monodromy Charge in D7-brane Inflation. 2018.
- [230] Elias Kiritsis and Vasilis Niarchos. Large-N limits of 2d CFTs, quivers and  $\text{AdS}_3$  duals. *Journal of High Energy Physics*, 2011:113, April 2011.
- [231] Alexei Kitaev and S. Josephine Suh. Statistical mechanics of a two-dimensional black hole. *Journal of High Energy Physics*, 2019(5), May 2019.
- [232] Igor R. Klebanov and Arvind Murugan. Gauge/Gravity Duality and Warped Resolved Conifold. *JHEP*, 03:042, 2007.
- [233] Igor R. Klebanov and Matthew J. Strassler. Supergravity and a confining gauge theory: Duality cascades and chi SB resolution of naked singularities. *JHEP*, 08:052, 2000.
- [234] Igor R. Klebanov and Edward Witten. Superconformal field theory on three-branes at a Calabi-Yau singularity. *Nucl. Phys.*, B536:199–218, 1998.
- [235] Albrecht Klemm and Eric Zaslow. Local mirror symmetry at higher genus. *AMS/IP Stud. Adv. Math.*, 23:183–207, 2001.

- [236] A. Klimyk and K. Schmudgen. *Quantum groups and their representations*. 1997.
- [237] Joachim Kock. *Frobenius algebras and 2-d topological quantum field theories*, volume 59. Cambridge University Press, 2004.
- [238] Paul Koerber. Stable D-branes, calibrations and generalized Calabi-Yau geometry. *JHEP*, 08:099, 2005.
- [239] Paul Koerber. Lectures on Generalized Complex Geometry for Physicists. *Fortsch. Phys.*, 59:169–242, 2011.
- [240] Paul Koerber and Luca Martucci. From ten to four and back again: How to generalize the geometry. *JHEP*, 08:059, 2007.
- [241] Axel Krause and Enrico Pajer. Chasing brane inflation in string-theory. *JCAP*, 0807:023, 2008.
- [242] C.I. Lazaroiu. On the structure of open - closed topological field theory in two-dimensions. *Nucl. Phys. B*, 603:497–530, 2001.
- [243] Aitor Lewkowycz and Juan Maldacena. Generalized gravitational entropy. *Journal of High Energy Physics*, 2013:90, August 2013.
- [244] Aitor Lewkowycz and Juan Maldacena. Exact results for the entanglement entropy and the energy radiated by a quark. *JHEP*, 05:025, 2014.
- [245] Chang-Shou Lin and Chin-Lung Wang. Elliptic functions, green functions and the mean field equations on tori. *Annals of Mathematics*, pages 911–954, 2010.
- [246] Jennifer Lin. Ryu-Takayanagi Area as an Entanglement Edge Term. *arXiv e-prints*, page arXiv:1704.07763, April 2017.
- [247] Jennifer Lin. Entanglement entropy in Jackiw-Teitelboim Gravity. *arXiv e-prints*, page arXiv:1807.06575, July 2018.
- [248] Jan Louis, Markus Rummel, Roberto Valandro, and Alexander Westphal. Building an explicit de Sitter. *JHEP*, 10:163, 2012.
- [249] Dieter Lust, Fernando Marchesano, Luca Martucci, and Dimitrios Tsimpis. Generalized non-supersymmetric flux vacua. *JHEP*, 11:021, 2008.



- [250] J. Maldacena and L. Susskind. Cool horizons for entangled black holes. *Fortschritte der Physik*, 61(9):781–811, September 2013.
- [251] Juan Maldacena. Wilson Loops in Large N Field Theories. *prl*, 80(22):4859–4862, Jun 1998.
- [252] Juan Maldacena. The Large-N Limit of Superconformal Field Theories and Supergravity. *International Journal of Theoretical Physics*, 38:1113–1133, January 1999.
- [253] Juan Maldacena. Eternal black holes in anti-de Sitter. *Journal of High Energy Physics*, 2003(4):021, April 2003.
- [254] Juan Martin Maldacena and Carlos Nunez. Supergravity description of field theories on curved manifolds and a no go theorem. *Int. J. Mod. Phys. A*, 16:822–855, 2001.
- [255] Fernando Marchesano and Luca Martucci. Non-perturbative effects on seven-brane Yukawa couplings. *Phys. Rev. Lett.*, 104:231601, 2010.
- [256] Fernando Marchesano, Gary Shiu, and Angel M. Uranga. F-term Axion Monodromy Inflation. *JHEP*, 09:184, 2014.
- [257] M. Marino. *Chern-Simons theory, matrix models, and topological strings*, volume 131. 2005.
- [258] Marcos Marino. Chern-Simons theory and topological strings. *Rev. Mod. Phys.*, 77:675–720, 2005.
- [259] Marcos Marino, Ruben Minasian, Gregory W. Moore, and Andrew Strominger. Nonlinear instantons from supersymmetric p-branes. *JHEP*, 01:005, 2000.
- [260] Donald Marolf and Henry Maxfield. Transcending the ensemble: baby universes, spacetime wormholes, and the order and disorder of black hole information. *Journal of High Energy Physics*, 2020(8):44, August 2020.
- [261] Luca Martucci. Warping the Kähler potential of F-theory/IIB flux compactifications. *JHEP*, 03:067, 2015.
- [262] Luca Martucci. Warped Kähler potentials and fluxes. *JHEP*, 01:056, 2017.

- [263] D. Maulik, A. Oblomkov, A. Okounkov, and R. Pandharipande. Gromov-Witten/Donaldson-Thomas correspondence for toric 3-folds. *arXiv e-prints*, page arXiv:0809.3976, September 2008.
- [264] Liam McAllister. de Sitter Vacua from Ten Dimensions. talk presented at String Phenomenology 2019, June 2019.
- [265] Liam McAllister. An Inflaton mass problem in string inflation from threshold corrections to volume stabilization. *JCAP*, 0602:010, 2006.
- [266] Liam McAllister, Pedro Schwaller, Geraldine Servant, John Stout, and Alexander Westphal. Runaway Relaxion Monodromy. *JHEP*, 02:124, 2018.
- [267] Liam McAllister, Pedro Schwaller, Geraldine Servant, John Stout, and Alexander Westphal. Runaway Relaxion Monodromy. *JHEP*, 02:124, 2018.
- [268] Liam McAllister and Eva Silverstein. String Cosmology: A Review. *Gen. Rel. Grav.*, 40:565–605, 2008.
- [269] Liam McAllister, Eva Silverstein, and Alexander Westphal. Gravity Waves and Linear Inflation from Axion Monodromy. *Phys. Rev.*, D82:046003, 2010.
- [270] Liam McAllister, Eva Silverstein, and Alexander Westphal. Gravity Waves and Linear Inflation from Axion Monodromy. *Phys. Rev.*, D82:046003, 2010.
- [271] Liam McAllister, Eva Silverstein, Alexander Westphal, and Timm Wrase. The Powers of Monodromy. *JHEP*, 09:123, 2014.
- [272] Lauren McGough and Herman Verlinde. Bekenstein-Hawking entropy as topological entanglement entropy. *Journal of High Energy Physics*, 2013:208, November 2013.
- [273] Paul McGuirk, Gary Shiu, and Yosuke Sumitomo. Non-supersymmetric infrared perturbations to the warped deformed conifold. *Nucl. Phys.*, B842:383–413, 2011.
- [274] Jacob McNamara and Cumrun Vafa. Cobordism Classes and the Swampland. 9 2019.
- [275] Jacob McNamara and Cumrun Vafa. Baby Universes, Holography, and the Swampland. *arXiv e-prints*, page arXiv:2004.06738, April 2020.

- [276] Thomas G. Mertens and Gustavo J. Turiaci. Liouville quantum gravity – holography, JT and matrices. *arXiv e-prints*, page arXiv:2006.07072, June 2020.
- [277] Andrei Micu, Eran Palti, and Gianmassimo Tasinato. Towards Minkowski Vacua in Type II String Compactifications. *JHEP*, 03:104, 2007.
- [278] Gregory W. Moore and Graeme Segal. D-branes and K-theory in 2D topological field theory. 8 2006.
- [279] Jakob Moritz, Ander Retolaza, and Alexander Westphal. Toward de Sitter space from ten dimensions. *Phys. Rev.*, D97(4):046010, 2018.
- [280] Andrew Neitzke and Cumrun Vafa. Topological strings and their physical applications. 10 2004.
- [281] Nikita A. Nekrasov. Seiberg-Witten Prepotential From Instanton Counting. *arXiv e-prints*, pages hep-th/0206161, June 2002.
- [282] Nikita A. Nekrasov and Samson L. Shatashvili. Quantization of Integrable Systems and Four Dimensional Gauge Theories. In *XVITH INTERNATIONAL CONGRESS ON MATHEMATICAL PHYSICS. Held 3-8 August 2009 in Prague*, pages 265–289, March 2010.
- [283] Georges Obied, Hiroshi Ooguri, Lev Spodyneiko, and Cumrun Vafa. De Sitter Space and the Swampland. 6 2018.
- [284] Mathematical Society of Japan. *Encyclopedic Dictionary of Mathematics: A-E*. Number v. 1 in *Encyclopedic Dictionary of Mathematics*. MIT Press, 1987.
- [285] Hiroshi Ooguri and Cumrun Vafa. Knot invariants and topological strings. *Nucl. Phys.*, B577:419–438, 2000.
- [286] Hiroshi Ooguri and Cumrun Vafa. World sheet derivation of a large N duality. *Nucl. Phys.*, B641:3–34, 2002.
- [287] Hiroshi Ooguri and Cumrun Vafa. On the Geometry of the String Landscape and the Swampland. *Nucl. Phys.*, B766:21–33, 2007.
- [288] Hiroshi Ooguri, Cumrun Vafa, and Erik P. Verlinde. Hartle-Hawking wave-function for flux compactifications. *Lett. Math. Phys.*, 74:311–342, 2005.

- [289] Eran Palti. The Swampland: Introduction and Review. *Fortsch. Phys.*, 67(6):1900037, 2019.
- [290] Geoff Penington, Stephen H. Shenker, Douglas Stanford, and Zhenbin Yang. Replica wormholes and the black hole interior. *arXiv e-prints*, page arXiv:1911.11977, November 2019.
- [291] J. Polchinski. *String Theory. Vol. 1: An Introduction to the Bosonic String*. Cambridge Monographs on Mathematical Physics. Cambridge University Press, 2007.
- [292] Joseph Polchinski. *String theory. Vol. 2: Superstring theory and beyond*. Cambridge University Press, 2007.
- [293] Joseph Polchinski and Matthew J. Strassler. The String dual of a confining four-dimensional gauge theory. 2000.
- [294] Joseph Polchinski and Edward Witten. Evidence for heterotic - type I string duality. *Nucl. Phys. B*, 460:525–540, 1996.
- [295] Thomas Quella. Symmetry protected topological phases beyond groups: The q-deformed aklt model. 05 2020.
- [296] Fernando Quevedo. Local String Models and Moduli Stabilisation. *Mod. Phys. Lett.*, A30(07):1530004, 2015.
- [297] Lisa Randall. The Boundaries of KKLT. *Fortsch. Phys.*, 68(3-4):1900105, 2020.
- [298] Lisa Randall and Raman Sundrum. A Large mass hierarchy from a small extra dimension. *Phys. Rev. Lett.*, 83:3370–3373, 1999.
- [299] Ander Retolaza and Angel Uranga. De Sitter Uplift with Dynamical Susy Breaking. *JHEP*, 04:137, 2016.
- [300] S. J. Rey and J. T. Yee. Macroscopic strings as heavy quarks: Large-  $N$  gauge theory and anti-de Sitter supergravity. *European Physical Journal C*, 22(2):379–394, Nov 2001.
- [301] Fabian Ruehle and Clemens Wieck. One-loop Pfaffians and large-field inflation in string theory. *Phys. Lett.*, B769:289–298, 2017.

- [302] Ingo Runkel and Lóránt Szegedy. Area-dependent quantum field theory with defects, 2018.
- [303] Shinsei Ryu and Tadashi Takayanagi. Holographic Derivation of Entanglement Entropy from the anti de Sitter Space/Conformal Field Theory Correspondence. *Phys. Rev. Lett.*, 96(18):181602, May 2006.
- [304] Phil Saad, Stephen H. Shenker, and Douglas Stanford. JT gravity as a matrix integral. *arXiv e-prints*, page arXiv:1903.11115, March 2019.
- [305] Nathan Seiberg and Edward Witten. String theory and noncommutative geometry. *Journal of High Energy Physics*, 1999(9):032, September 1999.
- [306] Sarah Shandera, Benjamin Shlaer, Horace Stoica, and S. H. Henry Tye. Interbrane interactions in compact spaces and brane inflation. *JCAP*, 0402:013, 2004.
- [307] C.L. Siegel. *Zur Theorie Der Quadratischen Formen, Von C.L. Siegel.* Akademie der Wissenschaften, Göttingen. Mathematisch-Physikalische Klasse. Nachrichten, Jahrg. 1972, Nr. 3. 1972.
- [308] Eva Silverstein. TASI / PiTP / ISS lectures on moduli and microphysics. In *Progress in string theory. Proceedings, Summer School, TASI 2003, Boulder, USA, June 2-27, 2003*, pages 381–415, 2004.
- [309] Eva Silverstein and Alexander Westphal. Monodromy in the CMB: Gravity Waves and String Inflation. *Phys. Rev.*, D78:106003, 2008.
- [310] J. K. Slingerland and F. A. Bais. Quantum groups and nonabelian braiding in quantum hall systems. *Nucl.Phys.*, B612:229–290, 2001.
- [311] Paul J. Steinhardt and Daniel Wesley. Dark Energy, Inflation and Extra Dimensions. *Phys. Rev.*, D79:104026, 2009.
- [312] Andrew Strominger. Massless black holes and conifolds in string theory. *Nucl. Phys. B*, 451:96–108, 1995.
- [313] Andrew Strominger and Cumrun Vafa. Microscopic origin of the Bekenstein-Hawking entropy. *Phys. Lett. B*, 379:99–104, 1996.
- [314] Leonard Susskind. The Anthropic landscape of string theory. 2 2003.

- [315] Leonard Susskind and John Uglum. Black hole entropy in canonical quantum gravity and superstring theory. *Phys. Rev.*, D50:2700–2711, 1994.
- [316] Gerard 't Hooft. A Planar Diagram Theory for Strong Interactions. *Nucl. Phys. B*, 72:461, 1974.
- [317] Tadashi Takayanagi and Kotaro Tamaoka. Gravity edges modes and Hayward term. *Journal of High Energy Physics*, 2020(2):167, February 2020.
- [318] Clifford Henry Taubes. Lagrangians for the Gopakumar-Vafa conjecture. *arXiv Mathematics e-prints*, page math/0201219, January 2002.
- [319] John Terning. *Modern supersymmetry: Dynamics and duality*. Oxford: Clarendon, 2006.
- [320] J. Teschner. TOPICAL REVIEW: Liouville theory revisited. *Classical and Quantum Gravity*, 18(23):R153–R222, December 2001.
- [321] The Sage Developers. *SageMath, the Sage Mathematics Software System (Version 9.0)*, 2020. <https://www.sagemath.org>.
- [322] Arkady A. Tseytlin. Mobius Infinity Subtraction and Effective Action in  $\sigma$  Model Approach to Closed String Theory. *Phys. Lett. B*, 208:221–227, 1988.
- [323] Jon Urrestilla, Neil Bevis, Mark Hindmarsh, and Martin Kunz. Cosmic string parameter constraints and model analysis using small scale Cosmic Microwave Background data. *JCAP*, 1112:021, 2011.
- [324] Cumrun Vafa. Gas of d-branes and Hagedorn density of BPS states. *Nucl. Phys. B*, 463:415–419, 1996.
- [325] Cumrun Vafa. Brane/anti-Brane Systems and  $U(N-M)$  Supergroup. *arXiv e-prints*, pages hep-th/0101218, January 2001.
- [326] Cumrun Vafa. Two dimensional Yang-Mills, black holes and topological strings. 6 2004.
- [327] Cumrun Vafa. Two Dimensional Yang-Mills, Black Holes and Topological Strings. *arXiv e-prints*, pages hep-th/0406058, June 2004.
- [328] Cumrun Vafa and Edward Witten. A Strong coupling test of S duality. *Nucl. Phys. B*, 431:3–77, 1994.

- [329] Irene Valenzuela. Backreaction Issues in Axion Monodromy and Minkowski 4-forms. *JHEP*, 06:098, 2017.
- [330] Antoine Van Proeyen. Tools for supersymmetry. *Ann. U. Craiova Phys.*, 9(I):1–48, 1999.
- [331] Mark van Raamsdonk. Building up spacetime with quantum entanglement. *General Relativity and Gravitation*, 42(10):2323–2329, October 2010.
- [332] Herman Verlinde. ER = EPR revisited: On the Entropy of an Einstein-Rosen Bridge. *arXiv e-prints*, page arXiv:2003.13117, March 2020.
- [333] Marcel Vonk. A mini-course on topological strings. *arXiv e-prints*, pages hep-th/0504147, April 2005.
- [334] C.T.C. Wall. Classification Problems in Differential Topology V. On Certain 6-Manifolds. *Inventiones Mathematicae*, 1:355–374, 1966.
- [335] Steven Weinberg. The Cosmological Constant Problem. *Rev. Mod. Phys.*, 61:1–23, 1989.
- [336] Xueda Wen, Shunji Matsuura, and Shinsei Ryu. Edge theory approach to topological entanglement entropy, mutual information and entanglement negativity in Chern-Simons theories. *Phys. Rev.*, B93(24):245140, 2016.
- [337] Edward Witten. Interacting field theory of open superstrings. *Nuclear Physics B*, 276(2):291–324, 1986.
- [338] Edward Witten. Noncommutative Geometry and String Field Theory. *Nucl. Phys. B*, 268:253–294, 1986.
- [339] Edward Witten. (2+1)-Dimensional Gravity as an Exactly Soluble System. *Nucl. Phys. B*, 311:46, 1988.
- [340] Edward Witten. Topological Sigma Models. *Commun. Math. Phys.*, 118:411, 1988.
- [341] Edward Witten. Quantum Field Theory and the Jones Polynomial. *Commun. Math. Phys.*, 121:351–399, 1989.
- [342] Edward Witten. Quantum Background Independence In String Theory. *arXiv e-prints*, pages hep-th/9306122, June 1993.

- [343] Edward Witten. Chern-Simons gauge theory as a string theory. *Prog. Math.*, 133:637–678, 1995.
- [344] Edward Witten. String theory dynamics in various dimensions. *Nucl. Phys. B*, 443:85–126, 1995.
- [345] Edward Witten. String theory dynamics in various dimensions. *Nuclear Physics B*, 443(1):85–126, February 1995.
- [346] Edward Witten. Nonperturbative superpotentials in string theory. *Nucl. Phys.*, B474:343–360, 1996.
- [347] Edward Witten. Strong coupling expansion of Calabi-Yau compactification. *Nucl. Phys. B*, 471:135–158, 1996.
- [348] Edward Witten. Anti-de Sitter space and holography. *Advances in Theoretical and Mathematical Physics*, 2:253–291, January 1998.
- [349] Edward Witten. Mirror manifolds and topological field theory. *AMS/IP Stud. Adv. Math.*, 9:121–160, 1998.
- [350] Edward Witten. Quantum gravity in de Sitter space. In *Strings 2001: International Conference*, 6 2001.
- [351] Edward Witten. Open strings on the Rindler horizon. *Journal of High Energy Physics*, 2019:126, Jan 2019.
- [352] Gabriel Wong. A note on entanglement edge modes in Chern Simons theory. *JHEP*, 08:020, 2018.
- [353] SL. Woronowicz. Compact matrix pseudogroups. *Communications in Mathematical Physics* 111 (4), 613-665, 1987.
- [354] Timm Wrase and Marco Zagermann. On Classical de Sitter Vacua in String Theory. *Fortsch. Phys.*, 58:906–910, 2010.
- [355] Barton Zwiebach. Closed string field theory: Quantum action and the Batalin-Vilkovisky master equation. *Nuclear Physics B*, 390(1):33–152, January 1993.